THE 13TH RESCEU INTERNATIONAL SYMPOSIUM

JGRG31

October 24 - 28, 2022

The 31st Workshop on General Relativity and Gravitation
Koshiba Hall, The University of Tokyo
(Online-hybrid style)

Volume III: Contributed Talks 2

Contributed talks

C41 – C86

C41

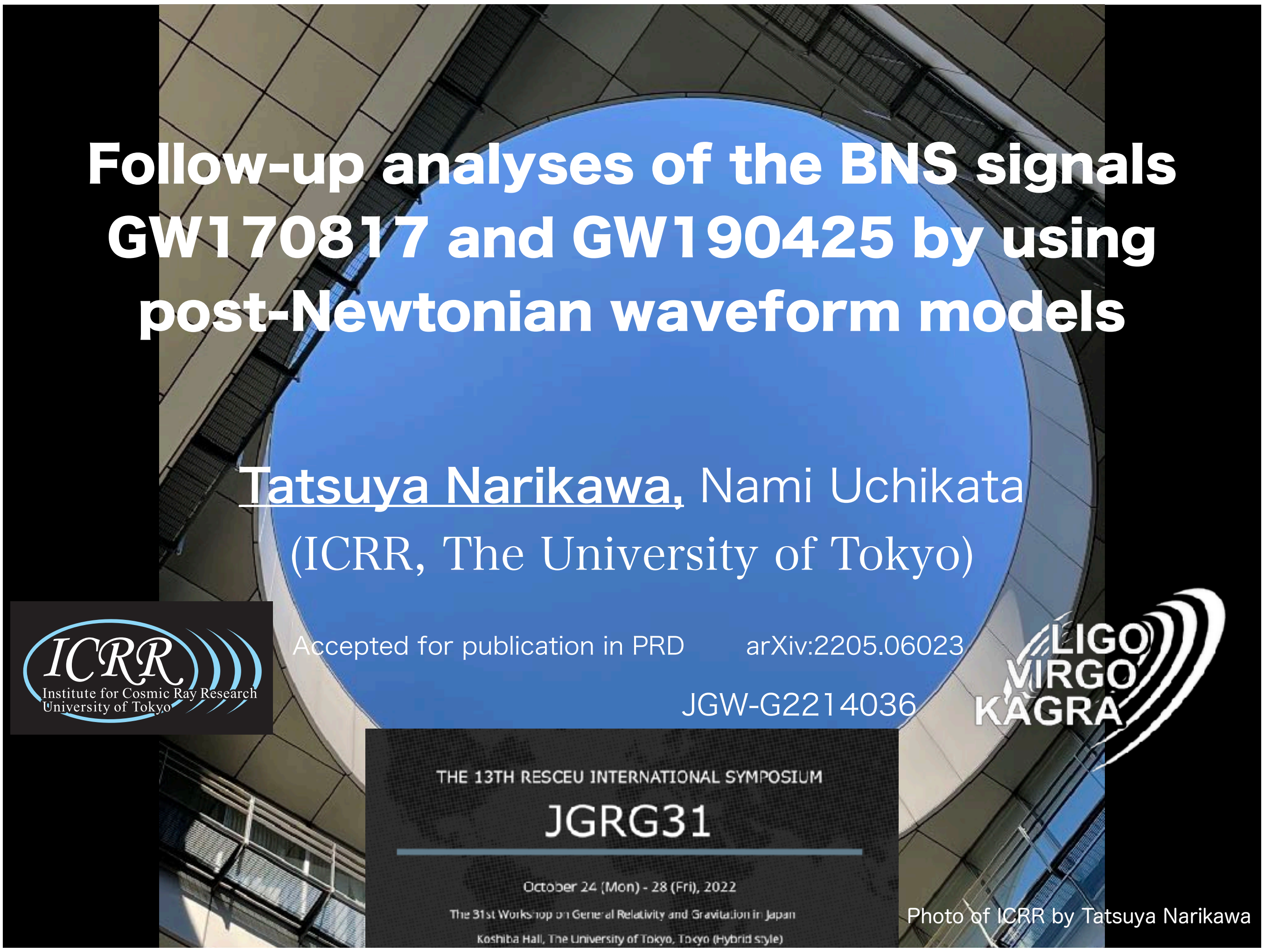

Follow-up analyses of the BNS signals GW170817 and GW190425 by using post-Newtonian waveform models

Tatsuya Narikawa, Nami Uchikata
(ICRR, The University of Tokyo)

ICRR Institute for Cosmic Ray Research University of Tokyo

Accepted for publication in PRD arXiv:2205.06023

JGW-G2214036

LIGO VIRGO KAGRA

THE 13TH RESCEU INTERNATIONAL SYMPOSIUM
JGRG31
October 24 (Mon) - 28 (Fri), 2022
The 31st Workshop on General Relativity and Gravitation in Japan
Koshiba Hall, The University of Tokyo, Tokyo (Hybrid style)

Photo of ICRR by Tatsuya Narikawa

Post-Newtonian (PN) theory

PN approximation: solve the Einstein eqs. by a series in v/c.
PN theory is theoretically rigid and can efficiently describe the GW emission in the inspiral regime. (valid for slow motion v<<1 and weak field M/R<<1)

The energy balance The GW phase

$$\dot{E}_{\rm bind} = -F_{\rm GW} \quad \longrightarrow \quad \frac{d\Psi_{\rm SPA}(f)}{df} - 2\pi t(f) = 0$$

PN tidal theory

PN tidal phase has been derived up to 2.5PN (relative 5+2.5PN) order [Flanagan&Hinderer08; Damour, Nagar, Villain2012]. (**PNTidal**)

Recently, the complete and correct tidal phase up to 2.5PN has been derived [Henry, Faye, Blanchet 2020; Narikawa, Uchikata, Tanaka 2021].

However, the correct **PNTidal** model has not been used in BNS analyses yet.
In this work, we first use it in BNS analyses.

Sophisticated models (EOB, IMRPhenom and NR calibrated models) are constructed by extension of the PN theory.

Post-Newtonian phase

modeling has advanced in recent years.

TaylorF2_PNTidal

$\chi_{\rm eff}$: spin
Difficult to measure well

η: symmetric mass ratio
Difficult to measure well

$$\Psi_{\rm BNS}(f) = \Psi_{\rm BBH}(f) + \Psi_{\rm Tidal}(f)$$

$$\sim \mathscr{M}^{-5/3} f^{-5/3} \left[1 + a_{\rm 1PN}(\eta) x^2 + a_{\rm 1.5PN}(\eta, \chi_{\rm eff}) x^3 \right.$$

$\mathscr{M}$:chirp mass
Measurable very well

$$\left. + a_{\rm 2PN}(\eta, \chi_i^2, \kappa_s) x^4 + \ldots + a_{\rm 5PN}(\tilde{\Lambda}) x^{10} + \ldots \right]$$

κ: spin-induced QM
NS EOSs

Λ: tidal deformability
NS EOSs

v: orbital velocity

$$x = (\pi M f)^{2/3} = v^2$$

PN formalism review [Blanchet2014; Poisson&Will2014; Isoyama, Nakano, Sturani 2020]
TF2 (3.5PN) [Dhurandhar+1994; Buonanno+2009] **Spin** summarized in [Khan+2016]
PNTidal [Flanagan&Hinderer08; Damour, Nagar, Villain 2012; Henry+2020; Narikawa+2021]

Tidal deformability λ

When binary orbital separations are small, each star is tidally distorted by its companion.

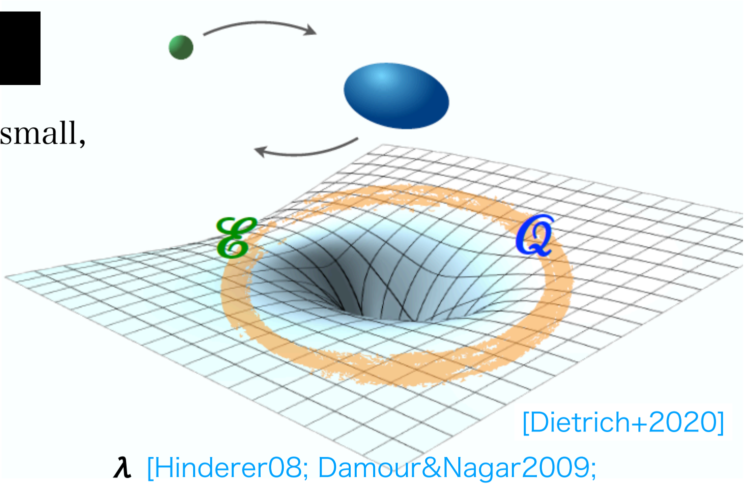

[Dietrich+2020]

$$\lambda := -\frac{Q_{ij}}{E_{ij}}$$

Q_{ij}: tidally induced quadrupole moment
E_{ij}: companion's tidal field

λ [Hinderer08; Damour&Nagar2009; Postnikov+2010]

The tidal deformability of NS matter affects the GW signals and characterizes NS EOS models.

Binary tidal deformability $\tilde{\Lambda} = \frac{16}{13}\left[(1+11X_2)X_1^4\Lambda_1 + (1 \leftrightarrow 2)\right]$

$\Lambda_{1,2} = \lambda_{1,2}/m_{1,2}^5$: individual ones $\quad X_{1,2} = m_{1,2}/(m_1+m_2)$: mass ratio

PNTidal [Flanagan&Hinderer08; Damour, Nagar, Villain 2012; Henry, Faye, Blanchet 2020; Narikawa, Uchikata, Tanaka 2021]

Tidal effects on waveform

[Chatziioannou, 2006.03168]

Evolution depends on NS EOS.

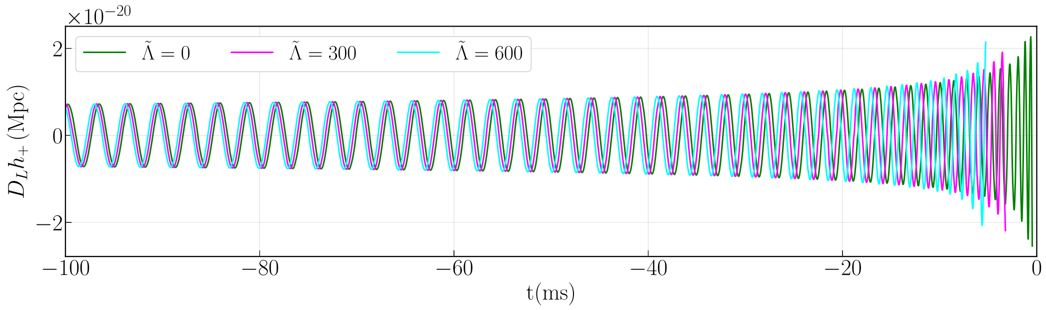

Less Compact NS -> fast evolution (large Λ)

More Compact NS -> slow evolution (small Λ)

BBH -> slowest evolution (Λ=0)

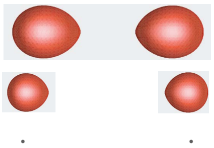

GW inference on GW170817

[LVC 2017, 2018]

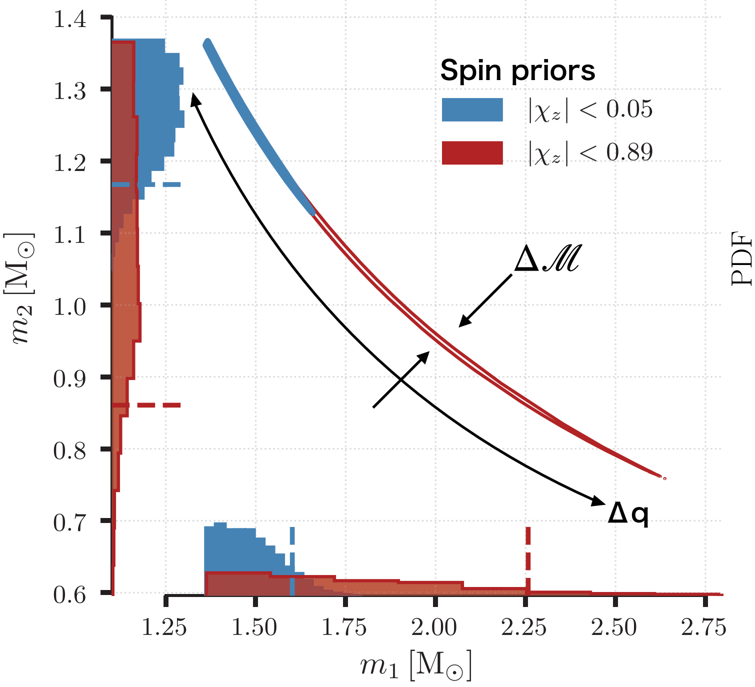

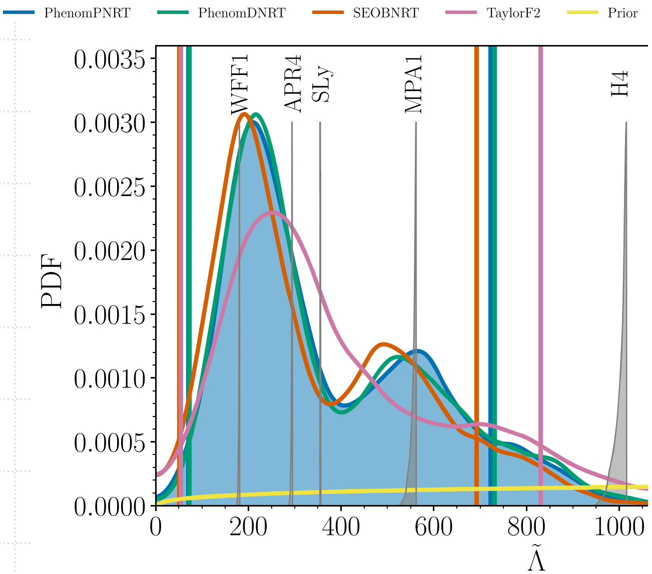

$\mathscr{M}$: measured well.

q: not measured well.

q-χ_{eff} correlation

$\tilde{\Lambda}$: measured, less compact EOS models are disfavored.

NRTidal might bias $\tilde{\Lambda}$ smaller.

[De+2018; Dai+2018; LVC2019; Narikawa+2018,2019; Chatziioannou2020]

NRTidal [Dietrich+2017]

Our analysis setup - parameter estimation

- **Post-Newtonian (PN) inspiral waveform model:**
  BBH (PP+Spin) + Tidal

- Phase $\Psi(f) = \Psi_{\rm BBH} + \Psi_{\rm tidal}$

Adding higher-order PN terms prevent $\tilde{\Lambda}$ biasing

- Point-particle: **TaylorF2+** (up to 6PN)
- Aligned-spin, Spin-Orbit: 1.5-3.5 PN, Spin-Spin: 2-3 PN,
- **Tidal effects: 5-5+2.5PN.**

Spin terms at other PN orders help to break degeneracies, e.g., $q - \chi_{\rm eff}$

We have implemented the correct **PNTidal** model.

- Amplitude up to 3PN for BBH (PP+spin), up to 5+1PN for Tidal

- Priors: **low-spin prior: $|\chi_{1z,2z}|<0.05$;** uniform in [0, 3000] on $\tilde{\Lambda}$
  astrophysically motivated

- **$f_{\rm high}$=1000 Hz to restrict to the inspiral regime**

- Bayesian inference library: Nested sampling in LALSUITE (LALInferenceNest)

Tidal phasing

different PN orders, from 5PN through 5+2.5PN, in PNTidal

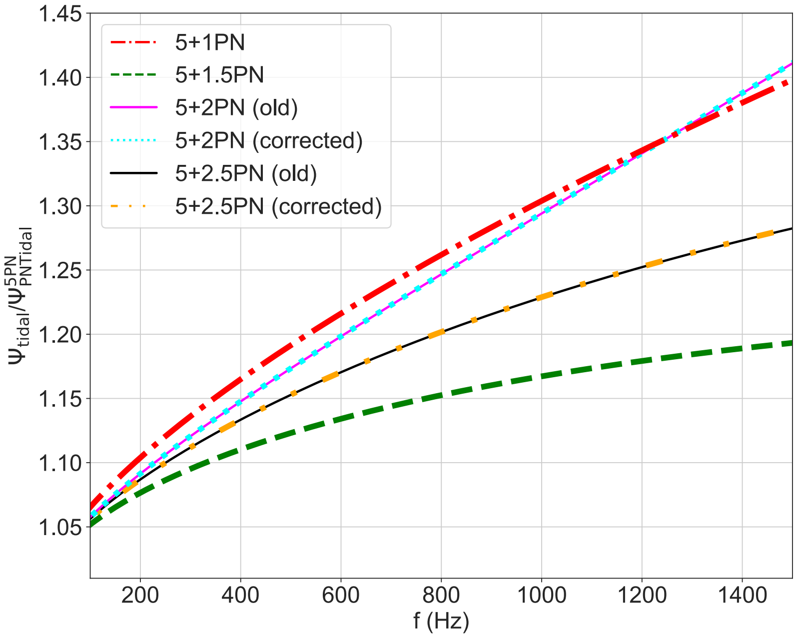

5+2PN
5+1PN

5+2.5PN

5+1.5PN

larger shift

demonstrated for un-equal mass binary, 1.68+1.13 $M_\odot$

PNTidal (old): [Agathos+, 2015].
PNTidal (corrected): [Henry+, 2020; Narikawa+, 2020].

An increase of PN order does not lead to a monotonic change in the phase shift.

The terms at 5+1PN and 5+2PN give larger phase shift. This is related to the half-PN orders at 5+1.5PN and 5+2.5PN being repulsive.

Tidal phasing
different PN orders in PNTidal and NR calibrated models

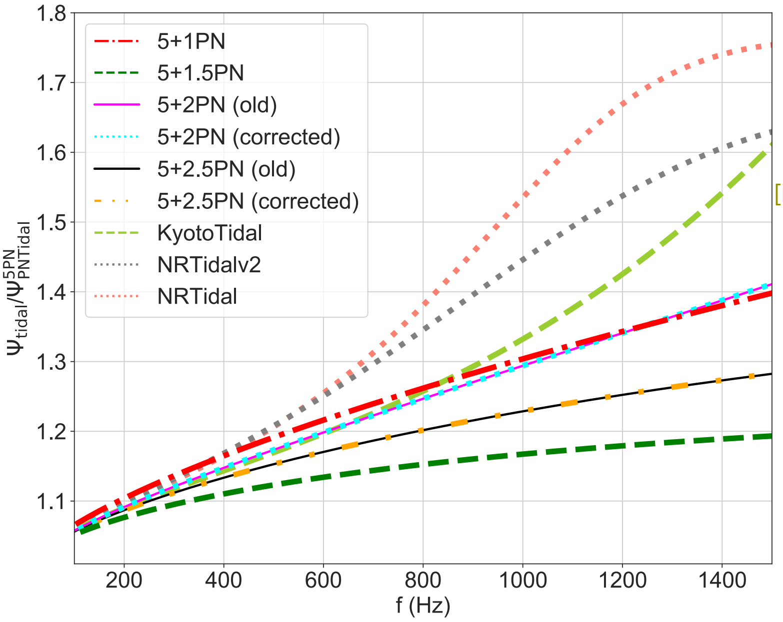

NRTidal

NRTidalv2

KyotoTidal

[Kawaguchi+]

NR calibrated models

5+2PN

5+1PN

5+2.5PN

5+1.5PN

PNTidal

larger shift

demonstrated for un-equal mass binary, 1.68+1.13 M⊙ and $\tilde{\Lambda} = 292$

NR calibrated models: **KyotoTidal**, **NRTidalv2**, and **NRTidal** give larger phase shift (more attractive) than **PNTidal.**

The terms at 5+1PN and 5+2PN give closer to NR calibrated models than the half-PN orders at 5+1.5PN and 5+2.5PN due to being repulsive.

---

❶ Comparison among the estimates of tidal deformability $\tilde{\Lambda}$ with different PN orders in PNTidal

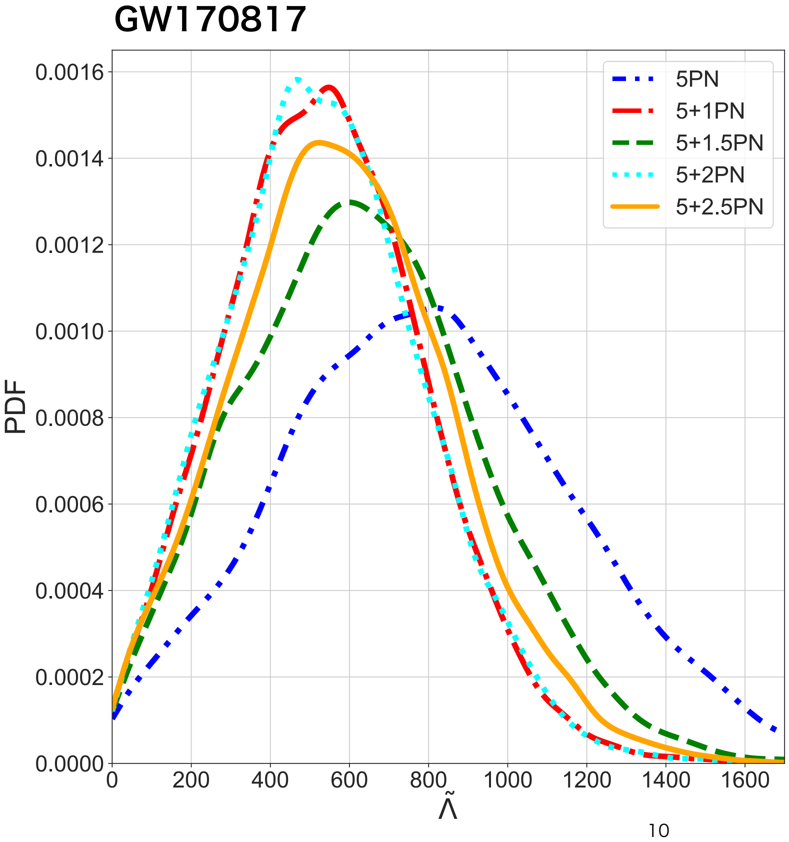

BBH baseline: **TF2+**, low-spin prior, $f_{\rm high}$=1000 Hz

An increase of PN order does not lead to a monotonic change in the estimates of $\tilde{\Lambda}$.

The terms up to 5+1PN and 5+2PN give smaller estimates on $\tilde{\Lambda}$. This is related to the half-PN orders at 5+1.5PN and **5+2.5PN** being repulsive.

Estimates of $\tilde{\Lambda}$ are consistent with the phase shift.

❷ Comparison between estimates of $\tilde{\Lambda}$ for PNTidal and NR calibrated models

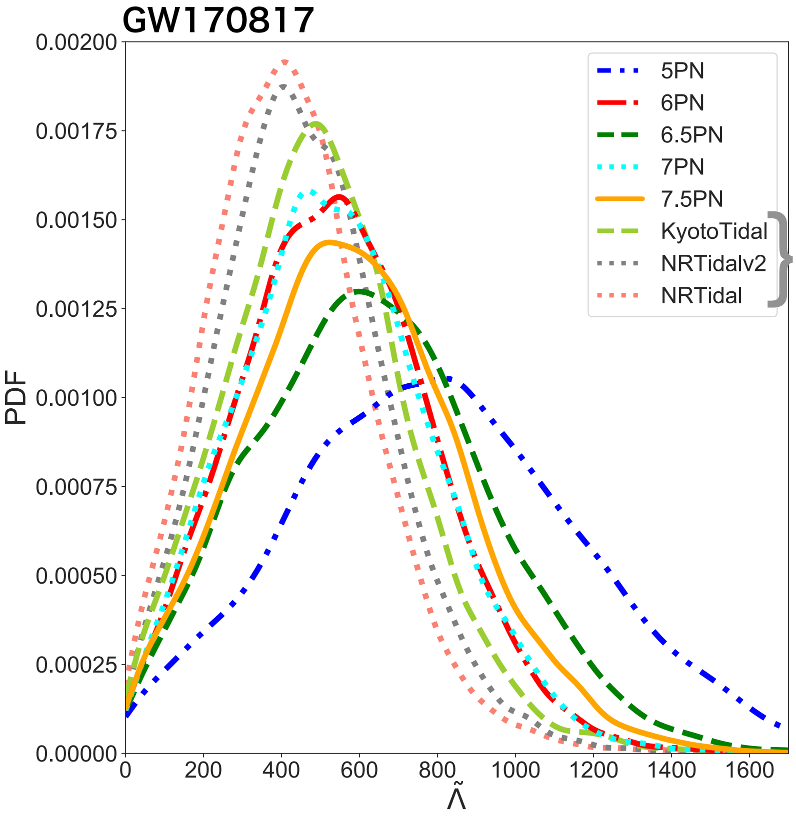

BBH baseline: **TF2+**,
low-spin prior, f_{high}=1000 Hz

NR calibrated models give smaller estimates of $\tilde{\Lambda}$ than PNTidal.

The terms up to 5+1PN and 5+2PN give closer estimates of $\tilde{\Lambda}$ with NR calibrated models, which is related to the half-PN orders at 5+1.5PN and **5+2.5PN** being repulsive.

Estimates of $\tilde{\Lambda}$ are consistent with the phase shift.

---

❸ Waveform model comparison among PNTidal and NR calibrated models

BBH baseline: **TF2+**,
low-spin prior, f_{high}=1000 Hz

The log Bayes factor

$$\log \mathrm{BF}_{\text{PNTidal/NR calibrated models}}$$

Waveform	GW170817
KyotoTidal	$0.25^{+0.14}_{-0.14}$
NRTidalv2	$0.23^{+0.14}_{-0.14}$
NRTidal	$0.46^{+0.14}_{-0.14}$
BBH (nontidal)	$0.79^{+0.13}_{-0.13}$

The log Bayes factors are less than 1, but positive values.

No preference among NR calibrated models over PNTidal. However, PNTidal is mildly preferred compared to NR calibrated models.

This is consistent with [Gamba+, 2021].

Summary

Post-Newtonian (PN) approximation is theoretically rigid and can efficiently describe the inspiral regime.

Follow-up analyses of GW170817 and GW190425 with **PNTidal** focusing on the inspiral regime (f_{high}=1000 Hz).

Results

Waveform systematics & Waveform model comparison:

➊ Different PN orders in PNTidal: **An increase of PN order does not lead to a monotonic change in the estimates of $\tilde{\Lambda}$.**

➋ PNTidal vs NR calibrated models: **NR calibrated models give smaller $\tilde{\Lambda}$ than PNTidal. No preference among NR calibrated models over PNTidal. However, PNTidal is mildly preferred compared to NR calibrated models.**

Since KAGRA has recently joined the international GW network [O3GK 2020] and the Adv. LIGO and Adv. Virgo detectors are improving their sensitivities now, they will detect BNS signals with high SNR and provide more information on the sources in coming observation runs.

Induced stochastic gravitational waves associated with primordial black holes as dark matter in the exponential-tailed case

2022 /10/25　Ryoto Inui　　C42

Collaboration with　Abe(Nagoya U.), Tada(IAR, KEK, Nagoya U.), and Yokoyama(KMI, Nagoya U.)

arXiv: 2209.13891v1

Primordial black hole (PBH)

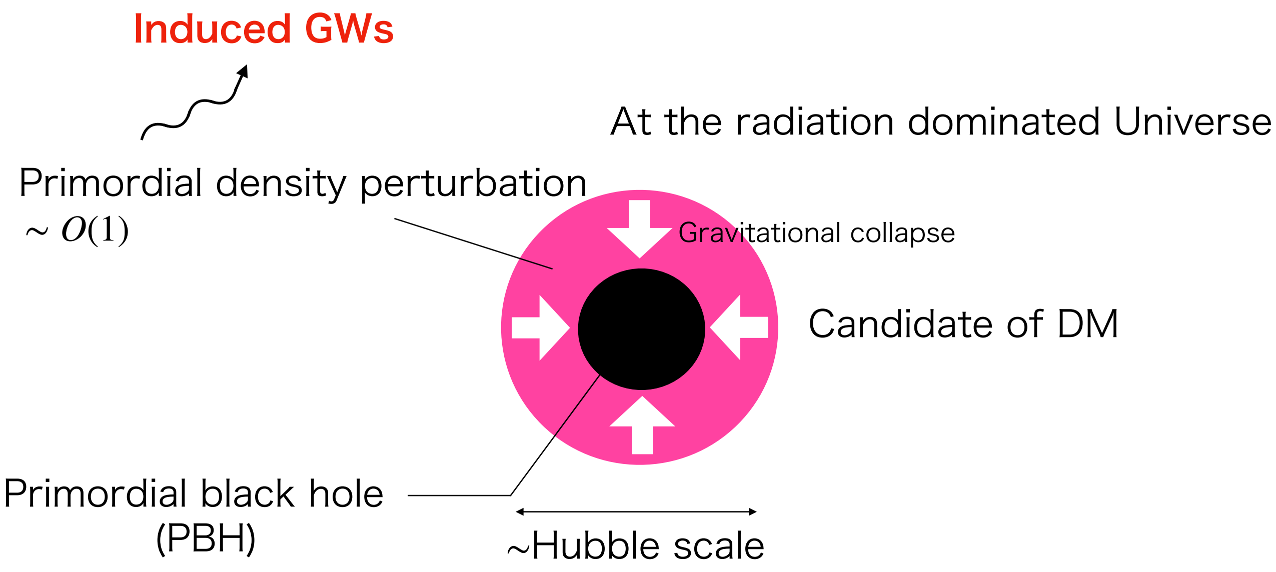

Induced GWs

At the radiation dominated Universe

Primordial density perturbation
$\sim O(1)$

Gravitational collapse

Candidate of DM

Primordial black hole
(PBH)

~Hubble scale

Observational quantity of PBH

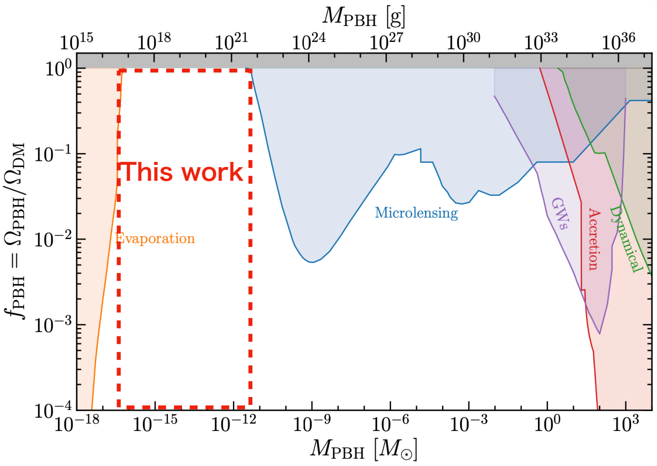

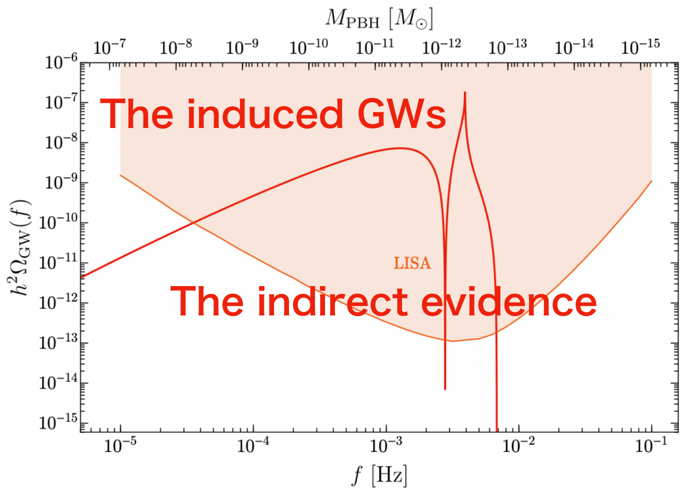

$$10^{-15}M_\odot \leq M_{\rm PBH} \lesssim 10^{-11}M_\odot$$

If PBH accounts for 100% of DM…

M.Green and J.Kavanagh '20
N.Bartolo et al. '19
R.Saito et al. '11

Exponential tail perturbation

Exponential tail $\zeta = -\frac{1}{\beta}\ln(1-\beta\zeta_g)$

ζ_g : Gaussian field

β : Parameter

Atal, Cid, Escriv`a and Garriga '19

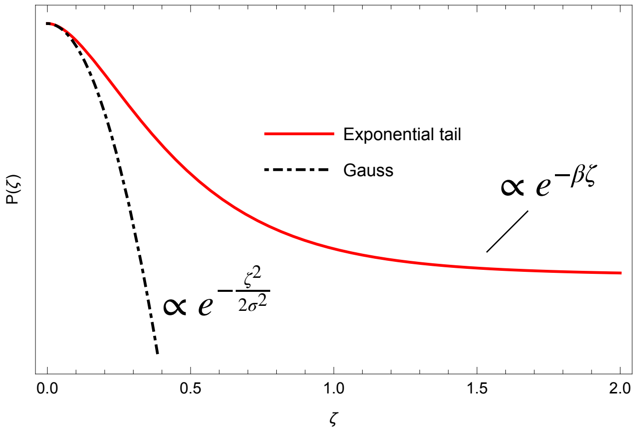

The GWs induced by the exponential tail perturbation

The induced GWs can be detected by LISA?

PBH abundance $(\beta = 3)$

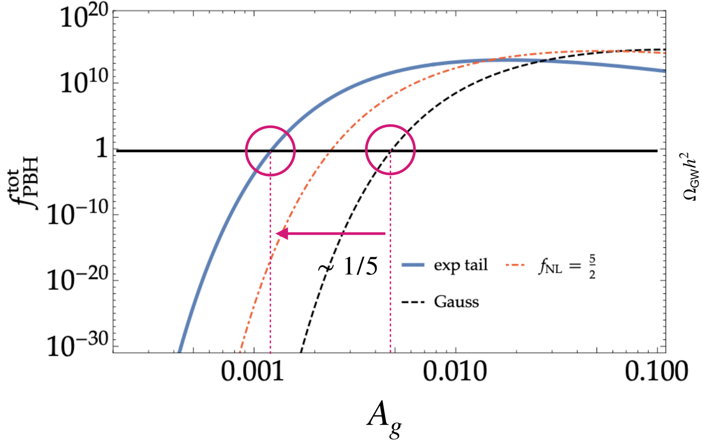

Induced GWs $(\beta = 3)$

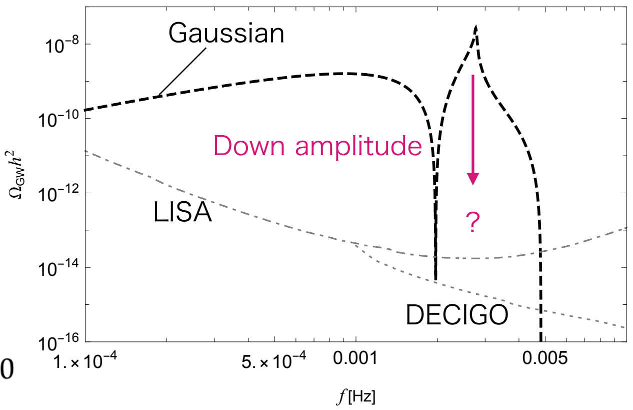

$$f_{\rm PBH}^{\rm tot} = 1,\ M_{\rm PBH} = 10^{-11} M_\odot$$

$$A_g = 1.32 \times 10^{-3}$$ Kitajima et al.2021

$$P_g(k) = \frac{2\pi^2 A_g}{k^3}\delta(\ln k - \ln k_*)$$

Scalar induced GWs

- Equation of motion for tensor perturbation

$$\Box h_\lambda(\tau, \boldsymbol{k}) = 4S_\lambda(\tau, \boldsymbol{k}) \propto \zeta\zeta \quad \longrightarrow \quad \text{The solution : } h_\lambda(\tau, \boldsymbol{k}) \propto \zeta\zeta$$

$(\lambda = +, \times)$ Source

- The power spectrum of tensor perturbation

$$(2\pi)^3 P_\lambda(\tau, k)\delta^{(3)}(\mathbf{k} + \mathbf{k}') = \left\langle h_\lambda(\tau, \mathbf{k}) h_\lambda(\tau, \mathbf{k}') \right\rangle \propto \left\langle \zeta(\boldsymbol{q}_1)\zeta(\boldsymbol{k} - \boldsymbol{q}_1)\zeta(\boldsymbol{q}_2)\zeta(\boldsymbol{k} - \boldsymbol{q}_2) \right\rangle$$

ex) : $\zeta = \zeta_g$ (Gaussian case)

$$\left\langle \zeta_g(\boldsymbol{q}_1)\zeta_g(\boldsymbol{k} - \boldsymbol{q}_1)\zeta_g(\boldsymbol{q}_2)\zeta_g(\boldsymbol{k} - \boldsymbol{q}_2) \right\rangle \sim O(A_g^2)$$

$$P_g(k) = \frac{2\pi^2 A_g}{k^3}\delta(\ln k - \ln k_*)$$

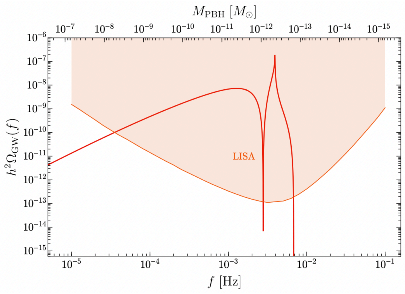

N.Bartolo et al. 2019

R.Saito et al. 2011

Scalar induced GWs

▷In the case of non-Gaussian perturbation

Perturbative expansion

$\zeta = \zeta_g + f_{\rm NL}\zeta_g^2 + g_{\rm NL}\zeta_g^3 \cancel{+\cdots}$

parametrize the non-Gaussianity with $f_{\rm NL}$ and $g_{\rm NL}$

Adshead et al 2105.01659 Yuan and Hung 2007.10686

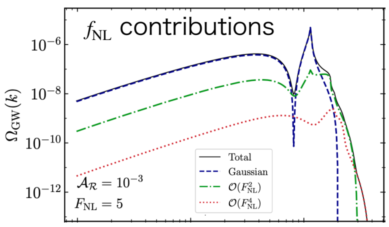

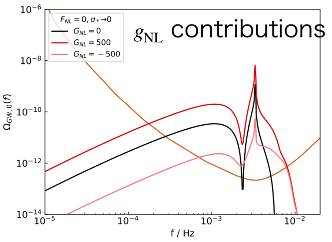

Exponential tail : $\zeta = -\dfrac{1}{3}\ln(1-3\zeta_g) = \zeta_g + \dfrac{3}{2}\zeta_g^2 + 3\zeta_g^3 + \dfrac{27}{4}\zeta_g^4 + \dfrac{81}{5}\zeta_g^5 + \cdots$

However, they are remaining another terms with same order up to $O(A_g^4)$

Crossing term $\propto f_{\rm NL}^2 g_{\rm NL} A_g^4,\ f_{\rm NL} h_{\rm NL} A_g^4$

Other non-considered terms $O(A_g^3),\ g_{\rm NL}^2 A_g^4, \cdots$

The tool for the calculation

▷ Diagrammatic approach···Corresponding a diagram and formula

Representation of $\langle h_\lambda(\tau,\boldsymbol{k}) h_{\lambda'}(\tau,\boldsymbol{k}')\rangle$

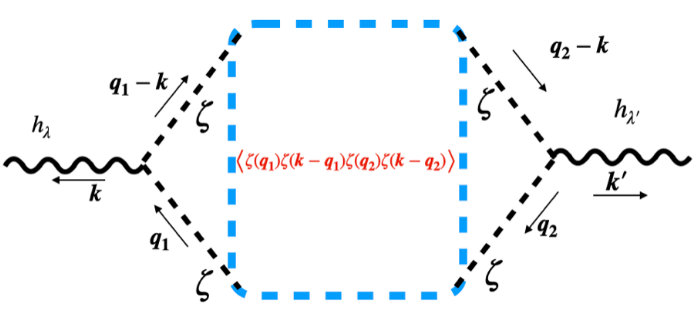

Building blocks

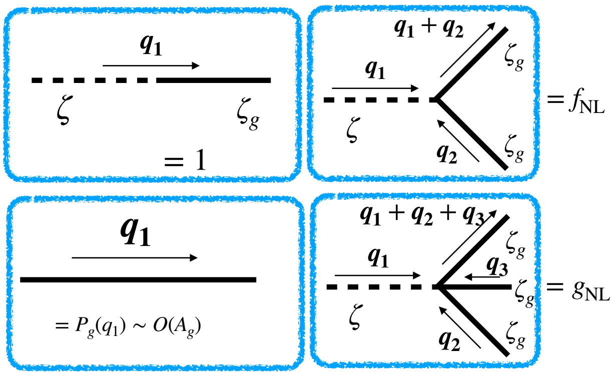

Adshead et al 2105.01659

The leading contribution

$$\left\langle \zeta_g(\boldsymbol{q_1})\zeta_g(\boldsymbol{k}-\boldsymbol{q_1})\zeta_g(\boldsymbol{q_2})\zeta_g(\boldsymbol{k}-\boldsymbol{q_2}) \right\rangle \sim O(A_g^2)$$

$O(A_g^2)$

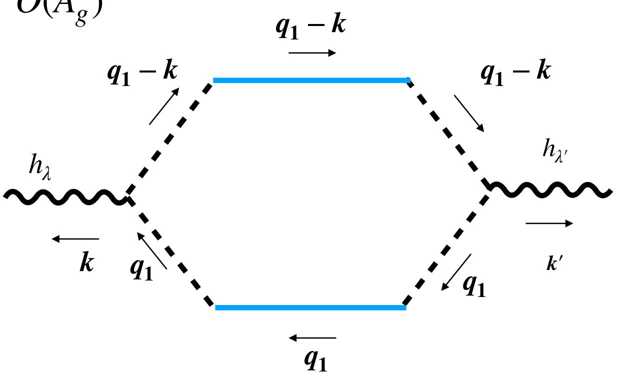

Vanilla

R.Saito et al. 2011

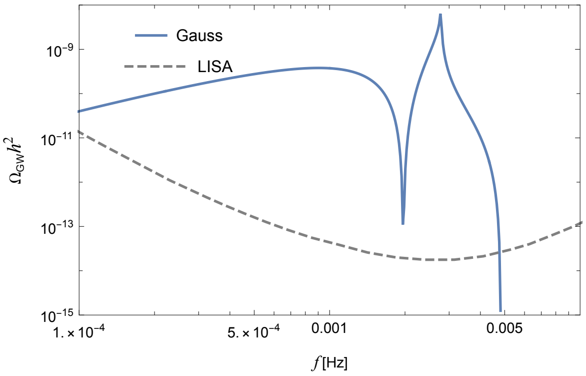

$f_{\rm PBH}^{\rm tot}=1,\ M_{\rm PBH}=10^{-11}M_\odot$

$\longleftrightarrow\ A_g=1.32\times10^{-3}$

$$P_g(k)=\frac{2\pi^2 A_g}{k^3}\delta(\ln k-\ln k_*)$$

$$k_*=1.56\times10^{12}\ {\rm Mpc}^{-1}$$

Higher order contributions

$O(A_g^3)$

Adshead et al 2105.01659

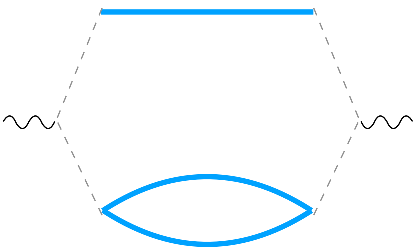

1-convolution

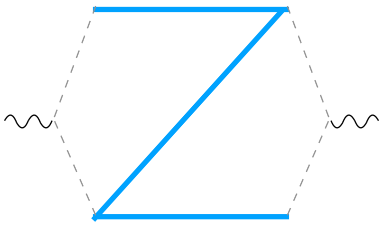

Z

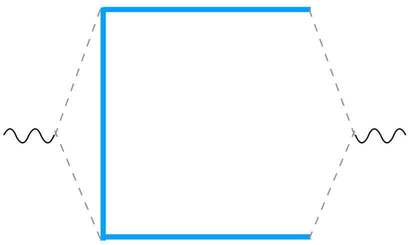

C

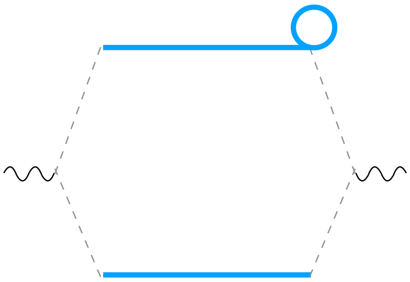

1 loop
Abe, Inui, Tada, Yokoyama

Higher order contributions

$O(A_g^4)$

Yuan and Huang, 2007.10686

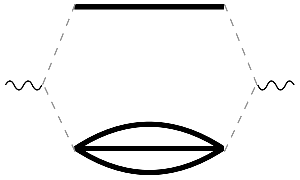

2-conv

Adshead et al 2105.01659

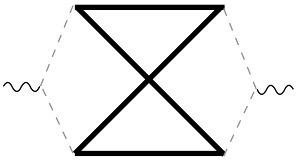

X

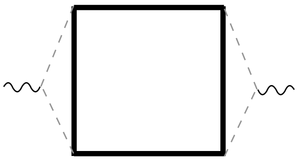

Box

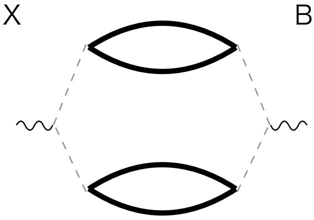

(1,1)-conv

New

$\propto f_{\rm NL}^2 g_{\rm NL}$ Abe, Inui, Tada, Yokoyama

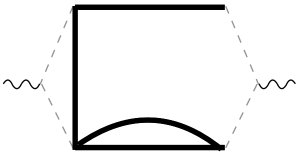

1-conv. C 1

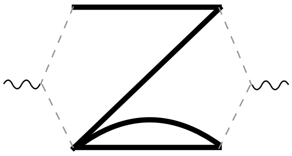

1-conv. Z 1

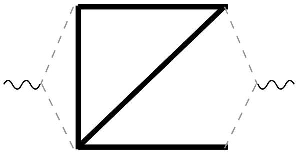

CZ

$\propto g_{\rm NL}^2$

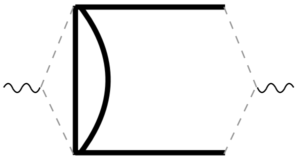

1-conv. C 2

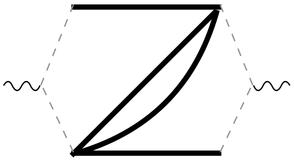

1-conv. Z 2

Higher order contributions

$O(A_g^4)$

Abe, Inui, Tada, Yokoyama

New

$\propto g_{\rm NL}^2$

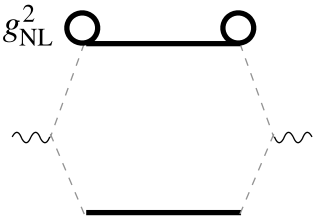

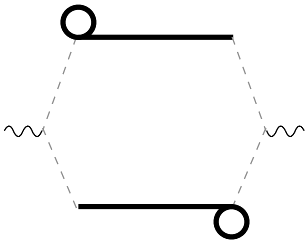

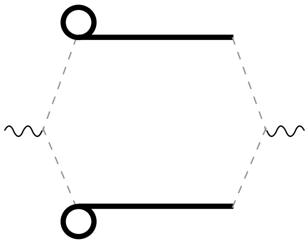

$\propto I_{\rm NL}$

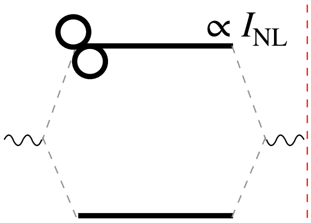

$\propto f_{\rm NL}^2 g_{\rm NL}$

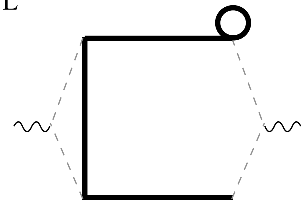

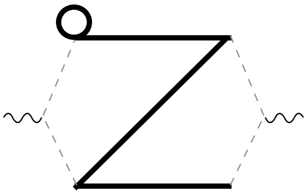

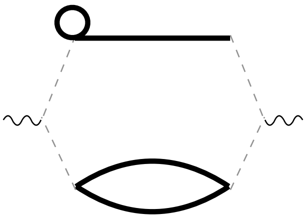

$\propto f_{\rm NL} h_{\rm NL}$

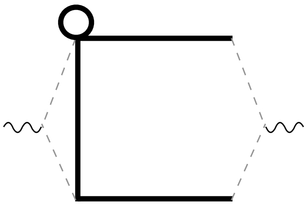

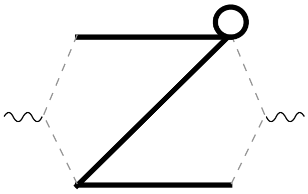

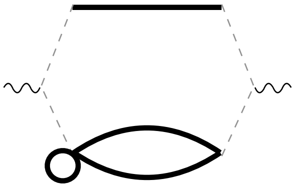

Result

GWs spectrum is well converged

GWs can be detected by LISA

Detect the footprint of the non-G : difficult in LISA

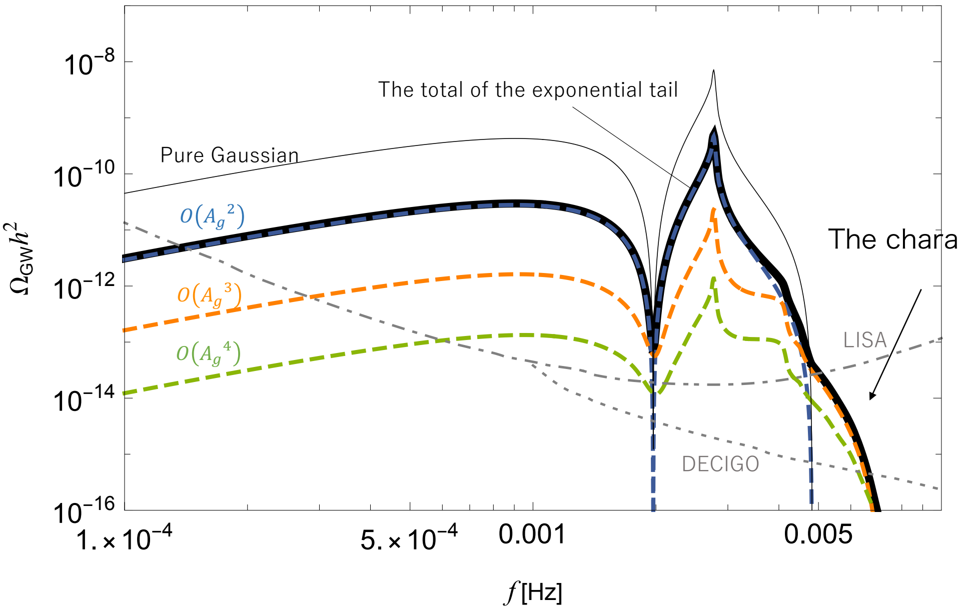

$f_{\rm PBH}^{\rm tot} = 1,\ M_{\rm PBH} = 10^{-11} M_\odot$

$\longleftrightarrow\quad A_g = 1.32 \times 10^{-3}$

$P_g(k) = \frac{2\pi^2 A_g}{k^3}\delta(\ln k - \ln k_*)$

$k_* = 1.56 \times 10^{12}\ \mathrm{Mpc}^{-1}$

Conclusion

Can GWs investigate the scenario where PBH = 100% DM?

We calculated the GWs induced by the exponential tail

We computed up to $O(A_g^4)$ contributions perturbatively

Exponential tail-type in LISA

GWs would be detectable

Detect the footprint of the non-G is difficult

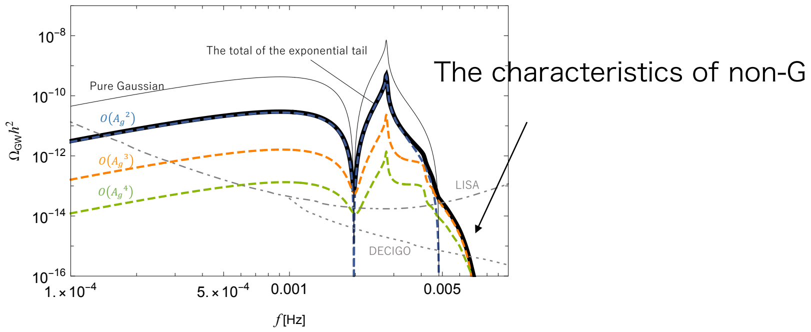

Appendix

USR (Ultra slow-roll models)

PBH can be realized in USR

Primordial density perturbation

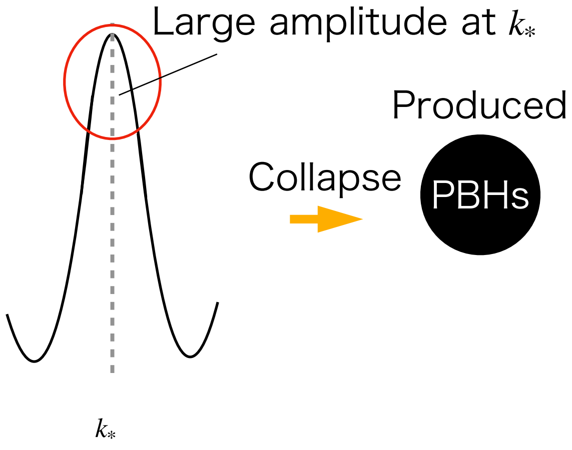

Large amplitude at k_*

Produced

Collapse

PBHs

k_*

High peak spectrum

$$P_{\zeta_g}(k) \propto \frac{H^2}{M_{\rm pl}^2 \epsilon k^3} \qquad \epsilon \equiv \frac{M_{\rm pl}}{2}\left(\frac{V_\phi}{V}\right)^2$$

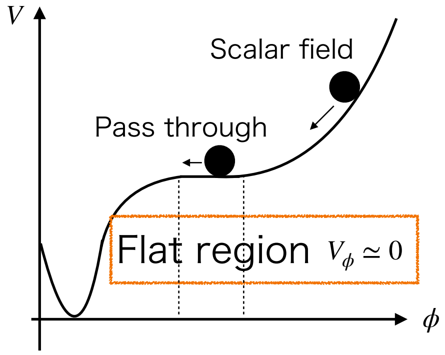

V

Scalar field

Pass through

Flat region $V_\phi \simeq 0$

ϕ

PBH abundance

Primordial perturbation：$\zeta = \frac{1}{\beta}\ln(1-\beta\zeta_g)$

Spacial distribution

Peak theory

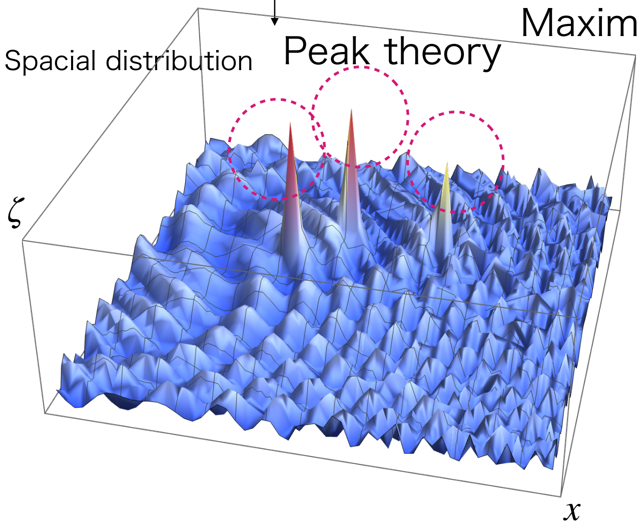

Determination of PBH formation

Maximum mean compaction > threshold

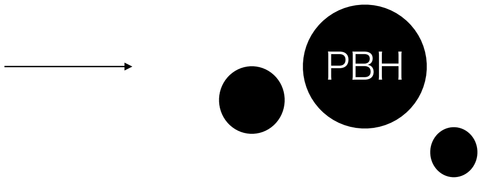

PBH abundance

Peak theory

Peak number density

$n_{\rm pk}(\mu,\tilde{k})d\mu d\tilde{k}$

$\zeta_g(x)$: Gaussian field

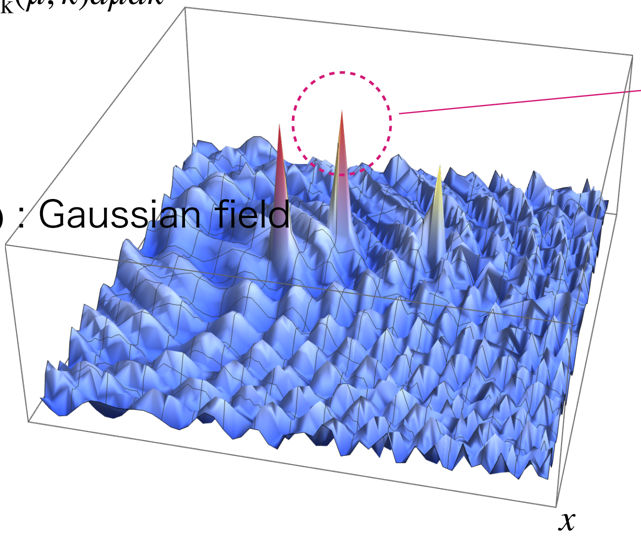

Around peak：spherical symmetric

$$\hat{\zeta}_g(r) = \hat{\zeta}_g(\psi(r),\mu,\tilde{k}) = \mu\frac{\sin k_* r}{k_* r}$$

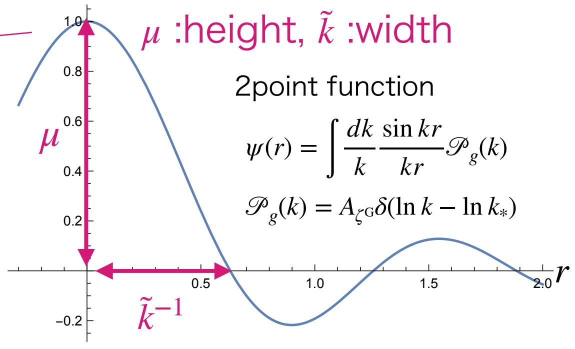

μ :height, $\tilde{k}$:width

2point function

$$\psi(r) = \int \frac{dk}{k}\frac{\sin kr}{kr}\mathscr{P}_g(k)$$

$$\mathscr{P}_g(k) = A_{\zeta G}\delta(\ln k - \ln k_*)$$

Yoo, Harada, Garriga, and Kohri ’18

Compaction function

Overdensity Spacial mean value Conserved at super horizon

$$C = \frac{M_{MS} - M_{bg}}{4\pi M_{\rm pl}^2 R} = \frac{1}{V(R)}\int_0^R \delta 4\pi R^2 dR\bigg|_{R=H^{-1}} = \frac{2}{3}[1-(1+r\zeta')^2] \overset{?}{>} C_{\rm th}$$

— Type I : $R =$ monotonic

- - - Type II : $R \neq$ monotonic

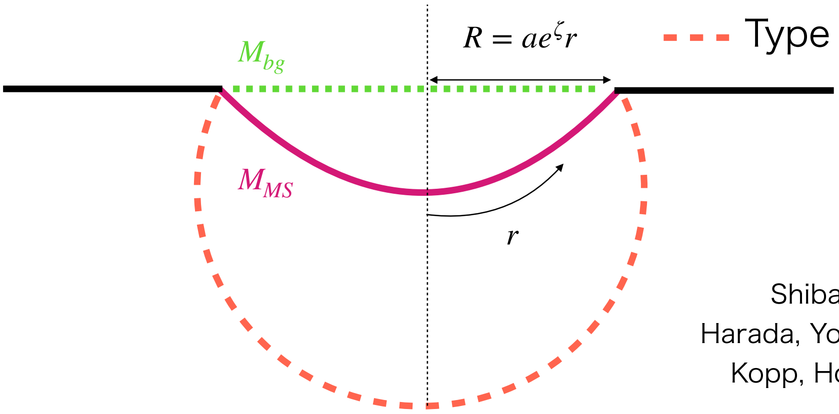

Shibata & Sasaki '99
Harada, Yoo, Nakama, Koga '15
Kopp, Hofmann, Weller '11

Mean compaction function

Threshold value of the compaction function

$$\frac{1}{5} \leq C_{\rm th} \leq \frac{1}{3}$$

Changed by the peak profile

Mean compaction function

$$\bar{C} = \frac{1}{V(R)}\int_0^R C(R) \times 4\pi R^2 dR$$

Almost universal

$$\bar{C}_{\rm m} > \boxed{\bar{C}_{\rm th} \simeq \frac{2}{5}}$$

Atal, Cid, Escrivà, Garriga '19
Escriv`a, Germani, Sheth '19

Diagrammatic approach

Diagrammatic rules

1.

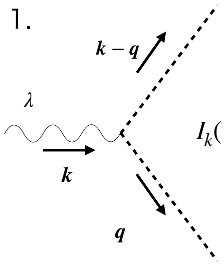

$I_k(|\boldsymbol{k}-\boldsymbol{q}|, q, k)Q(\boldsymbol{k}, \boldsymbol{q})$

2.

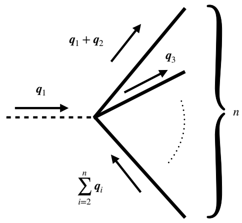

$n!F_{\rm NL}^{(n-1)}$

3.

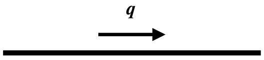

$P_g(q)$

4. Integrate over each undetermined momentum

$$\int \frac{d^3q}{(2\pi)^3}$$

5. Divide by the symmetric factor

arXiv: 2209.13891v1

Diagrammatic approach

Loop structures

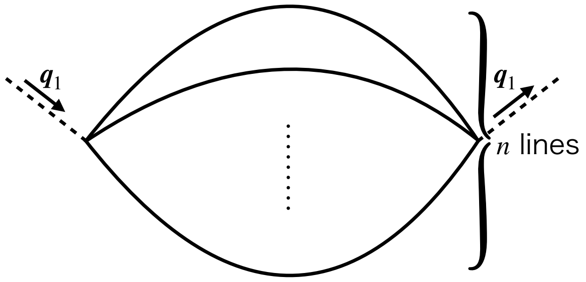

Symmetric factor $n!$

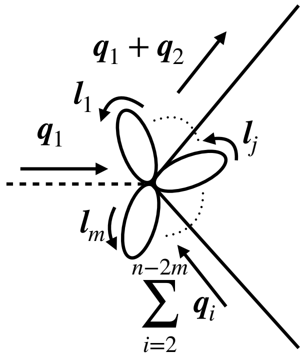

Symmetric factor $2^m m!$

arXiv: 2209.13891v1

Diagrammatic approach

Renormalized propagator

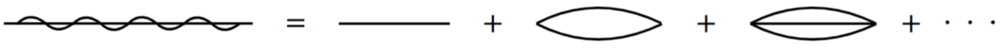

Renormalized vertex

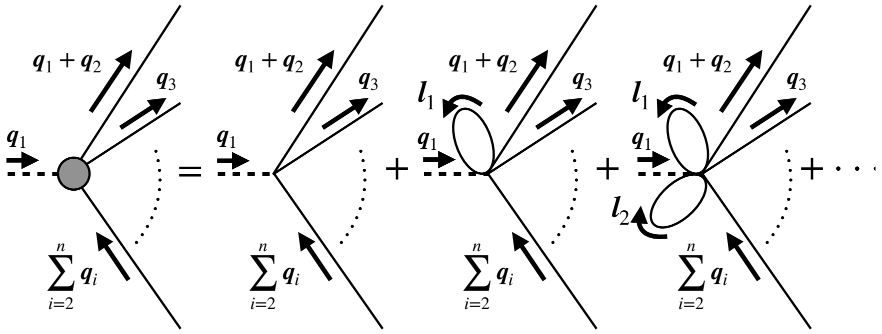

arXiv: 2209.13891v1

Diagrammatic approach

Prohibited structure

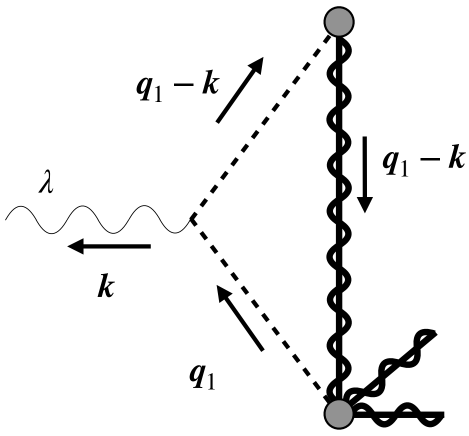

$$\int \frac{d^3q}{(2\pi)^3}\, Q_\lambda(\mathbf{k},\mathbf{q})\, I(\,|\,\mathbf{k}-\mathbf{q}\,|\,,\mathbf{q},\tau)\, P_g(q)$$

$$= \int_0^{2\pi} d\phi \begin{cases} \cos 2\phi & (\lambda = +\,) \\ \sin 2\phi & (\lambda = \times\,) \end{cases} \times \mathscr{F}(k,q,\theta,\tau)$$

$$= 0$$

Diagrammatic approach

Vanilla term

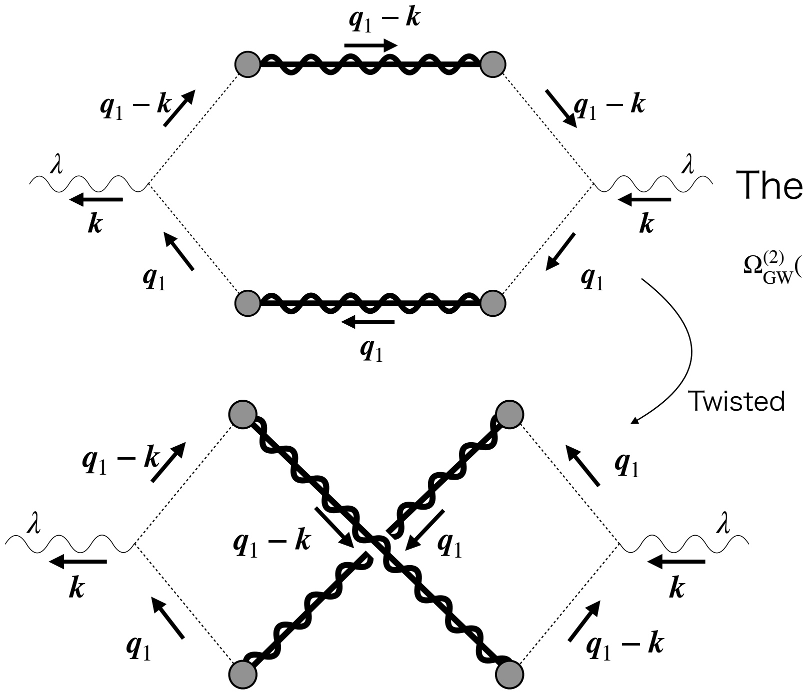

They give the same contribution

$$\Omega_{\rm GW}^{(2)}(k) = 2 \times \frac{1}{48}\left(\frac{k}{aH}\right)^2 \sum_{\lambda=+,\times} \overline{P_{\lambda\lambda}^{\rm Vanilla}(\tau \to \infty, k)}$$

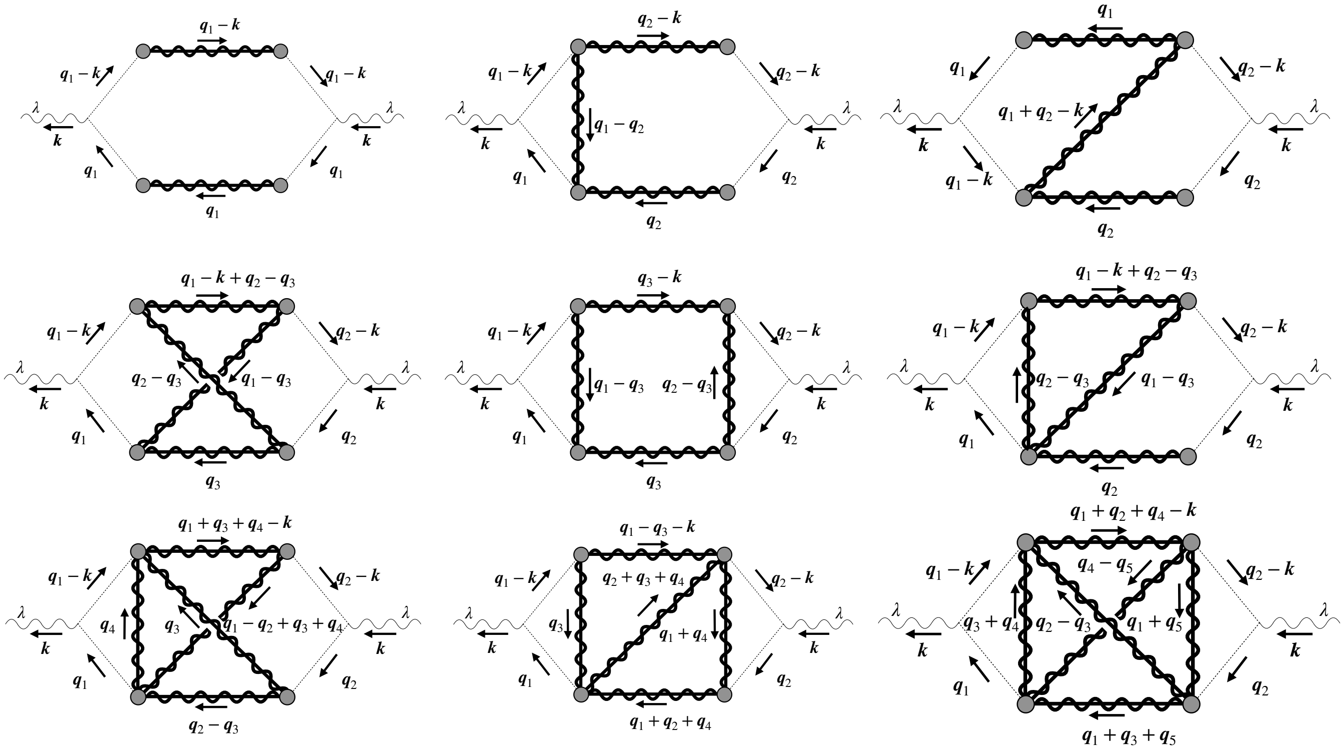

JGRG31
October 25, 2022 @ RESCEU, University of Tokyo

Thermal ringdown and the excitation of Kerr overtones

Naritaka Oshita

RIKEN, iTHEMS

RIKEN Interdisciplinary
Theoretical and Mathematical
Sciences Program

RIKEN

N.O. arXiv: 2208.02923

Ringdown for an extreme-mass-ratio merger

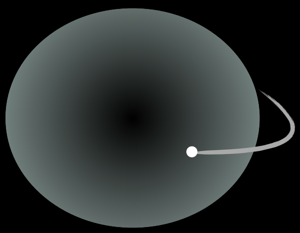

Do overtones dominate the signal?

Destructive Interference of Overtones

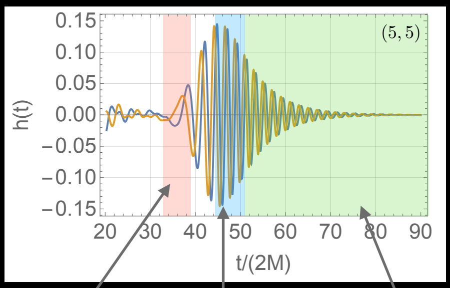

Strain Peak
(Overtones getting suppressed)

Beginning of Ringdown
(Destructive Interference)

Exponential Damping
(Fundamental Mode)

How are they excited?

Ringdown for a near-extremal BH
→ Fermi gas??
(Thermal Excitation of Overtones)

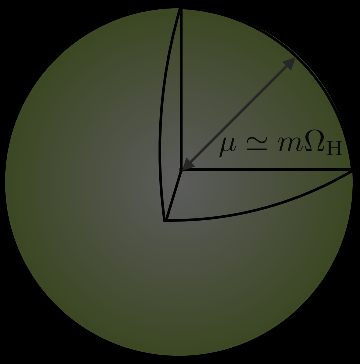

Black Hole Ringing

B. P. Abbott et al. (2016)

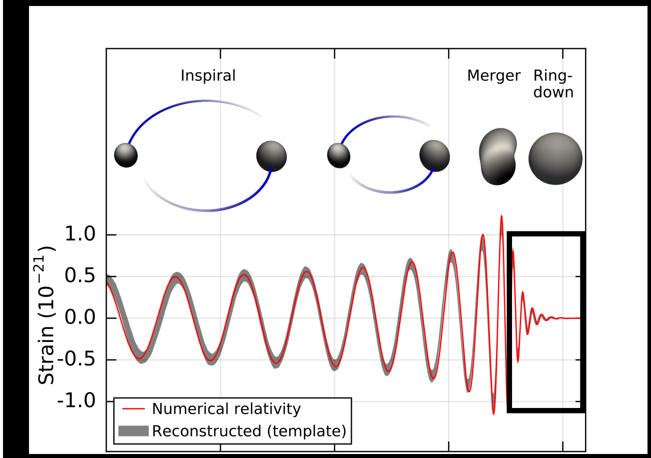

relaxation process of a BH
=ringdown phase
= superposition of quasi-normal modes

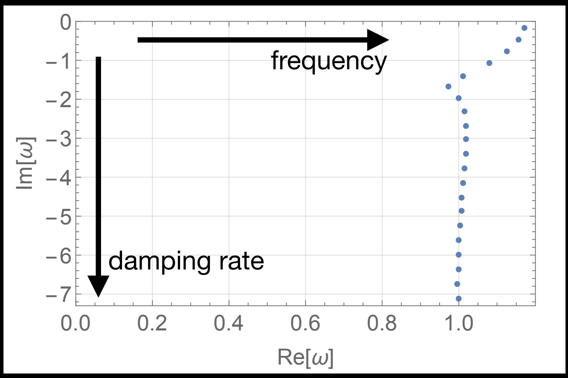

$$h_{\rm ringdown} \sim \sum_n A_n e^{-t/\tau_n} \cos[f_n(t-r^*-t_0)+\delta_n]$$

determined only by mass and angular momentum (no-hair theorem)

Quasi-Normal Modes (QNMs)

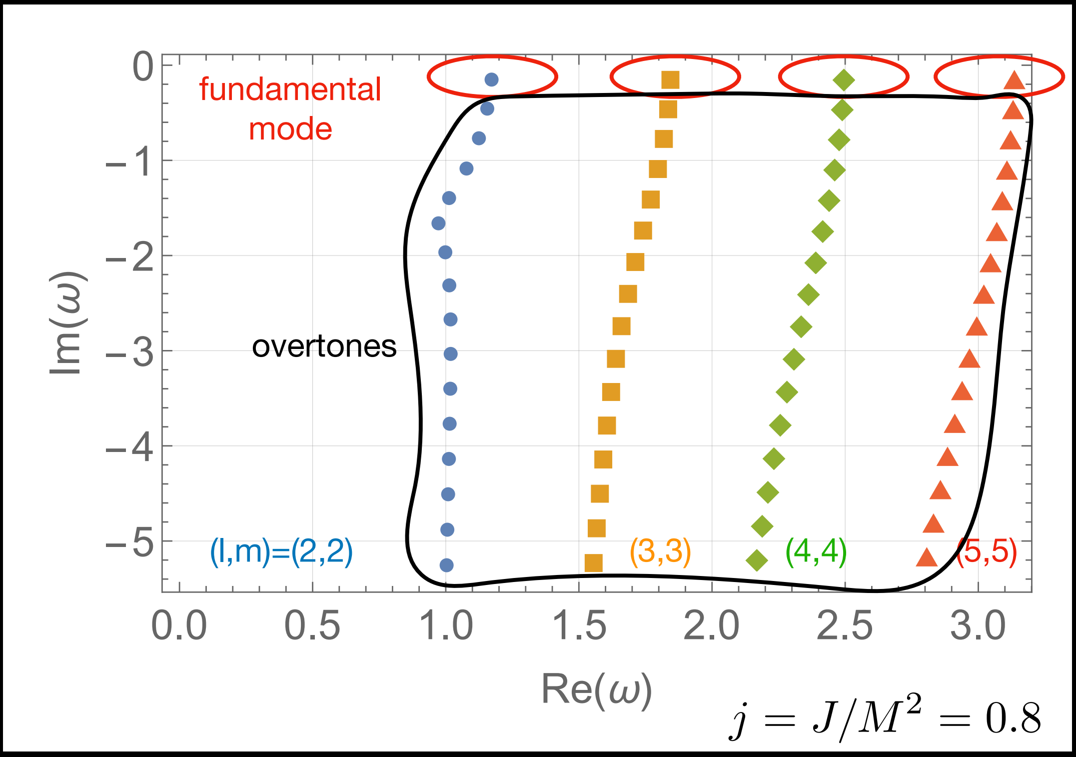

$$\omega_q = \underset{\text{(frequency)}}{\mathrm{Re}[\omega_q]} + i\underset{\text{(damping rate)}}{\mathrm{Im}[\omega_q]}$$

Why is a BH ringing important?

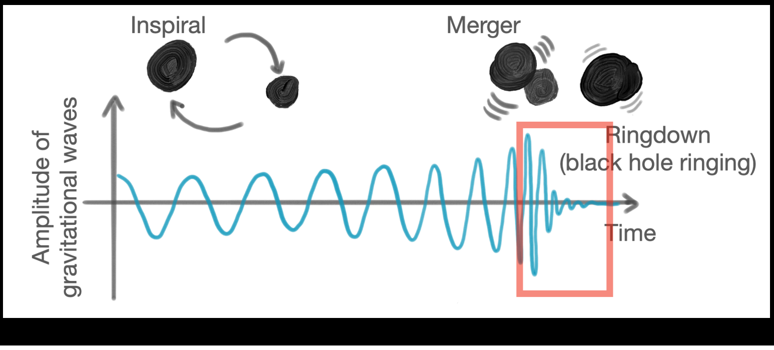

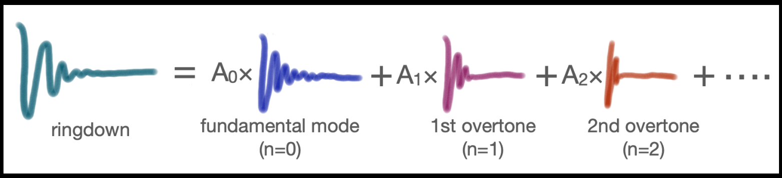

→**Measurement of the remnant mass and spin**

→**Test of GR in strong gravity regime**

(Test of the BH no-hair theorem)

Binary Black Hole with the comparable mass ratio

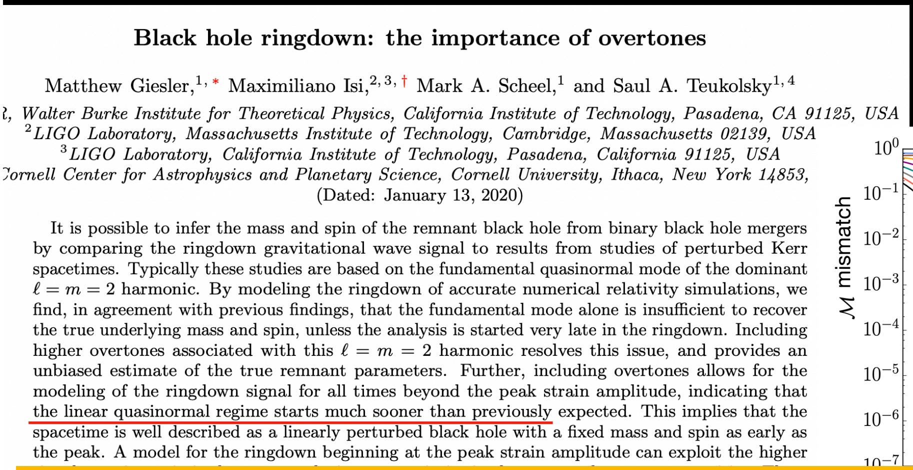

Black hole ringdown: the importance of overtones

Matthew Giesler,[1,*] Maximiliano Isi,[2,3,†] Mark A. Scheel,[1] and Saul A. Teukolsky[1,4]

Walter Burke Institute for Theoretical Physics, California Institute of Technology, Pasadena, CA 91125, USA
[2]*LIGO Laboratory, Massachusetts Institute of Technology, Cambridge, Massachusetts 02139, USA*
[3]*LIGO Laboratory, California Institute of Technology, Pasadena, California 91125, USA*
Cornell Center for Astrophysics and Planetary Science, Cornell University, Ithaca, New York 14853,
(Dated: January 13, 2020)

It is possible to infer the mass and spin of the remnant black hole from binary black hole mergers by comparing the ringdown gravitational wave signal to results from studies of perturbed Kerr spacetimes. Typically these studies are based on the fundamental quasinormal mode of the dominant $\ell = m = 2$ harmonic. By modeling the ringdown of accurate numerical relativity simulations, we find, in agreement with previous findings, that the fundamental mode alone is insufficient to recover the true underlying mass and spin, unless the analysis is started very late in the ringdown. Including higher overtones associated with this $\ell = m = 2$ harmonic resolves this issue, and provides an unbiased estimate of the true remnant parameters. Further, including overtones allows for the modeling of the ringdown signal for all times beyond the peak strain amplitude, indicating that the linear quasinormal regime starts much sooner than previously expected. This implies that the spacetime is well described as a linearly perturbed black hole with a fixed mass and spin as early as the peak. A model for the ringdown beginning at the peak strain amplitude can exploit the higher

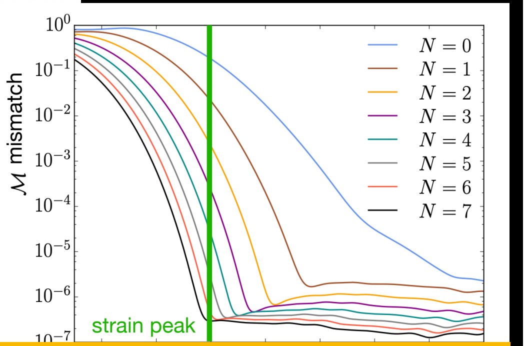

Do multiple overtones highly excited at the early stage of ringdown (or merger phase)?
To answer this question is one of the current challenges in gravitational physics

Giesler, Isi, Scheel, Teukolsky (2019)

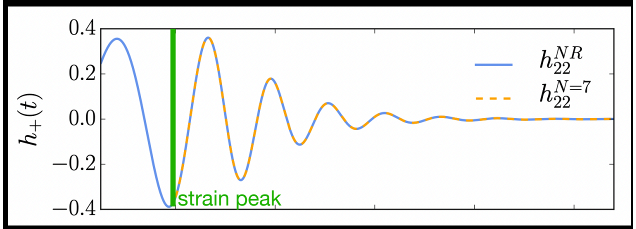

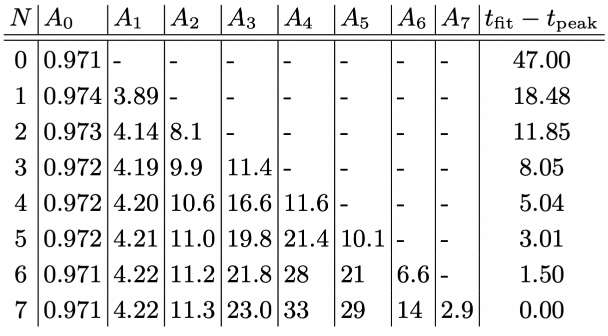

N	A_0	A_1	A_2	A_3	A_4	A_5	A_6	A_7	$t_{\rm fit} - t_{\rm peak}$
0	0.971	-	-	-	-	-	-	-	47.00
1	0.974	3.89	-	-	-	-	-	-	18.48
2	0.973	4.14	8.1	-	-	-	-	-	11.85
3	0.972	4.19	9.9	11.4	-	-	-	-	8.05
4	0.972	4.20	10.6	16.6	11.6	-	-	-	5.04
5	0.972	4.21	11.0	19.8	21.4	10.1	-	-	3.01
6	0.971	4.22	11.2	21.8	28	21	6.6	-	1.50
7	0.971	4.22	11.3	23.0	33	29	14	2.9	0.00

Are BH overtones well excited for an extreme-mass-ratio merger?

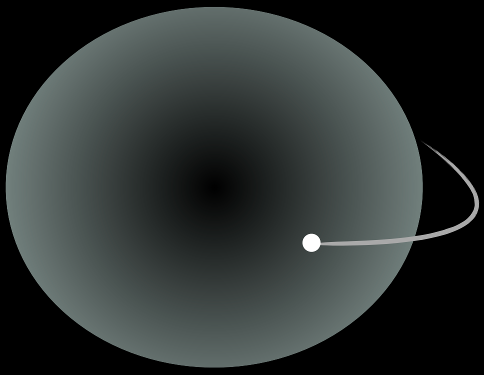

Binary black hole mergers: large mass ratio

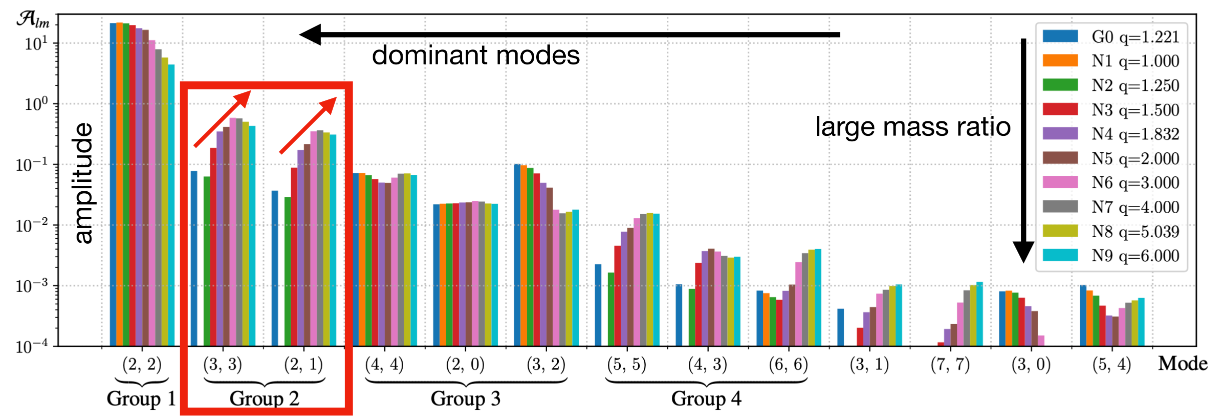

FIG. 4. The relative importance $\mathcal{A}_{lm}$, defined in Eq. (16) as the strain component in spin-weighted spherical mode (l, m) squared and integrated from t_{peak} to $t_{\text{peak}} + 100M$. Groups 1–4 of the (l, m) modes are defined according to their relative importance in the QNM expansion, and are added to the fitting models in order. See details in Sec. III A.

Xian Li et al. (2022)

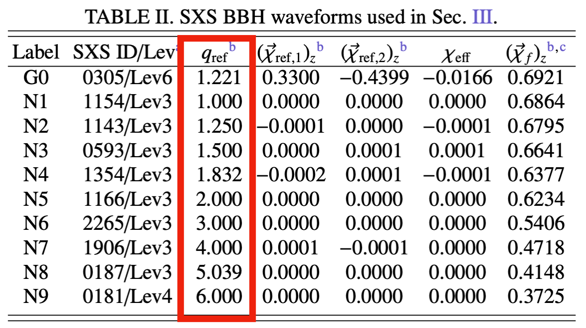

TABLE II. SXS BBH waveforms used in Sec. III.

Label	SXS ID/Lev	q_{ref}[b]	$(\vec{\chi}_{\text{ref},1})_z$[b]	$(\vec{\chi}_{\text{ref},2})_z$[b]	χ_{eff}	$(\vec{\chi}_f)_z$[b,c]
G0	0305/Lev6	1.221	0.3300	−0.4399	−0.0166	0.6921
N1	1154/Lev3	1.000	0.0000	0.0000	0.0000	0.6864
N2	1143/Lev3	1.250	−0.0001	0.0000	−0.0001	0.6795
N3	0593/Lev3	1.500	0.0000	0.0001	0.0001	0.6641
N4	1354/Lev3	1.832	−0.0002	0.0001	−0.0001	0.6377
N5	1166/Lev3	2.000	0.0000	0.0000	0.0000	0.6234
N6	2265/Lev3	3.000	0.0000	0.0000	0.0000	0.5406
N7	1906/Lev3	4.000	0.0001	−0.0001	0.0000	0.4718
N8	0187/Lev3	5.039	0.0000	0.0000	0.0000	0.4148
N9	0181/Lev4	6.000	0.0000	0.0000	0.0000	0.3725

Data analysis of numerical relativity waveforms
(SXS collaboration)

Larger Mass Ratio
→Excitation of Higher Harmonics

Fitting analysis in frequency domain

Solving the Sasaki-Nakamura equation

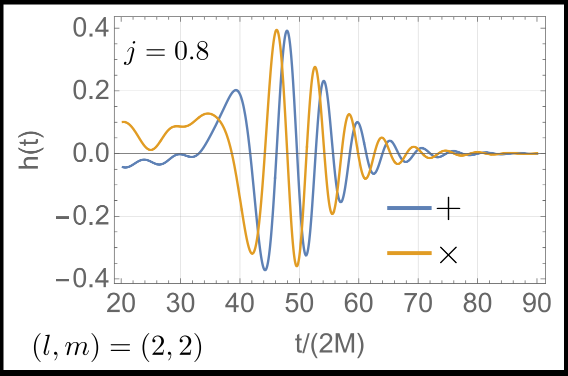

Fourier transform

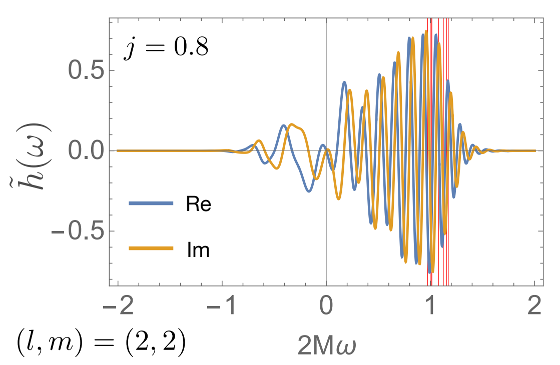

$$h_{\mathrm{QNM},lm}(t) = \sum_n \boxed{C_n} e^{-i\omega_{lmn}t}\theta(t - \boxed{t^*})$$

$$\tilde{h}_{\mathrm{QNM},lm}(\omega) = \frac{i}{2\pi}\sum_n \frac{\boxed{\tilde{C}_n}}{\omega - \omega_{lmn}} e^{i\omega \boxed{t^*}}$$

$$\tilde{C}_n = C_n e^{-i\omega_{lmn}t^*}$$

QNM fitting in time-domain waveform

see e.g. Giesler, et al. (2019)
Mourier et al. (2020)
Ma, et al. (2021)

c.f. Finch, et al. (2021)

QNM fitting in frequency domain

Fitting in *Frequency* vs *Time* Domain

N. O. arXiv:2208.02923

$(l,m) = (5,5)$

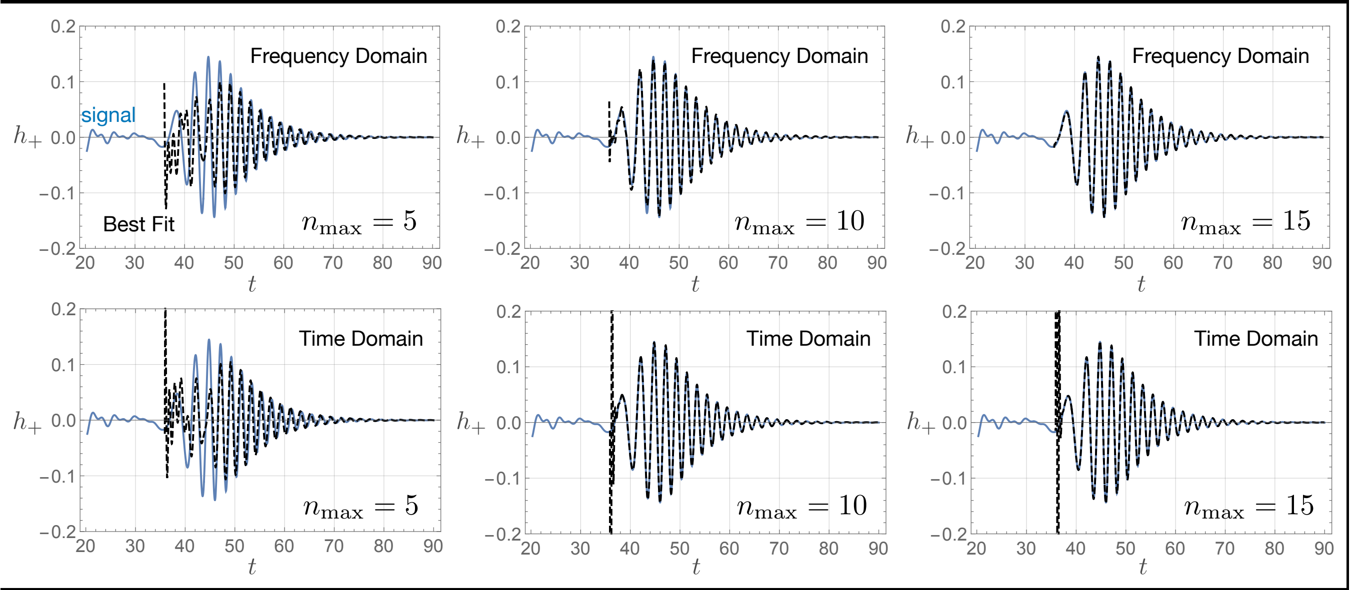

Each overtone has an exponentially large amplitude in the early ringdown
→Difficult to control such modes in time domain

Start time of ringdown

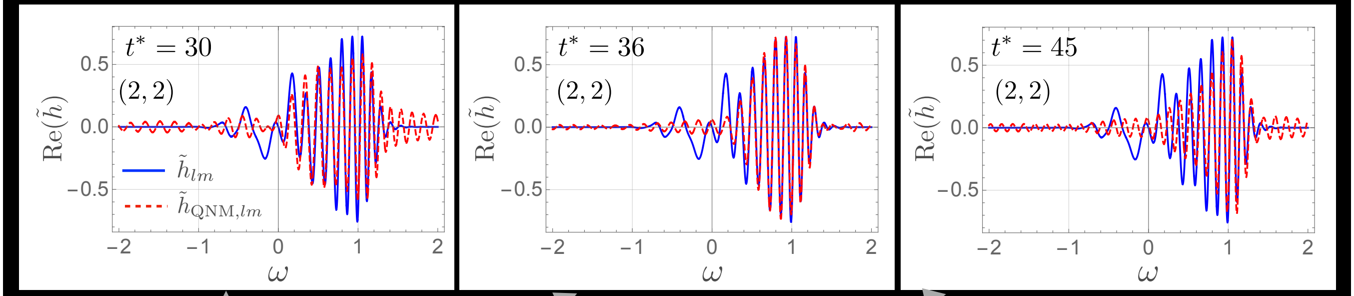

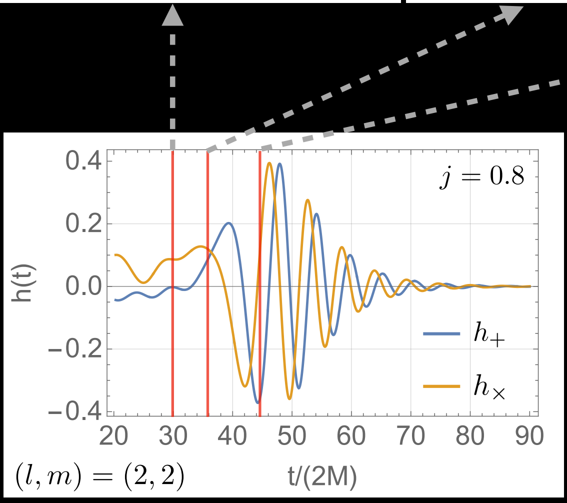

$n_{\max} = 15$

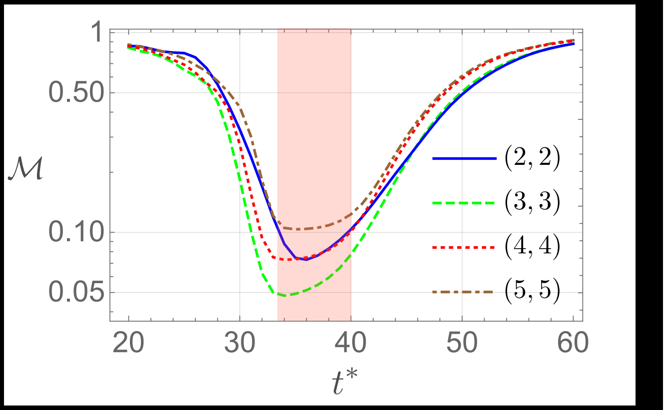

$$\mathcal{M} \equiv \left| 1 - \frac{\langle h | h_Q \rangle}{\sqrt{\langle h | h \rangle \langle h_Q | h_Q \rangle}} \right|$$

h : original

h_Q : QNM model

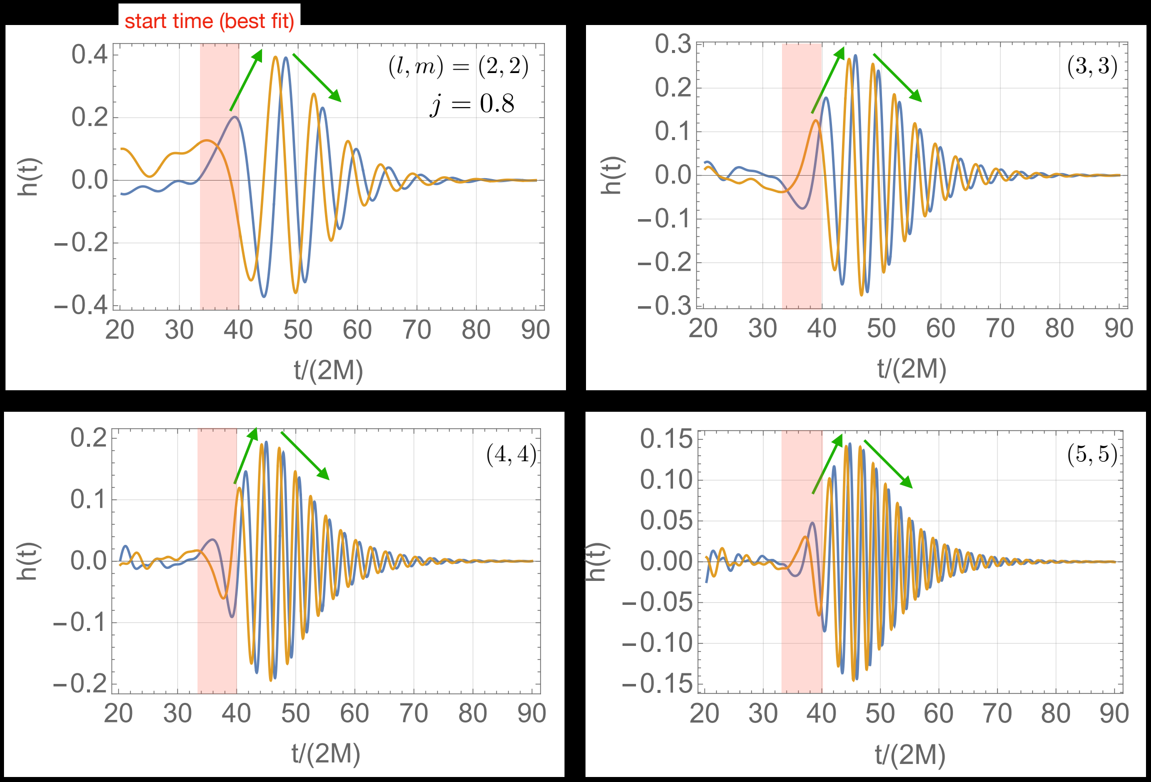

Ringdown starts before the strain peak.

→Overtones are excited.

Do overtones dominate the signal?

Destructive Interference of Overtones

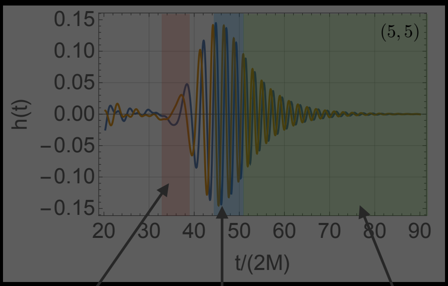

Strain Peak
(Overtones getting
suppressed)

Beginning of Ringdown
(Destructive Interference)

Exponential Damping
(Fundamental Mode)

How are they excited?

Ringdown for a near-extremal BH
→ Fermi gas??

(Thermal Excitation of Overtones)

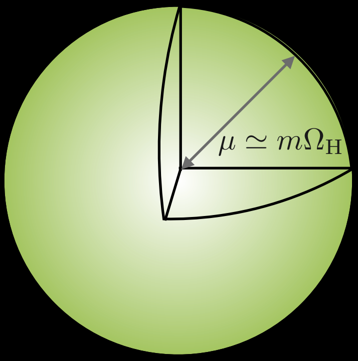

Fermi-Dirac statistics and Kerr Ringdown

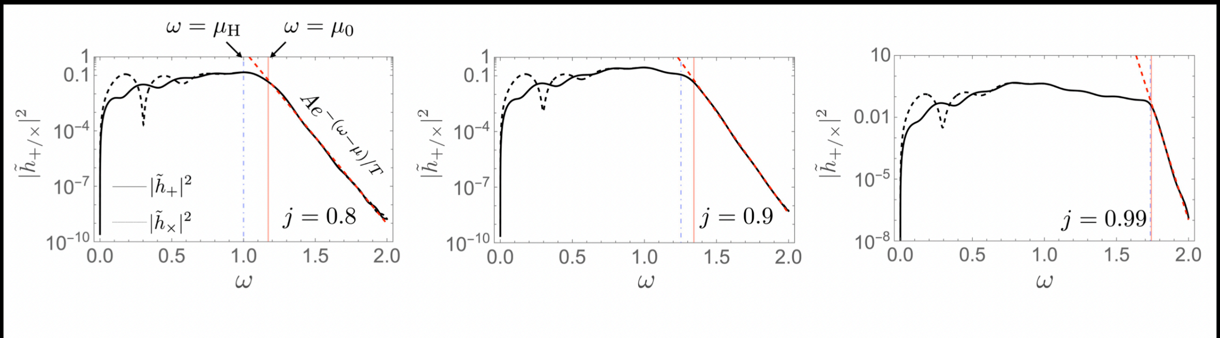

FIG. 8: The absolute square of the spectral amplitude of the GW signals for $j = 0.8$, $j = 0.9$, and $j = 0.99$ with $l = m = 2$. The Boltzmann distribution (fitted with the red dashed line) appears at higher frequencies than $\omega = \mu_0$ (red solid line). The blue dot-dashed line indicates $\omega = \mu_{\rm H}$.

N. O. arXiv:2208.02923

$(l, m) = (2, 2)$

$$\frac{1}{e^{(\omega-\mu)/T}+1}$$

Fermi-Dirac distribution

chemical potential

$\mu_{\rm H} = m\Omega_{\rm H}$ superradiant frequency

“temperature (frequency)” T

→obtained by fitting analysis

$\mu_0 = {\rm Re}(\omega_{lm0})$ fundamental QN frequency

Fitting the Boltzmann factor to GW data

$$\frac{1}{e^{(\omega-\mu)/T}+1} \sim e^{-(\omega-\mu)/T}$$

at higher frequencies

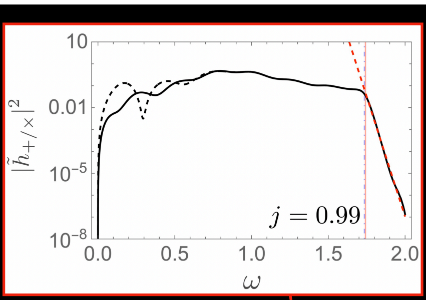

(l,m)	$j=0.8$ $(T_{\rm H}\simeq 0.0597)$			$j=0.9$ $(T_{\rm H}\simeq 0.0483)$			$j=0.99$ $(T_{\rm H}\simeq 0.0197)$		
	T	Δ_0	$\Delta_{\rm H}$	T	Δ_0	$\Delta_{\rm H}$	T	Δ_0	$\Delta_{\rm H}$
$(2,2)$	0.0462(2)	**4%**	23%	0.0397(2)	**3%**	18%	0.0198(2)	**6%**	**0.6%**
$(3,3)$	0.0493(2)	**0.6%**	17%	0.0375(1)	10%	22%	0.0196(3)	**5%**	**0.4%**
$(4,4)$	0.0565(1)	14%	**5%**	0.0454(2)	**8%**	**6%**	0.0200(3)	**6%**	**2%**
$(5,5)$	0.0552(2)	10%	**8%**	0.0483(1)	14%	**0.03%**	0.0196(4)	**4%**	**0.4%**

N. O. arXiv:2208.02923

Relative Error

$$\Delta_0 \equiv |T - T_0|/T_0, \;\; \Delta_{\rm H} \equiv |T - T_{\rm H}|/T_{\rm H}$$

$$T_0 \equiv |{\rm Im}(\omega_{lm0})|/\pi$$

temperature defined by the fundamental QN damping

$$T_{\rm H} \equiv \frac{\sqrt{1-j^2}}{4\pi r_+}$$

Hawking "frequency"

Fermi degeneracy of Kerr ringdown

j=0.99 (low Hawking temperature) $T_{\rm H} = \frac{\sqrt{1-j^2}}{4\pi r_+}$ $\Omega_{\rm H} = \frac{j}{2r_+}$

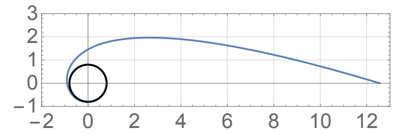

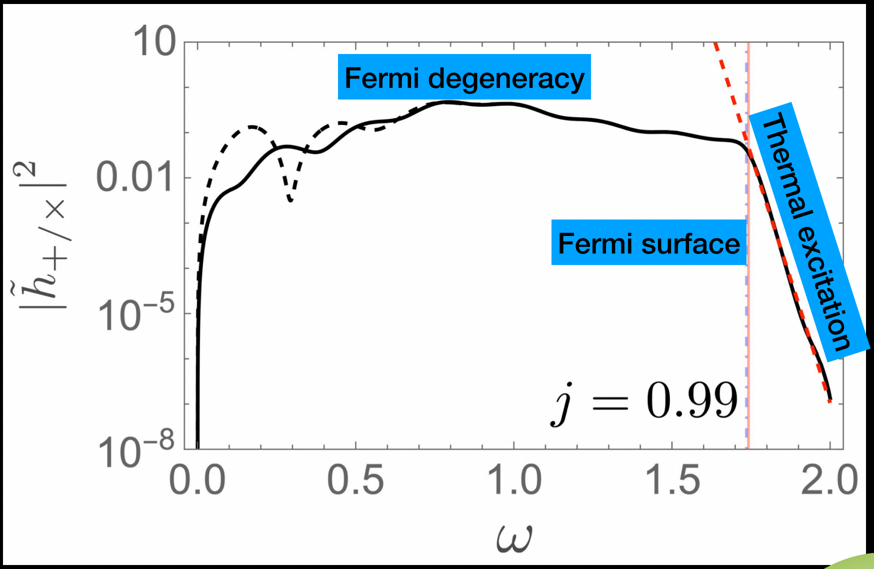

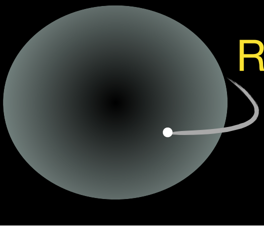

Ringdown of a near-extremal BH
→ Thermal Fermi system??

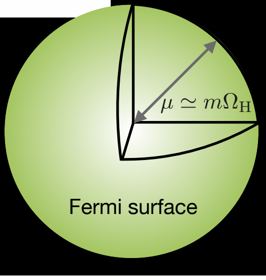

Green’s function of BH perturbations has infinite poles (i.e. QN modes).

Fermi-Dirac distribution also has infinite poles (i.e. Matsubara modes).

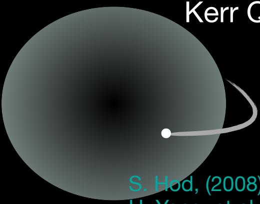

Kerr QN frequencies
for j~1

$$\omega \simeq \mu_{\rm H} - i\left(\frac{1}{2}+n\right)2\pi T_{\rm H}$$

Matsubara
frequencies

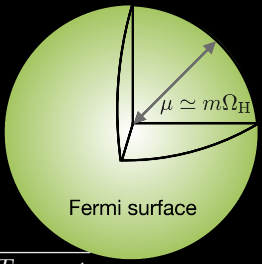

$$\frac{1}{e^{(\omega-\mu_{\rm H})/T_{\rm H}}+1}$$

S. Hod, (2008)
H. Yang, et al. (2013)

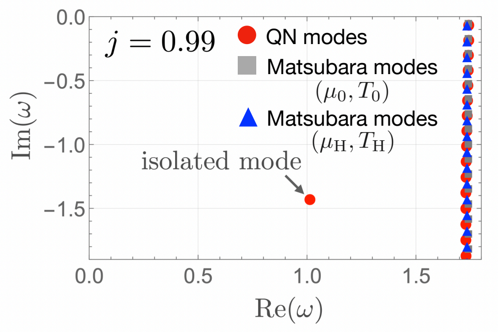

Can ringdown be thermal?

The suggestive frequency cutoff
for an extreme-mass-ratio merger is NOT surprising
once we admit the excitation of multiple overtones.

Summary

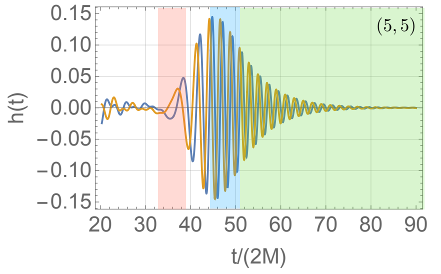

Ringdown of an extreme-mass-ratio merger

Destructive Interference of overtones

Close values of real parts of QN frequencies may lead to the destructive and constructive interference.

Beginning of Ringdown (Destructive Interference)	Strain Peak (Constructive Interference)	Exponential Damping (Fundamental Mode)

Exponential Cutoff in the Ringdown Spectrum → Fermi-Dirac Distribution?

Another supporting evidence
of the excitation of multiple overtones

near-extremal BH -> Fermi surface at

QN modes ~ Matsubara modes
in the near-extremal limit

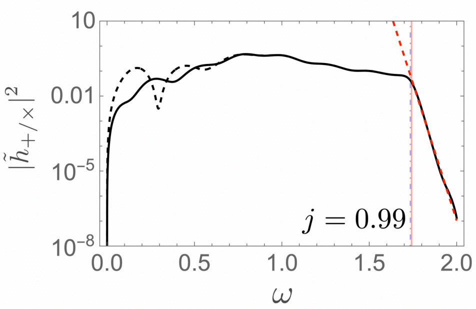

C44

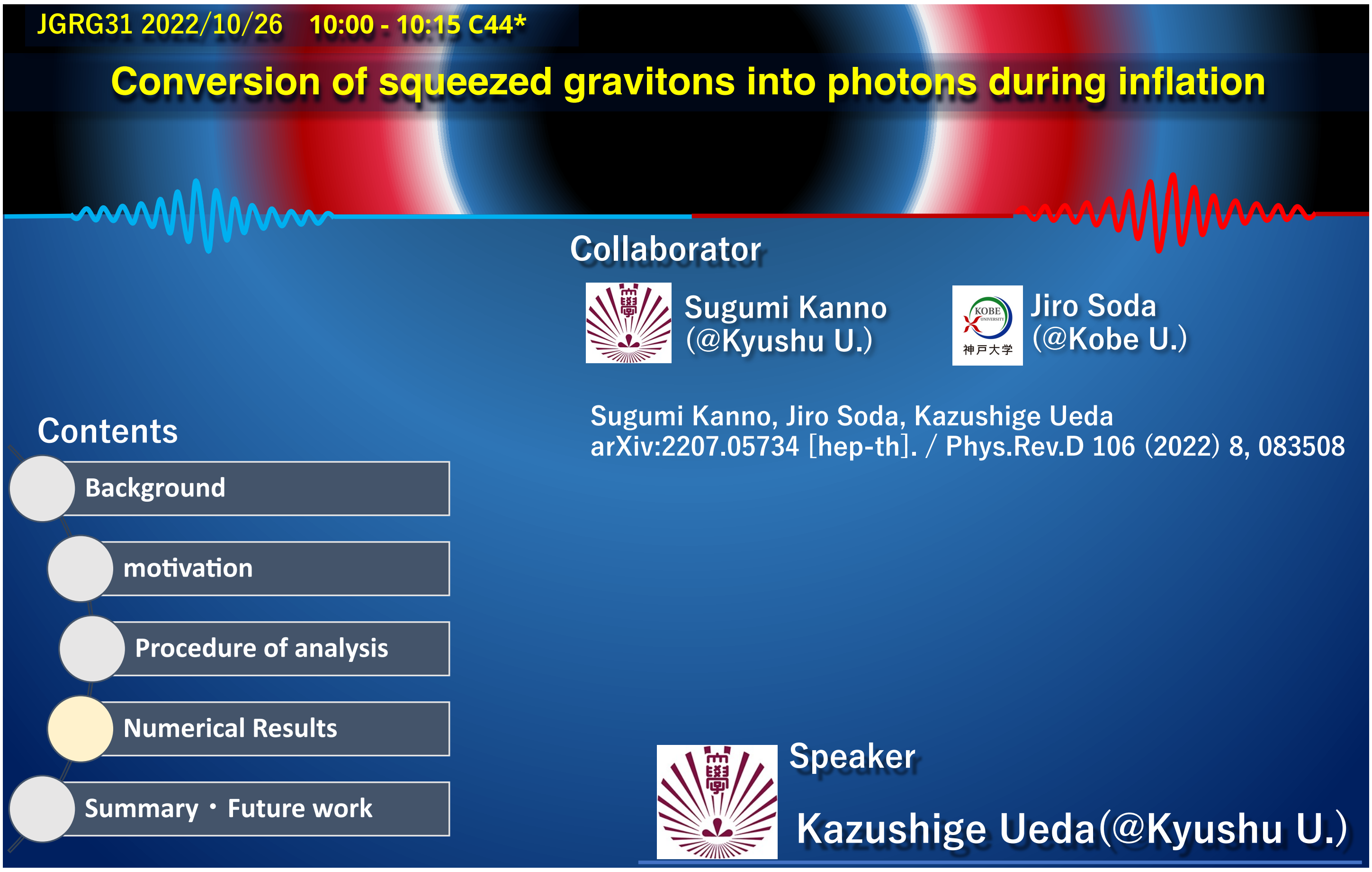

JGRG31 2022/10/26 10:00 - 10:15 C44*

Conversion of squeezed gravitons into photons during inflation

Collaborator

Sugumi Kanno (@Kyushu U.)

Jiro Soda (@Kobe U.)

Sugumi Kanno, Jiro Soda, Kazushige Ueda
arXiv:2207.05734 [hep-th]. / Phys.Rev.D 106 (2022) 8, 083508

Contents

- Background
- motivation
- Procedure of analysis
- Numerical Results
- Summary・Future work

Speaker

Kazushige Ueda(@Kyushu U.)

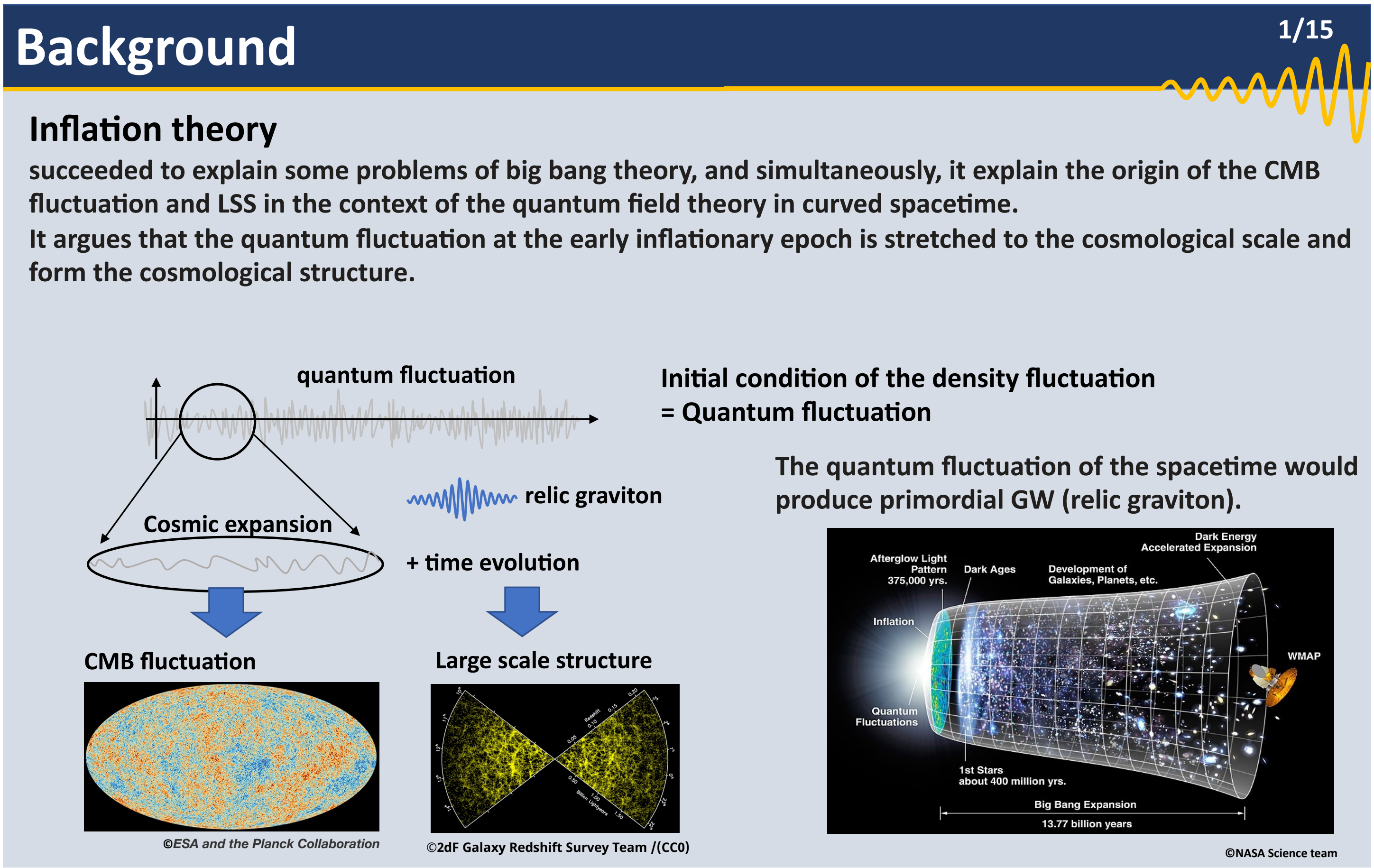

Background

Inflation theory

succeeded to explain some problems of big bang theory, and simultaneously, it explain the origin of the CMB fluctuation and LSS in the context of the quantum field theory in curved spacetime.
It argues that the quantum fluctuation at the early inflationary epoch is stretched to the cosmological scale and form the cosmological structure.

CMB fluctuation

©ESA and the Planck Collaboration

Large scale structure

©2dF Galaxy Redshift Survey Team /(CC0)

Initial condition of the density fluctuation
= Quantum fluctuation

The quantum fluctuation of the spacetime would produce primordial GW (relic graviton).

©NASA Science team

Background

It is important to explore quantum nature of the primordial gravitational wave.

The state of the relic graviton is written as some squeezed state during inflation.

However, decoherence of the gravitons during cosmic history may change the degree of squeezing.

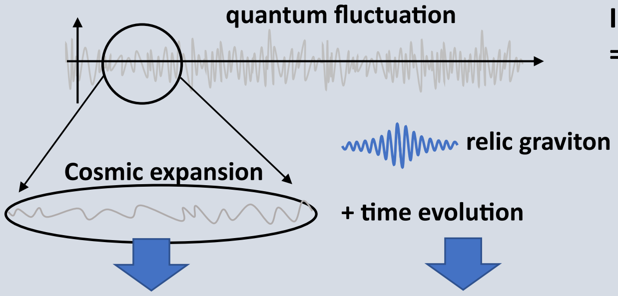

quantum fluctuation

relic graviton

Cosmic expansion

+ time evolution

Initial condition of the density fluctuation
= Quantum fluctuation

CMB fluctuation

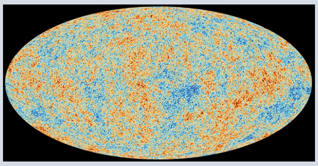

©ESA and the Planck Collaboration

Large scale structure

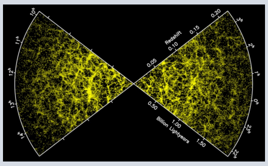

©2dF Galaxy Redshift Survey Team /(CC0)

The quantum fluctuation of the spacetime would produce primordial GW (relic graviton).

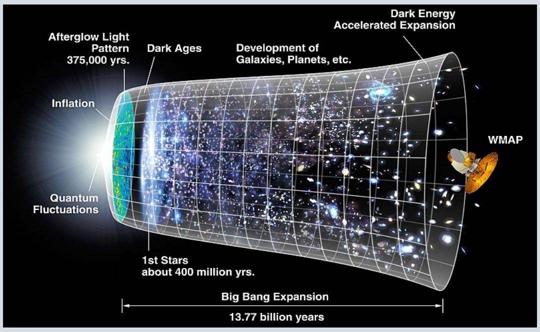

©NASA Science team

Graviton photon conversion

As the first step of the analysis of decoherence of the quantum state of the relic graviton, we consider the influence of the background magnetic field during inflation, since the existence of the tiny background magnetic field is not excluded by the observation. And the existence of the background magnetic field induces the graviton to photon conversion and vice versa.

In the presence of the magnetic field, graviton is converted to the photon and verse versa.

L. Maiani, R. Petronzio, and E. Zavattini, Phys. Lett. B 175, 359 (1986).
G. Raffelt and L. Stodolsky, Phys. Rev. D 37, 1237 (1988).

E. Masaki, J. Soda, PRD98, 023540 (2018)

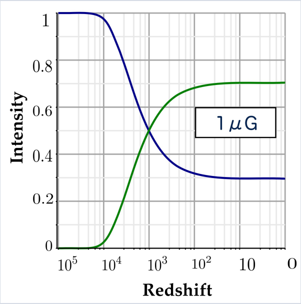

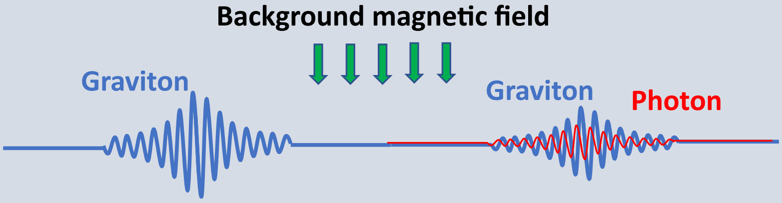

Background magnetic field

Graviton

Graviton

Photon

Besides the expansion of the universe, the existence of the cosmic magnetic field seems to have a big influence.

Introduction and motivation

Whether the squeezing of the gravitons survives or not during inflation ?
Under the presence of the background magnetic field.

Procedure of analysis

1. **Make a setup and derive the field equation of photon and graviton**
2. **Solve perturbatively** with Green's function
3. **Bogoliubov transformation**
4. **Define vacuum state and derive squeezing parameter**

Setup

1. Make a setup and derive the field equation of photon and graviton

2. Solve perturbatively with Green's function

3. Bogoliubov transformation

4. Define vacuum state and derive squeezing parameter

Part of the Action

$$S_g + S_A = \frac{M_{\rm pl}^2}{2} \int d^4x \sqrt{-g}\, R - \frac{1}{4} \int d^4x \sqrt{-g}\, F^{\mu\nu} F_{\mu\nu}$$

TT-gauge $h_{ij}{}^{,j} = h^i{}_i = 0$ **Radiation-gauge** $A_\mu = (0, \boldsymbol{A})\ ,\quad \nabla \cdot \boldsymbol{A} = 0$

de-Sitter background

$$ds^2 = a^2(\eta) \left[-d\eta^2 + (\delta_{ij} + h_{ij})\, dx^i dx^j \right]$$

Scale factor $a(\eta) = -\dfrac{1}{H\eta}$ **Conformal time** $-\infty < \eta < 0$

Setup

1. Make a setup and derive the field equation of photon and graviton

2. Solve perturbatively with Green's function

3. Bogoliubov transformation

4. Define vacuum state and derive squeezing parameter

We can decompose the action with the degree of freedom of the graviton and photons and their mixing,

Graviton part

$$\delta S_g = \frac{M_{\rm pl}^2}{8} \int d^4x\, a^2 \left[h^{ij\prime}\, h^\prime_{ij} - h^{ij,k} h_{ij,k} \right]$$

Photon part

$$\delta S_A = \frac{1}{2} \int d^4x \left[A_i^{\prime\,2} - A_{k,i}^2 \right]$$

Interaction part

$$\delta S_{\rm I} = \int d^4x \left[\varepsilon_{i\ell m} B_m h^{ij} \left(\partial_j A_\ell - \partial_\ell A_j \right) \right]$$

$$\downarrow$$

$$B_m = \varepsilon_{mj\ell}\, \partial_j A_\ell$$

Constant sizable background magnetic field that we assumed the presence at the beginning of inflation.

Decomposition of the solutions

1. Make a setup and derive the field equation of photon and graviton

2. Solve perturbatively with Green's function

3. Bogoliubov transformation

4. Define vacuum state and derive squeezing parameter

We defined the polarization tensor representing the vector component of the electromagnetic wave

Electromagnetic wave

mode function

$$A_i(\eta, x^i) = \sum_P \frac{\pm i}{(2\pi)^{3/2}} \int d^3k \, A^P_{\boldsymbol{k}}(\eta) \, e^P_i(\boldsymbol{k}) \, e^{i\boldsymbol{k}\cdot\boldsymbol{x}}$$

Polarization vector

We defined the polarization tensor representing the tensor component of the gravitational wave

Gravitational wave

mode function

$$h_{ij}(\eta, x^i) = \frac{2}{M_{\rm pl}} \sum_P \frac{1}{(2\pi)^{3/2}} \int d^3k \, h^P_{\boldsymbol{k}}(\eta) \, e^P_{ij}(\boldsymbol{k}) \, e^{i\boldsymbol{k}\cdot\boldsymbol{x}}$$

Polarization tensor

Analysis

1. Make a setup and derive the field equation of photon and graviton

2. Solve perturbatively with Green's function

3. Bogoliubov transformation

4. Define vacuum state and derive squeezing parameter

Field Eqs of graviton and photons

$$\begin{cases} h''^P_{\boldsymbol{k}}(\eta) + 2\frac{a'}{a} h'^P_{\boldsymbol{k}}(\eta) + k^2 h^P_{\boldsymbol{k}}(\eta) = -\frac{\lambda}{a^2} A^P_{\boldsymbol{k}}(\eta) \\ A''^P_{\boldsymbol{k}}(\eta) + k^2 A'^P_{\boldsymbol{k}}(\eta) = -\lambda h^P_{\boldsymbol{k}}(\eta) \end{cases}$$

Conformal time derivative

$$' = \frac{d}{d\eta}$$

Coupling constant

$$\lambda(\boldsymbol{k}) \equiv \frac{\sqrt{2}}{M_{\rm pl}} \varepsilon^{ilm} \, e^+_i \, k_\ell \, B_m$$

After the conformal transformation, we obtain the simplified field equation

$$y_{\boldsymbol{k}}(\eta) = a(\eta) h_{\boldsymbol{k}}(\eta)$$

$$\begin{cases} y''_{\boldsymbol{k}} + \left(k^2 - \frac{2}{\eta^2}\right) y_{\boldsymbol{k}} = \lambda H \eta A_{\boldsymbol{k}} \\ A''_{\boldsymbol{k}} + k^2 A_{\boldsymbol{k}} = \lambda H \eta \, y_{\boldsymbol{k}} \end{cases}$$

Procedure of analysis

1. Make a setup and derive the field equation of photon and graviton
2. **Solve perturbatively with Green’s function**
3. Bogoliubov transformation
4. Define vacuum state and derive squeezing parameter

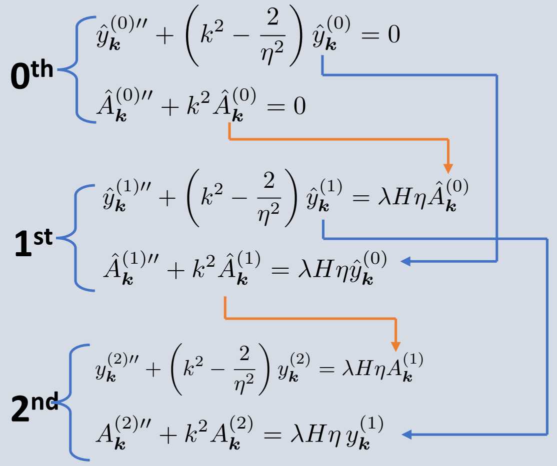

0th

$$\hat{y}_{\boldsymbol{k}}^{(0)\prime\prime} + \left(k^2 - \frac{2}{\eta^2}\right)\hat{y}_{\boldsymbol{k}}^{(0)} = 0$$

$$\hat{A}_{\boldsymbol{k}}^{(0)\prime\prime} + k^2 \hat{A}_{\boldsymbol{k}}^{(0)} = 0$$

1st

$$\hat{y}_{\boldsymbol{k}}^{(1)\prime\prime} + \left(k^2 - \frac{2}{\eta^2}\right)\hat{y}_{\boldsymbol{k}}^{(1)} = \lambda H \eta \hat{A}_{\boldsymbol{k}}^{(0)}$$

$$\hat{A}_{\boldsymbol{k}}^{(1)\prime\prime} + k^2 \hat{A}_{\boldsymbol{k}}^{(1)} = \lambda H \eta \hat{y}_{\boldsymbol{k}}^{(0)}$$

2nd

$$y_{\boldsymbol{k}}^{(2)\prime\prime} + \left(k^2 - \frac{2}{\eta^2}\right)y_{\boldsymbol{k}}^{(2)} = \lambda H \eta A_{\boldsymbol{k}}^{(1)}$$

$$A_{\boldsymbol{k}}^{(2)\prime\prime} + k^2 A_{\boldsymbol{k}}^{(2)} = \lambda H \eta\, y_{\boldsymbol{k}}^{(1)}$$

$$\hat{y}_{\boldsymbol{k}}^{(0)}(\eta) = u_{\boldsymbol{k}}^{(0)}(\eta)\,\hat{c} + u_{\boldsymbol{k}}^{(0)*}(\eta)\,\hat{c}^\dagger$$

$$\hat{A}_{\boldsymbol{k}}^{(0)}(\eta) = v_{\boldsymbol{k}}^{(0)}(\eta)\hat{d} + v_{\boldsymbol{k}}^{(0)*}(\eta)\hat{d}^\dagger$$

$$\begin{aligned}\hat{y}_{\boldsymbol{k}}^{(1)}(\eta) &= -\int_{\eta_i}^{\eta} d\eta' G_{\mathrm{dS}}(\eta,\eta')\lambda H \eta' \hat{A}_{\boldsymbol{k}}^{(0)}(\eta') \\ &\equiv u_{\boldsymbol{k}}^{(1)}(\eta)\ \hat{d} + u_{\boldsymbol{k}}^{(1)*}(\eta)\ \hat{d}^\dagger\end{aligned}$$

$$\begin{aligned}\hat{A}_{\boldsymbol{k}}^{(1)}(\eta) &= -\int_{\eta_i}^{\eta} d\eta' G_{\mathrm{M}}(\eta,\eta')\lambda H \eta' \hat{y}_{\boldsymbol{k}}^{(0)}(\eta') \\ &\equiv v_{\boldsymbol{k}}^{(1)}(\eta)\ \hat{c} + v_{\boldsymbol{k}}^{(1)*}(\eta)\ \hat{c}^\dagger\end{aligned}$$

At initial time, only 0th order of the solution appear.

The constant operator can be written by the creation and annihilation operator at the initial time of the inflation.

Procedure of analysis

1. Make a setup and derive the field equation of photon and graviton
2. Solve perturbatively with Green’s function
3. **Bogoliubov transformation**
4. Define vacuum state and derive squeezing parameter

Time development of the operators are described by the Bogoliubov transformation

$$\begin{pmatrix} a_y(\eta) \\ a_y^\dagger(\eta) \\ a_A(\eta) \\ a_A^\dagger(\eta) \end{pmatrix} = M \begin{pmatrix} a_y(\eta_i) \\ a_y^\dagger(\eta_i) \\ a_A(\eta_i) \\ a_A^\dagger(\eta_i) \end{pmatrix} = \left\{ \underset{0^{\text{th}}}{\begin{pmatrix} A_0 & 0 \\ 0 & D_0 \end{pmatrix}} + \underset{1^{\text{st}}}{\begin{pmatrix} 0 & B_1 \\ C_1 & 0 \end{pmatrix}} + \underset{2^{\text{nd}}}{\begin{pmatrix} A_2 & 0 \\ 0 & D_2 \end{pmatrix}} \right\} \begin{pmatrix} a_y(\eta_i) \\ a_y^\dagger(\eta_i) \\ a_A(\eta_i) \\ a_A^\dagger(\eta_i) \end{pmatrix}$$

Operators at arbitrary time at inflation ⇕ **Instant vacuum state**

Operators at initial time ⇕ **Bunch Davies vacuum state**

$$\hat{a}_y(\eta,\boldsymbol{k})|0\rangle = \hat{a}_A(\eta,\boldsymbol{k})|0\rangle = 0$$

Bogoliubov transformation ⟺

$$\hat{a}_y(\eta_i,\boldsymbol{k})|\mathrm{BD}\rangle = \hat{a}_A(\eta_i,\boldsymbol{k})|\mathrm{BD}\rangle = 0$$

The inverse matrix of the time evolution $M^{-1} = \begin{pmatrix} \alpha_y & \beta_y & \gamma_A & \delta_A \\ \beta_y^* & \alpha_y^* & \delta_A^* & \gamma_A^* \\ \gamma_y & \delta_y & \alpha_A & \beta_A \\ \delta_y^* & \gamma_y^* & \beta_A^* & \alpha_A^* \end{pmatrix}$

Procedure of analysis

1. Make a setup and derive the field equation of photon and graviton
2. Solve perturbatively with Green's function
3. Bogoliubov transformation
4. **Define vacuum state and derive squeezing parameter**

Definition of Bunch Davies vacuum for graviton

$$\hat{a}_y(\eta_i, \boldsymbol{k})|\mathrm{BD}\rangle = 0 \quad \alpha_y\Lambda + \beta_y + \gamma_A\Xi = 0$$
$$\alpha_y\Xi + \gamma_A\Omega + \delta_A = 0$$

Definition of Bunch Davies vacuum for photon

$$\hat{a}_A(\eta_i, \boldsymbol{k})|\mathrm{BD}\rangle = 0 \quad \alpha_A\Xi + \gamma_y\Lambda + \delta_y = 0$$
$$\alpha_A\Omega + \beta_A + \gamma_y\Xi = 0$$

Since the photon and graviton behaves independently, their operator commutes,

$$[\hat{a}_y(\eta, \boldsymbol{k})\ \ , \hat{a}_A(\eta, \boldsymbol{k})] = -\alpha_A\delta_A + \beta_A\gamma_A - \gamma_y\beta_y + \alpha_y\delta_y = 0$$

Solving above simultaneous equations, we obtain each squeezing operators as

$$\Lambda = \frac{\gamma_A\delta_y - \beta_y\alpha_A}{\alpha_y\alpha_A - \gamma_y\gamma_A} \qquad \Xi = \frac{\beta_y\gamma_y - \alpha_y\delta_y}{\alpha_y\alpha_A - \gamma_y\gamma_A} \qquad \Omega = \frac{\gamma_y\delta_A - \beta_A\alpha_y}{\alpha_y\alpha_A - \gamma_y\gamma_A}$$

We assume the Bunch Davies vacuum as

$$|\mathrm{BD}\rangle = \prod_{k=-\infty}^{\infty} \exp\left[\frac{\Lambda}{2}\,\hat{a}_y^\dagger(\eta, \boldsymbol{k})\hat{a}_y^\dagger(\eta, -\boldsymbol{k}) + \Xi\,\hat{a}_y^\dagger(\eta, \boldsymbol{k})\hat{a}_A^\dagger(\eta, -\boldsymbol{k}) + \frac{\Omega}{2}\,\hat{a}_A^\dagger(\eta, \boldsymbol{k})\hat{a}_A^\dagger(\eta, -\boldsymbol{k})\right]|0\rangle$$

Numerical result

$$|\mathrm{BD}\rangle = \prod_{k=-\infty}^{\infty} \exp\left[\boxed{\frac{\Lambda}{2}\,\hat{a}_y^\dagger(\eta, \boldsymbol{k})\hat{a}_y^\dagger(\eta, -\boldsymbol{k})} + \Xi\,\hat{a}_y^\dagger(\eta, \boldsymbol{k})\hat{a}_A^\dagger(\eta, -\boldsymbol{k}) + \frac{\Omega}{2}\,\hat{a}_A^\dagger(\eta, \boldsymbol{k})\hat{a}_A^\dagger(\eta, -\boldsymbol{k})\right]|0\rangle$$

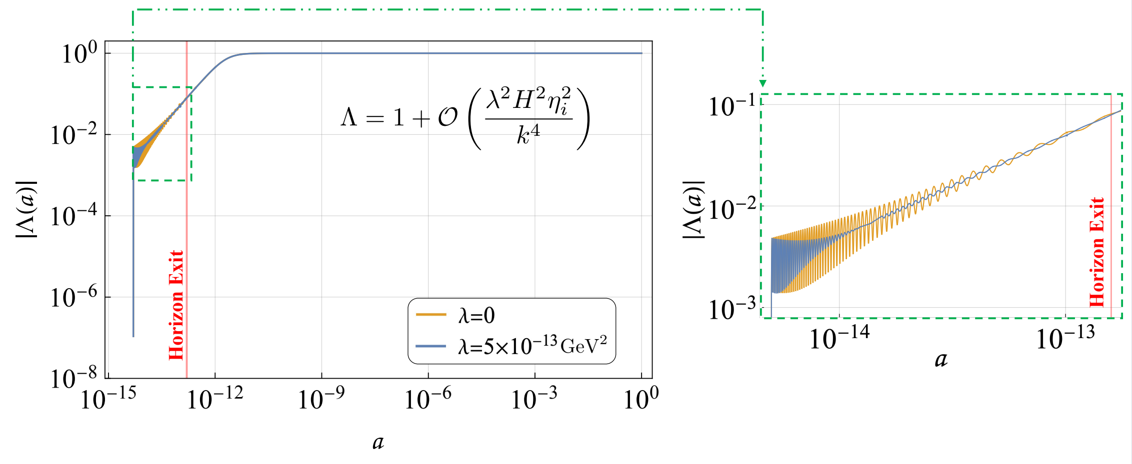

$\lambda = 5\times10^{-13}\,\mathrm{GeV}^2$

$k = 10^2\,\mathrm{GeV}$

$H = 10^{14}\,\mathrm{GeV}$

$\eta_i = -2\,\mathrm{GeV}^{-1}$

$a(\eta_i) = (2\times10^{14})^{-1}$

$\Omega \simeq \frac{B^2}{a_i^4 M_{\mathrm{pl}}^2 H^2}\frac{1}{k\eta_i}$

$B^2/a_i^4 \ll M_{\mathrm{pl}}^2 H^2$

$1/k \ll \eta_i$

The squeezing operator for graviton reduces 1 after the horizon exit.

The amplitude of the oscillation before the horizon exit is weakened by the conversion.
i.e. some part of the graviton is converted to the photon.

Numerical result

$$|\mathrm{BD}\rangle = \prod_{k=-\infty}^{\infty} \exp\left[\frac{\Lambda}{2}\,\hat{a}_y^\dagger(\eta,\boldsymbol{k})\hat{a}_y^\dagger(\eta,-\boldsymbol{k}) + \boxed{\Xi\,\hat{a}_y^\dagger(\eta,\boldsymbol{k})\hat{a}_A^\dagger(\eta,-\boldsymbol{k})} + \frac{\Omega}{2}\,\hat{a}_A^\dagger(\eta,\boldsymbol{k})\hat{a}_A^\dagger(\eta,-\boldsymbol{k})\right]|0\rangle$$

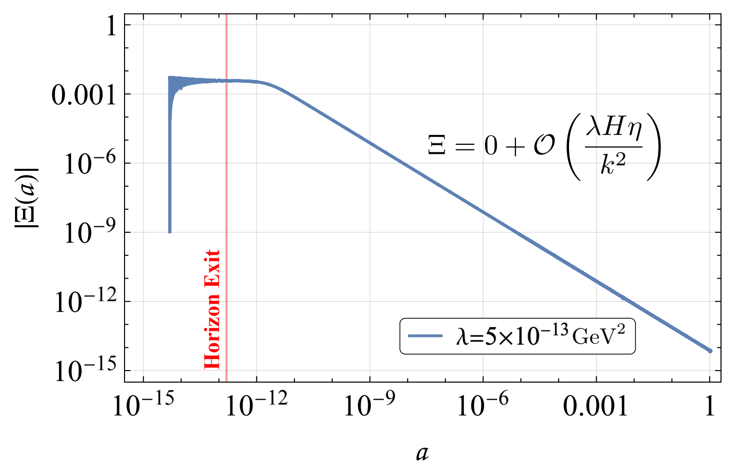

$\lambda = 5 \times 10^{-13}\,\mathrm{GeV}^2$

$k = 10^2\,\mathrm{GeV}$

$H = 10^{14}\,\mathrm{GeV}$

$\eta_i = -2\,\mathrm{GeV}^{-1}$

$a(\eta_i) = (2 \times 10^{14})^{-1}$

$\Omega \simeq \frac{B^2}{a_i^4 M_{\mathrm{pl}}^2 H^2}\frac{1}{k\eta_i}$

$B^2/a_i^4 \ll M_{\mathrm{pl}}^2 H^2$

$1/k \ll \eta_i$

The mixing state go down after the horizon exit.

Numerical result

$$|\mathrm{BD}\rangle = \prod_{k=-\infty}^{\infty} \exp\left[\frac{\Lambda}{2}\,\hat{a}_y^\dagger(\eta,\boldsymbol{k})\hat{a}_y^\dagger(\eta,-\boldsymbol{k}) + \Xi\,\hat{a}_y^\dagger(\eta,\boldsymbol{k})\hat{a}_A^\dagger(\eta,-\boldsymbol{k}) + \boxed{\frac{\Omega}{2}\,\hat{a}_A^\dagger(\eta,\boldsymbol{k})\hat{a}_A^\dagger(\eta,-\boldsymbol{k})}\right]|0\rangle$$

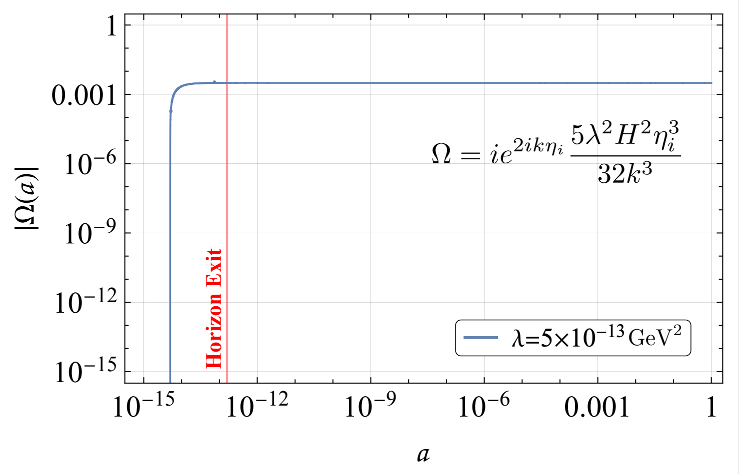

$\lambda = 5 \times 10^{-13}\,\mathrm{GeV}^2$

$k = 10^2\,\mathrm{GeV}$

$H = 10^{14}\,\mathrm{GeV}$

$\eta_i = -2\,\mathrm{GeV}^{-1}$

$a(\eta_i) = (2 \times 10^{14})^{-1}$

$\Omega \simeq \frac{B^2}{a_i^4 M_{\mathrm{pl}}^2 H^2}\frac{1}{k\eta_i}$

$B^2/a_i^4 \ll M_{\mathrm{pl}}^2 H^2$

$1/k \ll \eta_i$

The photon originated by the graviton is generated at early time of the inflation.
It is consistent with other results.

Summary・Future work

Will the squeezing of the gravitons survives or not during inflation ?
Under the presence of the background magnetic field.

- ✓ Derived the field equation of the graviton field and that of photon field under the influence of the background magnetic field.
- ✓ Obtain solutions by using perturbative approach and Green's function.
- ✓ Performed the Bogoliubov transformation to follow the time evolution of squeezing parameter.
- ✓ Plotted the squeezing parameter of GG, GP, and PP state during inflation.

A. The gravitons are robust against the decoherence by the cosmological magnetic fields.

Future work

- ☐ How to include the small anisotropy of the spacetime background ?
- ☐ Are there some model which the squeezing of the graviton broken at the inflation end ?
- ☐ How about
  - other spacetime background, background magnetic field, or systems to consider.
  - after the inflation era, (radiation, matter, cosmological constant dominant era)

E N D

Thank you for your listening!

Analysis

We adopted the perturbative approach to solve field equation of graviton and photon

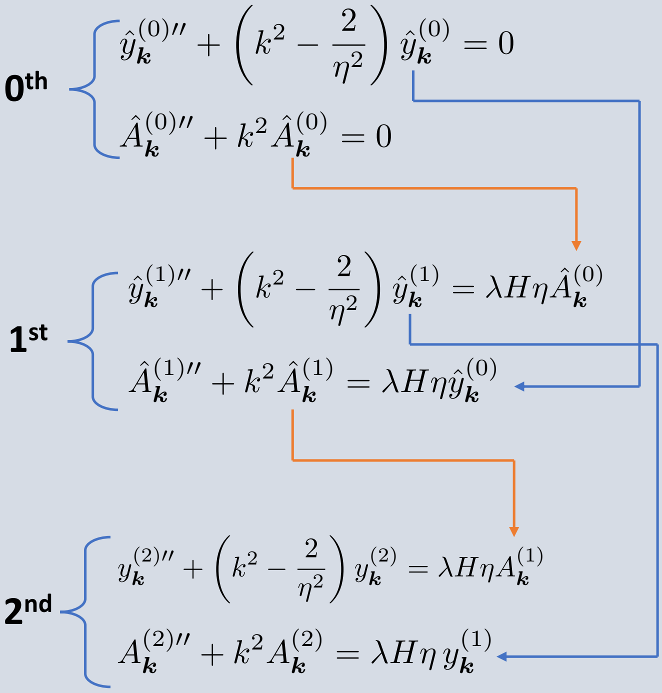

0th

$$\begin{cases} \hat{y}_{\boldsymbol{k}}^{(0)\prime\prime} + \left(k^2 - \dfrac{2}{\eta^2}\right) \hat{y}_{\boldsymbol{k}}^{(0)} = 0 \\ \hat{A}_{\boldsymbol{k}}^{(0)\prime\prime} + k^2 \hat{A}_{\boldsymbol{k}}^{(0)} = 0 \end{cases}$$

1st

$$\begin{cases} \hat{y}_{\boldsymbol{k}}^{(1)\prime\prime} + \left(k^2 - \dfrac{2}{\eta^2}\right) \hat{y}_{\boldsymbol{k}}^{(1)} = \lambda H \eta \hat{A}_{\boldsymbol{k}}^{(0)} \\ \hat{A}_{\boldsymbol{k}}^{(1)\prime\prime} + k^2 \hat{A}_{\boldsymbol{k}}^{(1)} = \lambda H \eta \hat{y}_{\boldsymbol{k}}^{(0)} \end{cases}$$

2nd

$$\begin{cases} y_{\boldsymbol{k}}^{(2)\prime\prime} + \left(k^2 - \dfrac{2}{\eta^2}\right) y_{\boldsymbol{k}}^{(2)} = \lambda H \eta A_{\boldsymbol{k}}^{(1)} \\ A_{\boldsymbol{k}}^{(2)\prime\prime} + k^2 A_{\boldsymbol{k}}^{(2)} = \lambda H \eta \, y_{\boldsymbol{k}}^{(1)} \end{cases}$$

Solve iteratively with Green's function

Minkowski

$$G_{\mathrm{M}}(\eta, \eta') = -\frac{1}{k} \sin k(\eta - \eta')$$

de Sitter

$$G_{\mathrm{dS}}(\eta, \eta') = \frac{1}{2ik}\left(1 + \frac{i}{k\eta'}\right)\left(1 - \frac{i}{k\eta}\right) e^{-ik(\eta-\eta')} - \frac{1}{2ik}\left(1 - \frac{i}{k\eta'}\right)\left(1 + \frac{i}{k\eta}\right) e^{ik(\eta-\eta')}$$

Analysis

Perturbative solutions of the graviton field

$$\hat{y}_{\boldsymbol{k}}^{(0)}(\eta) = u_{\boldsymbol{k}}^{(0)}(\eta)\, \hat{c} + u_{\boldsymbol{k}}^{(0)*}(\eta)\, \hat{c}^\dagger$$

Constant operator of the integration of graviton

$$\hat{y}_{\boldsymbol{k}}^{(1)}(\eta) = -\int_{\eta_i}^{\eta} d\eta' G_{\mathrm{dS}}(\eta, \eta') \lambda H \eta' \hat{A}_{\boldsymbol{k}}^{(0)}(\eta') \equiv u_{\boldsymbol{k}}^{(1)}(\eta)\ \hat{d} + u_{\boldsymbol{k}}^{(1)*}(\eta)\ \hat{d}^\dagger$$

$$\hat{y}_{\boldsymbol{k}}^{(2)}(\eta) = -\int_{\eta_i}^{\eta} d\eta' G_{\mathrm{dS}}(\eta, \eta') \lambda H \eta' \hat{A}_{\boldsymbol{k}}^{(1)}(\eta') \equiv u_{\boldsymbol{k}}^{(2)}(\eta)\ \hat{c} + u_{\boldsymbol{k}}^{(2)*}(\eta)\ \hat{c}^\dagger$$

Perturbative solutions of the photon field

$$\hat{A}_{\boldsymbol{k}}^{(0)}(\eta) = v_{\boldsymbol{k}}^{(0)}(\eta) \hat{d} + v_{\boldsymbol{k}}^{(0)*}(\eta) \hat{d}^\dagger$$

Constant operator of the integration of photon

$$\hat{A}_{\boldsymbol{k}}^{(1)}(\eta) = -\int_{\eta_i}^{\eta} d\eta' G_{\mathrm{M}}(\eta, \eta') \lambda H \eta' \hat{y}_{\boldsymbol{k}}^{(0)}(\eta') \equiv v_{\boldsymbol{k}}^{(1)}(\eta)\ \hat{c} + v_{\boldsymbol{k}}^{(1)*}(\eta)\ \hat{c}^\dagger$$

$$\hat{A}_{\boldsymbol{k}}^{(2)}(\eta) = -\int_{\eta_i}^{\eta} d\eta' G_{\mathrm{M}}(\eta, \eta') \lambda H \eta'\ \hat{y}_{\boldsymbol{k}}^{(1)}(\eta') = v_{\boldsymbol{k}}^{(2)}(\eta)\ \hat{d} + v_{\boldsymbol{k}}^{(2)*}(\eta)\ \hat{d}^\dagger$$

Analysis

Since only the 0^{th} order solution contributes solutions at initial time, we can derive the explicit form of the annihilation operator at the initial time.

$$\hat{a}_y(\eta_i, \boldsymbol{k}) = \left(1 - \frac{i}{2k\eta_i}\right) e^{-ik\eta_i}\,\hat{c} + \frac{i}{2k\eta_i} e^{ik\eta_i}\,\hat{c}^\dagger$$

$$\hat{a}_A(\eta_i, \boldsymbol{k}) = e^{-ik\eta_i}\,\hat{d}$$

We can easily solve inversely to obtain

$$\hat{c} = \left(1 + \frac{i}{2k\eta_i}\right) e^{ik\eta_i}\,\hat{a}_y(\eta_i, \boldsymbol{k}) - \frac{i}{2k\eta_i} e^{ik\eta_i}\,\hat{a}_y^\dagger(\eta_i, -\boldsymbol{k})$$

$$\hat{d} = e^{ik\eta_i}\,\hat{a}_A(\eta_i, \boldsymbol{k})$$

After plugging these operators into equations in previous slide, we obtain the time evolution of the annihilation opeartors.

Bogoliubov transformation

Time development of the operators are described by the Bogoliubov transformation

$$\begin{pmatrix} a_y(\eta) \\ a_y^\dagger(\eta) \\ a_A(\eta) \\ a_A^\dagger(\eta) \end{pmatrix} = M \begin{pmatrix} a_y(\eta_i) \\ a_y^\dagger(\eta_i) \\ a_A(\eta_i) \\ a_A^\dagger(\eta_i) \end{pmatrix} = \left\{ \underset{0^{\text{th}}}{\begin{pmatrix} A_0 & 0 \\ 0 & D_0 \end{pmatrix}} + \underset{1^{\text{st}}}{\begin{pmatrix} 0 & B_1 \\ C_1 & 0 \end{pmatrix}} + \underset{2^{\text{nd}}}{\begin{pmatrix} A_2 & 0 \\ 0 & D_2 \end{pmatrix}} \right\} \begin{pmatrix} a_y(\eta_i) \\ a_y^\dagger(\eta_i) \\ a_A(\eta_i) \\ a_A^\dagger(\eta_i) \end{pmatrix}$$

The inverse matrix of the time evolution

$$M^{-1} = \begin{pmatrix} \alpha_y & \beta_y & \gamma_A & \delta_A \\ \beta_y^* & \alpha_y^* & \delta_A^* & \gamma_A^* \\ \gamma_y & \delta_y & \alpha_A & \beta_A \\ \delta_y^* & \gamma_y^* & \beta_A^* & \alpha_A^* \end{pmatrix}$$

$$\hat{a}_y(\eta_i, \boldsymbol{k}) = \alpha_y\,\hat{a}_y(\eta, \boldsymbol{k}) + \beta_y\,\hat{a}_y^\dagger(\eta, -\boldsymbol{k}) + \gamma_A\,\hat{a}_A(\eta, \boldsymbol{k}) + \delta_A\,\hat{a}_A^\dagger(\eta, -\boldsymbol{k})$$

$$\hat{a}_A(\eta_i, \boldsymbol{k}) = \gamma_y\,\hat{a}_y(\eta, \boldsymbol{k}) + \delta_y\,\hat{a}_y^\dagger(\eta, -\boldsymbol{k}) + \alpha_A\,\hat{a}_A(\eta, \boldsymbol{k}) + \beta_A\,\hat{a}_A^\dagger(\eta, -\boldsymbol{k})$$

The Bunch Davies vacuum is defined by the ground state at the initial time,

$$\hat{a}_y(\eta_i, \boldsymbol{k})|\mathrm{BD}\rangle = \hat{a}_A(\eta_i, \boldsymbol{k})|\mathrm{BD}\rangle = 0$$

Bunch Davies vacuum state

Commutation relations of operators

$$[\hat{a}_y(\eta,\boldsymbol{k}),\hat{a}_y^\dagger(\eta,-\boldsymbol{k}')]=\delta(\boldsymbol{k}+\boldsymbol{k}')\quad[\hat{a}_A(\eta,\boldsymbol{k}),\hat{a}_A^\dagger(\eta,-\boldsymbol{k}')]=\delta(\boldsymbol{k}+\boldsymbol{k}')$$

$$[\hat{a}_y(\eta,\boldsymbol{k}),\hat{a}_A(\eta,-\boldsymbol{k}')]=0$$

Since the quantum state of the current system is consisted by the photon and graviton,

$$\mathcal{H}_{y,\boldsymbol{k}}\otimes\mathcal{H}_{y,-\boldsymbol{k}}\otimes\mathcal{H}_{A,\boldsymbol{k}}\otimes\mathcal{H}_{A,-\boldsymbol{k}}$$

We assume the Bunch Davies vacuum as

$$|\mathrm{BD}\rangle=\prod_{k=-\infty}^{\infty}\exp\left[\frac{\Lambda}{2}\,\hat{a}_y^\dagger(\eta,\boldsymbol{k})\hat{a}_y^\dagger(\eta,-\boldsymbol{k})+\Xi\,\hat{a}_y^\dagger(\eta,\boldsymbol{k})\hat{a}_A^\dagger(\eta,-\boldsymbol{k})+\frac{\Omega}{2}\,\hat{a}_A^\dagger(\eta,\boldsymbol{k})\hat{a}_A^\dagger(\eta,-\boldsymbol{k})\right]|0\rangle$$

$$=\prod_{\boldsymbol{k}}\sum_{p\,,q\,,r=0}^{\infty}\frac{\Lambda^p\,\Xi^q\,\Omega^r}{2^{p+r}p!\,q!\,r!}|p+q\rangle_{y,\boldsymbol{k}}\otimes|p\rangle_{y,-\boldsymbol{k}}\otimes|r\rangle_{A,\boldsymbol{k}}\otimes|q+r\rangle_{A,-\boldsymbol{k}}$$

Instant vacuum state

$$\hat{a}_y(\eta,\boldsymbol{k})|0\rangle=\hat{a}_A(\eta,\boldsymbol{k})|0\rangle=0$$

Polarization tensor

Polarization tensor

$$e^{ijP}(\boldsymbol{k})e^Q_{ij}(\boldsymbol{k})=\delta^{PQ}$$

$$e^{iP}(\boldsymbol{k})e^Q_{i}(\boldsymbol{k})=\delta^{PQ}$$

$$P,Q=+,\times$$

$$e^{+}_{ij}(\boldsymbol{k})=\frac{1}{\sqrt{2}}\left\{e^+_i(\boldsymbol{k})e^+_j(\boldsymbol{k})-e^\times_i(\boldsymbol{k})e^\times_j(\boldsymbol{k})\right\}$$

$$e^{\times}_{ij}(\boldsymbol{k})=\frac{1}{\sqrt{2}}\left\{e^+_i(\boldsymbol{k})e^\times_j(\boldsymbol{k})+e^\times_i(\boldsymbol{k})e^+_j(\boldsymbol{k})\right\}$$

Configuration of the momentum, polarization vectors, background magnetic field, and direction of propagation is illustrated as

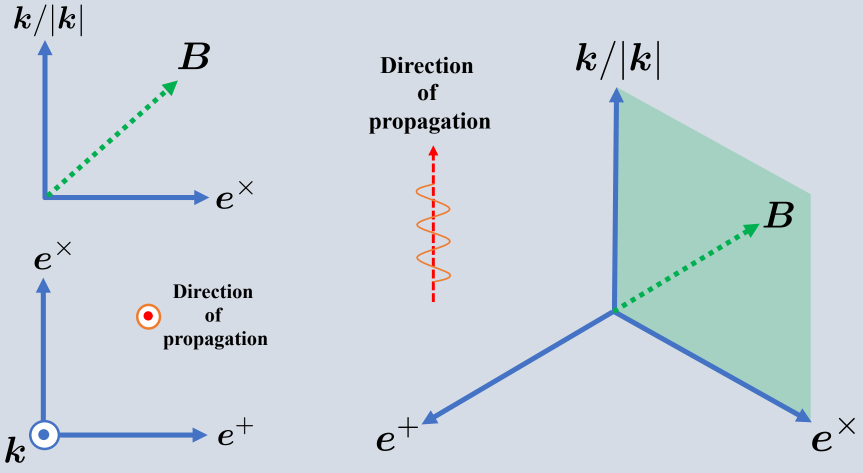

Analysis

Solutions are written as

$$\hat{y}_{\boldsymbol{k}}(\eta) = \left(u_{\boldsymbol{k}}^{(0)} + u_{\boldsymbol{k}}^{(2)}\right)\hat{c} + u_{\boldsymbol{k}}^{(1)}\,\hat{d} + \mathrm{h.c.} \qquad \hat{A}_{\boldsymbol{k}}(\eta) = \left(v_{\boldsymbol{k}}^{(0)} + v_{\boldsymbol{k}}^{(2)}\right)\hat{d} + v_{\boldsymbol{k}}^{(1)}\,\hat{c} + \mathrm{h.c.}$$

After the derivation of solutions, we define the conjugate momentum of each modes,

Conjugate momentum of the graviton

$$\begin{aligned} p_{\boldsymbol{k}}(\eta) &= \frac{\partial L_g}{\partial y'_{-\boldsymbol{k}}} = y'_{\boldsymbol{k}}(\eta) + \frac{1}{\eta}y_{\boldsymbol{k}}(\eta) \\ &= \left(u_{\boldsymbol{k}}^{(0)\,\prime} + u_{\boldsymbol{k}}^{(2)\,\prime}\right)\hat{c} + u_{\boldsymbol{k}}^{(1)\,\prime}\,\hat{d} + \frac{1}{\eta}\left\{\left(u_{\boldsymbol{k}}^{(0)} + u_{\boldsymbol{k}}^{(2)}\right)\hat{c} + u_{\boldsymbol{k}}^{(1)}\,\hat{d}\right\} + \mathrm{h.c.} \end{aligned}$$

Conjugate momentum of the photon

$$\begin{aligned} \pi_{\boldsymbol{k}}(\eta) &= \frac{\partial L_A}{\partial A'_{-\boldsymbol{k}}} = A'_{\boldsymbol{k}}(\eta) \\ &= \left(v_{\boldsymbol{k}}^{(0)\,\prime} + v_{\boldsymbol{k}}^{(2)\,\prime}\right)\hat{d} + v_{\boldsymbol{k}}^{(1)\,\prime}\,\hat{c} + \mathrm{h.c.} \end{aligned}$$

Instant vacuum state is defined by the annihilation operator for each time

$$\hat{a}(\eta, \boldsymbol{k})|0\rangle = 0$$

Analysis

Annihilation operator is defined by the solution and its momentum,

$$\hat{a}_y(\eta, \boldsymbol{k}) = \sqrt{\frac{k}{2}}\hat{y}_{\boldsymbol{k}}(\eta) + \frac{i}{\sqrt{2k}}\hat{p}_{\boldsymbol{k}}(\eta) \qquad \hat{a}_A(\eta, \boldsymbol{k}) = \sqrt{\frac{k}{2}}\hat{A}_{\boldsymbol{k}}(\eta) + \frac{i}{\sqrt{2k}}\hat{\pi}_{\boldsymbol{k}}(\eta)$$

After simplify the coefficient function of the operators, we obtain

$$\hat{a}_y(\eta, \boldsymbol{k}) = \left(\psi_p^{(0)} + \psi_p^{(2)}\right)\hat{c} + \left(\psi_m^{(0)*} + \psi_m^{(2)*}\right)\hat{c}^\dagger + \psi_p^{(1)}\hat{d} + \psi_m^{(1)*}\hat{d}^\dagger$$

$$\hat{a}_A(\eta, \boldsymbol{k}) = \left(\phi_p^{(0)} + \phi_p^{(2)}\right)\hat{d} + \left(\phi_m^{(0)*} + \phi_m^{(2)*}\right)\hat{d}^\dagger + \phi_p^{(1)}\hat{c} + \phi_m^{(1)*}\hat{c}^\dagger$$

where we defined coefficient functions as

$$\psi_p^{(j)} = \sqrt{\frac{k}{2}}u_{\boldsymbol{k}}^{(j)}(\eta) + \frac{i}{\sqrt{2k}}\left(u_{\boldsymbol{k}}^{(j)\prime}(\eta) + \frac{1}{\eta}u_{\boldsymbol{k}}^{(j)}(\eta)\right) \qquad \phi_p^{(j)} = \sqrt{\frac{k}{2}}v_{\boldsymbol{k}}^{(j)}(\eta) + \frac{i}{\sqrt{2k}}v_{\boldsymbol{k}}^{(j)\prime}(\eta)$$

$$\psi_m^{(j)} = \sqrt{\frac{k}{2}}u_{\boldsymbol{k}}^{(j)}(\eta) - \frac{i}{\sqrt{2k}}\left(u_{\boldsymbol{k}}^{(j)\prime}(\eta) + \frac{1}{\eta}u_{\boldsymbol{k}}^{(j)}(\eta)\right) \qquad \phi_m^{(j)} = \sqrt{\frac{k}{2}}v_{\boldsymbol{k}}^{(j)}(\eta) - \frac{i}{\sqrt{2k}}v_{\boldsymbol{k}}^{(j)\prime}(\eta)$$

Thus, the time evolution of the annihilation operators of graviton and photon is expressed with the constant operators of the integration.

Analysis

The time evolution of each annihilation operator for graviton

$$\begin{aligned}\hat{a}_y(\eta,\boldsymbol{k}) =& \left[\left(\psi_p^{(0)}+\psi_p^{(2)}\right)\left(1+\frac{i}{2k\eta_i}\right)e^{ik\eta_i}+\left(\psi_m^{(0)*}+\psi_m^{(2)*}\right)\frac{i}{2k\eta_i}e^{-ik\eta_i}\right]\hat{a}_y(\eta_i,\boldsymbol{k})\\ &+\left[\left(\psi_p^{(0)}+\psi_p^{(2)}\right)\left(-\frac{i}{2k\eta_i}\right)e^{ik\eta_i}+\left(\psi_m^{(0)*}+\psi_m^{(2)*}\right)\left(1-\frac{i}{2k\eta_i}\right)e^{-ik\eta_i}\right]\hat{a}_y^\dagger(\eta_i,-\boldsymbol{k})\\ &+\psi_p^{(1)}e^{ik\eta_i}\hat{a}_A(\eta_i,\boldsymbol{k})+\psi_m^{(1)*}e^{-ik\eta_i}\hat{a}_A^\dagger(\eta_i,-\boldsymbol{k})\end{aligned}$$

The time evolution of each annihilation operator for photon

$$\begin{aligned}\hat{a}_A(\eta,\boldsymbol{k}) =& \left(\phi_p^{(1)}\left(1+\frac{i}{2k\eta_i}\right)e^{ik\eta_i}+\phi_m^{(1)*}\frac{i}{2k\eta_i}e^{-ik\eta_i}\right)\hat{a}_y(\eta_i,\boldsymbol{k})\\ &+\left(-\phi_p^{(1)}\frac{i}{2k\eta_i}e^{ik\eta_i}+\phi_m^{(1)*}\left(1-\frac{i}{2k\eta_i}\right)e^{-ik\eta_i}\right)\hat{a}_y^\dagger(\eta_i,-\boldsymbol{k})\\ &+\left(\phi_p^{(0)}+\phi_p^{(2)}\right)e^{ik\eta_i}\hat{a}_A(\eta_i,\boldsymbol{k})+\left(\phi_m^{(0)*}+\phi_m^{(2)*}\right)e^{-ik\eta_i}\hat{a}_A^\dagger(\eta_i,-\boldsymbol{k})\end{aligned}$$

Bunch Davies vacuum state

Commutation relations of operators

$[\hat{a}_y(\eta,\boldsymbol{k}),\hat{a}_y^\dagger(\eta,-\boldsymbol{k}')]=\delta(\boldsymbol{k}+\boldsymbol{k}')$ $[\hat{a}_A(\eta,\boldsymbol{k}),\hat{a}_A^\dagger(\eta,-\boldsymbol{k}')]=\delta(\boldsymbol{k}+\boldsymbol{k}')$

$[\hat{a}_y(\eta,\boldsymbol{k}),\hat{a}_A(\eta,-\boldsymbol{k}')]=0$

Since the quantum state of the current system is consisted by the photon and graviton,

$$\mathcal{H}_{y,\boldsymbol{k}}\otimes\mathcal{H}_{y,-\boldsymbol{k}}\otimes\mathcal{H}_{A,\boldsymbol{k}}\otimes\mathcal{H}_{A,-\boldsymbol{k}}$$

We assume the Bunch Davies vacuum as

$$\begin{aligned}|\mathrm{BD}\rangle =& \prod_{k=-\infty}^{\infty}\exp\left[\frac{\Lambda}{2}\,\hat{a}_y^\dagger(\eta,\boldsymbol{k})\hat{a}_y^\dagger(\eta,-\boldsymbol{k})+\Xi\,\hat{a}_y^\dagger(\eta,\boldsymbol{k})\hat{a}_A^\dagger(\eta,-\boldsymbol{k})+\frac{\Omega}{2}\,\hat{a}_A^\dagger(\eta,\boldsymbol{k})\hat{a}_A^\dagger(\eta,-\boldsymbol{k})\right]|0\rangle\\ =&\prod_{\boldsymbol{k}}\sum_{p\,,q\,,r=0}^{\infty}\frac{\Lambda^p\,\Xi^q\,\Omega^r}{2^{p+r}p!\,q!\,r!}|p+q\rangle_{y,\boldsymbol{k}}\otimes|p\rangle_{y,-\boldsymbol{k}}\otimes|r\rangle_{A,\boldsymbol{k}}\otimes|q+r\rangle_{A,-\boldsymbol{k}}\end{aligned}$$

Instant vacuum state

$$\hat{a}_y(\eta,\boldsymbol{k})|0\rangle=\hat{a}_A(\eta,\boldsymbol{k})|0\rangle=0$$

C45

Consistency between **causality** and **complementarity** guaranteed by Robertson inequality in quantum field theory

contents

☑Superposition of Newtonian potential and a paradox

☑Resolution of the paradox

☑Analysis of paradox based on QFT

☑Conclusions

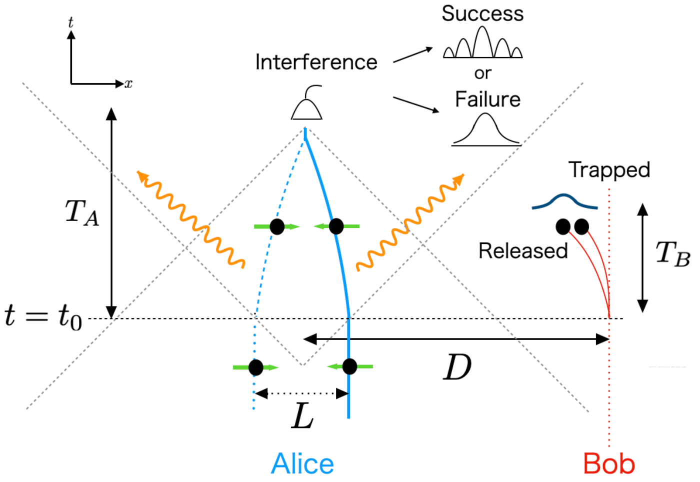

Yuuki Sugiyama

Based on arXiv: 2206.02506

Collaboration : A. Matsumura, K. Yamamoto

JGRG31 2022/10/26 @ U. Tokyo

Introduction

The unification of **gravity** and **quantum mechanics** is one of the most important problems in modern physics

However, we do **not know** even whether gravitational interaction obeys the framework of quantum mechanics

Introduction

What happens, if massive particle **is in a superposition state**

Dose **superposition state of Newtonian potential** realize?


Superposition state of a particle A

Introduction

What happens, if massive particle **is in a superposition state**

Dose **superposition state of Newtonian potential** realize?


Superposition state of a particle A

Quantum superposition state of
Newtonian potential due to a particle A?

Introduction

Does a massive quantum particle generate the quantum superposition of Newtonian potential?

How is the quantum superposition of Newtonian potential consistent with the QFT of gravity and graviton?

Gedanken experiment

Mari et al. (2016)
Belenchia et al.(2018)

Considering two systems (Alice and Bob) interact through Newtonian potential

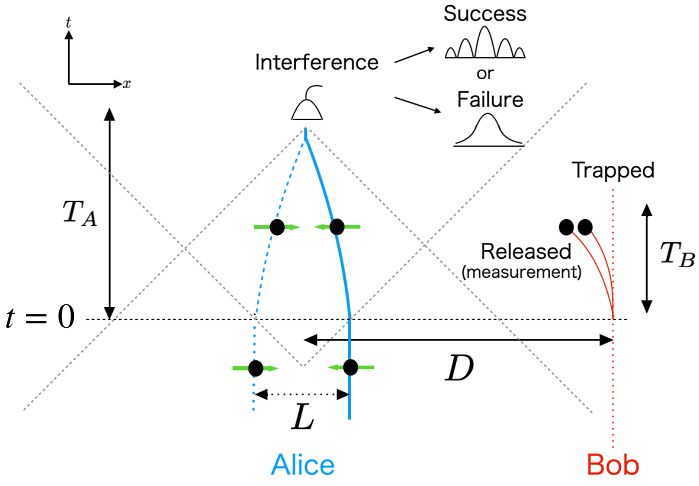

(A) Alice’s system

Alice’s particle is in a superposition of two states and starts to recombine at $t=0$.

At $t=T_A$, an interference experiment is performed and judges whether it is success or not.

Gedanken experiment

Mari et al. (2016)
Belenchia et al.(2018)

Considering two systems (Alice and Bob) interact through Newtonian potential

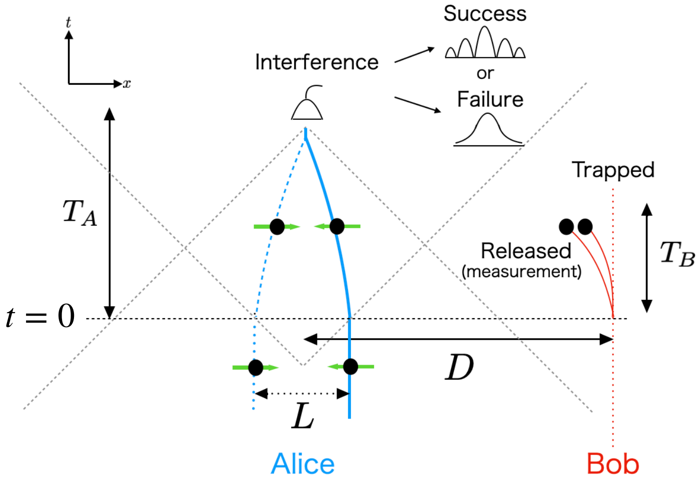

(B) Bob's system

Bob chooses whether he releases his particle or not at $t = 0$.

(Alice's particle and Bob's particle interact with each other through Newtonian potential.)

When he releases his particle, he measures the position of his particle.

We can judge which-path Alice's particle took by using Bob's particle

Gedanken experiment

Mari et al. (2016)
Belenchia et al.(2018)

In this system, we consider **causality** and **complementarity**

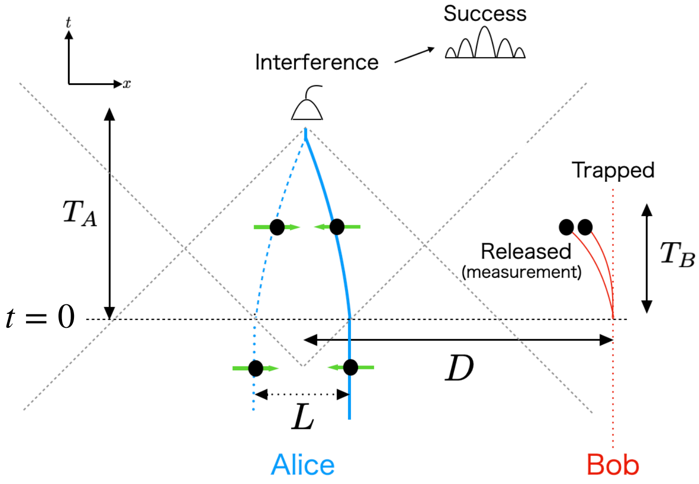

If causality holds, Alice's interference experiments succeed no matter what Bob measures

(Causality: properties of GR)

Here, complementarity means Alice's interference experiments fail due to Bob's measurement

(Complementarity: properties of QM)

Gedanken experiment

Mari et al. (2016)
Belenchia et al.(2018)

In this system, we consider **causality** and **complementarity**

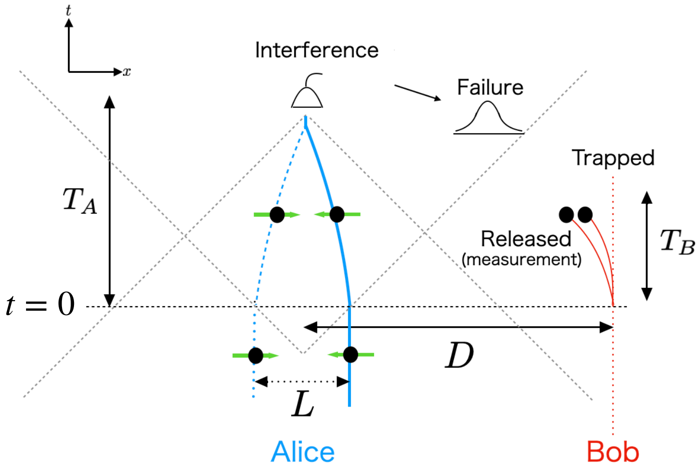

If causality holds, Alice’s interference experiments succeed no matter what Bob measures

(Causality: properties of GR)

Here, complementarity means Alice's interference experiments fail due to Bob's measurement

(Complementarity: properties of QM)

Gedanken experiment

Mari et al. (2016)
Belenchia et al.(2018)

In this system, we consider **causality** and **complementarity**

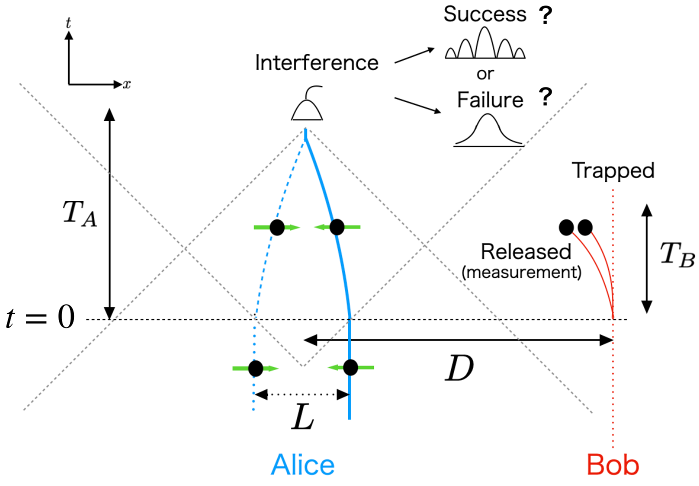

$D > T_A$ and $D > T_B$,

If causality holds, Alice’s interference experiments succeed no matter what Bob measures

(Causality: properties of GR)

Here, complementarity means Alice's interference experiments fail due to Bob's measurement

(Complementarity: properties of QM)

Newtonian potential only,

Causality and Complementarity contradict ! ?

Resolution for paradox

Belenchia et al.(2018)
Danielson et al. (2022)

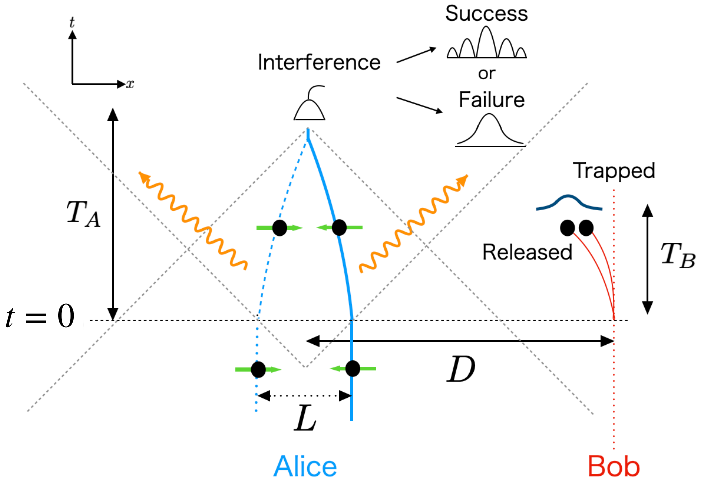

Paradox is solved by order estimation

(A i) vacuum fluctuation

Bob's measurement of Alice's which-path information is limited

(Through superposition of Newtonian potential)

(A ii) quantum radiation

Alice's experiments are failure due to decoherence

Thanks to the quantum gravitational field, the paradox does not appear

→ Quantized gravitational field is **necessary** !

Our motivation

We want to understand causality and complementarity are consistent based on QFT

Use a model of QED: gauge field interacting with two charged particles

YS, Matsumura, Yamamoto, PRD 106, 045009 (2022)

, arXiv: 2206.02506

EM		Gravity
Charge	⟷	Mass
EM wave	⟷	GWs

Setup

- Particle A combines during time T_A
- Particle B performs interference experiment during time T_B and measures which path A took
- initial state

$$|\Psi(0)\rangle = \frac{1}{2}\left(|R\rangle_A + |L\rangle_A\right)\left(|R\rangle_B + |L\rangle_B\right)|0\rangle_{ph}$$

$$\hat{U}(T) = e^{-i(\hat{H}_0+\hat{V})T} \quad , \hat{V} = \int d^3x\left(\hat{J}^\mu_A(\mathbf{x}) + \hat{J}^\mu_B(\mathbf{x})\right)\hat{A}^\mu(\mathbf{x})$$

$$|\Psi(T)\rangle = e^{-i(\hat{H}_0+\hat{V})T}|\Psi(0)\rangle$$

$$\approx \frac{1}{\sqrt{2}}|R\rangle_A|\Phi_{BR}\rangle + \frac{1}{\sqrt{2}}|L\rangle_A|\Phi_{BL}\rangle$$

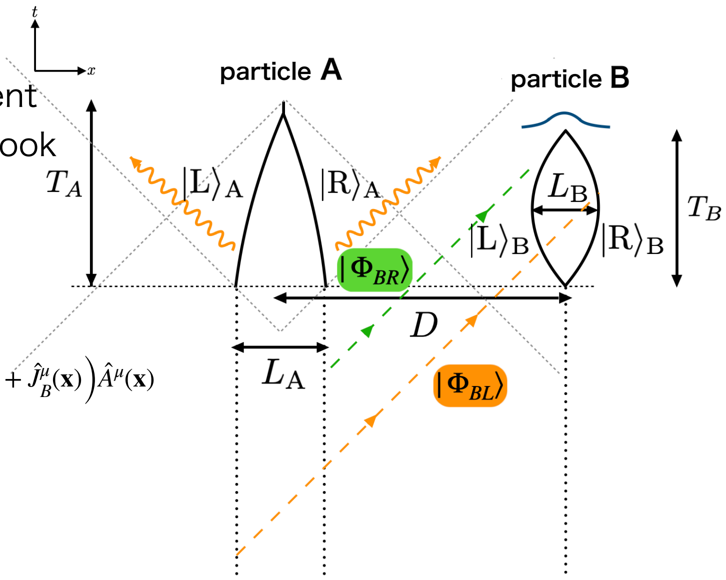

Causality

If causality holds, Bob should not affect Alice's experiments…

retarded Green's function from Bob

$$A_{B(R/L)\mu}(x) = \int d^4y G^r_{\mu\nu}(x,y) J^\nu_{B(R/L)}(y)$$

- Alice's density matrix

$$\rho_A = Tr_{B,ph}[|\Psi(T)\rangle\langle\Psi(T)|]$$

$$= \frac{1}{2}\begin{pmatrix} 1 & \frac{1}{2}e^{-\Gamma_A+i\Phi_A}\left(e^{-i\int d^4x(J^\mu_{AR}-J^\mu_{AL})A_{BR\mu}} + e^{-i\int d^4x(J^\mu_{AR}-J^\mu_{AL})A_{BL\mu}}\right) \\ * & 1 \end{pmatrix}$$

Causality

If causality holds, Bob should not affect Alice's experiments…

retarded Green's function from Bob

$$A_{B(R/L)\mu}(x) = \int d^4y G^r_{\mu\nu}(x,y) J^\nu_{B(R/L)}(y)$$

$D > T_A$ **&** $D > T_B$

- Alice's density matrix

$$\rho_A = Tr_{B,ph}[\,|\Psi(T)\rangle\langle\Psi(T)|\,]$$

$$= \frac{1}{2}\begin{pmatrix} 1 & \frac{1}{2}e^{-\Gamma_A+i\Phi_A}\left(e^{-i\int d^4x(J^\mu_{AR}-J^\mu_{AL})\cancel{A_{BR\mu}}} + e^{-i\int d^4x(J^\mu_{AR}-J^\mu_{AL})\cancel{A_{BL\mu}}}\right) \\ * & \end{pmatrix}$$

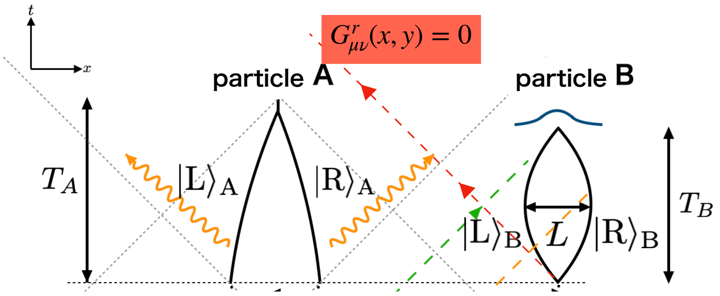

$G^r_{\mu\nu}(x,y) = 0$

Causality

If causality holds, Bob should not affect Alice's experiments…

- Alice's density matrix

$$\rho_A = Tr_{B,ph}[\,|\Psi(T)\rangle\langle\Psi(T)|\,]$$

$$= \frac{1}{2}\begin{pmatrix} 1 & e^{-\underline{\Gamma_A}+i\underline{\Phi_A}} \\ e^{-\underline{\Gamma_A}-i\underline{\Phi_A}} & 1 \end{pmatrix}$$

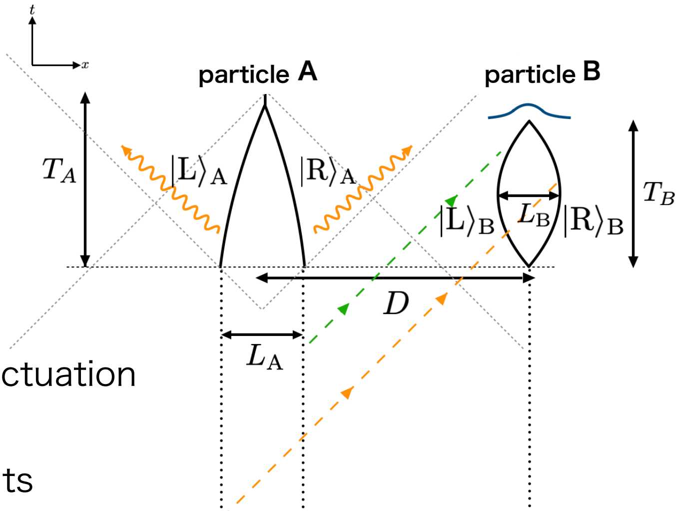

$\underline{\Gamma_A} > 0$: decoherence induced by vacuum fluctuation

➡ Photon radiation

$\underline{\Phi_A}$: cause phase shift in Alice's experiments

Bob does not affect Alice's density matrix !

Hidaka, Iso, Shimada (2022)

Complementarity

Jaeger et al. (1995)
Englert PRL (1996)

Complementarity is evaluated by

$$V_A^2 + D_B^2 \leq 1$$

Visibility V_A : coherence of particle A

Distinguishability D_B : how Bob’s state can distinguish the trajectory of A

e.g.) If $D_B = 1, \ \ V_A = 0$

We can judge which-path A took

But the coherence of particle A is lost

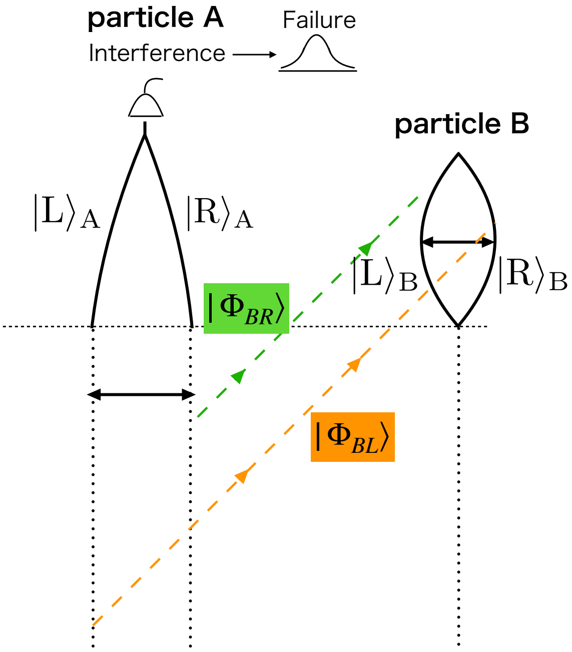

Complementarity

Jaeger et al. (1995)
Englert PRL (1996)

Complementarity is evaluated by

$$V_A^2 + D_B^2 \leq 1$$

Visibility V_A : coherence of particle A

Distinguishability D_B : how Bob’s state can distinguish the trajectory of A

e.g.) If $D_B = 0, \ \ V_A \leq 1$

We cannot judge which-path A took

The experiment of particle A can be success

V_A and D_B are complementary

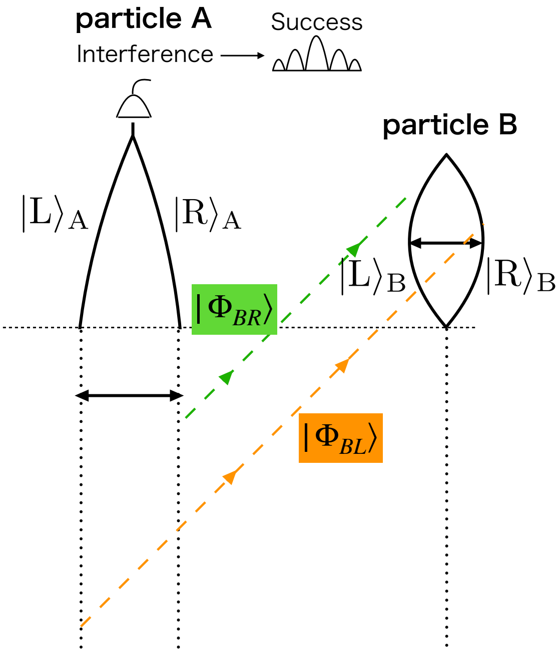

Complementarity

Jaeger et al. (1995)
Englert PRL (1996)

- Visibility

$$V_A = 2 |_A \langle L_f | \rho_A | R_f \rangle_A |$$

interference term of Alice's density matrix

- Distinguishability

$$D_B = \frac{1}{2} Tr_B | \rho_{BR} - \rho_{BL} | = \frac{1}{2} \sum_i |\lambda_i|$$

$$\rho_{BP} = Tr_{ph}[|\Phi_{BP}\rangle\langle\Phi_{BP}|]$$

- Result

$$V_A^2 + D_B^2 = e^{-2\Gamma_A} \cos^2 \left(\frac{\Phi_{AB}}{2} \right) + e^{-2\Gamma_B} \sin^2 \left(\frac{\Phi_{BA}}{2} \right) \leq 1$$

$\Phi_{AB} = \int d^4x (J^\mu_{AR} - J^\mu_{AL})(A_{BR\mu} - A_{BL\mu})$ $\Phi_{BA} = \int d^4x (J^\mu_{BR} - J^\mu_{BL})(A_{AR\mu} - A_{AL\mu})$

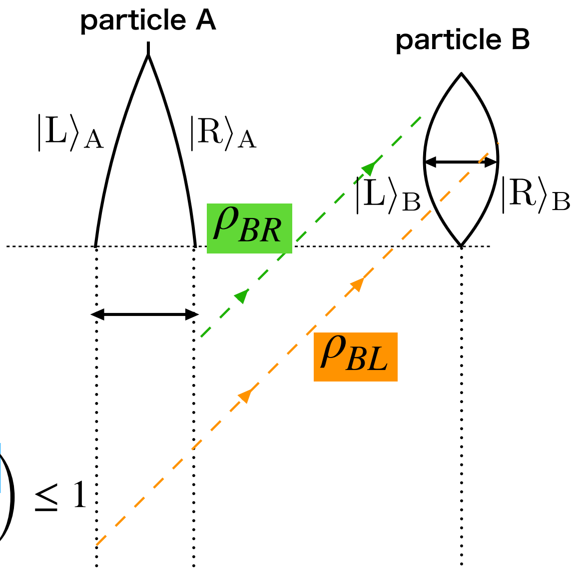

Complementarity

Jaeger et al. (1995)
Englert PRL (1996)

- Visibility

$$V_A = 2 |_A \langle L_f | \rho_A | R_f \rangle_A |$$

interference term of Alice's density matrix

- Distinguishability

$$D_B = \frac{1}{2} Tr_B | \rho_{BR} - \rho_{BL} | = \frac{1}{2} \sum_i |\lambda_i|$$

$$\rho_{BP} = Tr_{ph}[|\Phi_{BP}\rangle\langle\Phi_{BP}|]$$

- Result When A and B are space-like,

$$V_A^2 + D_B^2 = e^{-2\Gamma_A} \cos^2 \left(\cancel{\frac{\Phi_{AB}}{2}} \right) + e^{-2\Gamma_B} \sin^2 \left(\frac{\Phi_{BA}}{2} \right) \leq 1$$

$\Phi_{AB} = \int d^4x (J^\mu_{AR} - J^\mu_{AL})(\cancel{A_{BR\mu}} - \cancel{A_{BL\mu}})$ $\Phi_{BA} = \int d^4x (J^\mu_{BR} - J^\mu_{BL})(A_{AR\mu} - A_{AL\mu})$

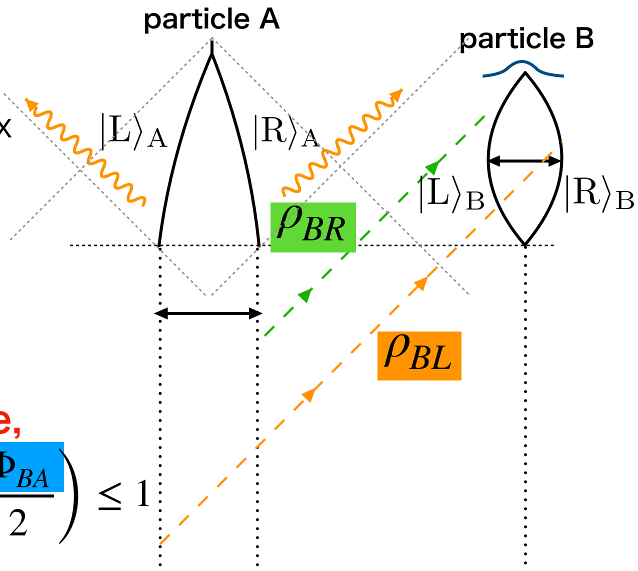

Complementarity

Jaeger et al. (1995)
Englert PRL (1996)

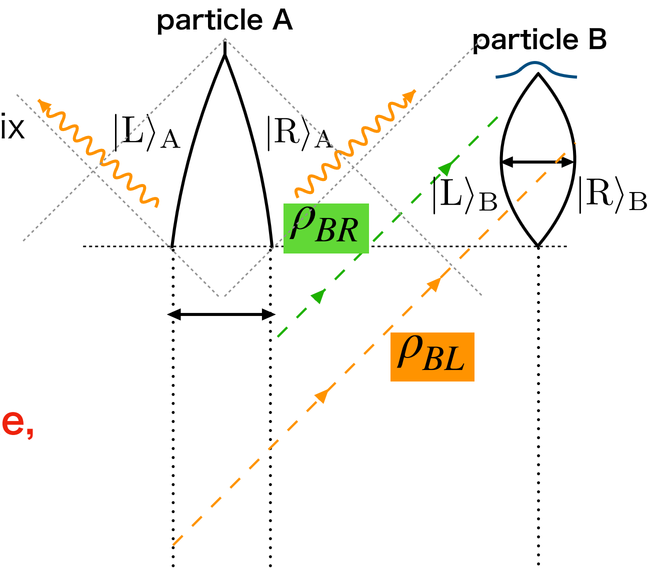

- Visibility

$$V_A = 2\,|{}_A\langle L_f|\rho_A|R_f\rangle_A|$$

interference term of Alice's density matrix

- Distinguishability

$$D_B = \frac{1}{2}Tr_B|\rho_{BR} - \rho_{BL}| = \frac{1}{2}\sum_i |\lambda_i|$$

$$\rho_{BP} = Tr_{ph}[\,|\Phi_{BP}\rangle\langle\Phi_{BP}|\,]$$

- Result **When A and B are space-like,**

$$V_A^2 + D_B^2 = e^{-2\underline{\Gamma_A}} + e^{-2\underline{\Gamma_B}}\sin^2\left(\frac{\Phi_{BA}}{2}\right) \le 1$$

$$\Phi_{AB} = \int d^4x(J^\mu_{AR} - J^\mu_{AL})(\cancel{A_{BR\mu}} - \cancel{A_{BL\mu}}) \qquad \Phi_{BA} = \int d^4x(J^\mu_{BR} - J^\mu_{BL})(A_{AR\mu} - A_{AL\mu})$$

Complementarity

Jaeger et al. (1995)
Englert PRL (1996)

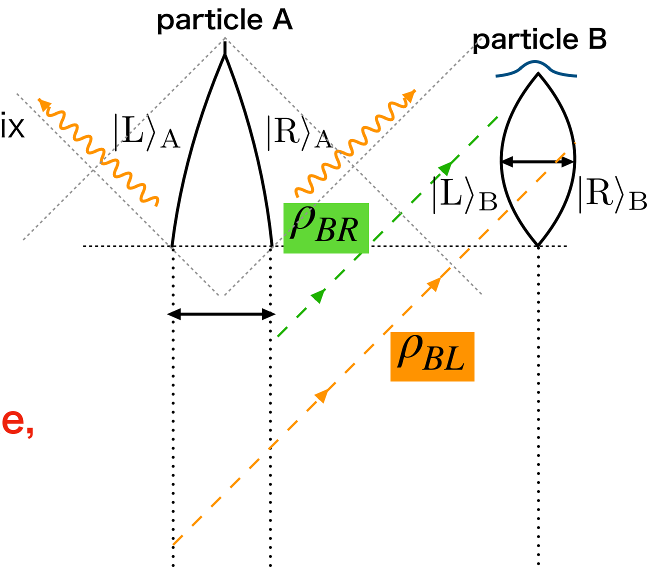

- Visibility

$$V_A = 2\,|{}_A\langle L_f|\rho_A|R_f\rangle_A|$$

interference term of Alice's density matrix

- Distinguishability

$$D_B = \frac{1}{2}Tr_B|\rho_{BR} - \rho_{BL}| = \frac{1}{2}\sum_i |\lambda_i|$$

$$\rho_{BP} = Tr_{ph}[\,|\Phi_{BP}\rangle\langle\Phi_{BP}|\,]$$

- Result **When A and B are space-like,**

$$V_A^2 + D_B^2 = e^{-2\underline{\Gamma_A}} + e^{-2\underline{\Gamma_B}}\sin^2\left(\frac{\Phi_{BA}}{2}\right) \le 1$$

This inequality violates if $\Gamma_A = \Gamma_B = 0$

Robertson inequality

- Robertson inequality

For arbitrary observables $\hat{A}$, $\hat{B}$,

$$(\Delta\hat{A})^2(\Delta\hat{B})^2 \geq \frac{1}{4}\left|\left\langle [\hat{A},\hat{B}] \right\rangle\right|^2$$

$\Delta\hat{A}$, $\Delta\hat{B}$ are fluctuation

Formulas

$$\langle 0|e^{i\hat{\phi}_i}|0\rangle = e^{-\frac{1}{2}\langle 0|\hat{\phi}_i^2|0\rangle} = e^{-\Gamma_i}$$

$$\underline{\hat{\phi}_i} = \int d^4x(J^\mu_{iR}(x) - J^\mu_{iL}(x))\hat{A}_\mu(x)$$

(phase shift due to vacuum fluctuation of $\hat{A}_\mu(x)$)

- Result

$$\Gamma_A\Gamma_B \geq \frac{1}{16}\Phi_{BA}^2$$

$$\Phi_{BA} \neq 0 \leftarrow G^r_{\mu\nu}(x,y) \sim \underline{[\hat{A}_\mu(x),\hat{A}_\nu(y)]}\theta(x^0-y^0) \neq 0$$

(non-commutative property of $\hat{A}_\mu(x)$)

➡ Γ_A and Γ_B **cannot** be 0 at the **same time**, if $\Phi_{BA} \neq 0$!

- Relation to complementarity

$$\Gamma_A\Gamma_B \geq \frac{1}{16}\Phi_{BA}^2 \Longrightarrow e^{-2\Gamma_A} + e^{-2\Gamma_B}\sin^2\left(\frac{\Phi_{BA}}{2}\right) \leq 1$$

(sufficient condition)

Complementarity is guaranteed by Robertson inequality !

Conclusion

- We investigated the paradox based on QED

Bob's operations do not affect Alice's interference experiments due to causality

We derived an inequality representing complementarity

↑

Complementarity is guaranteed by **Robertson inequality**

Causality and complementarity are **consistent !**

- Similar result is expected for the gravitational field:

$$\Gamma^g_A\Gamma^g_B \geq \frac{1}{16}(\Phi^g_{BA})^2 \Longrightarrow e^{-2\Gamma^g_A} + e^{-2\Gamma^g_B}\sin^2\left(\frac{\Phi^g_{BA}}{2}\right) \leq 1$$

For the paradox not to appear, not only Newtonian potential, but also

the non-commutative property of the gravitational field is expected to be necessary

Thank you for listening!

I’d like to say the message from Yamamoto-san.

Congratulations on your 60’s birthday,
Prof. Jun’ichi Yokoyama!!

Backup

Backup : Larmor radiation formula

Energy radiation W using Larmor formula

$$W \sim e^2 \left(\frac{L}{T^2} \right)^2$$

The number of emitted photon N during time T

$$N = \frac{WT}{\nu} \sim e^2 \left(\frac{L}{T} \right)^2 \sim \underline{\langle 0 | \hat{\phi}_i^2 | 0 \rangle}$$

Vacuum fluctuation of photon

Energy of one photon

Backup : Formulas

$$\Gamma_A = \frac{1}{4} \int d^4x d^4y \left(J^\mu_{AR}(x) - J^\mu_{AL}(x) \right) \left(J^\mu_{AR}(y) - J^\mu_{AL}(y) \right) \langle \{ \hat{A}^I_\mu(x), \hat{A}^I_\mu(y) \} \rangle$$

$$\Phi_A = \int d^4x (J^\mu_{AR}(x) - J^\mu_{AL}(x)) A_\mu(x) - \frac{1}{2} \int d^4x d^4y (J^\mu_{AR}(x) - J^\mu_{AL}(x))(J^\nu_{AR}(y) + J^\nu_{AL}(y)) G^r_{\mu\nu}(x, y)$$

$$\begin{aligned} |\Psi(T)\rangle &= \exp\left[- i\hat{H}T \right] |\Psi(0)\rangle \\ &= e^{-i\hat{H}_0 T} T \exp\left[- i \int_0^T dt \hat{V}_I(t) \right] |\Psi(0)\rangle \\ &\approx e^{-i\hat{H}_0 T} \frac{1}{2} \sum_{P,Q=R,L} |P\rangle_A |Q\rangle_B \hat{U}_{PQ} |\alpha\rangle_{ph} \\ &= \frac{1}{2} \sum_{P,Q=R,L} |P_f\rangle_A |Q_f\rangle_B \, e^{-i\hat{H}_{ph} T} \hat{U}_{PQ} |\alpha\rangle_{ph} \end{aligned}$$

$$\hat{H} = H_0 + \hat{V}$$

$$\hat{V} = \int d^3x \left(\hat{J}^\mu_A(\mathbf{x}) + \hat{J}^\mu_B(\mathbf{x}) \right) \hat{A}^\mu(\mathbf{x})$$

$$\hat{U}_{PQ} = T \exp \left[-i \int_0^T dt \int d^3x \left(J^\mu_{AP} + J^\mu_{BQ} \right) \hat{A}^I_\mu(x) \right]$$

$$V_A = e^{-\Gamma_A} \left| \cos\left(\frac{\Phi_{AB}}{2} \right) \right| \quad D_B = e^{-\Gamma_B} \left| \sin\left(\frac{\Phi_{BA}}{2} \right) \right|$$

Accelerating Expansion of the Universe by Porcupinefish spacetime

Yoshiyuki WATABIKI
watabiki@th.phys.titech.ac.jp
(in collaboration with Jan Ambjørn)

Talk @ JGRG31
held at Univ. of Tokyo
on 26/10/2022

Conclusion

- The topology of universe is 3D torus.
  - → The spacetime is flat.
- Accelerating expansion of universe is caused by Porcupinefish spacetime.
  - → The late time observables are explained from the early time ones (CMB).

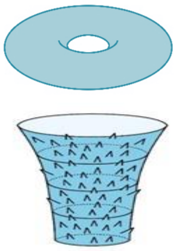

1- b

b. From the birth of universes to the Big Bang

● Hamiltonian for the evolution of Universe

$$[\phi_m, \phi_n^\dagger] = \delta_{m,n}$$

$$\alpha_n = \phi_n^\dagger$$

$$\alpha_{-n} = n\phi_n + \frac{1}{2g}\delta_{n,3} - \frac{\mu}{2g}\delta_{n,1}$$

$$\alpha_0 = 1$$

$$\begin{aligned}
H_W &= -\frac{g}{3}\sum_{k+l+m=-2} \mathrm{Tr} :\alpha_k\alpha_l\alpha_m: \\
&= \left.\begin{aligned} &-g\sum_{n=4}^{\infty}\sum_{k=1}^{n-3}\phi_k^\dagger\phi_{n-k-2}^\dagger n\phi_n \\ &-g\sum_{n=4}^{\infty}\sum_{k=\max(3-n,1)}^{\infty}\phi_{n+k-2}^\dagger k\phi_k n\phi_n \end{aligned}\right\} \text{Knitting Mechanism} \\
&\quad \underbrace{-\sum_{n=1}^{\infty}\phi_{n+1}^\dagger n\phi_n + \mu\sum_{n=2}^{\infty}\phi_{n-1}^\dagger n\phi_n - 2g\sum_{n=3}^{\infty}\phi_{n-2}^\dagger n\phi_n}_{\text{Expansion of Universes}} \\
&\quad + (\mu\phi_1 - 2g\phi_2 - g\phi_1\phi_1) \underbrace{-\left(\frac{1}{4g}\phi_4^\dagger - \frac{\mu}{2g}\phi_2^\dagger + \phi_1^\dagger\right)}_{\text{Creation of Universes}} - \frac{\mu\mu}{4g}
\end{aligned}$$

- **Knitting mechanism** (Dimension Enhancement)

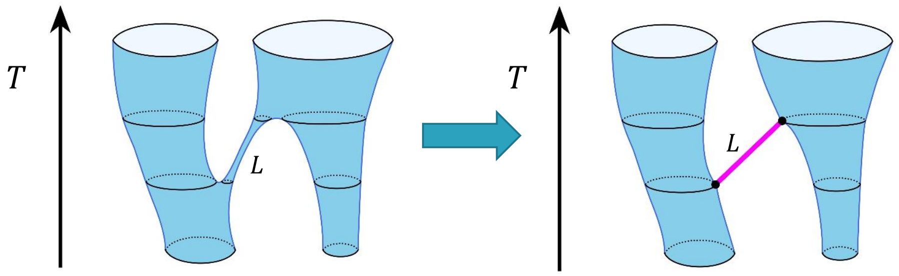

(A wormhole with Length L is shown by purple line.)

High−dimensional space is formed after the birth of space.

Contributions by tiny wormholes are dominant. $G(L,L;T) \sim \frac{1}{\sqrt{4\pi LT}}$

$[T \sim 0]$

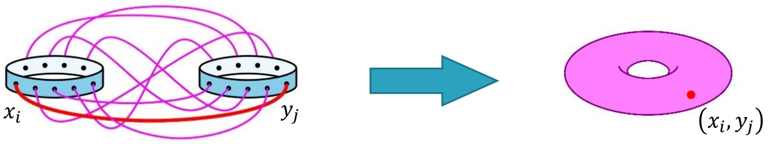

(The set of tiny wormholes gives a topology.)

---

2. Modified Friedmann Equation

a. The derivation of Modified Friedmann equation

- **The classical Hamiltonian from**

$$-\sum \phi^{\dagger}_{n+1} n \phi_n + \mu \sum \phi^{\dagger}_{n-1} n \phi_n - 2g \sum \phi^{\dagger}_{n-2} n \phi_n$$

is

$$\mathcal{H}_{\mathrm{c}} = -L\left(\Pi^2 - \mu + \frac{2g}{\Pi}\right) \qquad \{L\,,\Pi\} = 1$$

then, we obtain

μ is replaced by Matter Energy at the end of inflation.

$$\left(\dot{L}/L\right)^2 = 4\mu + \frac{B}{\dot{L}/L}\frac{1+3F(x)}{(F(x))^2} \qquad 4\mu \rightarrow \frac{\kappa\rho}{3}$$

$$(F(x))^3 - (F(x))^2 + x = 0 \qquad x \overset{\mathrm{def}}{=} \frac{B}{\left(\dot{L}/L\right)^3} \qquad B \overset{\mathrm{def}}{=} -8g$$

b. The origin of accelerating expansion of Universe

- **The geometrical meaning of** $-2g\alpha_0 \sum \phi_{n-2}^{\dagger} n \phi_n$

This term comes from the leading term of disk amplitude $F(L)$

$$F(L) = \delta(V) + \cdots$$

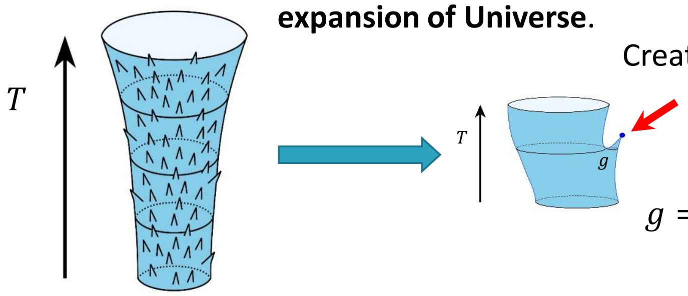

Negative g gives accelerating expansion of Universe.

Creation of baby universe

$F(L) = \delta(V)$

$$g = -\frac{B}{8} < 0$$

Porcupinefish diagram

---

3. Cosmic Tensions caused by Accelerating Expansion of Universe

- **Boundary Condition** (CDM is assumed)

Data from Planck satellite

$t_0^{(\mathrm{CMB})}$ = 13.8 × 10^9 [year]

$H_0^{(\mathrm{CMB})}$ = 67.3 ± 0.6 [km/sec/Mpc]

$z_{\mathrm{LS}}^{(\mathrm{CMB})}$ = 1089.95

↓

$$\frac{L_{\Lambda(\mathrm{CMB})}\left(t_0^{(\mathrm{CMB})}\right)}{L_{\Lambda(\mathrm{CMB})}\left(t_{\mathrm{LS}}^{(\mathrm{CMB})}\right)} = 1 + z_{\mathrm{LS}}^{(\mathrm{CMB})} \qquad H_{\Lambda(\mathrm{CMB})}\left(t_0^{(\mathrm{CMB})}\right) = H_0^{(\mathrm{CMB})}$$

$t_{\mathrm{LS}}^{(\mathrm{CMB})}$ and $\Lambda^{(\mathrm{CMB})}$ are determined.

● **Boundary Condition** (CDM is assumed)

Data from Standard candles

$H_0^{(\mathrm{SC})}$ = 73.0 ±1.0 [km/sec/Mpc] ⬅ 5σ from Planck Satellite

(ArXiv:2112.04510)

We also use $t_{\mathrm{LS}}^{(\mathrm{CMB})}$ and $z_{\mathrm{LS}}^{(\mathrm{CMB})}$. ⬅ No difference between ΛCDM model and our model before $t_{\mathrm{LS}}^{(\mathrm{CMB})}$

$$\frac{L_{\Lambda^{(\mathrm{SC})}}\left(t_0^{(\mathrm{SC})}\right)}{L_{\Lambda^{(\mathrm{SC})}}\left(t_{\mathrm{LS}}^{(\mathrm{CMB})}\right)} = 1 + z_{\mathrm{LS}}^{(\mathrm{CMB})} \qquad H_{\Lambda^{(\mathrm{SC})}}\left(t_0^{(\mathrm{SC})}\right) = H_0^{(\mathrm{SC})}$$

$$\frac{L_B\left(t_0^{(\mathrm{B})}\right)}{L_B\left(t_{\mathrm{LS}}^{(\mathrm{CMB})}\right)} = 1 + z_{\mathrm{LS}}^{(\mathrm{CMB})} \qquad H_B\left(t_0^{(\mathrm{B})}\right) = H_0^{(\mathrm{SC})}$$

$t_0^{(\mathrm{SC})}$, $\Lambda^{(\mathrm{SC})}$, $t_0^{(\mathrm{B})}$, B are determined.

=13.3 =13.9

● $\frac{H(z)}{1+z}$

Blue is our model using Standard Candle data.
Orange is ΛCDM model using Standard Candle data.
Green is ΛCDM model by Planck satellite data only.

H_0 tension
(5σ difference)

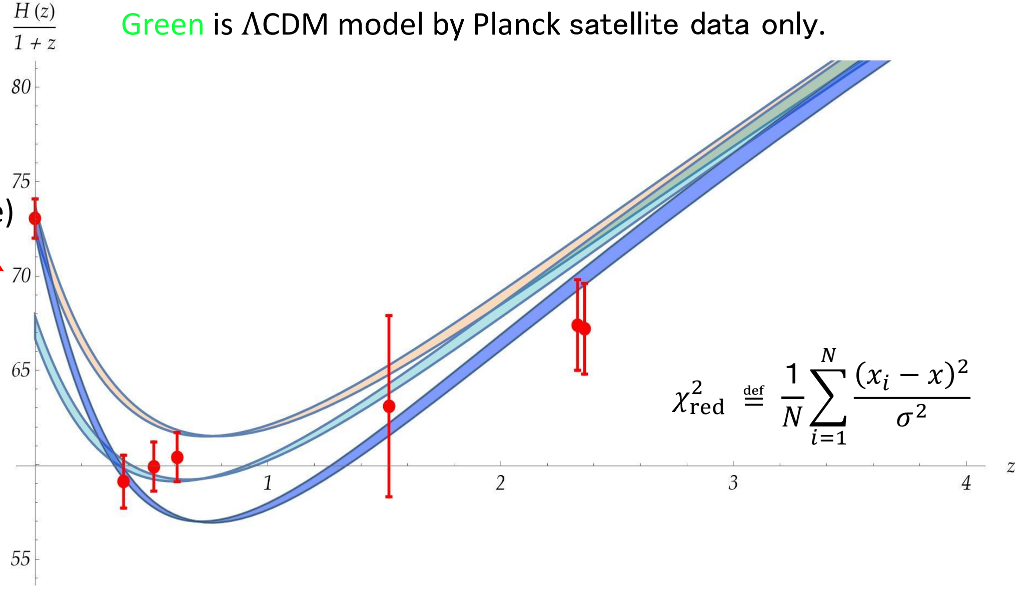

$$\chi_{\mathrm{red}}^2 \overset{\mathrm{def}}{=} \frac{1}{N}\sum_{i=1}^{N}\frac{(x_i - x)^2}{\sigma^2}$$

$$\chi_{\mathrm{red}}^{(\mathrm{B})2} = 1.3^2 \qquad \chi_{\mathrm{red}}^{(\mathrm{SC})2} = 1.9^2 \qquad \chi_{\mathrm{red}}^{(\mathrm{CMB})2} = 2.3^2$$

- $\boldsymbol{\frac{D_V(z)}{r_s}}$ **(BAO)**

$$r_S^{(B)} \backsim r_S^{(SC)} \sim r_S^{(CMB)} = 147.05 \pm 0.30 \text{ [Mpc]}$$

Data from Planck satellite

r_s is the sound horizon at $z = z_{\text{drag}}$

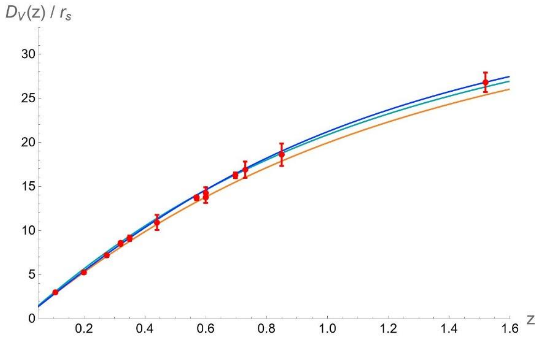

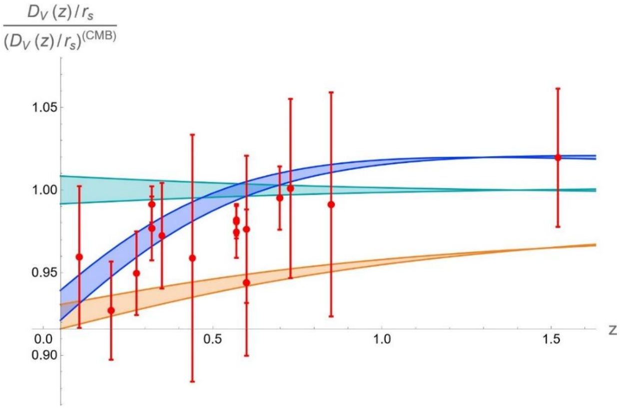

$$\chi_{\text{red}}^{(B)2} = 1.0^2 \qquad \chi_{\text{red}}^{(SC)2} = 2.1^2 \qquad \chi_{\text{red}}^{(CMB)2} = 1.3^2$$

- $\boldsymbol{f_{\mathrm{m}}(z)\, \sigma_8(z)}$

$$\sigma_8^{(B)}(z_0) \sim \sigma_8^{(SC)}(z_0) \sim \sigma_8^{(CMB)}(z_0) = 0.8120 \pm 0.0073$$

Data from Planck satellite

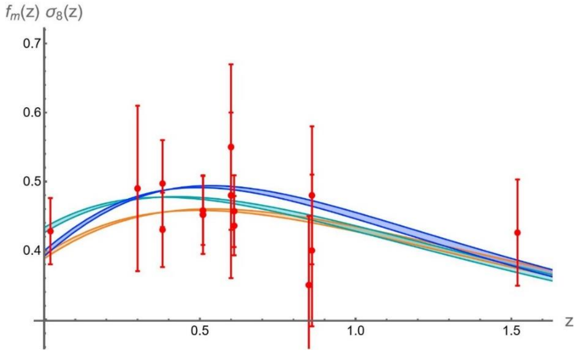

$$\chi_{\text{red}}^{(B)2} = 0.70^2 \qquad \chi_{\text{red}}^{(SC)2} = 0.51^2 \qquad \chi_{\text{red}}^{(CMB)2} = 0.54^2$$

- $\boldsymbol{S_8} \overset{\text{def}}{=} S_8(0), \quad S_8(z) \overset{\text{def}}{=} \sigma_8(z)\sqrt{\Omega_{\mathrm{m}}(z)/0.3}$

$$\chi_{\text{red}}^{(B)2} = 0.75^2 \qquad \chi_{\text{red}}^{(SC)2} = 0.75^2 \qquad \chi_{\text{red}}^{(CMB)2} = 3.35^2$$

σ_8 problem

4. Conclusions

a. Emergence of space

- High-dimensional space is formed
  by the direct product of several 1D loop spaces S^1.
- The topology of our universe is 3D torus.
  Therefore, the spacetime is flat.

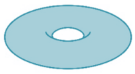

b. Identity of Dark energy

- Accelerating expansion of Universe is explained
  by Porcupinefish spacetime.
- No tensions appear in $(H_0$, BAO, $f\sigma_8$, $S_8)$.
- Dark energy does not exist.

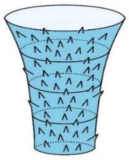

C47

October 26, 2022
JGRG31 (Tokyo-U)
Lecture Number：c47

Non-singular bouncing universe under the null energy condition

Presenter : **Yuki Hashimoto** (*Fukushima University*)

Collaboration with : Kazuharu Bamba (*Fukushima University*)

What is the Bounce Universe Model?

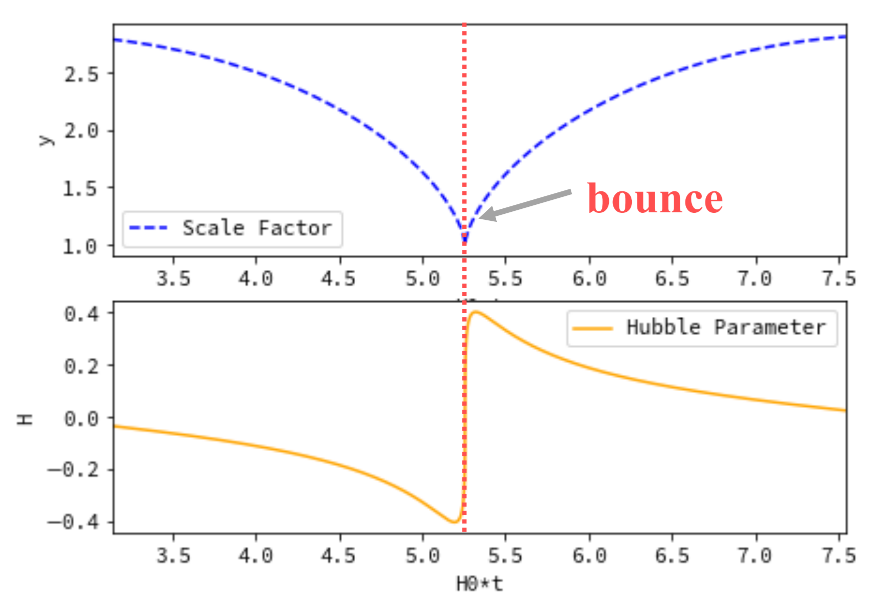

The universe transitions from contraction to expansion.

Bounce and Null Energy Condition

- Requirements for bouncing:.
  - $\dot{H} = -\frac{1}{2M_P^2}(\rho + p) + \frac{k}{a^2} > 0$, when $H = 0$.
- Null Energy Condition (NEC):.
  - Condition on energy positivity

M. Novello and S. E. Perez Bergliaffa. Bouncing Cosmologies. *Phys. Rept.*, 463

  - $NEC \Leftrightarrow \rho + p \geq 0$

The bounce universe requires a violation of null energy condition.

Previous Studies

Conventional Study ($k = 0$):

- Bounce has achieved by violation of the null energy condition.

Yi-Fu Cai, Damien A. Easson, and Robert Brandenberger. *JCAP*, 08:020, 2012.

- The violation of null energy condition means that ”ghosts” exist.
  - Cosmological solutions without singularity are unstable for linear perturbations.

Tsutomu Kobayashi, *Phys.Rev.D*, 94 (2016) 4

Latest Study ($k > 0$):

- A classical model that does not require violation of the null energy condition has proposed.
  - Stable bounce without instability due to violation of the condition can be realized.

Özenç Güngör and Glenn D. Starkman *JCAP* 04 (2021) 003.

Contents of this work

For the non-singular bouncing universe under the null energy condition, we solve the next equations numerically:

- Equation of motion for a scalar field
- Friedmann equations

Also, we analyze the evolution of the universe before and after the bounce.

Bounce Universe Model under the NEC

To build a model that satisfies the null energy condition…

We consider a scalar field (Jordan frame action) with a canonical kinetic energy term coupled with a scalar curvature R .

The coupling of the scalar field and the scalar curvature facilitates the bounce that occurs when dominating the kinematics of the scale factor and plays an important role in the evolution of the universe.

Özenç Güngör and Glenn D. Starkman *JCAP* 04 (2021) 003

Bounce Universe Model under the NEC

- Jordan frame action：

An action that couples general relativity with real scalar field.

$$S = \int \sqrt{-g} d^4x \left(\frac{1}{2} M_P^2 R - \frac{1}{2} g^{\mu\nu} \nabla_\mu \varphi \nabla_\nu \varphi - \left(\frac{\alpha}{2} R \varphi^2 + \bar{V}(\varphi) \right) \right)$$

M_P ：Plank mass
α ：Parameter
R ：Scalar curvature
$\bar{V}(\varphi)$ ：Scalar field potential

Özenç Güngör and Glenn D. Starkman *JCAP* 04 (2021) 003

Bounce Universe Model under the NEC

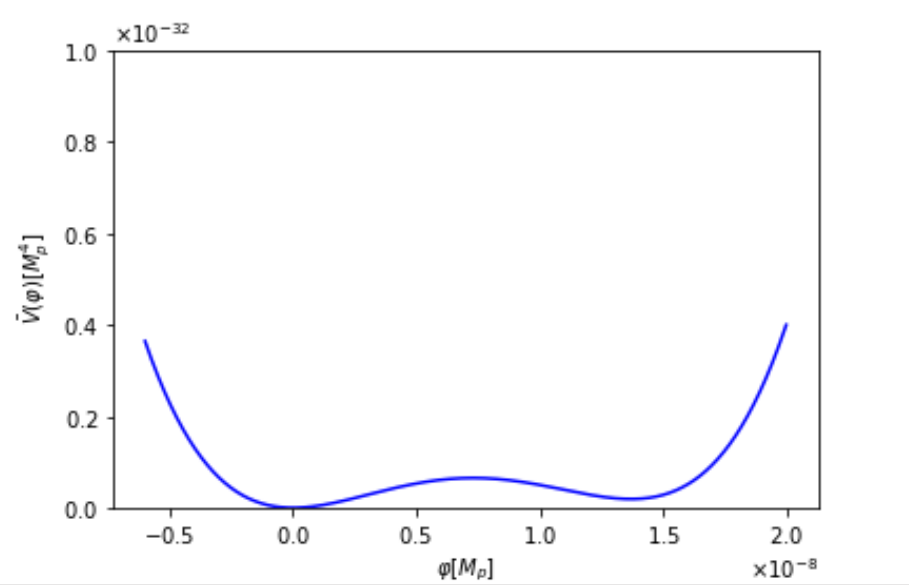

Scalar field potential : $\bar{V}(\varphi) = V_0 + \frac{m^2}{2}\varphi^2 + \frac{\beta}{3}\varphi^3 + \frac{\lambda}{4}\varphi^4$

Scalar potential : $V(\varphi) = \bar{V}(\varphi) + \frac{\alpha}{2} R \varphi^2$ $(V_0, \alpha, \beta, \lambda : \text{constant},\ m = 10^{-8} M_P)$

Özenç Güngör and Glenn D. Starkman *JCAP* 04 (2021) 003

Bounce Universe Model under the NEC

$$T_{\mu\nu} \equiv \frac{-2}{\sqrt{-g}}\frac{\delta S}{\delta g^{\mu\nu}} = (1-2\alpha)\nabla_\mu\varphi\nabla_\nu\varphi - \frac{1}{2}(1-4\alpha)g_{\mu\nu}g^{\alpha\beta}\nabla_\alpha\varphi\nabla_\beta\varphi$$
$$-g_{\mu\nu}V(\varphi) + \alpha R_{\mu\nu}\varphi^2 - 2\alpha\varphi\nabla_\mu\nabla_\nu\varphi + 2g_{\mu\nu}\alpha\varphi\varphi$$

$$\rho = \frac{1}{2}\dot{\varphi}^2 + V(\varphi) - 3\alpha\frac{\ddot{a}}{a}\varphi^2$$

$$p = \frac{1}{2}(1-4\alpha)\dot{\varphi}^2 - V(\varphi) + \alpha\left(\frac{\ddot{a}}{a} + 2H^2 + 2\frac{k}{a^2}\right)\varphi^2 - 2\alpha\varphi\ddot{\varphi}$$

$$R = 6\left(\dot{H} + 2H^2 + \frac{k}{a^2}\right)$$

Özenç Güngör and Glenn D. Starkman *JCAP* 04 (2021) 003

Numerical Simulation

- Equation of motion for a scalar field : $\ddot{\varphi} + 3H\dot{\varphi} + \frac{\partial V(\varphi)}{\partial\varphi} = 0$

- Friedmann equations : $\dot{H} = -\frac{1}{2M_P^2}(\rho + p) + \frac{k}{a^2}$

$$\frac{\ddot{a}}{a} = -\frac{1}{6M_P^2}(\rho + 3p)$$

- Initial conditions :

$$V_0 = 1.0 \times 10^{-4}m^4,\ \varphi_0 = \frac{-\beta+\sqrt{\beta^2-4m^2\lambda}}{2\lambda},\ \dot{\varphi}_0 = 1.0 \times 10^{-4},\ H_0 = -\sqrt{\frac{\bar{V}(\varphi_0)}{3(M_P^2-\alpha\varphi_0^2)}},$$

$$a_0 = 10^{16},\ \dot{a}_0 = a_0H_0,\ M_P = 1,\ m = 10^{-8}M_P,\ \alpha = \frac{1}{6},\ \beta = 2.1m,\ \lambda = 1,\ \ k = 1.0m^2$$

Result and discussion

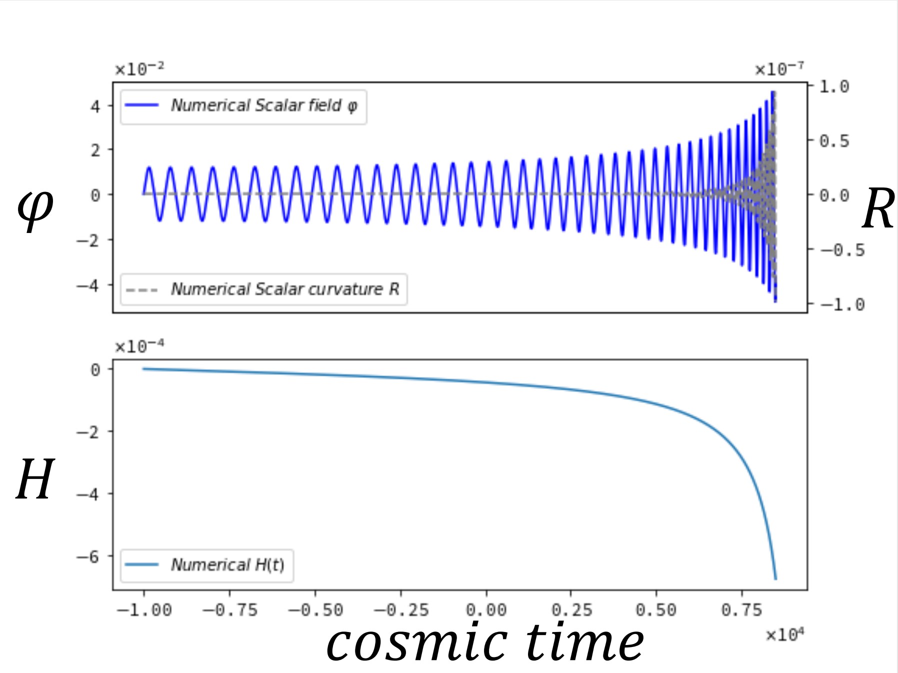

Numerical plots of a scalar field φ, scalar curvature R, and Hubble parameter H.

Result and discussion

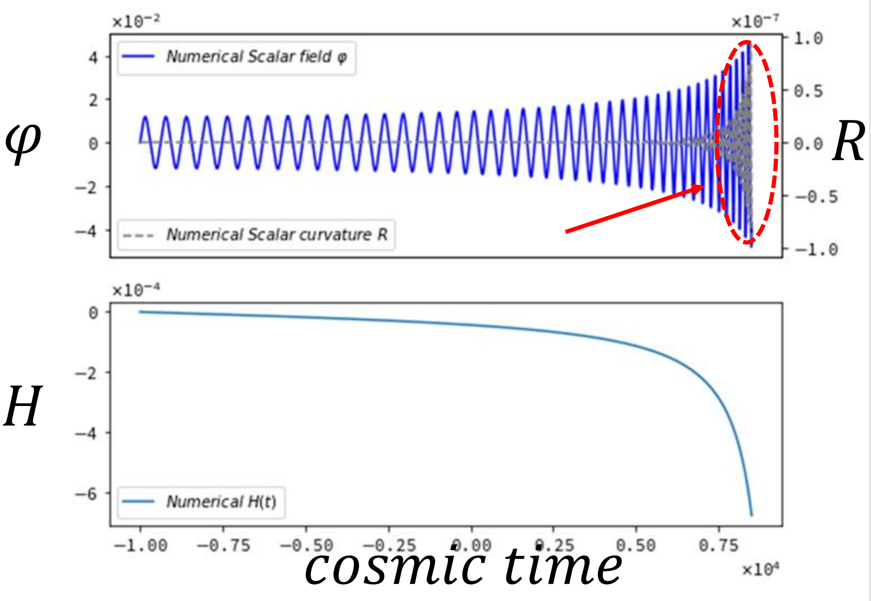

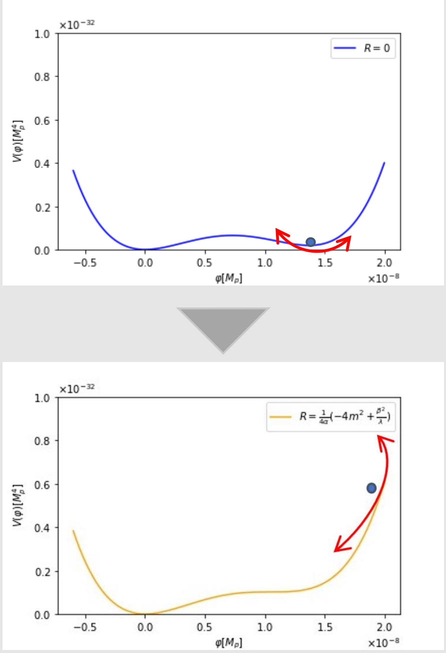

- Scalar curvature R eventually diverged.
- The behavior of H was also affected and did not bounce.

Result and discussion

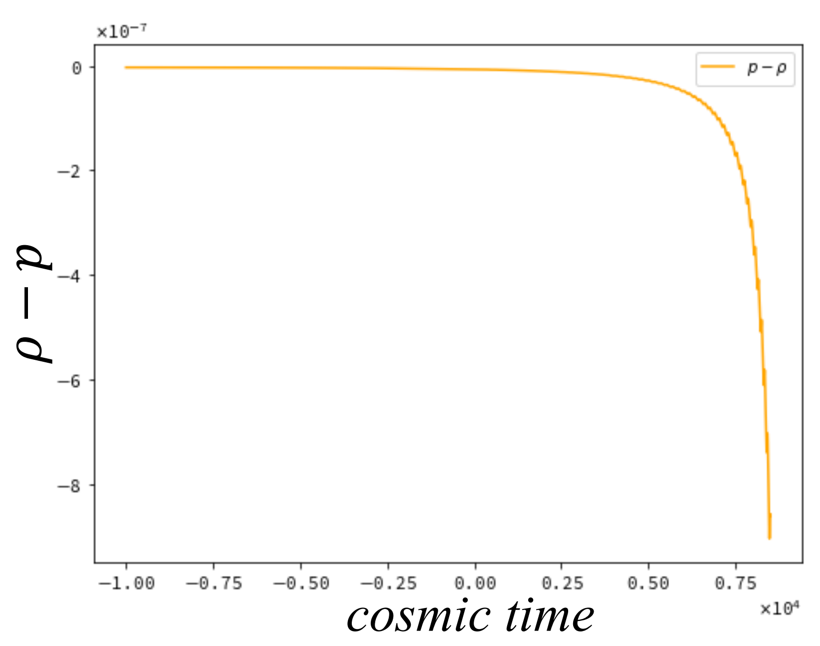

Numerical plots of $\rho - p$.

This implies that as the universe contracts, the BKL instability also grows.

Conclusion

- We have solved the equation of motion and Friedmann equations for a scalar field numerically in non-singular bouncing universe model under the null energy condition, and analyzed their evolution.
- Numerical results showed that the scalar curvature diverged just before the bounce.
  - ▶ **It is difficult to achieve stable bounce with a classical model that does not violate the null energy condition.**
- For a detailed analysis, an evaluation of the stability of the model for linear perturbation is required.

C48

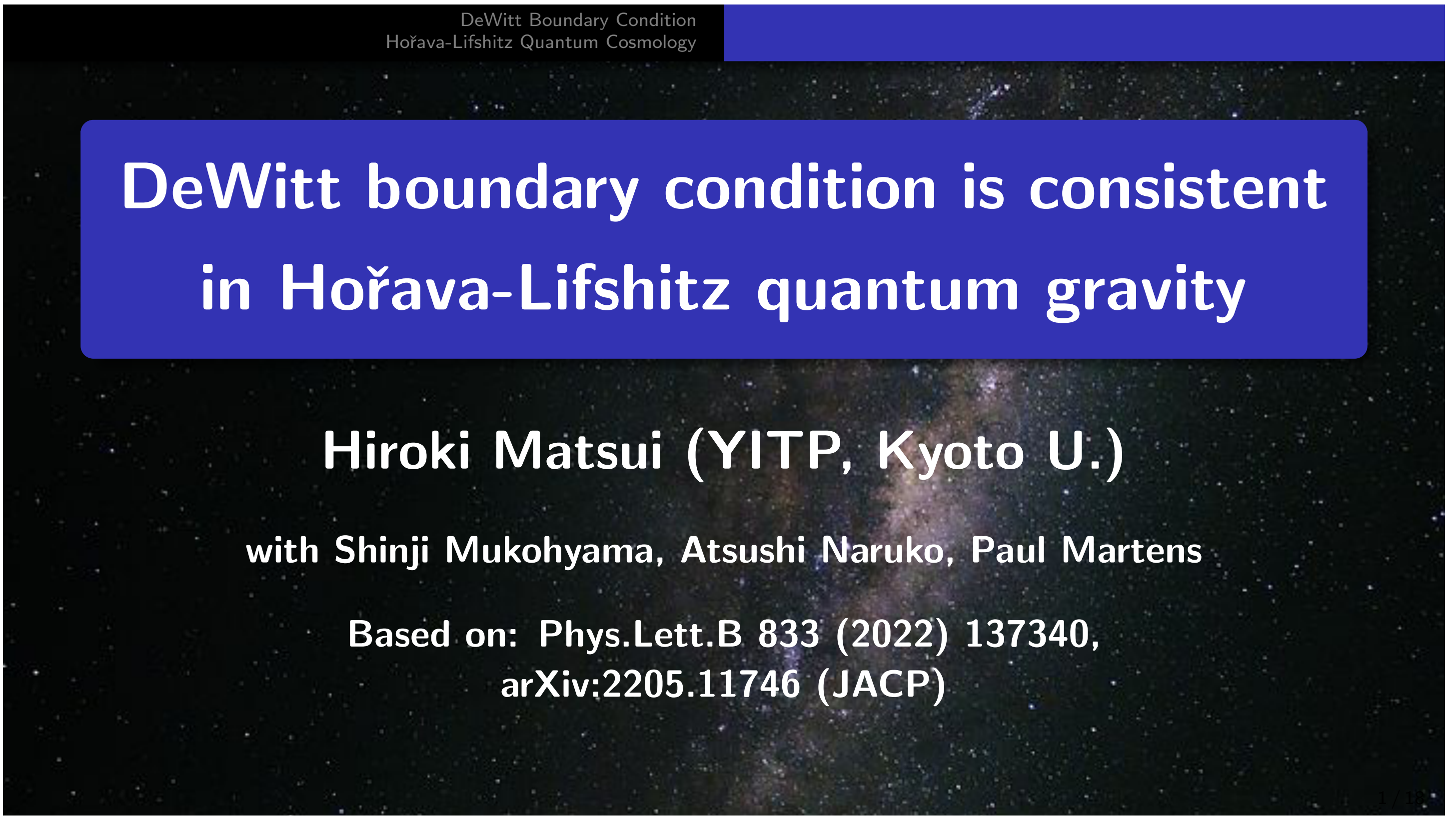

DeWitt boundary condition is consistent in Hořava-Lifshitz quantum gravity

Hiroki Matsui (YITP, Kyoto U.)

with Shinji Mukohyama, Atsushi Naruko, Paul Martens

Based on: Phys.Lett.B 833 (2022) 137340,
arXiv:2205.11746 (JACP)

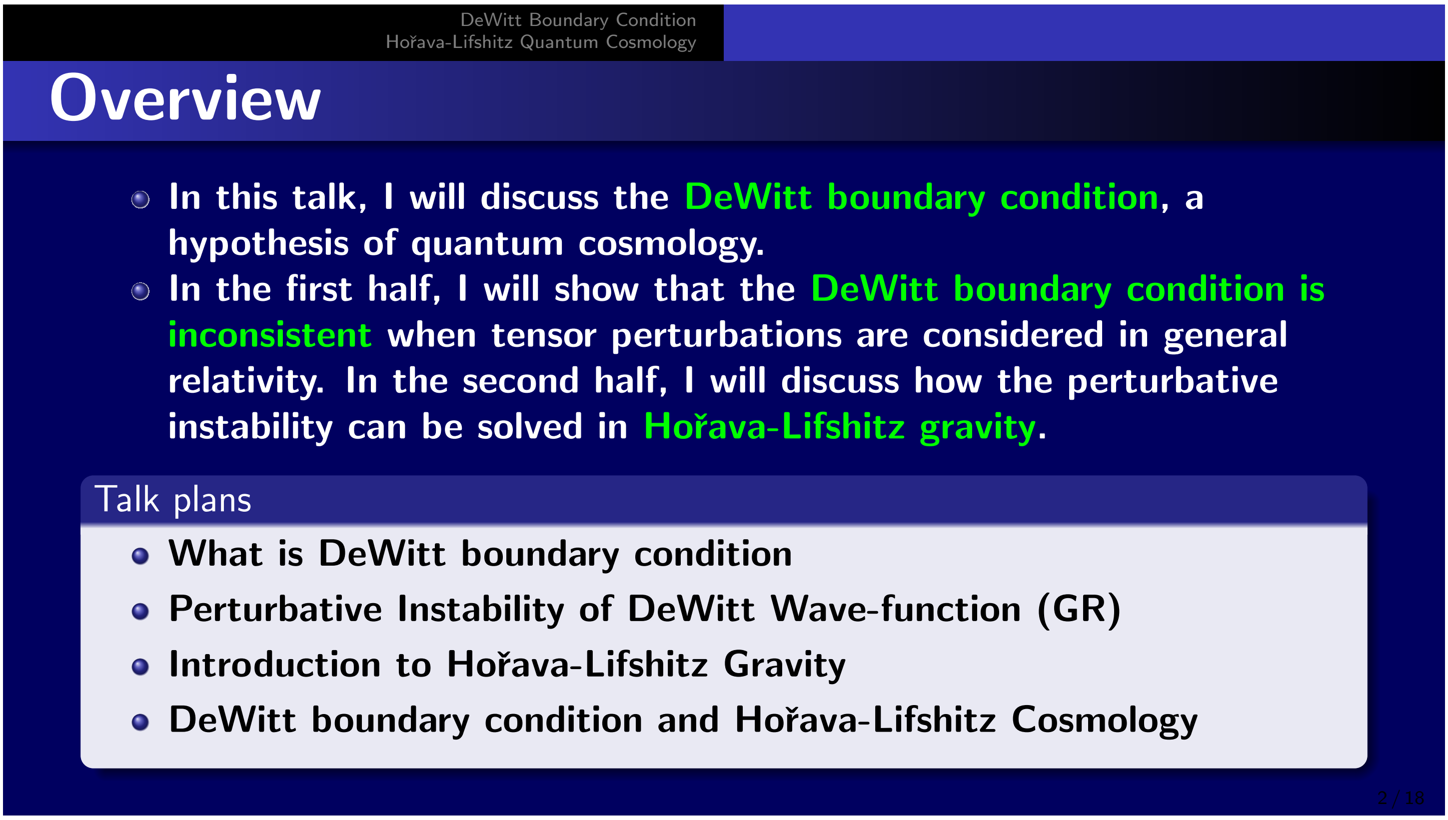

Overview

- In this talk, I will discuss the DeWitt boundary condition, a hypothesis of quantum cosmology.
- In the first half, I will show that the DeWitt boundary condition is inconsistent when tensor perturbations are considered in general relativity. In the second half, I will discuss how the perturbative instability can be solved in Hořava-Lifshitz gravity.

Talk plans

- What is DeWitt boundary condition
- Perturbative Instability of DeWitt Wave-function (GR)
- Introduction to Hořava-Lifshitz Gravity
- DeWitt boundary condition and Hořava-Lifshitz Cosmology

Quantum Cosmology

Quantum cosmology tries to describe how the universe was created and evolve within the framework of quantum gravity.

1. Wheeler-DeWitt equation (canonical quantization)

$$\mathcal{H}\,\Psi = \left[-16\pi\, G_N\, \mathcal{G}_{ijkl}\frac{\partial^2}{\partial g_{ij}\partial g_{kl}} + \frac{\sqrt{g}}{16\pi\, G_N}(-R+2\Lambda)\right]\Psi = 0$$

2. Path integral of quantum gravity (path integral quantization)

$$\Psi(g_{\mu\nu}, \phi) = \int^{(g_{\mu\nu},\phi)} \mathcal{D}g_{\mu\nu}\,\mathcal{D}\phi\; e^{iS[g_{\mu\nu},\phi]/\hbar}$$

$\Psi(g_{\mu\nu}, \phi)$ is the wave function of the universe

---

Einstein Gravity in ADM formalism

1. Arnowitt-Deser-Misner (ADM) formalism

$$ds^2 = -N^2 dt^2 + g_{ij}(dx^i + N^i dt)(dx^j + N^j dt)$$

$$\text{Lapse function}: N = N(t,\vec{x}),\ \text{Shift vector}: N^i = N^i(t,\vec{x}),\ \text{3D metric}: g_{ij} = g_{ij}(t,\vec{x})$$

2. Einstein-Hilbert action in ADM formalism

$$S_{\rm GR} = \frac{M_{\rm Pl}^2}{2}\int dt d^3x N\sqrt{g}\left(K^{ij}K_{ij} - K^2 + R - 2\Lambda\right)$$

$$\text{Extrinsic curvature}: K_{ij} = \frac{1}{2N}(\partial_t g_{ij} - g_{jk}\nabla_i N^k - g_{ik}\nabla_j N^k),$$

3. A homogenous and isotropic universe with tensor perturbations (closed universe $K = +1$)

$$N^i = 0, \quad g_{ij} = a^2(t)\left[\Omega_{ij}(\mathbf{x}) + h_{ij}(t\,,\mathbf{x})\right], \quad h_{ij}(t\,,\mathbf{x}) = \sum_{snlm} h^s_{nlm}(t)Q^{snlm}_{ij},$$

Wheeler-DeWitt equation in Einstein Gravity

B. S. DeWitt, Phys. Rev. 160, 1113-1148 (1967)

1. Expand Einstein-Hilbert action to the second-order perturbation

$$S_{\mathrm{GR}} = V\int dt \left\{ \left(\frac{3N}{a}\right)\left[-\left(\frac{a}{N}\dot{a}\right)^2 + a^2 - \frac{\Lambda a^4}{3}\right] + \sum_{snlm} (Na)\left[\frac{1}{8}\left(\frac{a}{N}\dot{h}^s_{nlm}\right)^2 - \frac{1}{8}\left[(n^2-3)+6\right]\left(h^s_{nlm}\right)^2\right]\right\} \Rightarrow H_{\mathrm{GR}}$$

2. Canonical Quantization

$$\Pi_a \mapsto -i\frac{\partial}{\partial a}, \quad \Pi_h \mapsto -i\frac{\partial}{\partial h}, \quad \Longrightarrow \quad \Pi_a^2 = -\frac{1}{a^p}\frac{\partial}{\partial a}\left(a^p\frac{\partial}{\partial a}\right), \quad \Pi_h^2 = -\frac{\partial^2}{\partial h^2},$$

3. Wheeler-DeWitt equation

$$\left\{\frac{1}{2}\left(\frac{\partial^2}{\partial a^2} + \frac{p}{a}\frac{\partial}{\partial a}\right) + \left(-3g_1 a^2 + g_0 a^4\right) - \frac{1}{2V^2 a^2}\frac{\partial^2}{\partial \mathfrak{h}^2} + \frac{\mathfrak{h}^2}{2}\left(f_1 a^2\right)\right\}\Psi(a, \mathfrak{h}) = 0,$$

$$\mathfrak{h} = \frac{h}{2\sqrt{\gamma}}, \ \gamma = 6V^2, \ g_1 = \gamma, \ g_0 = \gamma\Lambda, \ f_1 = \gamma^2\left[(n^2-3)+6\right],$$

What is the DeWitt boundary condition?

DeWitt Boundary Condition

$$\Psi(a=0, h) = 0$$

B. S. DeWitt, Phys. Rev. 160, 1113-1148 (1967) **55 years ago**

DeWitt boundary condition: $\Psi(0)=0$, $\left[\frac{1}{2}\left(\frac{\partial^2}{\partial a^2}+\frac{p}{a}\frac{\partial}{\partial a}\right)+\left(-3g_1a^2+g_0a^4\right)\right]\Psi(a)=0$

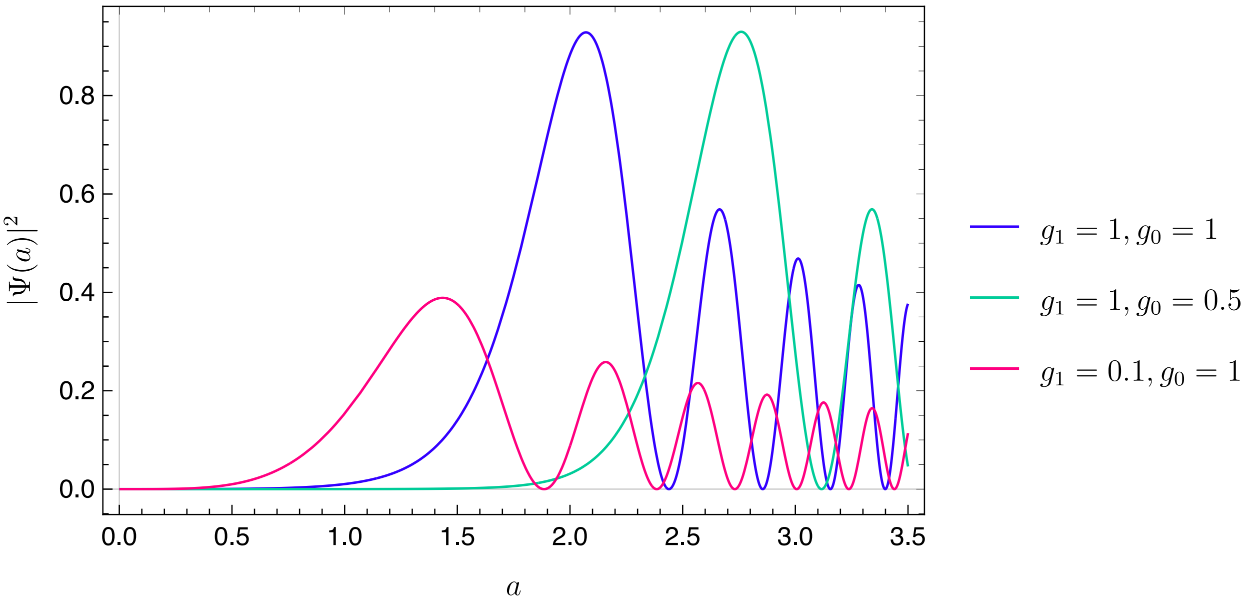

Tensor perturbations around Big Bang singularity

1. Wheeler-DeWitt equation (background+tensor perturbations)

$$\left\{\frac{1}{2}\left(\frac{\partial^2}{\partial a^2}+\frac{p}{a}\frac{\partial}{\partial a}\right)+\left(-3g_1a^2+g_0a^4\right)-\frac{1}{2V^2a^2}\frac{\partial^2}{\partial \mathfrak{h}^2}+\frac{\mathfrak{h}^2}{2}\left(f_1a^2\right)\right\}\Psi(a,\mathfrak{h})=0\,,$$

2. DeWitt wave function satisfying $\Psi(a=0,\mathfrak{h})=0$ around Big Bang singularity takes

$$\Psi(a,\mathfrak{h})=a^c\sum_{i=0}^{\infty}F_i(\mathfrak{h})\,a^i\simeq a^cF_0(\mathfrak{h})+O(a^{c+1})\,,$$

$$\lim_{\mathfrak{h}\to\pm\infty}F_i(\mathfrak{h})=0\,,\quad (i=0,1,\cdots)\,.$$

3. Around the singularity, the wave equation for the tensor fields and the solutions are

$$\partial_{\mathfrak{h}}^2F_0-V^2\left[(c+p-1)c\right]F_0=0\,,$$

$$F_0(\mathfrak{h})=b_1e^{-\mathfrak{h}\sqrt{V^2[(c+p-1)c]}}+b_2e^{+\mathfrak{h}\sqrt{V^2[(c+p-1)c]}}\to\infty\quad(\mathfrak{h}\to\pm\infty)$$

NO-GO ?

DeWitt Boundary Condition

$$\Psi(a=0,h)=0$$

$$\Rightarrow \lim_{h\to\pm\infty}\Psi(a,h)\to\infty$$

H. Matsui, S. Mukohyama and A. Naruko, Phys. Lett. B 833 (2022) 137340

Hořava-Lifshitz Gravity

P. Hořav, JHEP 03 (2009) 020, Phys.Rev.D 79 (2009) 084008

- A candidate of quantum gravity theories, higher-order derivative gravity theory satisfying renormalizability and unitarity (proposed by P. Hořav in 2009)
- Anisotropic scaling between space and time:

$$\begin{cases} t\to b^{z}t \\ \vec{x}\to b\vec{x} \end{cases} \quad\Longrightarrow\quad \text{Lorentz-invariance is broken at UV (for } z\neq 1)$$

- Power-counting renormalizability at UV ($z=3$)

$$\frac{1}{2}\int dt d^3x\left[\dot{h}^2-h\,(-\Delta)^z\,h\right]\quad\Longrightarrow\quad h\to b^{\frac{z-3}{2}}h,\ \ (z=3)$$

- Projectable-version, Non-projectable-version, U(1) extension, etc.

- **Cosmological consequences like gravitational dark matter, scale-invariant perturbations through anisotropic scaling ($z=3$)**
  (see e.g. S. Mukohyama, Class.Quant.Grav. 27 (2010) 223101)

Hořava-Lifshitz Gravity in $3+1$ Dimensions

P. Hořav, JHEP 03 (2009) 020, Phys.Rev.D 79 (2009) 084008

Hořava-Lifshitz gravitational action

$$S_{\rm HL} = \frac{\mathcal{M}_{\rm HL}^2}{2}\int dt d^3\vec{x}\, N\sqrt{g}\,(K^{ij}K_{ij} - \lambda K^2 + c_g^2 R - 2\Lambda + \mathcal{O}_{z>1})\,,$$

$$\frac{\mathcal{O}_{z>1}}{2} = (c_1 \nabla_i R_{jk}\nabla^i R^{jk} + c_2 \nabla_i R \nabla^i R + c_3 R_i^j R_j^k R_k^i + c_4 R R_i^j R_j^i + c_5 R^3) + (c_6 R_i^j R_j^i + c_7 R^2)\,,$$

UV action with z=3

- **Kinetic terms (2nd-time derivative)**

$$\int dt d^3\vec{x}\, N\sqrt{g}\,(K^{ij}K_{ij} - \lambda K^2)$$

- **Potential terms (6th spatial derivative)**

$$\int dt d^3\vec{x}\, N\sqrt{g}\,(c_1 \nabla_i R_{jk}\nabla^i R^{jk} + c_2 \nabla_i R \nabla^i R + c_3 R_i^j R_j^k R_k^i + c_4 R R_i^j R_j^i + c_5 R^3)$$

Wheeler-DeWitt equation in Hořava-Lifshitz gravity

Wheeler-DeWitt equation for scale factor a and tensor perturbations h

$$\left\{\frac{1}{2}\left(\frac{\partial^2}{\partial a^2} + \frac{p}{a}\frac{\partial}{\partial a}\right) + \left(\mathcal{C}a - \frac{g_3}{a^2} - 3g_2 - 3g_1 a^2 + g_0 a^4\right) - \frac{1}{2V^2 a^2}\frac{\partial^2}{\partial \mathfrak{h}^2} + \frac{\mathfrak{h}^2}{2}\left(f_1 a^2 + f_2 + \frac{f_3}{a^2}\right)\right\}\Psi(a,\mathfrak{h}) = 0\,,$$

$$\mathfrak{h} = \frac{h}{2\sqrt{\gamma}}\,,\ \mathcal{C} = \gamma C\,,\ g_3 = 24\gamma(c_3 + 3c_4 + 9c_5)\,,\ g_2 = 4\gamma(c_6 + 3c_7)\,,\ g_1 = \gamma c_g^2\,,\ g_0 = \gamma\Lambda\,,$$

$$f_1 = \gamma^2\left[(n^2-3)+6\right]\,,\ f_2 = -8\gamma^2\left[18(2c_6 - c_7) + 6(2c_6 + 3c_7)(n^2-3) + c_6(n^2-3)^2\right]\,,$$

$$f_3 = -8\gamma^2\Big[18(12c_3 + 11c_4 - 9c_5) + 18(2c_1 + 4c_3 + 5c_4 + 9c_5)(n^2-3) + 6(c_3+c_4)(n^2-3)^2 - c_1(n^2-3)^3\Big]\,,$$

Hořava-Lifshitz DeWitt wave function $(z = 3)$

Anisotropic scaling $z = 3$ ($a \to 0$)

Wheeler-DeWitt equation

$$\left\{\frac{1}{2}\left(\frac{\partial^2}{\partial a^2}+\frac{p}{a}\frac{\partial}{\partial a}\right)+\left(-\frac{g_3}{a^2}\right)-\frac{1}{2V^2a^2}\frac{\partial^2}{\partial \mathfrak{h}^2}+\frac{\mathfrak{h}^2}{2}\left(\frac{f_3}{a^2}\right)\right\}\Psi(a,\mathfrak{h})=0\,.$$

DeWitt wave function

$$\Psi(a,\mathfrak{h}) = \begin{cases} \frac{Aa^c}{\sqrt{\mathfrak{h}}}W_{N+1/4,1/4}(w)\,, & (\mathfrak{h}>0) \\ -\frac{Aa^c}{\sqrt{-\mathfrak{h}}}W_{N+1/4,1/4}(w)\,, & (\mathfrak{h}<0) \end{cases}$$

$$w = V\sqrt{f_3}\mathfrak{h}^2, \quad c^2+(p-1)c+\left[\frac{\sqrt{f_3}}{V}(4N+1)-2g_3\right]=0\,,\ (N=0,1,\cdots)\,,$$

$W_{\mu,\nu}(w)$ **is Whittaker function**

Scale-invariant tensor perturbations

DeWitt wave function

$$\Psi(a,\mathfrak{h}) = \begin{cases} \frac{Aa^c}{\sqrt{\mathfrak{h}}}W_{N+1/4,1/4}(w)\,, & (\mathfrak{h}>0) \\ -\frac{Aa^c}{\sqrt{-\mathfrak{h}}}W_{N+1/4,1/4}(w)\,, & (\mathfrak{h}<0) \end{cases}$$

$$w = V\sqrt{f_3}\mathfrak{h}^2, \quad c^2+(p-1)c+\left[\frac{\sqrt{f_3}}{V}(4N+1)-2g_3\right]=0\,,\ (N=0,1,\cdots)\,,$$

DeWitt wave function for ground state $(N = 0)$

$$\Psi(a,\mathfrak{h}) = A(V\sqrt{f_3})^{1/4}a^c e^{-\frac{V\sqrt{f_3}\mathfrak{h}^2}{2}}$$

Correlation Functions

$$\langle \mathfrak{h}^2\rangle = \frac{\int d\mathfrak{h}\,\mathfrak{h}^2\,|\Psi(a,\mathfrak{h})|^2}{\int d\mathfrak{h}\,|\Psi(a,\mathfrak{h})|^2}\propto \mathcal{M}^2 n^{-3} \qquad f_3\propto n^6,$$

Hořava-Lifshitz DeWitt wave function

DeWitt wave function is written in power series,

$$\Psi(a,\mathfrak{h}) = a^{c}F_0(h) + a^{c+1}F_1(h) + a^{c+2}F_2(h) + \cdots$$

$$w = V\sqrt{f_3}\mathfrak{h}^2, \quad c^2 + (p-1)c + \left[\frac{\sqrt{f_3}}{V}(4N+1) - 2g_3\right] = 0\,, \ (N = 0, 1, \cdots)\,,$$

$$\partial_{\mathfrak{h}}^2 F_0 - V^2\left[f_3\mathfrak{h}^2 + (c+p-1)c - 2g_3\right]F_0 = 0, \quad F_0(\mathfrak{h}) = \left\{\begin{array}{ll} \frac{A}{\sqrt{\mathfrak{h}}}W_{N+1/4,1/4}(w)\,, & (\mathfrak{h} > 0) \\ -\frac{A}{\sqrt{-\mathfrak{h}}}W_{N+1/4,1/4}(w)\,, & (\mathfrak{h} < 0) \end{array}\right. ,$$

$$\partial_{\mathfrak{h}}^2 F_1 - V^2\left[f_3\mathfrak{h}^2 + (c+p)(c+1) - 2g_3\right]F_1 = 0, \quad F_1(\mathfrak{h}) = 0\,,$$

$$\partial_{\mathfrak{h}}^2 F_2 - V^2\left[f_3\mathfrak{h}^2 + (c+p+1)(c+2) - 2g_3\right]F_2 = V^2(f_2\mathfrak{h}^2 - 6g_2)F_0$$

$$F_0(\mathfrak{h}) = \begin{cases} A_0 \exp\left(-\frac{1}{2}w\right)\,, & (N=0) \\ (1-2w)A_1 \exp\left(-\frac{1}{2}w\right)\,, & (N=1) \\ \left(1 - 4w + \frac{4}{3}w^2\right)A_2 \exp\left(-\frac{1}{2}w\right)\,, & (N=2) \end{cases} \quad F_2(\mathfrak{h}) = \sum_{\tilde{N}=0}^{N+1} a_{N,\tilde{N}} w^{\tilde{N}} A_N \exp\left(-\frac{1}{2}w\right)\,,$$

Numerical simulation: $p = 1,\ g_3 = 2,\ f_3 = 1,\ g_2 = g_1 = f_1 = f_0 = 0$

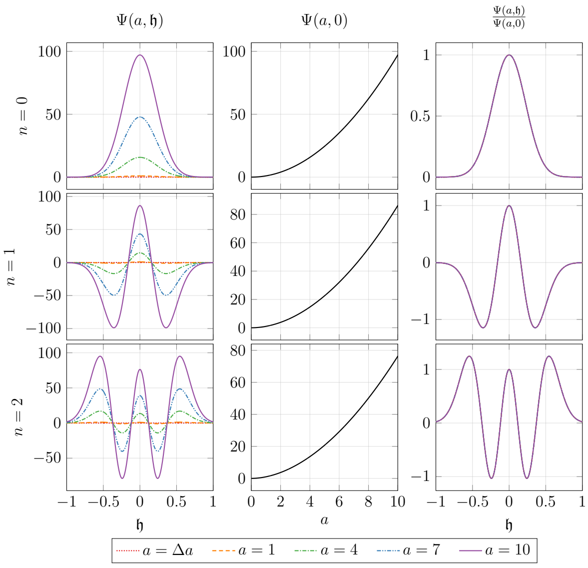

(a) $f_2 = 0,\ \mathcal{C} = 0,\ g_0 = 0$

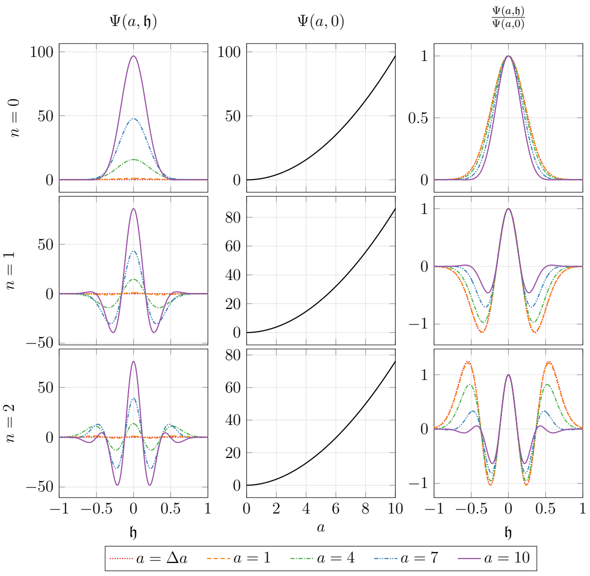

(b) $f_2 = 1,\ \mathcal{C} = 0,\ g_0 = 0$

Numerical simulation: $p = 1,\ g_3 = 2,\ f_3 = 1,\ g_2 = g_1 = f_1 = f_0 = 0$

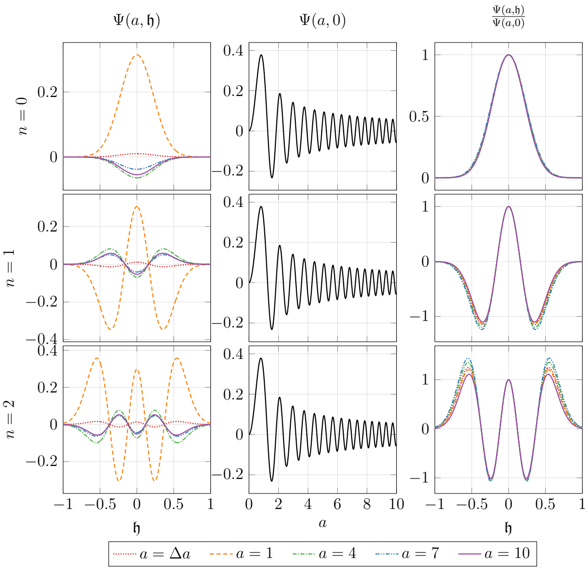

(c) $f_2 = 1,\ \mathcal{C} = 10,\ g_0 = 0$

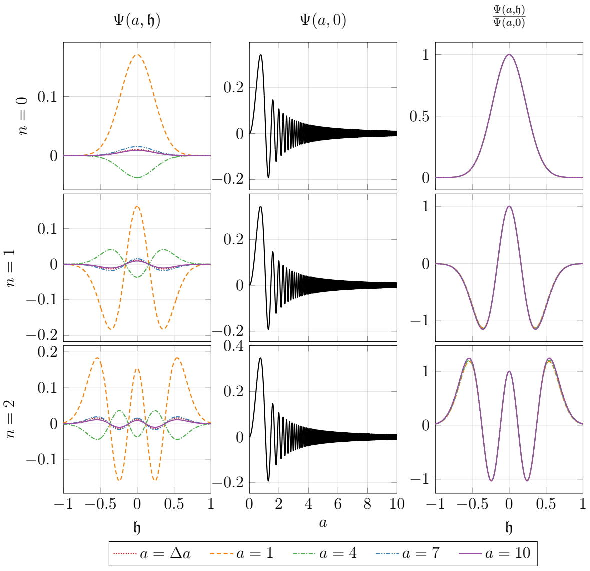

(d) $f_2 = 1,\ \mathcal{C} = 10,\ g_0 = 10$

Summary and Future issues

- DeWitt boundary condition is a hypothesis of quantum cosmology to solve the initial singularity problem
- In many theories of gravity, including general relativity DeWitt wave function predicts instability of tensor perturbations (NO-GO!)
- DeWitt boundary condition is consistent in Hořava-Lifshitz gravity
- Hořava-Lifshitz DeWitt wave function predicts the quantum creation with perturbatively stable from the initial singularity, scale-invariant fluctuations through anisotropic scaling, and then a universe dominated by gravitational dark matter

- Renormalization in Wheeler-DeWitt equation, Inner-product, Path integral formulation of the DeWitt wave function, etc.

C49

The magneto-hydrodynamic evolution of the cosmological magnetic fields

JGRG31, 2022.10.26

Fumio UCHIDA (RESCEU, U-Tokyo)

Fujiwara–Kamada–**FU**–Yokoyama, in preparation

Cosmological magnetic fields as a probe into the early universe

Everywhere in the present universe

The intergalactic magnetic field in voids
Neronov–Vovk 2010

Primordial magnetic field as the origin

Interplay with the physics in the early universe

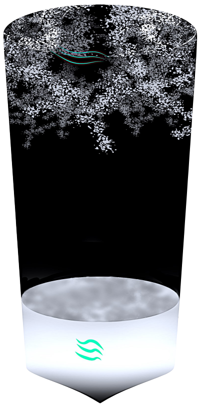

Cosmological evolution

Cosmic expansion

$$\text{(energy density)} \propto \text{(scale factor)}^{-4}, \quad \text{(length)} \propto \text{(scale factor)}$$

Magneto-hydrodynamics

$$\begin{cases} \text{Cosmological: homogeneous and isotropic} \\ \text{Astrophysical: absent at large scales in voids} \end{cases}$$

Cosmological evolution

Cosmic expansion

$$\text{(energy density)} \propto \text{(scale factor)}^{-4}, \quad \text{(length)} \propto \text{(scale factor)}$$

Magneto-hydrodynamics

$$\begin{cases} \text{Cosmological: homogeneous and isotropic} \\ \text{Astrophysical: absent at large scales in voids} \end{cases}$$

Outline

Introduction

Description of the magnetic field decay

Reconnection-driven turbulence

Discussion

Parametrization of homogeneous and isotropic magnetic field

Assumption:

Homogeneity and isotropy in a stochastic sense

$$\begin{cases} \text{Typical strength } \; B := \sqrt{\langle \boldsymbol{B}^2(\boldsymbol{x}) \rangle}, \\ \text{Coherence length } \; \xi := \dfrac{1}{B^2} \displaystyle\int dk \frac{2\pi}{k} \frac{\partial B^2}{\partial k}. \end{cases}$$

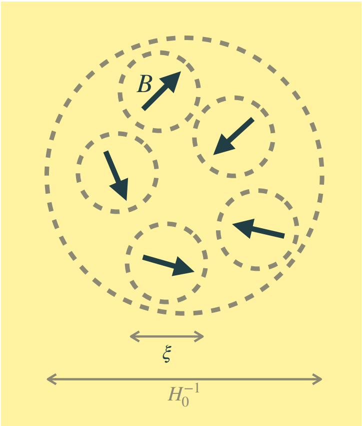

Description of the decay law

$\begin{cases} \text{Conserved quantity} \\ \text{Time scale of the decay} \end{cases}$

→ decay law, $B(T)$ and $\xi(T)$, is determined.

Initial conditions of the plot:

non-helical magnetic field
kinetically-driven turbulence,

assuming magnetogenesis during the first-order electroweak phase transition.

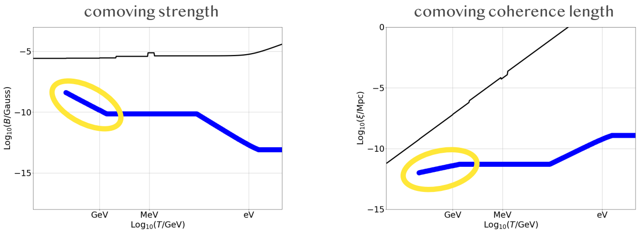

Fujiwara–Kamada–**FU**–Yokoyama, in prep.

Description of the decay law

$\begin{cases} \text{Conserved quantity} \\ \text{Time scale of the decay} \end{cases}$

→ decay law, $B(T)$ and $\xi(T)$, is determined.

Initial conditions of the plot:

non-helical magnetic field
kinetically-driven turbulence,

assuming magnetogenesis during the first-order electroweak phase transition.

Subsequent regimes:

viscous due to neutrino viscosity,
. . . ,

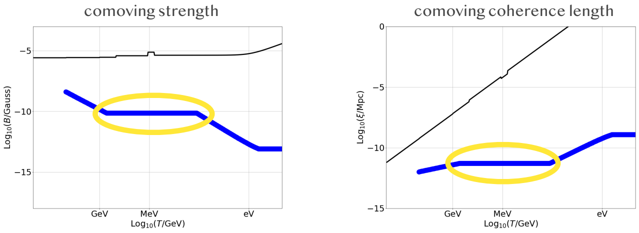

Fujiwara–Kamada–**FU**–Yokoyama, in prep.

Description of the decay law

Conserved quantity
Time scale of the decay

→ decay law, $B(T)$ and $\xi(T)$, is determined.

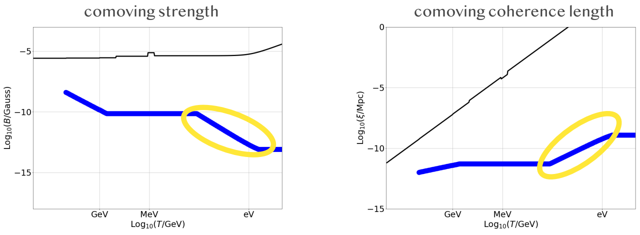

Fujiwara–Kamada–**FU**–Yokoyama, in prep.

Initial conditions of the plot:

non-helical magnetic field
kinetically-driven turbulence,

assuming magnetogenesis during the first-order electroweak phase transition.

Subsequent regimes:

viscous due to neutrino viscosity,
…,
reconnection-driven turbulence

Outline

Introduction

Description of the magnetic field decay

Reconnection-driven turbulence

Discussion

Conserved quantity: Saffman helicity invariant

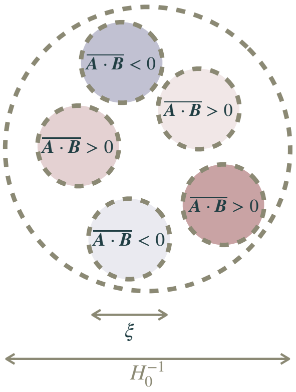

Variance of magnetic helicity distribution

$$I := \int d^3r \langle h(\boldsymbol{x})h(\boldsymbol{x}+\boldsymbol{r})\rangle \sim \xi^3 \langle h^2 \rangle \sim B^4\xi^5,$$

$h(\boldsymbol{x}) = \boldsymbol{A}(\boldsymbol{x}) \cdot \boldsymbol{B}(\boldsymbol{x})$: magnetic helicity density

is approximately conserved.

Hosking–Schekochihin 2021, Zhou+ 2022

Fast magnetic reconnection timescale

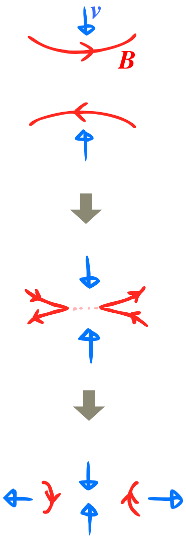

Magnetic field lines reconnect,
and the released energy accelerates the plasma.

When magnetic energy is decaying through magnetic reconnection,

$$\tau_{\text{reconnection}} \left(\simeq 10^2 \sqrt{1+\sigma\eta}\, \frac{\xi}{B/\sqrt{\rho+p}} \right) = \text{(Hubble time)}$$

Hosking–Schekochihin 2021, 2022

Reconnection-driven turbulence

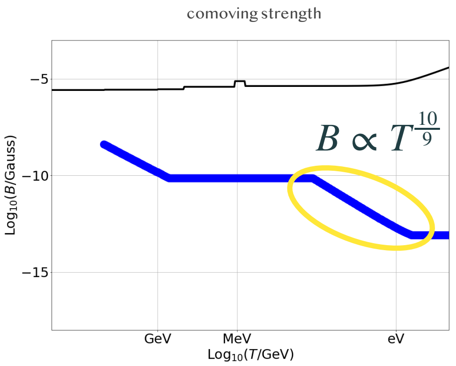

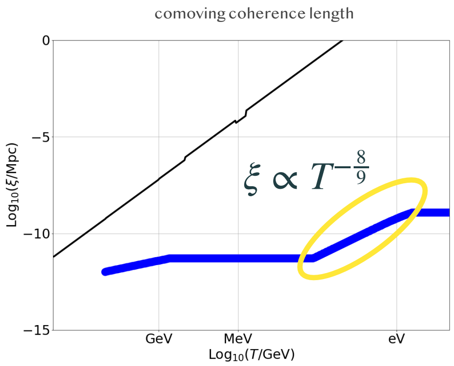

Fujiwara–Kamada–**FU**–Yokoyama, in prep.

Outline

Introduction

Description of the magnetic field decay

Reconnection-driven turbulence

Discussion

Comparison with the previous analysis

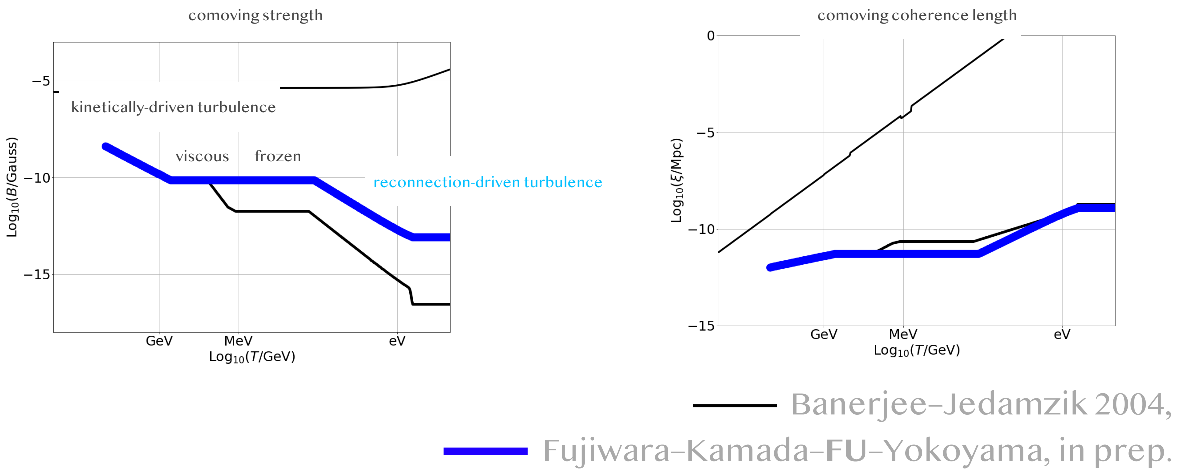

Summary

The evolution of the cosmological magnetic field is determined by

conserved quantities and time scales for the decay,

which are different according to the regimes.

The comprehensive description becomes possible, by employing the Saffman helicity invariant and reconnection time scale.

Hemispherical asymmetry of primordial power spectra

K. Sravan Kumar

Department of Physics, Tokyo Institute of Technology, Tokyo, Japan

Based on **arXiv:2209.03928 [gr-qc]** in collaboration with **João Marto**

October 26, 2022

Hemispherical power asymmetry (HPA)

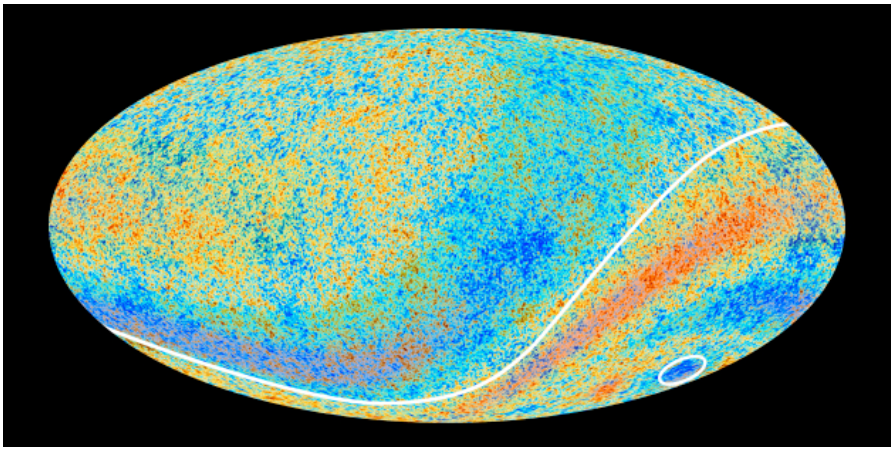

Figure: HPA breaks the isotropy of primordial fluctuations and CMB appears to be asymmetric with slightly higher temperatures in the north and slightly lower temperatures in the south.

- HPA is observed to be significant at low multipoles $\ell \sim 2 - 64$ or large angular scales or $k \lesssim 0.0045\mathrm{Mpc}^{-1}$.
- HPA can be parameterized as

$$\mathcal{P}_{\mathcal{R}}\left(k,\ \hat{\boldsymbol{n}}\right) \simeq \mathcal{P}_{\mathcal{R}\ iso}(k)\left(1+2A(k)\hat{\mathbf{p}}\cdot\hat{\mathbf{n}}\right)\ ,$$

which implies

$$A(k) = \frac{\mathcal{P}_{\mathcal{R}}\left(k,\ \hat{\mathbf{n}}\right) - \mathcal{P}_{\mathcal{R}}\left(k,\ -\hat{\mathbf{n}}\right)}{4\mathcal{P}_{\mathcal{R}\ iso}}\,.$$

$\hat{\boldsymbol{p}}$ is the direction of maximal symmetry and $\hat{\mathbf{n}} = \frac{\boldsymbol{x}}{x_{\rm ls}}$ is the line of sight from earth and $x_{\rm ls} = 14,000\mathrm{Mpc}^{-1}$ is the co-moving distance to the surface of last scattering.

- The constraint on HPA is $|A| = 0.066 \pm 0.021$ (3.3σ) for $\ell < 64$ and the Planck data reports the existence of asymmetry even up to $\ell \sim 600$ (Planck 2013, 2015 and 2019 and Y. Akrami et al (2014)).
- From the latest Planck data 2019 HPA suspected to be present even in the 3-point correlations.

Attempts to explain HPA

- HPA is most often seen as a signature of Non-Gaussianity at large scales.
- Most explanations for HPA invoked existence of an **additional** scalar field whose amplitude is modulated on super-horizon scales at the onset of inflation. See A. L. Erickcek et al 2008

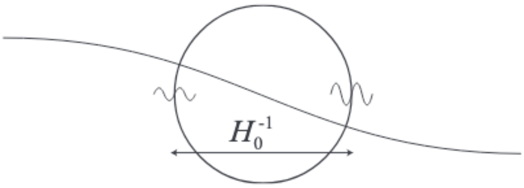

- Another explanation for HPA came from introducing asymmetric space-dependent initial conditions for the quantum fluctuations A. Ashoorioon and T. Koivisto (2015)

- A best theoretical explanation is which introduces less new parameters and explain more data points.

Can we explain HPA within the context of standard single-field slow-roll inflation? Can the answer lies somewhere in the our understanding of inflationary "quantum fluctuations"?

Standard formulation of inflationary quantum fluctuations

- Finding background solutions corresponding to quasi-de Sitter.
- We perturb metric and matter degrees of freedom around the given background

$$g_{\mu\nu} = \bar{g}_{\mu\nu} + \hat{h}_{\mu\nu}, \quad \phi = \bar{\phi}(t) + \hat{\delta\phi}\,.$$

- We quantize the effective gravitational degrees of freedom

$$\delta\hat{G}_{\mu\nu} = \delta\hat{T}_{\mu\nu}$$

- Through inflationary quantum fluctuations we witness the linearized "quantum gravity" J. Martin (2004).

Open questions

Understanding inflationary quantum fluctuations require a robust formulation of QFT in curved space-time.

- Standard QFT: Particles that propagate forward and backward in time (anti- particle). What happens to particles and anti-particle states in a curved spacetime? What is time reversal operation in curved spacetime?
- What happens to $(\mathcal{C})\mathcal{PT}$ in curved spacetime?
- In GR time is a coordinate and in quantum theory time is a parameter. What is the consistent way to quantize gravitational degrees of freedom?
- (Quantum) gravity is special and surprising: Wheeler-De Witt equation is timeless: $\mathcal{H}\Psi = 0$. The problem of time in quantum cosmology (C. Keifer, 2nd ed. 2007, Carlo Rovelli 2004.)

Formulating new set of rules for quantization (in the context of inflation)

- Separate completely classical and quantum mechanical notion of time
- Expansion of Universe: Shrinking Horizon $r_H = |\frac{1}{aH}|$ when $|H| \approx \text{const}$ (classical arrow of time).
- Quantum theory requires understanding of discrete symmetries. Notion of observers, regions of spacetime, Penrose diagrams are classical concepts J. F. Donogue, G. Menezes 2021. and they must be important only we after we quantize fields respecting discrete symmetries.
- In a quantum theory an arrow of time only emerges only after we specify initial and final states otherwise quantum theory is time symmetric (J. Hartle 2013).

Doubling the number of quantum states: $\mathcal{PT}$ transformations in gravitational context

- Respecting discrete symmetries $\mathcal{PT}$ we propose quantum fields are always created as $\mathcal{PT}$ pairs.

We represent the total vacuum as direct sum of two different vacua related by $\mathcal{PT}$ transformations.

$$|0\rangle = \frac{1}{\sqrt{2}}\Big(|0\rangle_{\mathrm{I}} \oplus |0\rangle_{\mathrm{II}}\Big) .$$

In the vacuum $|0\rangle_{\mathrm{I}}$ we create quantum fields at the position $\mathbf{x}$ that evolve forward in time and in the vacuum $|0\rangle_{\mathrm{II}}$ we create quantum fields at $-\mathbf{x}$ which evolve backward in time.

Quantization in de Sitter spacetime

$$ds^2 = -dt^2 + a(t)^2 d\mathbf{x}^2 \quad = \frac{1}{H^2\tau^2}\left(-d\tau^2 + d\mathbf{x}^2\right) .$$

where $d\tau = \frac{dt}{a}$,

$$a(t) = e^{Ht}, \quad R = 12H^2 = \left(\frac{1}{a}\frac{da}{dt}\right)^2 = \mathrm{const}\,.$$

The metric is $\mathcal{PT}$ symmetric.

$$t : -\infty \to \infty,\ H > 0 \implies \tau < 0, \quad t : \infty \to -\infty,\ H < 0 \implies \tau > 0.$$

Expanding Universe means $\tau : \pm\infty \to 0$.

Quantization in de Sitter space-time

- For a state evolving forward in time $\tau < 0$ and for a state that is evolving backward in time $\tau > 0$.
- Let us take a massless field in de Sitter space. We split the field operator into two parts

$$\hat{\phi}\left(\tau,\,\mathbf{x}\right) = \frac{1}{\sqrt{2}}\hat{\varphi}_{\rm I}\left(\tau,\,\mathbf{x}\right) \oplus \frac{1}{\sqrt{2}}\hat{\varphi}_{\rm II}\left(-\tau,\,-\mathbf{x}\right)\,,$$

corresponding to two vacua

$$a_{\mathbf{k}}|0\rangle_{\rm I} = 0, \quad b_{\mathbf{k}}|0\rangle_{\rm II} = 0, \quad \left[\hat{\varphi}_{\rm I}\left(\tau,\,\mathbf{x}\right),\,\hat{\varphi}_{\rm II}\left(-\tau,\,-\mathbf{x}\right)\right] = 0\,.$$

Quantum mechanically $\hat{\varphi}_{\rm I}\left(\tau,\,\mathbf{x}\right)|0\rangle_{\rm I}$ is the postive energy state that propagate forward in time at $\mathbf{x}$ while $\hat{\varphi}_{\rm II}\left(-\tau,\,-\mathbf{x}\right)|0\rangle_{\rm II}$ is the postive energy state that propagate backward in time at -**x**.

$\mathcal{PT}$ symmetry in dS spacetime

Since dS spacetime is perfectly $\mathcal{PT}$ symmetric we have that the quantum fields $\hat{\varphi}_{\rm I}\left(\tau,\,\mathbf{x}\right)|0\rangle_{\rm I}$ and $\hat{\varphi}_{\rm II}\left(-\tau,\,-\mathbf{x}\right)|0\rangle_{\rm II}$ behave identically, which can be seen from the fact that their equal time correlations are the same

$$\frac{1}{a^2}{}_{\rm I}\langle 0|\hat{\varphi}_{\rm I}\left(\tau,\,\mathbf{x}\right)\hat{\varphi}_{\rm I}\left(\tau,\,\mathbf{x}'\right)|0\rangle_{\rm I} =$$
$$\frac{1}{a^2}{}_{\rm II}\langle 0|\hat{\varphi}_{\rm II}\left(-\tau,\,-\mathbf{x}\right)\hat{\varphi}_{\rm II}\left(-\tau,\,-\mathbf{x}'\right)|0\rangle_{\rm II} = \frac{H^2}{4\pi^2k^3}\,.$$

For more details about QFT in dS spacetime KSK, Joao Marto (arXiv: 2211.XXXX)

Quantization in quasi-de Sitter space-time: Single field inflation case

- Inflationary space-time is not $\mathcal{PT}$ symmetric like dS. Expectation is $\mathcal{PT}$ symmetry must be spontaneously broken at the quantum level.
- $$\hat{v}\left(\tau,\,\mathbf{x}\right)=\frac{1}{\sqrt{2}}\hat{v}_{\rm I}\left(\tau,\,\mathbf{x}\right)\oplus\frac{1}{\sqrt{2}}\hat{v}_{\rm II}\left(-\tau,\,-\mathbf{x}\right)\,.$$
  corresponding to $\vert 0\rangle_{\rm qdS}=\vert 0\rangle_{\rm qdS_I}\oplus\vert 0\rangle_{\rm qdS_{II}}$.
- $\hat{v}_{\rm II}\left(-\tau,\,-\mathbf{x}\right)$ is the fluctuation that goes backward in time. Logically, if the fluctuation propagates forward in time in a slow-roll background, the fluctuation that goes backward in time experience space-time as a "slow-climb". Therefore "quantum mechanically" we solve for $v_{\rm II,\,k}\left(\tau\right)$ following the time reversal operation

$$t\to -t\implies H\to -H,\quad \epsilon\to-\epsilon,\quad \eta\to-\eta\,.$$

Hemispherical asymmetry of scalar power spectra

$$A(k)=\frac{P_{\zeta 1}-P_{\zeta 2}}{4P_{\zeta}}$$

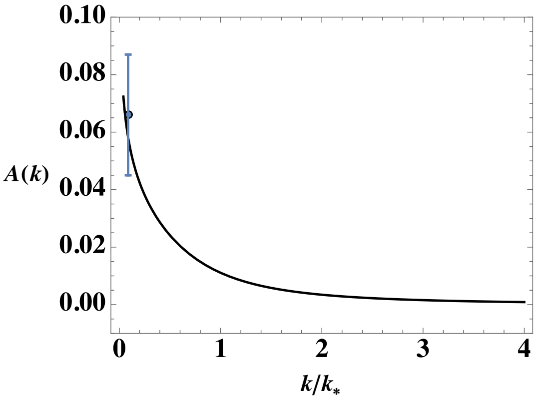

Figure: Here $k_*=a_*H_*=0.05\mathrm{Mpc}^{-1}$ and we are within $|A|=0.066\pm0.021$ for $k\lesssim10^{-1}k_*$.

Hemispherical asymmetry for tensor power spectra

Similarly, double vacuum scheme of quantization predicts the power asymmetry of the tensor-power spectrum

$$T(k) = \frac{P_{h1} - P_{h2}}{4P_h}$$

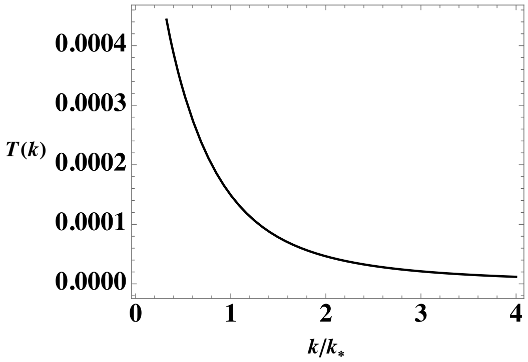

Figure: This plot is obtained for the case of Starobinsky and Higgs inflation.

Conclusions

- Based on several open theoretical questions about QFT in curved space-time and the surprising anomalies we proposed a new vacua structure for inflationary quantum fluctuations.
- Our scheme of quantization naturally produces HPA for both scalar and tensor power spectra. If detected we greatly learn about nature of QFT in curved space-time

Thank you very much for your attention.

C51

Weak lensing of gravitational waves in wave optics: Beyond the Born approximation

Morifumi Mizuno
Tokyo Institute of Technology

Collaborator: Teruaki Suyama
Physical Review D in review [arXiv:2210.02062]

Tokyo Tech

Gravitational lensing (GL) of gravitational waves (GWs)

Dark matter inhomogeneity→lensed waveform

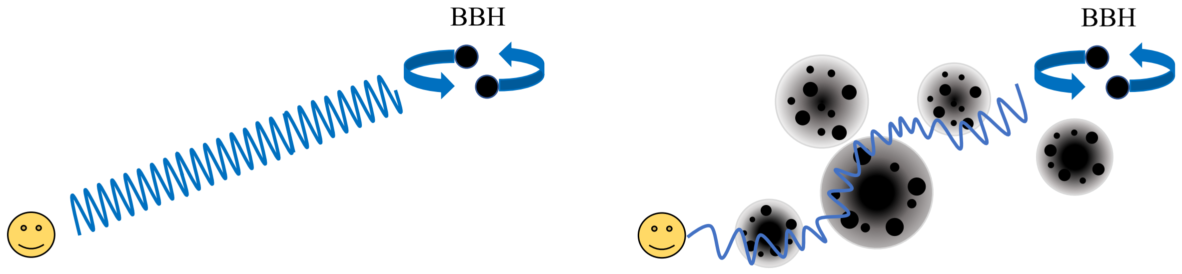

Unlensed GWs **Lensed GWs**

We can probe the dark matter distribution by GL of GWs!

Gravitational lensing (GL) of gravitational waves (GWs)

GL of EM waves and GWs

GL of GWs has…

- Information about **phase**
- Frequency dependency

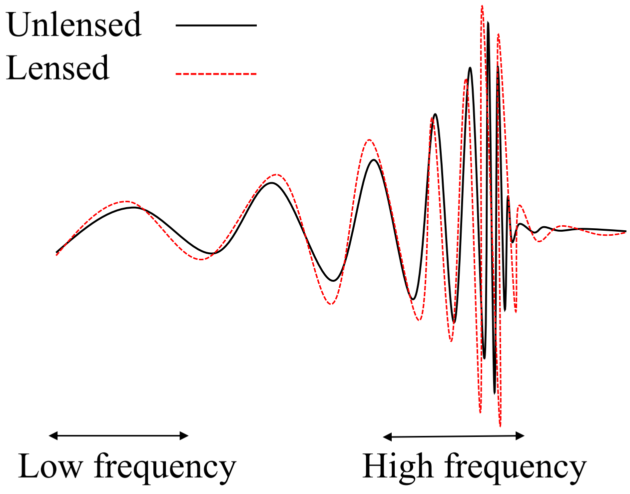

Wave equation

Frequency

T.Nakamura, S.Deguchi (1999)

$$\boxed{(\nabla^2 + \omega^2)\tilde{\phi}(\omega,\boldsymbol{r}) = 4\omega^2\Phi\tilde{\phi}\ (\omega,\boldsymbol{r})}$$

Amplitude

Potential

Amplification factor: $F(\omega) \equiv \dfrac{\tilde{\phi}(\omega)}{\tilde{\phi}_0(\omega)}$ ← Lensed ← Unlensed

Lensing effect is encoded in the amplification factor

Weak lensing

- Lensing effect is small
- Dark matter distribution is random

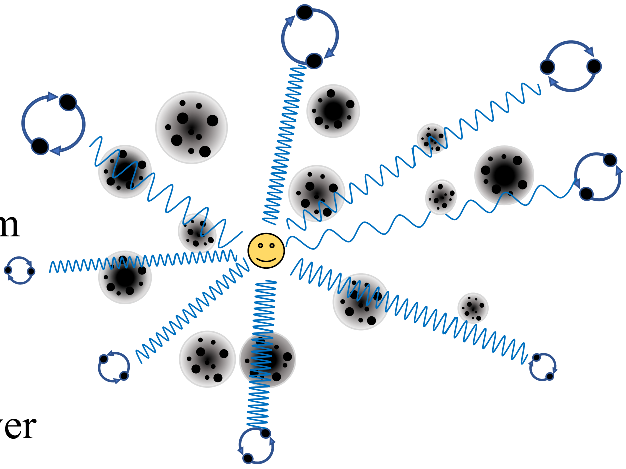

We need to take the average $\langle \cdots \rangle$ over many GW events

---

Born approximation in wave optics

First order approximation R. Takahashi, [astro-ph/0511517]

magnification K_{Born} $\sim \mathcal{O}(\Phi)$ **phase modulation S_{Born}** $\sim \mathcal{O}(\Phi)$

$$F(\omega) = \frac{\tilde{\phi}(\omega)}{\tilde{\phi}_0(\omega)} \sim 1 + K_{\mathrm{Born}} + iS_{\mathrm{Born}} \sim (1 + K_{\mathrm{Born}}) e^{iS_{\mathrm{Born}}}$$

$$S_{\mathrm{Born}} = -2\omega \int_0^{\chi_s} d\chi \left[\cos\left[\frac{\chi_s - \chi}{2\omega\chi_s\chi} \nabla_\theta^2 \right] - 1 \right] \Phi$$

$$K_{\mathrm{Born}} = 2\omega \int_0^{\chi_s} d\chi \sin\left[\frac{\chi_s - \chi}{2\omega\chi_s\chi} \nabla_\theta^2 \right] \Phi$$

$$\langle S_{\mathrm{Born}} \rangle = \langle K_{\mathrm{Born}} \rangle = 0$$

$$\langle S_{\mathrm{Born}}^2 \rangle = 4\omega^2 \left(\frac{3H_0^2\Omega_m}{2} \right)^2 \int_0^{\chi_s} d\chi \int \frac{d^2\boldsymbol{k}_\perp}{(2\pi)^2} \left(1 - \cos\left[\frac{(\chi_s - \chi)\chi}{2\chi_s\omega} k_\perp^2 \right] \right)^2 \frac{1}{k^4} P_\delta(k_\perp, \chi_1)$$

$$\langle K_{\mathrm{Born}}^2 \rangle = 4\omega^2 \left(\frac{3H_0^2\Omega_m}{2} \right)^2 \int_0^{\chi_s} d\chi \frac{1}{a^2(\chi)} \int \frac{d^2\boldsymbol{k}_\perp}{(2\pi)^2} \sin^2\left[\frac{(\chi_s - \chi)\chi}{2\chi_s\omega} k_\perp^2 \right] \frac{1}{k^4} P_\delta(k_\perp, \chi_1)$$

Matter power spectrum

We can determine matter power spectrum by $\langle S_{\mathrm{Born}}^2 \rangle$, $\langle K_{\mathrm{Born}}^2 \rangle$

Why beyond Born approximation?

Accuracy of the Born approximation?

Missing phenomena?

↓

Beyond the Born approximation

Post-Born approximation (Our work!)

new variable J: $$\frac{\tilde{\phi}(\omega)}{\tilde{\phi}_0(\omega)} = e^{i\omega J(\omega)} = e^{K(\omega)} e^{iS(\omega)}$$

$(\nabla^2 + \omega^2)\tilde{\phi} = 4\omega^2 \Phi \tilde{\phi}$ becomes…

$$\boxed{J(\chi_s, \boldsymbol{\theta}, \omega) = \int_0^{\chi_s} d\chi \exp\left[i \frac{\chi_s - \chi}{2\omega\chi_s\chi} \nabla_\theta^2 \right] \left(-2\Phi(\chi, \boldsymbol{\theta}) - \frac{1}{2\chi^2} (\nabla_\theta J)^2 \right)}$$

Higher order terms…

$$\omega J = S - iK \quad \Rightarrow \quad \begin{aligned} S &= \boxed{S_{\mathrm{Born}}} + \boxed{S^{(2)} + S^{(3)}} + \cdots \\ K &= \boxed{K_{\mathrm{Born}}} + \boxed{K^{(2)} + K^{(3)}} + \cdots \end{aligned}$$

The Born approximation

The post-Born approximation

$S_{\mathrm{Born}}, K_{\mathrm{Born}} \sim \mathcal{O}(\Phi)$

$S^{(2)}, K^{(2)} \sim \mathcal{O}(\Phi^2)$

$S^{(3)}, K^{(3)} \sim \mathcal{O}(\Phi^3)$

Post-Born approximation

1st order in Φ

$$S_{\mathrm{Born}} = -2\omega \int_0^{\chi_s} d\chi \left[\cos\left[\frac{\chi_s - \chi}{2\omega\chi_s\chi}\nabla_\theta^2\right] - 1\right]\Phi$$

$$K_{\mathrm{Born}} = 2\omega \int_0^{\chi_s} d\chi \sin\left[\frac{\chi_s - \chi}{2\omega\chi_s\chi}\nabla_\theta^2\right]\Phi$$

The Born approximation
R. Takahashi, [astro-ph/0511517]

2nd order in Φ

$$S^{(2)} = -2\omega \int_0^{\chi_s}\frac{d\chi}{\chi^2}\int_0^{\chi} d\chi_1 \int_0^{\chi} d\chi_2 \left[\cos\left[\frac{(W\nabla)^{(2)}}{2\omega}\right] - 1\right]\nabla_{\theta 1}\Phi_1 \cdot \nabla_{\theta 2}\Phi_2$$

$$K^{(2)} = 2\omega \int_0^{\chi_s}\frac{d\chi}{\chi^2}\int_0^{\chi} d\chi_1 \int_0^{\chi} d\chi_2 \sin\left[\frac{(W\nabla)^{(2)}}{2\omega}\right]\nabla_{\theta 1}\Phi_1 \cdot \nabla_{\theta 2}\Phi_2$$

$$(W\nabla)^{(2)} = W(\chi, \chi_s)\nabla_{\theta 12}^2 + W(\chi_1, \chi)\nabla_{\theta 1}^2 + W(\chi_2, \chi)\nabla_{\theta 2}^2$$

The post-Born approximation
New results!

3rd order in Φ

$$S^{(3)} = -4\omega \int_0^{\chi_s}\frac{d\chi}{\chi^2}\int_0^{\chi} d\chi_3 \int_0^{\chi}\frac{d\chi'}{\chi'^2}\int_0^{\chi'} d\chi_1 \int_0^{\chi'} d\chi_2 \left[\cos\left[\frac{(W\nabla)^{(3)}}{2\omega}\right] - 1\right]\nabla_{\theta 12}(\nabla_{\theta 1}\Phi_1 \cdot \nabla_{\theta 2}\Phi_2)\cdot\nabla_{\theta 3}\Phi_3$$

$$K^{(3)} = 4\omega \int_0^{\chi_s}\frac{d\chi}{\chi^2}\int_0^{\chi} d\chi_3 \int_0^{\chi}\frac{d\chi'}{\chi'^2}\int_0^{\chi'} d\chi_1 \int_0^{\chi'} d\chi_2 \sin\left[\frac{(W\nabla)^{(3)}}{2\omega}\right]\nabla_{\theta 12}(\nabla_{\theta 1}\Phi_1 \cdot \nabla_{\theta 2}\Phi_2)\cdot\nabla_{\theta 3}\Phi_3$$

$$(W\nabla)^{(3)} = W(\chi, \chi_s)\nabla_{\theta 123}^2 + W(\chi_3, \chi)\nabla_{\theta 3}^2 + W(\chi', \chi)\nabla_{\theta 12}^2 + W(\chi_1, \chi')\nabla_{\theta 1}^2 + W(\chi_2, \chi')\nabla_{\theta 2}^2$$

$$W(\chi, \chi_s) = \frac{1}{\chi} - \frac{1}{\chi_s}$$

Average and Variance

Variance (the Born approximation)

$$\langle S_{\mathrm{Born}}\rangle = \langle K_{\mathrm{Born}}\rangle = 0$$

$$\langle S_{\mathrm{Born}}^2\rangle = 4\omega^2\left(\frac{3H_0^2\Omega_m}{2}\right)^2 \int_0^{\chi_s} d\chi \int \frac{d^2\boldsymbol{k}_\perp}{(2\pi)^2}\left(1 - \cos\left[\frac{(\chi_s - \chi)\chi}{2\chi_s\omega}k_\perp^2\right]\right)^2 \frac{1}{k_\perp^4}P_\delta(k_\perp, \chi_1)$$

$$\langle K_{\mathrm{Born}}^2\rangle = 4\omega^2\left(\frac{3H_0^2\Omega_m}{2}\right)^2 \int_0^{\chi_s} d\chi \frac{1}{a^2(\chi)}\int \frac{d^2\boldsymbol{k}_\perp}{(2\pi)^2}\sin^2\left[\frac{(\chi_s - \chi)\chi}{2\chi_s\omega}k_\perp^2\right]\frac{1}{k_\perp^4}P_\delta(k_\perp, \chi_1)$$

The Born approximation
R. Takahashi, [astro-ph/0511517]

Nonzero Average (the post-Born approximation)

$$\langle S\rangle = 2\omega\left(\frac{3H_0^2\Omega_m}{2}\right)^2 \int_0^{\chi_s}\frac{d\chi}{\chi^2}\int_0^{\chi} d\chi_1\, \chi_1^2 \frac{1}{a^2(\chi_1)}\int \frac{d^2\boldsymbol{k}_\perp}{(2\pi)^2}\left(1 - \cos\left[\frac{(\chi - \chi_1)\chi_1}{\chi\omega}k_\perp^2\right]\right)\frac{1}{k_\perp^2}P_\Phi(k_\perp, \chi_1)$$

$$\langle K\rangle = -2\omega\left(\frac{3H_0^2\Omega_m}{2}\right)^2 \int_0^{\chi_s}\frac{d\chi}{\chi^2}\int_0^{\chi} d\chi_1\, \chi_1^2 \frac{1}{a^2(\chi_1)}\int \frac{d^2\boldsymbol{k}_\perp}{(2\pi)^2}\sin\left[\frac{(\chi - \chi_1)\chi_1}{\chi\omega}k_\perp^2\right]\frac{1}{k_\perp^2}P_\Phi(k_\perp, \chi_1)$$

New results!

Average

Nonzero Average $\langle K\rangle, \langle S\rangle \neq 0,\ \langle K_{\mathrm{Born}}\rangle, \langle S_{\mathrm{Born}}\rangle = 0$

Magnification $\langle K\rangle$ and $\langle K^2_{\mathrm{Born}}\rangle^{1/2}$

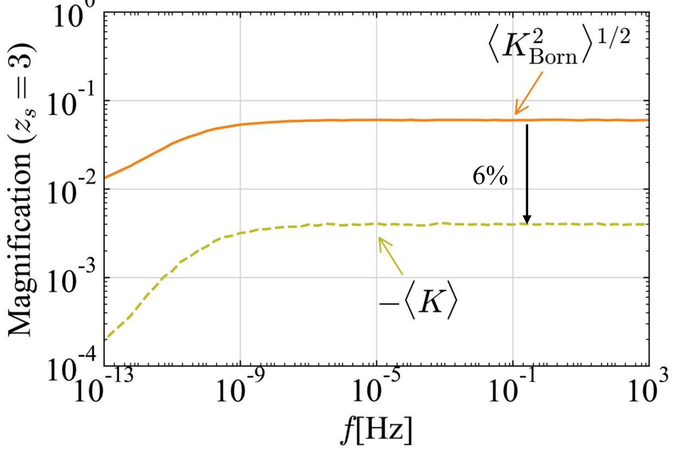

Phase modulation $\langle S\rangle$ and $\langle S^2_{\mathrm{Born}}\rangle^{1/2}$

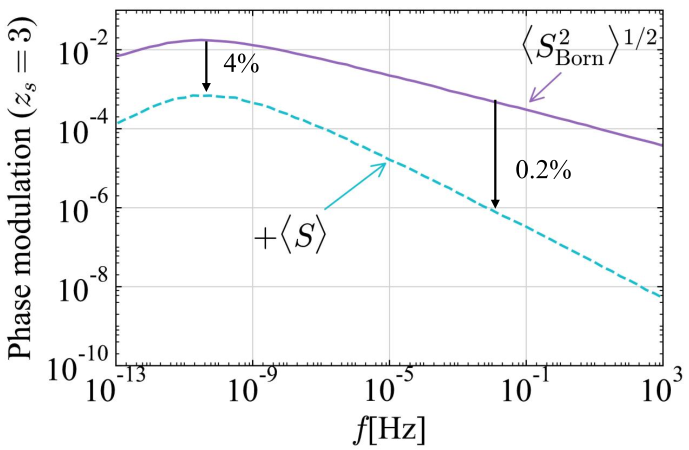

We can use $\langle K\rangle$, $\langle S\rangle$ as a new probe for the matter power spectrum

Validity of the Born approximation

Source redshift: $z_s = 1(3)$, f: frequency of GWs

	$f \leq 10^{-2}$ Hz	$10^{-2} \leq f \leq 10^1$ Hz	$10^1 \leq f \leq 10^3$ Hz
$\langle K\rangle / \langle K^2_{\mathrm{Born}}\rangle^{1/2}$	$\leq 2.4(6)\%$		$\leq 2.4(6)\%$
$\langle S\rangle / \langle S^2_{\mathrm{Born}}\rangle^{1/2}$	$\leq 1.5(4)\%$	$\leq 1(3)\%$	$\leq 8(25)\%$
Post Born variance K	$\leq 0.035(0.25)\%$		$\leq 0.035(0.25)\%$
Post Born variance S	$\leq 0.05(0.4)\%$	$\leq 0.02(0.2)\%$	$\leq 2(14)\%$

Detectable!

small

The shot noise (point mass) effect

Summary

Weak lensing of gravitational waves
↓
probing **dark matter distribution**

We derived…

S and ***K*** up to **3rd order** in Φ

We found that…

Born approximation is **good!**

$\langle S \rangle$ and $\langle K \rangle$ can be used as an **additional probe!**

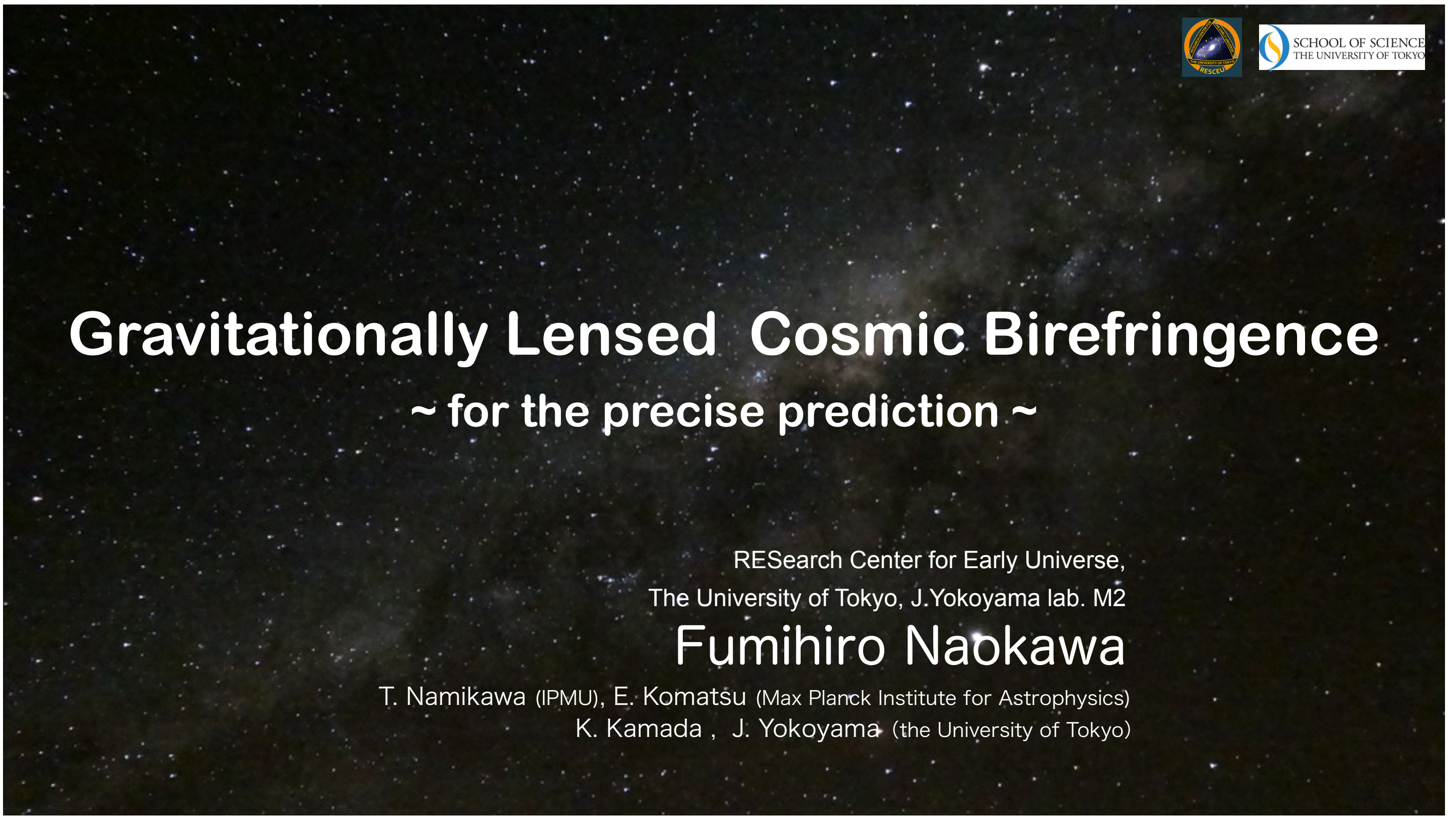

Gravitationally Lensed Cosmic Birefringence

~ for the precise prediction ~

RESearch Center for Early Universe,
The University of Tokyo, J.Yokoyama lab. M2

Fumihiro Naokawa

T. Namikawa (IPMU), E. Komatsu (Max Planck Institute for Astrophysics)
K. Kamada , J. Yokoyama (the University of Tokyo)

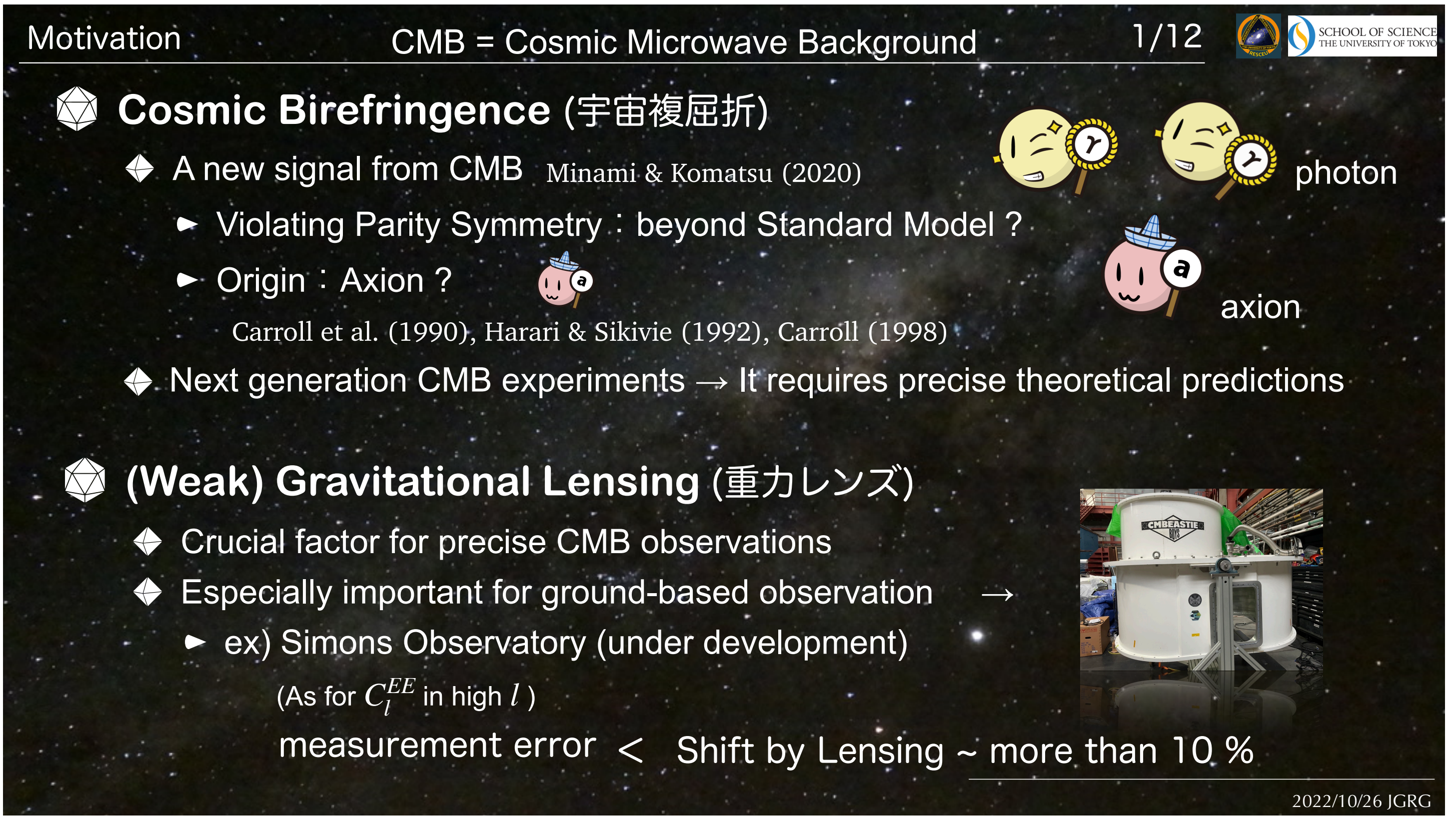

Motivation CMB = Cosmic Microwave Background

Cosmic Birefringence (宇宙複屈折)

- A new signal from CMB Minami & Komatsu (2020)
  - Violating Parity Symmetry：beyond Standard Model ?
  - Origin：Axion ?

    Carroll et al. (1990), Harari & Sikivie (1992), Carroll (1998)
- Next generation CMB experiments → It requires precise theoretical predictions

photon

axion

(Weak) Gravitational Lensing (重力レンズ)

- Crucial factor for precise CMB observations
- Especially important for ground-based observation →
  - ex) Simons Observatory (under development)

(As for C_l^{EE} in high l)

measurement error < Shift by Lensing ~ more than 10 %

Today's Contents

- Introduction to CMB
- Cosmic Birefringence
- Gravitational Lensing

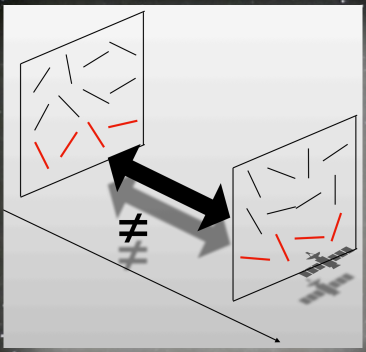

+

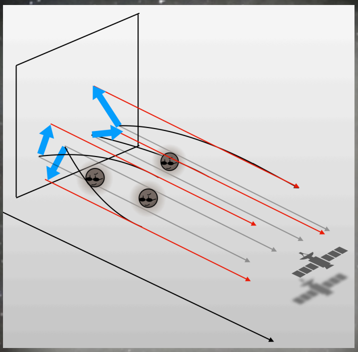

=

- Gravitationally Lensed Cosmic Birefringence (←My work)

CMB (Cosmic Microwave Background)

Data → Observables → Power Spectra

Temperature Θ

Polarization

E mode B mode

$C_l^{\Theta\Theta}$ $C_l^{\Theta E}$ $\cancel{C_l^{\Theta B}}$

C_l^{EE} C_l^{BB} $\cancel{C_l^{EB}}$

Cosmological Model

Power Spectra

$C_l^{\Theta\Theta}$ $C_l^{\Theta E}$ $\cancel{C_l^{\Theta B}}$

C_l^{EE} C_l^{BB} $\cancel{C_l^{EB}}$

Comparison

What is Cosmic Birefringence ?

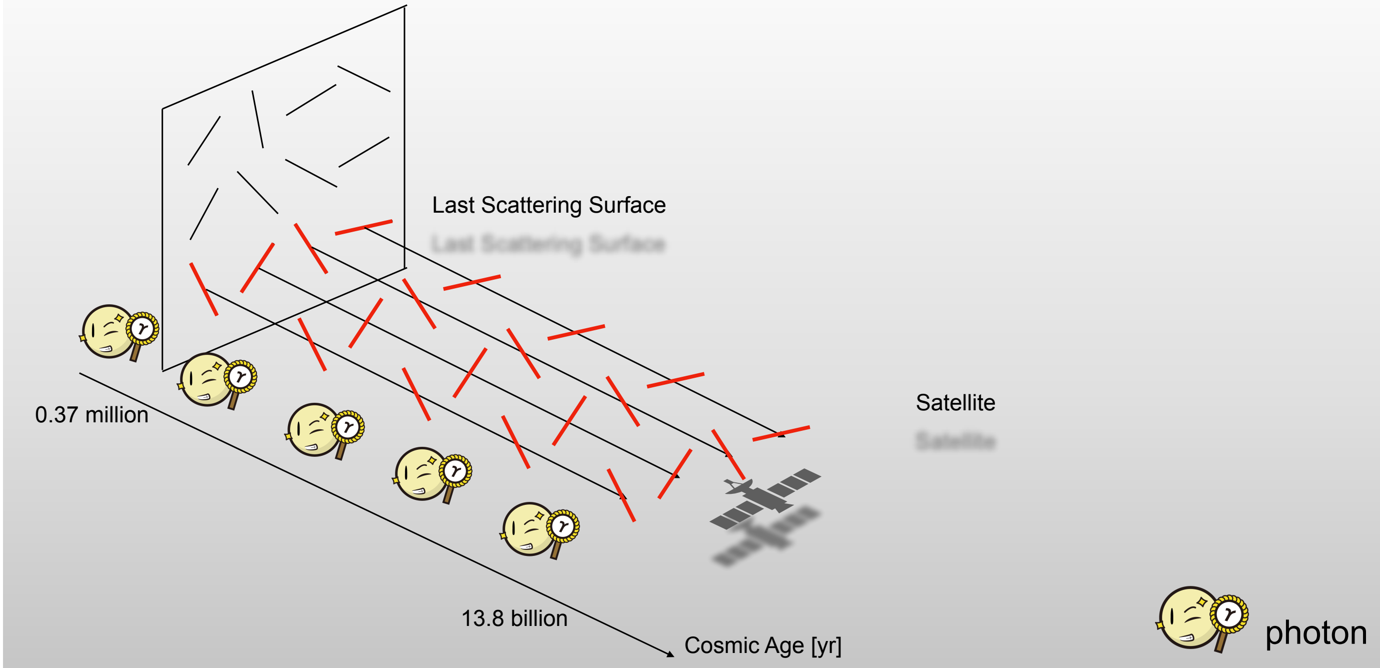

What is Cosmic Birefringence ?

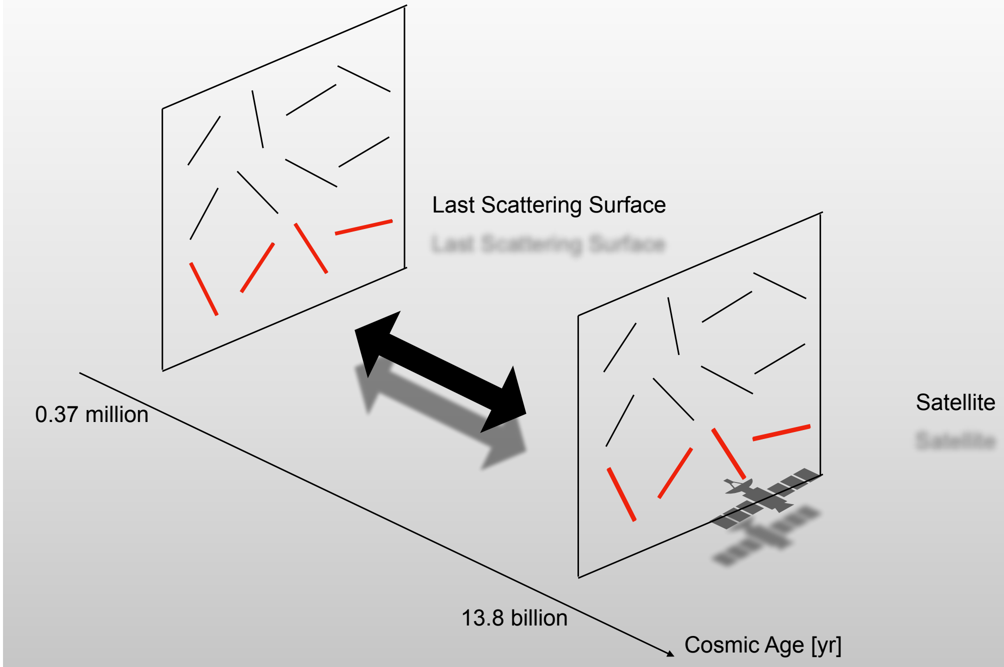

What is Cosmic Birefringence ?

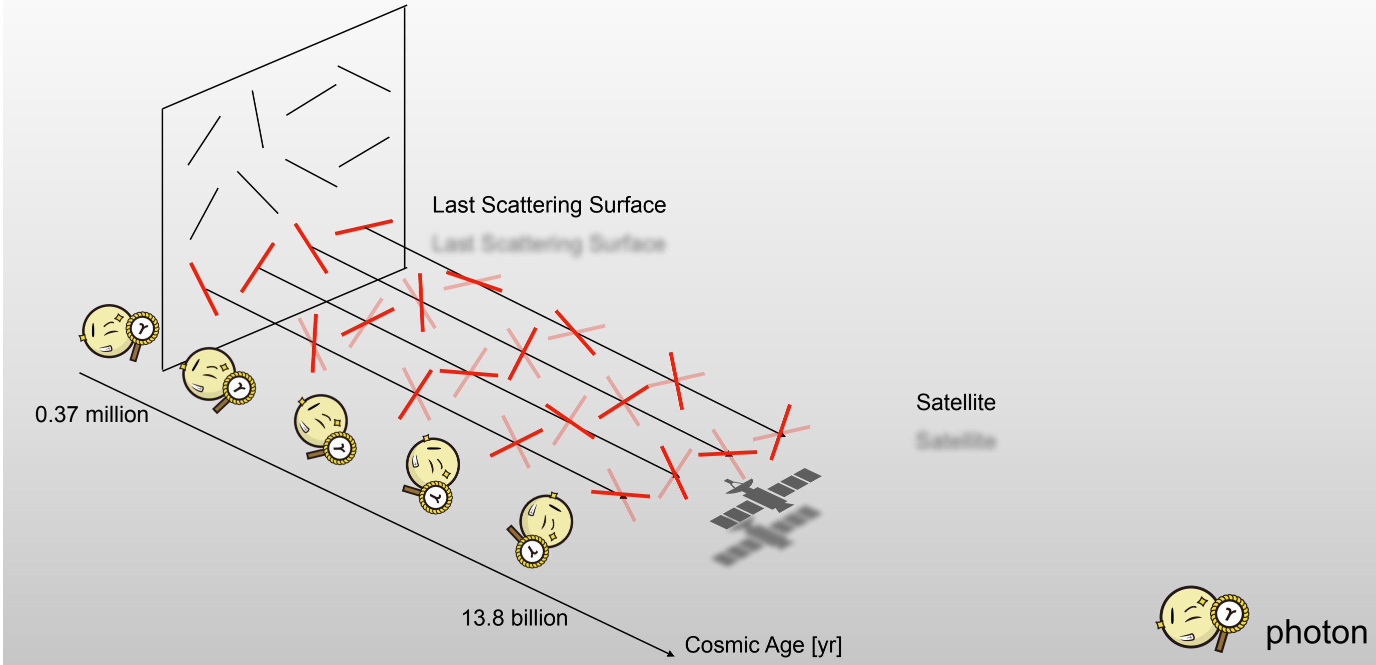

Last Scattering Surface

Satellite

0.37 million

13.8 billion

Cosmic Age [yr]

photon

What is Cosmic Birefringence ?

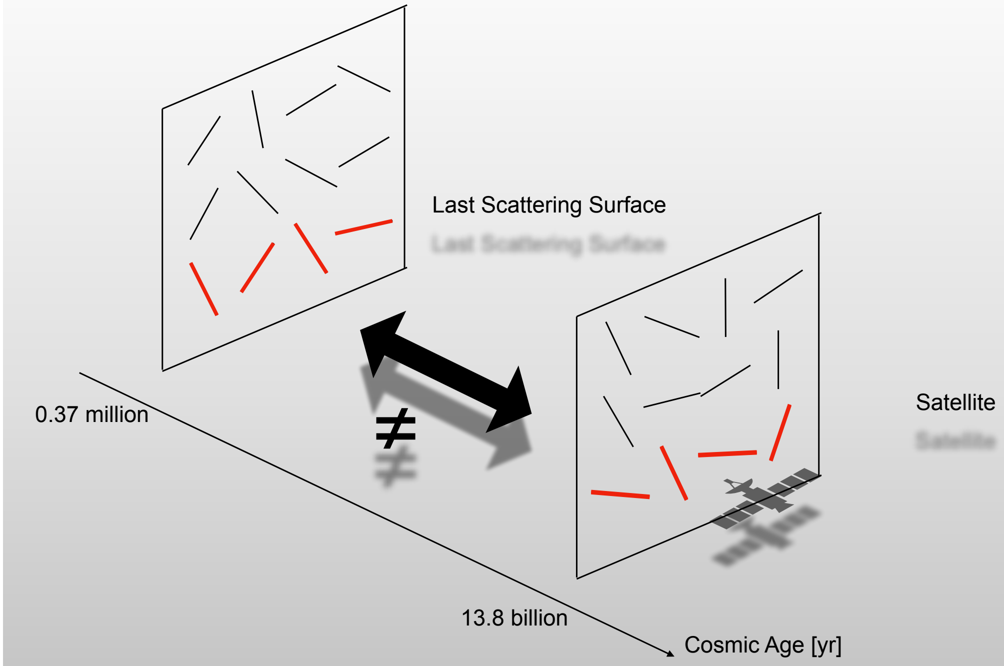

Last Scattering Surface

Satellite

≠

0.37 million

13.8 billion

Cosmic Age [yr]

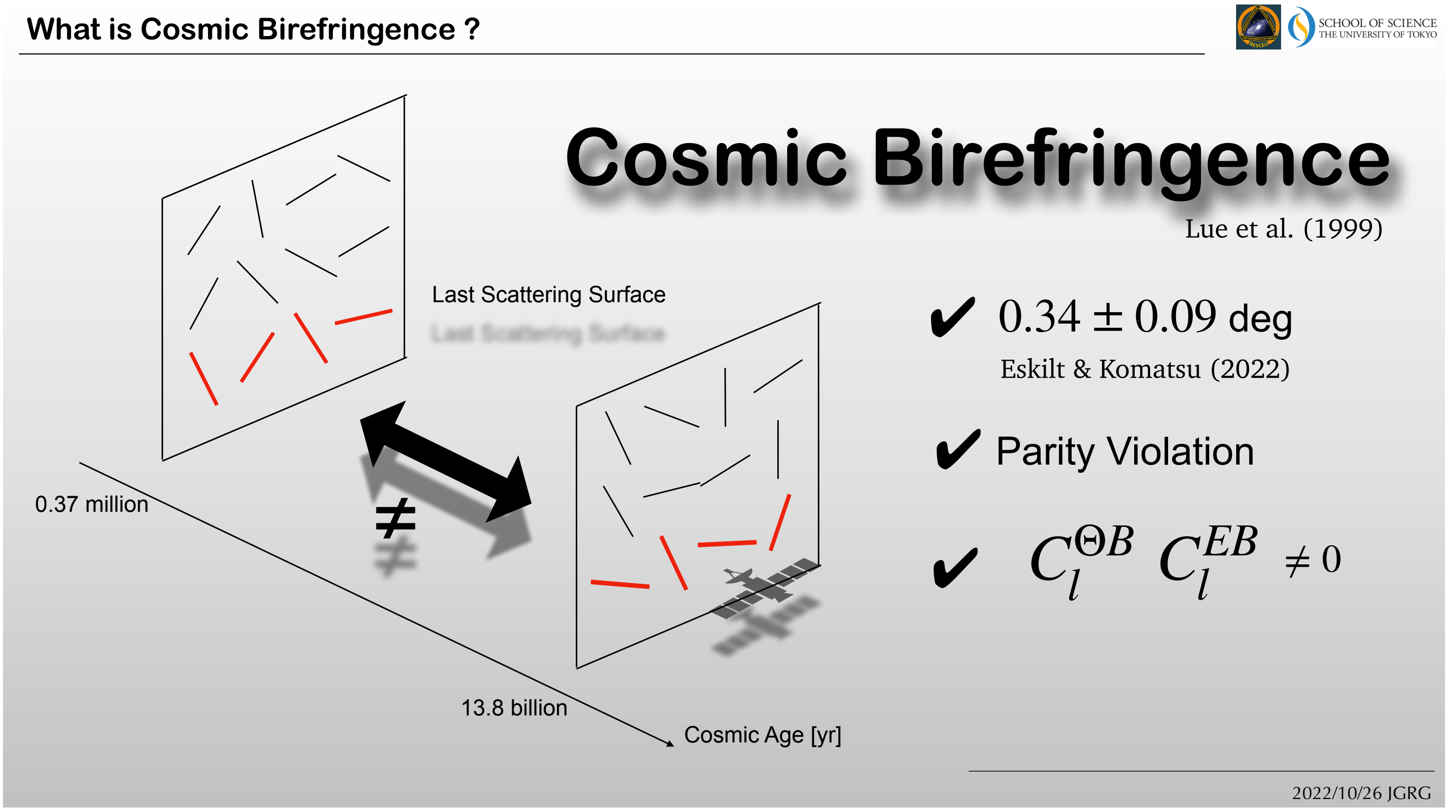

What is Cosmic Birefringence ?

Cosmic Birefringence

Lue et al. (1999)

- ✔ 0.34 ± 0.09 deg

  Eskilt & Komatsu (2022)

- ✔ Parity Violation

- ✔ $C_l^{\Theta B}$ C_l^{EB} $\neq 0$

Last Scattering Surface

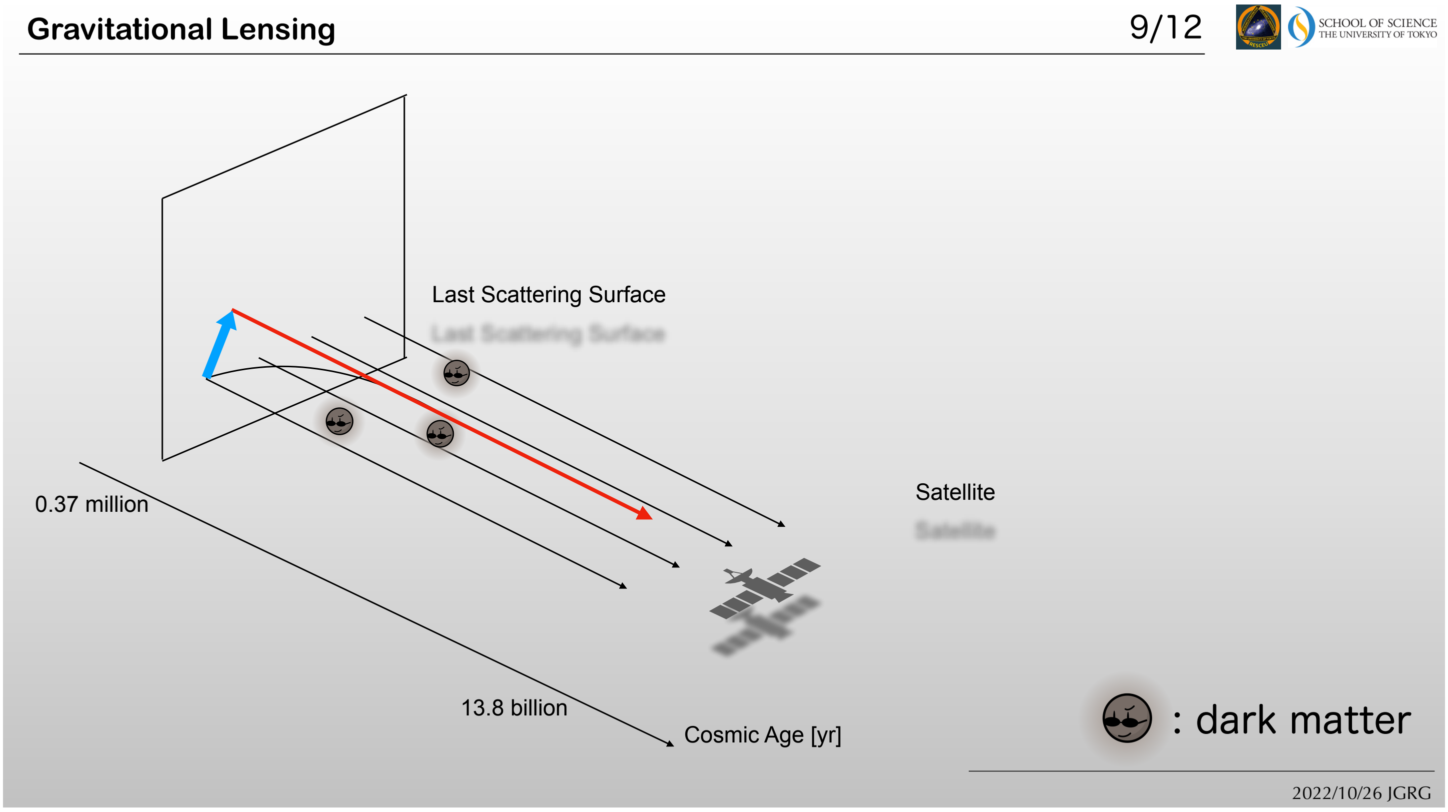

Gravitational Lensing

Last Scattering Surface
Satellite

Gravitational Lensing

CMB photons are deflected

Gravitational Lensing

Challinor & Lewis (2005)

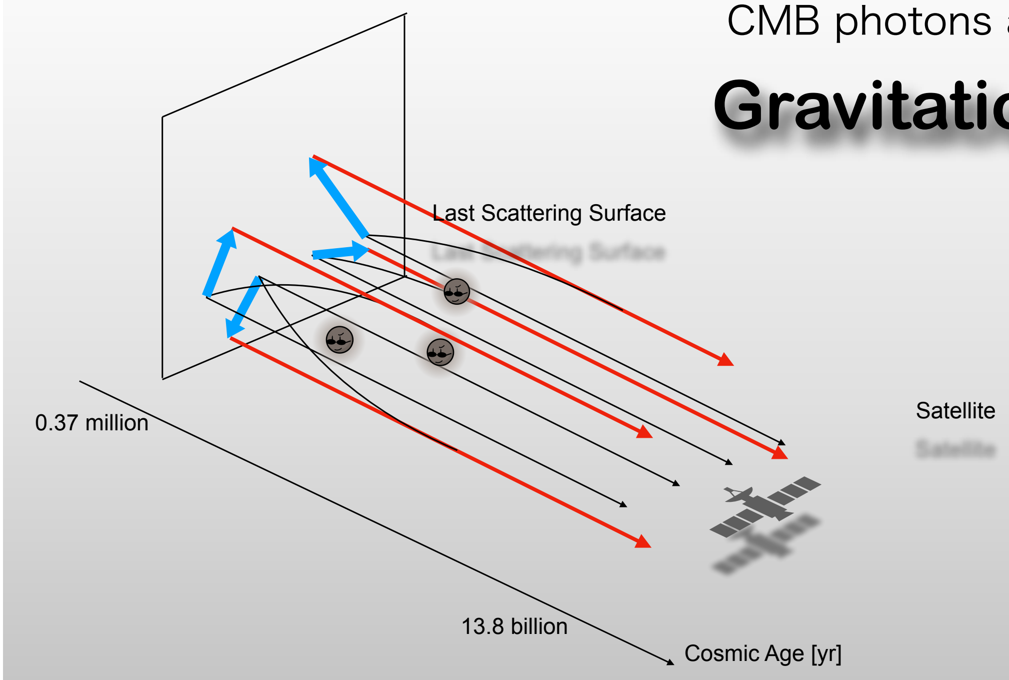

● : dark matter

Gravitational Lensing

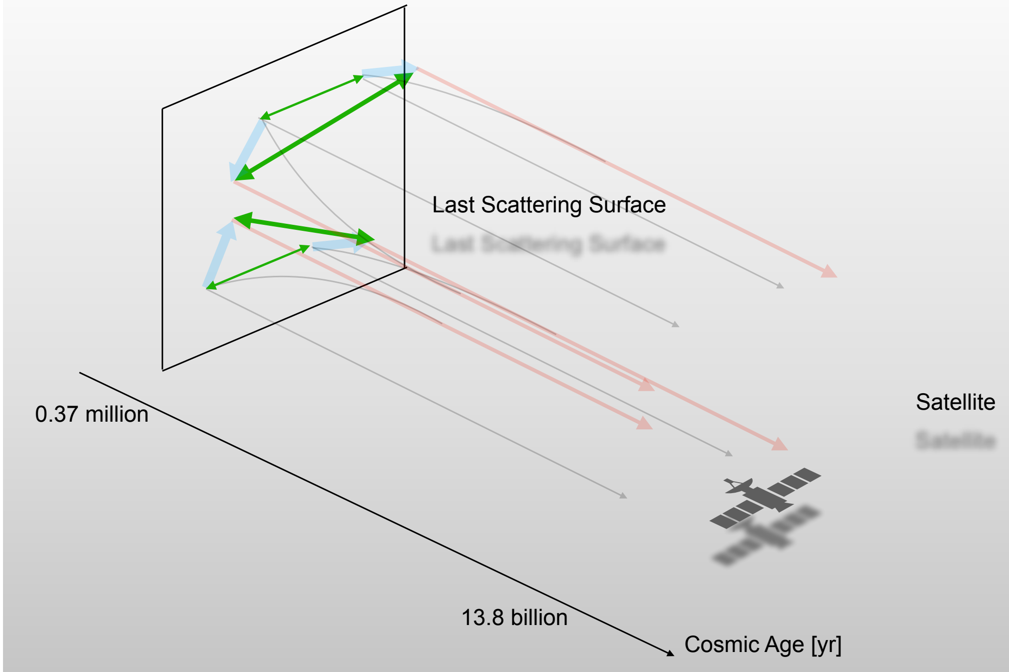

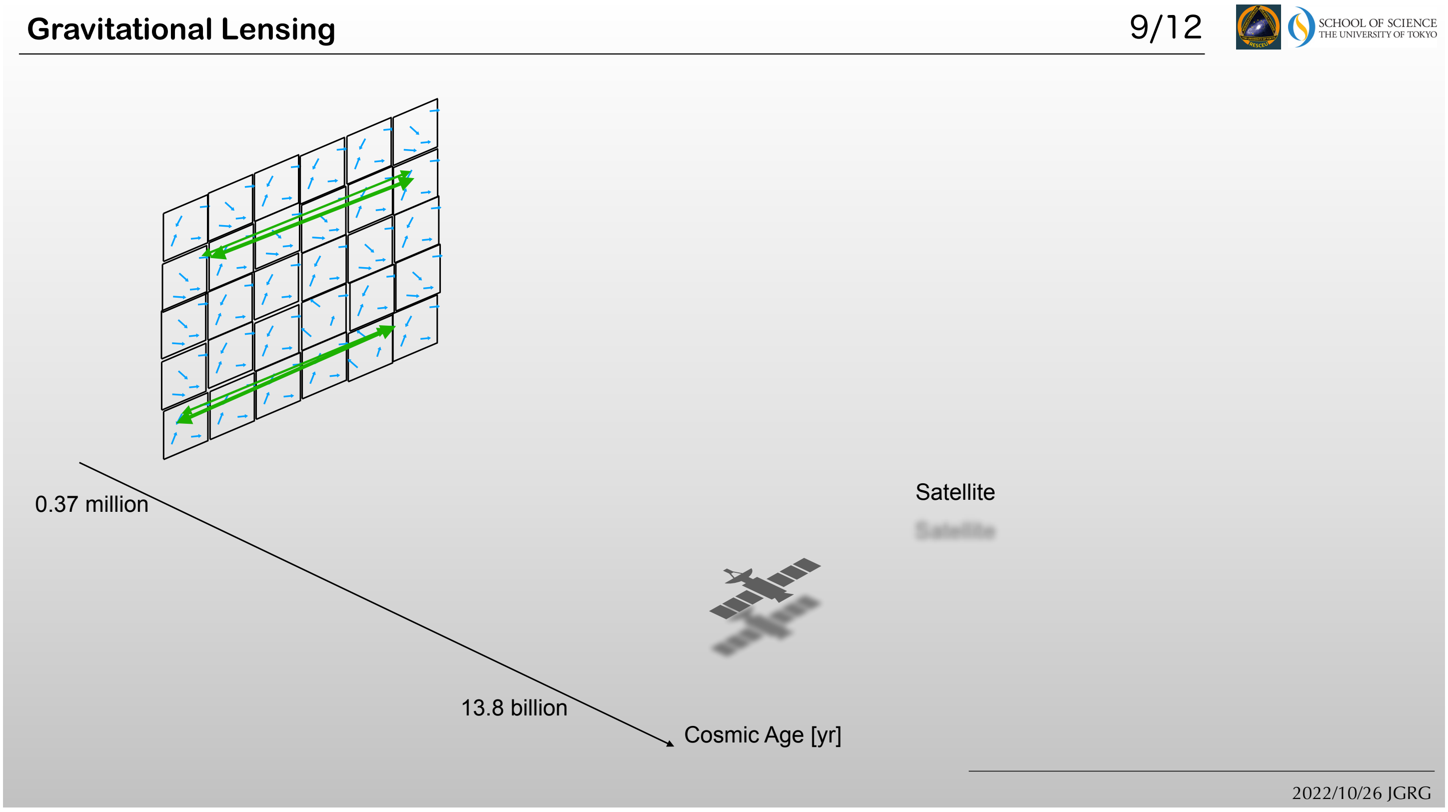

Gravitational Lensing

0.37 million

Satellite

13.8 billion

Cosmic Age [yr]

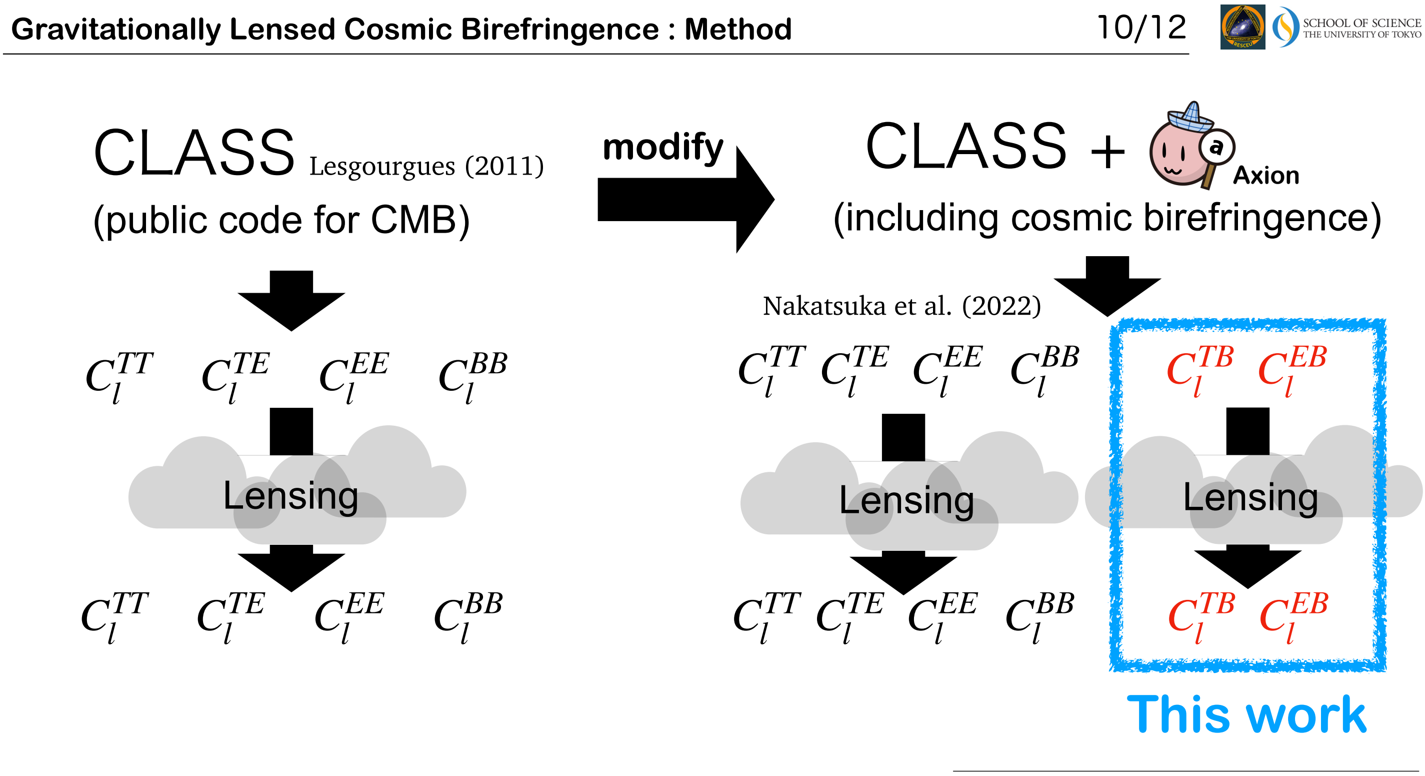

Gravitationally Lensed Cosmic Birefringence : Method

CLASS Lesgourgues (2011)
(public code for CMB)

C_l^{TT} C_l^{TE} C_l^{EE} C_l^{BB}

Lensing

C_l^{TT} C_l^{TE} C_l^{EE} C_l^{BB}

modify

CLASS + Axion
(including cosmic birefringence)

Nakatsuka et al. (2022)

C_l^{TT} C_l^{TE} C_l^{EE} C_l^{BB}

Lensing

C_l^{TT} C_l^{TE} C_l^{EE} C_l^{BB}

C_l^{TB} C_l^{EB}

Lensing

C_l^{TB} C_l^{EB}

This work

Summary & Prospects

Summary

- Cosmic Birefringence can be a clue to new physics.
- Now, precise theoretical predictions are needed.
- I've developed a lensing correction tool,
  which will becomes important in the near future.

Prospects (about lensing correction)

- Doing forecasts for future observations using my developing code.
- Seeking unique behaviors of lensed C_l^{EB} or C_l^{TB}

Hubble tension and local environment of SNe Ia host galaxies

Shao-Jiang Wang

2022-10-26 16:25-16:40 (JST)
JGRG31@ Tokyo University
Based on arXiv:2209.14732

“First detection of the Hubble variation correlation and its scale dependence”

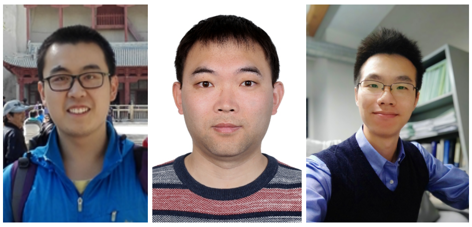

Wang-Wei Yu **Li Li** **Shao-Jiang Wang**

Hubble tension

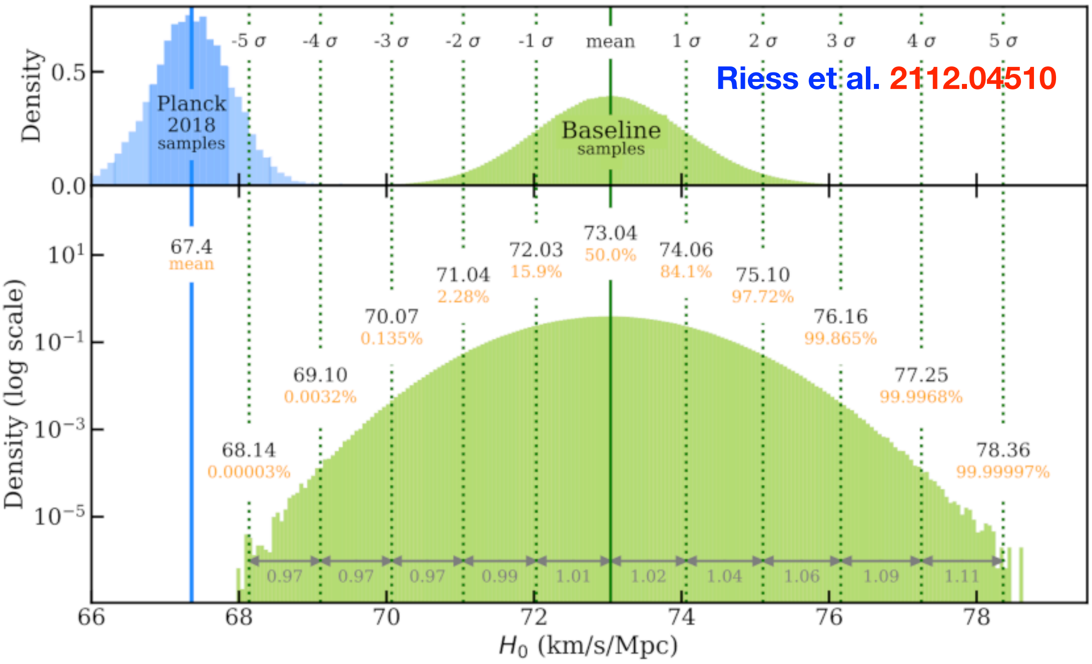

67 → 73 **New physics?** 67 ← 73

Modified early/&late Universe **Unknown local systematics**

Hubble variation

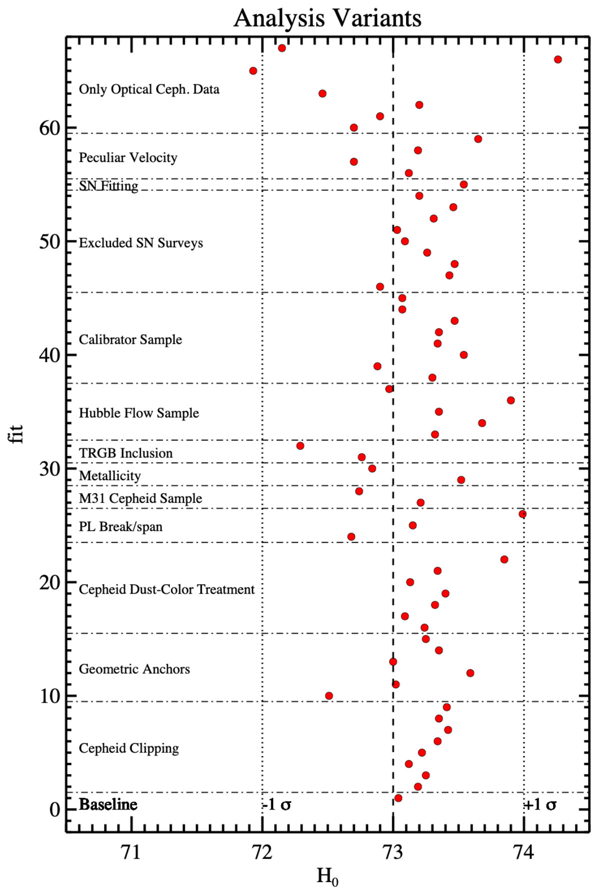

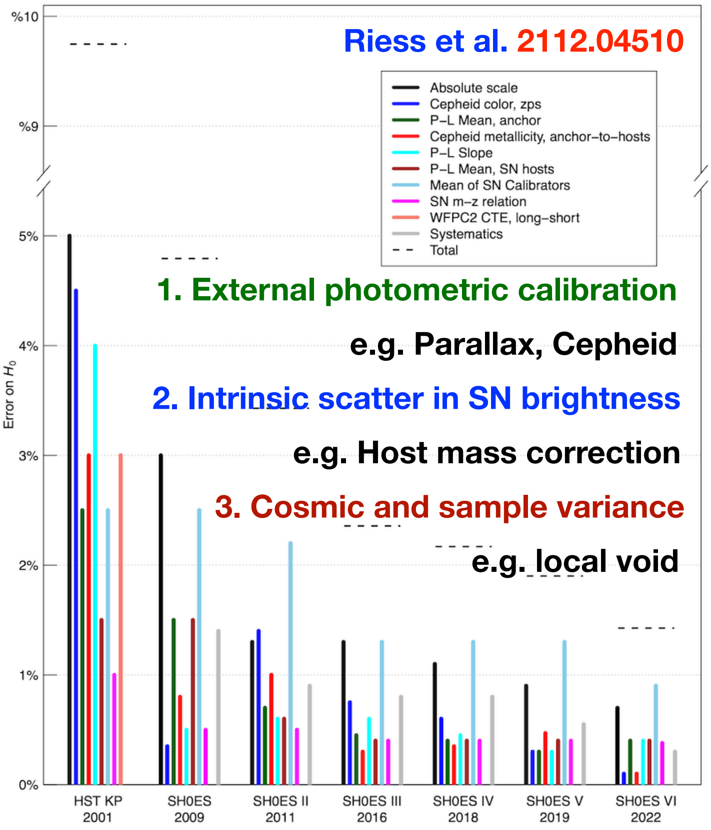

Riess et al. 2112.04510

1. External photometric calibration

e.g. Parallax, Cepheid

2. Intrinsic scatter in SN brightness

e.g. Host mass correction

3. Cosmic and sample variance

e.g. local void

Hubble variation

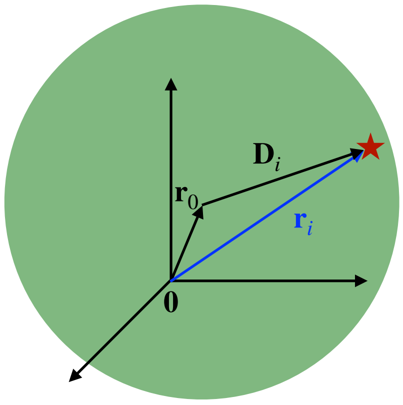

Local H0 Measurement

$$c\tilde{z}_i^{\rm cos} \equiv (cz_i - c\tilde{z}_i^{\rm pec}) = H_0^{\rm bac} D_i + \mathbf{\Delta v}_i \cdot \hat{\mathbf{D}}_i$$

$$\Rightarrow H_0^{\rm loc} = H_0^{\rm bac} + \frac{\mathbf{\Delta v}_i \cdot \hat{\mathbf{D}}_i}{D_i} \neq H_0^{\rm bac}$$

Hubble variation $H_0^{\rm loc} = cz_i/D_i$

$$\delta_H(\mathbf{r}_0; \{\mathbf{r}_i\}) \equiv \frac{H_0^{\rm loc} - H_0^{\rm bac}}{H_0^{\rm bac}} = \frac{\mathbf{v}_i \cdot (\mathbf{r}_i - \mathbf{r}_0)}{H_0^{\rm bac} |\mathbf{r}_i - \mathbf{r}_0|^2}$$

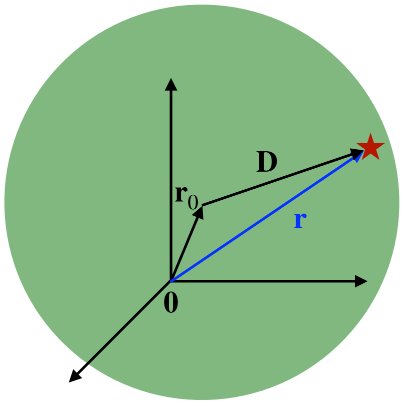

Continuous sample

$$\bar{\delta}_H(\mathbf{r}_0; B_R^3(\mathbf{r}_0)) = \frac{1}{H_0^{\rm bac}} \int \mathrm{d}^3\mathbf{r} \frac{\mathbf{v}(\mathbf{r}) \cdot (\mathbf{r} - \mathbf{r}_0)}{|\mathbf{r} - \mathbf{r}_0|^2} W_R(\mathbf{r} - \mathbf{r}_0)$$

Window function $W_R(\mathbf{D} \equiv \mathbf{r} - \mathbf{r}_0) = \Theta(R - D) \Big/ \left(\frac{4}{3}\pi R^3\right)$

Hubble variation

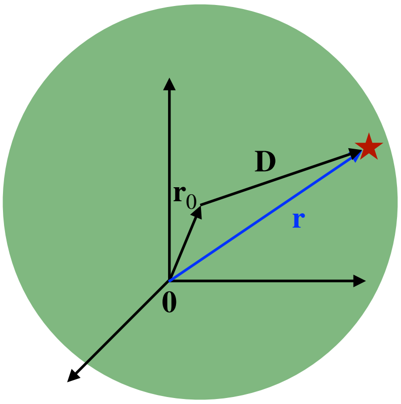

Local ball

$$\bar{\delta}_H(\mathbf{r}_0; B_R^3(\mathbf{r}_0)) = f(\Omega_\mathrm{m}) \int \mathrm{d}^3\mathbf{D}\, \delta_\mathrm{m}(\mathbf{r}_0 + \mathbf{D}) W_R(\mathbf{D}) \ln \frac{D}{R}$$

Local position $0 < D < R \to 0 : \delta_\mathrm{m}(\mathbf{r}_0 + \mathbf{D}) \to \delta_\mathrm{m}(\mathbf{r}_0)$

$$\bar{\delta}_H(\mathbf{r}_0; B_{R\to 0}^3(\mathbf{r}_0)) = f(\Omega_\mathrm{m})\delta_\mathrm{m}(\mathbf{r}_0) \int_0^R \frac{4\pi D^2 \mathrm{d}D}{\frac{4}{3}\pi R^3} \ln \frac{D}{R} = -\frac{f(\Omega_\mathrm{m})}{3}\delta_\mathrm{m}(\mathbf{r}_0)$$

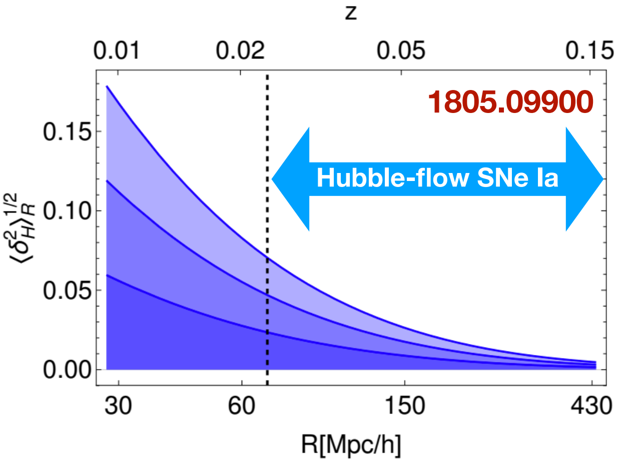

Turner, Cen, Ostriker (TCO 1992)
Xiang-Dong Shi et al 1996 Shi & Turner 9707101
Yun Wang, Spergel, Turner 9708014

Implications

local void $\delta_\mathrm{m}(\mathbf{r}_0) < 0 \Rightarrow \bar{\delta}_H(\mathbf{r}_0; B_{R\to 0}^3(\mathbf{r}_0)) > 0$

Sample selection $R > 70$ **Mpc/h** $\Leftrightarrow z > 0.023$

Observational tests

Hubble variation at r0 from a local ball at r0 leads to a local slope

$$K_\mathrm{local} = \frac{\bar{\delta}_H(\mathbf{r}_0; B_R^3(\mathbf{r}_0))}{\bar{\delta}_\mathrm{m}^R(\mathbf{r}_0)} = f(\Omega_\mathrm{m}) \frac{\int \mathrm{d}^3\mathbf{D}\, \delta_\mathrm{m}(\mathbf{r}_0 + \mathbf{D}) W_R(\mathbf{D}) \ln D/R}{\int \mathrm{d}^3\mathbf{D}\, \delta_\mathrm{m}(\mathbf{r}_0 + \mathbf{D}) W_R(\mathbf{D})}$$

the probability $p(\delta_\mathrm{m}, R)$ **for the density contrast field** $\delta_\mathrm{m}(\mathbf{r}_0 + \mathbf{D})$ **to take a given value** δ_m **within** R

$$p(\delta_\mathrm{m}, R) = \frac{1}{\sqrt{2\pi\sigma_R^2}} e^{-\frac{\delta_\mathrm{m}^2}{2\sigma_R^2}} \qquad \sigma_R^2 = \int \frac{k^2 \mathrm{d}k}{2\pi^2} P(k) \left[\frac{3 j_1(kR)}{kR}\right]^2$$

One can define a statistical local slope

$$\langle K_\mathrm{local} \rangle = f(\Omega_\mathrm{m}) \frac{\int \mathrm{d}^3\mathbf{D} \int \mathrm{d}\delta_\mathrm{m}\, \delta_\mathrm{m} p(\delta_\mathrm{m}, R) W_R(\mathbf{D}) \ln D/R}{\int \mathrm{d}^3\mathbf{D} \int \mathrm{d}\delta_\mathrm{m}\, \delta_\mathrm{m} p(\delta_\mathrm{m}, R) W_R(\mathbf{D})} = -\frac{1}{3} f(\Omega_\mathrm{m})$$

There is only one point $(\bar{\delta}_\mathrm{m}^R(\mathbf{r}_0), \bar{\delta}_H(\mathbf{r}_0; B_R^3(\mathbf{r}_0)))$ **for a given** R, **not enough to fit this local slope**

→ **averaging over** $(\bar{\delta}_\mathrm{m}^R(\mathbf{r}_i), \bar{\delta}_H(\mathbf{r}_i; B_R^3(\mathbf{r}_i)))$

Observational test

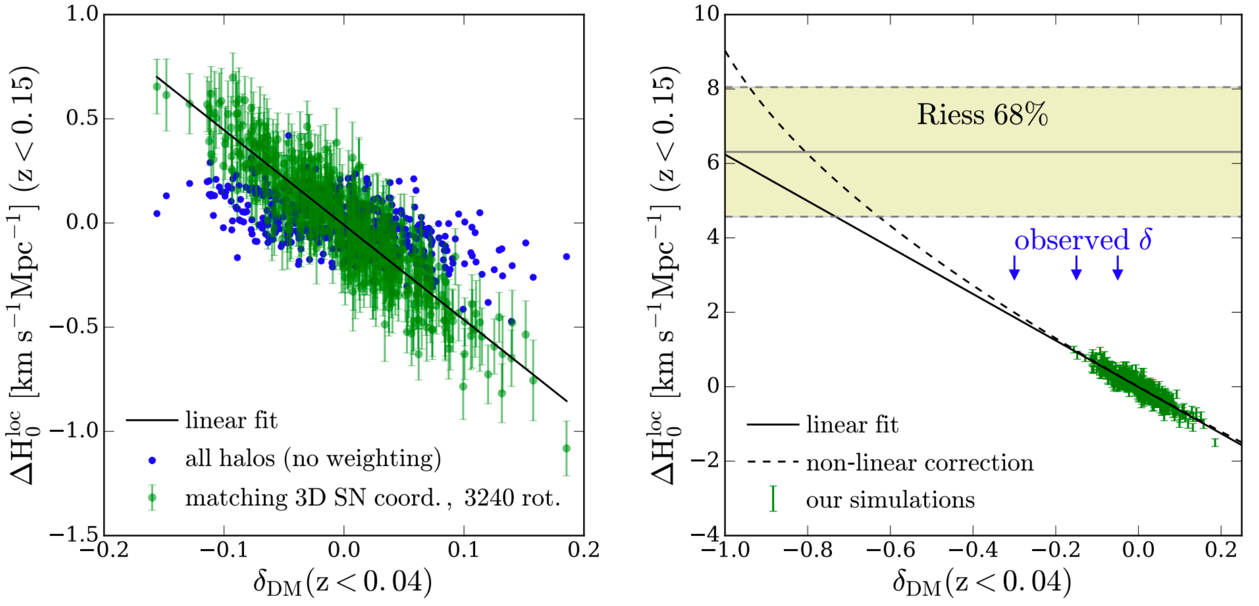

Figure 4. Correlation between $\Delta H_0^{\rm loc}$ for $z_{\rm max} = 0.15$ (corresponding to the SN sample) and dark matter density contrast δ for $z_{\rm max} = 0.04$ (corresponding to the distance scale for local density measurements); both are measured from 512 sub-volumes of the Dark Sky simulations. *Left*: $\Delta H_0^{\rm loc}$ measurements from matching the 3D coordinates of SNe and haloes in sub-volumes (green points with error bars), compared to inference from all haloes in sub-volumes (blue points). The error bars on the green points reflect the variances from rotations of the SN coordinate system within each sub-volume. The solid line shows the linear fit to the green points. *Right*: zoomed-out version of the left-hand panel. We additionally mark the location of several δ values from observations, as well as the 1-σ range favoured by the R16 analysis. We note that none of the observations of δ can account for the 6 km s^{-1}Mpc^{-1} difference between $H_0^{\rm loc}$ and $H_0^{\rm CMB}$.

Hao-Yi Wu & Dragan Huterer 1706.09723

Hubble variation from distant discrete sample

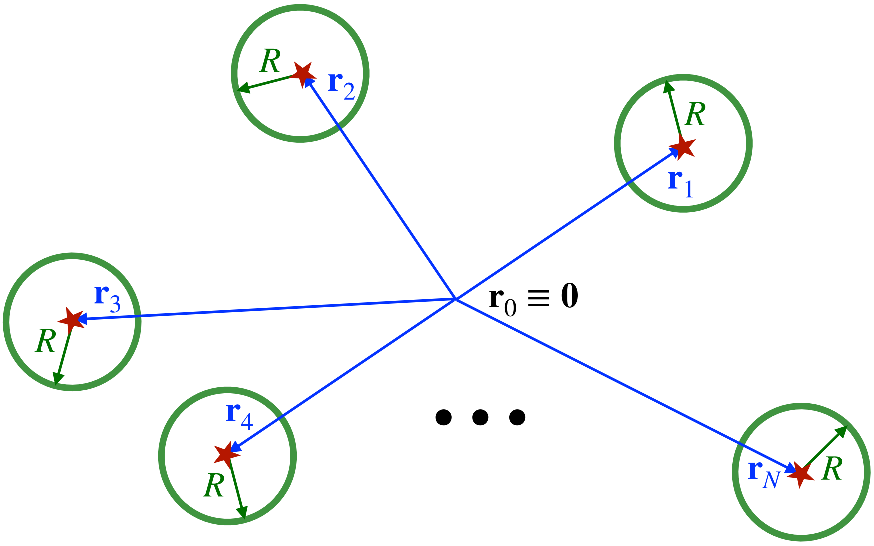

$$\bar{\delta}_H(\mathbf{0}; \{\mathbf{r}_i \,|\, r_i \gg R\}) \equiv \frac{1}{N}\sum_{i=1}^{N} \frac{\mathbf{v}(\mathbf{r}_i)\cdot\mathbf{r}_i}{H_0^{\rm bac} r_i^2} \approx \frac{1}{N}\sum_{i=1}^{N}\left[\bar{\delta}_H(\mathbf{0}; S_R^2(\mathbf{r}_i)) + \frac{f(\Omega_{\rm m})}{3}\bar{\delta}_{\rm m}^{\rm lin}(\mathbf{r}_i)\frac{R^2}{r_i^2}\right]$$

$$\approx \frac{1}{N}\sum_{i=1}^{N}\left[-\frac{f(\Omega_{\rm m})}{3}\bar{\delta}_{\rm m}^{R}(\mathbf{r}_i)\frac{R^2}{r_i^2} + \frac{f(\Omega_{\rm m})}{3}\bar{\delta}_{\rm m}^{\rm lin}(\mathbf{r}_i)\frac{R^2}{r_i^2}\right]$$

$$\equiv -\frac{f}{3}\left\langle \left[\bar{\delta}_{\rm m}^{R}(\mathbf{r}_i) - \bar{\delta}_{\rm m}^{\rm lin}(\mathbf{r}_i)\right]\frac{R^2}{r_i^2}\right\rangle_i$$

Hubble variation correlation

Hubble variation from an arbitrary discrete sample of distant SNe Ia (firstly derived)

$$\bar{\delta}_H(\mathbf{0};\{\mathbf{r}_i\,|\,r_i \gg R\}) \approx -\frac{f}{3}\left\langle \left[\bar{\delta}^R_{\rm m}(\mathbf{r}_i)-\bar{\delta}^{\rm lin}_{\rm m}(\mathbf{r}_i)\right]\frac{R^2}{r_i^2}\right\rangle_i$$

Selecting distant SNe Ia with the same ambient density contrast at a scale R

$$\bar{\delta}_H(\mathbf{0};\{\mathbf{r}_i\,|\,\bar{\delta}^R_{\rm m}(\mathbf{r}_i)=\delta^R_{\rm m}\}) \approx -\frac{f(\Omega_{\rm m})}{3}\left\langle\frac{R^2}{r_i^2}\right\rangle_i \delta^R_{\rm m} \equiv -\frac{f}{3}Q$$

$$K_{\rm non-local} \equiv \frac{\bar{\delta}_H(\mathbf{0};\{\mathbf{r}_i\,|\,\bar{\delta}^R_{\rm m}(\mathbf{r}_i)=\delta^R_{\rm m}\})}{\delta^R_{\rm m}} = -\frac{f}{3}\left\langle\frac{R^2}{r_i^2}\right\rangle_i \equiv -\frac{f}{3}Q$$

There are enough data points to fit this non-local slope by selecting different discrete samples of distant SNe Ia with different ambient density contrasts at the same scale R

Observational tests

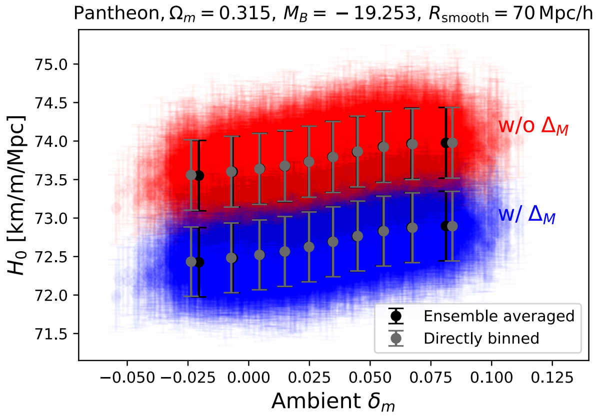

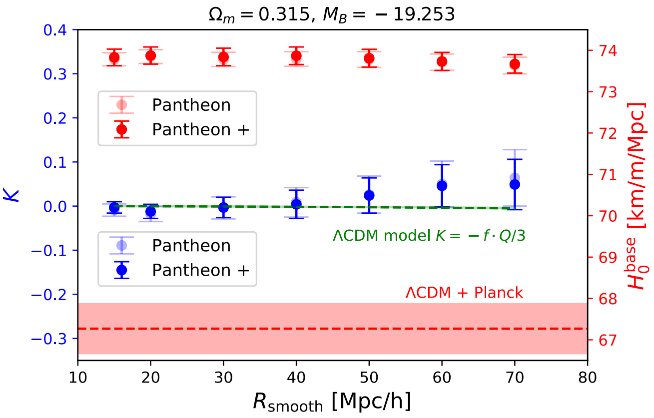

Density field of I-th ensemble $\delta^I_{\rm m}(\mathbf{r}_i) \equiv \frac{\rho^I_{\rm m}(\mathbf{r}_i)-\bar{\rho}_{\rm m}}{\bar{\rho}_{\rm m}}, I = 1,\cdots,N$

Ambient density contrast from I-th ensemble

$$\bar{\delta}^I_{\rm m}(\mathbf{d}_i) = \frac{1}{m_i}\sum_{j=1}^{m_i}\delta^I_{\rm m}(\mathbf{r}_j(\mathbf{d}_i)) \qquad |\mathbf{r}_j(\mathbf{d}_i)-\mathbf{d}_i|^2 < R^2$$

Put all SNe in an ascending order

$$\bar{\delta}^I_{\rm m}(\mathbf{d}_{P^I_1}) \le \bar{\delta}^I_{\rm m}(\mathbf{d}_{P^I_2}) \le \cdots \le \bar{\delta}^I_{\rm m}(\mathbf{d}_{P^I_n})$$

Ambient density contrast of k-th group

$$\langle\bar{\delta}^I_{\rm m}\rangle_k \equiv \frac{1}{100}\sum_{j=1}^{100}\bar{\delta}^I_{\rm m}(\mathbf{d}_{P^I_{j+(k-1)s}})$$

Ensemble averaged H0 from k-th group

$$\overline{H}_0\left(\langle\bar{\delta}_{\rm m}\rangle_k \equiv \frac{1}{N}\sum_{I=1}^{N}\langle\bar{\delta}^I_{\rm m}\rangle_k\right) \equiv \frac{1}{N}\sum_{I=1}^{N}H_0(\langle\bar{\delta}^I_{\rm m}\rangle_k)$$

Slope $\delta_H \equiv \frac{\overline{H}_0(\langle\bar{\delta}_{\rm m}\rangle_k)-H_0^{\rm base}}{H_0^{\rm base}} = K\langle\bar{\delta}_{\rm m}\rangle_k$

Conclusions and discussions

1. We have derived for the first time a theoretical estimation for our local Hubble variation from an arbitrary discrete sample of distant SNe Ia

2. We have found a residual linear correlation between our local Hubble constants fitted from different groups of SNe and their corresponding ambient density contrast of SN-host galaxies at a given scale

3. This residual linear trend becomes more and more positively correlated with the ambient density contrasts of SN-host galaxies estimated at larger and larger scales, on the contrary to but still marginally consistent with the theoretical expectation from the LCDM model

4. This might indicate some unknown corrections to the peculiar velocity of the SN-host galaxy from the density contrasts at larger scales or the smoking gun for the new physics

Thank you

JGRG31 Workshop

October 27, 2022

Cosmology with cross-correlation of Gravitational Waves

Lorenzo Valbusa Dall'Armi

Third-year PhD Student in Padova, Italy

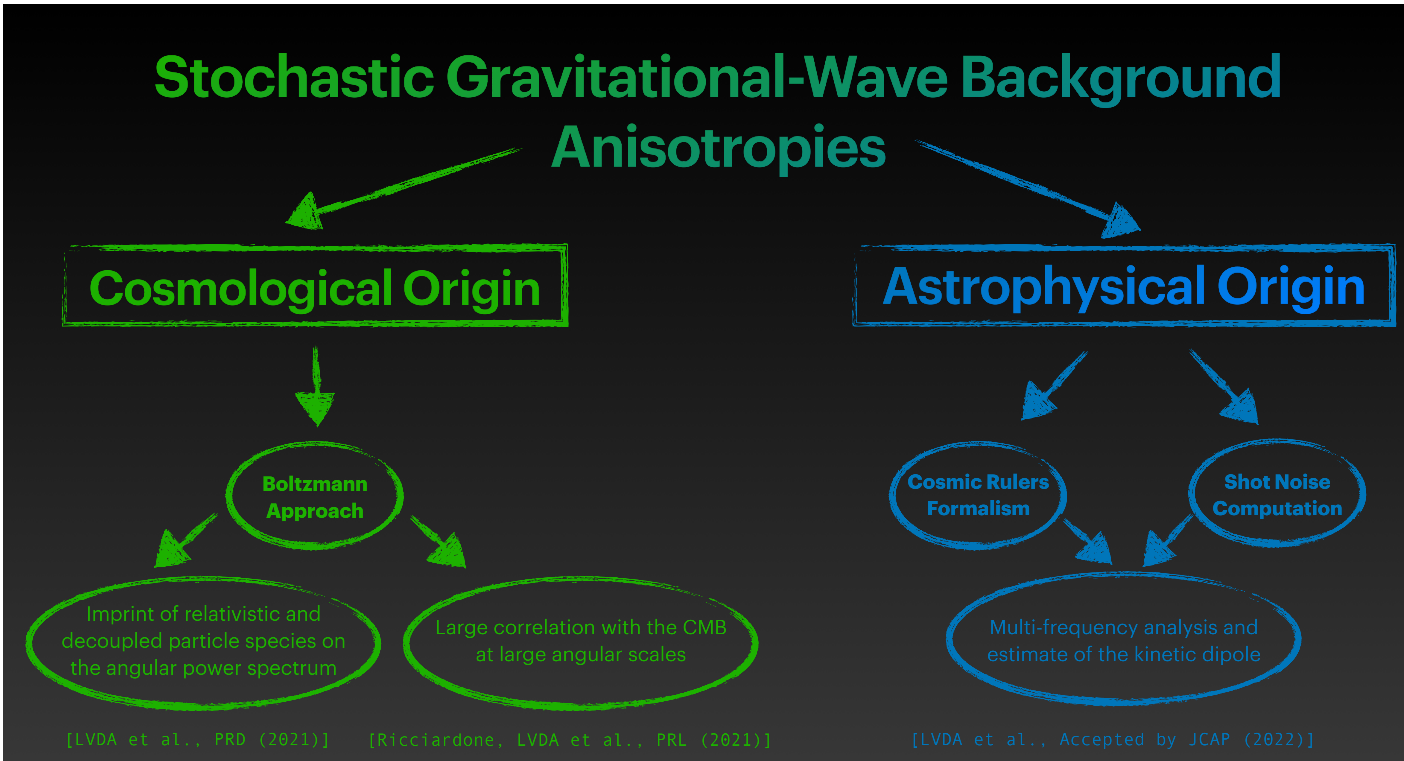

Stochastic Gravitational-Wave Background Anisotropies

Cosmological Origin

Boltzmann Approach

Imprint of relativistic and decoupled particle species on the angular power spectrum

Large correlation with the CMB at large angular scales

[LVDA et al., PRD (2021)]

[Ricciardone, LVDA et al., PRL (2021)]

Astrophysical Origin

Cosmic Rulers Formalism

Shot Noise Computation

Multi-frequency analysis and estimate of the kinetic dipole

[LVDA et al., Accepted by JCAP (2022)]

Cosmological Background

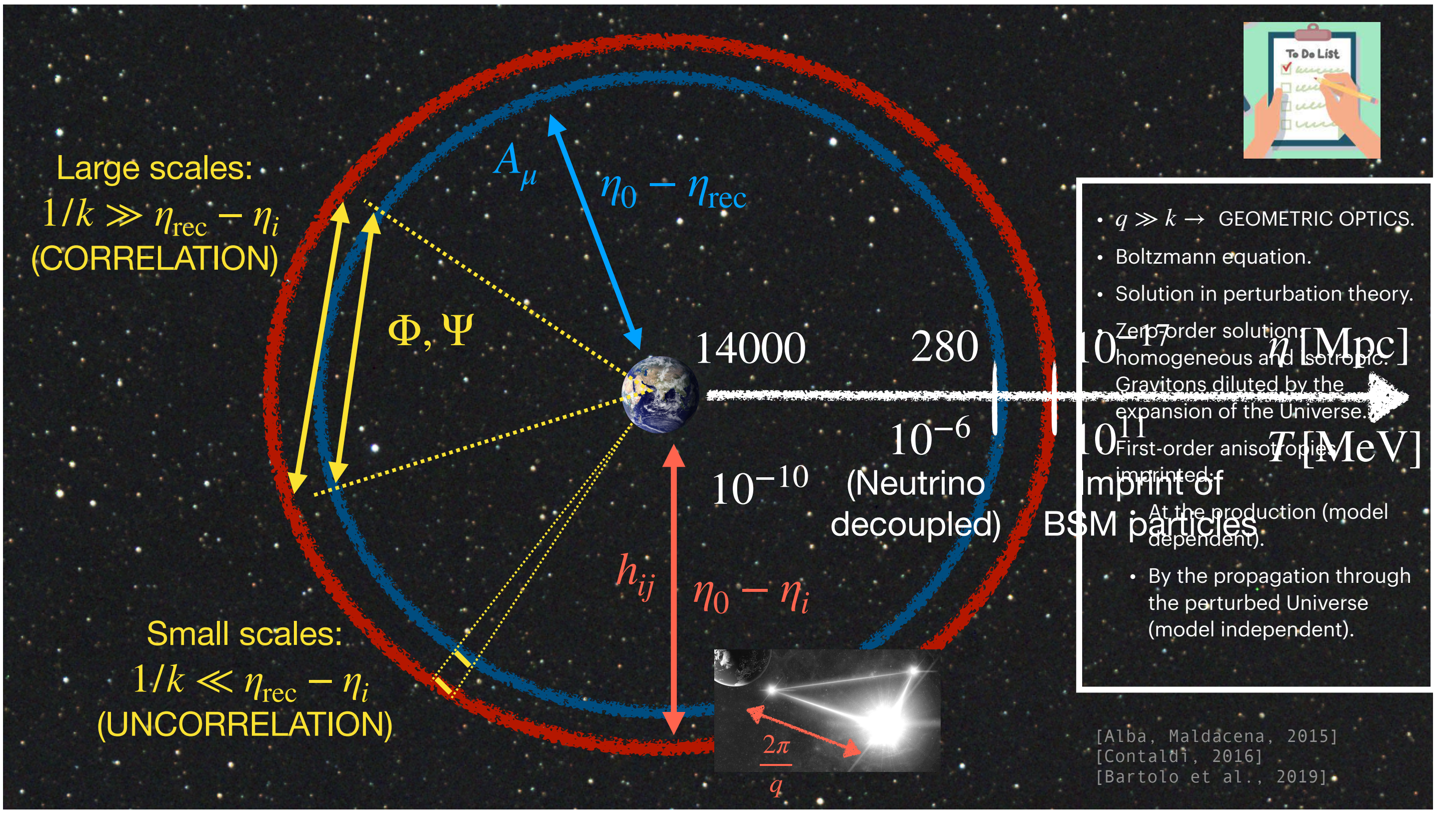

- $q \gg k \rightarrow$ GEOMETRIC OPTICS.
- Boltzmann equation.
- Solution in perturbation theory.
- Zero-order solution: homogeneous and isotropic. Gravitons diluted by the expansion of the Universe.
- First-order anisotropies imprinted:
  - At the production (model dependent).
  - By the propagation through the perturbed Universe (model independent).

[Alba, Maldacena, 2015]
[Contaldi, 2016]
[Bartolo et al., 2019]

CGWB Angular Power Spectrum

- The angular power spectrum is the sum of three contributions:

- $$C_{\ell,I}^{\mathrm{CGWB}}(\eta_0) = \int_0^{+\infty} \frac{dk}{k} P(k) \left[\int_{\eta_i}^{\eta_0} d\eta j_\ell [k(\eta_0 - \eta)] \underbrace{\boxed{T_\Gamma(\eta_i, k)}}_{\rightarrow\ \mathrm{SW}} \right]^2$$

- $$C_{\ell,S}^{\mathrm{CGWB}}(\eta_0) = \int_0^{+\infty} \frac{dk}{k} P(k) \left\{ \int_{\eta_i}^{\eta_0} d\eta j_\ell [k(\eta_0 - \eta)] \left[\underbrace{\boxed{T_\Phi(\eta, k)\delta(\eta - \eta_i)}}_{\rightarrow\ \mathrm{SW}} + \underbrace{\boxed{T'_\Phi(\eta, k) + T'_\Psi(\eta, k)}}_{\rightarrow\ \mathrm{ISW}} \right] \right\}^2$$

- $$C_{\ell,T}^{\mathrm{CGWB}}(\eta_0) = \int_0^{+\infty} \frac{dk}{k} P(k) \left[\int_{\eta_i}^{\eta_0} d\eta \frac{1}{4} \sqrt{\frac{(\ell + 2)!}{(\ell - 2)!}} j_\ell [k(\eta_0 - \eta)] \underbrace{\boxed{T'_h(\eta, k)}}_{\rightarrow\ \mathrm{ISW}} \right]^2$$

SW

ISW

IMPRINT OF BEYOND STANDARD MODEL PARTICLES

- At large angular scales, the angular power spectrum is sensitive to the number of relativistic and decoupled particle species

$$C_\ell^{\mathrm{SW}} \sim T_\phi^2(\eta_i, k) \sim \left(1 + \frac{4}{15} f_{\mathrm{dec}}(\eta_i) \right)^{-2} .$$

- Observations of the CGWB anisotropies at different frequencies (i.e. at different initial times of propagation) could allow to reconstruct the timeline of the particle content of the Universe.

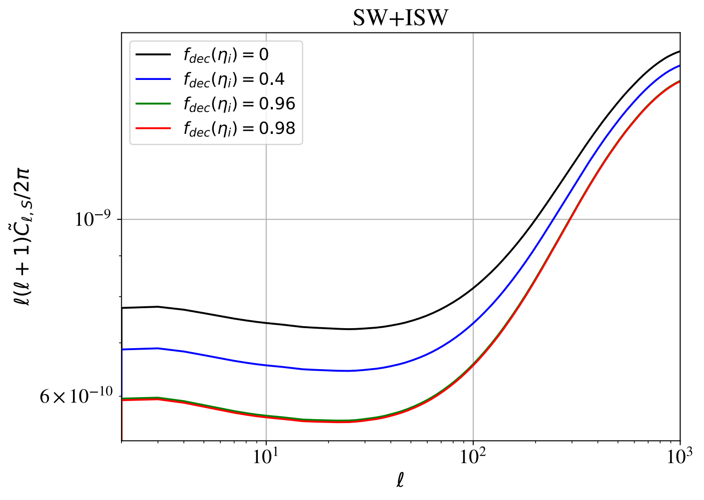

[LVDA et al., 2021]

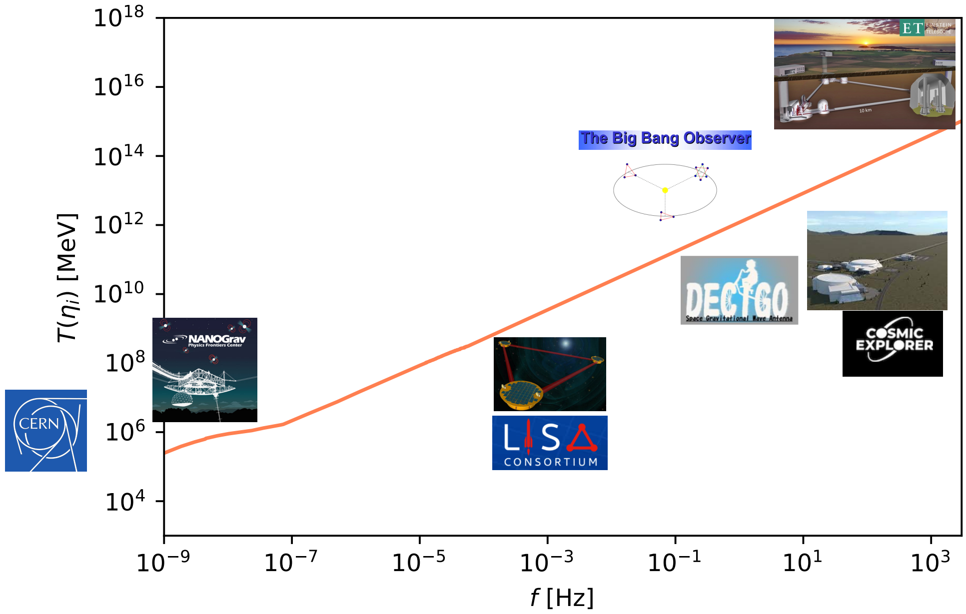

CGWB x CMB

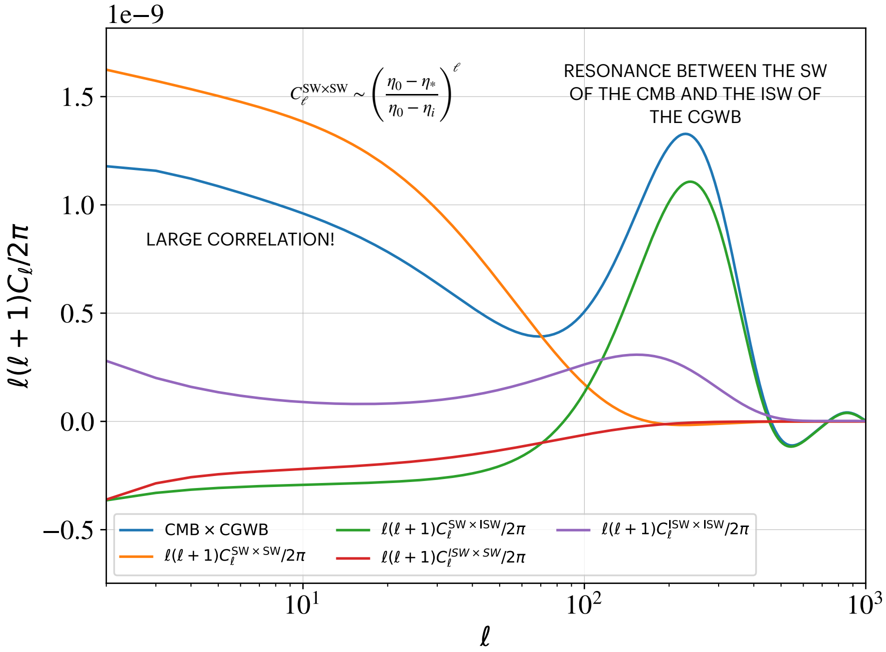

[Ricciardone, LVDA et al., 2021]

CONSTRAINED REALIZATIONS

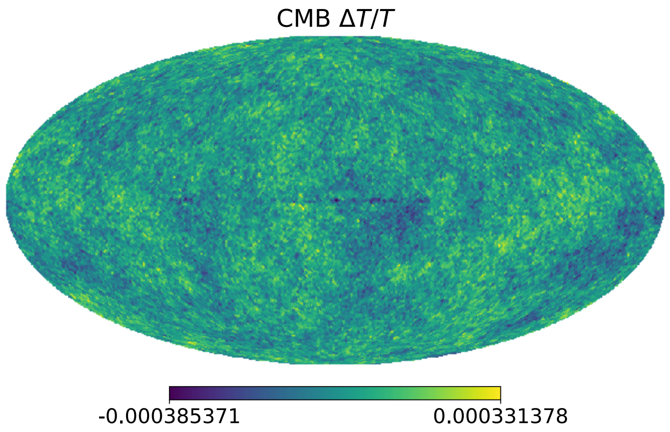

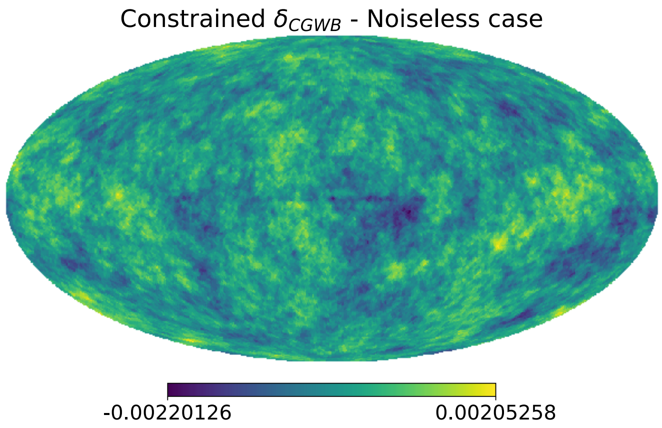

The CGWB map at large angular scales is univocally determined by the CMB one.

The constrained realizations can be used to test foreground or systematic contamination in the data.

[Ricciardone, LVDA et al., 2021]

Astrophysical Background

A BACKGROUND FROM UNRESOLVED SOURCES

- The energy density of the AGWB is obtained by summing all the contributions from GW unresolved sources along the past GW-cone,

$$\bar{\Omega}_{\rm AGWB}(f) = \frac{f^2}{\rho_{\rm crit}c^2}\int \frac{dz}{(1+z)H(z)}\int d\vec{\theta}\, p(\vec{\theta})\, w(\vec{\theta},z)\, R(z)\frac{dE}{df_e d\Omega_e}(\vec{\theta},f_e)\Big|_{f_e=(1+z)f}.$$

- The capability of the detector to resolve the sources has been taken into account in the window function w,

$$w(\vec{\theta},z) = \frac{\frac{dN_{\rm GW}}{d\vec{\theta}}(\vec{\theta},z,{\rm SNR}<{\rm SNR_{thr}})}{\frac{dN_{\rm GW}}{d\vec{\theta}}(\vec{\theta},z)},$$

where the signal-to-noise ratio has been computed by using

$$\mathrm{SNR} = \sqrt{4\int df\,\frac{|h(f)|^2}{N(f)}}.$$

Population of BBH

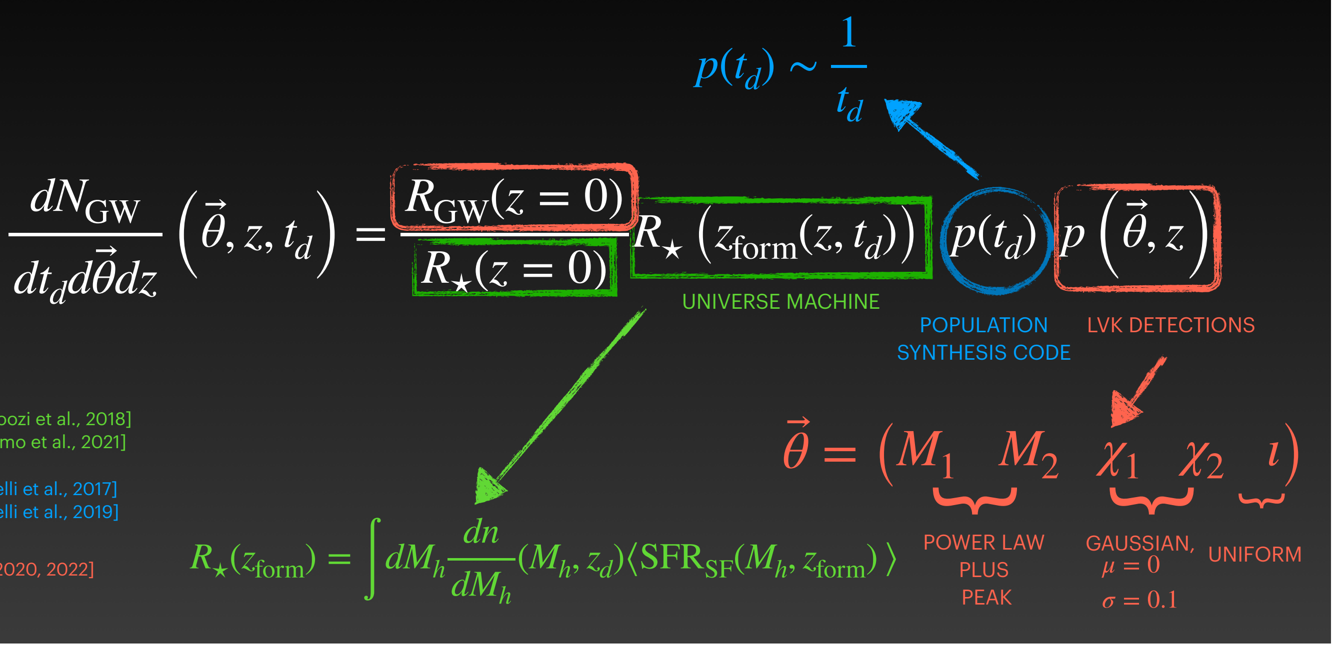

$$p(t_d) \sim \frac{1}{t_d}$$

$$\frac{dN_{\rm GW}}{dt_d d\vec{\theta} dz}\left(\vec{\theta},z,t_d\right) = \frac{\boxed{R_{\rm GW}(z=0)}}{\boxed{R_\star(z=0)}}\boxed{R_\star\left(z_{\rm form}(z,t_d)\right)}\,\boxed{p(t_d)}\,\boxed{p\left(\vec{\theta},z\right)}$$

UNIVERSE MACHINE

POPULATION
SYNTHESIS CODE

LVK DETECTIONS

$$\vec{\theta} = \left(\underbrace{M_1 \quad M_2}\ \ \underbrace{\chi_1 \quad \chi_2}\ \ \underbrace{\iota}\right)$$

POWER LAW
PLUS
PEAK

GAUSSIAN,
$\mu = 0$
$\sigma = 0.1$

UNIFORM

$$R_\star(z_{\rm form}) = \int dM_h \frac{dn}{dM_h}(M_h, z_d)\langle {\rm SFR_{SF}}(M_h, z_{\rm form})\rangle$$

[Behroozi et al., 2018]
[Bellomo et al., 2021]

[Mapelli et al., 2017]
[Mapelli et al., 2019]

[LVK 2020, 2022]

Contributions to the anisotropies

- There are three contributions to the AGWB anisotropies: the intrinsic, the kinetic and the shot noise fluctuations.
- The intrinsic anisotropies are due to clustering, to the relative velocity of the sources and to the metric perturbations.
- The kinematic dipole is induced by the observer motion w.r.t. the rest frame of the sources.
- The AGWB is generated by discrete sources, which are distributed according to a Poisson PDF, therefore shot noise fluctuations in the sky are expected.

[Cusin et al., 2018]
[Bertacca et al., 2019]

[Cusin, Tasinato, 2022]
[LVDA et al., 2022]
[Chung et al., 2022]

[Jenkins, Romano, Sakellariadou, 2019]
[Jenkins, Sakellariadou, 2019]
[Alonso et al., 2020]
[Bellomo et al. 2021]

Kinetic Dipole

Many estimates of our peculiar velocity from many independent probes

Tensions between the estimates from different surveys (plus CMB anomalies)

$\vec{v}_{\rm LSS} \neq \vec{v}_{\rm CMB}$?

Add the AGWB as another, independent, observable, with:
- Sky coverage almost equal to one;
- Many frequencies accessible, thus we can measure the signals produced by different kind of sources;
- Better component separation from shot noise and the intrinsic anisotropies.

[Planck, 2013]
[Gibelyou, Huterer, 2012]
[Rubart, Schwartz, 2013]
[Secrest, 2020]

The dipole at different frequencies

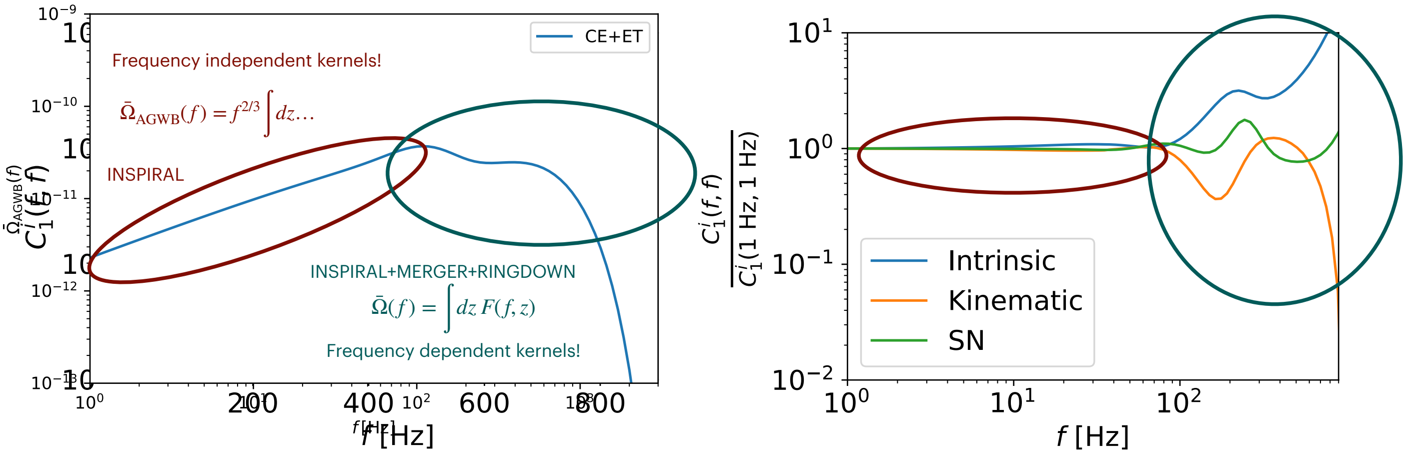

- The SN dominates the angular power spectrum of orders of magnitude.
- At small frequencies, the contributions to the anisotropies do not depend on the frequencies, but at larger frequencies (accessible by ET or CE) they exhibit different frequency shapes.

[LVDA et al., 2021]

Component Separation (without instrumental noise)

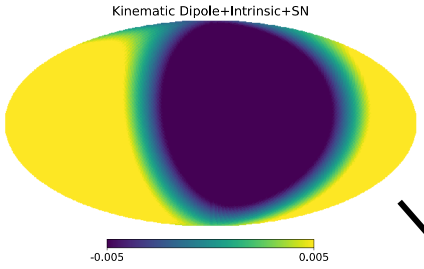

$\vec{d}_{\rm obs}(30\,{\rm Hz})$

"Hidden Contribution"

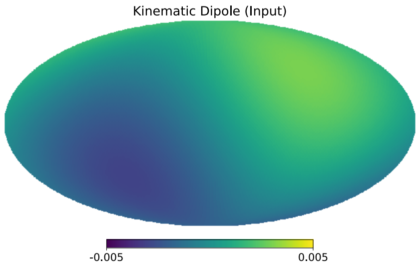

$\vec{d}_{\rm KD}(30\,{\rm Hz})$

Component Separation
with ILC

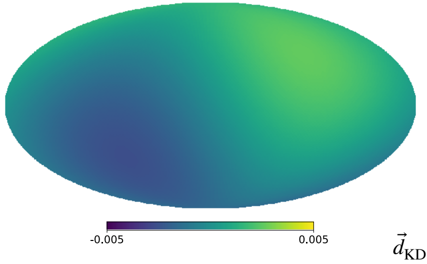

$\vec{d}_{\rm KD}(30\,{\rm Hz})$

✓ The reconstruction of the KD agrees with the input one ($\mathrm{SNR} \approx 10$)

[LVDA et al., 2021]

Component Separation (with instrumental noise)

- We define an estimator by multiplying the signals by some weights and by adding it a bias

$$\tilde{I}^{\rm KD}_{{\rm piv},\vartheta} = \sum_{A,B,f,f'} d_{f,A} E^{ff'}_{\vartheta,AB} d_{f',B} - b_\vartheta \,.$$

- We find E , b by imposing that the estimator is unbiased and by minimizing the covariance which comes not only from instrumental noise, but also from the contaminations of the other contributions to the signal (SN + intrinsic noise).

- The covariance we have found for our estimator of the dipole is

$$\mathrm{cov}_{ij} = \mathrm{cov}(v_{o,i}, v_{o,j}) = T_{\rm obs} \sum_\vartheta \Delta\Omega^2 \hat{n}^i_\vartheta \hat{n}^j_\vartheta \left(\frac{1}{\bar{\Omega}_{\rm AGWB}(f_{\rm piv})} \frac{4\pi^2 f^3}{3H_0^2} \right)^2 \mathrm{cov}_{\vartheta\vartheta'} \,,$$

Contribution canceled by the different shapes in frequency between the dipole and the SN

$$\mathrm{cov}_{\vartheta\vartheta'} = \underline{\frac{2\delta_{\vartheta\vartheta'}}{\sum_f \mathrm{Tr}\left(S_f^{-1} B^{\rm KD}_{f,\vartheta} S_f^{-1} B^{\rm KD}_{f,\vartheta}\right)}} + \delta_{\vartheta\vartheta'} \sum_{f,f',\vartheta''} \cancel{\frac{\mathrm{Tr}\left(S_f^{-1} B^{\rm KD}_{f,\vartheta''} S_f^{-1} B^{\rm KD}_{f,\vartheta'}\right) \mathrm{Tr}\left(S_{f'}^{-1} B^{\rm KD}_{f',\vartheta} S_{f'}^{-1} B^{\rm KD}_{f',\vartheta''}\right)}{\left[\sum_f \mathrm{Tr}\left(S_f^{-1} B^{\rm KD}_{f,\vartheta} S_f^{-1} B^{\rm KD}_{f,\vartheta}\right)\right]^2}} \frac{C^{\rm SN+int}_{ff'}}{\mathscr{E}^{\rm KD}_f \mathscr{E}^{\rm KD}_{f'}} \,.$$

The detection of the dipole depends just on the instrumental noise

[LVDA et al., 2021]

Improvements w.r.t. the standard approach

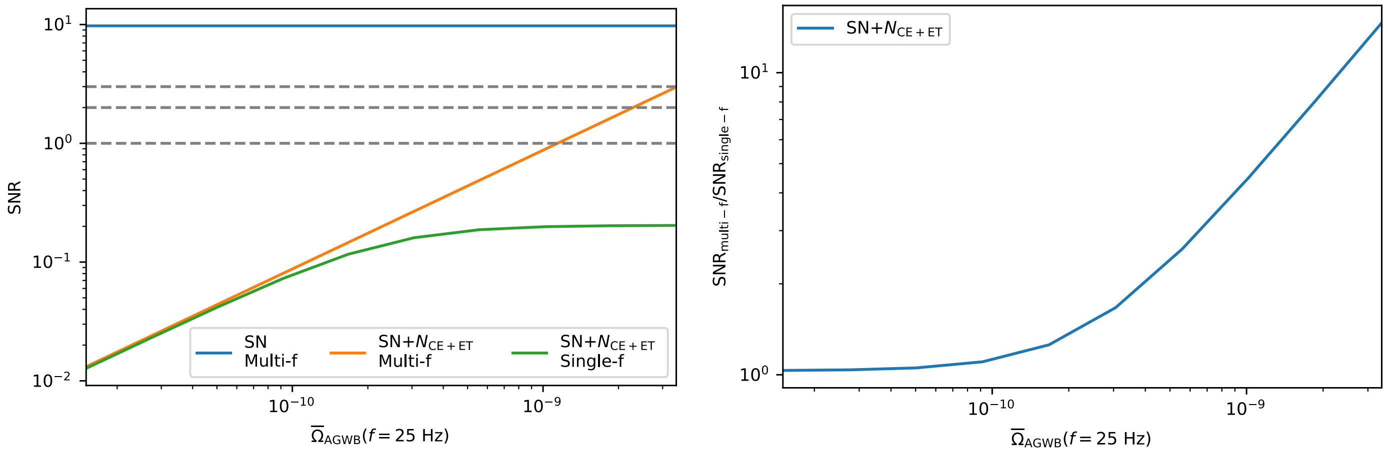

- Plot of the SNR of the kinematic dipole with the old (auto+cross) and the new technique (auto).
- With a multi-frequency analysis, we are able to increase, in the limit of low instrumental noise, the precision of the detection by an order of magnitude.

Summary

- The angular power spectrum of the cosmological background can constrain the fraction of relativistic and decoupled particle species at a different epochs (before BBN).
- The cross correlation between the CMB and the CGWB at large angular scales is almost one; this fact could be exploited in a future analysis of the anisotropies.

- By exploiting the frequency dependence of the anisotropies of the AGWB, we are able to separate the components that contribute to the total signal. An example is the cleaning of the kinematic dipole map w.r.t. the shot noise contamination.
- By using this new multi-frequency analysis, we are able to constrain the observer's motion with $\mathrm{SNR} \approx 3$ with the detector network ET+CE for a BBH signal consistent with the upper bounds of LVK.

THANK YOU
FOR YOUR ATTENTION

C55

Angular Correlations of the Inflationary Stochastic Gravitational-wave Background

Oct 27th, 2022
The 31st Workshop on General Relativity and Gravitation in Japan @The Univ. of Tokyo

Zhen-Yuan Wu, Ryo Saito, Nobuyuki Sakai (Yamaguchi University)

arXiv:2207.04669

Motivation

Primordial Gravitational-waves (PGWs)

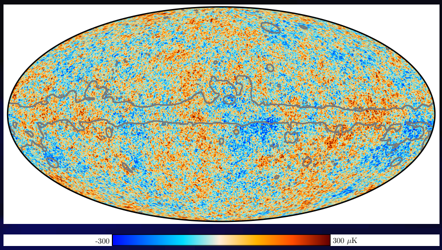

Credit: ESA & the Planck Collaboration

Cosmic Microwave Background
(CMB)

?

Stochastic Gravitational-wave Background
(SGWB)

- General prediction of inflation
- Observed as one kind of SGWB

⇨

Rich information about the early universe
&
Directly verify inflation

Difficulties in directly measuring the inflationary SGWB

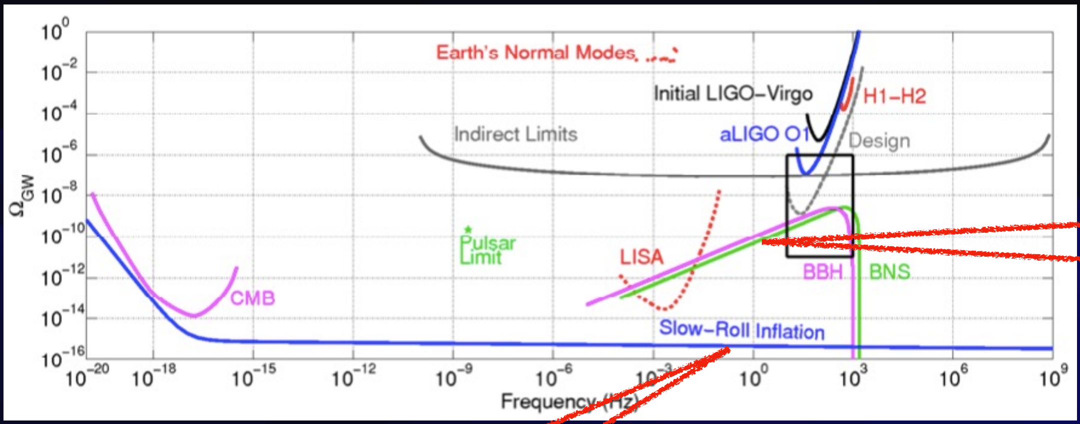

[Abbott, B. P. et al. Physical Review Letter (2017)]

easily covered by an *astrophysical background* (e.g. Binary Black-holes and Binary Neutron Stars)

predicted energy density is *weak*

Many studies on distinguishing SGWB

- Spectral separation

  Ungarelli & Vecchio, 04; Adams & Cornish, 14; Parida+, 16, Boileau+, 21; Poletli, 21, ...
- Spectral subtraction

  Regimbau+, 17; Pan & Yang, 20; Martinovic+, 21; Sachdev+, 20; ...
- Anisotropies

  Adshead+, 21; Bartolo+, 22; Malhotra+, 21; ...
- PGW polarizations

  Seto, 06; Seto, 09; Smith & Caldwell, 17; Domcke+, 19;…
- ***and more…***

These methods cannot guarantee that the *remaining component is from inflation* without *assuming an exact inflation model*.

This work asks:

Is there any *unique feature of the inflationary SGWB* without an *a priori assumption on the exact model*?

Results

Good news

- Yes, there is an unique angular correlation, the *antipodal angular correlation (AAC)* in the inflationary SGWB, resulting from the *standing-wave nature* after *horizon re-entry*.
- AAC is *not expected in the astrophysical SGWB* because the GWs are in the *sub-horizon region all the time*.

Bad news

- AAC is *not measurable* in direct GW observations under the standard assumptions *(statistically isotropic* or *Gaussian)*.
  - Strain correlation
  - Intensity correlation
  - Time-domain analysis

but intensity AAC is an indicator of statistical *anisotropic* inflation.

Antipodal Angular Correlation (AAC)

Characterizing the SGWB

- Plane wave expansion

random variables

$$h_{ij}(t,\mathbf{x}) = \sum_{P=+,-} \int_{-\infty}^{\infty} df \int_{S^2} d^2\hat{\mathbf{n}}\, \underbrace{h_P(f,\hat{\mathbf{n}})}_{\text{strain}}\, \underbrace{e^P_{ij}(\hat{\mathbf{n}})}_{\text{polarization tensors}}\, e^{-i\,2\pi f\,(t-\hat{\mathbf{n}}\cdot\mathbf{x})}$$

- Correlation Functions

$$\langle h^*_P(f,\hat{\mathbf{n}}_1)\, h_{P'}(f',\hat{\mathbf{n}}_2)\rangle$$

higher orders…

$= ?$ for the inflationary SGWB

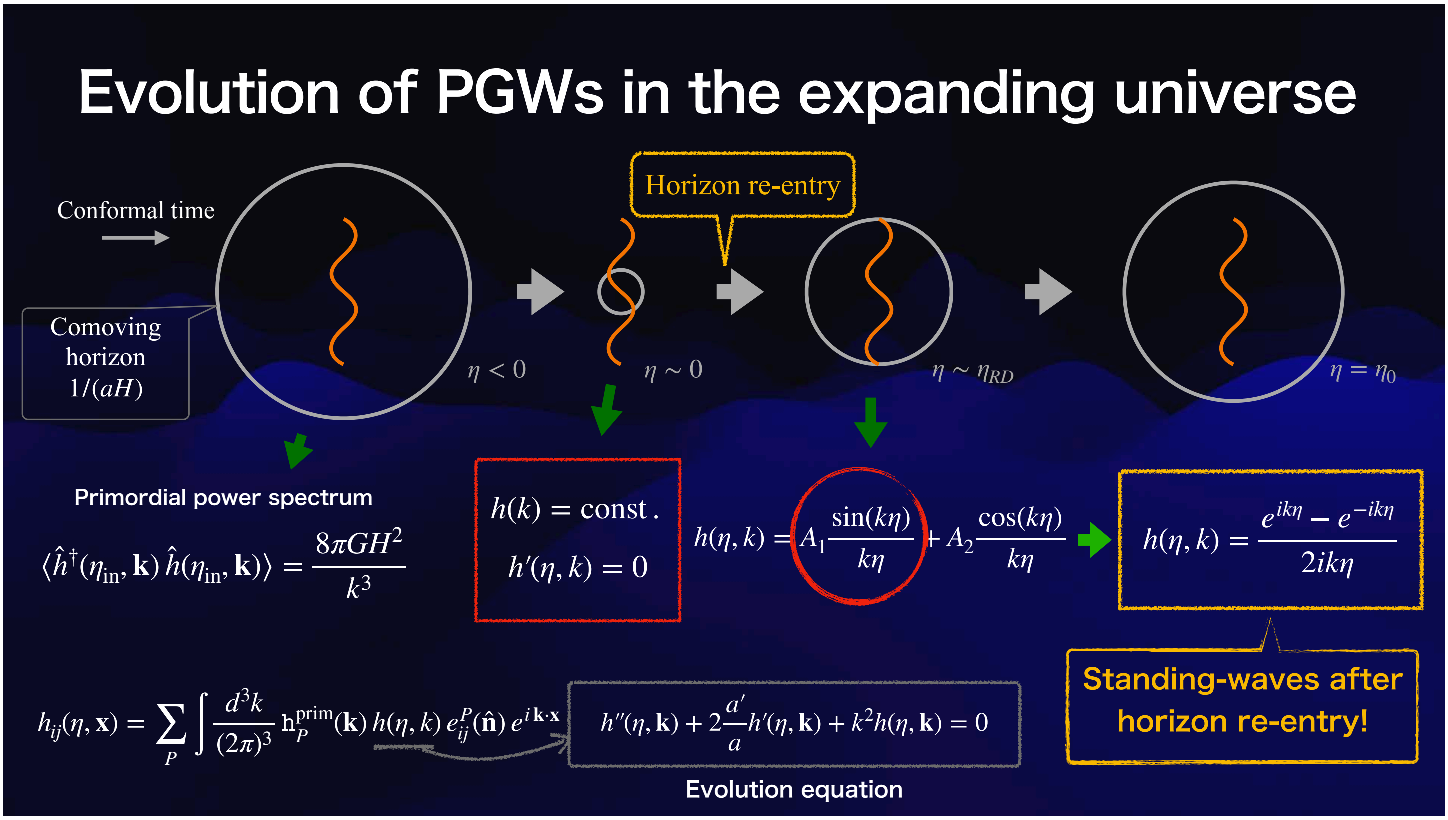

Evolution of PGWs in the expanding universe

Primordial power spectrum

$$\langle \hat{h}^\dagger(\eta_{\rm in}, \mathbf{k})\, \hat{h}(\eta_{\rm in}, \mathbf{k}) \rangle = \frac{8\pi G H^2}{k^3}$$

$$h(k) = \text{const}\,.$$

$$h'(\eta, k) = 0$$

$$h(\eta, k) = A_1 \frac{\sin(k\eta)}{k\eta} + A_2 \frac{\cos(k\eta)}{k\eta}$$

$$h(\eta, k) = \frac{e^{ik\eta} - e^{-ik\eta}}{2ik\eta}$$

Standing-waves after horizon re-entry!

$$h_{ij}(\eta, \mathbf{x}) = \sum_P \int \frac{d^3k}{(2\pi)^3} \mathrm{h}_P^{\rm prim}(\mathbf{k})\, h(\eta, k)\, e_{ij}^P(\hat{\mathbf{n}})\, e^{i\,\mathbf{k}\cdot\mathbf{x}}$$

$$h''(\eta, \mathbf{k}) + 2\frac{a'}{a} h'(\eta, \mathbf{k}) + k^2 h(\eta, \mathbf{k}) = 0$$

Evolution equation

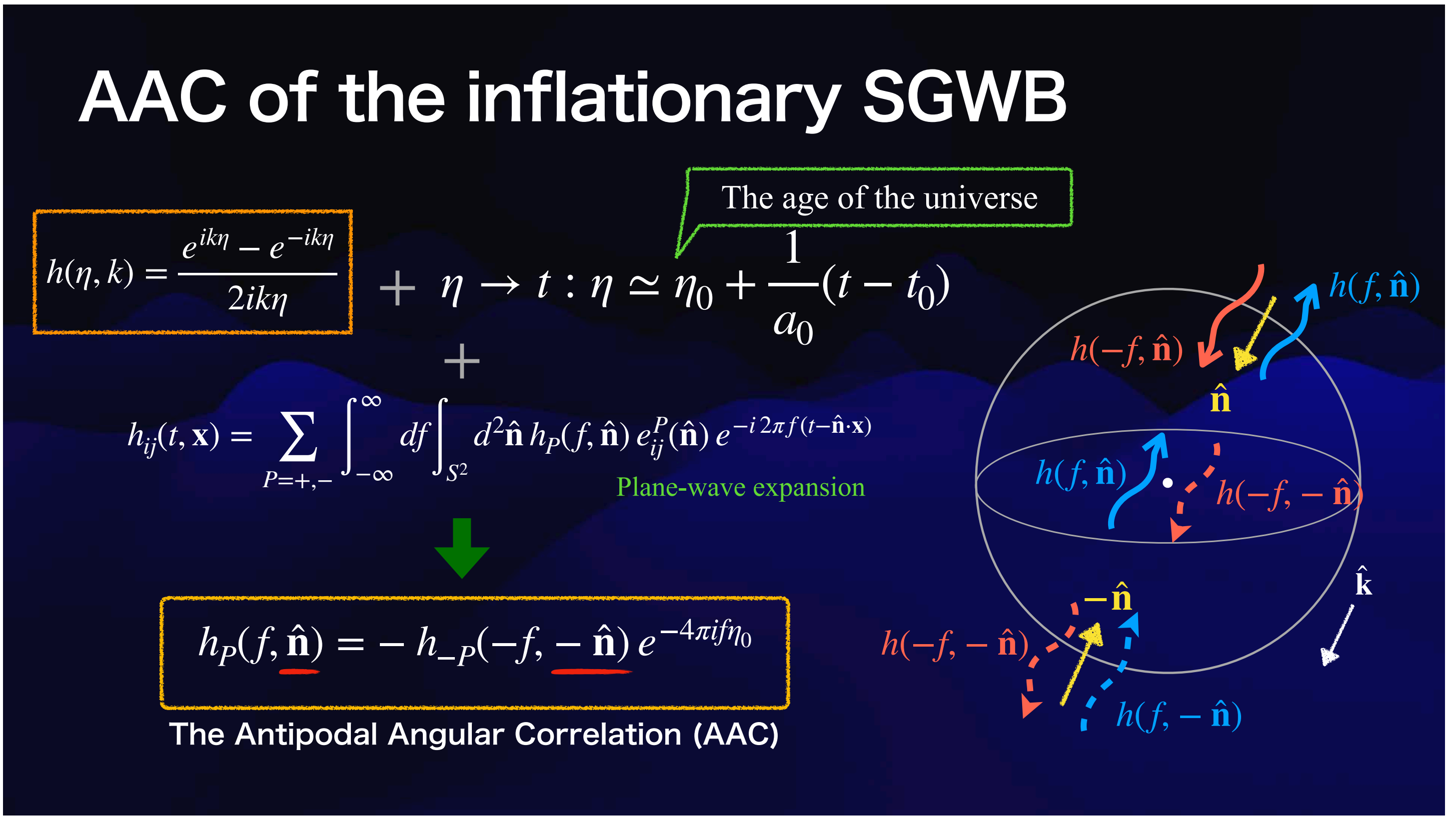

AAC of the inflationary SGWB

$$h(\eta, k) = \frac{e^{ik\eta} - e^{-ik\eta}}{2ik\eta}$$

$$+ \ \eta \to t : \eta \simeq \eta_0 + \frac{1}{a_0}(t - t_0)$$

The age of the universe

$$+$$

$$h_{ij}(t, \mathbf{x}) = \sum_{P=+,-} \int_{-\infty}^{\infty} df \int_{S^2} d^2\hat{\mathbf{n}}\, h_P(f, \hat{\mathbf{n}})\, e_{ij}^P(\hat{\mathbf{n}})\, e^{-i\,2\pi f (t - \hat{\mathbf{n}}\cdot\mathbf{x})}$$

Plane-wave expansion

$$h_P(f, \underline{\hat{\mathbf{n}}}) = -\, h_{-P}(-f, \underline{-\,\hat{\mathbf{n}}})\, e^{-4\pi i f \eta_0}$$

The Antipodal Angular Correlation (AAC)

AAC of the inflationary SGWB

2-point Correlation Function

$$\langle h_P(f,\hat{\mathbf{n}}_1)\, h^*_{P'}(f',\hat{\mathbf{n}}_2)\rangle$$

$$= \delta(f-f')\,\underbrace{\delta_{PP'}\,\delta^2(\hat{\mathbf{n}}_1,\hat{\mathbf{n}}_2)\frac{1}{2}S_h(f)}_{\text{Normal contribution in SGWB}} + \delta(f+f')\,\delta_{P(-P')}\,\underbrace{\delta^2(\hat{\mathbf{n}}_1,-\hat{\mathbf{n}}_2)\frac{1}{2}A_h(f)}_{\text{The antipodal contribution only results from PGWs}}$$

$$h_P(f,\hat{\mathbf{n}}) = -h_{-P}(-f,-\hat{\mathbf{n}})\,e^{-4\pi i f\eta_0}$$

AAC

$$\boxed{A_h(f) = -S_h(f)\,e^{-4\pi i f\eta_0}}$$

- ○ $|A_h(f)| \sim |S_h(f)|$
- ○ $\Delta f \sim 1/\eta_0 \sim 1/T_{\rm age} \sim 10^{-18}\,\mathrm{Hz}$

The measurability of AAC

Strain Correlation

- Cross Correlation for detecting an SGWB [Allen & Romano 99]

$$\langle S \rangle = \int_{T/2}^{-T/2} dt\, \langle s_1(t)\, s_2(t) \rangle = \int_{T/2}^{-T/2} dt\, \langle h^2(t) + h(t)\, s_2(t) + h(t)\, s_1(t) + s_1(t)\, s_2(t) \rangle = \int_{T/2}^{-T/2} dt\, \langle h^2(t) \rangle$$

- The observable quantity for the strain

$$\underset{\times}{h_P(f, \hat{\mathbf{n}})} \rightarrow \underset{\bigcirc}{h_{P;T}(f, \hat{\mathbf{n}})} = \int_{-\infty}^{\infty} df'\, h_P(f', \hat{\mathbf{n}})\, W_T(f - f')$$

Frequency resolution is limited! $|f' - f| \simeq 1/T_{\rm obs}$

[Allen+ 00; Bartolo+ 19]

- The AAC in the strain correlation

“Problematic” phase factor

$$\langle h_{P;T}(f, \hat{\mathbf{n}})\, h^*_{-P;T}(-f, -\hat{\mathbf{n}}) \rangle = \int_{-\infty}^{\infty} df'\, \frac{1}{2} S_h(f')\, |W_T(f - f')|^2\, e^{-4\pi i f' \eta_0} \simeq 0$$

Intensity Correlation (This work)

Undesired phase factor $e^{-4\pi i f \eta_0}$ ⇨

&

Phase-decoherence effect during propagation [*Margalit+, 20*] ⇨

phase-incoherent methods
e.g., *intensity* map
[*Mitra+, 08; Renzini & Contaldi, 18*]

- Antipodal correlation in intensity

$$I_P \equiv |h_P(f, \hat{\mathbf{n}})|^2 \;\Rightarrow\; \boxed{I_P(f, \hat{\mathbf{n}}) = I_{-P}(-f, -\hat{\mathbf{n}})}$$

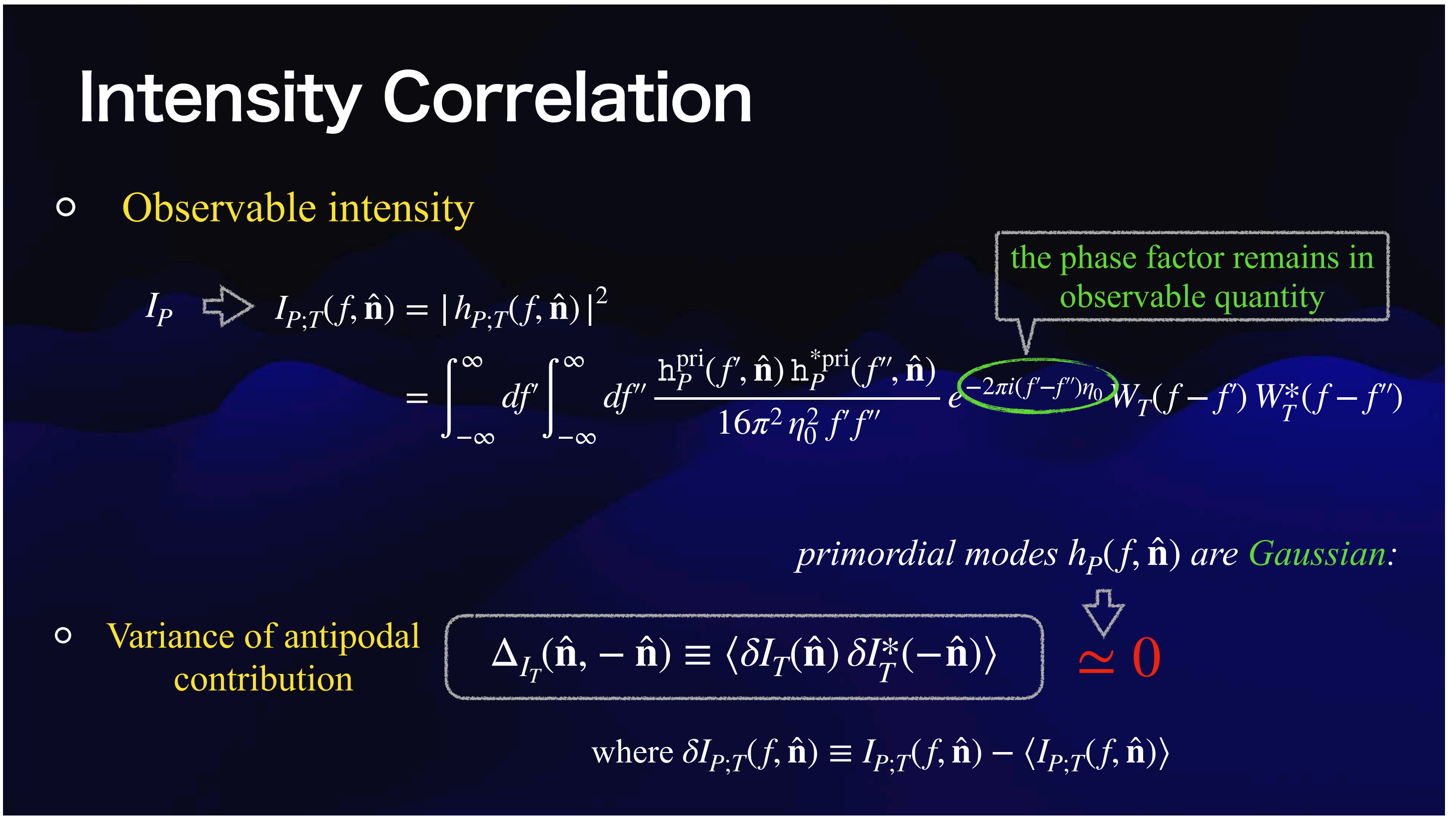

Intensity Correlation

- Observable intensity

$$I_P \;⇨\; I_{P;T}(f,\hat{\mathbf{n}}) = |\,h_{P;T}(f,\hat{\mathbf{n}})\,|^2$$

$$= \int_{-\infty}^{\infty} df' \int_{-\infty}^{\infty} df'' \frac{\mathrm{h}_P^{\mathrm{pri}}(f',\hat{\mathbf{n}})\,\mathrm{h}_P^{*\mathrm{pri}}(f'',\hat{\mathbf{n}})}{16\pi^2\,\eta_0^2\,f'\,f''}\, e^{-2\pi i(f'-f'')\eta_0}\, W_T(f-f')\, W_T^*(f-f'')$$

the phase factor remains in observable quantity

primordial modes $h_P(f,\hat{\mathbf{n}})$ are Gaussian:

⇩

- Variance of antipodal contribution

$$\boxed{\Delta_{I_T}(\hat{\mathbf{n}},-\hat{\mathbf{n}}) \equiv \langle \delta I_T(\hat{\mathbf{n}})\,\delta I_T^*(-\hat{\mathbf{n}})\rangle} \simeq 0$$

where $\delta I_{P;T}(f,\hat{\mathbf{n}}) \equiv I_{P;T}(f,\hat{\mathbf{n}}) - \langle I_{P;T}(f,\hat{\mathbf{n}})\rangle$

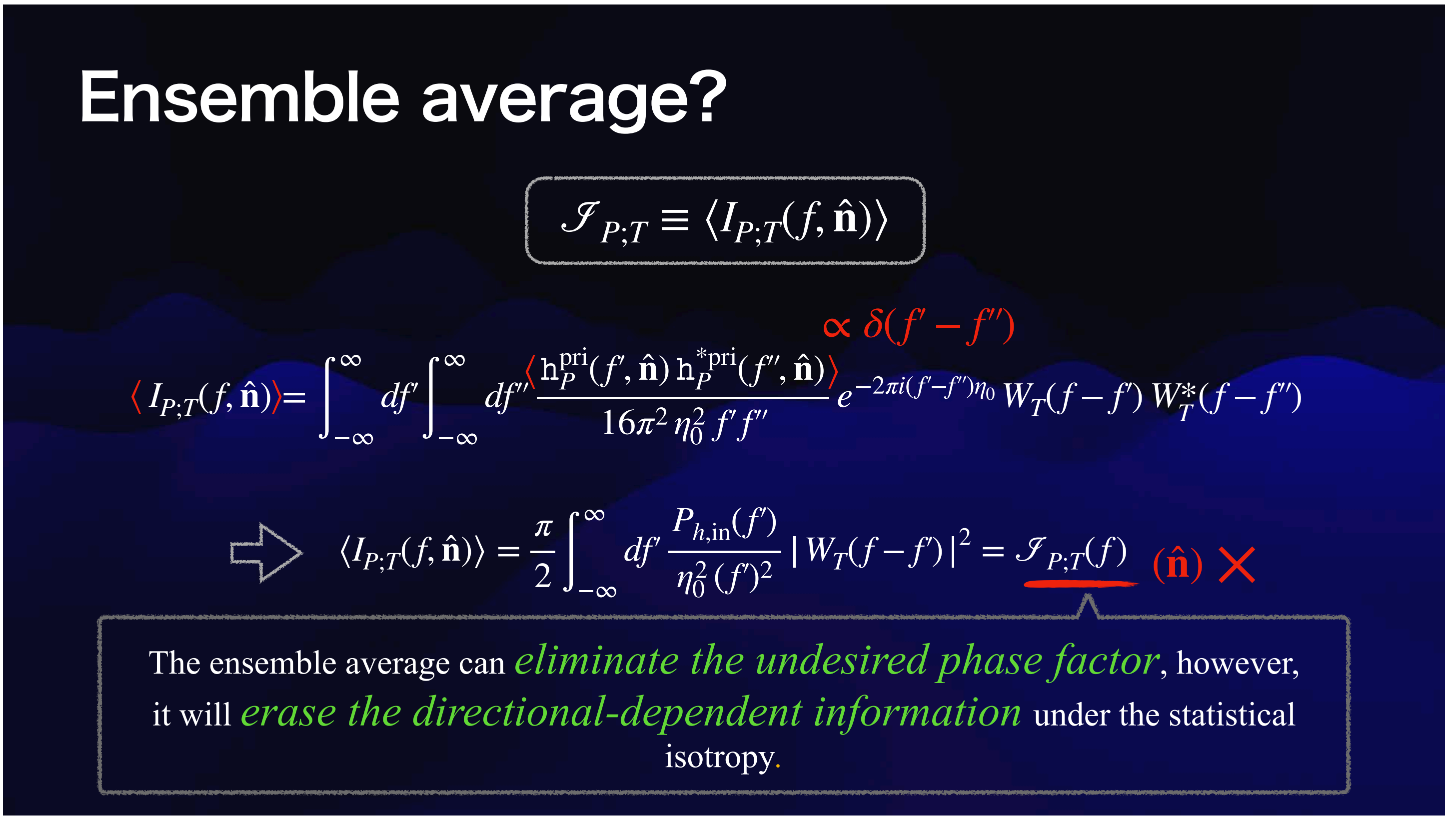

Ensemble average?

$$\boxed{\mathscr{I}_{P;T} \equiv \langle I_{P;T}(f,\hat{\mathbf{n}})\rangle}$$

$$\propto \delta(f'-f'')$$

$$\langle I_{P;T}(f,\hat{\mathbf{n}})\rangle = \int_{-\infty}^{\infty} df' \int_{-\infty}^{\infty} df'' \frac{\langle \mathrm{h}_P^{\mathrm{pri}}(f',\hat{\mathbf{n}})\,\mathrm{h}_P^{*\mathrm{pri}}(f'',\hat{\mathbf{n}})\rangle}{16\pi^2\,\eta_0^2\,f'\,f''}\, e^{-2\pi i(f'-f'')\eta_0}\, W_T(f-f')\, W_T^*(f-f'')$$

$$⇨ \quad \langle I_{P;T}(f,\hat{\mathbf{n}})\rangle = \frac{\pi}{2}\int_{-\infty}^{\infty} df' \frac{P_{h,\mathrm{in}}(f')}{\eta_0^2\,(f')^2}\,|\,W_T(f-f')\,|^2 = \underline{\mathscr{I}_{P;T}(f)} \quad (\hat{\mathbf{n}}) \times$$

The ensemble average can *eliminate the undesired phase factor*, however, it will *erase the directional-dependent information* under the statistical isotropy.

Indicator of anisotropic inflation

Statistical anisotropy

$$\propto \delta(f' - f'')P_{h,\mathrm{in}}(2\pi f\hat{\mathbf{n}})$$

$$\langle I_{P;T}(f,\hat{\mathbf{n}})\rangle = \int_{-\infty}^{\infty} df' \int_{-\infty}^{\infty} df'' \frac{\langle \mathrm{h}_P^{\mathrm{pri}}(f',\hat{\mathbf{n}})\, \mathrm{h}_P^{*\mathrm{pri}}(f'',\hat{\mathbf{n}})\rangle}{16\pi^2\,\eta_0^2\, f' f''} e^{-2\pi i(f'-f'')\eta_0}\, W_T(f-f')\, W_T^*(f-f'')$$

$$\Rightarrow \langle I_{P;T}(f,\hat{\mathbf{n}})\rangle = \frac{\pi}{2}\int_{-\infty}^{\infty} df' \frac{P_{h,\mathrm{in}}(f'\hat{\mathbf{n}})}{\eta_0^2\,(f')^2}\,|\,W_T(f-f')\,|^2 = \mathcal{I}_{P;T}(\underline{f,\hat{\mathbf{n}}})$$

Variance of antipodal contribution

$$\Delta_{I_T}(\hat{\mathbf{n}}, -\hat{\mathbf{n}})/\Delta_{I_T}(\hat{\mathbf{n}},\hat{\mathbf{n}}) = 1 \Rightarrow$$

Antipodal correlation as an indicator of *an*isotropic inflation

$$\Delta_{I_T}(\hat{\mathbf{n}},\hat{\mathbf{n}}) \equiv \langle \delta I_T(\hat{\mathbf{n}})\, \delta I_T^*(\hat{\mathbf{n}})\rangle$$

$$\delta I_{P;T}(f,\hat{\mathbf{n}}) \equiv I_{P;T}(f,\hat{\mathbf{n}}) - \langle I_{P;T}(f,\hat{\mathbf{n}})\rangle$$

Summary

- Antipodal angular correlation (AAC) as *a distinguishable feature b/t inflationary and astrophysical SGWB*.
- It is unfortunately *unmeasurable* in the direct GW observations

  under some standard assumptions (*Gaussian* or *statistical isotropy*) on PGWs.
- The intensity AAC as an indicator of statistical *an*isotropic inflation.

Future works

- Classification of the *(un)measurable angular correlations* in SGWB
  - Perturbed background induced
  - Fossil field induced (Scalar-tensor-tensor primordial non-Gaussianity)

    [Malhotra+, 21; Adshead+, 21; ...]
  - …
- The *replacement/explanation of the ensemble average* in practice.

Thank you for your attention!

Material supply

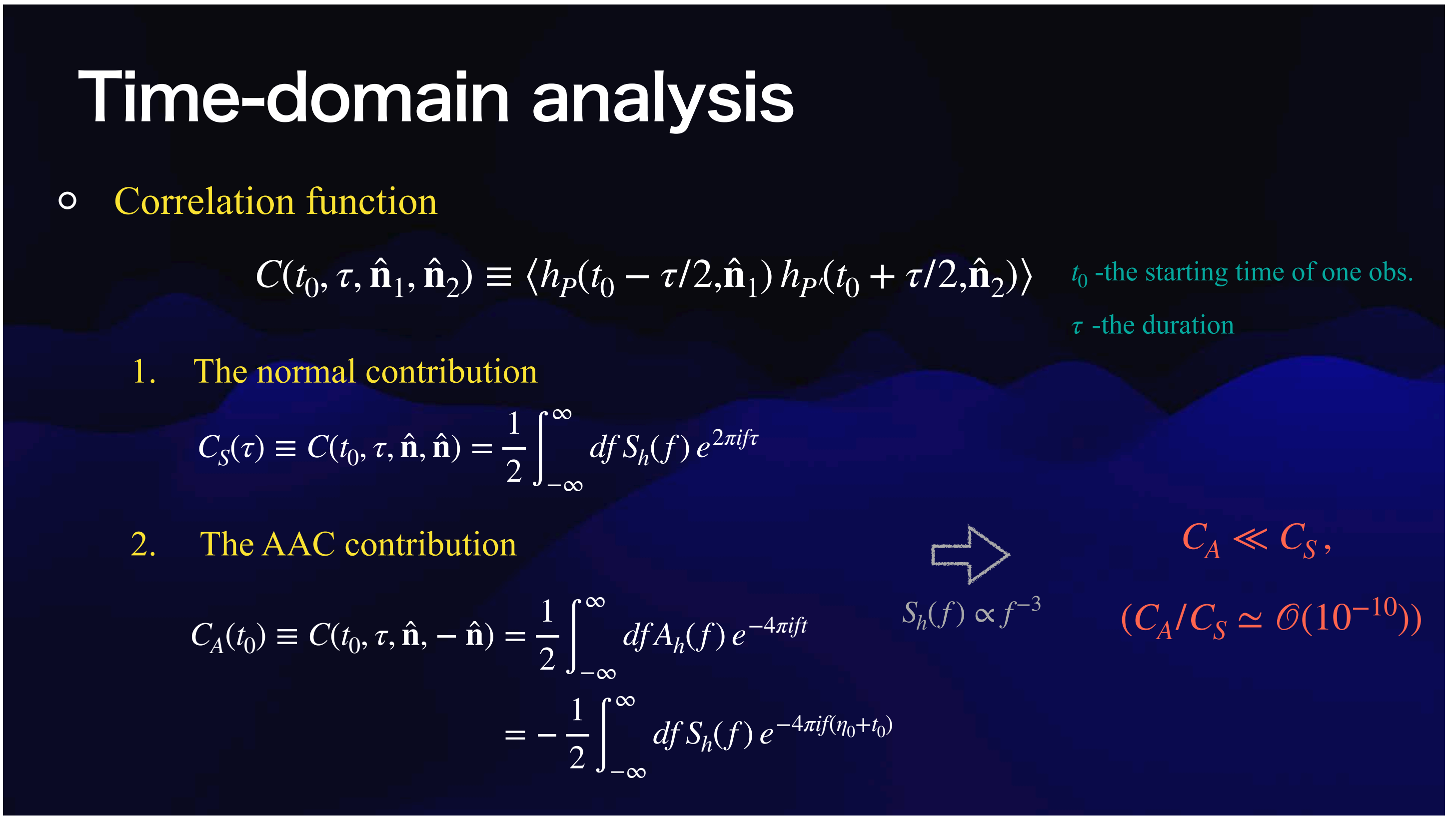

Time-domain analysis

- Correlation function

$$C(t_0, \tau, \hat{\mathbf{n}}_1, \hat{\mathbf{n}}_2) \equiv \langle h_P(t_0 - \tau/2, \hat{\mathbf{n}}_1)\, h_{P'}(t_0 + \tau/2, \hat{\mathbf{n}}_2)\rangle$$

t_0 -the starting time of one obs.

τ -the duration

1. The normal contribution

$$C_S(\tau) \equiv C(t_0, \tau, \hat{\mathbf{n}}, \hat{\mathbf{n}}) = \frac{1}{2}\int_{-\infty}^{\infty} df\, S_h(f)\, e^{2\pi i f \tau}$$

2. The AAC contribution

$$C_A(t_0) \equiv C(t_0, \tau, \hat{\mathbf{n}}, -\hat{\mathbf{n}}) = \frac{1}{2}\int_{-\infty}^{\infty} df\, A_h(f)\, e^{-4\pi i f t}$$
$$= -\frac{1}{2}\int_{-\infty}^{\infty} df\, S_h(f)\, e^{-4\pi i f(\eta_0 + t_0)}$$

$\Rightarrow$

$S_h(f) \propto f^{-3}$

$C_A \ll C_S$,

$(C_A / C_S \simeq \mathcal{O}(10^{-10}))$

October 27th, 2022

Multi-messenger constraints on the Abelian-Higgs cosmic string model

The 31st JGRG workshop @ University of Tokyo

[C56] Jun’ya Kume (Univ. of Tokyo, RESCEU)

In collaboration with
Mark Hindmarsh (Univ. of Helsinki, Univ. of Sussex)
arXiv:2210.06178

---

particle emission + GWB

October 27th, 2022

Multi-messenger constraints on the Abelian-Higgs cosmic string model

The 31st JGRG workshop @ University of Tokyo

[C56] Jun’ya Kume (Univ. of Tokyo, RESCEU)

In collaboration with
Mark Hindmarsh (Univ. of Helsinki, Univ. of Sussex)
arXiv:2210.06178

Contents

➢Multi-messenger from Abelian-Higgs strings

➢Particle emission from string network

➢Gravitational wave background from loops

➢Summary & Discussion

Multi-messenger from Abelian-Higgs strings

- **Abelian-Higgs model** (Nielsen & Olesen 1967)

$$\mathcal{L} = -\frac{1}{4}F_{\mu\nu}F^{\mu\nu} + |D_\mu\Phi|^2 - V(\Phi) \qquad V(\Phi) = \frac{1}{4}\lambda\left(|\Phi|^2 - \eta^2\right)$$

→topologically stable "string" defect

– tension: $G\mu \sim 10^{-6}(\eta/10^{16}\mathrm{GeV})^2$

✓simplest realization of cosmic strings

→ large-scale lattice simulations of the field theory

(from Ringeval 2010)

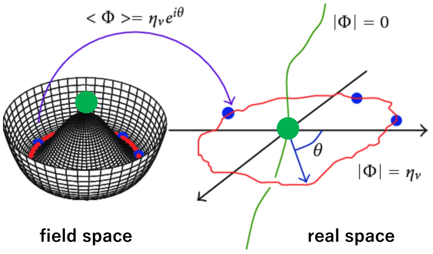

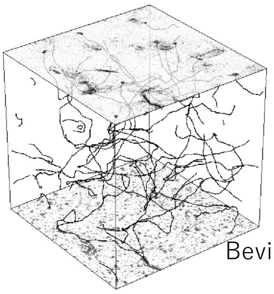

Bevis+ 2007

Multi-messenger from Abelian-Higgs strings

- **Abelian-Higgs model** (Nielsen & Olesen 1967)

$$\mathcal{L} = -\frac{1}{4}F_{\mu\nu}F^{\mu\nu} + |D_\mu\Phi|^2 - V(\Phi) \qquad V(\Phi) = \frac{1}{4}\lambda\left(|\Phi|^2 - \eta^2\right)$$

→topologically stable “string” defect

– tension: $G\mu \sim 10^{-6}(\eta/10^{16}\mathrm{GeV}\,)^2$

(from Ringeval 2010)

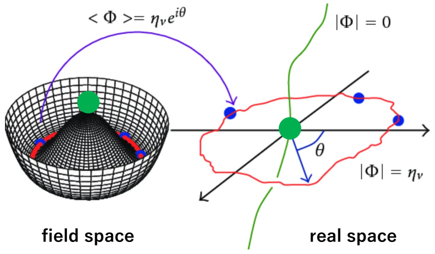

✓simplest realization of cosmic strings

→ large-scale lattice simulations of the field theory

– loops rapidly evaporates by **classical field radiation**

– No observable GWB…!?

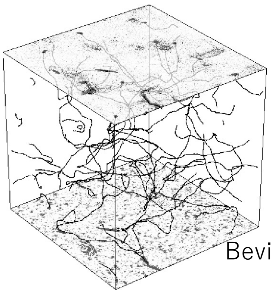

Bevis+ 2007

Multi-messenger from Abelian-Higgs strings

- **Recent simulation of individual loops** (Matsunami+ 2019, Hindmarsh+ 2021)

For loops created with a special initial condition, classical radiation can be suppressed until l_{crit}.

→large loops radiate gravitational waves!

($\simeq$ Nambu-Goto dynamics)

Multi-messenger investigation of AH strings!?

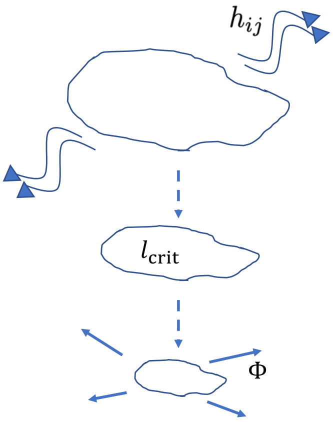

Multi-messenger from Abelian-Higgs strings

- **Recent simulation of individual loops** (Matsunami+ 2019, Hindmarsh+ 2021)

For loops created with a special initial condition,
classical radiation can be suppressed until l_{crit}.
→large loops radiate gravitational waves!
(≃ Nambu-Goto dynamics)

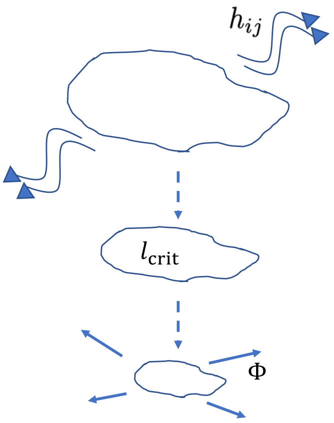

Multi-messenger investigation of AH strings!?

– Production rate of such loops is quite uncertain…
GWB from AH loops needs to be quantified.

Multi-messenger from Abelian-Higgs strings

AH string network

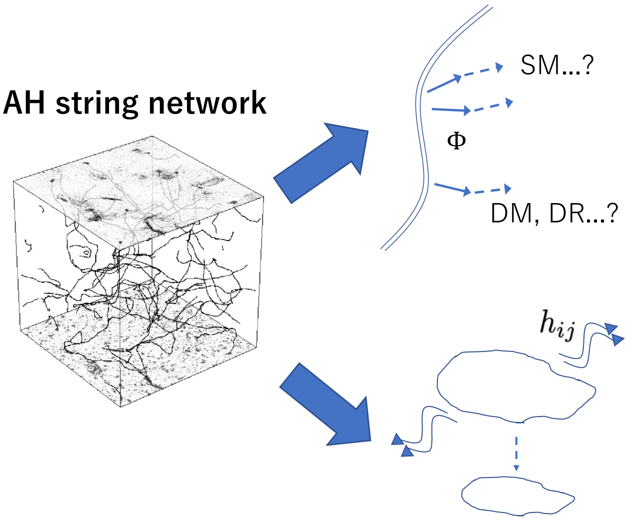

particle emission
from the network

GWs from a certain
fraction of large loops

Multi-messenger from Abelian-Higgs strings

(Mota & Hindmarsh 2014)

AH string network

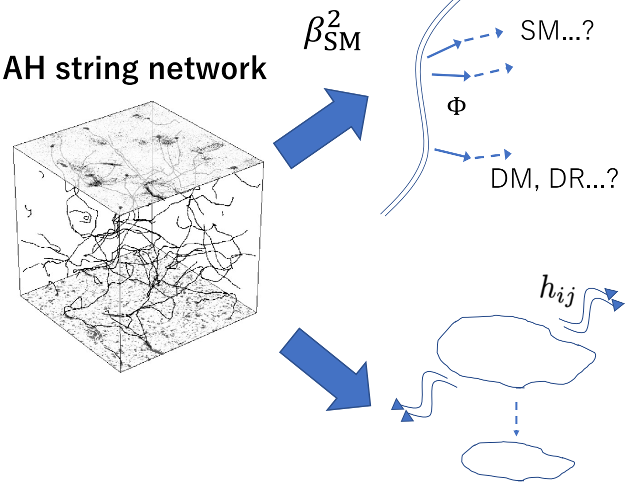

particle emission from the network

– energy injection into visible sector


©NASA
Fermi-LAT

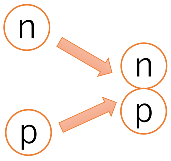

BBN

GWs from a certain fraction of large loops

Multi-messenger from Abelian-Higgs strings

(Mota & Hindmarsh 2014)

AH string network

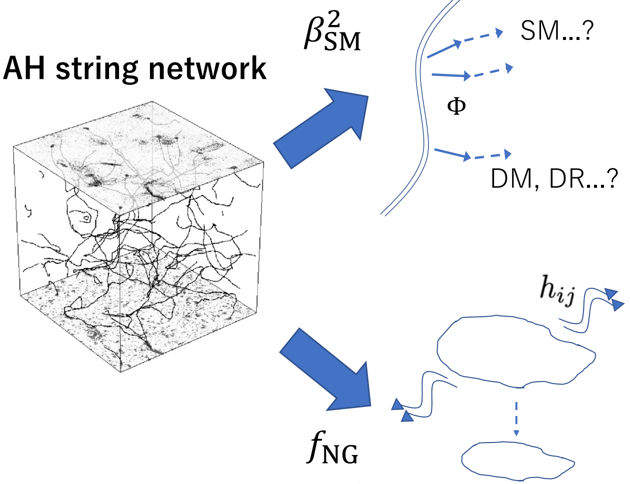

$f_{\rm NG}$

(Hindmarsh+ 2021)

particle emission from the network

– energy injection into visible sector


©NASA
Fermi-LAT

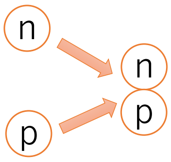

BBN

GWs from a certain fraction of large loops

– GWB observation

recent PTA…?

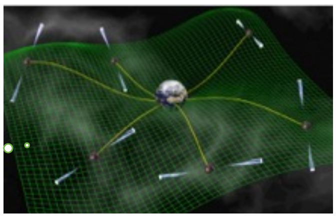

Contents

- ➢Multi-messenger from Abelian-Higgs strings
- ➢Particle emission from string network
- ➢Gravitational wave background from loops
- ➢Summary & Discussion

Particle emission from string network

- **Characterizing particle emission** (Mota & Hindmarsh 2014)

Introducing $\beta^2_{\rm SM}$ as a fraction of energy transfer

$Q_h = -\beta^2_{\rm SM}\left[\dot{\rho}_s + 3H(1+w_s)\rho_s\right]$: total power/unit volume

Injected energy density until t

$$\Delta\rho_h(t) \simeq Q_h t \simeq 3\beta^2_{\rm SM}(w - \underline{\underline{w_s}})\underline{\underline{\rho_s}}/\alpha^2$$

w_s: eq. of state parameter of strings

ρ_s: energy density of string network

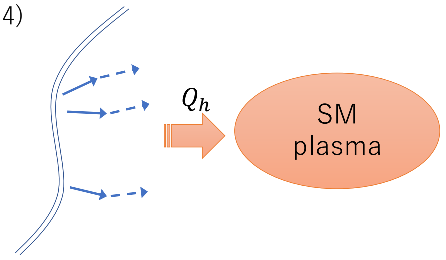

Particle emission from string network

- **Characterizing particle emission** (Mota & Hindmarsh 2014)

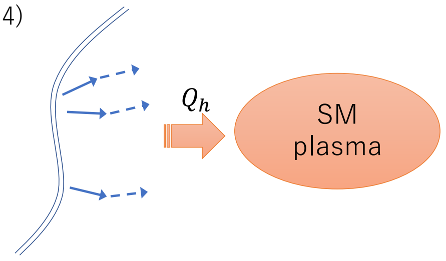

Introducing $\beta_{\rm SM}^2$ as a fraction of energy transfer

$Q_h = -\beta_{\rm SM}^2 \left[\dot{\rho}_s + 3H(1+w_s)\rho_s\right]$: total power/unit volume

Injected energy density until t

$$\Delta\rho_h(t) \simeq Q_h t \simeq 3\beta_{\rm SM}^2(w - \underline{\underline{w_s}})\underline{\underline{\rho_s}}/\alpha^2$$

w_s: eq. of state parameter of strings
ρ_s: energy density of string network

inferred from numerical simulations
(Bevis+ 2007, Hindmarsh+ 2008, …)

$$\Delta\rho_h(t) = \bar{\gamma}_{\rm h,ft}\frac{\mu}{t^2} \qquad \bar{\gamma}_{\rm h,ft} \simeq \begin{cases} 2.8\beta_{\rm SM}^2 & (\text{RD era}) \\ 0.5\beta_{\rm SM}^2 & (\text{MD era}) \end{cases}$$

Particle emission from string network

- **Possible decay channel of strings** (Mota & Hindmarsh 2014)

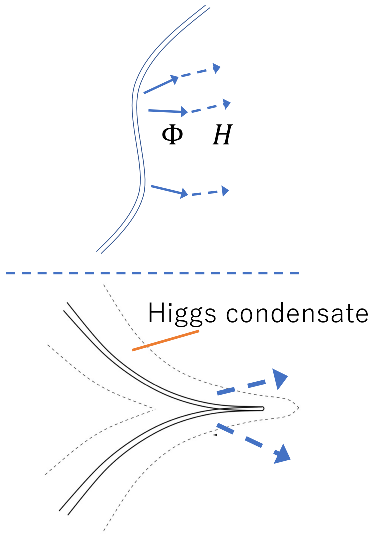

Portal coupling to SM Higgs can be introduced:

$$S = S_0[\Phi, H, \ldots] + \kappa \int d^4x(\Phi^\dagger\Phi - M^2)H^\dagger H$$ (Vachaspati 2009)

string → (string field Φ) → SM Higgs H
(*e.g.* condensate of H → cusp annihilation)

Shower of energetic SM Higgs might alter…
– Big Bang Nucleosynthesis (primordial constraint)
– Diffuse γ -ray background (late-time constraint)

Particle emission from string network

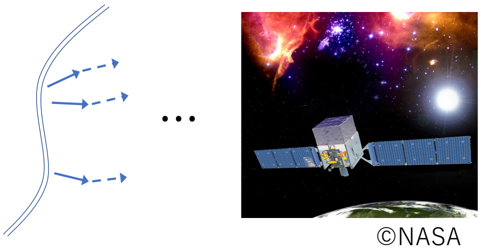

©NASA

- **Constraint from the cascade energy density**

Injection that ends up in the EM cascade:

$$\omega_{\rm em}(t) = f_{\rm em}\Delta\rho_h(t) \simeq 0.5 f_{\rm em}\beta_{\rm SM}^2\frac{\mu}{t^2}$$

Primally ch.: Higgs $\to b\bar{b} \to \cdots$

many photons via pion decay $\to f_{\rm em} \simeq 1$ (Bhattacharjee+ 2000)

From the DGRB measurement by Fermi-LAT

$$\omega_{\rm em} \lesssim 8.3\times 10^{-8}{\rm eV/cm^3}$$

(Berezinsky+ 2016)

$$\xrightarrow[t\,\sim\, t_0]{}$$

(M. Hindmarsh, **JK** 2022)

$$\boxed{G\mu \lesssim 4\times 10^{-12}\,\beta_{\rm SM}^{-2}}$$

※BBN constraint becomes the same order.

→Upper bound on $\Delta\rho_h/s$ at t_{BBN} to avoid dissociation

---

Contents

Gravitational wave background from loops

- **GW emission from Nambu-Goto-like loops**

fraction of loops obeying NG dynamics: $f_{\mathrm{NG}}(\lesssim 0.1)$ (Hindmarsh+ 2022)

→SGWB from $f_{\mathrm{NG}} \cdot \underline{\mathrm{n}(l,t)}$ loops

loop dist. not quantified in AH simulation...

Gravitational wave background from loops

- **GW emission from Nambu-Goto-like loops**

fraction of loops obeying NG dynamics: $f_{\mathrm{NG}}(\lesssim 0.1)$ (Hindmarsh+ 2022)

→SGWB from $f_{\mathrm{NG}} \cdot \underline{\mathrm{n}(l,t)}$ loops

loop dist. not quantified in AH simulation...

For $\mathrm{n}(l,t)$, we adopt BOS model based on NG-simulation.(Blanco-Pillado+ 2017)

$$\boxed{\Omega_{\mathrm{gw}}^{(\mathrm{AH})}(f) = f_{\mathrm{NG}}\Omega_{\mathrm{gw}}^{(\mathrm{BOS})}(f)}$$

※Instead, LRS model (Lorentz+ 2010) can also be adopted as a reference.

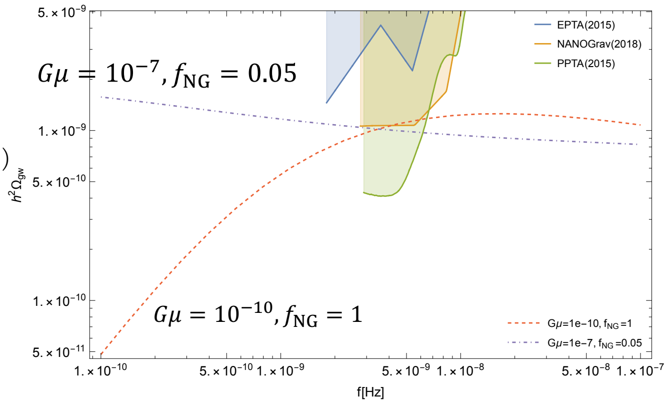

Gravitational wave background from loops

- **Recent PTA results and string GWB**

"common stochastic process" was observed! ⚠Lack of HD correlation(= may not GWB)

→ power-law search of GWB

$$\Omega_{\rm gw}^{\rm (pow)}(f) = \frac{2\pi^2}{3H_0^2}A^2 f_{\rm yr}^2\left(\frac{f}{f_{\rm yr}}\right)^{5-\gamma}$$

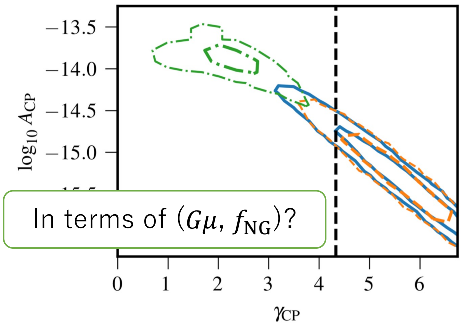

In terms of $(G\mu,\, f_{\rm NG})$?

(The NANOGrav collaboration 2020)

Gravitational wave background from loops

- **Recent PTA results and string GWB**

"common stochastic process" was observed! ⚠Lack of HD correlation(= may not GWB)

→ power-law search of GWB

$$\Omega_{\rm gw}^{\rm (pow)}(f) = \frac{2\pi^2}{3H_0^2}A^2 f_{\rm yr}^2\left(\frac{f}{f_{\rm yr}}\right)^{5-\gamma}$$

Modeling likelihood to map:$(G\mu,\, f_{\rm NG})\rightarrow(A,\, \gamma)$

$$P(S_{\rm gw}^{\rm (pow)}|S_{\rm gw}^{\rm (AH)}) \propto \prod_{f_i\in[f_{\rm min},f_{\rm max}]} \frac{\sqrt{\left[S_n(f_i)+S_{\rm gw}^{\rm (pow)}(f_i)\right]\left[S_n(f_i)+S_{\rm gw}^{\rm (AH)}(f_i)\right]}}{\left[S_n(f_i)+S_{\rm gw}^{\rm (pow)}(f_i)\right]+\left[S_n(f_i)+S_{\rm gw}^{\rm (AH)}(f_i)\right]}.$$

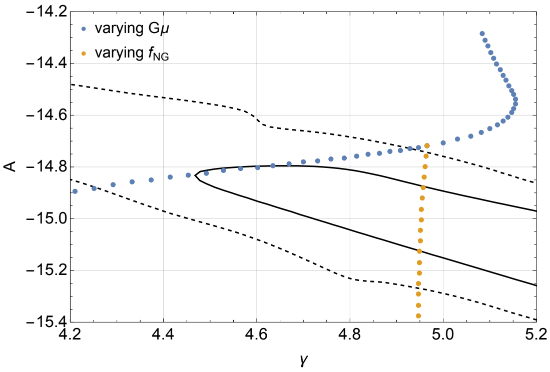

→project contours by using mapped points

(Gowling+ 2022)

Gravitational wave background from loops

- **Combining PTA result with DGRB constraint** (M. Hindmarsh, **JK** 2022)

PTA constraints in $(G\mu, f_{\rm NG})$ plane:

※$G\mu \lesssim 10^{-7}$ by CMB (Planck 2013) & $f_{\rm NG} \lesssim 0.1$

$$G\mu f_{\rm NG}^{2.6} \gtrsim 3.2 \times 10^{-13}\ (95\%)$$

To account for NANOGrav result,

$$f_{\rm NG} \gtrsim 10^{-2}$$

– motivates further loop simulations

$$\beta_{\rm SM}^2 \lesssim 10^{-3}$$

– implication to model building

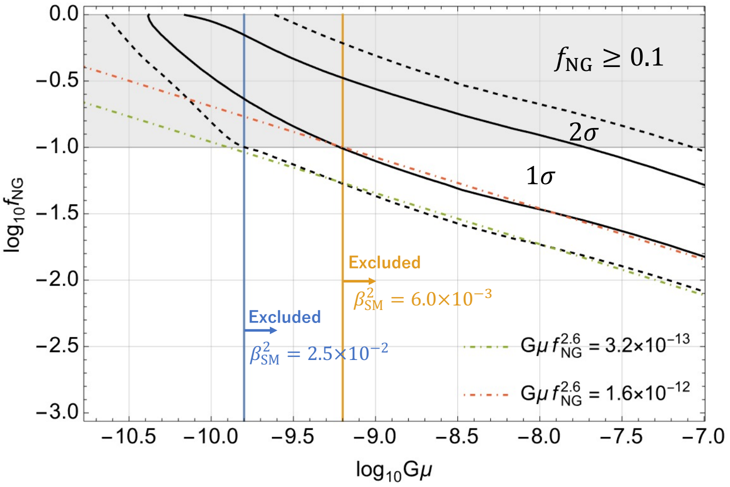

Contents

➢Multi-messenger from Abelian-Higgs strings

➢Particle emission from string network

➢Gravitational wave background from loops

➢Summary & Discussion

Summary

✓AH string network may radiate both **particles & GWB**
→multi-messenger constraints by characterizing two signals

✓Assuming that strings dominantly decay into SM Higgs,
$G\mu \lesssim 4\times10^{-12}\beta_{SM}^{-2}$ from DGRB & BBN constraint.

✓NANOGrav result requires $G\mu f_{NG}^{2.6} \gtrsim 3.2\times10^{-13}$ at 95%.
→ $f_{\mathrm{NG}} \gtrsim 10^{-2}$ & $\beta_{SM}^{2} \lesssim 10^{-3}$ are favored to avoid other constraints.

Discussion

- Not conclusive constraints but **offering multi-messenger study**
  - too early to claim GWB detection by PTA.
  - creation of NG-like loops in AH model is quite uncertain…

- Implications to the model building
  - Dark Matter (Radiation) can also be produced: $\beta_{\mathrm{SM}}^2 + \beta_{\mathrm{DM}}^2 + \beta_{\mathrm{DR}}^2 \simeq 1$
  - β_{DM}^2 can be tightly constrained but β_{DR}^2 is not. (see *e.g.* Hindmarsh +2013)

- Extension to other models, e.g. $U(1)_{B-L}$ breaking…?

Nambu-Goto loop distibution

- **Two different results** (Blanco-Pillado+ 2013, Lorentz+ 2010)

Gravitational backreaction are differently treated:

BOS model

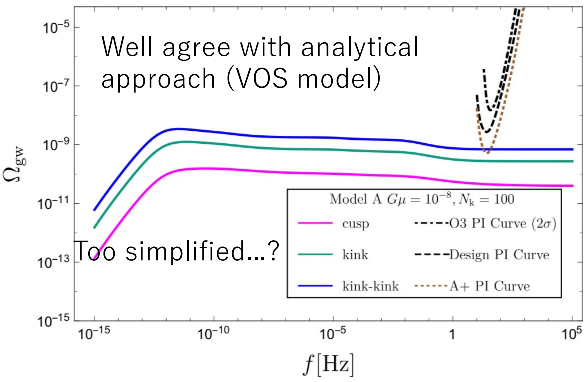

Well agree with analytical approach (VOS model)

Too simplified…?

LRS model

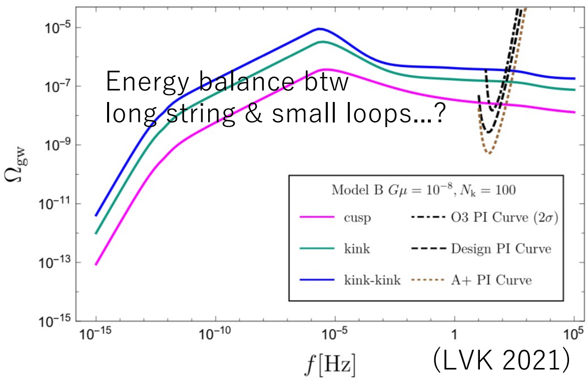

Energy balance btw long string & small loops…?

(LVK 2021)

GWB in the BOS model

- **GWB spectrum from NG simulation** (Blanco-Pillado+ 2017)

scaling

− contribution from oscillating loop distribution: $n(l,t) = t^{-4}\mathrm{n}(l/t)$

$$\Omega_{\rm gw}^{\rm (NG)}(f) \equiv \frac{1}{\rho_c}\frac{d\ln\rho_{\rm gw}^{\rm (NG)}}{d\ln f} = \frac{8\pi f G^2\mu^2}{3H_0^2}\sum_{n=1}^{\infty} C_n(f)P_n$$

power spectrum of n-th mode

$$C_n(f) = \frac{2n}{f^2}\int_0^\infty \frac{dz}{H(z)(1+z)^6}\mathrm{n}\left(\frac{2n}{(1+z)f}, t(z)\right)$$

Continuously generated with $l/t \sim 0.1$ through out the history of universe.

(For a different loop distribution (LRS model), see Lorentz+ 2010)

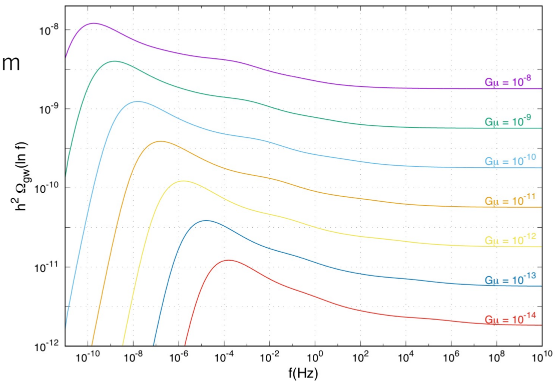

Gravitational wave background from loops

- **Effect of particle emission to the loop creation** (Auclair+ 2019)

Loops in AH model dominantly emit GWs until l_{crit} → high freq. cutoff

dominated by kinks

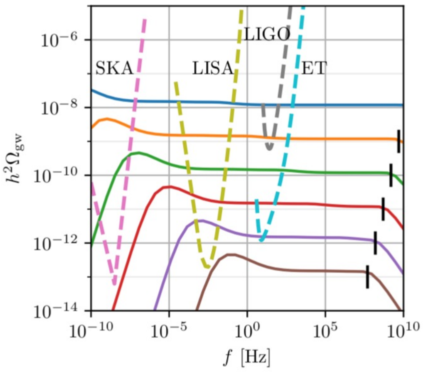

dominated by cusps

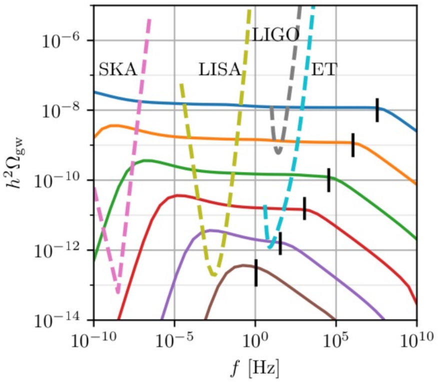

BBN constraint on decaying massive particle

- **Light element abundance**

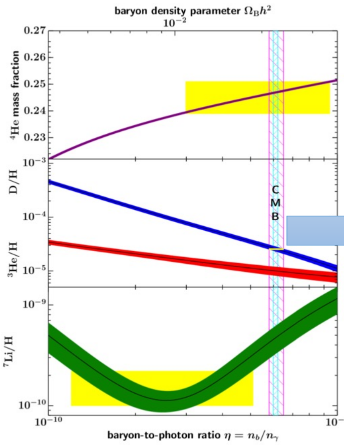

Particle Data Group

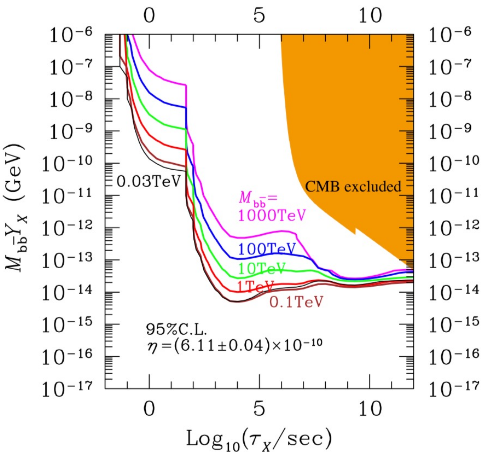

(Kawasaki+ 2017)

$$\underbrace{\text{string} \to \Phi \to H \to}_{\text{Effectively, a specie } X} b\bar{b}$$

$$M_X Y_X \sim \frac{\Delta\rho_h(t)}{s(t)} \simeq 22\beta_{\text{SM}}^2 G\mu \left(\frac{m_p}{t}\right)^{1/2}$$

$t \sim \tau_X$

$$G\mu \lesssim 3.6 \times 10^{-12}\beta_{\text{SM}}^{-2}$$

(M. B. Hindmarsh, **JK** 2022)

Abelian-Higgs model

- **Nambu-Goto VS large-scale lattice simulation**

typically, treated as infinitely thin 1d-object: NG action

$$S_0 = -\mu \int \mathrm{d}^2\sigma \sqrt{-\gamma}. \quad \gamma_{ab} = \partial_a X^\mu \partial_b X^\nu g_{\mu\nu}$$

relativistically oscillating loops → **SGWB**

+ re-connection rules → scaling behavior

However, in the lattice simulation,
loops rapidly evaporate by the **particle emission**!

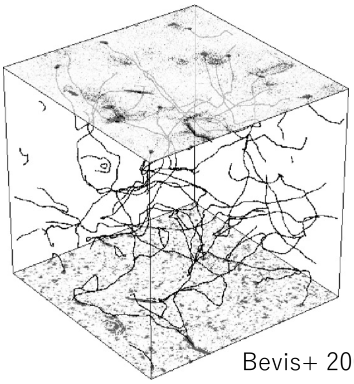

Bevis+ 2007

C57

The prospect of distinguishing stellar-mass compact objects in extreme mass ratio inspiral system with LISA

Mostafizur Rahman

Dept. of Physics
Indian Institute of Technology, Gandhinagar
Gujarat-382355, India

[2112.13869] with Arpan Bhattacharyya

31st Workshop on General Relativity and Gravitation in Japan (JGRG31)

Table of Contents

Extreme Mass Ratio Inspiral (EMRI)

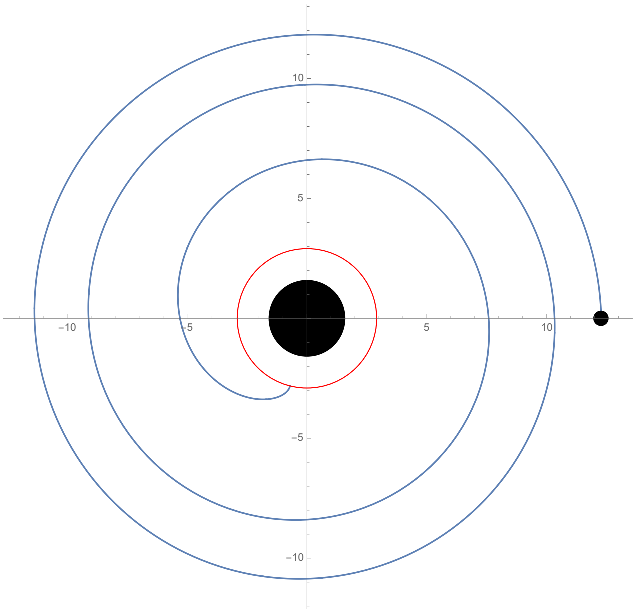

- EMRI:
  - System: Super Massive Compact object : the primary,
    Stellar- Mass compact Object: the secondary
  - $q \approx 10^{-4} - 10^{-7}$
  - The system emit gravitational waves in millihertz frequencies.

- Goal: Whether we identify the nature of secondary with LISA observation?

Modeling the EMRI system and MPD equations

- Model:
  - The primary: Super massive Kerr BH
  - The secondary: Spinning extended object subject to quadrupolar deformation

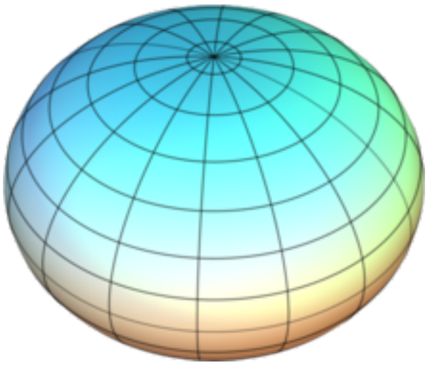

[Image Source: google]

The SET of secondary object allows for a multipolar expansion.

$$\boxed{\begin{aligned} T^{\alpha\beta} = \int \mathrm{d}\tau \Big[\Big\{ \delta^{(4)} p^{(\alpha} v^{\beta)} \Big\} - \Big\{ \nabla_\gamma \Big(S^{\gamma(\alpha} v^{\beta)} \delta^{(4)} \Big) \Big\} \\ - \frac{1}{3} \Big\{ \delta^{(4)} J^{\gamma\delta\epsilon(\alpha} R^{\beta)}{}_{\epsilon\gamma\delta} + 2 \nabla_\gamma \nabla_\delta \Big(J^{\delta(\alpha\beta)\gamma} \delta^{(4)} \Big) \Big\} \Big] \end{aligned}}$$

Spin Induced Quadrupolar Tensor (SIQT)

$$\boxed{J^{\alpha\beta\gamma\delta} = -\frac{3}{m^2} p^{[\alpha} Q^{\beta][\gamma} p^{\delta]}}$$

- $Q^{\alpha\beta} = C_Q S^{\alpha}_{\mu} S^{\beta\mu}/m$: Mass quadrupole tensor

Secondary	C_Q
Black hole	1
Neutron star	3 – 20
Boson star	10 – 150
White Dwarf	$10^3 - 10^5$
Brown Dwarf	$\sim 10^6$

[Phys. Rev. D 104, 084056 (2021)]

An order of magnitude analysis:

Force due to SIQT

$$\frac{D^2 z^\alpha}{d\tau^2} = q f^\alpha_{(1)} + q^2 f^\alpha_{(2)} + \ldots$$

$$\mathcal{E} \sim m, \qquad \dot{\mathcal{E}} \sim (qh^{(1)})^2, \qquad T_i = \frac{\mathcal{E}}{\dot{\mathcal{E}}} \sim \frac{M}{q} \gg 1$$

Over the inspiral period $f^\alpha_{(2)}$ produces a shift

$$z^\alpha \sim q^2 f^\alpha_{(2)} T_i^2 \sim q^0$$

We can not neglect the effect of second order force terms

Dynamics of EMRI sytem and adiabatic approximation

- Dynamics of the secondary governed by Mathisson-Papapetrou-Dixon (MPD) equation
- Assumptions: The secondary moves on the equatorial plane of the primary and their spin is aligned
- From MPD equation, we get $\boxed{\dot{r}^2 = V}$, from which we get the energy and angular momentum of stable circular obrits and the position of ISCO

Adiabatic Approximation:

- Inspiral time scale $T_e (\sim M/q) \gg$ Orbital time scale $T_o (\sim M)$

$$\boxed{\left(\frac{dE}{dt}\right)^{\text{orbit}} = -\left\langle \frac{dE}{dt} \right\rangle_{\text{GW}}}$$

- Inspiral $\equiv$ Flow through a sequence of circular orbit.
- The flow determined by the rate of change of energy E.

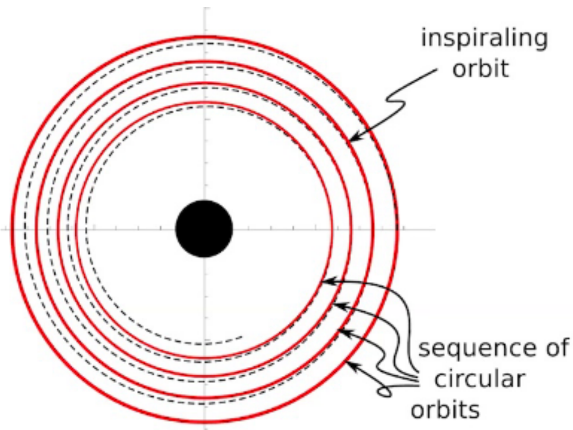

[Image Credit: Adam Pound]

Teukolsky Equation

- GW flux at specific radius r_0 $(dE/dt) \propto \langle(\dot{h}_+)^2 + (\dot{h}_\times)^2\rangle$

$$\boxed{\left(\frac{dE}{dt}\right)^{\infty,\mathrm{H}}_{\mathrm{GW}} = \sum_{\ell=2}^{\infty}\sum_{m=-\ell}^{\ell} \frac{|\mathcal{A}^{H,\infty}_{\ell m\omega}|^2}{2\pi(m\Omega)^2},}$$

where,

$$\mathcal{A}^{H,\infty}_{\ell m\omega} = \text{Const.}\ \left[A_0 - A_1\partial_r + A_2\partial_r^2 - A_3\partial_r^3 + A_4\partial_r^4\right] R^{\text{in,up}}_{\ell m\omega}\Big|_{r_0,\pi/2}$$

- Total flux, $\mathcal{F} = (\dot{E})^\infty + (\dot{E})^H$
- Adiabatic evolution of orbital radius $r(t)$ and phase $\Phi(t)$

$$\boxed{\frac{dr}{dt} = -\mathcal{F}(r)\left(\frac{dE}{dr}\right)^{-1}, \qquad \frac{d\phi}{dt} = \Omega(r(t))}$$

- GW phase $\boxed{\Phi_{GW} = 2\phi}$

GW phase

- Throughout the inspiral, the phase can be written as

$$\boxed{\Phi_{\mathrm{GW}}(t) = \Phi^{(0)}(t) + \chi\Phi^{(1)}(t) + q\chi^2\delta\Phi^{(2)}(t) + \mathcal{O}(\sigma^3)}$$

$$\boxed{\delta\Phi^{(2)}(t) = \Phi^{(2)}_\chi(t) + C_Q\Phi^{(2)}_Q(t)}$$

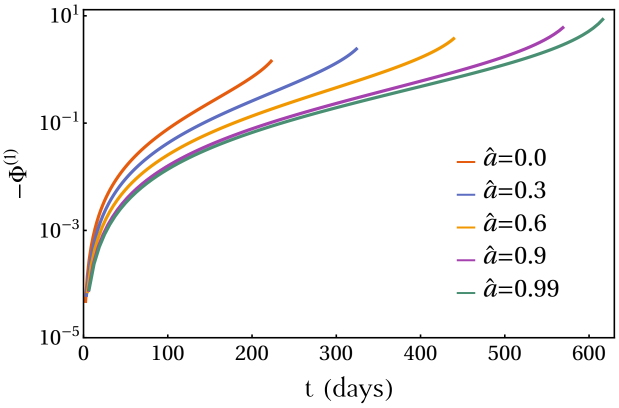

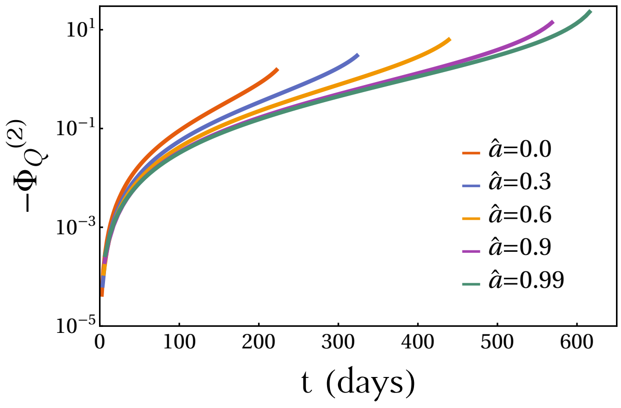

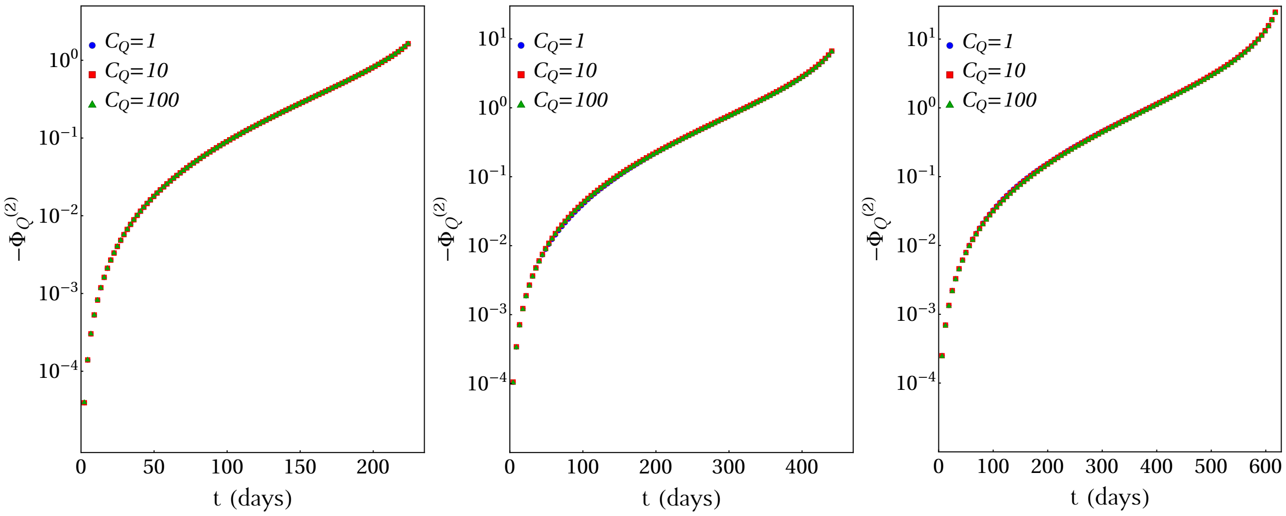

- Total accumulated GW phase

$$\boxed{\Phi_{\mathrm{GW}}(t_{\mathrm{end}}) = \Phi^0(t_{\mathrm{end}}) + \chi\Phi^{(1)}(t_{\mathrm{end}}) + q\chi^2\left(\Phi_\chi^{(2)}(t_{\mathrm{end}}) + C_Q\Phi_Q^{(2)}(t_{\mathrm{end}})\right)}$$

- Deviation in the orbital phase caused by quadrupolar deformation

$$\boxed{\Delta\Phi(t_{\mathrm{end}}) = C_Q q\chi^2\Phi_Q^{(2)}(t_{\mathrm{end}}), \qquad \Phi^{(2)}(t_{\mathrm{end}}) \approx \mathcal{O}(1-25)}$$

Possible values of Spin

a	$\Phi_Q^{(2)}(t_{\mathrm{end}})$
0	1.63344
0.3	3.17133
0.6	6.65017
0.9	14.8259
0.99	24.5308

Secondary	$\chi_{\max}$
Black hole	1
Neutron star	0.7 [1]
Boson star	$\gtrsim 1$ [2]
Gravastar	~ 1.2 [3]
Superspinar	> 1 [4]

[[1]Astrophys. J. 424 (Apr., 1994) 823]

[[2]arXiv:2203.07442 [gr-qc].]

[[3]Phys. Rev. D 78 (Oct, 2008) 084011.]

[[4] Phys. Lett. B 672 (2009) 299–302]

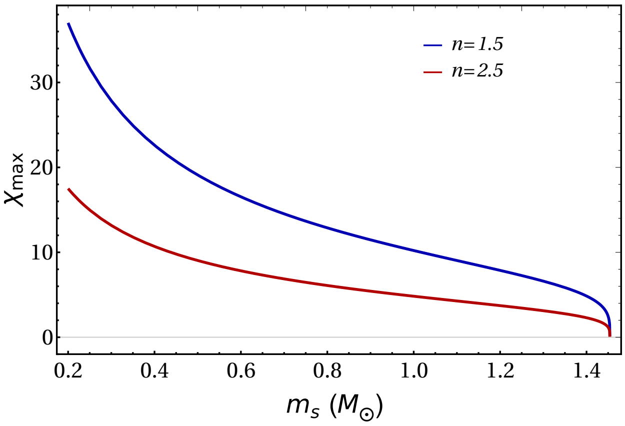

[Phys. Rev. D 67 (2003) 024005]

Prospect of Detection

The systematic errors due to the inaccuracy in modeling should be less than the statistical errors due to detector noise

- The phase shift is resolvable if

$$\boxed{\Delta\Phi(t_{\text{end}}) = C_Q q \chi^2 \Phi^{(2)}(t_{\text{end}}) \geq \sqrt{D-1}/\rho = 0.1 \text{ rad}}$$

[PRL 123,101103 (2019)]

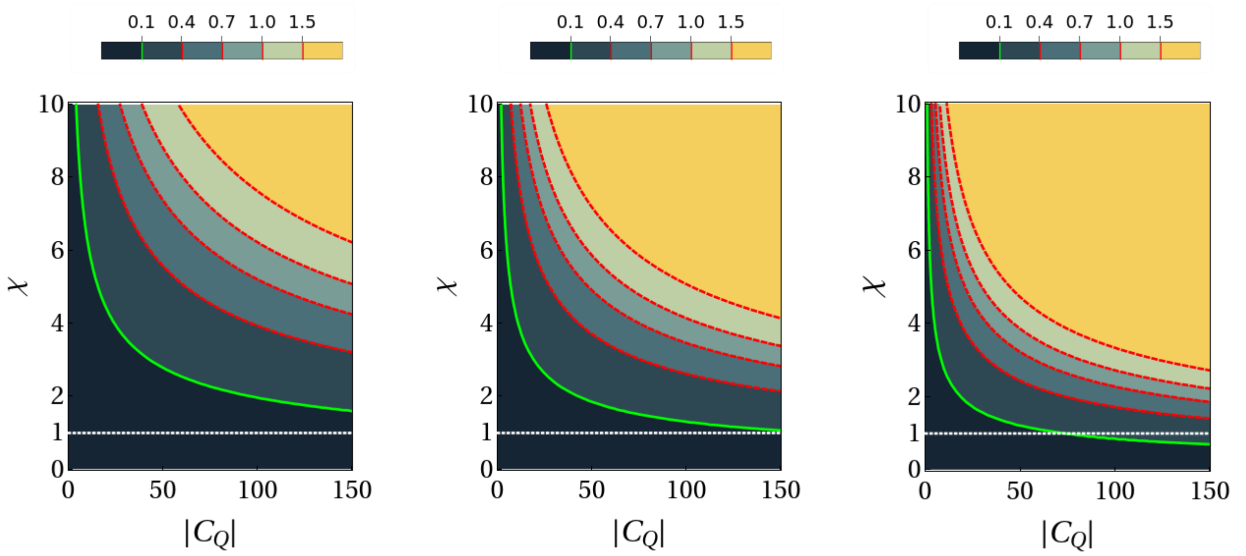

Case Study

Case-I Neutron Star:

$$\boxed{\Delta\Phi^{\text{NS}} = 0.0216 \left(\frac{q}{10^{-4}}\right)\left(\frac{C_Q}{20}\right)\left(\frac{\chi}{0.7}\right)^2\left(\frac{\Phi^{(2)}_{\text{Q,end}}(a)}{24.5308}\right)}$$

$$(q_{\text{ref}}, C_Q^{\text{ref}}, \chi_{\text{ref}}) = (10^{-4}, 20, 0.7)$$

Case-II Boson Star:

$$\boxed{\Delta\Phi^{\text{ECO}} = 0.4411 \left(\frac{q}{10^{-4}}\right)\left(\frac{C_Q}{50}\right)\left(\frac{\chi}{2}\right)^2\left(\frac{\Phi^{(2)}_{\text{Q,end}}(a)}{24.5308}\right)}$$

$$(q_{\text{ref}}, C_Q^{\text{ref}}, \chi_{\text{ref}}) =(10^{-4}, 50, 2)$$

Case Study:

Case III: White dwarf

$$\boxed{\Delta\Phi^{\mathrm{WD}} = 0.882\left(\frac{q}{10^{-6}}\right)\left(\frac{C_Q}{10^4}\right)\left(\frac{\chi}{2}\right)^2\left(\frac{\Phi^{(2)}_{\mathrm{Q,end}}(a)}{24.5308}\right)}$$

$$(q_{\mathrm{ref}}, C_Q^{\mathrm{ref}}, \chi_{\mathrm{ref}}) = (10^{-6}, 10^4, 2),$$

Case IV: Brown dwarf

$$\boxed{\Delta\Phi^{\mathrm{BD}} = 4.5\left(\frac{q}{10^{-10}}\right)\left(\frac{C_Q}{2\times10^5}\right)\left(\frac{\chi}{80}\right)^2\left(\frac{\Phi^{(2)}_{\mathrm{Q,end}}(a)}{3.17}\right)}$$

$$(q_{\mathrm{ref}}, C_Q^{\mathrm{ref}}, \chi_{\mathrm{ref}}) = (10^{-10}, 2\times10^5, 80, 0.3),$$

Conclusion and Future Directions

Take away massage:

- The effect of quadrupolar deformation can be quite significant of some ECOs like boson star, white dwarfs, brown dwarfs and superspinors etc.
- LISA can detect (if they exist!) these objects
- The parameter space for detection increaases with primary’s spin

Future Directions:

- Relaxing equatorial, circular orbit assumption
- Consider of the effect of tidal field
- Considering the effect of self-force
- Whether we can do the same for equal mass binary system

THANK
YOU
GRACIAS
ARIGATO
SHUKURIA
MERCI
BOLZÏN
GRAZIE
MEHRBANI
DANKSCHEEN
BÏYAN
SHUKRIA
TASHAKKUR ATU
YAQHANYELAY
SUKSAMA
EKHMET
GOZAIMASHITA
EFCHARISTO
JUSPAXAR
KOMAPSUMNIDA
MAAKE
PALDIES
TINGKI

Time evolution and quasinormal modes of odd parity perturbations of stealth black holes in DHOST theory

Keisuke Nakashi (Kochi KOSEN・Rikkyo U.)

with **M. Kimura** (Daiichi Tech.)
H. Motohashi (Kogakuin U.)
K. Takahashi (YITP, Kyoto U.)

in progress

JGRG31 @ Koshiba Hall 2022/10/24 - 28

Introduction

- (Schwarzschild) Black hole perturbation in GR
  - ■ Master equation : 2-dimensional wave equation

$$\left(\frac{\partial^2}{\partial x^2}-\frac{\partial^2}{\partial t^2}-V_{\rm eff}(x)\right)\Psi(t,x)=0$$

  - ■ Characteristic modes : quasinormal modes (QNMs)

$$\Psi(t,x)=e^{-i\omega t}\psi(x)$$

$$\left(\frac{{\rm d}^2}{{\rm d}x^2}+\omega^2-V_{\rm eff}\right)\psi=0$$

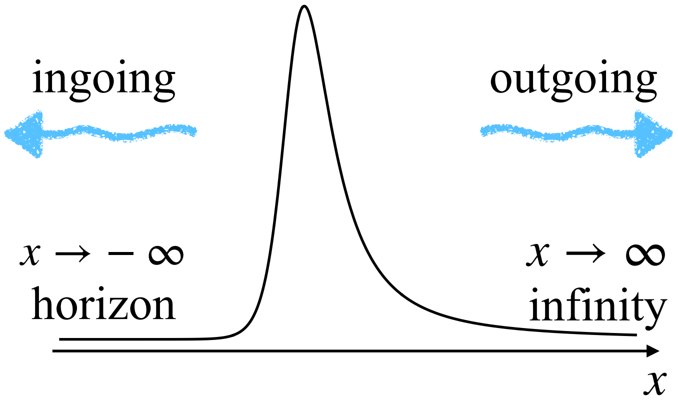

Introduction

- Why are the QNMs important in GR ?
  - ■ QNMs dominate the late time behavior of perturbations.

[Vishveshwara (1970)], [Leaver (1986)]

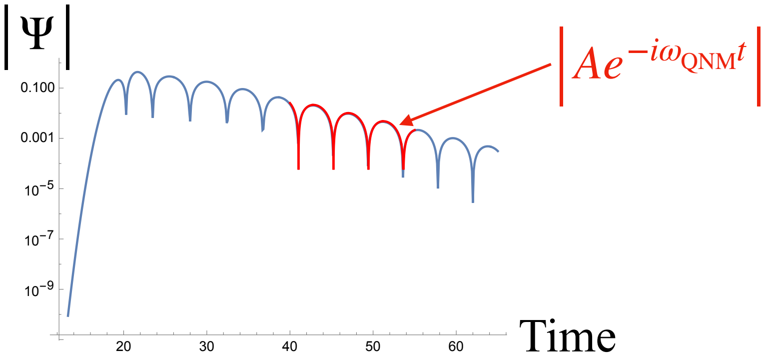

  - ■ Ringdown phase can be fitted by the superposition of QNMs.

[Giesler, Isi, Scheel, & Teukolsky (2019)]
[Sago, Isoyama, & Nakano (2021)], etc.

Introduction

- How about in modified gravity ?
  - ■ Do QNMs always dominate the late time behavior ?
    For some solutions in a scalar-tensor theory, the monopole perturbations do not exhibit a damping oscillation.

[KN, Kimura, Motohashi, & Takahashi (2022)]

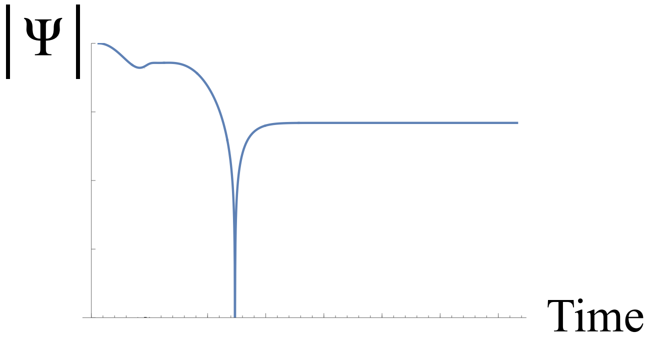

It is important examine not only QNM frequencies

but also time evolution

Gravity theory

- Degenerate Higher-Order Scalar Tensor (DHOST) theory

[Langlois&Noui, (2015), Crisostomi+, (2016), Ben Achour+, (2016)]

$$\mathscr{L} = F_0(\phi, X) + F_1(\phi, X)\Box\phi + F_2(\phi, X)R + \sum_{I=1}^{5} A_I(\phi, X)\, L_I^{(2)},\ X \equiv \phi_\mu \phi^\mu$$

$$L_1 \equiv \phi_{\mu\nu}\phi^{\mu\nu},\ L_2 \equiv (\Box\phi)^2,\ L_3 \equiv \phi^\mu \phi_{\mu\nu}\phi^\nu \Box\phi,\ L_4 \equiv \phi^\mu \phi_{\mu\nu}\phi^{\nu\lambda}\phi_\lambda,\ L_5 \equiv (\phi^\mu \phi_{\mu\nu}\phi^\nu)^2$$

+ degeneracy conditions

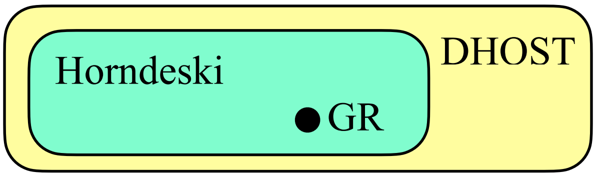

■ 2 tensor DOFs. + 1 scalar DOF.

■ No Ostrogradsky ghost instability

Gravity theory

- Degenerate Higher-Order Scalar Tensor (DHOST) theory

[Langlois&Noui, (2015), Crisostomi+, (2016), Ben Achour+, (2016)]

$$\mathscr{L} = F_0(\cancel{\phi}, X) + \cancel{F_1(\phi, X)\Box\phi} + F_2(\cancel{\phi}, X)R + \sum_{I=1}^{5} A_I(\cancel{\phi}, X)\, L_I^{(2)},\ X \equiv \phi_\mu \phi^\mu$$

$$L_1 \equiv \phi_{\mu\nu}\phi^{\mu\nu},\ L_2 \equiv (\Box\phi)^2,\ L_3 \equiv \phi^\mu \phi_{\mu\nu}\phi^\nu \Box\phi,\ L_4 \equiv \phi^\mu \phi_{\mu\nu}\phi^{\nu\lambda}\phi_\lambda,\ L_5 \equiv (\phi^\mu \phi_{\mu\nu}\phi^\nu)^2$$

+ degeneracy conditions

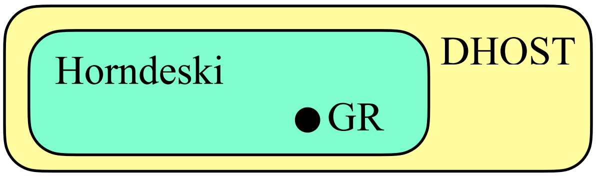

■ 2 tensor DOFs. + 1 scalar DOF.

■ No Ostrogradsky ghost instability

Gravity theory

- subclass of DHOST theory

[Langlois&Noui, (2015), Crisostomi+, (2016), Ben Achour+, (2016)]

$$\mathscr{L} = F_0(X) + F_2(X)R + \sum_{I=1}^{5} A_I(X)\, L_I^{(2)},\ X \equiv \phi_\mu \phi^\mu$$

$$L_1 \equiv \phi_{\mu\nu}\phi^{\mu\nu},\ L_2 \equiv (\Box\phi)^2,\ L_3 \equiv \phi^\mu \phi_{\mu\nu}\phi^\nu \Box\phi\,,\ L_4 \equiv \phi^\mu \phi_{\mu\nu}\phi^{\nu\lambda}\phi_\lambda\,,\ L_5 \equiv (\phi^\mu \phi_{\mu\nu}\phi^\nu)^2$$

\+ degeneracy conditions

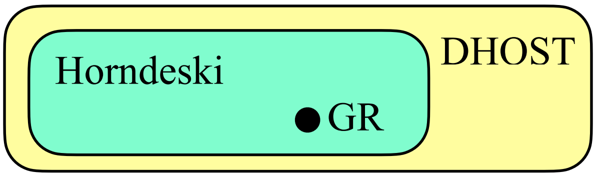

- 2 tensor DOFs. + 1 scalar DOF.
- No Ostrogradsky ghost instability
- Symmetries : $\phi \to \phi + \mathrm{const}.$ & $\phi \to -\phi$

Background

- Stealth Schwarzschild black hole

[Motohashi & Minamitsuji (2019)]
[Charmousis+, (2019)]
[Takahashi & Motohashi (2020)], etc.

  - Metric : Schwarzschild metric

$$\bar{g}_{\mu\nu}\mathrm{d}x^\mu \mathrm{d}x^\nu = -A(r)\,\mathrm{d}t^2 + A(r)^{-1}\,\mathrm{d}r^2 + r^2\mathrm{d}\Omega^2, \quad A(r) = 1 - \frac{r_\mathrm{s}}{r}$$

  - Scalar field : nontrivial configuration with $X = -q^2$

$$\bar{\phi} = q\left(t + 2\sqrt{r_\mathrm{s} r} + r_\mathrm{s} \ln \frac{\sqrt{r} - \sqrt{r_\mathrm{s}}}{\sqrt{r} + \sqrt{r_\mathrm{s}}}\right)$$

  - Existence conditions of stealth solutions

$$F_0(-q^2) = 0, \quad \partial_X F_0(-q^2) = 0$$

※ Perturbations of a stealth solution are strong coupled in general.
In the odd parity sector, we ignore the effect of such terms for simplicity.

Odd parity perturbation

- Quadratic Lagrangian [Takahashi, Motohashi, & Minamitsuji (2019)]

$$\mathcal{L}^{(2)} \sim b_1(\partial_t\chi)^2 - b_2(\partial_r\chi)^2 + \partial_t\chi\partial_r\chi - [\ell(\ell+1)b_4 + V_{\rm eff}(r)]\chi^2$$

■ Introduce new time coordinate $\tilde{t}$

$$\tilde{t} = t\sqrt{\frac{r_{\rm s}}{r_{\rm g}}} + 2\sqrt{\frac{r}{r_{\rm g}}}(r_{\rm s} - r_{\rm g}) - \frac{1}{\sqrt{r_{\rm g}}}\left(r_{\rm g}^{3/2}\ln\frac{\sqrt{r}-\sqrt{r_{\rm g}}}{\sqrt{r}+\sqrt{r_{\rm g}}} - r_{\rm s}^{3/2}\ln\frac{\sqrt{r}-\sqrt{r_{\rm s}}}{\sqrt{r}+\sqrt{r_{\rm s}}}\right)$$

$r_{\rm g} = \left(1 + \frac{q^2A_1}{F_2}\right)r_{\rm s}$: Killing horizon for graviton

■ Diagonalized quadratic Lagrangian

$$\mathcal{L}^{(2)} \sim \tilde{b}_1(\partial_{\tilde{t}}\chi)^2 - b_2(\partial_r\chi)^2 - [\ell(\ell+1)b_4 + V_{\rm eff}(r)]\chi^2$$

EOM & QNM frequency

- Introduce generalized tortoise coordinate x & new variable Ψ

$$\frac{\partial^2\Psi}{\partial x^2} - \frac{\partial^2\Psi}{\partial\tilde{t}^2} - V_{\rm eff}(r)\Psi = 0$$

$$x = r + r_{\rm g}\ln\left(\frac{r}{r_{\rm g}} - 1\right) \qquad V_{\rm eff} = \left(1 - \frac{r_{\rm g}}{r}\right)\left[\frac{\ell(\ell+1)}{r^2} - \frac{3r_{\rm g}}{r^3}\right]$$

→ Regge-Wheeler equation replaced $r_{\rm s}$ by $r_{\rm g}$

- QNM frequency : $\omega^{\rm DHOST} = \frac{r_{\rm s}}{r_{\rm g}}\omega^{\rm GR} = \left(1 + \frac{q^2A_1}{F_2}\right)^{-1}\omega^{\rm GR}$

Initial surface ($r_\mathrm{s} < r_\mathrm{g}$ case)

- Time evolution of Ψ

$$\frac{\partial^2\Psi}{\partial x^2} - \frac{\partial^2\Psi}{\partial \tilde{t}^2} - V_\mathrm{eff}\Psi = 0 \quad + \quad \text{initial condition}$$

■ Initial surface : $\tilde{t} = $ const. surface

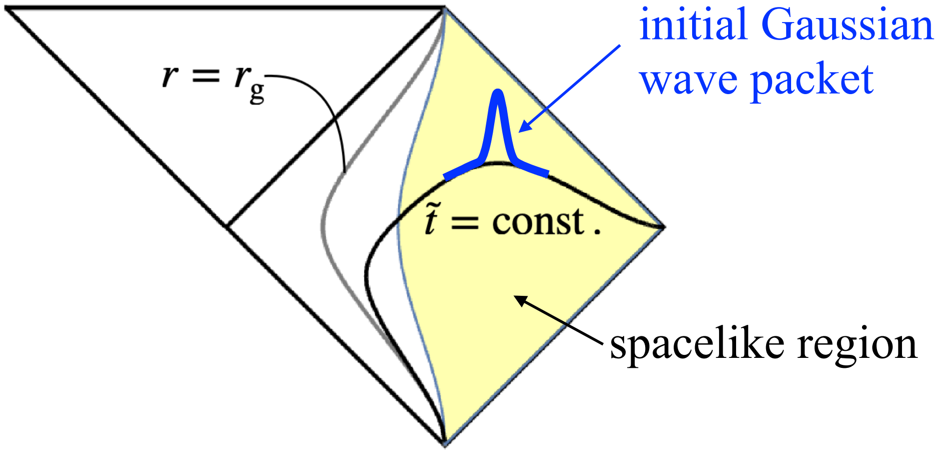

Time evolution ($r_\mathrm{g} = 1.5r_\mathrm{s}$, $\ell = 2$)

- QNM dominates the late time behavior.

  QNM frequency is $\omega^\mathrm{DHOST} = \dfrac{r_\mathrm{s}}{r_\mathrm{g}}\omega^\mathrm{GR}$ as expected.

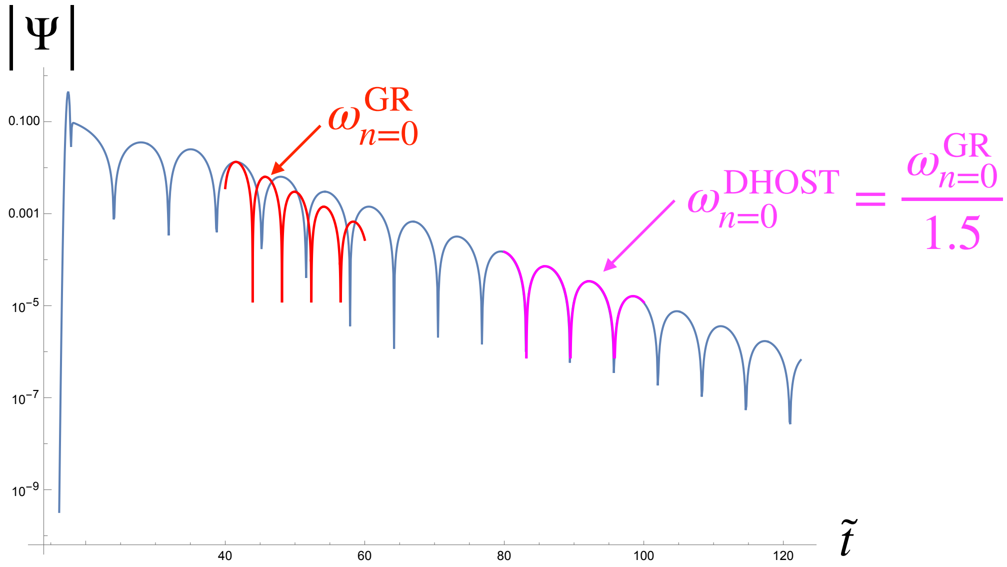

Summary

- We investigate the time evolution of odd parity perturbations in a subclass of DHOST theory.
  - ■ EOM becomes Regge-Wheeler equation replaced r_s by r_g.
  - ■ QNM frequency is $\omega^{\mathrm{DHOST}} = \frac{r_s}{r_g}\omega^{\mathrm{GR}}$.
  - ■ QNMs dominate the late time behavior of the perturbations.

C59

The Effective Field Theory of Vector-Tensor Theories

Katsuki Aoki (YITP, Kyoto University)

KA, M. A. Gorji, S, Mukohyama, K. Takahashi, JCAP01(2022)059 [2111.08119]
KA, A. De Felice, M. A. Gorji, T. Hiramatsu, S, Mukohyama, M. C. Pookkillath, K. Takahashi, in progress.

Introduction

☐ **Dark energy?**

There are a lot of models…

e.g. Λ, canonical scalar, Brans–Dicke, Galileon, and more…

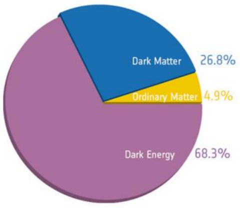

☐ **How do we distinguish various dark energy models?**

✓ Concrete models: definite predictions, but model dependent.

✓ EFT approach: try to extract model-independent predictions

Creminelli+ 2006, Cheung+ 2008, Gubitosi+ 2013, Bloomfield+ 2013, …

$$S=\int \mathrm{d}^4x\sqrt{-g}\left[\frac{M_*^2}{2}f(t)R\underbrace{-\Lambda(t)-c(t)g^{00}}_{\text{Canonical scalar}}-\frac{1}{2}\bar{M}_1^3(t)\delta g^{00}\delta K+\cdots\right]$$

Non-minimal coupling

Galileon (KGB)

EFT coefficients universally characterize the models.

EFT of dark energy

☐ Scalar dark energy or vector dark energy?
(≃ Horndeski) (≃ Generalized Proca)

*The formulation itself is applicable to any ST/VT theories for cosmology.

☐ **How do we distinguish these dark energy models?**
Or, how do we distinguish the spin of dark energy?

☐ **"The EFT of dark energy" is not "EFT of ALL dark energy"!**

$$S=\int \mathrm{d}^4x\sqrt{-g}\left[\frac{M_*^2}{2}f(t)R\underbrace{-\Lambda(t)-c(t)g^{00}}_{\text{Canonical scalar}}-\frac{1}{2}\bar{M}_1^3(t)\delta g^{00}\delta K+\cdots\right]$$

Non-minimal coupling

Galileon (KGB)
= scalar-tensor theories!

Extensions are required!

Cosmology = SSB of spacetime sym.

Universe is filled with unknown (inflation/dark energy)
= part(s) of spacetime symmetries are spontaneously broken.

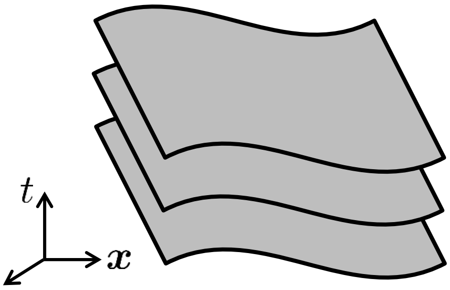

Preferred slices
= scalar condensate
(EFT of scalar-tensor)

Creminelli+ 2006, Cheung+ 2008,
Gubitosi+ 2013, Bloomfield+ 2013, ...

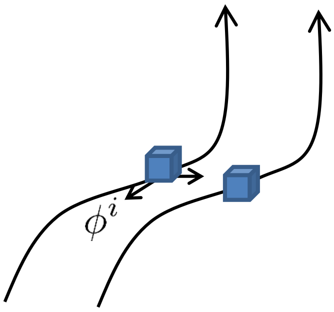

Preferred coordinates
= fluid/solid
(EFT of continuum)

Dubovsky+ 2006, Endlich+ 2013,
KA+ 2204.06672.

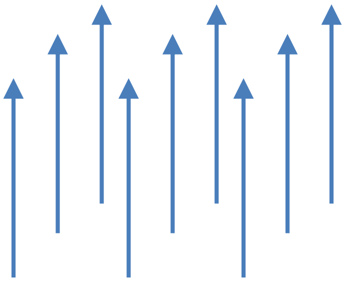

Preferred direction
= vector condensate
(EFT of vector-tensor)

KA+ 2111.08119

Cosmology = SSB of spacetime sym.

☐ In this talk, we focus on scalar-tensor theories and vector-tensor theories.

ST: Preferred spacelike slices

$$\langle \tilde{t}(t,\boldsymbol{x})\rangle = t$$

A clock field

VT: Preferred timelike direction

$$\langle v_\mu \rangle = \bar{v}_\mu(t) \propto \delta^0_\mu$$

☐ The difference is clarified by the use of internal symmetry.

✓ General scalar-tensor theory: no symmetry associated with $\tilde{t}$

✓ Shift-symmetric theory: invariant under $\tilde{t}(t,\boldsymbol{x}) \to \tilde{t}(t,\boldsymbol{x}) - \chi_0$

✓ Localized shift symmetry: invariant under $\tilde{t}(t,\boldsymbol{x}) \to \tilde{t}(t,\boldsymbol{x}) - g_M\chi(t,\boldsymbol{x})$

Covariant derivative of the clock field: $v_\mu = \partial_\mu \tilde{t} + g_M A_\mu$ ← Gauge field

↖ Gauge coupling

*The vector may be massive because of SSB.

Web of EFTs

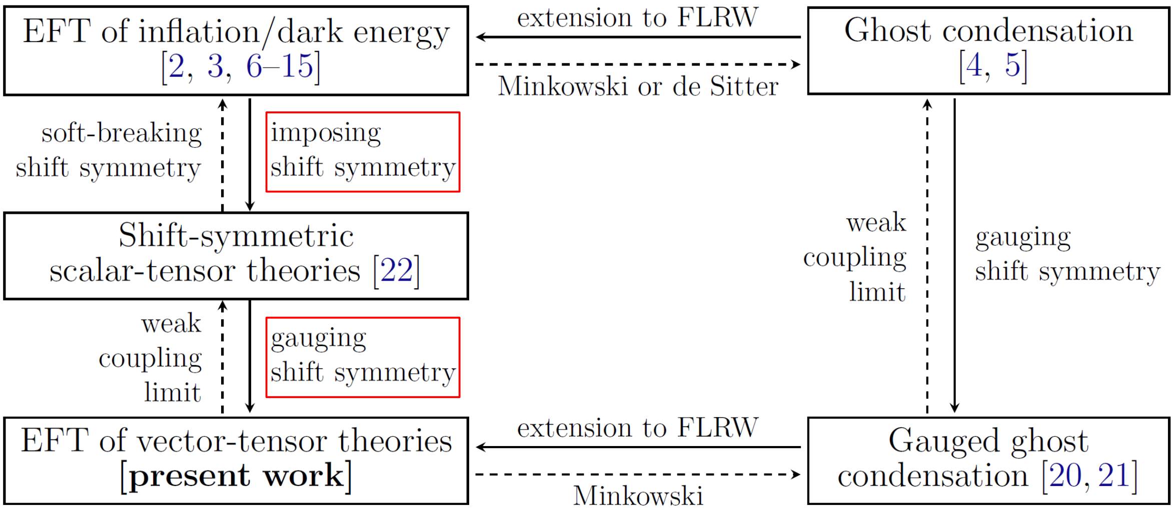

Therefore, STEFT and VTEFT are distinguished by

1. the existence of shift symmetry and
2. global shift symmetry ($g_M = 0$) or local shift symmetry ($g_M \neq 0$).

Scalar and tensor perturbations

- Symmetry, field contents, and expansion parameters are known
  → We can systematically construct the EFT Lagrangian.
- Let's make the Lagrangian user-friendly.
  Easy to understand existence/absence of shift sym. and gauge coupling.
- We finally find the following form in the absence of vorticity.
  = no vector perturbations in cosmology

$$\delta_2 S = \int \frac{\mathrm{d}t\mathrm{d}^3k}{(2\pi)^3}\bar{N}a^3\frac{M^2}{2}$$

$$\times\Bigg[(1+\tilde{\alpha}_H)\frac{\delta N}{\bar{N}}\delta_1{}^{(3)}R + 4H\tilde{\alpha}_B\frac{\delta N}{\bar{N}}\delta_1 K + \delta_1 K^{\alpha}{}_{\beta}\delta_1 K^{\beta}{}_{\alpha} - (1+\tilde{\alpha}_B^{\mathrm{GLPV}})(\delta_1 K)^2$$

$$+\tilde{\alpha}_K H^2\left(\frac{\delta N}{\bar{N}}\right)^2 + (1+\alpha_T)\delta_2\left({}^{(3)}R\frac{\sqrt{h}}{a^3}\right) + \frac{\tilde{\alpha}_M^{\mathrm{GC}}}{H^2}(\delta_1{}^{(3)}R)^2 + \frac{\tilde{\alpha}_B^{\mathrm{GC}}}{H}\delta_1 K\delta_1{}^{(3)}R\Bigg] + \delta_2 S_{\mathrm{m}} + \cdots,$$

The action is formally the same as the standard EFTofDE.
All information are embedded in the EFT coefficients with tilde.

Scalar and tensor perturbations

- α without tilde and α with tilde are

$$\begin{aligned}
\tilde{\alpha}_B(t,k) &= [1-\mathcal{G}(t,k)]\alpha_B(t)\,,\\
\tilde{\alpha}_K(t,k) &= [1-\mathcal{G}(t,k)]\alpha_K(t)\,,\\
\tilde{\alpha}_H(t,k) &= [1-\mathcal{G}(t,k)]\alpha_H(t) + \mathcal{G}(t,k)\alpha_T(t)\,,\\
\tilde{\alpha}_B^{\mathrm{GLPV}}(t,k) &= \alpha_B^{\mathrm{GLPV}}(t) + 4\mathcal{G}(t,k)\frac{\alpha_B^2(t)}{\alpha_K(t)}\,,\\
\tilde{\alpha}_M^{\mathrm{GC}}(t,k) &= \alpha_M^{\mathrm{GC}}(t) - \frac{1}{4}\mathcal{G}(t,k)\frac{[\alpha_H(t)-\alpha_T(t)]^2}{\alpha_K(t)}\,,\\
\tilde{\alpha}_B^{\mathrm{GC}}(t,k) &= \alpha_B^{\mathrm{GC}}(t) - 2\mathcal{G}(t,k)\frac{\alpha_B(t)[\alpha_H(t)-\alpha_T(t)]}{\alpha_K(t)}\,.
\end{aligned}$$

where $\mathcal{G}(t,k) = \dfrac{\alpha_V\alpha_K}{\alpha_V\alpha_K + k^2/(a^2H^2)}$

$\alpha_V(t) \propto g_M^2$ is the effective gauge coupling

- STEFT corresponds to $\alpha_V = 0$ in which $\tilde{\alpha}_X(t,k) \rightarrow \alpha_X(t)$.

Universal predictions

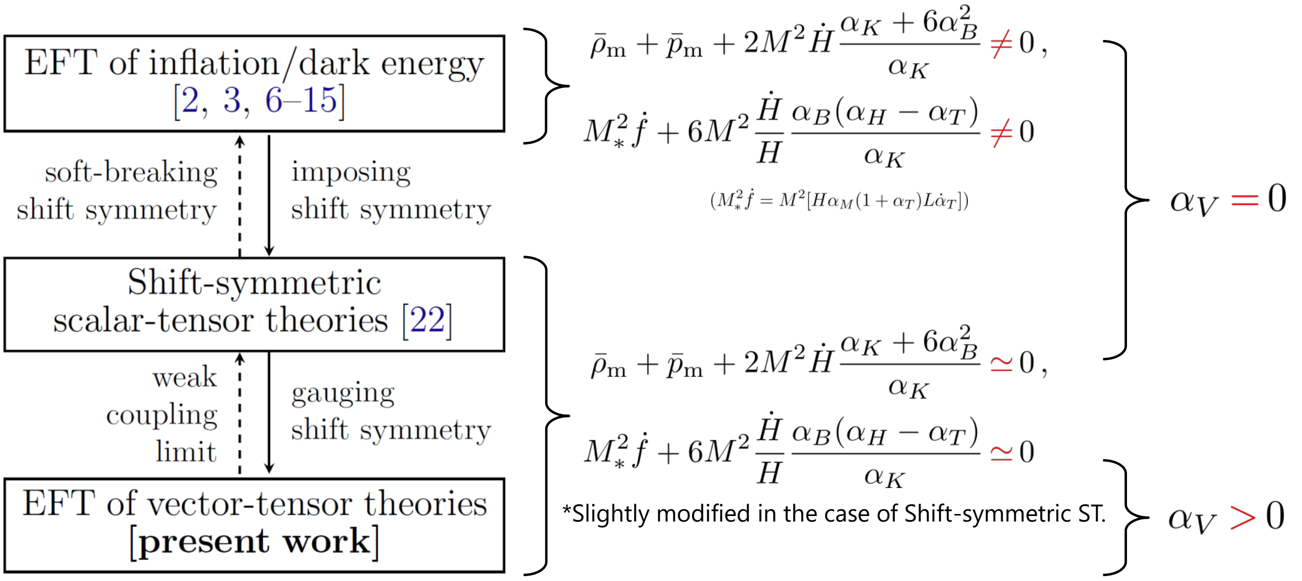

EFT of inflation/dark energy [2, 3, 6–15]

soft-breaking shift symmetry

imposing shift symmetry

Shift-symmetric scalar-tensor theories [22]

weak coupling limit

gauging shift symmetry

EFT of vector-tensor theories **[present work]**

$$\bar{\rho}_{\rm m} + \bar{p}_{\rm m} + 2M^2\dot{H}\frac{\alpha_K + 6\alpha_B^2}{\alpha_K} \neq 0\,,$$

$$M_*^2\dot{f} + 6M^2\frac{\dot{H}}{H}\frac{\alpha_B(\alpha_H - \alpha_T)}{\alpha_K} \neq 0$$

$$(M_*^2\dot{f} = M^2[H\alpha_M(1+\alpha_T)L\dot{\alpha}_T])$$

$$\bar{\rho}_{\rm m} + \bar{p}_{\rm m} + 2M^2\dot{H}\frac{\alpha_K + 6\alpha_B^2}{\alpha_K} \simeq 0\,,$$

$$M_*^2\dot{f} + 6M^2\frac{\dot{H}}{H}\frac{\alpha_B(\alpha_H - \alpha_T)}{\alpha_K} \simeq 0$$

*Slightly modified in the case of Shift-symmetric ST.

$\alpha_V = 0$

$\alpha_V > 0$

Consistency relations

Gauge coupling

Scalar and tensor perturbations

☐ Using the so-called α-basis, the EFT action becomes

$$\delta_2 S = \int \frac{{\rm d}t{\rm d}^3k}{(2\pi)^3}\bar{N}a^3\frac{M^2}{2}$$
$$\times\Bigg[(1+\tilde{\alpha}_H)\frac{\delta N}{\bar{N}}\delta_1{}^{(3)}R + 4H\tilde{\alpha}_B\frac{\delta N}{\bar{N}}\delta_1 K + \delta_1 K^\alpha{}_\beta\delta_1 K^\beta{}_\alpha - (1+\tilde{\alpha}_B^{\rm GLPV})(\delta_1 K)^2$$
$$+ \tilde{\alpha}_K H^2\left(\frac{\delta N}{\bar{N}}\right)^2 + (1+\alpha_T)\delta_2\left({}^{(3)}R\frac{\sqrt{h}}{a^3}\right) + \frac{\tilde{\alpha}_M^{\rm GC}}{H^2}(\delta_1{}^{(3)}R)^2 + \frac{\tilde{\alpha}_B^{\rm GC}}{H}\delta_1 K\delta_1{}^{(3)}R\Bigg] + \delta_2 S_{\rm m} + \cdots\,,$$

No tilde in α_T = the operator relevant for tensor modes (GWs).
GWs cannot distinguish ST&VT (or GWs give universal constraints).

Scalar perturbations can discriminate ST&VT by the gauge coupling α_V.

Modification of Poisson equation

- ☐ Effective gravitational coupling in quasi-static approximation:

$$\frac{k^2}{a^2}\Psi = -\mu(t)4\pi G\bar{\rho}_{\rm m}\Delta$$

$$8\pi G = 1/M^2(t_0)$$

Gravitational const. of GWs@$t = t_0$

- ☐ Horndeski/Generalized Proca Class ($\alpha_H = 0$)

$$\mu(t) = \frac{M^2(t_0)}{M^2(t)}\left[1+\alpha_T - 2\alpha_T^2\alpha_V + \frac{2}{V_S}(\alpha_M + \mathcal{A} - 2\mathcal{A}\alpha_T\alpha_V)^2\right]$$

$$V_S = 4\alpha_V\mathcal{A}^2 + (\text{terms independent of } \alpha_V)$$

Stability conditions: $M^2 > 0,\ 1+\alpha_T > 0,\ \alpha_V > 0,\ V_S > 0$

The gauge coupling ($\alpha_V > 0$) generically prevents the enhancement of μ.

"5th force in ST > 5th force in VT"

CMB constraints

- ☐ We are currently developing Boltzmann solvers.

$\alpha_T = \alpha_H = 0$

$D_\ell^{TT} = \ell(\ell+1)C_\ell/(2\pi)$

ST limit

Vector DE

Computed by **T. Hiramatsu**.

Summary

☐ The Effective Field Theory of Vector-Tensor Theories
= Unified formulation of not only VT but also ST.

☐ In practice, all you need is replacement of EFT coefficients

$$\alpha_B(t) \to \tilde{\alpha}_B(t,k) = [1 - \mathcal{G}(t,k)]\alpha_B(t), \ldots \qquad \mathcal{G}(t,k) = \frac{\alpha_V\alpha_K}{\alpha_V\alpha_K + k^2/(a^2H^2)}$$

☐ ST&VT are distinguished by consistency relations and gauge coupling

$$\bar{\rho}_{\rm m} + \bar{p}_{\rm m} + 2M^2\dot{H}\frac{\alpha_K + 6\alpha_B^2}{\alpha_K} \neq 0 \;\; \text{or} \;\; \simeq 0\,,$$

$$M_*^2\dot{f} + 6M^2\frac{\dot{H}}{H}\frac{\alpha_B(\alpha_H - \alpha_T)}{\alpha_K} \neq 0 \;\; \text{or} \;\; \simeq 0$$

Existence/absence of “potential”

$$\alpha_V = 0 \;\; \text{or} \;\; > 0$$

Scalar field or Vector field

☐ Boltzmann solver is under development.

We can understand how the shift sym. and the spin affect observables!

C60

Gravitational field of scalar lumps in higher-derivative gravity

based on Phys. Rev. D 103, 124068 [arXiv:2103.14313/gr-qc]

Yuichi Miyashita
(Tokyo Tech)
Collaboration with Luca Buoninfante (NORDITA)

JGRG31 October 2022

OUTLINE

1. Introduction and setup
   - Actions for higher-derivative gravity with scalar field
   - Linearized field equation with gravitational potential
2. Analysis for gravitational potentials
   i. Free massive scalar case
   ii. Polynomial scalar field case
   iii. Tachyon potential case
3. Summary & Future Directions

$c = \hbar = 1$ & $\eta = \mathrm{diag}(-,+,+,+)$

Introduction

Einstein’s GR: the most successful theory of gravity

- Several experiments verifying predictions
  …… Gravitational Wave (LIGO/Virgo, 2016), …
- Fundamental theory for gravity in modern physics

Open problems: incompleteness in UV-regime

- The predictivity breaks down in UV regime, high-energy & short distance
  Classical : BH & cosmological singularity
  Quantum: non-renormalizability

We want to modify GR in UV-regime…

Extension of GR

1. Four-derivative gravity

- Introducing **four-derivative term** (->quadratic curvature)

$$S = \int \frac{d^4x}{16\pi G}\sqrt{-g}\left[R + \alpha R^2 + \beta R_{\mu\nu}^2\right]$$

- Higher derivative terms expected from EFT perspective

2. Nonlocal gravity

Infinite derivative!

$$F_i(-\Box) = \sum_{n=0}^{\infty} f_{i,n}(-\Box)^n$$

- Introducing **infinitely higher derivative term**

$$S = \frac{2}{\kappa^2}\int d^4x\,\sqrt{-g}\left[R + \frac{1}{2}\left(RF_1(-\Box)R + R_{\mu\nu}F_2(-\Box)R^{\mu\nu}\right)\right]$$

- Nonlocality from infinite derivatives

Setup

Consider the action $S = S_g + S_\phi$ $\kappa^2 = 32\pi G$ $F_1(\Box) = -\frac{F_2(\Box)}{2} = \frac{1 - f(\Box)}{\Box}$

$$\begin{cases} S_g = \frac{2}{\kappa^2}\int d^4x\sqrt{-g}\left[R + \frac{1}{2}\left(RF_1(-\Box_g)R + R_{\mu\nu}F_2(-\Box_g)R^{\mu\nu}\right)\right] \\ S_\phi = \int d^4x\sqrt{-g}\left[\frac{1}{2}\phi(\Box_g - m^2)\phi - V(\phi)\right] \end{cases}$$

Field equation

$$\boxed{(\Box^2 - m^2)\phi = -\frac{dV(\phi)}{d\phi}}$$

Form factor characterizing the gravity sector:

1. $f = 1$: General Relativity
2. $f = 1 - \frac{\alpha}{2}\Box$: fourth-derivative gravity α>0: constant
3. $f = e^{-\Box/\mu^2}$: nonlocal gravity μ : Nonlocal Scale

---

Linearized field equations

Field equations for metric perturbation $h_{\mu\nu}$ and scalar field ϕ

$$f(\Box)\Box\left(h_{\mu\nu} - \frac{1}{2}\eta_{\mu\nu}h\right) = -\frac{\kappa}{2}T_{\mu\nu}$$

Harmonic gauge

$$\partial^\mu\left(h_{\mu\nu} - \frac{1}{2}\eta_{\mu\nu}h\right) = 0$$

Assumption: <u>static</u> and <u>spherically symmetric</u> configuration

- The isotropic coordinate $\mathrm{d}s^2 = -\left(1 + 2\Phi(r)\right)\mathrm{d}t^2 + (1 - 2\Psi(r))\mathrm{d}\vec{r}^2$

$$\Rightarrow \begin{cases} f(\nabla^2)\nabla^2\Phi(r) = 4\pi G\{T[\phi](r) + 2T_{00}[\phi](r)\} \\ f(\nabla^2)\nabla^2\Psi(r) = 4\pi G\, T_{00}[\phi](r) \end{cases}$$

$T[\phi] = T^\mu_\mu[\phi]$

$T_{00}[\phi](r)$ and $T[\phi](r)$ are determined from the solution ϕ of field equation

Gravitational potential generated by scalar field

Consider **scalar lump** generating gravitational potential

- **Lump**: localized scalar field configuration

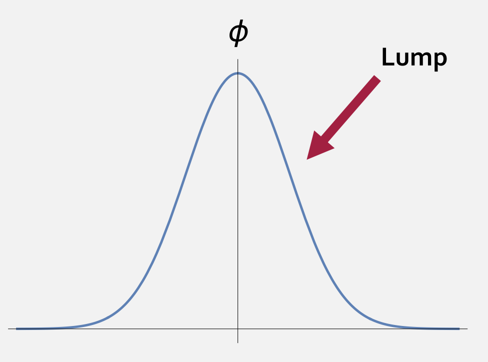

Three cases for scalar field ϕ

1. Free massive scalar
$$V(\phi) = 0$$
2. Polynomial potential with $\lambda > 0,\ g > 0$
$$V(\phi) = -\frac{\lambda}{4}\phi^4 + \frac{g}{3}\phi^3$$
3. Tachyon potential
$$V(\phi) = -m_s^2\phi^2 \log\left(\frac{\phi^2}{m_s^2 e}\right)$$

---

1. Free massive scalar field

The action for scalar field: $S = \int dx\, \phi(\Box - m^2)\phi$

Equation $(\nabla^2 - m^2)\phi = 0$ ⇒ Lump $\phi = \frac{C}{r}e^{-mr}$ (C: constant)

Localized source radius $R \sim 1/m$

⇒ Substituting
$$\begin{cases} f(\nabla^2)\nabla^2\Phi(r) = 4\pi G\{T[\phi](r) + 2T_{00}[\phi](r)\} \\ f(\nabla^2)\nabla^2\Psi(r) = 4\pi G\, T_{00}[\phi](r) \end{cases}$$

Solutions of equations given in integral representation

- Asymptotically flat solution (boundary condition)

1. Free massive scalar field

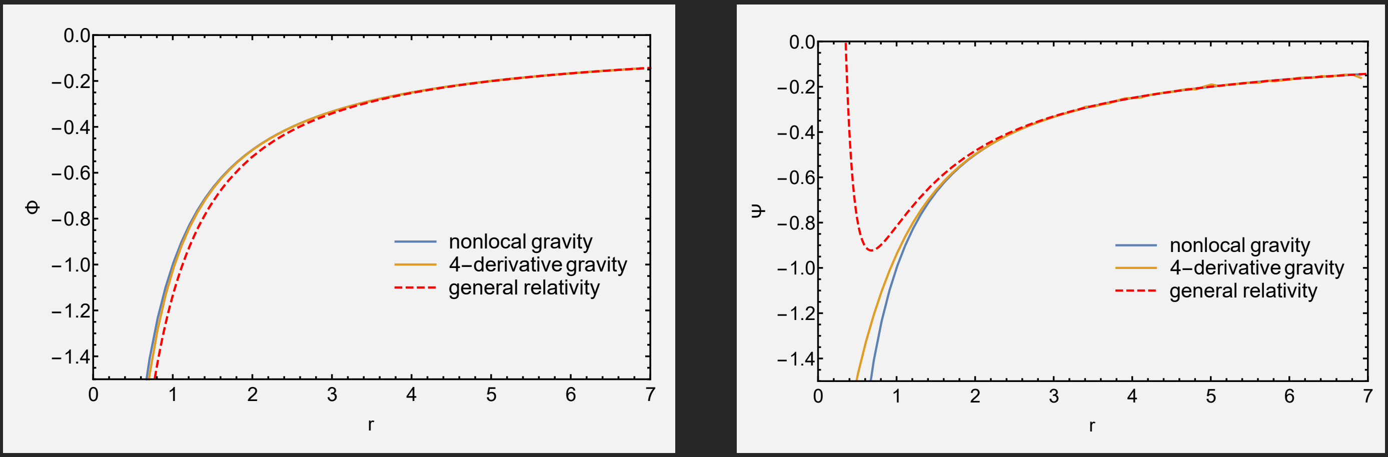

- Singularity at the origin $r = 0$ in all theories

  (This singularity is not regularized by nonlocality)

- No repulsive behavior of the potential $\Psi(r)$ in higher derivative gravity

---

2. Polynomial scalar field potential

The potential: $V(\phi) = \frac{g}{3}\phi^3 - \frac{\lambda}{4}\phi^4$

Radius of system $R = \frac{1}{g}\sqrt{\frac{\lambda}{2}}$

Equation $\left(\partial_r^2 + \frac{2}{r}\partial_r\right)\phi = g\phi^2 - \lambda\phi^3$ Lump $\phi = \frac{2}{g}\frac{1}{r^2+R^2}$ (regular)

Mass energy M of lump config:

$$M = \int d^3r\ T_{00}(r) = \frac{2\pi}{3g^2R^3}$$

Corresponding Schwarzschild radius:

$$R_{\rm sch} = 2GM = \frac{4\pi^2 G}{3g^2R^3}$$

Validity for weak field approx.

$$\boldsymbol{R \gtrsim R_{\rm Sch}}$$

$$\boldsymbol{\lambda \lesssim \left(4\pi\sqrt{\frac{G}{3}}\right) g}$$

2. Polynomial scalar field potential

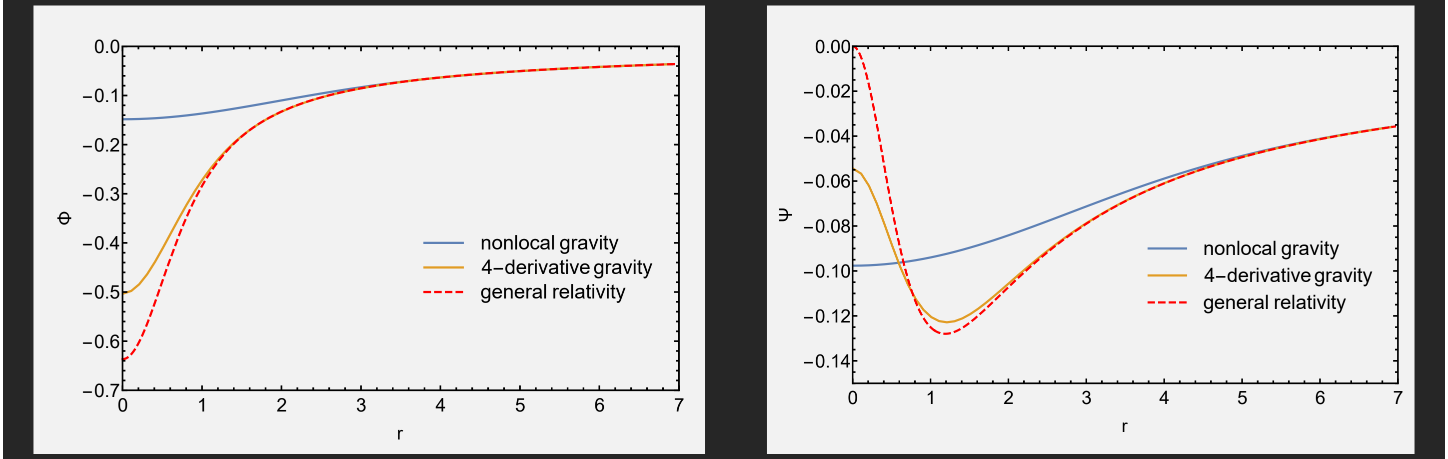

- Nonsingular potentials from nonsingular scalar field
- No repulsive behavior of the potential $\Psi(r)$ in nonlocal gravity

  → Only true for sufficiently small scale μ (for large μ, monotonicity is lost)

---

3. Tachyon potential

Tachyon potential: $V(\phi) = m_s^2 \phi^2 \log\left(\frac{\phi^2}{m_s^2 e}\right)$

Equation $\left(\partial_r^2 + \frac{2}{r}\partial_r\right)\phi = -2m_s^2 \phi \log\left(\frac{\phi^2}{m_s^2}\right)$ → Lump $\phi = e^{3/2} m_s e^{-m_s r}$

Mass energy M of lump config:

$$M = \int d^3r \; T_{00}(r) = \frac{e^3 \pi^{3/2} m_s}{2\sqrt{2}}$$

Corresponding Schwarzschild radius:

$$R_{\text{sch}} = 2GM = \frac{e^3 \pi^{3/2} G m_s}{\sqrt{2}}$$

→

Validity for weak field approx.

$$\boldsymbol{R \gtrsim R_{\text{Sch}}}$$

↓

$$\boldsymbol{m_s^2 \lesssim \left(\frac{e^3 \pi^{3/2}}{\sqrt{2}}\right) M_p^2}$$

3. Tachyon potential

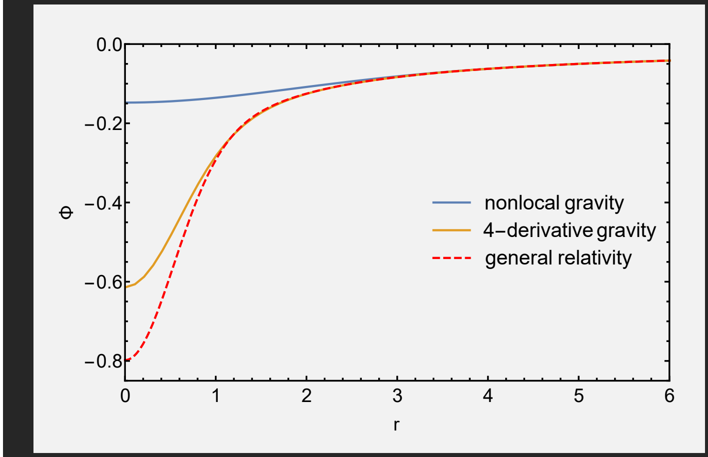

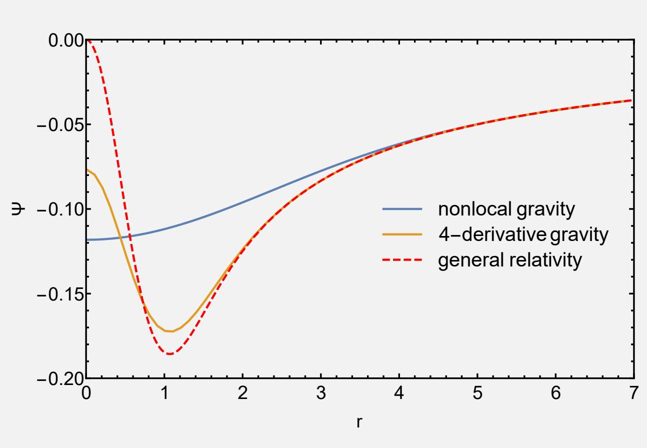

- Nonsingular potentials from nonsingular scalar field in all theories
- No repulsive behavior of the potential $\Psi(r)$ in nonlocal gravity

➡ Range of monotonicity: $\mu \leq 2m_s$ (from analytic solution)

Compactness

Conditions for weak field regime: $2|\Phi|, 2|\Psi| < 1$

- For case 2 & 3, conditions are satisfied from $r = 0$ to $r = \infty$

⟶ In this sense these solution can describe **horizonless** compact objects

Compactness $\mathcal{C} \equiv GM/R$ with effective radius R for localized mass M

- Blackhole : $\mathcal{C} = GM/2GM = 1/2$
- Compact object : $\mathcal{C} < 1/2$

From the results of analysis:

- Compactness is proportional to potential at the origin: $\mathcal{C} \propto \Phi(0)$
- Nonlocality give less compact configuration as compared to other theories
- Higher derivative plays crucial role even for regular configuration

Summary & Future Directions

◆ Summary:

- Linearized metric sourced by scalar lump in different theories of gravity
- Nonlocality avoids repulsive contribution for sufficiently small scale μ
- Less compactness configuration in nonlocal gravity

◆ Future Directions:

- Study for some phenomenology of horizonless compact object
- Horizonless compact objects as remnant of binary merger
  ...introducing higher multipole & non-zero velocity, making stability analysis, ...

C61

New black hole solutions with a dynamical traceless nonmetricity tensor in Metric-Affine Gravity

Sebastián Bahamonde

JSPS Postdoctoral Researcher at Tokyo Institute of Technology, Japan

JGRG31, 27/Oct/2022
Based on JCAP **09** (2020), 057 and 2210.05998;
Jointly with Jorge Gigante Valcarcel.

Fundamental variables and characteristic tensors

- In the most general metric-affine setting, the fundamental variables are a **metric** $g_{\mu\nu}$ (10 comp.) as well as the coefficients $\tilde{\Gamma}^{\rho}{}_{\mu\nu}$ (64 comp.) of an **affine connection**.

Fundamental variables and characteristic tensors

- In the most general metric-affine setting, the fundamental variables are a **metric** $g_{\mu\nu}$ (10 comp.) as well as the coefficients $\tilde{\Gamma}^{\rho}{}_{\mu\nu}$ (64 comp.) of an **affine connection**.
- The most general connection can be written as

Fundamental variables and characteristic tensors

- In the most general metric-affine setting, the fundamental variables are a **metric** $g_{\mu\nu}$ (10 comp.) as well as the coefficients $\tilde{\Gamma}^{\rho}{}_{\mu\nu}$ (64 comp.) of an **affine connection**.
- The most general connection can be written as

Connection decomposition

$$\tilde{\Gamma}^{\lambda}{}_{\mu\nu} = \Gamma^{\lambda}{}_{\mu\nu} + N^{\lambda}{}_{\mu\nu} = \overbrace{\Gamma^{\lambda}{}_{\mu\nu}}^{\textbf{Levi-Civita}}$$

Fundamental variables and characteristic tensors

- In the most general metric-affine setting, the fundamental variables are a **metric** $g_{\mu\nu}$ (10 comp.) as well as the coefficients $\tilde{\Gamma}^\rho{}_{\mu\nu}$ (64 comp.) of an **affine connection**.
- The most general connection can be written as

Connection decomposition

$$\tilde{\Gamma}^\lambda{}_{\mu\nu} = \Gamma^\lambda{}_{\mu\nu} + N^\lambda{}_{\mu\nu} = \overbrace{\Gamma^\lambda{}_{\mu\nu}}^{\text{Levi-Civita}}$$

Fundamental variables and characteristic tensors

- In the most general metric-affine setting, the fundamental variables are a **metric** $g_{\mu\nu}$ (10 comp.) as well as the coefficients $\tilde{\Gamma}^\rho{}_{\mu\nu}$ (64 comp.) of an **affine connection**.
- The most general connection can be written as

Connection decomposition

$$\tilde{\Gamma}^\lambda{}_{\mu\nu} = \Gamma^\lambda{}_{\mu\nu} + N^\lambda{}_{\mu\nu} = \overbrace{\Gamma^\lambda{}_{\mu\nu}}^{\text{Levi-Civita}} + \overbrace{\frac{1}{2}T^\lambda{}_{\mu\nu} - T_{(\mu}{}^\lambda{}_{\nu)}}^{\text{Torsion part}}$$

Fundamental variables and characteristic tensors

- In the most general metric-affine setting, the fundamental variables are a **metric** $g_{\mu\nu}$ (10 comp.) as well as the coefficients $\tilde{\Gamma}^\rho{}_{\mu\nu}$ (64 comp.) of an **affine connection**.
- The most general connection can be written as

Connection decomposition

$$\tilde{\Gamma}^\lambda{}_{\mu\nu} = \Gamma^\lambda{}_{\mu\nu} + N^\lambda{}_{\mu\nu} = \overbrace{\Gamma^\lambda{}_{\mu\nu}}^{\text{Levi-Civita}} + \overbrace{\frac{1}{2} T^\lambda{}_{\mu\nu} - T_{(\mu}{}^{\lambda}{}_{\nu)}}^{\text{Torsion part}} + \overbrace{\frac{1}{2} Q^\lambda{}_{\mu\nu} - Q_{(\mu}{}^{\lambda}{}_{\nu)}}^{\text{Nonmetricity part}} .$$

Curvature decomposition, torsion and nonmetricity

$$\begin{aligned}
\tilde{R}^\lambda{}_{\rho\mu\nu} &= R^\lambda{}_{\rho\mu\nu} + 2\nabla_{[\mu|} N^\lambda{}_{\rho|\nu]} + 2N^\lambda{}_{\sigma[\mu|} N^\sigma{}_{\rho|\nu]} \,, \\
\tilde{T}^\mu{}_{\nu\rho} &= \tilde{\Gamma}^\mu{}_{\rho\nu} - \tilde{\Gamma}^\mu{}_{\nu\rho} \,, \\
\tilde{Q}_{\mu\nu\rho} &= \tilde{\nabla}_\mu g_{\nu\rho} = \partial_\mu g_{\nu\rho} - \tilde{\Gamma}^\sigma{}_{\nu\mu} g_{\sigma\rho} - \tilde{\Gamma}^\sigma{}_{\rho\mu} g_{\nu\sigma} \,.
\end{aligned}$$

Tildes=General, nothing=Riemannian $\to$ ∇_μ(Levi-Civita), $\tilde{\nabla}_\mu$(General)

Decomposition into irreducible parts

- Irreducible decomposition of the torsion tensor:

$$T^\lambda{}_{\mu\nu} = \frac{1}{3}\left(\delta^\lambda{}_\nu T_\mu - \delta^\lambda{}_\mu T_\nu\right) + \frac{1}{6}\varepsilon^\lambda{}_{\rho\mu\nu} S^\rho + t^\lambda{}_{\mu\nu} \,,$$

Decomposition into irreducible parts

- Irreducible decomposition of the torsion tensor:

$$T^{\lambda}{}_{\mu\nu} = \frac{1}{3}\left(\delta^{\lambda}{}_{\nu}T_{\mu} - \delta^{\lambda}{}_{\mu}T_{\nu}\right) + \frac{1}{6}\varepsilon^{\lambda}{}_{\rho\mu\nu}S^{\rho} + t^{\lambda}{}_{\mu\nu}\,,$$

  - vector part $T_{\mu} = T^{\lambda}{}_{\mu\lambda}$,

Decomposition into irreducible parts

- Irreducible decomposition of the torsion tensor:

$$T^{\lambda}{}_{\mu\nu} = \frac{1}{3}\left(\delta^{\lambda}{}_{\nu}T_{\mu} - \delta^{\lambda}{}_{\mu}T_{\nu}\right) + \frac{1}{6}\varepsilon^{\lambda}{}_{\rho\mu\nu}S^{\rho} + t^{\lambda}{}_{\mu\nu}\,,$$

  - vector part $T_{\mu} = T^{\lambda}{}_{\mu\lambda}$,

  - axial vector part $S_{\mu} = \varepsilon_{\mu\nu\rho\sigma}T^{\nu\sigma\rho}$,

Decomposition into irreducible parts

- Irreducible decomposition of the torsion tensor:

$$T^{\lambda}{}_{\mu\nu}=\frac{1}{3}\left(\delta^{\lambda}{}_{\nu}T_{\mu}-\delta^{\lambda}{}_{\mu}T_{\nu}\right)+\frac{1}{6}\varepsilon^{\lambda}{}_{\rho\mu\nu}S^{\rho}+t^{\lambda}{}_{\mu\nu}\,,$$

  - vector part $T_{\mu}=T^{\lambda}{}_{\mu\lambda}$,
  - axial vector part $S_{\mu}=\varepsilon_{\mu\nu\rho\sigma}T^{\nu\sigma\rho}$,
  - tensor part $t^{\lambda}{}_{\mu\nu}=T^{\lambda}{}_{\mu\nu}-\frac{1}{3}\left(\delta^{\lambda}{}_{\nu}T_{\mu}-\delta^{\lambda}{}_{\mu}T_{\nu}\right)-\frac{1}{6}\varepsilon^{\lambda}{}_{\rho\mu\nu}S^{\rho}$.

Decomposition into irreducible parts

- Irreducible decomposition of the torsion tensor:

$$T^{\lambda}{}_{\mu\nu}=\frac{1}{3}\left(\delta^{\lambda}{}_{\nu}T_{\mu}-\delta^{\lambda}{}_{\mu}T_{\nu}\right)+\frac{1}{6}\varepsilon^{\lambda}{}_{\rho\mu\nu}S^{\rho}+t^{\lambda}{}_{\mu\nu}\,,$$

  - vector part $T_{\mu}=T^{\lambda}{}_{\mu\lambda}$,
  - axial vector part $S_{\mu}=\varepsilon_{\mu\nu\rho\sigma}T^{\nu\sigma\rho}$,
  - tensor part $t^{\lambda}{}_{\mu\nu}=T^{\lambda}{}_{\mu\nu}-\frac{1}{3}\left(\delta^{\lambda}{}_{\nu}T_{\mu}-\delta^{\lambda}{}_{\mu}T_{\nu}\right)-\frac{1}{6}\varepsilon^{\lambda}{}_{\rho\mu\nu}S^{\rho}$.

- Irreducible decomposition of the nonmetricity tensor:

$$Q_{\lambda\mu\nu}=\text{Weyl part }+\text{ Traceless part}=g_{\mu\nu}W_{\lambda}+\not{Q}_{\lambda\mu\nu}\,,$$

$$\not{Q}_{\lambda\mu\nu}=\frac{1}{2}\left(g_{\lambda\mu}\Lambda_{\nu}+g_{\lambda\nu}\Lambda_{\mu}\right)-\frac{1}{4}g_{\mu\nu}\Lambda_{\lambda}+\frac{1}{3}\varepsilon_{\lambda\rho\sigma(\mu}\Omega_{\nu)}{}^{\rho\sigma}+q_{\lambda\mu\nu}\,.$$

Decomposition into irreducible parts

- Irreducible decomposition of the torsion tensor:

$$T^{\lambda}{}_{\mu\nu} = \frac{1}{3}\left(\delta^{\lambda}{}_{\nu}T_{\mu} - \delta^{\lambda}{}_{\mu}T_{\nu}\right) + \frac{1}{6}\varepsilon^{\lambda}{}_{\rho\mu\nu}S^{\rho} + t^{\lambda}{}_{\mu\nu}\,,$$

  - vector part $T_{\mu} = T^{\lambda}{}_{\mu\lambda}$,
  - axial vector part $S_{\mu} = \varepsilon_{\mu\nu\rho\sigma}T^{\nu\sigma\rho}$,
  - tensor part $t^{\lambda}{}_{\mu\nu} = T^{\lambda}{}_{\mu\nu} - \frac{1}{3}\left(\delta^{\lambda}{}_{\nu}T_{\mu} - \delta^{\lambda}{}_{\mu}T_{\nu}\right) - \frac{1}{6}\varepsilon^{\lambda}{}_{\rho\mu\nu}S^{\rho}$.
- Irreducible decomposition of the nonmetricity tensor:

$$Q_{\lambda\mu\nu} = \text{Weyl part } + \text{ Traceless part} = g_{\mu\nu}W_{\lambda} + \not{Q}_{\lambda\mu\nu}\,,$$

$$\not{Q}_{\lambda\mu\nu} = \frac{1}{2}\left(g_{\lambda\mu}\Lambda_{\nu} + g_{\lambda\nu}\Lambda_{\mu}\right) - \frac{1}{4}g_{\mu\nu}\Lambda_{\lambda} + \frac{1}{3}\varepsilon_{\lambda\rho\sigma(\mu}\Omega_{\nu)}{}^{\rho\sigma} + q_{\lambda\mu\nu}\,.$$

  - Weyl vector $W_{\mu} = \frac{1}{4}Q_{\mu\nu}{}^{\nu}$,

Decomposition into irreducible parts

- Irreducible decomposition of the torsion tensor:

$$T^{\lambda}{}_{\mu\nu} = \frac{1}{3}\left(\delta^{\lambda}{}_{\nu}T_{\mu} - \delta^{\lambda}{}_{\mu}T_{\nu}\right) + \frac{1}{6}\varepsilon^{\lambda}{}_{\rho\mu\nu}S^{\rho} + t^{\lambda}{}_{\mu\nu}\,,$$

  - vector part $T_{\mu} = T^{\lambda}{}_{\mu\lambda}$,
  - axial vector part $S_{\mu} = \varepsilon_{\mu\nu\rho\sigma}T^{\nu\sigma\rho}$,
  - tensor part $t^{\lambda}{}_{\mu\nu} = T^{\lambda}{}_{\mu\nu} - \frac{1}{3}\left(\delta^{\lambda}{}_{\nu}T_{\mu} - \delta^{\lambda}{}_{\mu}T_{\nu}\right) - \frac{1}{6}\varepsilon^{\lambda}{}_{\rho\mu\nu}S^{\rho}$.
- Irreducible decomposition of the nonmetricity tensor:

$$Q_{\lambda\mu\nu} = \text{Weyl part } + \text{ Traceless part} = g_{\mu\nu}W_{\lambda} + \not{Q}_{\lambda\mu\nu}\,,$$

$$\not{Q}_{\lambda\mu\nu} = \frac{1}{2}\left(g_{\lambda\mu}\Lambda_{\nu} + g_{\lambda\nu}\Lambda_{\mu}\right) - \frac{1}{4}g_{\mu\nu}\Lambda_{\lambda} + \frac{1}{3}\varepsilon_{\lambda\rho\sigma(\mu}\Omega_{\nu)}{}^{\rho\sigma} + q_{\lambda\mu\nu}\,.$$

  - Weyl vector $W_{\mu} = \frac{1}{4}Q_{\mu\nu}{}^{\nu}$,
  - Second vector part $\Lambda_{\mu} = \frac{4}{9}\left(Q^{\nu}{}_{\mu\nu} - W_{\mu}\right)$,

Decomposition into irreducible parts

- Irreducible decomposition of the torsion tensor:

$$T^{\lambda}{}_{\mu\nu} = \frac{1}{3}\left(\delta^{\lambda}{}_{\nu}T_{\mu} - \delta^{\lambda}{}_{\mu}T_{\nu}\right) + \frac{1}{6}\varepsilon^{\lambda}{}_{\rho\mu\nu}S^{\rho} + t^{\lambda}{}_{\mu\nu}\,,$$

  - vector part $T_{\mu} = T^{\lambda}{}_{\mu\lambda}$,
  - axial vector part $S_{\mu} = \varepsilon_{\mu\nu\rho\sigma}T^{\nu\sigma\rho}$,
  - tensor part $t^{\lambda}{}_{\mu\nu} = T^{\lambda}{}_{\mu\nu} - \frac{1}{3}\left(\delta^{\lambda}{}_{\nu}T_{\mu} - \delta^{\lambda}{}_{\mu}T_{\nu}\right) - \frac{1}{6}\varepsilon^{\lambda}{}_{\rho\mu\nu}S^{\rho}$.
- Irreducible decomposition of the nonmetricity tensor:

$$Q_{\lambda\mu\nu} = \text{Weyl part} \;+\; \text{Traceless part} = g_{\mu\nu}W_{\lambda} + \not{Q}_{\lambda\mu\nu}\,,$$

$$\not{Q}_{\lambda\mu\nu} = \frac{1}{2}\left(g_{\lambda\mu}\Lambda_{\nu} + g_{\lambda\nu}\Lambda_{\mu}\right) - \frac{1}{4}g_{\mu\nu}\Lambda_{\lambda} + \frac{1}{3}\varepsilon_{\lambda\rho\sigma(\mu}\Omega_{\nu)}{}^{\rho\sigma} + q_{\lambda\mu\nu}\,.$$

  - Weyl vector $W_{\mu} = \frac{1}{4}Q_{\mu\nu}{}^{\nu}$,
  - Second vector part $\Lambda_{\mu} = \frac{4}{9}\left(Q^{\nu}{}_{\mu\nu} - W_{\mu}\right)$,
  - First (pseudo)tensor part $\Omega_{\lambda}{}^{\mu\nu} = -\left[\varepsilon^{\mu\nu\rho\sigma}Q_{\rho\sigma\lambda} + \varepsilon^{\mu\nu\rho}{}_{\lambda}\left(\frac{3}{4}\Lambda_{\rho} - W_{\rho}\right)\right]$,

---

Decomposition into irreducible parts

- Irreducible decomposition of the torsion tensor:

$$T^{\lambda}{}_{\mu\nu} = \frac{1}{3}\left(\delta^{\lambda}{}_{\nu}T_{\mu} - \delta^{\lambda}{}_{\mu}T_{\nu}\right) + \frac{1}{6}\varepsilon^{\lambda}{}_{\rho\mu\nu}S^{\rho} + t^{\lambda}{}_{\mu\nu}\,,$$

  - vector part $T_{\mu} = T^{\lambda}{}_{\mu\lambda}$,
  - axial vector part $S_{\mu} = \varepsilon_{\mu\nu\rho\sigma}T^{\nu\sigma\rho}$,
  - tensor part $t^{\lambda}{}_{\mu\nu} = T^{\lambda}{}_{\mu\nu} - \frac{1}{3}\left(\delta^{\lambda}{}_{\nu}T_{\mu} - \delta^{\lambda}{}_{\mu}T_{\nu}\right) - \frac{1}{6}\varepsilon^{\lambda}{}_{\rho\mu\nu}S^{\rho}$.
- Irreducible decomposition of the nonmetricity tensor:

$$Q_{\lambda\mu\nu} = \text{Weyl part} \;+\; \text{Traceless part} = g_{\mu\nu}W_{\lambda} + \not{Q}_{\lambda\mu\nu}\,,$$

$$\not{Q}_{\lambda\mu\nu} = \frac{1}{2}\left(g_{\lambda\mu}\Lambda_{\nu} + g_{\lambda\nu}\Lambda_{\mu}\right) - \frac{1}{4}g_{\mu\nu}\Lambda_{\lambda} + \frac{1}{3}\varepsilon_{\lambda\rho\sigma(\mu}\Omega_{\nu)}{}^{\rho\sigma} + q_{\lambda\mu\nu}\,.$$

  - Weyl vector $W_{\mu} = \frac{1}{4}Q_{\mu\nu}{}^{\nu}$,
  - Second vector part $\Lambda_{\mu} = \frac{4}{9}\left(Q^{\nu}{}_{\mu\nu} - W_{\mu}\right)$,
  - First (pseudo)tensor part $\Omega_{\lambda}{}^{\mu\nu} = -\left[\varepsilon^{\mu\nu\rho\sigma}Q_{\rho\sigma\lambda} + \varepsilon^{\mu\nu\rho}{}_{\lambda}\left(\frac{3}{4}\Lambda_{\rho} - W_{\rho}\right)\right]$,
  - Second tensor part $q_{\lambda\mu\nu} = Q_{(\lambda\mu\nu)} - g_{(\mu\nu}W_{\lambda)} - \frac{3}{4}g_{(\mu\nu}\Lambda_{\lambda)}$.

Dynamics of metric-affine geometry

- Gravitational action with dynamical torsion and nonmetricity:

$$S = \int d^4x\sqrt{-g}\left[\mathcal{L}_m - \frac{1}{16\pi}\mathcal{L}_g(\tilde{\mathcal{R}}, \mathcal{T}, \mathcal{Q})\right] .$$

Dynamics of metric-affine geometry

- Gravitational action with dynamical torsion and nonmetricity:

$$S = \int d^4x\sqrt{-g}\left[\mathcal{L}_m - \frac{1}{16\pi}\mathcal{L}_g(\tilde{\mathcal{R}}, \mathcal{T}, \mathcal{Q})\right] .$$

- Correspondence between geometry and matter:

$$\begin{aligned}\frac{\delta S_g}{\delta e^a{}_\nu} &= 16\pi\theta_a{}^\nu ,\\ \frac{\delta S_g}{\delta \omega^a{}_{b\nu}} &= 16\pi\Delta_a{}^{b\nu} .\end{aligned}$$

  Here $\theta_a{}^\nu$ is the energy-momentum tensor (canonical) and $\Delta_a{}^{b\nu}$ is the hypermomentum density tensor.

Dynamics of metric-affine geometry

- Gravitational action with dynamical torsion and nonmetricity:

$$S=\int d^4x\sqrt{-g}\left[\mathcal{L}_m-\frac{1}{16\pi}\mathcal{L}_g(\tilde{\mathcal{R}},\mathcal{T},\mathcal{Q})\right].$$

- Correspondence between geometry and matter:

$$\begin{aligned}\frac{\delta S_g}{\delta e^a{}_\nu} &= 16\pi\theta_a{}^\nu\,,\\ \frac{\delta S_g}{\delta\omega^a{}_{b\nu}} &= 16\pi\Delta_a{}^{b\nu}\,.\end{aligned}$$

  Here $\theta_a{}^\nu$ is the energy-momentum tensor (canonical) and $\Delta_a{}^{b\nu}$ is the hypermomentum density tensor.
- Three independent contractions of the curvature tensor and only one independent scalar curvature:

$$\tilde{R}_{\mu\nu}=\tilde{R}^\lambda{}_{\mu\lambda\nu}\,,\quad \hat{R}_{\mu\nu}=\tilde{R}_\mu{}^\lambda{}_{\nu\lambda}\,,\quad \tilde{R}^\lambda{}_{\lambda\mu\nu}=4\nabla_{[\nu}W_{\mu]}\,,$$
$$\tilde{R}=\tilde{R}^{\lambda\rho}{}_{\lambda\rho}\,.$$

Dynamics of metric-affine geometry

- Gravitational action with dynamical torsion and nonmetricity:

$$S=\int d^4x\sqrt{-g}\left[\mathcal{L}_m-\frac{1}{16\pi}\mathcal{L}_g(\tilde{\mathcal{R}},\mathcal{T},\mathcal{Q})\right].$$

- Correspondence between geometry and matter:

$$\begin{aligned}\frac{\delta S_g}{\delta e^a{}_\nu} &= 16\pi\theta_a{}^\nu\,,\\ \frac{\delta S_g}{\delta\omega^a{}_{b\nu}} &= 16\pi\Delta_a{}^{b\nu}\,.\end{aligned}$$

  Here $\theta_a{}^\nu$ is the energy-momentum tensor (canonical) and $\Delta_a{}^{b\nu}$ is the hypermomentum density tensor.
- Three independent contractions of the curvature tensor and only one independent scalar curvature:

$$\tilde{R}_{\mu\nu}=\tilde{R}^\lambda{}_{\mu\lambda\nu}\,,\quad \hat{R}_{\mu\nu}=\tilde{R}_\mu{}^\lambda{}_{\nu\lambda}\,,\quad \tilde{R}^\lambda{}_{\lambda\mu\nu}=4\nabla_{[\nu}W_{\mu]}\,,$$
$$\tilde{R}=\tilde{R}^{\lambda\rho}{}_{\lambda\rho}\,.$$

- $GL(4,R)$ group allows the definition of a large number of scalars.

MAG theory with shears

- Let us first consider a simple model where torsion is not propagating and the traceless part of nonmetricity is dynamical:

$$S=\frac{1}{16\pi}\int d^4x\sqrt{-g}\Big[-R+2f_1\tilde{R}_{(\lambda\rho)\mu\nu}\tilde{R}^{(\lambda\rho)\mu\nu} \\ +2f_2\left(\tilde{R}_{(\mu\nu)}-\hat{R}_{(\mu\nu)}\right)\left(\tilde{R}^{(\mu\nu)}-\hat{R}^{(\mu\nu)}\right)\Big]\,,$$

MAG theory with shears

- Let us first consider a simple model where torsion is not propagating and the traceless part of nonmetricity is dynamical:

$$S=\frac{1}{16\pi}\int d^4x\sqrt{-g}\Big[-R+2f_1\tilde{R}_{(\lambda\rho)\mu\nu}\tilde{R}^{(\lambda\rho)\mu\nu} \\ +2f_2\left(\tilde{R}_{(\mu\nu)}-\hat{R}_{(\mu\nu)}\right)\left(\tilde{R}^{(\mu\nu)}-\hat{R}^{(\mu\nu)}\right)\Big]\,,$$

- As can be seen, the propagation of the nonmetricity field described in the action is carried out by the symmetric part of the curvature tensor and its symmetric contraction:

$$\tilde{R}^{(\lambda\rho)}{}_{\mu\nu}=\tilde{\nabla}_{[\nu}Q_{\mu]}{}^{\lambda\rho}+\frac{1}{2}T^{\sigma}{}_{\mu\nu}Q_{\sigma}{}^{\lambda\rho}\,,$$

$$\tilde{R}_{(\mu\nu)}-\hat{R}_{(\mu\nu)}=\tilde{\nabla}_{(\mu}Q^{\lambda}{}_{\nu)\lambda}-\tilde{\nabla}_{\lambda}Q_{(\mu\nu)}{}^{\lambda}-Q^{\lambda\rho}{}_{\lambda}Q_{(\mu\nu)\rho}+Q_{\lambda\rho(\mu}Q_{\nu)}{}^{\lambda\rho} \\ +T_{\lambda\rho(\mu}Q^{\lambda\rho}{}_{\nu)}\,,$$

which in turn constitute deviations from the third Bianchi of GR.

Spherical symmetry in metric-affine geometry

- Metric, torsion and nonmetricity tensors in symmetric space-times:

$$\mathcal{L}_\xi g_{\mu\nu} = \mathcal{L}_\xi T^\lambda{}_{\mu\nu} = \mathcal{L}_\xi Q^\lambda{}_{\mu\nu} = 0 \implies \mathcal{L}_\xi \tilde{R}^\lambda{}_{\rho\mu\nu} = 0\,.$$

Spherical symmetry in metric-affine geometry

- Metric, torsion and nonmetricity tensors in symmetric space-times:

$$\mathcal{L}_\xi g_{\mu\nu} = \mathcal{L}_\xi T^\lambda{}_{\mu\nu} = \mathcal{L}_\xi Q^\lambda{}_{\mu\nu} = 0 \implies \mathcal{L}_\xi \tilde{R}^\lambda{}_{\rho\mu\nu} = 0\,.$$

- Killing vectors in static and spherically symmetric space-times:

$$\begin{aligned}\eta_0 &= \partial_t\,,\\ \xi_1 &= \sin\varphi\,\partial_\vartheta + \cot\vartheta\cos\varphi\,\partial_\varphi\,,\\ \xi_2 &= -\cos\varphi\,\partial_\vartheta + \cot\vartheta\sin\varphi\,\partial_\varphi\,,\\ \xi_3 &= -\partial_\varphi\,.\end{aligned}$$

Spherical symmetry in metric-affine geometry

- Metric, torsion and nonmetricity tensors in symmetric space-times:

$$\mathcal{L}_\xi g_{\mu\nu} = \mathcal{L}_\xi T^{\lambda}{}_{\mu\nu} = \mathcal{L}_\xi Q^{\lambda}{}_{\mu\nu} = 0 \implies \mathcal{L}_\xi \tilde{R}^{\lambda}{}_{\rho\mu\nu} = 0\,.$$

- Killing vectors in static and spherically symmetric space-times:

$$\begin{aligned} \eta_0 &= \partial_t\,, \\ \xi_1 &= \sin\varphi\,\partial_\vartheta + \cot\vartheta\cos\varphi\,\partial_\varphi\,, \\ \xi_2 &= -\,\cos\varphi\,\partial_\vartheta + \cot\vartheta\sin\varphi\,\partial_\varphi\,, \\ \xi_3 &= -\,\partial_\varphi\,. \end{aligned}$$

- Metric:

$$\#10\,\text{dof} \to \#2\,\text{dof}\left\{ ds^2 = \Psi_1(r)\,dt^2 - \frac{dr^2}{\Psi_2(r)} - r^2\left(d\vartheta^2 + \sin\vartheta^2 d\varphi^2\right)\right. .$$

Spherical symmetry in metric-affine geometry

- Torsion contains $\#8$ dof:

$$\begin{gathered} T^{t}{}_{tr} = t_1(r)\,,\quad T^{r}{}_{tr} = t_2(r)\,,\quad T^{\vartheta}{}_{t\vartheta} = T^{\varphi}{}_{t\varphi} = t_3(r)\,,\quad T^{\vartheta}{}_{r\vartheta} = T^{\varphi}{}_{r\varphi} = t_4(r)\,, \\ T^{\vartheta}{}_{t\varphi} = T^{\varphi}{}_{\vartheta t}\sin^2\vartheta = t_5(r)\sin\vartheta\,,\quad T^{\vartheta}{}_{r\varphi} = T^{\varphi}{}_{\vartheta r}\sin^2\vartheta = t_6(r)\sin\vartheta\,, \\ T^{t}{}_{\vartheta\varphi} = t_7(r)\sin\vartheta\,,\quad T^{r}{}_{\vartheta\varphi} = t_8(r)\sin\vartheta\,. \end{gathered}$$

Spherical symmetry in metric-affine geometry

- Torsion contains $\#8$ dof:

$$\begin{gathered}T^{t}{}_{tr}=t_1(r)\,,\quad T^{r}{}_{tr}=t_2(r)\,,\quad T^{\vartheta}{}_{t\vartheta}=T^{\varphi}{}_{t\varphi}=t_3(r)\,,\quad T^{\vartheta}{}_{r\vartheta}=T^{\varphi}{}_{r\varphi}=t_4(r)\,,\\ T^{\vartheta}{}_{t\varphi}=T^{\varphi}{}_{\vartheta t}\sin^2\vartheta=t_5(r)\sin\vartheta\,,\quad T^{\vartheta}{}_{r\varphi}=T^{\varphi}{}_{\vartheta r}\sin^2\vartheta=t_6(r)\sin\vartheta\,,\\ T^{t}{}_{\vartheta\varphi}=t_7(r)\sin\vartheta\,,\quad T^{r}{}_{\vartheta\varphi}=t_8(r)\sin\vartheta\,.\end{gathered}$$

- Nonmetricity contains $\#12$ dof:

$$\begin{gathered}Q_{ttt}=q_1(r)\,,\quad Q_{trr}=q_2(r)\,,\quad Q_{ttr}=q_3(r)\,,\\ Q_{t\vartheta\vartheta}=Q_{t\varphi\varphi}\csc^2\vartheta=q_4(r)\,,\quad Q_{rtt}=q_5(r)\,,\quad Q_{rrr}=q_6(r)\,,\\ Q_{rtr}=q_7(r)\,,\quad Q_{r\vartheta\vartheta}=Q_{r\varphi\varphi}\csc^2\vartheta=q_8(r)\,,\\ Q_{\vartheta t\vartheta}=Q_{\varphi t\varphi}\csc^2\vartheta=q_9(r)\,,\quad Q_{\vartheta r\vartheta}=Q_{\varphi r\varphi}\csc^2\vartheta=q_{10}(r)\,,\\ Q_{\vartheta t\varphi}=-Q_{\varphi t\vartheta}=q_{11}(r)\sin\vartheta\,,\quad Q_{\vartheta r\varphi}=-Q_{\varphi r\vartheta}=q_{12}(r)\sin\vartheta\,.\end{gathered}$$

Spherical symmetry in metric-affine geometry

- Torsion contains $\#8$ dof:

$$\begin{gathered}T^{t}{}_{tr}=t_1(r)\,,\quad T^{r}{}_{tr}=t_2(r)\,,\quad T^{\vartheta}{}_{t\vartheta}=T^{\varphi}{}_{t\varphi}=t_3(r)\,,\quad T^{\vartheta}{}_{r\vartheta}=T^{\varphi}{}_{r\varphi}=t_4(r)\,,\\ T^{\vartheta}{}_{t\varphi}=T^{\varphi}{}_{\vartheta t}\sin^2\vartheta=t_5(r)\sin\vartheta\,,\quad T^{\vartheta}{}_{r\varphi}=T^{\varphi}{}_{\vartheta r}\sin^2\vartheta=t_6(r)\sin\vartheta\,,\\ T^{t}{}_{\vartheta\varphi}=t_7(r)\sin\vartheta\,,\quad T^{r}{}_{\vartheta\varphi}=t_8(r)\sin\vartheta\,.\end{gathered}$$

- Nonmetricity contains $\#12$ dof:

$$\begin{gathered}Q_{ttt}=q_1(r)\,,\quad Q_{trr}=q_2(r)\,,\quad Q_{ttr}=q_3(r)\,,\\ Q_{t\vartheta\vartheta}=Q_{t\varphi\varphi}\csc^2\vartheta=q_4(r)\,,\quad Q_{rtt}=q_5(r)\,,\quad Q_{rrr}=q_6(r)\,,\\ Q_{rtr}=q_7(r)\,,\quad Q_{r\vartheta\vartheta}=Q_{r\varphi\varphi}\csc^2\vartheta=q_8(r)\,,\\ Q_{\vartheta t\vartheta}=Q_{\varphi t\varphi}\csc^2\vartheta=q_9(r)\,,\quad Q_{\vartheta r\vartheta}=Q_{\varphi r\varphi}\csc^2\vartheta=q_{10}(r)\,,\\ Q_{\vartheta t\varphi}=-Q_{\varphi t\vartheta}=q_{11}(r)\sin\vartheta\,,\quad Q_{\vartheta r\varphi}=-Q_{\varphi r\vartheta}=q_{12}(r)\sin\vartheta\,.\end{gathered}$$

- This means that not only the field equations are very difficult to treat but we need to find a solution of a system with $\#2(\text{metric})+\#8(\text{torsion})+\#12(\text{nonmetricity})=22$ dof!

How to find a solution with all of these dof?

- We are only interested in the traceless part of $Q_{\alpha\mu\nu}$ (containing shears), so that:

How to find a solution with all of these dof?

- We are only interested in the traceless part of $Q_{\alpha\mu\nu}$ (containing shears), so that:

  1. We eliminate the Weyl part of nonmetricity $W_\mu = \frac{1}{4}\,Q_{\mu\nu}{}^{\nu} = 0$ by setting

$$\begin{aligned} q_1(r) &= \frac{\Psi_1(r)}{r^2}\left(r^2 q_2(r)\Psi_2(r) + 2q_4(r)\right)\,, \\ q_5(r) &= \frac{\Psi_1(r)}{r^2}\left(r^2 q_6(r)\Psi_2(r) + 2q_8(r)\right)\,. \end{aligned}$$

How to find a solution with all of these dof?

- We are only interested in the traceless part of $Q_{\alpha\mu\nu}$ (containing shears), so that:
  1. We eliminate the Weyl part of nonmetricity $W_\mu = \frac{1}{4} Q_{\mu\nu}{}^{\nu} = 0$ by setting

$$
\begin{aligned}
q_1(r) &= \frac{\Psi_1(r)}{r^2}\left(r^2 q_2(r)\Psi_2(r) + 2q_4(r)\right) ,\\
q_5(r) &= \frac{\Psi_1(r)}{r^2}\left(r^2 q_6(r)\Psi_2(r) + 2q_8(r)\right) .
\end{aligned}
$$

  2. We imposed $N_{[\lambda\rho]\mu} = 0$ which is equivalent to $T_{\lambda\mu\nu} = Q_{[\mu\nu]\lambda}$:
     → Shear transformations in the general linear group involves the part of the anholonomic connection describing a shear current or charge to take values in the **symmetric traceless part** of the Lie algebra.

How to find a solution with all of these dof?

- We are only interested in the traceless part of $Q_{\alpha\mu\nu}$ (containing shears), so that:
  1. We eliminate the Weyl part of nonmetricity $W_\mu = \frac{1}{4} Q_{\mu\nu}{}^{\nu} = 0$ by setting

$$
\begin{aligned}
q_1(r) &= \frac{\Psi_1(r)}{r^2}\left(r^2 q_2(r)\Psi_2(r) + 2q_4(r)\right) ,\\
q_5(r) &= \frac{\Psi_1(r)}{r^2}\left(r^2 q_6(r)\Psi_2(r) + 2q_8(r)\right) .
\end{aligned}
$$

  2. We imposed $N_{[\lambda\rho]\mu} = 0$ which is equivalent to $T_{\lambda\mu\nu} = Q_{[\mu\nu]\lambda}$:
     → Shear transformations in the general linear group involves the part of the anholonomic connection describing a shear current or charge to take values in the **symmetric traceless part** of the Lie algebra.

  3. We demand the corresponding torsion and nonmetricity scalars of the solution to be regular.

How to find a solution with all of these dof?

- We are only interested in the traceless part of $Q_{\alpha\mu\nu}$ (containing shears), so that:
  1. We eliminate the Weyl part of nonmetricity $W_\mu = \frac{1}{4} Q_{\mu\nu}{}^{\nu} = 0$ by setting

$$\begin{aligned} q_1(r) &= \frac{\Psi_1(r)}{r^2}\left(r^2 q_2(r)\Psi_2(r) + 2q_4(r)\right) \,, \\ q_5(r) &= \frac{\Psi_1(r)}{r^2}\left(r^2 q_6(r)\Psi_2(r) + 2q_8(r)\right) \,. \end{aligned}$$

  2. We imposed $N_{[\lambda\rho]\mu} = 0$ which is equivalent to $T_{\lambda\mu\nu} = Q_{[\mu\nu]\lambda}$:
     → Shear transformations in the general linear group involves the part of the anholonomic connection describing a shear current or charge to take values in the **symmetric traceless part** of the Lie algebra.
  3. We demand the corresponding torsion and nonmetricity scalars of the solution to be regular.
- After following these three steps we end up with 2 dof (metric)+ 5 dof (torsion/nonmetricity) which is only 7 dof.

New solution only with shears

- By plugging these conditions in the field equations, there are several branches but only one has solutions with dynamical shears. This branch involves the constants of the theory as

$$f_2 = -\frac{1}{4} f_1 .$$

New solution only with shears

- By plugging these conditions in the field equations, there are several branches but only one has solutions with dynamical shears. This branch involves the constants of the theory as

$$f_2 = -\frac{1}{4} f_1 .$$

- The metric behaves as

New solution only with shears

- By plugging these conditions in the field equations, there are several branches but only one has solutions with dynamical shears. This branch involves the constants of the theory as

$$f_2 = -\frac{1}{4} f_1 .$$

- The metric behaves as

Solution - metric part

$$ds^2 = \Psi_1(r)\, dt^2 - \frac{dr^2}{\Psi_2(r)} - r^2 \left(d\theta_1^2 + \sin^2\theta_1 d\theta_2^2 \right) \,,$$

$$\Psi_1(r) = \Psi_2(r) = 1 - \frac{2m}{r} - \frac{2 f_1 \kappa_{\text{sh}}^2}{r^2} \,.$$

New solution only with shears

- By plugging these conditions in the field equations, there are several branches but only one has solutions with dynamical shears. This branch involves the constants of the theory as

$$f_2 = -\frac{1}{4} f_1 .$$

- The metric behaves as

Solution - metric part

$$ds^2 = \Psi_1(r)\, dt^2 - \frac{dr^2}{\Psi_2(r)} - r^2 \left(d\theta_1^2 + \sin^2\theta_1 d\theta_2^2 \right) ,$$

$$\Psi_1(r) = \Psi_2(r) = 1 - \frac{2m}{r} - \frac{2 f_1 \kappa_{\rm sh}^2}{r^2} .$$

New solution only with shears

- By plugging these conditions in the field equations, there are several branches but only one has solutions with dynamical shears. This branch involves the constants of the theory as

$$f_2 = -\frac{1}{4} f_1 .$$

- The metric behaves as

Solution - metric part

$$ds^2 = \Psi_1(r)\, dt^2 - \frac{dr^2}{\Psi_2(r)} - r^2 \left(d\theta_1^2 + \sin^2\theta_1 d\theta_2^2 \right) ,$$

$$\Psi_1(r) = \Psi_2(r) = 1 - \frac{2m}{r} - \frac{2 f_1 \kappa_{\rm sh}^2}{r^2} .$$

Here, $\kappa_{\rm sh}$ is interpreted as a new charge, ”shear charge”.

- See our paper to see the form of q_i and t_i. One component of nonmetricity is arbitrary (problem?).

Reissner-Nordström-like solutions with spin, dilation and shear charges

- After finding the shear part alone, we found a theory containing our previous result JCAP **09** (2020), 057 (with spin+dilation) plus the second (with only shears).

Reissner-Nordström-like solutions with spin, dilation and shear charges

- After finding the shear part alone, we found a theory containing our previous result JCAP **09** (2020), 057 (with spin+dilation) plus the second (with only shears).

- The action of the full model is

$$
\begin{aligned}
S = \frac{1}{64\pi}\int \Big[& -4R - 6d_1\tilde{R}_{\lambda[\rho\mu\nu]}\tilde{R}^{\lambda[\rho\mu\nu]} - 9d_1\tilde{R}_{\lambda[\rho\mu\nu]}\tilde{R}^{\mu[\lambda\nu\rho]} \\
& + 2d_1\left(\tilde{R}_{[\mu\nu]} + \hat{R}_{[\mu\nu]}\right)\left(\tilde{R}^{[\mu\nu]} + \hat{R}^{[\mu\nu]}\right) + 18d_1\tilde{R}_{\lambda[\rho\mu\nu]}\tilde{R}^{(\lambda\rho)\mu\nu} \\
& - 3d_1\tilde{R}_{(\lambda\rho)\mu\nu}\tilde{R}^{(\lambda\rho)\mu\nu} + 6d_1\tilde{R}_{(\lambda\rho)\mu\nu}\tilde{R}^{(\lambda\mu)\rho\nu} + 2\left(2e_1 - f_1\right)\tilde{R}^{\lambda}{}_{\lambda\mu\nu}\tilde{R}^{\rho}{}_{\rho}{}^{\mu\nu} \\
& + 8f_1\tilde{R}_{(\lambda\rho)\mu\nu}\tilde{R}^{(\lambda\rho)\mu\nu} - 2f_1\left(\tilde{R}_{(\mu\nu)} - \hat{R}_{(\mu\nu)}\right)\left(\tilde{R}^{(\mu\nu)} - \hat{R}^{(\mu\nu)}\right) \\
& + 3\left(1 - 2a_2\right)T_{[\lambda\mu\nu]}T^{[\lambda\mu\nu]}\Big] d^4x\sqrt{-g}\,.
\end{aligned}
$$

Reissner-Nordström-like solutions with spin, dilation and shear charges

- After finding the shear part alone, we found a theory containing our previous result JCAP **09** (2020), 057 (with spin+dilation) plus the second (with only shears).
- The action of the full model is

$$
\begin{aligned}
S = \frac{1}{64\pi}\int\Big[& -4R - 6d_1\tilde{R}_{\lambda[\rho\mu\nu]}\tilde{R}^{\lambda[\rho\mu\nu]} - 9d_1\tilde{R}_{\lambda[\rho\mu\nu]}\tilde{R}^{\mu[\lambda\nu\rho]} \\
& + 2d_1\left(\tilde{R}_{[\mu\nu]} + \hat{R}_{[\mu\nu]}\right)\left(\tilde{R}^{[\mu\nu]} + \hat{R}^{[\mu\nu]}\right) + 18d_1\tilde{R}_{\lambda[\rho\mu\nu]}\tilde{R}^{(\lambda\rho)\mu\nu} \\
& - 3d_1\tilde{R}_{(\lambda\rho)\mu\nu}\tilde{R}^{(\lambda\rho)\mu\nu} + 6d_1\tilde{R}_{(\lambda\rho)\mu\nu}\tilde{R}^{(\lambda\mu)\rho\nu} + 2\left(2e_1 - f_1\right)\tilde{R}^{\lambda}{}_{\lambda\mu\nu}\tilde{R}^{\rho}{}_{\rho}{}^{\mu\nu} \\
& + 8f_1\tilde{R}_{(\lambda\rho)\mu\nu}\tilde{R}^{(\lambda\rho)\mu\nu} - 2f_1\left(\tilde{R}_{(\mu\nu)} - \hat{R}_{(\mu\nu)}\right)\left(\tilde{R}^{(\mu\nu)} - \hat{R}^{(\mu\nu)}\right) \\
& + 3\left(1 - 2a_2\right)T_{[\lambda\mu\nu]}T^{[\lambda\mu\nu]}\Big]d^4x\sqrt{-g}\,.
\end{aligned}
$$

- When traceless part of nonmetricity is zero, the above action coincides with our previous study.

Reissner-Nordström-like solutions with spin, dilation and shear charges

- Since we already found the solution for each model independently, it was not so difficult to find the solution for the full model.

Reissner-Nordström-like solutions with spin, dilation and shear charges

- Since we already found the solution for each model independently, it was not so difficult to find the solution for the full model.
- In this case, all nonmetricity components are fully set by the field equations (remember that in the shear case, one component was free). See our paper to see the form of q_i, t_i and the field strength tensors in the irreducible modes.

Reissner-Nordström-like solutions with spin, dilation and shear charges

- Since we already found the solution for each model independently, it was not so difficult to find the solution for the full model.
- In this case, all nonmetricity components are fully set by the field equations (remember that in the shear case, one component was free). See our paper to see the form of q_i, t_i and the field strength tensors in the irreducible modes.

- The solution gives us the following metric

Reissner-Nordström-like solutions with spin, dilation and shear charges

- Since we already found the solution for each model independently, it was not so difficult to find the solution for the full model.
- In this case, all nonmetricity components are fully set by the field equations (remember that in the shear case, one component was free). See our paper to see the form of q_i, t_i and the field strength tensors in the irreducible modes.
- The solution gives us the following metric

Solution General - metric part

$$ds^2 = \Psi_1(r)\,dt^2 - \frac{dr^2}{\Psi_2(r)} - r^2\left(d\theta_1^2 + \sin^2\theta_1 d\theta_2^2\right)\,,$$

$$\Psi_1(r) = \Psi_2(r) = 1 - \frac{2m}{r} + \frac{d_1\kappa_{\rm s}^2 - 4e_1\kappa_{\rm d}^2 - 2f_1\kappa_{\rm sh}^2}{r^2}\,,$$

Reissner-Nordström-like solutions with spin, dilation and shear charges

- Since we already found the solution for each model independently, it was not so difficult to find the solution for the full model.
- In this case, all nonmetricity components are fully set by the field equations (remember that in the shear case, one component was free). See our paper to see the form of q_i, t_i and the field strength tensors in the irreducible modes.
- The solution gives us the following metric

Solution General - metric part

$$ds^2 = \Psi_1(r)\,dt^2 - \frac{dr^2}{\Psi_2(r)} - r^2\left(d\theta_1^2 + \sin^2\theta_1 d\theta_2^2\right)\,,$$

$$\Psi_1(r) = \Psi_2(r) = 1 - \frac{2m}{r} + \frac{d_1\kappa_{\rm s}^2 - 4e_1\kappa_{\rm d}^2 - 2f_1\kappa_{\rm sh}^2}{r^2}\,,$$

Sebastian Bahamonde (*) Black Holes in metric-affine 11 / 15

Reissner-Nordström-like solutions with spin, dilation and shear charges

- Since we already found the solution for each model independently, it was not so difficult to find the solution for the full model.
- In this case, all nonmetricity components are fully set by the field equations (remember that in the shear case, one component was free). See our paper to see the form of q_i, t_i and the field strength tensors in the irreducible modes.
- The solution gives us the following metric

Solution General - metric part

$$ds^2 = \Psi_1(r)\, dt^2 - \frac{dr^2}{\Psi_2(r)} - r^2 \left(d\theta_1^2 + \sin^2\theta_1 d\theta_2^2\right) \,,$$

$$\Psi_1(r) = \Psi_2(r) = 1 - \frac{2m}{r} + \frac{d_1\kappa_{\rm s}^2 - 4e_1\kappa_{\rm d}^2 - 2f_1\kappa_{\rm sh}^2}{r^2} \,,$$

having the three possible charges of MAG: spin, dilation and shear.

Solution with the geometrical charges, cosmological constant and electromagnetic field

On the other hand, the solution can also be trivially generalised to include the cosmological constant and Coulomb electromagnetic fields with electric and magnetic charges q_e and q_m, which are decoupled from torsion under the assumption of the minimal coupling principle. This natural extension is then described by a Reissner-Nordström-de Sitter-like geometry

Solution General - metric part

$$\Psi(r) = 1 - \frac{2m}{r} + \frac{d_1\kappa_{\rm s}^2 - 4e_1\kappa_{\rm d}^2 - 2f_1\kappa_{\rm sh}^2 + q_e^2 + q_m^2}{r^2} + \frac{\Lambda}{3}r^2 \,,$$

which turns out to represent **the broadest family of static and spherically symmetric black hole solutions obtained in MAG** so far.

What do these charges physically represent? - Torsion

- **Torsion part** $T^{\lambda}{}_{\mu\nu}$:

What do these charges physically represent? - Torsion

- **Torsion part** $T^{\lambda}{}_{\mu\nu}$:
  1. **Intrinsic spin** generates gravitation. This effect does not exist in GR.

What do these charges physically represent? - Torsion

- **Torsion part $T^{\lambda}{}_{\mu\nu}$:**
  1. **Intrinsic spin** generates gravitation. This effect does not exist in GR.
  2. We know that the spin is a fundamental property of particles. Since their masses contribute to gravity, why their spin do not in GR?

What do these charges physically represent? - Torsion

- **Torsion part $T^{\lambda}{}_{\mu\nu}$:**
  1. **Intrinsic spin** generates gravitation. This effect does not exist in GR.
  2. We know that the spin is a fundamental property of particles. Since their masses contribute to gravity, why their spin do not in GR?
  3. The solution is in vacuum and a charge κ_s appears (spin charge). Analogue to the case of Schwarzschild where the mass M appears.

What do these charges physically represent? - Torsion

- **Torsion part $T^{\lambda}{}_{\mu\nu}$:**

  1. **Intrinsic spin** generates gravitation. This effect does not exist in GR.
  2. We know that the spin is a fundamental property of particles. Since their masses contribute to gravity, why their spin do not in GR?
  3. The solution is in vacuum and a charge κ_s appears (spin charge). Analogue to the case of Schwarzschild where the mass M appears.
  4. We expect that the spin charge might be important in certain astrophysical scenarios such as: highly mangnetized neutron stars; supermassive black holes with endowed spin.

What do these charges physically represent? - Nonmetricity

- **Nonmetricity part - only Weyl W_{μ}:**

What do these charges physically represent? - Nonmetricity

- **Nonmetricity part - only Weyl W_μ:**
  1. **Intrinsic dilations** generates gravitation. This effect does not exist in GR.

What do these charges physically represent? - Nonmetricity

- **Nonmetricity part - only Weyl W_μ:**
  1. **Intrinsic dilations** generates gravitation. This effect does not exist in GR.

  2. dilation: deformation that involves only change of volume (in this case, intrinsic dilation!)

What do these charges physically represent? - Nonmetricity

- **Nonmetricity part - only Weyl W_μ:**
  1. **Intrinsic dilations** generates gravitation. This effect does not exist in GR.
  2. dilation: deformation that involves only change of volume (in this case, intrinsic dilation!)
  3. Weyl part of nonmetricity is ”scale invariant”

What do these charges physically represent? - Nonmetricity

- **Nonmetricity part - only Weyl W_μ:**
  1. **Intrinsic dilations** generates gravitation. This effect does not exist in GR.
  2. dilation: deformation that involves only change of volume (in this case, intrinsic dilation!)
  3. Weyl part of nonmetricity is ”scale invariant”

- **Nonmetricity part - Traceless part $\not{Q}_{\lambda\mu\nu}$:**

What do these charges physically represent? - Nonmetricity

- **Nonmetricity part - only Weyl W_μ:**
  1. **Intrinsic dilations** generates gravitation. This effect does not exist in GR.
  2. dilation: deformation that involves only change of volume (in this case, intrinsic dilation!)
  3. Weyl part of nonmetricity is ”scale invariant”
- **Nonmetricity part - Traceless part $\not{Q}_{\lambda\mu\nu}$:**
  1. **Intrinsic shears** generates gravitation. This effect does not exist in GR.

What do these charges physically represent? - Nonmetricity

- **Nonmetricity part - only Weyl W_μ:**
  1. **Intrinsic dilations** generates gravitation. This effect does not exist in GR.
  2. dilation: deformation that involves only change of volume (in this case, intrinsic dilation!)
  3. Weyl part of nonmetricity is ”scale invariant”
- **Nonmetricity part - Traceless part $\not{Q}_{\lambda\mu\nu}$:**
  1. **Intrinsic shears** generates gravitation. This effect does not exist in GR.
  2. Shears: Deformations without changing the volume.

What do these charges physically represent? - Nonmetricity

- **Nonmetricity part - only Weyl W_μ:**
  1. **Intrinsic dilations** generates gravitation. This effect does not exist in GR.
  2. dilation: deformation that involves only change of volume (in this case, intrinsic dilation!)
  3. Weyl part of nonmetricity is ”scale invariant”
- **Nonmetricity part - Traceless part $\not{Q}_{\lambda\mu\nu}$:**
  1. **Intrinsic shears** generates gravitation. This effect does not exist in GR.
  2. Shears: Deformations without changing the volume.
- **Solution:** $\kappa_{\rm d}$ and $\kappa_{\rm sh}$ appear which are the dilation and shear charges. Analogue to the case of Schwarzschild M.

What do these charges physically represent? - Nonmetricity

- **Nonmetricity part - only Weyl W_μ:**
  1. **Intrinsic dilations** generates gravitation. This effect does not exist in GR.
  2. dilation: deformation that involves only change of volume (in this case, intrinsic dilation!)
  3. Weyl part of nonmetricity is ”scale invariant”
- **Nonmetricity part - Traceless part $\not{Q}_{\lambda\mu\nu}$:**
  1. **Intrinsic shears** generates gravitation. This effect does not exist in GR.
  2. Shears: Deformations without changing the volume.
- **Solution:** $\kappa_{\rm d}$ and $\kappa_{\rm sh}$ appear which are the dilation and shear charges. Analogue to the case of Schwarzschild M.
- Do all particles in nature have different dilations and shears? are these properties important in particle physics?

Conclusions and what do to next

- We found the first solution with the traceless part of nonmetricity having a dynamical role where the shear charge appears in the metric.

Conclusions and what do to next

- We found the first solution with the traceless part of nonmetricity having a dynamical role where the shear charge appears in the metric.

- The general solution contains the three fundamental charges (spin,dilation and shear) and the mass which constitute the most general spherically symmetric solution with all the possible intrinsic geometrical properties of matter.

Conclusions and what do to next

- We found the first solution with the traceless part of nonmetricity having a dynamical role where the shear charge appears in the metric.
- The general solution contains the three fundamental charges (spin,dilation and shear) and the mass which constitute the most general spherically symmetric solution with all the possible intrinsic geometrical properties of matter.
- It is worth studying:

Conclusions and what do to next

- We found the first solution with the traceless part of nonmetricity having a dynamical role where the shear charge appears in the metric.
- The general solution contains the three fundamental charges (spin,dilation and shear) and the mass which constitute the most general spherically symmetric solution with all the possible intrinsic geometrical properties of matter.
- It is worth studying:

    1. Cosmology of the complete model: from inflation to dark energy.

Conclusions and what do to next

- We found the first solution with the traceless part of nonmetricity having a dynamical role where the shear charge appears in the metric.

- The general solution contains the three fundamental charges (spin,dilation and shear) and the mass which constitute the most general spherically symmetric solution with all the possible intrinsic geometrical properties of matter.

- It is worth studying:

    1. Cosmology of the complete model: from inflation to dark energy.

    2. Perturbations of this solution: Is it stable? quasinormal modes?

Conclusions and what do to next

- We found the first solution with the traceless part of nonmetricity having a dynamical role where the shear charge appears in the metric.

- The general solution contains the three fundamental charges (spin,dilation and shear) and the mass which constitute the most general spherically symmetric solution with all the possible intrinsic geometrical properties of matter.

- It is worth studying:

    1. Cosmology of the complete model: from inflation to dark energy.

    2. Perturbations of this solution: Is it stable? quasinormal modes?

    3. What is the role of dilations/shears in particle physics?

C62

Vector-tensor theories in the metric-affine formalism

@JGRG31 Oct. 27th (Thu.)

Tact Ikeda (Rikkyo University)

Based on ongoing work with T. Kobayashi (Rikkyo)

Introduction

- Modified gravity is actively studied
    - To better understand the nature of gravity
    - To understand mysteries in the universe
        - ☑ Inflation, dark matter, etc.
- How: Add new gravitational d.o.f.
    - Scalar-tensor theories: $g_{ab} + \phi$
    - Vector-tensor theories: $g_{ab} + A_a$
        - ☑ Generalized Proca theory [L. Heisenberg (2014)]

Generalized Proca theory

- **Generalized Proca theory** [L. Heisenberg (2014)]

$$S_{GP} = \int d^4x\sqrt{-g}\sum_n \mathcal{L}_n$$

$$X = -A^aA_a/2$$

$$F_{ab} = \partial_a A_b - \partial_b A_a$$

$$\tilde{F}_{ab} = \epsilon^{abcd}F_{cd}$$

$$\mathcal{L}_2 = G_2\left(A_a, F_{ab}, \tilde{F}_{ab}\right)$$

$$\mathcal{L}_3 = G_3(X)\nabla_a A^a$$

$$\mathcal{L}_4 = G_4(X)R + G_{4,X}\left[\left(\nabla_a A^a\right)^2 - \nabla_a A_b \nabla^b A^a\right]$$

$$\mathcal{L}_5 = G_5(X)G_{ab}\nabla^a A^b - \frac{1}{6}G_{5,X}\left[(\nabla\cdot A)^3 + 2\nabla_a A_b\nabla^c A^a \nabla^b A_c - 3(\nabla\cdot A)\nabla_a A_b \nabla^b A^a\right] - g_5(X)\tilde{F}^{ac}\tilde{F}^b{}_c\nabla_a A_b$$

$$\mathcal{L}_6 = G_6(X)\mathcal{L}^{abcd}\nabla_a A_b \nabla_c A_d + \frac{G_{6,X}}{2}\tilde{F}^{ab}\tilde{F}^{cd}\nabla_a A_c \nabla_b A_d$$

  - In the limit $A_a \to \partial_a\phi$,

    the theory reduces to (shift-symmetric) Horndeski

- This work:
  I would like to consider this in the metric-affine formalism

---

Metric v.s. Metric-affine formalism

- **Metric formalism** (GR, etc.):
  - $\Gamma^a{}_{bc} = \left\{{a \atop bc}\right\} := \frac{1}{2}g^{ad}(\partial_b g_{dc} + \partial_c g_{bd} - \partial_d g_{bc})$
    - ☑ Torsionless: $\Gamma^a{}_{bc} = \Gamma^a{}_{cb}$
    - ☑ Metricity: $D_a g_{bc} = 0$

$$D_aA_b = \partial_a A_b - \left\{{c \atop ab}\right\}A_c$$

$$\nabla_a A_b = \partial_a A_b - \Gamma^c{}_{ab}A_c$$

- **Metric-affine formalism**:
  - $\Gamma^a{}_{bc} \neq \left\{{a \atop bc}\right\} = \frac{1}{2}g^{ad}(\partial_b g_{dc} + \partial_c g_{bd} - \partial_d g_{bc})$
    - ☑ Geometrical variables: $T^a{}_{bc} = \Gamma^a{}_{bc} - \Gamma^a{}_{cb}, \ \ Q_{abc} = -\nabla_a g_{bc}$
  - g_{ab} and Γ^a_{bc} are independent variables

Integrating out Γ

- Theories in the metric-affine formalism: $L(g, \Gamma)$

- We can solve $\delta L / \delta \Gamma = 0$,
  it is algebraic equation in our cases

  - We can integrate out Γ:
    $L(g, \Gamma) \ \Rightarrow \ L(g)$

  - The metric-affine formalism reduces to the metric formalism

---

To avoid ghost instability

- In the metric-affine formalism,
  most theories without imposing any symmetry
  suffer form ghost instability

  - One of following 2 ways is useful
    e.g.) $F(g^{\mu\nu}, R_{\mu\nu})$ theories, etc. [Jiménez and Delhom (2019)]

    - ☑ Torsionless condition: $\Gamma^a{}_{bc} = \Gamma^a{}_{cb}$

    - ☑ projective symmetry: $\hat{\Gamma}^a{}_{bc} = \Gamma^a{}_{bc} + \delta^a_c U_b$

- We assumed torsionless condition/projective symmetry in our theories

[TI and Kobayashi (in preparation)]

This talk

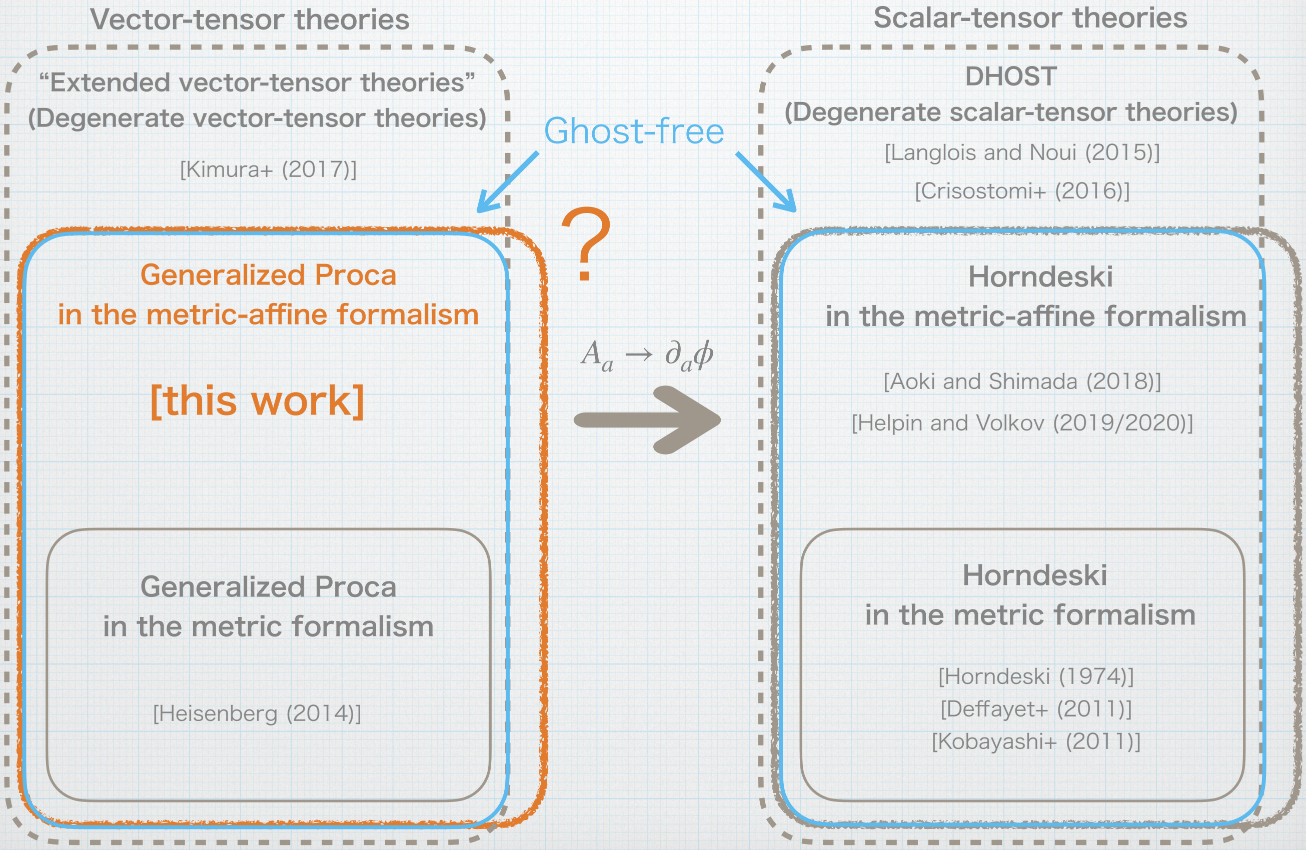

Vector-tensor theories

“Extended vector-tensor theories”
(Degenerate vector-tensor theories)

[Kimura+ (2017)]

Ghost-free

Scalar-tensor theories

DHOST
(Degenerate scalar-tensor theories)

[Langlois and Noui (2015)]

[Crisostomi+ (2016)]

?

Generalized Proca
in the metric-affine formalism

[this work]

$A_a \to \partial_a \phi$

Horndeski
in the metric-affine formalism

[Aoki and Shimada (2018)]

[Helpin and Volkov (2019/2020)]

Generalized Proca
in the metric formalism

[Heisenberg (2014)]

Horndeski
in the metric formalism

[Horndeski (1974)]
[Deffayet+ (2011)]
[Kobayashi+ (2011)]

Theory with torsionless cond.

[TI and Kobayashi (in preparation)]

- This theory is extension of [Helpin and Volkov (2019)]
  (all ϕ terms are extended to A_a)
  - We impose torsionless condition: $\Gamma^a{}_{bc} = \Gamma^a{}_{cb}$

$$\boxed{L = G_2(X) + G_3(X)\mathscr{L}_3 + G_4(X)g^{ab}R_{ab} + \sum_{i=1}^{3} H_i(X)\mathscr{L}^i_4}$$

$$R_{abc}{}^d = 2\Gamma^e{}_{[a|c|}\Gamma^d{}_{b]e} - 2\partial_{[a}\Gamma^d{}_{b]c}, \quad R_{ab} = R_{acb}{}^c$$

$$\mathscr{L}_3 = g^{ab}\nabla_a A_b, \quad \mathscr{L}^1_4 = (\nabla^a A_a)^2, \quad \mathscr{L}^2_4 = g^{ad}g^{bc}\nabla_a A_b \nabla_c A_d, \quad \mathscr{L}^3_4 = g^{ac}g^{bd}\nabla_a A_b \nabla_c A_d$$

- We can Integrate out Γ
  - The metric-affine formalism reduces to the metric formalism

Theory with torsionless cond.

[TI and Kobayashi (in preparation)]

$$\mathscr{L}(g,\Gamma,A) = G_2(X) + G_3(X)\mathscr{L}_3 + G_4(X)g^{ab}R_{ab} + \sum \boxed{H_i(X)}\mathscr{L}^i_4$$

$$\rightarrow \mathscr{L}(g,A) = (\text{up to linear in } D_aA_b) + G_4(X)\overset{g}{R} + \sum \boxed{\alpha_i(X)}L_i$$

integrating out Γ

$$L_1 = g^{a(c}g^{d)b}D_aA_bD_cA_d, \quad L_2 = g^{ab}g^{cd}D_aA_bD_cA_d,$$
$$L_3 = \left(A^aA^bg^{cd} + A^cA^dg^{ab}\right)D_aA_bD_cA_d, \quad L_4 = \left(A^aA^{(c}g^{d)b} + A^bA^{(c}g^{d)a}\right)D_aA_bD_cA_d,$$
$$L_5 = A^aA^bA^cA^dD_aA_bD_cA_d, \quad L_6 = g^{a[c}g^{d]b}D_aA_bD_cA_d, \quad L_7 = \left(A^aA^{[c}g^{d]b} - A^bA^{[c}g^{d]a}\right)D_aA_bD_cA_d,$$
$$L_8 = \left(A^aA^cg^{bd} - A^bA^dg^{ac}\right)D_aA_bD_cA_d, \quad L_9 = \epsilon^{abcd}D_aA_bD_cA_d,$$

[Kimura+ (2017)]

- To avoid ghost instability,
  coefficient functions α_i must satisfy degeneracy conditions
  - Degeneracy requires a certain constraint among H_i
    (but it does not completely fix H_i)
  - This theory is described in the framework of degenerate vector-tensor theories, not generalized Proca theory

---

Theory with projective symm.

[TI and Kobayashi (in preparation)]

- This theory is extension of [K. Aoki and K. Shimada (2018)]
  (all ϕ terms are extended to A_a)
  - We impose projective symmetry: $\hat{\Gamma}^a{}_{bc} = \Gamma^a{}_{bc} + \delta^a_cU_b$

$$\boxed{\begin{aligned} L = {} & G_4(X)g^{ab}R_{ab} + F(X)G^{ab}A_aA_b \\ & + G_2(X) + G_3(X)\mathscr{L}^{gal}_3 + H_1(X)\mathscr{L}^{gal}_4 + H_2(X)\mathscr{L}^{gal'}_4 \end{aligned}}$$

$$G^{bb'} = \epsilon^{abcd}\epsilon_a{}^{b'c'd'}R_{cdc'd'}, \quad \mathscr{L}^{gal}_3 = \epsilon^{abcd}\epsilon^{a'b'}{}_{cd}A_aA_{a'}\nabla_bA_{b'}$$
$$\mathscr{L}^{gal}_4 = \epsilon^{abcd}\epsilon^{a'b'c'}{}_dA_aA_{a'}\nabla_bA_{b'}\nabla_cA_{c'}, \quad \mathscr{L}^{gal'}_4 = \epsilon^{abcd}\epsilon^{a'b'c'}{}_dA_aA_{a'}\nabla_bA_{b'}\nabla_{c'}A_c$$

- We can also Integrate out Γ
  - The theory is always ghost-free and described in the framework of degenerate vector-tensor theories

Theory with projective symm.

[TI and Kobayashi (in preparation)]

- We can also construct a theory with projective symmetry in a different way
  - The theory depends on $D_a A_b$ through a projective-invariant combination: $\mathscr{A}^a{}_b$

$$D_a A_b = \partial_a A_b - \{{}^{\,c}_{ab}\} A_c$$
$$\nabla_a A_b = \partial_a A_b - \Gamma^c{}_{ab} A_c$$

$$\boxed{L = G_2(X) + G_3(X)\mathscr{L}_3 + G_4(X) g^{ab} R_{ab} + \sum_{i=1}^{3} Q_i(X)\mathscr{L}^i_4}$$

$$\mathscr{A}^a{}_b = (\nabla^a A_b + g_{bc}\nabla^a A^c)/2, \quad \mathscr{L}_3 = \mathscr{A}^a{}_a$$
$$\mathscr{L}^1_4 = \delta^b_a \delta^d_c \mathscr{A}^a{}_b \mathscr{A}^c{}_d, \quad \mathscr{L}^2_4 = \delta^b_a \delta^d_c \mathscr{A}^a{}_d \mathscr{A}^c{}_b, \quad \mathscr{L}^3_4 = g_{ac} g^{bd} \mathscr{A}^a{}_b \mathscr{A}^c{}_d$$

- We can also Integrate out Γ
  - Degeneracy requires $Q_3 = 0$
    - ☑ The theory is also described in the framework of degenerate vector-tensor theories

---

Summary

[TI and Kobayashi (in preparation)]

- We investigated what is the metric-affine version of generalized Proca theories
  - The theory with torsionless condition
    - ☑ Under a certain constraint
      one gets ghost-free degenerate vector-tensor theories
  - Constricting the epsilon tensor (with projective symm.)
    - ☑ Always ghost-free degenerate vector-tensor theories
  - Using the projective-invariant combination (with projective symm.)
    - ☑ Under a certain constraint
      one gets ghost-free degenerate vector-tensor theories
- torsionless condition / projective symm. alone is not perfect!
- Future work
  - Adding higher curvature terms to action, etc.

[TI and Kobayashi (in preparation)]

This talk

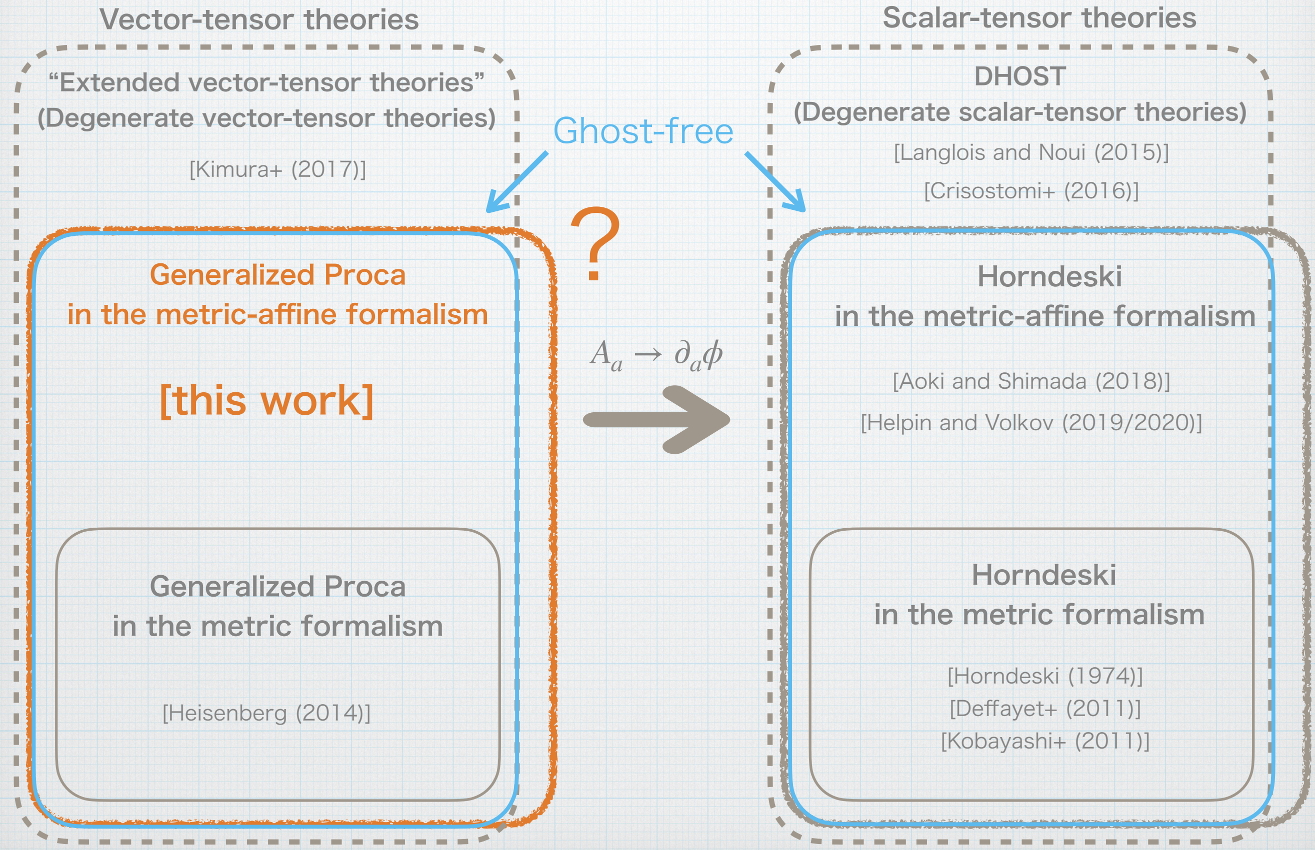

Vector-tensor theories

"Extended vector-tensor theories"
(Degenerate vector-tensor theories)

[Kimura+ (2017)]

Ghost-free

Scalar-tensor theories

DHOST
(Degenerate scalar-tensor theories)

[Langlois and Noui (2015)]

[Crisostomi+ (2016)]

Generalized Proca
in the metric-affine formalism

[this work]

?

$A_a \to \partial_a \phi$

Horndeski
in the metric-affine formalism

[Aoki and Shimada (2018)]

[Helpin and Volkov (2019/2020)]

Generalized Proca
in the metric formalism

[Heisenberg (2014)]

Horndeski
in the metric formalism

[Horndeski (1974)]
[Deffayet+ (2011)]
[Kobayashi+ (2011)]

"Modification to the Hawking temperature of a dynamical black hole by a time-dependent supertranslation," JHEP 20 (2020) 089 arXiv:2004.05045

asinormal modes and photon orbits of deformed Schwarzschild black holes," PRD 106 (2022) 044068 arXiv:2205.02433

Long-lived Quasinormal Modes of Black hole with Matter Inflow

Hsu-Wen Chiang

based on works in collaboration with

Yu-Hsein Kung, Che-Yu Chen, Jie-Shiun Tsao and Pisin Chen

and acknowledgment to Keisuke Izumi, Feng-Li Lin, Misao Sasaki and Bill Unruh

Leung Center for Cosmology and Particle Astrophysics (LeCosPA)
National Taiwan University (NTU)

Image credit (Left) LIGO/Virgo/Georgia Tech/S. Ghonge & K. Jani. (Right) A. Chael etal. ApJ. 918 (2021) 1, 6

Era of Black Hole Observation

- Multi-messenger astronomy?

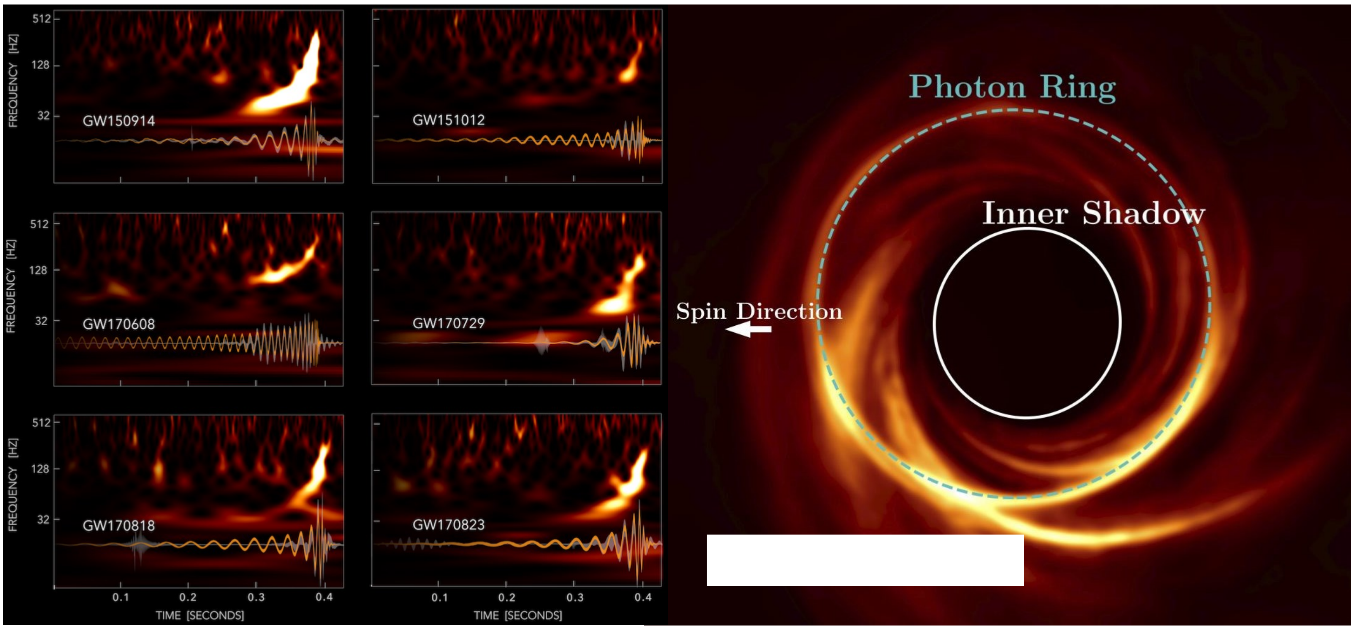

Matter Inflow Toy Model

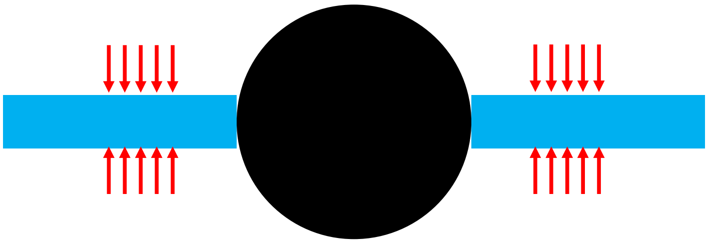

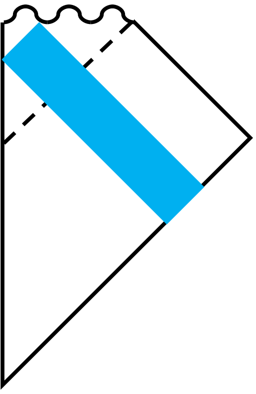

- For simplicity, let’s neglect the spin of the black hole and the gas stream orbital angular momentum.
- The system is described exactly by the dynamical soft hair model.
  JHEP 20 (2020) 089 arXiv:2004.05045 (Yu-Hsein Kung, HWC, Pisin Chen)
- The flow stretches the horizon and leads to grav. lensing, forming an ergosphere.
- No gravitational wave (GW) is emitted though.

Extreme Mass Ratio Inspiral

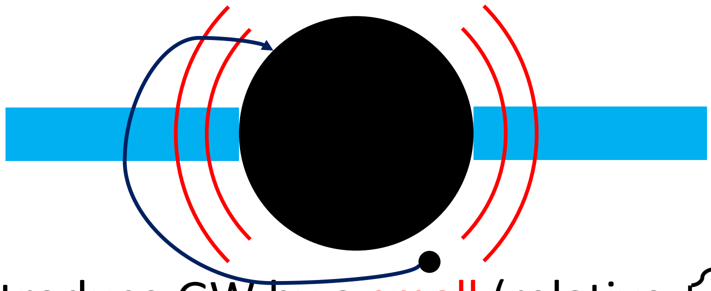

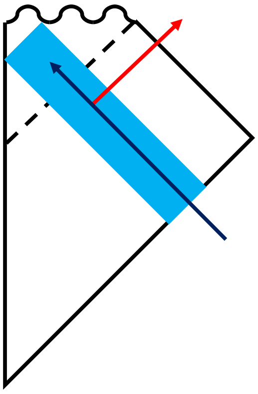

- Let us introduce GW by a small (relative to the matter inflow) companion BH.

Image credit (Left) LIGO/Virgo/Georgia Tech/S. Ghonge & K. Jani. (Right) A. Chael etal. ApJ. 918 (2021) 1, 6

Era of Black Hole Observation

- Multi-messenger astronomy?

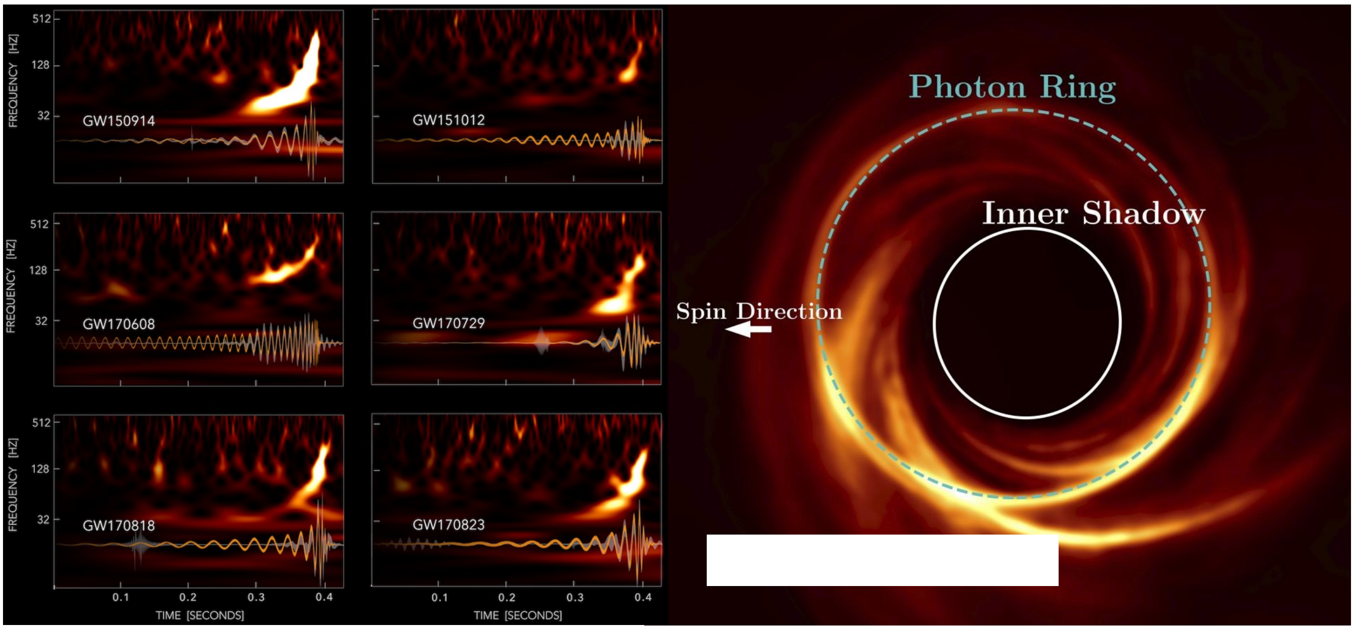

Extreme Mass Ratio ~~Inspiral~~ Ring down

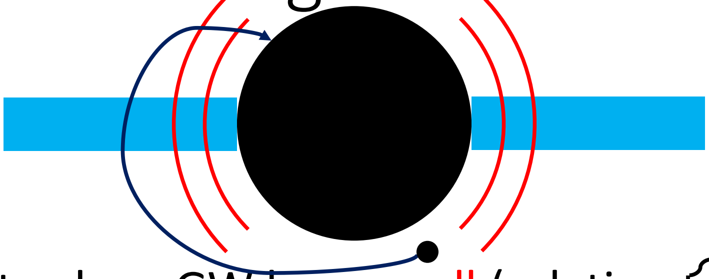

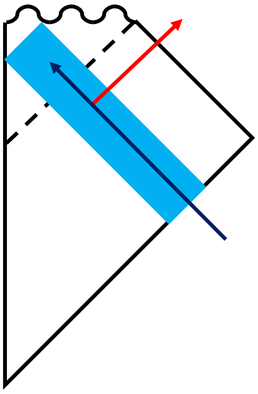

- Let us introduce GW by a small (relative to the matter inflow) companion BH.
- Focus on ring-down GWs and utilize quasinormal modes (QNM) of minimally coupled scalar field as the test bed:

$$\partial_\mu(\sqrt{-g}g^{\mu\nu}\partial_\nu\phi) = 0$$

$$\phi = r^{-1}\sum_{lm}\Phi_{\rm lm}(r^*)Y_{lm}e^{i\omega_{lm}(v-r^*)+Z_{lm}}$$

Deformed Quasinormal Modes

- Expand around smallness of flow density ϵ:

$$g_{\mu\nu} = g_{\mu\nu}^{(0)} + \epsilon g_{\mu\nu}^{(1)}$$

- Consider time scale where the horizon growth and the flow variation can be neglected.

$$\dot{\epsilon}^{-1} \gg T \ll \mathrm{M}$$

- Assume an axisymmetric flow.
- KG eq. can be cast into Schrödinger form

$$\Phi_{\mathrm{lm}}''(r^*) + \left(\omega_{lm}^2 - V_{lm}(r^*)\right)\Phi_{\mathrm{lm}}(r^*)$$

- C.f. PRD 102 (2020) 044047 (Cano etal.), PRD 106 (2022) 044068 (Che-Yu Chen, HWC, Jie-Hsiun Tsao) and Che-Yu Chen's talk later ☺.

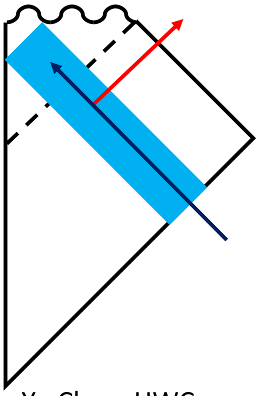

Deformed Effective Potential

- Anisotropic density: $\frac{\epsilon Y_{s0}}{4\pi r^2}$, $s \geq 2$.
- Deform factor is roughly $\epsilon\frac{rs^2+4\mathrm{M}}{s^4(r-2\mathrm{M})}$. → Spectrum is modified.
- Expansion fails at $\frac{r-2\mathrm{M}}{2\mathrm{M}} \approx \epsilon$.
- Divergence is either physical → Echo.
- Or regularizable.
  → Theoretic interest.

🟧 s=2 🟦 s=3 🟩 s=5

V at eikonal limit ($\mathrm{M}\omega_R \gg 1$)

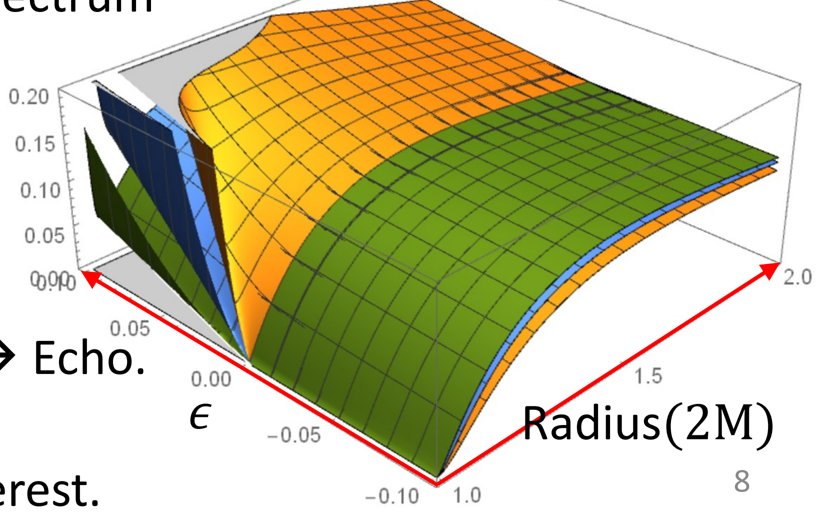

Near-horizon Expansion

- Let us zoom into $r - r_H = o(\epsilon)$ and $\epsilon > 0$.

  $V_{lm} = \sum_{n=0,k} l^2 (2\mathrm{M})^{k-2} \epsilon^n (r - r_H)^{-k} \, F^n_{k,slm}$,

  where n is the order in ϵ and k is r^* divergence.

$k = -3$	$k = -2$	$k = -1$	$k = 0$	$k > 0$	F^n_k
6	-3	1	$e^{-\epsilon^{-1}}$	0	$n = 0$
Irrelevant	Irrelevant	$\log(r - r_H)$	Irrelevant	0	$n = 1$
Irrelevant	Irrelevant	$-\log(r - r_H)^2$	Irrelevant	0	$n = 2$
Irrelevant	Irrelevant	$\log(r - r_H)^3$		0	$n = 3$

Regularized by pushing r_H outward

Near-horizon Expansion

- Let us zoom into $r - r_H = o(\epsilon)$ and $\epsilon > 0$.

  $V_{lm} = \sum_{n=0,k} l^2 (2\mathrm{M})^{k-2} \epsilon^n (r - r_H)^{-k} \, F^n_{k,slm}$,

  where n is the order in ϵ and k is r^* divergence.

$k = -3$	$k = -2$	$k = -1$	$k = 0$	$k > 0$	F^n_k
6	-3	1	$e^{-\epsilon^{-1}}$	0	$n = 0$
Irrelevant	Irrelevant	$\log(r - r_H)$	Irrelevant	0	$n = 1$
Irrelevant	Irrelevant	$-\log(r - r_H)^2$	Irrelevant	0	$n = 2$
Irrelevant	Irrelevant	$\log(r - r_H)^3$		0	$n = 3$

Regularized by pushing r_H outward

Near-horizon Expansion

- Let us zoom into $r - r_H = o(\epsilon)$ and $\epsilon > 0$.

  $V_{lm} = \sum_{n=0,k} l^2 (2\mathrm{M})^{k-2} \epsilon^n (r - r_H)^{-k} F^n_{k,slm}$,

  where n is the order in ϵ and k is r^* divergence.

$k=-3$	$k=-2$	$k=-1$	$k=0$	$k>0$	F_k^n
6	-3	1	$e^{-\epsilon^{-1}}$	0	$n=0$
Irrelevant	Irrelevant	$\log(r-r_H)$	Irrelevant	0	$n=1$
Irrelevant	Irrelevant	$-\log(r-r_H)^2$	Irrelevant	0	$n=2$
Irrelevant	Irrelevant	$\log(r-r_H)^3$		0	$n=3$

Sch.

Regularized by pushing r_H outward

Decay Time Estimate

- $V(r) \propto Ae^{-\frac{1}{\epsilon}} + \frac{r-r_H}{2\mathrm{M}}\left(1 + B\epsilon \log\left(\frac{r-r_H}{2\mathrm{M}}\right)\right).$

- Weakly trapped at $\frac{r-r_H}{2\mathrm{M}} \sim e^{-\frac{1}{B\epsilon}}$, with $\Delta V \sim \frac{l^2 e^{-\frac{1}{B\epsilon}}}{(2M)^2}$.

$k=-3$	$k=-2$	$k=-1$	$k=0$	$k>0$	F_k^n
6	-3	1	$e^{-\epsilon^{-1}}$	0	$n=0$
Irrelevant	Irrelevant	$\log(r-r_H)$	Irrelevant	0	$n=1$
Irrelevant	Irrelevant	$-\log(r-r_H)^2$	Irrelevant	0	$n=2$
Irrelevant	Irrelevant	$\log(r-r_H)^3$		0	$n=3$

Sch.

Regularized by pushing r_H outward

Decay Time Estimate

- $V(r) \propto Ae^{-\frac{1}{\epsilon}} + \frac{r-r_H}{2\mathrm{M}}\left(1 + B\epsilon\log\left(\frac{r-r_H}{2\mathrm{M}}\right)\right).$
- Weakly trapped at $\frac{r-r_H}{2\mathrm{M}} \sim e^{-\frac{1}{B\epsilon}}$, with $\Delta V \sim \frac{l^2 e^{-\frac{1}{B\epsilon}}}{(2M)^2}$.
- Rough estimate of decay time by WKB $\sqrt{\frac{\Delta r^*}{\sqrt{\Delta V}}}\, e^{W_\mathrm{p}\sqrt{V_\mathrm{p}}}$.
- These modes correspond to geodesics trapped inside the photon sphere by gravitational lensing. → Ergosphere!

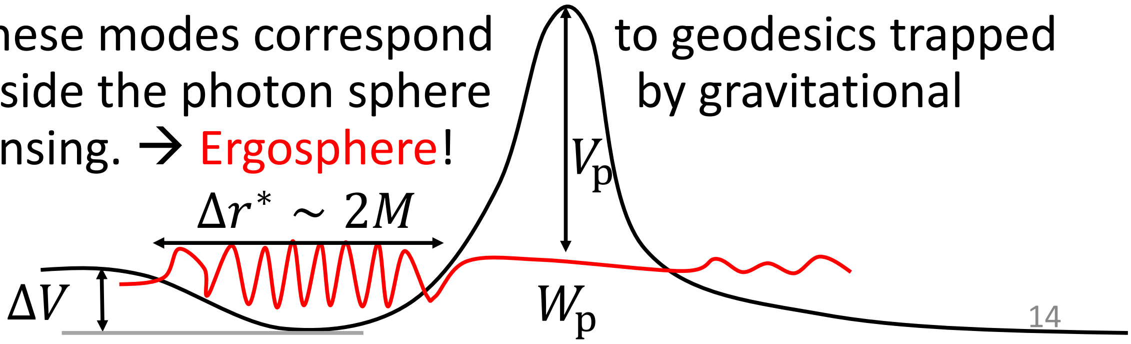

Conclusion and Future Work

- Our toy model suggests that QNM potential is deformed by transient matter flow.
- Series analysis leads to a diverging potential
- After careful a to small dip o
- Relate these n to trapped geodesics insi ergosphere.

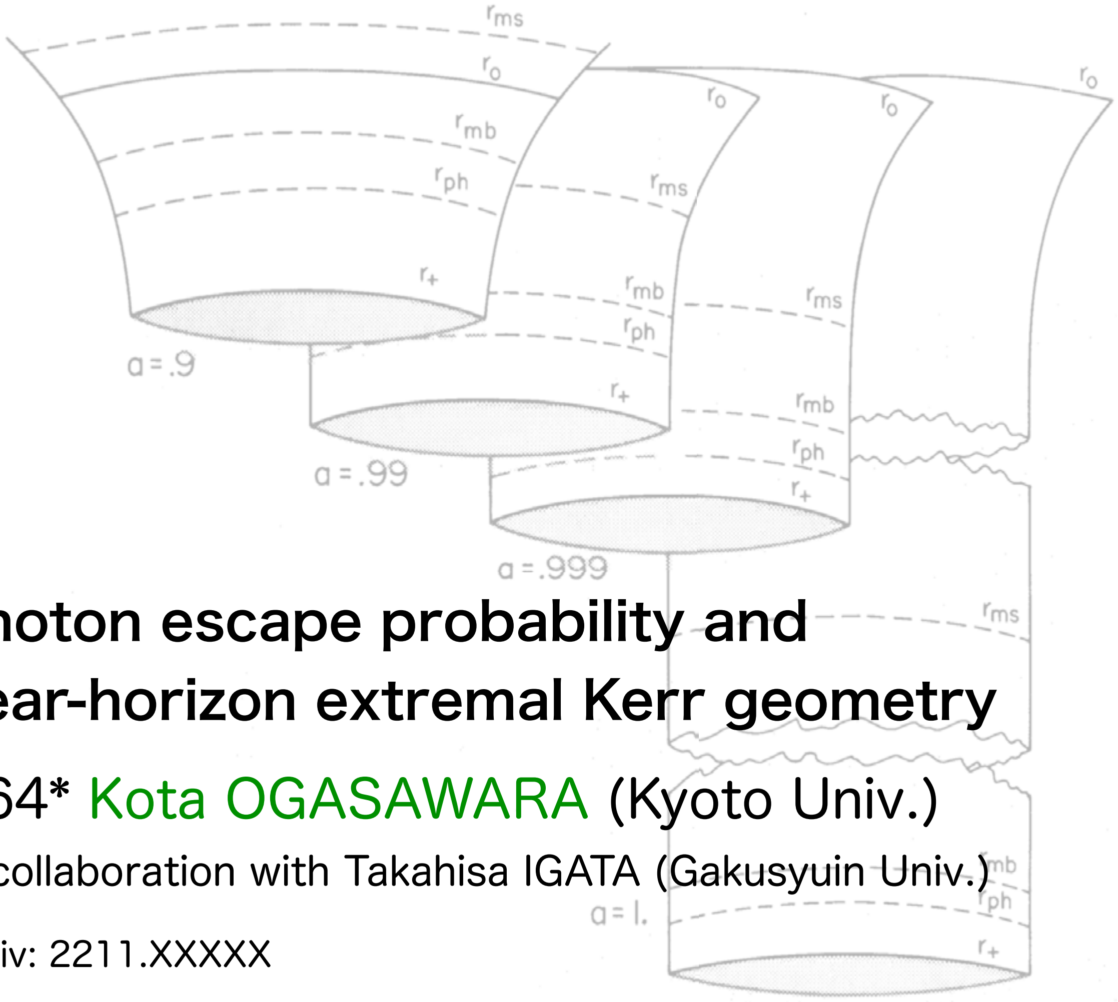

Photon escape probability and near-horizon extremal Kerr geometry

C64* Kota OGASAWARA (Kyoto Univ.)

In collaboration with Takahisa IGATA (Gakusyuin Univ.)

arXiv: 2211.XXXXX

Black Hole (BH) Observations

[EHT Collaboration]

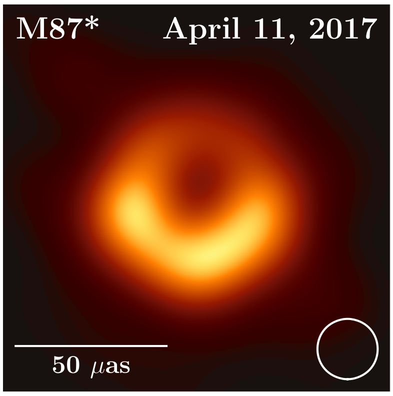

[LVK Collaboration]

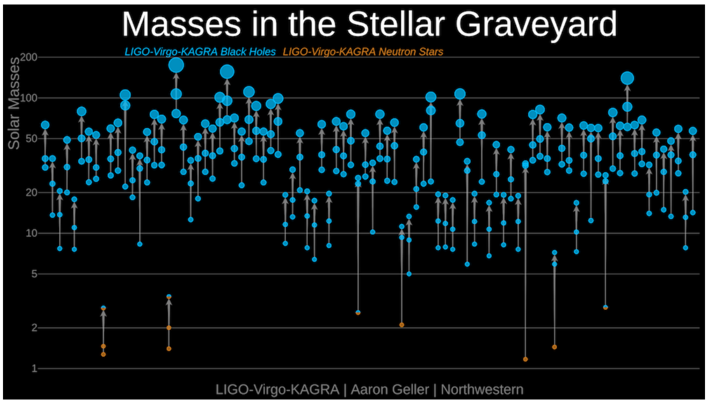

- BH observation: receiving signals emitted from its vicinity.
- How visible is the neighborhood of BH?

Photon Escape Cone

[Synge (1966), Semerak (1996), Takahashi+(2010)]

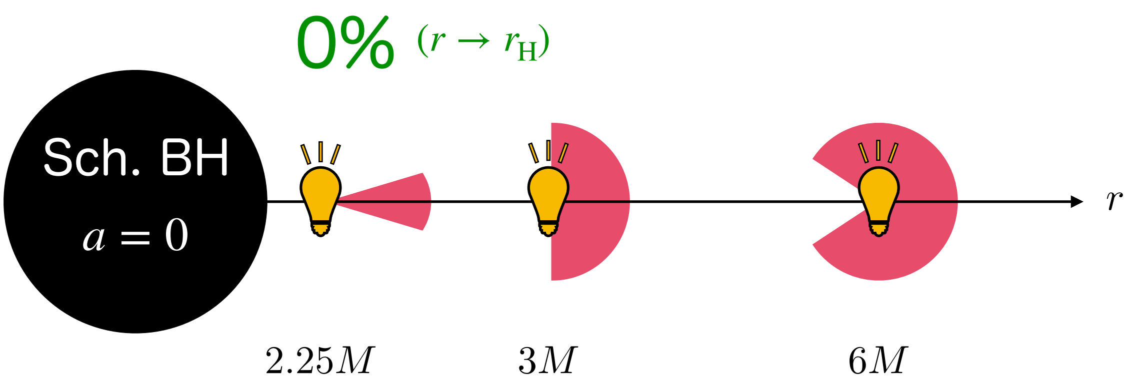

Photon sphere

- As the source approaches BH, the probability of photon escape decreases. → It's hard to see near BH···

BH Spin & Proper Motion of Emitter

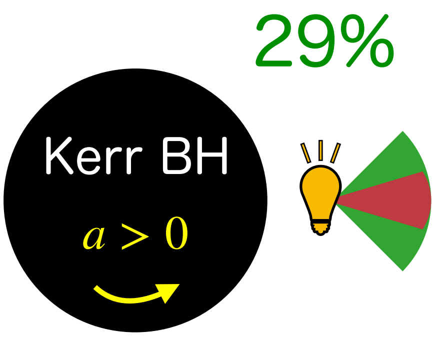

- High spin BH is more visible than non-spining BH.
- Proper motion of the emitter increases the escape probability.

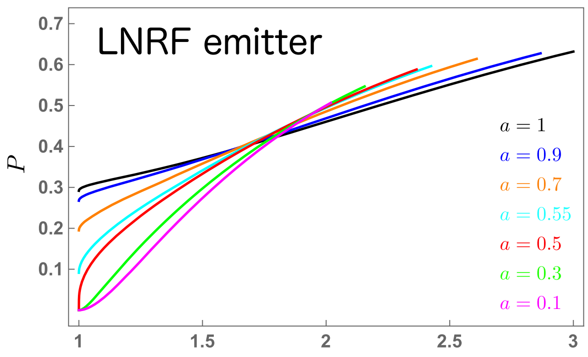

[KO+(2020)]

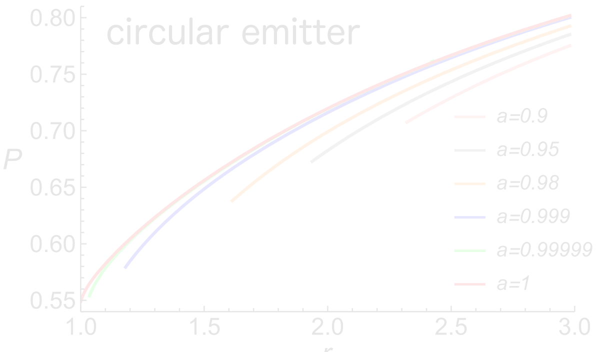

[Igata+(2020)]

BH Spin & Proper Motion of Emitter

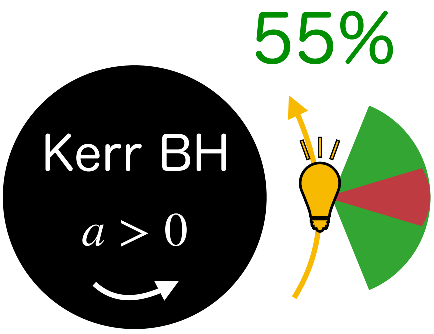

- High spin BH is more visible than non-spining BH.
- Proper motion of the emitter increases the escape probability.

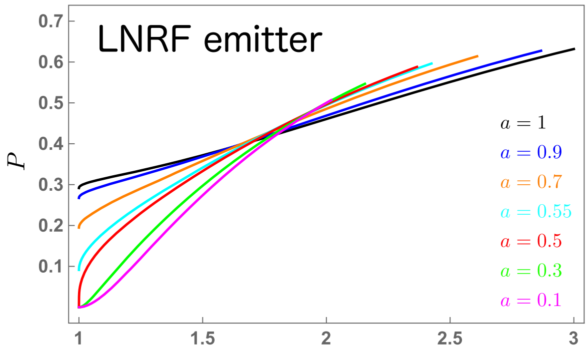

[KO+(2020)]

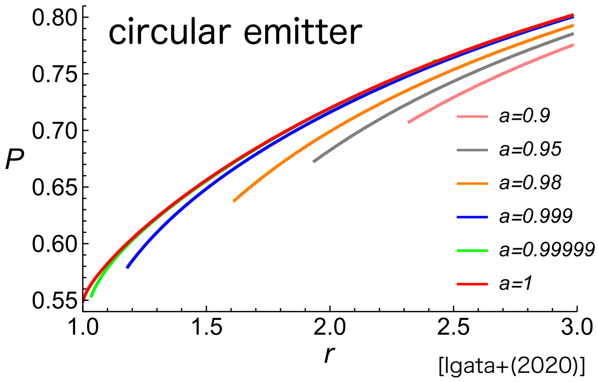

[Igata+(2020)]

BH Spin & Proper Motion of Emitter

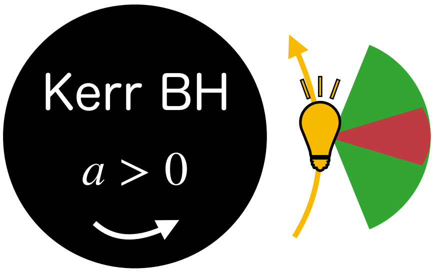

Near-Horizon $(r \to r_{\rm H})$

& Near-Extremal $(a \to M)$

look interesting!!

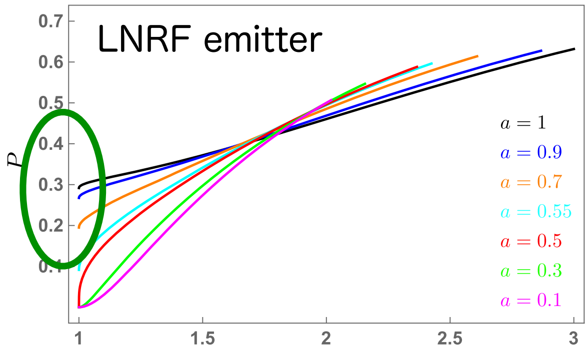

[KO+(2020)]

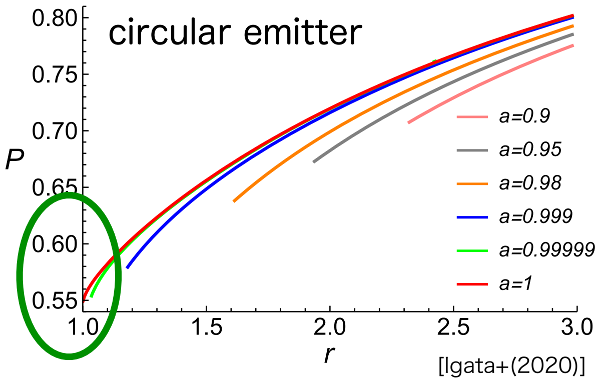

[Igata+(2020)]

Typical Radii around a Kerr BH

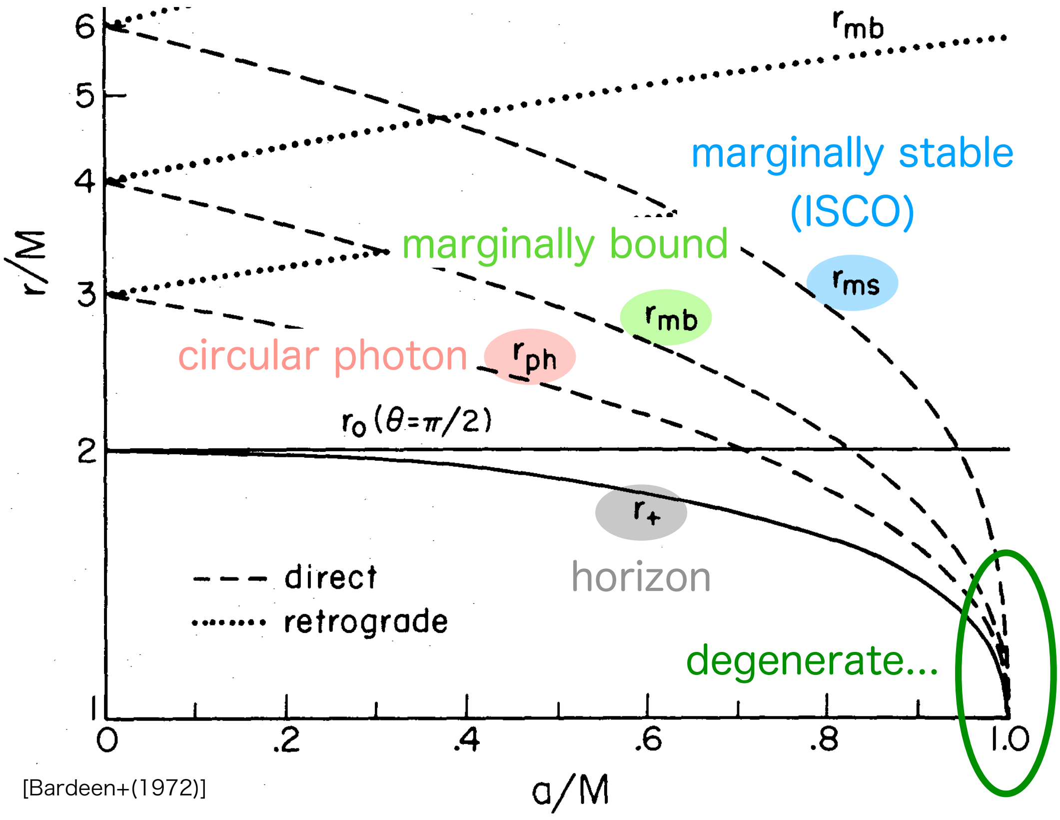

[Bardeen+(1972)]

Near-Horizon Extremal Kerr Geometry

- B.L. (t, r, ϕ) → Bardeen–Horowitz (T, R, Φ)

$$T = \frac{\varepsilon t}{2M},\ R = \frac{r-M}{\varepsilon M},\ \Phi = \phi - \frac{t}{2M},\ (\varepsilon \to 0) \qquad ✓\ \Omega_{\mathrm{H}}\partial_T = \partial_t + \Omega_{\mathrm{H}}\partial_\phi$$

- NHEK metric

$$\Gamma = \frac{1+\cos^2\theta}{2},\ \Lambda = \frac{2\sin\theta}{1+\cos^2\theta}$$

$$g^{\mathrm{NHEK}}_{\mu\nu}\mathrm{d}X^\mu \mathrm{d}X^\nu = 2M^2\Gamma\left[-R^2\mathrm{d}T^2 + \frac{\mathrm{d}R^2}{R^2} + \mathrm{d}\theta^2 + \Lambda^2(\mathrm{d}\Phi + R\mathrm{d}T)^2\right]$$

- symmetry：Kerr exterior R×U(1) → Kerr throat SL(2,R)×U(1)

$$[H_0, H_\pm] = \mp H_\pm,\ [H_+, H_-] = 2H_0$$

$$H_0 = T\partial_T - R\partial_R,\ H_+ = \partial_T,\ W_0 = \partial_\Phi,$$

$$H_- = \left(T^2 + \frac{1}{R^2}\right)\partial_T - 2TR\partial_R - \frac{2}{R}\partial_\Phi$$

Extremal Kerr Throat

- extremal limit

$$a = M\sqrt{1-\kappa^2}, \quad 0 < \kappa \ll 1$$

- near horizon radii

$$r = M(1+\kappa^p R), \quad 0 < p \leq 1$$

$$r_{\rm ms} = M(1+2^{1/3}\kappa^{2/3})$$
$$r_{\rm mb} = M(1+\sqrt{2}\kappa)$$
$$r_{\rm ph} = M(1+2/\sqrt{3}\kappa)$$
$$r_+ = M(1+\kappa)$$

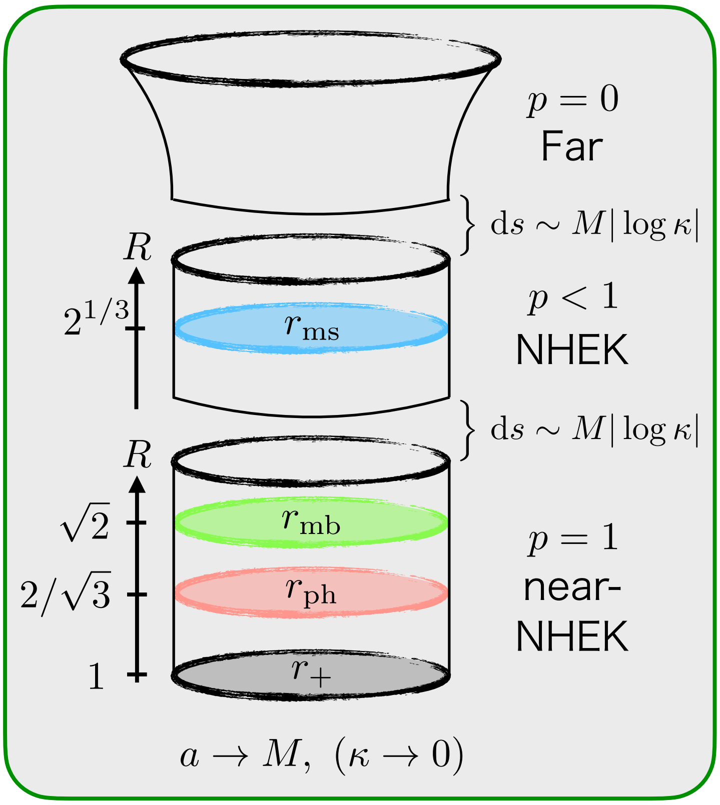

Extremal Kerr Throat

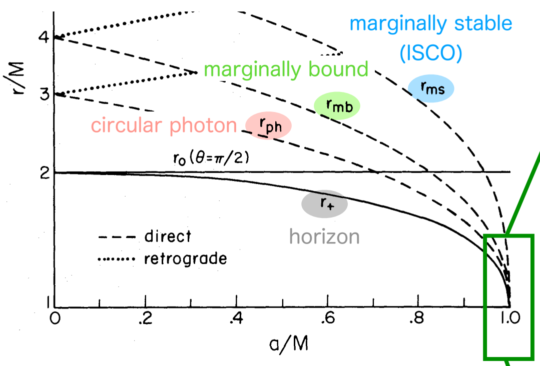

Degeneracy of radii
is resolved!!

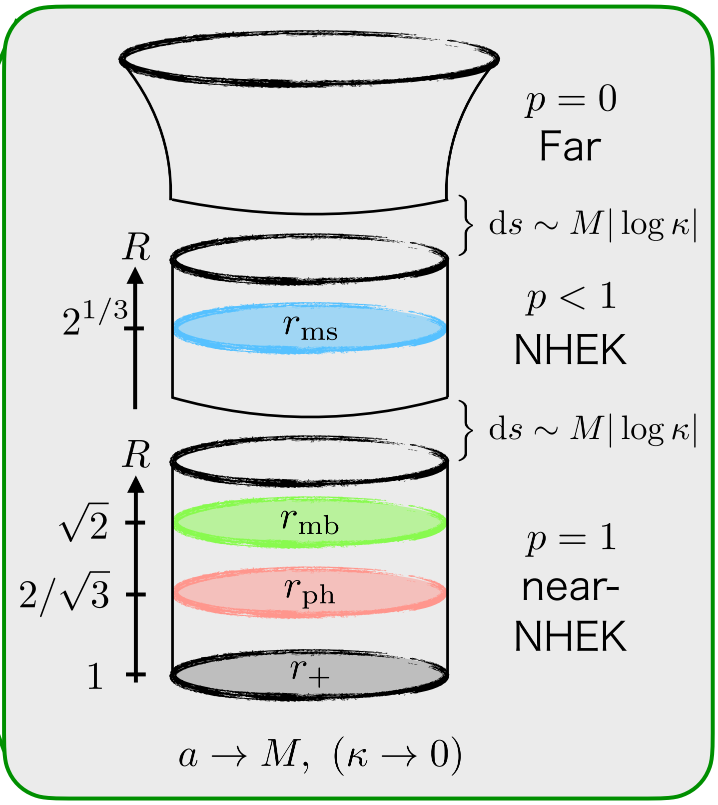

Calculation Procedure

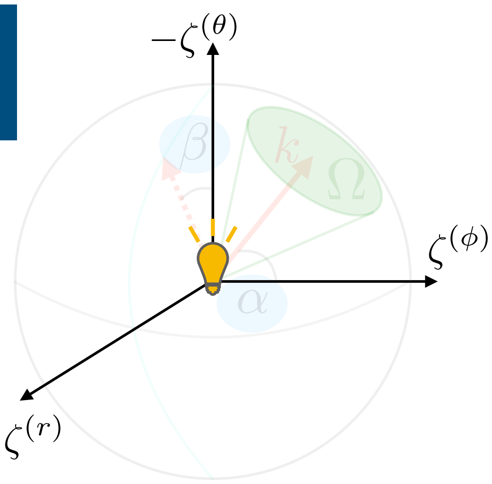

① rest frame of the emitter $\{\zeta_a^{(\mu)}\}$

② emission angles (α, β)

$$\cos\alpha = \frac{k^{(\phi)}}{k^{(t)}}, \quad \cos\beta = \frac{-k^{(\theta)}}{\sqrt{(k^{(t)})^2 - (k^{(\phi)})^2}}$$

✓ Ω : escapable region

③ area-preserving projection (ρ, φ)

$$\mathrm{d}\mathcal{A} = \rho\mathrm{d}\rho \wedge \mathrm{d}\varphi = \sin\alpha\mathrm{d}\alpha \wedge \mathrm{d}\beta = \mathrm{d}\Omega$$

$$\rho = 2\cos\left(\frac{\alpha}{2}\right), \quad \varphi = \frac{\pi}{2} - \beta$$

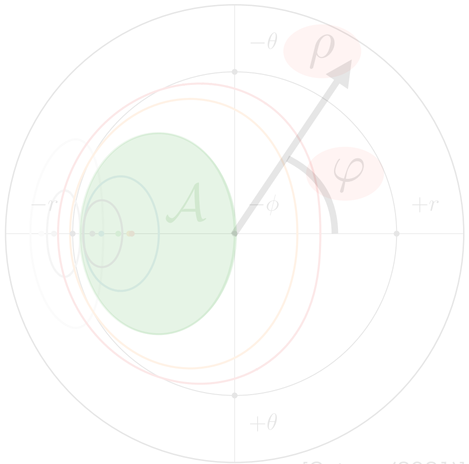

④ integrate $P = \frac{\mathcal{A}}{4\pi} = \frac{\int \rho\mathrm{d}\rho \wedge \mathrm{d}\varphi}{4\pi}$

[Gates+ (2021)]

Calculation Procedure

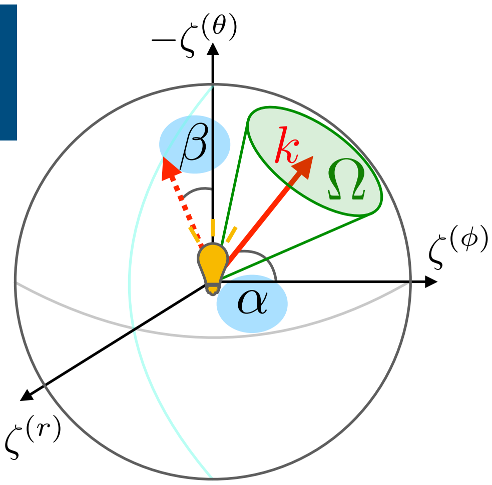

① rest frame of the emitter $\{\zeta_a^{(\mu)}\}$

② emission angles (α, β)

$$\cos\alpha = \frac{k^{(\phi)}}{k^{(t)}}, \quad \cos\beta = \frac{-k^{(\theta)}}{\sqrt{(k^{(t)})^2 - (k^{(\phi)})^2}}$$

✓ Ω : escapable region

boundary

= photon unstable circular orbit

(in general, Spherical Photon Orbits)

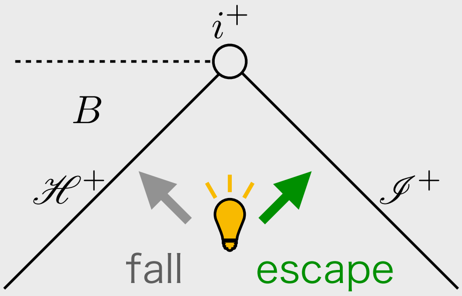

[Gates+ (2021)]

Calculation Procedure

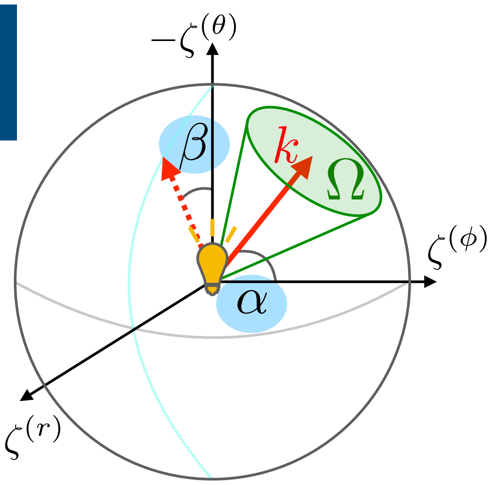

① rest frame of the emitter $\{\zeta_a^{(\mu)}\}$

② emission angles (α, β)

$$\cos\alpha = \frac{k^{(\phi)}}{k^{(t)}}, \quad \cos\beta = \frac{-k^{(\theta)}}{\sqrt{(k^{(t)})^2 - (k^{(\phi)})^2}}$$

✓ Ω : escapable region

③ area-preserving projection (ρ, φ)

$$\mathrm{d}\mathcal{A} = \rho \mathrm{d}\rho \wedge \mathrm{d}\varphi = \sin\alpha \mathrm{d}\alpha \wedge \mathrm{d}\beta = \mathrm{d}\Omega$$

$$\rho = 2\cos\left(\frac{\alpha}{2}\right), \quad \varphi = \frac{\pi}{2} - \beta$$

④ integrate $\quad P = \dfrac{\mathcal{A}}{4\pi} = \dfrac{\int \rho \mathrm{d}\rho \wedge \mathrm{d}\varphi}{4\pi}$

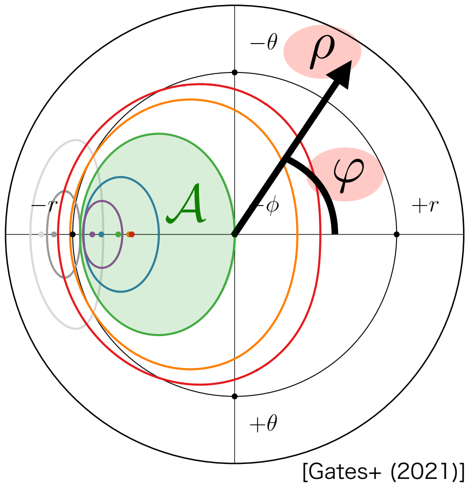

[Gates+ (2021)]

Three Emitters Motion

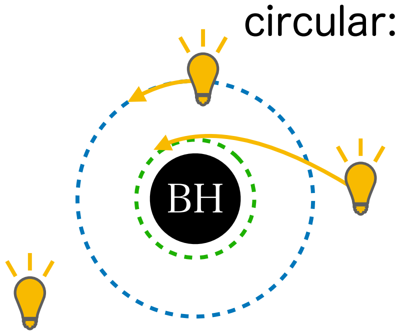

circular: $r > r_{\mathrm{ms}}$

marginally bounded: $r > r_{\mathrm{mb}}$

Locally non rotating frame:

$r > r_+$ (no proper motion)

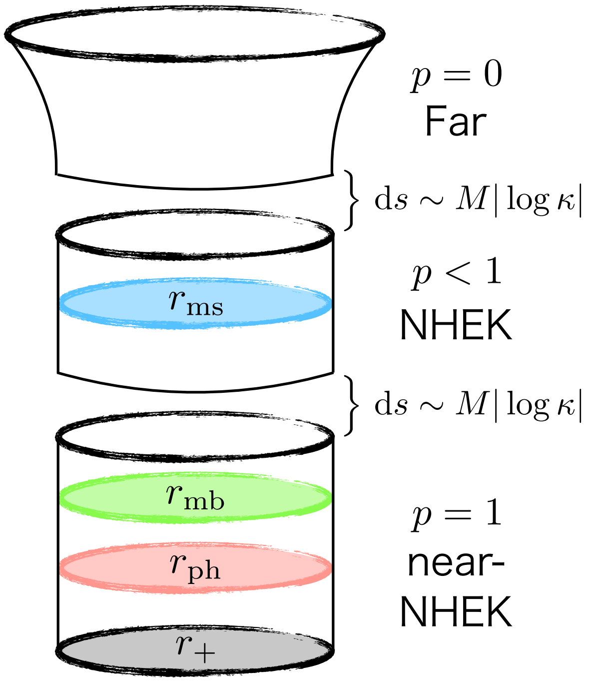

$a \to M, \ (\kappa \to 0)$

Escape Probability in NHEK (p<1)

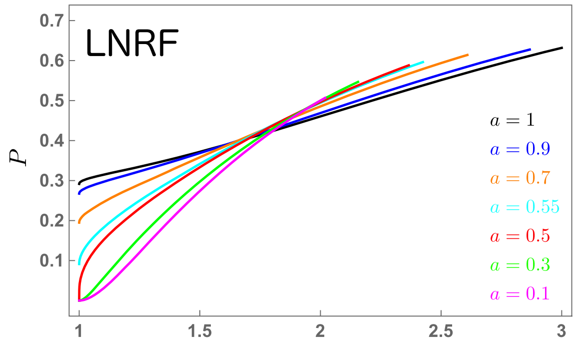

$$P_{\rm LNRF} = \frac{7}{24} \simeq 29.17\%$$

$$P_{\rm ms} = \frac{5}{12} + \frac{\arctan\sqrt{5/3}}{\sqrt{5}\pi} \simeq 54.65\%$$

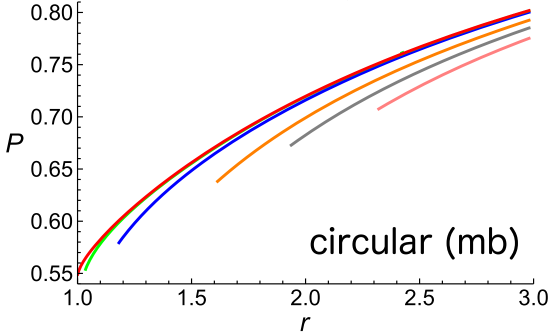

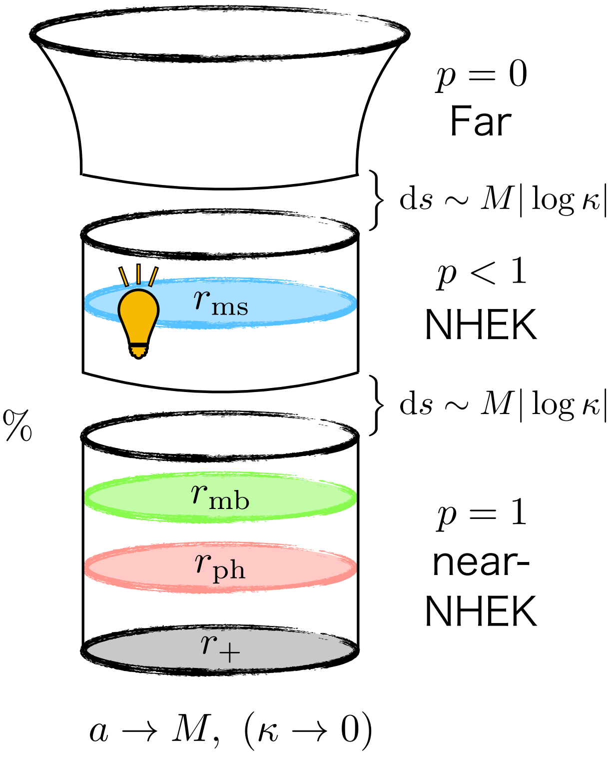

Escape Probability in near-NHEK (p=1)

Deleted due to preliminary results.

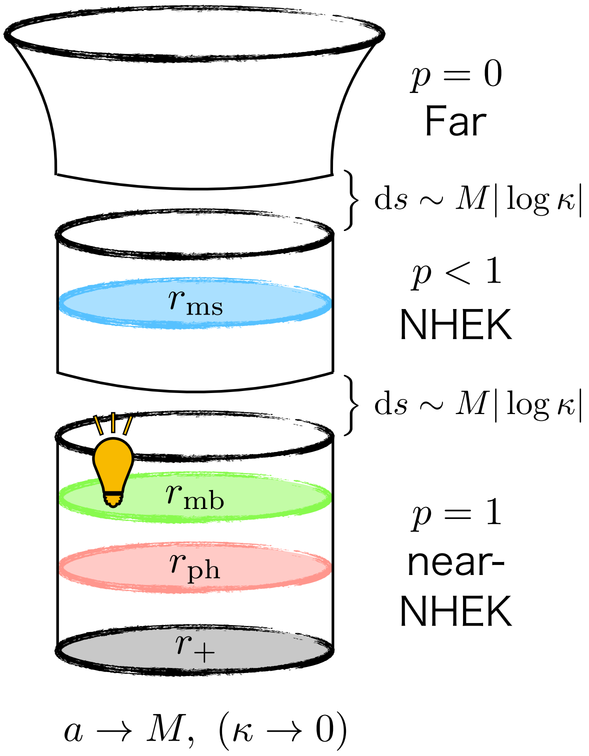

Limit of P as a Function of Energy

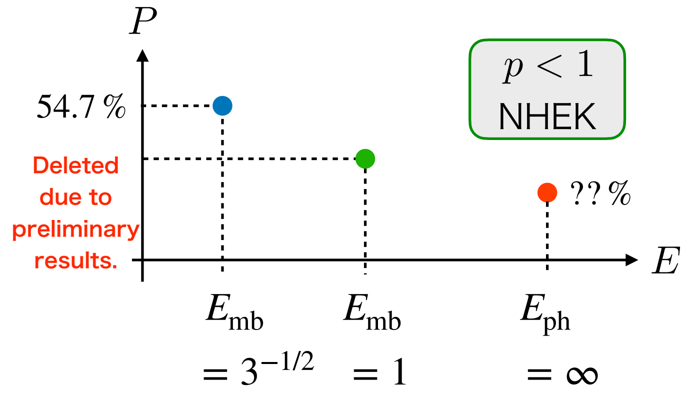

Deleted due to preliminary results.

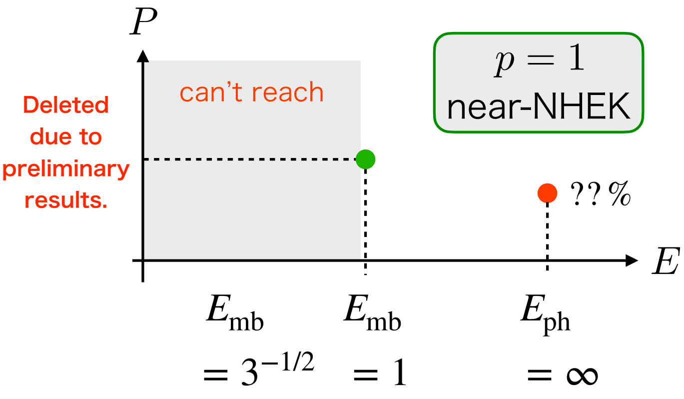

Deleted due to preliminary results.

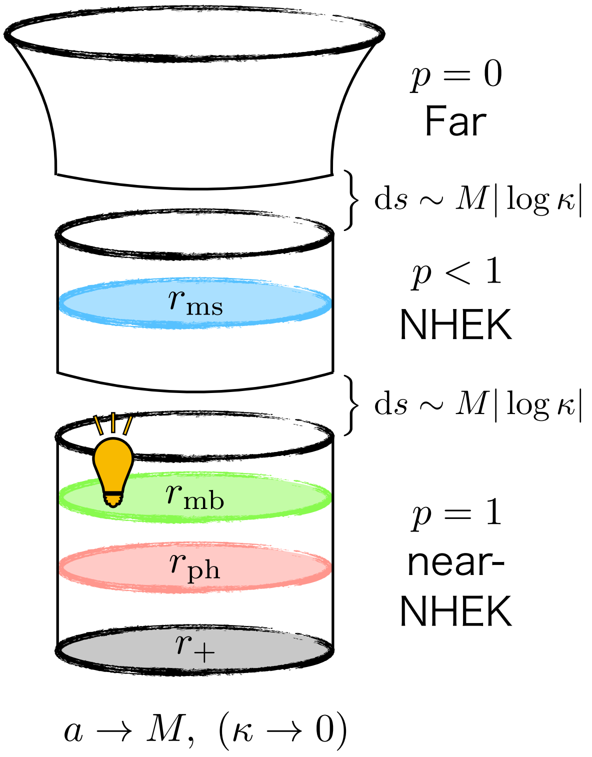

Summary

✓ How visible is the neighborhood of BH ? → Escape Probability

✓ Focus on the near BH region
→ near-NHEK throat

✓ Deepest part of the NHEK throat
→ emitter asymptotic to $\mathscr{H}^+$
→ we want to find the limit of P as a function of energy:
$P(E), \ (r \to r_+)$

- Nature of extremal Kerr BH
- Kerr (AdS) CFT? ...

Deleted due to preliminary results.

Thank you for your attention
Feel free to comment me

Maximum size of black holes in the accelerating Universe

from T. Shiromizu, K. Izumi, K. Lee and D. S. , Phys. Rev. D **106**, 084041 (2022)

Diego Soligon

Graduate School of Mathematics, Nagoya University

JGRG, 27th October 2022

Outline

Introduction

- It has been shown in previous studies that in a spacetime with positive cosmological constant the area of a black hole horizon has an upper bound
- For example, in Hayward, Shiromizu and Nakao (1994) it was shown that for an apparent horizon $A \leq 4\pi/\Lambda$
- Further development took into consideration the angular momentum of a rotating black hole (eg. Clement, Reiris and Simon, 2015), leading to a more refined inequality
- This study took into consideration all the variables previously considered separately (angular momentum, matter, gravitational waves) to produce an even more accurate upper bound

---

Outline

Definitions

Given a four-dimensional spacetime (M, g_{ab}) with a three-dimensional hypersurface (Σ, q_{ab}), we consider a compact 2-surface in it denoted (S, h_{ab}).

$$g_{ab} = h_{ab} + r_a r_b - n_a n_b = q_{ab} - n_a n_b$$

with n^a the future-directed normal to Σ and r^a the spacelike normal to S.

Definitions

The second fundamental forms of Σ and S respectively are

$$K_{ab} = q_a^c q_b^d \nabla_c n_d$$

and

$$k_{ab} = h_a^c h_b^d \nabla_c r_d$$

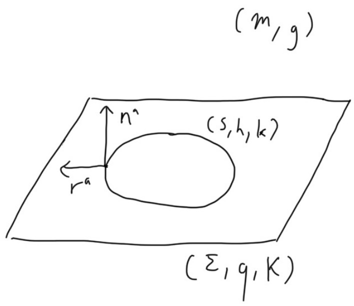

Setup

We can decompose the second fundamental form K_{ab} as

$$K_{ab} = K_{(r)} r_a r_b + \kappa_{ab} + v_a r_b + v_b r_a$$

where

$$K_{(r)} := K_{ab} r^a r^b$$

$$\kappa_{ab} := h_a^c h_b^d K_{cd}$$

$$v_a := h_a^c r^b K_{bc}$$

Setup

Defining $\theta_+ = \kappa + k$ we obtain the key equation

$$r^a \nabla_a \theta_+ = -\frac{1}{2}\theta_{+ab}\theta_+^{ab} - \frac{1}{2}\theta_+^2 + \theta_+ (K_{(r)} + \kappa) + \frac{1}{2}R + \mathcal{D}_a V^a - V_a V^a - G_{ab} k^a n^b$$

with

$$V_a := v_a - \mathcal{D}_a \ln \varphi$$

a spacelike vector tangent to S and

$$k^a := n^a + r^a$$

a future-directed null vector

Definitions

θ_+ as defined before is the outgoing null expansion rate associated with k^a, with $\theta_+ = h^{ab}\nabla_a k_b = h^{ab}\theta_{+ab}$. Then, a stable marginally outer trapped surface can be defined as a compact 2-surface S satisfying

$$\theta_+|_S = 0 \qquad \text{and} \qquad \mathrm{r}^{\mathrm{a}}\nabla_{\mathrm{a}}\theta_+|_{\mathrm{S}} \geq 0$$

Outline

Area of a stable MOTS

If we consider a spacetime with a positive cosmological constant Λ, the Einstein equation reads $G_{ab} = 8\pi T_{ab} - \Lambda g_{ab}$. Then, if we integrate the key equation over S we obtain

$$\frac{1}{2}\int_S R\, dA \geq \Lambda A + \int_S \left[V_a V^a + 8\pi(\rho_+ + \rho_{+\mathrm{gw}})\right] dA$$

with

$$\rho_+ := T_{ab}k^a n^b = T_{ab}n^a n^b + T_{ab}r^a n^b$$

$$8\pi\rho_{+\mathrm{gw}} := \frac{1}{2}\tilde{\theta}_{+ab}\tilde{\theta}_+^{ab} = \frac{1}{2}(\tilde{\kappa}_{ab}\tilde{\kappa}^{ab} + \tilde{k}_{ab}\tilde{k}^{ab}) + \tilde{\kappa}_{ab}\tilde{k}^{ab}$$

The tilde indicates traceless part.

Area of a stable MOTS

If the dominant energy condition holds, i. e. $\rho_+ \geq 0$, then the RHS in the integral equation is non-negative. From the Gauss-Bonnet theorem we can then infer that a stable MOTS is topologically a 2-sphere, so that $\int_S R dA = 8\pi$. The integral equation then becomes

$$A \leq \frac{4\pi}{\Lambda} - \frac{1}{\Lambda}\int_S \left[V_a V^a + 8\pi(\rho_+ + \rho_{+\mathrm{gw}})\right] dA.$$

or

$$\int_S \left[V^a V_a + 8\pi\left(\rho_+ + \rho_{+\mathrm{gw}}\right)\right] dA \leq 4\pi - \Lambda A$$

Simplification with surface-averaged quantities

Defining the surface-averaged total density

$$\bar{\rho}_{+\mathrm{tot}} = \frac{1}{A}\int_S \rho_{+\mathrm{tot}} dA$$

the inequality is simplified as

$$A \leq \frac{4\pi}{\Lambda_+} - \frac{1}{\Lambda_+}\int_S V^a V_a dA$$

where

$$\Lambda_+ := \Lambda + 8\pi\bar{\rho}_{+\mathrm{tot}}$$

Application to Kerr-de Sitter metric

If we consider a Kerr-de Sitter metric, integrating over the surface of the horizon we obtain

$$\int_{S_H} V_a V^a dA = 24\pi \frac{(am)^2}{r_H^4} + O(a^4)$$

Note that there is no dependence on the cosmological constant at the leading order. While higher order computation is possible, the physical or geometrical meaning of higher order terms would not be immediately clear.

Outline

Consequence for black hole event horizons

- Since we can describe a black hole horizon as a marginally outer trapped surface, our result effectively impose an upper bound to the size of a black hole.
- The results can be applied in various models, but given the scale of the quantities in consideration it is especially relevant in the study of the early Universe.
- However, when considering black hole formation higher order perturbations become relevant, so the surface-averaged approach becomes less viable.

Further applications

Another interesting case is if we consider n dimensions. The following equation holds:

$$\frac{1}{2}\int_S {}^{(n-1)}R dA \geq \Lambda A + \int_S \left[V_a V^a + 8\pi(\rho_+ + \rho_{+gw})\right] dA$$

For $n \geq 4$ we cannot use Gauss-Bonnet theorem to evaluate the integral.

C66

Rotating black holes at large D in Einstein-Gauss-Bonnet theory

Ryotaku Suzuki

with

Shinya Tomizawa

Toyota Technological Institute (豊田工業大学)

arXiv: 2202.12649 [PRD106, 024018(2022)]

JGRG31, The University of Tokyo, 24-28 Oct. 2022

Introduction

- String Theory predicts Higher Curvature Corrections to GR
  Einstein-Gauss-Bonnet theory is one of the simplest

$$S = -\frac{1}{16\pi G}\int (R + \alpha_{\rm GB}\mathcal{L}_{\rm GB}) d^d x \qquad \mathcal{L}_{\rm GB} = R^2 - 4R_{\mu\nu}R^{\mu\nu} + R_{\mu\nu\rho\sigma}R^{\mu\nu\rho\sigma}$$

- However, only static spherically symmetric BH [Boulware-Deser (1985)] is found in EGB theory so far

  No exact solutions like Myers-Perry or black string as in GR

Stationary BH in EGB theory

Stationary solutions are important. But finding sols is not successful.

- D=5 Kerr-Schild ansatz does not include rotating solution in general

Anabalon+ (2008)

Instead, numerical or perturbative approaches have been used

- D=5 equally-rotating BH

numerical Brihaye-Radu (2008) MP+small α_{GB} approx Ma-Li-Lu (2021)

- Singly-rotating BH with small Ω Kim-Cai (2007)

Then, we try to find analytic solutions beyond small parameter limit using the large D effective theory approach

---

Large D limit

Large D limit of General Relativity

Emparan, RS, Tanabe (2013)

$$S_{EH} = \int dx^{D} \sqrt{-g} R$$

Assume Large Spacetime Dimension $(D \to \infty)$

(Mostly consider large symmetric part like S^{D-p})

BH dynamics

→ Effective Theory@D=∞ + 1/D correction

(analogy to) Large N limit of SU(N) Super Yang-Mills

Localization of Gravity

Gravity is localized around BH at large D

$$r \simeq r_0 + \frac{r_0}{D} \ln \mathrm{R} \longleftrightarrow \mathrm{R} := (r/r_0)^{D-3}$$

Near horizon coordinate

ex) Schwarzschild

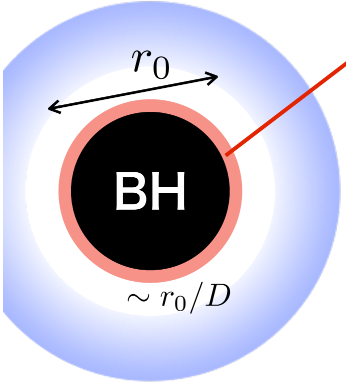

Near region

$$\boxed{r - r_0 \sim O(r_0/D)}$$

→1/D expansion as function of R

$$g = g_0(\mathrm{R}) + g_1(\mathrm{R})/D + \dots$$

Far region

$$\boxed{r - r_0 \sim O(r_0)}$$

→ post Minkowski

Overlap region $r_0/D \ll r - r_0 \ll r_0 \quad (1 \ll \mathrm{R} \ll e^{D})$

→Near sols. and Far sols. can be matched

Large D Effective Theory

Emparan-Shiromizu-RS-Tanabe-Tanaka (2015), Emparan-RS-Tanabe (2015)
Bhattacharyya-De-Minwalla-Mohan-Saha (2015)

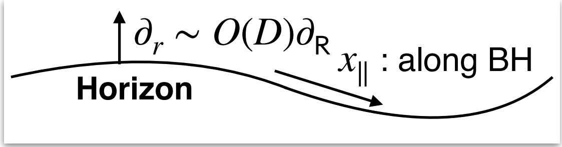

Consider general shape of BHs

Assume near region@D=∞ is solved with $\mathsf{R} := (r/r_0)^{D-\#} \longrightarrow \partial_r \sim O(D)\partial_{\mathsf{R}}$

$\Rightarrow$ $\partial_r \sim O(D) \gg \partial_{\|} \quad (\partial_{\|} = O(1) \sim O(\sqrt{D}))$

Radial gradient ∂_{R} is enhanced by D in Einstein equation

Large D Effective Theory

Emparan-Shiromizu-RS-Tanabe-Tanaka (2015), Emparan-RS-Tanabe (2015)
Bhattacharyya-De-Minwalla-Mohan-Saha (2015)

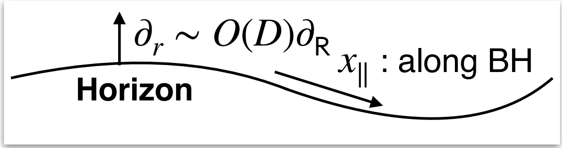

Consider general shape of BHs

Assume near region@D=∞ is solved with $\mathsf{R} := (r/r_0)^{D-\#} \longrightarrow \partial_r \sim O(D)\partial_{\mathsf{R}}$

$\Rightarrow$ $\partial_r \sim O(D) \gg \partial_{\|} \quad (\partial_{\|} = O(1) \sim O(\sqrt{D}))$

Radial gradient ∂_{R} is enhanced by D in Einstein equation

$$\begin{tikzcd}\text{Einstein equation@D=}\infty \arrow[r] \arrow[d] & \text{ODE w.r.t } \mathsf{R} \text{ (} \partial_{\|} \text{ is dropped)} \\ \text{Constraints w.r.t } x_{\|} & \end{tikzcd}$$

Large D Effective Theory

Emparan-Shiromizu-RS-Tanabe-Tanaka (2015), Emparan-RS-Tanabe (2015)
Bhattacharyya-De-Minwalla-Mohan-Saha (2015)

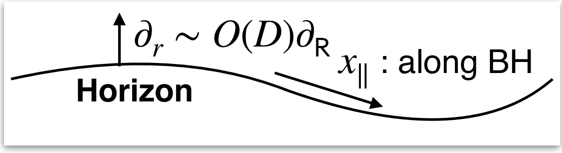

Consider general shape of BHs

Assume near region@D=∞ is solved with $\mathrm{R} := (r/r_0)^{D-\#} \longrightarrow \partial_r \sim O(D)\partial_{\mathrm{R}}$

➡ $\partial_r \sim O(D) \gg \partial_{\|} \quad (\partial_{\|} = O(1) \sim O(\sqrt{D}))$

Radial gradient ∂_{R} is enhanced by D in Einstein equation

Einstein equation@D=∞ ⟶ **ODE w.r.t R ($\partial_{\|}$ is dropped)**

Integrable in R → integration functions of $x_{\|}$

= Effective fields on the horizon

↓

Constraints w.r.t $x_{\|}$

Large D Effective Theory

Emparan-Shiromizu-RS-Tanabe-Tanaka (2015), Emparan-RS-Tanabe (2015)
Bhattacharyya-De-Minwalla-Mohan-Saha (2015)

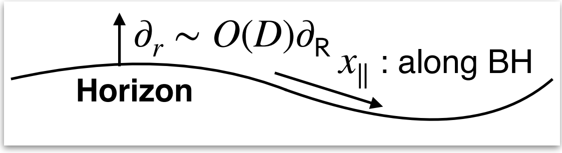

Consider general shape of BHs

Assume near region@D=∞ is solved with $\mathrm{R} := (r/r_0)^{D-\#} \longrightarrow \partial_r \sim O(D)\partial_{\mathrm{R}}$

➡ $\partial_r \sim O(D) \gg \partial_{\|} \quad (\partial_{\|} = O(1) \sim O(\sqrt{D}))$

Radial gradient ∂_{R} is enhanced by D in Einstein equation

Einstein equation@D=∞ ⟶ **ODE w.r.t R ($\partial_{\|}$ is dropped)**

Integrable in R → integration functions of $x_{\|}$

= Effective fields on the horizon

↓

Constraints w.r.t $x_{\|}$

⟵

→ Effective equation (theory) for the effective fields

Rotating BH@Large D

At large D, Myers-Perry has simple structure:

Myers-Perry@D=∞ = static black holes@D=∞

(with the line elements replaced by the boosted frame)

Emparan-Grumiller-Tanabe (2013), Emparan-RS-Tanabe (2014)

D=2n+3 Equally-rotating Myers-Perry@Large D $\mathsf{R} := r^{2n}$

$$ds^2_{\mathrm{MP}} \simeq -\left(1-\frac{1}{\mathsf{R}}\right)(e^{(0)})^2 + \left(1-\frac{1}{\mathsf{R}}\right)^{-1} dr^2 + \underbrace{(e^{(2)})^2 + d\Sigma^2_{\mathrm{CP^n}}}_{S^{2n+1}}$$

$$e^{(i)} := \Lambda^i{}_t dt + \Lambda^i{}_\phi (d\phi + \mathscr{A})$$

$\leftrightarrow (dt, d\phi + \mathscr{A})$ in Schwarzschild@Large D

Rotating BH@Large D

At large D, Myers-Perry has simple structure:

Myers-Perry@D=∞ = static black holes@D=∞

(with the line elements replaced by the boosted frame)

Emparan-Grumiller-Tanabe (2013), Emparan-RS-Tanabe (2014)

D=2n+3 Equally-rotating Myers-Perry@Large D $\mathsf{R} := r^{2n}$

$$ds^2_{\mathrm{MP}} \simeq -\left(1-\frac{1}{\mathsf{R}}\right)(e^{(0)})^2 + \left(1-\frac{1}{\mathsf{R}}\right)^{-1} dr^2 + \underbrace{(e^{(2)})^2 + d\Sigma^2_{\mathrm{CP^n}}}_{S^{2n+1}}$$

$$e^{(i)} := \Lambda^i{}_t dt + \Lambda^i{}_\phi (d\phi + \mathscr{A})$$

$\leftrightarrow (dt, d\phi + \mathscr{A})$ in Schwarzschild@Large D

This property simplifies the analysis of Myers-Perry at large D

- Leading order equation becomes that of static BHs
- Equation decouples to separate ODEs (then Integrable)

ex) perturbative analysis Myers-Perry BH **Emparan-RS-Tanabe (2014)** **RS-Tanabe (2015)**

Charged Myers-Perry **Tanabe (2016), Mandlik-Thakur (2018)**

Rotating BH@Large D

At large D, Myers-Perry has simple structure:

Myers-Perry@D=∞ = static black holes@D=∞

(with the line elements replaced by the boosted frame)

Emparan-Grumiller-Tanabe (2013), Emparan-RS-Tanabe (2014)

D=2n+3 Equally-rotating Myers-Perry@Large D $\mathsf{R} := r^{2n}$

$$ds^2_{\mathrm{MP}} \simeq -\left(1-\frac{1}{\mathsf{R}}\right)(e^{(0)})^2 + \left(1-\frac{1}{\mathsf{R}}\right)^{-1} dr^2 + \underbrace{(e^{(2)})^2 + d\Sigma^2_{\mathrm{CP^n}}}_{S^{2n+1}}$$

$$e^{(i)} := \Lambda^i{}_t dt + \Lambda^i{}_\phi (d\phi + \mathscr{A})$$

$\leftrightarrow (dt, d\phi + \mathscr{A})$ in Schwarzschild@Large D

This property simplifies the analysis of Myers-Perry at large D

- Leading order equation becomes that of static BHs
- Equation decouples to separate ODEs (then Integrable)

ex) perturbative analysis Myers-Perry BH Emparan-RS-Tanabe (2014)
RS-Tanabe (2015)
Charged Myers-Perry Tanabe (2016), Mandlik-Thakur (2018)

Main Strategy: assume the same property in EGB theory

EGB theory at large D

Large D limit in EGB Theory

Large D limit of EGB BH depends on how the GB coupling scales

$$R_{\mu\nu}+\frac{1}{2}Rg_{\mu\nu}+\underline{\alpha_{\rm GB}}H_{\mu\nu}=0 \qquad H_{\mu\nu}=-\frac{1}{2}\mathcal{L}_{\rm GB}g_{\mu\nu}+2RR_{\mu\nu}-4R_{\mu\alpha}R^{\alpha}{}_{\nu}$$
$$-4R_{\mu\alpha\nu\beta}R^{\alpha\beta}+2R_{\mu\alpha\beta\gamma}R_{\nu}{}^{\alpha\beta\gamma}.$$

Assume $\alpha_{\rm GB}=O(D^{-2})$ so that EH term∼GB term@D→∞

Near Horizon@D→∞ : $R\sim D^2/r_0^2$ (rad: r_0)

NOTE: EH≫GB or EH≪GB cases
are obtained as the parameter limit $D^2\alpha_{\rm GB}\to 0$ or $D^2\alpha_{\rm GB}\to\infty$

- Large D effective theory has been applied to several black hole analysis in EGB theory
  Black hole perturbation, Black String, Black Ring — $\Omega\sim 1/\sqrt{D}$
  Chen-Li (2017), Chen-Li-Zhang (2017,2018)

But not yet for (spherical) rotating black holes

Setup

For simplicity, we consider equally-rotating BH in D=2n+3.

Background : Minkowski in Eddington-Finkelstein coord.

$$ds^2=-dt^2+2dtdr+\underline{r^2(d\phi+\mathcal{A})^2+r^2d\Sigma^2_{CP^n}}$$

$S^{2n+1}\to$ a hopf fibration of S^1 on CP^n

Setup

For simplicity, we consider equally-rotating BH in D=2n+3.

Background : Minkowski in Eddington-Finkelstein coord.

$$ds^2 = -dt^2 + 2dtdr + \underbrace{r^2(d\phi + \mathscr{A})^2 + r^2 d\Sigma^2_{CP^n}}_{S^{2n+1} \rightarrow \text{a hopf fibration of } S^1 \text{ on } CP^n}$$

Assume the ansatz in the boosted frame
(expecting the same simplification as in Myers-Perry)

$$ds^2 = -A(r)(e^{(0)})^2 + 2U(r)e^{(0)}e^{(1)} + 2C(r)e^{(0)}e^{(2)} + H(r)(e^{(2)})^2 + r^2 d\Sigma^2$$

$(dt, dr, d\phi + \mathscr{A})$ → **boosted frame**

$$e^{(0)} = \frac{dt - \Omega r(d\phi + \mathcal{A})}{\sqrt{1-\Omega^2}} \qquad e^{(1)} = dr \qquad e^{(2)} = \frac{r(d\phi + \mathcal{A}) - \Omega dt}{\sqrt{1-\Omega^2}}$$

1/D expansion and Assumption

Ansatz

$$ds^2 = -A(r)(e^{(0)})^2 + 2U(r)e^{(0)}e^{(1)} + 2C(r)e^{(0)}e^{(2)} + H(r)(e^{(2)})^2 + r^2 d\Sigma^2$$

1/n-expansion with $\mathsf{R} := r^{2n}$ $(r_H = 1)$ (D=2n+3) $\alpha := (2n)^2 \alpha_{\mathrm{GB}}$

$$A = \sum_{i=0}^{\infty} \frac{1}{n^i} A_i(\mathsf{R}), \quad U = \sum_{i=0}^{\infty} \frac{1}{n^i} U_i(\mathsf{R}), \quad C = \sum_{i=0}^{\infty} \frac{1}{n^i} C_i(\mathsf{R}), \quad H = \sum_{i=0}^{\infty} \frac{1}{n^i} H_i(\mathsf{R}).$$

1/D expansion and Assumption

Ansatz

$$ds^2 = -A(r)(e^{(0)})^2 + 2U(r)e^{(0)}e^{(1)} + 2C(r)e^{(0)}e^{(2)} + H(r)(e^{(2)})^2 + r^2 d\Sigma^2$$

1/n-expansion with $\mathsf{R} := r^{2n}$ $(r_H = 1)$ (D=2n+3) $\alpha := (2n)^2\alpha_{\text{GB}}$

$$A = \sum_{i=0}^{\infty} \frac{1}{n^i} A_i(\mathsf{R}), \quad U = \sum_{i=0}^{\infty} \frac{1}{n^i} U_i(\mathsf{R}), \quad C = \sum_{i=0}^{\infty} \frac{1}{n^i} C_i(\mathsf{R}), \quad H = \sum_{i=0}^{\infty} \frac{1}{n^i} H_i(\mathsf{R}).$$

Assumption: LO-metric ≈ static BH (with boosted frame)

$$\boxed{\begin{array}{c} ds^2 \simeq -f(r)dt^2 + 2dtdr + (d\phi + \mathscr{A})^2 + d\Sigma^2 + \mathcal{O}(n^{-1}) \\ e^{(0)} \leftrightarrow dt, \quad e^{(1)} \leftrightarrow dr, \quad e^{(2)} \leftrightarrow d\phi + \mathscr{A} \end{array}}$$

➡ $C(r) = \mathcal{O}(1/n), \quad H(r) = 1 + \mathcal{O}(1/n)$

→ EGB equation decouples to
separate ODEs w.r.t R with source terms → Integrable

Leading order solution

$$A_0 = 1 + \frac{1}{2\alpha} - \frac{1}{2\alpha}\sqrt{1 + \frac{4\alpha(\alpha+1)m}{\mathsf{R}}}$$

$$U_0 = 1, \quad C_0 = 0, \quad H_0 = 1,$$

$$ds^2 \simeq -A_0(e^{(0)})^2 + 2e^{(0)}e^{(1)} + (e^{(2)})^2 + d\Sigma^2 + \mathcal{O}(n^{-1})$$

With $e^{(0)} \leftrightarrow dt, \quad e^{(1)} \leftrightarrow dr, \quad e^{(2)} \leftrightarrow d\phi + \mathscr{A}$

Identical to D=2n+3 Boulware-Deser @large D
(as expected)

Higher order corrections

Higher order corrections are obtained by solving the sourced ODEs w.r.t R

With an auxiliary variable $X := \sqrt{1 + \frac{4\alpha(\alpha+1)m}{\mathrm{R}}}$

Next-to-Leading order sols : A_1, C_1, H_1, U_1

$$A_1 = \frac{\left(X^2-1\right)\Omega^2 \log\left(X^2+1\right)}{16\alpha\left(2\alpha^2+3\alpha+1\right)X\left(\Omega^2-1\right)} + \frac{\left(X^2-1\right)\Omega^2(\arctan X - \arctan(1+2\alpha))}{8\alpha(\alpha+1)X\left(\Omega^2-1\right)} - \frac{(X-1)\left(X+2\Omega^2-1\right)\log(X-1)}{4\alpha X\left(\Omega^2-1\right)} - \frac{(X-1)\log(X+1)\left(\alpha\left(4\Omega^2-2\right)+X\left(2\alpha+\Omega^2+2\right)+5\Omega^2-2\right)}{8\alpha(\alpha+1)X\left(\Omega^2-1\right)} + a_0 + a_1 X + \frac{a_2}{X},$$

$$C_1 = \frac{\Omega(X-1)}{4\alpha(1-\Omega^2)} \log\left(\frac{4\alpha(1+\alpha)}{X^2-1}\right) \qquad U_1 = \frac{(X-1)\Omega^2(\alpha(X-1)-1)}{2(\alpha+1)(2\alpha+1)\left(X^2+1\right)\left(\Omega^2-1\right)}$$

$$H_1 = \frac{\Omega^2}{(\alpha+1)(1-\Omega^2)}\left[\log\left(\frac{X+1}{2}\right) - \arctan X + \frac{\pi}{4} - \frac{1}{2(2\alpha+1)}\log\left(\frac{X^2+1}{2}\right)\right],$$

NNLO is also obtained (much complicated)

Thermodynamics

Metric is solved up to NLO in 1/n-expansion
→ Thermodynamic variables are obtained up to the same order

Entropy ← Iyer-Wald formula

The 1st law is checked up to NLO

$$\mathcal{S} = \frac{1}{4G}\int_H (1 + 2\alpha_{\mathrm{GB}}\mathcal{R})\sqrt{h}\, d^{D-2}x$$

scalar curvature of horizon surface

1/n-expansion up to O(1/n) $\alpha_H := \alpha/m^{\frac{1}{2n}}$

$$M = \frac{n\Omega_{2n+1}}{8\pi G}\frac{(1+\alpha_H)m}{1-\Omega^2}$$

$$J = \frac{n\Omega_{2n+1}}{8\pi G}\frac{(1+\alpha_H)m^{\frac{2n+1}{2n}}\Omega}{1-\Omega^2}$$

$$T = \frac{n}{\pi}\frac{1+\alpha_H}{1+2\alpha_H}m^{-\frac{1}{2n}}\sqrt{1-\Omega^2}$$

$$S = \frac{\Omega_{2n+1}}{4G}\frac{(1+2\alpha_H)m^{\frac{2n+1}{2n}}}{\sqrt{1-\Omega^2}}$$

Thermodynamics

Metric is solved up to NLO in 1/n-expansion
→ Thermodynamic variables are obtained up to the same order

Entropy ← Iyer-Wald formula

The 1st law is checked up to NLO

$$\mathcal{S} = \frac{1}{4G}\int_H (1 + 2\alpha_{\mathrm{GB}}\mathcal{R})\sqrt{h}\, d^{D-2}x$$

\ scalar curvature of horizon surface

1/n-expansion up to O(1/n) $\alpha_H := \alpha/m^{\frac{1}{2n}}$

$$M = \frac{n\Omega_{2n+1}}{8\pi G}\frac{(1+\alpha_H)m}{1-\Omega^2}\Big[1 - \frac{1}{8n\,(1-\Omega^2)\,(\alpha_H+1)\,(2\alpha_H+1)}\,(4 - 8\Omega^2\alpha_H^2 + \left(-8\Omega^4 + 2(\pi-6)\Omega^2 + 8\right)\alpha_H$$
$$-2\Omega^2\log\left(2\alpha_H^2 + 2\alpha_H + 1\right) + 4\Omega^2\,(2\alpha_H+1)\,(\log(\alpha_H+1) - \arctan(2\alpha_H+1)) + \Omega^2(\pi-4))\Big]\,,$$

$$J = \frac{n\Omega_{2n+1}}{8\pi G}\frac{(1+\alpha_H)m^{\frac{2n+1}{2n}}\Omega}{1-\Omega^2}\Big[1 - \frac{1}{8n\,(1-\Omega^2)\,(\alpha_H+1)\,(2\alpha_H+1)}\,\big(8\left(2\Omega^2-1\right)\alpha_H^2 + 2\Omega^2\log\left(2\alpha_H^2 + 2\alpha_H + 1\right)$$
$$+4(1+2\alpha_H)\Omega^2(\arctan(2\alpha_H+1) - \log(\alpha_H+1)) - 2\alpha_H\left((\pi-16)\Omega^2 + 10\right) - (\pi-8)\Omega^2 - 8\big)\Big]\,,$$

$$T = \frac{n}{\pi}\frac{1+\alpha_H}{1+2\alpha_H}m^{-\frac{1}{2n}}\sqrt{1-\Omega^2}\left[1 - \frac{\left(4\Omega^2+1\right)\alpha_H + 4\alpha_H^2 + 2\Omega^2}{2n\,(1-\Omega^2)\,(\alpha_H+1)\,(2\alpha_H+1)}\right],$$

$$S = \frac{\Omega_{2n+1}}{4G}\frac{(1+2\alpha_H)m^{\frac{2n+1}{2n}}}{\sqrt{1-\Omega^2}}\Big[1 + \frac{1}{8n(1-\Omega^2)\,(\alpha_H+1)\,(2\alpha_H+1)}\,\big(8\left(1-2\Omega^2\right)\alpha_H^2 + 8\alpha_H\left(1-2\Omega^2\right)$$
$$+4(1+2\alpha_H)\Omega^2\left(\log(1+\alpha_H) - \arctan(2\alpha_H+1) + \pi/4\right) - 2\Omega^2\log\left(2\alpha_H^2 + 2\alpha_H + 1\right)\big)\Big]\,.$$

Phase diagram

Mass-Normalized Entropy and Angular momentum

$$j := \frac{8\pi GJ}{(n+1)\Omega_{2n+1}}\left(\frac{8\pi GM}{(n+1/2)\Omega_{2n+1}}\right)^{-\frac{2n+1}{2n}} \qquad s := \frac{4GS}{(n+1)\Omega_{2n+1}}\left(\frac{8\pi GM}{(n+1/2)\Omega_{2n+1}}\right)^{-\frac{2n+1}{2n}}$$

Thick：O(1)+O(1/n)

Dotted：O(1)

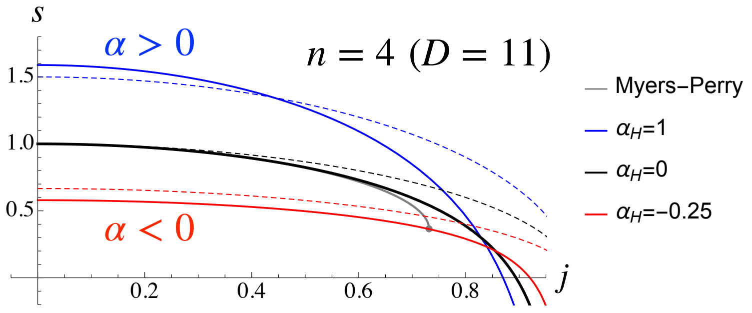

$$s = \frac{\sqrt{1-j^2}\,(2\alpha_H+1)}{\alpha_H+1}$$
$$\times\left[1 + \frac{1}{2n(1-j^2)}\left(\log\left(\frac{1-j^2}{1+\alpha_H}\right)\right.\right.$$
$$\left.\left.+\frac{\alpha_H\left(4\left(1-j^2\right)\alpha_H - 4j^2 + 3\right)}{(\alpha_H+1)\,(2\alpha_H+1)}\right)\right]$$

- 1/n expansion is bad around extremal limit
  (the same is true in GR)
- For any j, Entropy Increase for α>0
  Decrease for α<0

Summary

Summary

- The exact sols for rotating BHs in EGB theory are missing

- With an assumption (LO metric ≈ static metric with boosted frame) the metric functions are solved in Equally-rotating case in 1/D expansion
- The same assumption would apply to the singly rotating case (and more) **Large D would be a viable approach for rotating EGB BHs**

Future Work

- Dynamical analysis by Large D effective theory (Work in Progress)

$$m = \text{const}. \to m(t, \theta, \phi)$$

- More general cases (i.e. single rotation)

- Rotating BHs in Lovelock theory or more generic higher curvature theory

---

Large D Effective Theory of BS

Ex) Dynamical Black String Emparan-RS-Tanabe (2015)

$$ds^2 = -2dtdr - \left(1 - \frac{m(t,z)}{\mathsf{R}}\right)dt^2 - \frac{1}{D}\frac{2p(t,z)}{\mathsf{R}}dtdz + \frac{dz^2}{D} + \mathsf{R}^{2/D}d\Omega^2_{D-3}$$

with $\mathsf{R} = r^{D-4}$ undetermined functions :$m(t,z), p(t,z)$

Constraints eqs

→ **Simple theory of effective fields** $\{m(t,z), p(t,z)\}$

$$\begin{cases} \partial_t m(t,z) - \partial_z^2 m(t,z) = -\partial_z p(t,z) \\ \partial_t p(t,z) - \partial_z^2 p(t,z) = \partial_z\left(m(t,z) - \dfrac{p^2(t,z)}{m(t,z)}\right) \end{cases}$$

Appearance of Non-uniform BS as End point of GL@D = ∞

in a second with NDSolve on Laptop

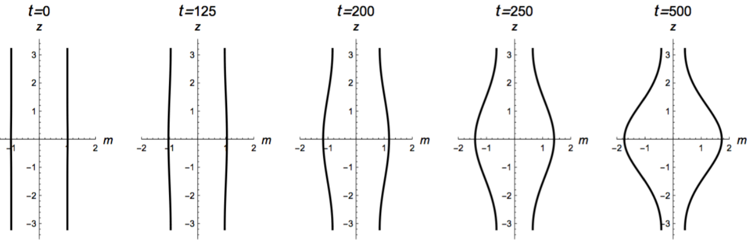

Ergo Region

Ergo radius is obtained by

$$0 = g_{tt} = (1-\Omega^2)^{-1}(-A - 2\Omega C + \Omega^2 H)$$

Using the leading order solution

$$\mathsf{R}_{\text{ergo}} = \frac{(1+\alpha)m}{(1-\Omega^2)(1+\alpha(1-\Omega^2))} + \mathcal{O}(n^{-1})$$

- Ergo region exists for any α
- Size of ergo region monotonically increases with α
  Reach a limit at α→∞

$$\mathsf{R}_{\text{ergo}}\Big|_{\alpha=0} = \frac{m}{1-\Omega^2} \Longrightarrow \mathsf{R}_{\text{ergo}}\Big|_{\alpha=\infty} = \frac{m}{(1-\Omega^2)^2}$$

Higher order equations

$$X := \sqrt{1 + \frac{4m\alpha(\alpha+1)}{\mathsf{R}}}$$

$$\partial_X\left(\frac{X}{X^2-1}A_i\right) = \mathrm{Src}_A^{(i)} \qquad \partial_X^2 C_i = \mathrm{Src}_C^{(i)}$$

$$\partial_X\left[(1+X^{-2})(1+2\alpha-X)\partial_X H_i\right] = \mathrm{Src}_H^{(i)}$$

$$\partial_X\left[U_i - \frac{X^2-1}{4X}\partial_X H_i\right] = \mathrm{src}_U^{(i)}$$

$$A_{i>0}(\mathsf{R}=m) = 0, \quad C_{i>0}(\mathsf{R}=m)$$

C67

Geometric-optics correspondence of deformed black holes

Che-Yu Chen

Institute of Physics, Academia Sinica, Taiwan

- **CYC,** Hsu-Wen Chiang (LeCosPA, NTU), Jie-Shiun Tsao (NTNU)
- *Phys. Rev. D* 106 (2022) 4, 044068

THE 13TH RESCEU INTERNATIONAL SYMPOSIUM

JGRG31

Geometric-Optics (Eikonal) Approximations

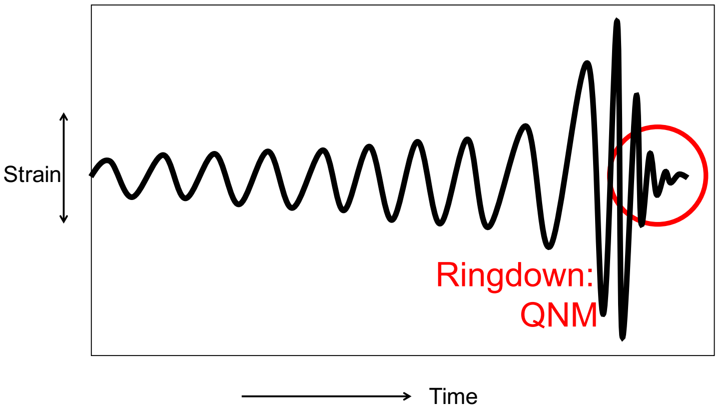

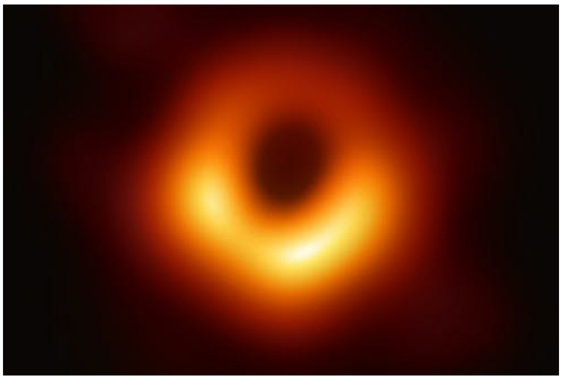

Field propagation in BH spacetimes

$\nabla^{\alpha}\nabla_{\alpha}A = \cdots$

Photon propagation in BH spacetimes

$k^{\alpha}k_{\alpha} = 0$

Geometric-Optics (Eikonal) Approximations

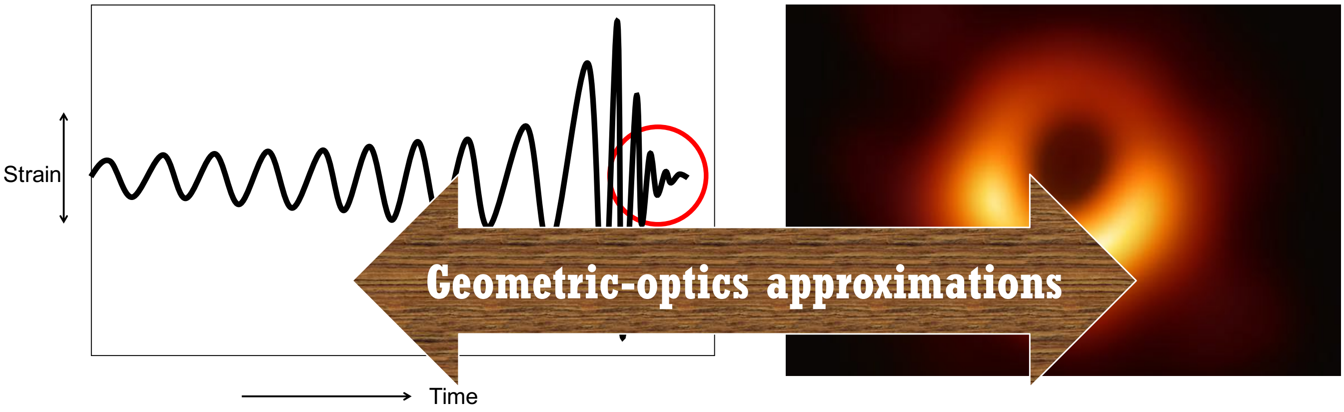

Geometric-optics approximations

Field propagation in BH spacetimes

$$\nabla^{\alpha}\nabla_{\alpha}A = \boldsymbol{O(\lambda/L)\sim 0}$$

Photon propagation in BH spacetimes

$$k^{\alpha}k_{\alpha} = 0$$

How does the correspondence manifest in BH spacetimes?

- <u>Spacetime symmetry is crucial</u>
- Non-rotating BH:

  Static and spherically symmetric

$$\left(\frac{d^2}{dr_*^2}+\omega^2\right)\Psi = V_g\Psi$$

- The peak of the QNM potential in the eikonal limit (high frequency limit, or $l \to \infty$) coincides with the photon sphere (PS)

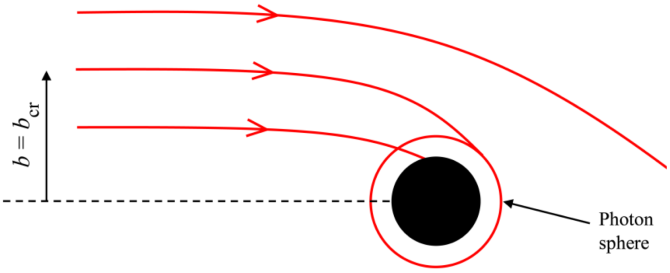

approach PS when $l \to \infty$

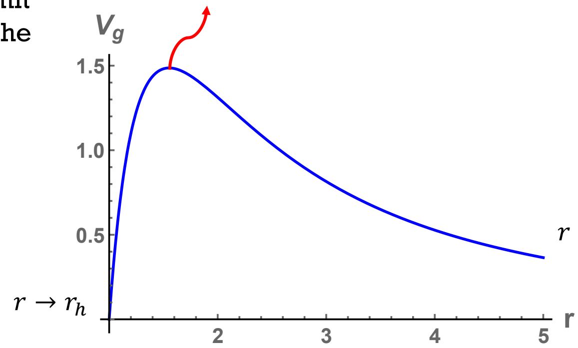

Correspondence in Kerr Spacetime

- Separable geodesic equations (Carter constant), and separable wave equations

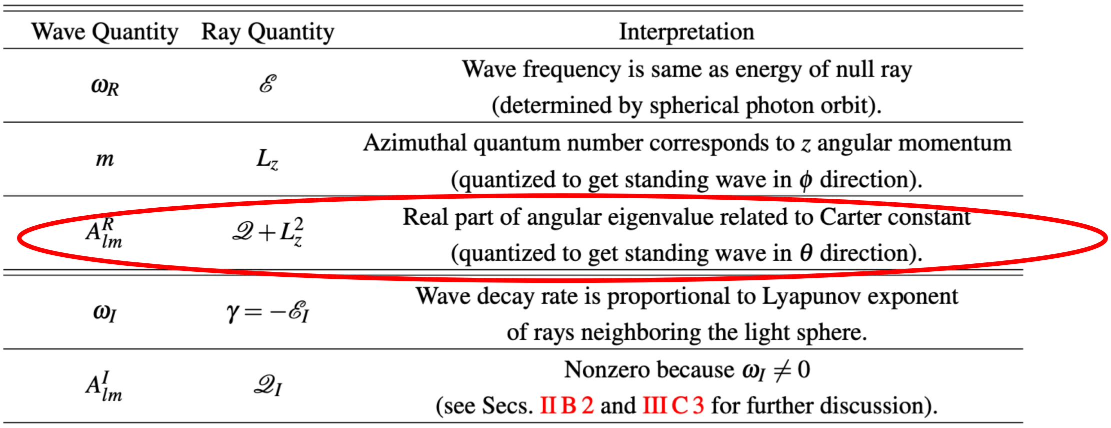

Wave Quantity	Ray Quantity	Interpretation
ω_R	$\mathscr{E}$	Wave frequency is same as energy of null ray (determined by spherical photon orbit).
m	L_z	Azimuthal quantum number corresponds to z angular momentum (quantized to get standing wave in ϕ direction).
A^R_{lm}	$\mathscr{Q}+L_z^2$	Real part of angular eigenvalue related to Carter constant (quantized to get standing wave in θ direction).
ω_I	$\gamma=-\mathscr{E}_I$	Wave decay rate is proportional to Lyapunov exponent of rays neighboring the light sphere.
A^I_{lm}	$\mathscr{Q}_I$	Nonzero because $\omega_I \neq 0$ (see Secs. II B 2 and III C 3 for further discussion).

Yang *et al.* (2012)

Recently extended to Kerr-Newman by Li *et al.* (2021)

Eikonal QNMs and BH Shadows

ω_R ↔ Angular frequency on PS ↔ Size of shadow image

ω_I ↔ Lyapunov exponent on PS ↔ Higher-order ring structures

Jusufi (2020), Cuadros-Melgar *et al.* (2020)

Jusufi (2020), Yang (2021)

- What if the black hole spacetime has less symmetry?

Deformed Schwarzschild Spacetime

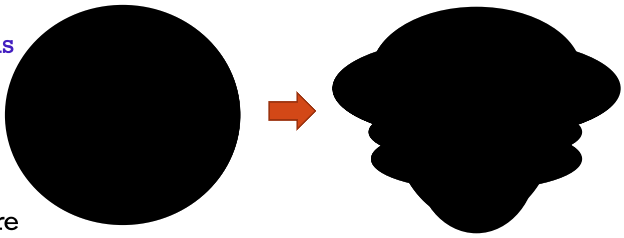

- Consider small but general axisymmetric deformations of Schwarzschild BHs

In the presence of deformations:

- Radial and latitudinal sectors of geodesic equations are NOT separable
- Generic photon orbits $r(\theta)$ do NOT have constant r
- Inseparable QNM equations if deformations are not small
  - Can be made separable if deformations are small

Cano, Fransen, Hertog (2020)

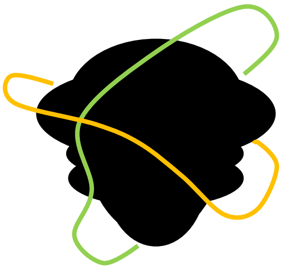

$$\boxed{(\partial_{r_*}^2 + \omega^2)\Psi_{lm} = V_{\text{eff}}(r,l,m)\Psi_{lm}} \qquad \boxed{V_{\text{eff}}(r,l,m) = V_{Sch} + \delta V}$$

Two Kinds of Photon Orbits

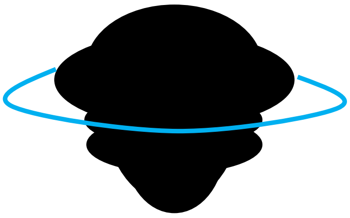

- Planar circular photon orbits with a constant radius:
  - The peak of $V_{\text{eff}}(r)$ is precisely on these orbits

$(|m| = l \gg 1)$

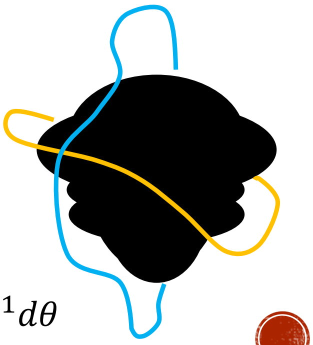

- Generic photon orbits do not have constant r
- These photon orbits should
  - be periodic
  - form a class of limit cycles
- We can integrate the orbits along full periods $\oint d\lambda = \oint \dot{\theta}^{-1} d\theta$

Generic Orbits

$$\left\langle \frac{d}{d\lambda}\left(g_{rr}\dot{r}\right)\right\rangle = \langle \partial_r F(r^*,\theta)(r - r^*)\rangle$$

definition of limit cycle

$$= 0$$

- The peak of $V_{\text{eff}}(r)$ coincides with the root of this integrated equation

($|m| < l$ and $l \gg 1$)

Generic Orbits

$$\left\langle \frac{d}{d\lambda}\left(g_{rr}\dot{r}\right)\right\rangle = \langle \partial_r F(r^*,\theta)(r - r^*)\rangle$$

definition of limit cycle

$$= \partial_r F_0(r_P)\boxed{\langle r - r^*\rangle} + o(\epsilon)$$

Lyapunov exponent is $O(1)$

averaged radius along one period

$$= 0$$

- The peak of $V_{\text{eff}}(r)$ coincides with the averaged radius of these orbits along one period

Conclusions

- Geometric-optics approximation adopted in BH spacetime
  - Correspondence between eikonal QNMs and photon orbits
- Schwarzschild and Kerr: Using their symmetries
- What if the black hole spacetime has less symmetry?
- Identify eikonal correspondence through the definition of averaged radius along full closed photon orbits
- Future:
  - Non-axisymmetric deformations
  - Deformed Kerr
  - Observational implications

Deformed Schwarzschild Spacetime

$$g_{tt} = -\left(1 - \frac{2M}{r}\right)\left(1 + \epsilon A_j(r)\cos^j\theta\right) ,$$

$$g_{rr} = \left(1 - \frac{2M}{r}\right)^{-1}\left(1 + \epsilon B_j(r)\cos^j\theta\right) ,$$

$$g_{\theta\theta} = r^2\left(1 + \epsilon C_j(r)\cos^j\theta\right) ,$$

$$g_{\varphi\varphi} = r^2\sin^2\theta\left(1 + \epsilon D_j(r)\cos^j\theta\right) ,$$

$$g_{tr} = \epsilon a_j(r)\cos^j\theta\,, \qquad g_{t\theta} = \epsilon b_j(r)\cos^j\theta\,,$$

$$g_{r\theta} = \epsilon c_j(r)\cos^j\theta \qquad g_{r\varphi} = \epsilon d_j(r)\cos^j\theta\,,$$

$$g_{\theta\varphi} = \epsilon e_j(r)\cos^j\theta\,.$$

- A general axisymmetric deformation which excludes frame-dragging effects

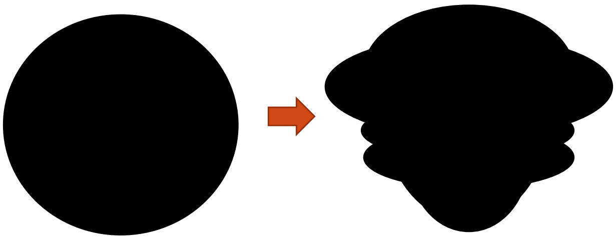

- Small deformation: $|\epsilon| \ll 1$

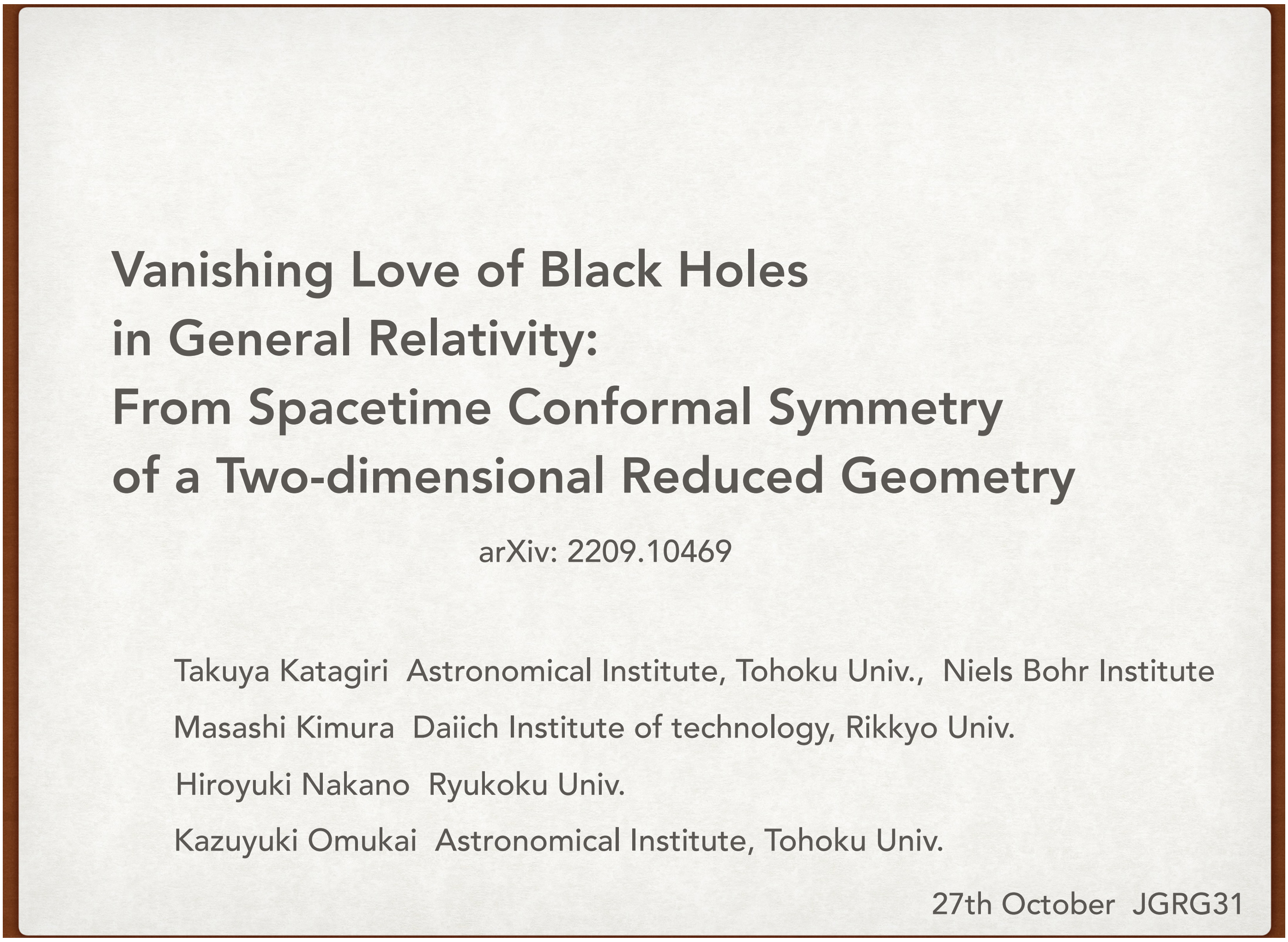

Vanishing Love of Black Holes in General Relativity: From Spacetime Conformal Symmetry of a Two-dimensional Reduced Geometry

arXiv: 2209.10469

Takuya Katagiri Astronomical Institute, Tohoku Univ., Niels Bohr Institute
Masashi Kimura Daiich Institute of technology, Rikkyo Univ.
Hiroyuki Nakano Ryukoku Univ.
Kazuyuki Omukai Astronomical Institute, Tohoku Univ.

27th October JGRG31

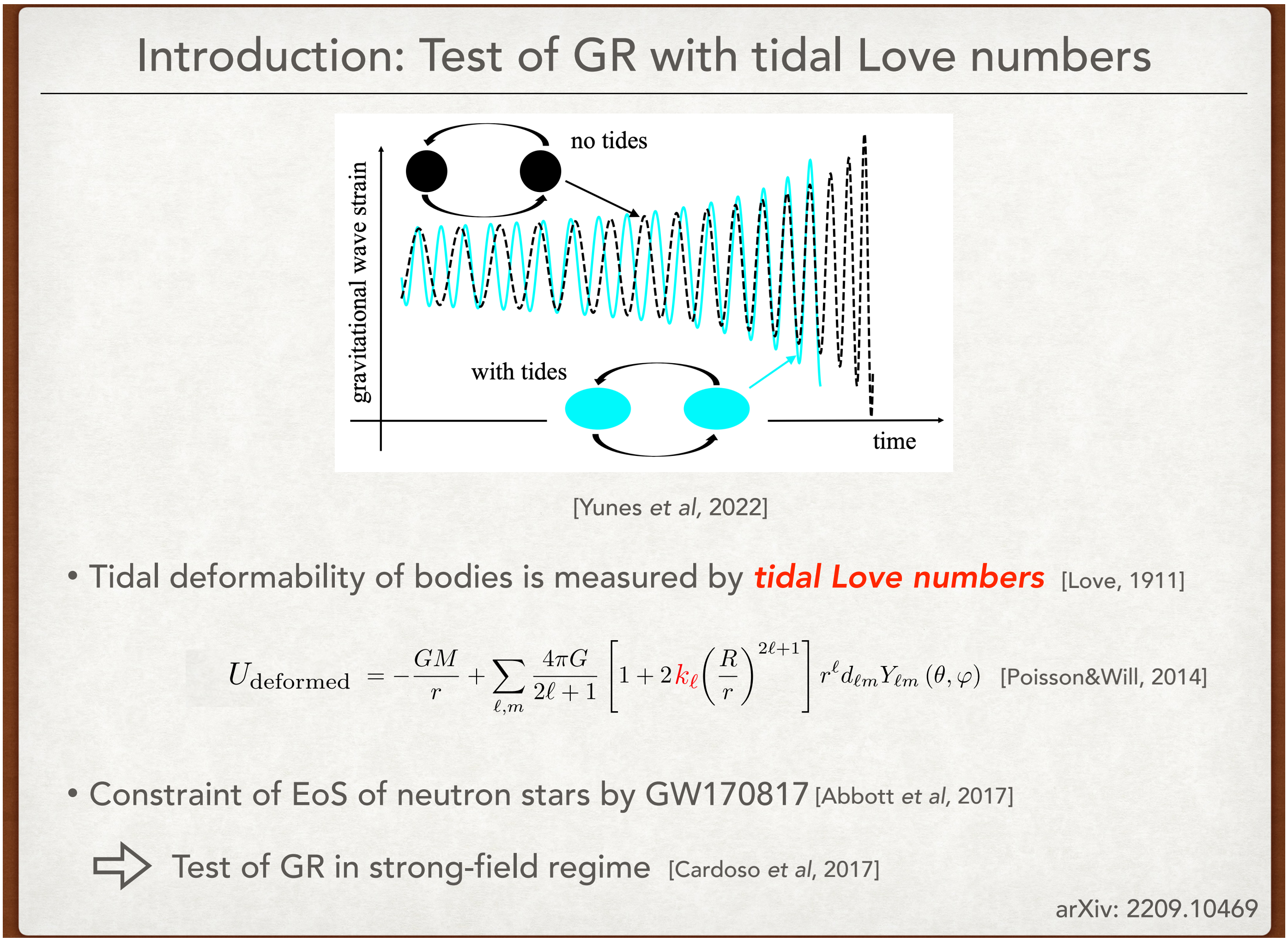

Introduction: Test of GR with tidal Love numbers

[Yunes *et al*, 2022]

- Tidal deformability of bodies is measured by ***tidal Love numbers*** [Love, 1911]

$$U_{\text{deformed}} = -\frac{GM}{r} + \sum_{\ell,m} \frac{4\pi G}{2\ell+1} \left[1 + 2 k_\ell \left(\frac{R}{r} \right)^{2\ell+1} \right] r^\ell d_{\ell m} Y_{\ell m} \left(\theta, \varphi \right)$$ [Poisson&Will, 2014]

- Constraint of EoS of neutron stars by GW170817 [Abbott *et al*, 2017]

⇨ Test of GR in strong-field regime [Cardoso *et al*, 2017]

arXiv: 2209.10469

Vanishing of tidal Love numbers of Schwarzschild BHs

- Situation:

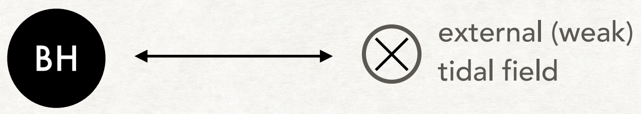

- Linear perturbation to Schwarzschild BHs in the static limit:

[Regge&Wheeler, 1957]

$$\frac{\Delta}{z^2}\frac{d}{dz}\left(\frac{\Delta}{z^2}\frac{d\Phi_\ell}{dz}\right) - \frac{\Delta}{z^2}\left[\frac{\ell(\ell+1)}{z^2} - \frac{3}{z^3}\right]\Phi_\ell = 0\,, \quad \Delta := z(z-1)\,, \quad z = \frac{r}{r_H}$$

- (Relativistic) ***tidal Love numbers*** are defined by: [Binnington&Poisson, 2009]

$$\boxed{\Phi_\ell|_{z\gg1} \sim z^{\ell+1}\left(1+2k_\ell z^{-2\ell-1}\right)}$$ under regularity at horizon

- Schwarzschild BH in 4 dim has **zero Love numbers** [Binnington&Poisson, 2009]

✻ This is also the case of enen-parity perturbation

arXiv: 2209.10469

Beyond GR or non-vacuum or higher dimensions

Some nontrivial underlying structure may prohibit acquiring Love numbers

- Schwarzschild BH in 4 dim has **zero** Love numbers for spin-s fields [Hui *et al*, 2021]

- Their vanishing is also the case for Kerr BHs [Tiec *et al*, 2021; Chia, 2021; Charalanbous *et al*, 2021]

- BHs in some modified theories of gravity, BHs in GR with matter fields, and higher-dim Schwarzschild BHs can have **nonzero** Love numbers

[Kol&Smolkin, 2012; Cardoso *et al*, 2020]

- Is **Love numbers = 0** a unique feature of BHs in vacuum in 4 dim GR?

⇨ No ! [Cardoso *et al*, 2017] [Cardoso *et al*, 2020]
Schwarzschild BH in Brans-Dicke, Riessner-Nordstrom BH also have **zero**

arXiv: 2209.10469

Previous works and our work

- Previous works argued

``hidden” symmetric structure is important

[Porto, 2016; Penna, 2018; Charalambou *et al*, 2021;
Hui *et al*, 2022; Achour *et al*, 2022; Charalambou *et al*, 2022]

- Our question

Why does such a hidden symmetric structure exist? Geometrical origin?

We study the **underlying symmetric structure** of Love numbers = 0
in terms of spacetime symmetry
in a unified manner for scalar $(s=0)$, vector $(s=1)$, and tidal fields $(s=2)$

arXiv: 2209.10469

Reduction to AdS2

- Regge-Wheeler eq. for spin-s fields in static limit:

$$\frac{\Delta}{z^2}\frac{d}{dz}\left(\frac{\Delta}{z^2}\frac{d\Phi_\ell}{dz}\right)-\frac{\Delta}{z^2}\left[\frac{\ell(\ell+1)}{z^2}-\frac{s^2-1}{z^3}\right]\Phi_\ell=0.$$

$$\big\downarrow$$

Field redefinition: $\phi_\ell(z)=\dfrac{\Phi_\ell}{z}$

$$\frac{d}{dz}\left(\Delta\frac{d\phi_\ell}{dz}\right)-\left(\ell(\ell+1)-\frac{s^2}{z}\right)\phi_\ell=0,$$

- This can be identified as an equation for static scalar fields in AdS2

2-dim spacetime
with negative constant curvature: $ds^2=-\Delta dt^2+\dfrac{1}{\Delta}dz^2\,,\quad \Delta:=z(z-1)\,,\quad R^{(2)}=-2$

$$\boxed{\left[\Box_{\mathrm{AdS}_2}-\left(\ell(\ell+1)-\frac{s^2}{z}\right)\right]\phi_\ell=0}$$ [Castro, *et al*, 2010]

✻Low-frequency perturbation can also be reduced

arXiv: 2209.10469

Generator of hidden symmetries: Ladder operators

- Ladder operators: $\mathcal{D}_{k_\pm} = \underline{z(z-1)\partial_z} - \frac{k_\pm}{2}\underline{\left(2z-1-\frac{s^2}{k_\pm^2}\right)}, \quad k_+ = -\ell - 1, \quad k_- = \ell$

🟥 : Closed conformal Killing vector field of AdS2, $\mathcal{L}_\zeta g_{ab}^{(\mathrm{AdS}_2)} = (\nabla_c \zeta^c)\, g_{ab}^{(\mathrm{AdS}_2)}$

with $\nabla_a \zeta_b = \nabla_b \zeta_a$

🟪 $:= \int dz\; g_{zz}^{(\mathrm{AdS}_2)} \zeta^z$

- Ladder operator shifts ℓ into $\ell \to \ell \pm 1$

$$\begin{tikzcd}
 & \left[\Box_{\mathrm{AdS}_2} - \left(\boxed{(\ell-1)\ell} - \frac{s^2}{z}\right)\right] \mathcal{D}_{k_-}\phi_\ell = 0 \\
\left[\Box_{\mathrm{AdS}_2} - \left(\ell(\ell+1) - \frac{s^2}{z}\right)\right] \phi_\ell = 0 \arrow[ur] \arrow[dr] & \\
 & \left[\Box_{\mathrm{AdS}_2} - \left(\boxed{(\ell+1)(\ell+2)} - \frac{s^2}{z}\right)\right] \mathcal{D}_{k_+}\phi_\ell = 0
\end{tikzcd}$$

arXiv: 2209.10469

Supersymmetric structure

- Let us consider a pair $(\phi_\ell, \phi_{\ell\pm1})$:

EoM: $\mathcal{H}_\ell \phi_\ell = 0, \quad \mathcal{H}_{\ell\pm1}\phi_{\ell\pm1} = 0$ where

$$\mathcal{H}_\ell := -\Delta \frac{d}{dz}\left(\Delta \frac{d}{dz}\right) + \Delta\left[\ell(\ell+1) - \frac{s^2}{z}\right]$$

$$\mathcal{H}_{\ell\pm1} := -\Delta \frac{d}{dz}\left(\Delta \frac{d}{dz}\right) + \Delta\left[(\ell\pm1)(\ell\pm1+1) - \frac{s^2}{z}\right]$$

- Hamiltonians can be ``factorized": $\boxed{\mathcal{H}_\ell = \mathcal{D}_{-k_\pm}\mathcal{D}_{k_\pm} + \beta_{k_\pm}^2, \quad \mathcal{H}_{\ell\pm1} = \mathcal{D}_{k_\pm}\mathcal{D}_{-k_\pm} + \beta_{k_\pm}^2}$

$k_+ = -\ell - 1, \quad k_- = \ell \qquad \beta_{k_\pm} = \frac{k_\pm^2 - s^2}{2k_\pm}$

$$\Rightarrow \quad \begin{aligned} \mathcal{D}_{k_\pm}\mathcal{H}_\ell\phi_\ell &= \mathcal{D}_{k_\pm}\left(\mathcal{D}_{-k_\pm}\mathcal{D}_{k_\pm} + \beta_{k_\pm}^2\right)\phi_\ell = \mathcal{H}_{\ell\pm1}\mathcal{D}_{k_\pm}\phi_\ell = 0, \\ \mathcal{D}_{-k_\pm}\mathcal{H}_{\ell\pm1}\phi_{\ell\pm1} &= \mathcal{D}_{-k_\pm}\left(\mathcal{D}_{k_\pm}\mathcal{D}_{-k_\pm} + \beta_{k_\pm}^2\right)\phi_{\ell\pm1} = \mathcal{H}_\ell\mathcal{D}_{-k_\pm}\phi_{\ell\pm1} = 0. \end{aligned}$$

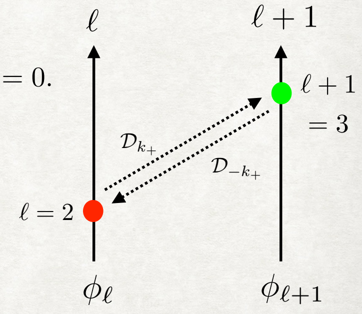

ϕ_ℓ and $\phi_{\ell\pm1}$ are **symmetric partners**

Inductively, all the modes are symmetric partners

arXiv: 2209.10469

Supersymmetry Algebra

- Hidden symmetric structure can be understood from **supersymmetry algebra**

$$[\mathcal{H}, \mathcal{Q}] = [\mathcal{H}, \bar{\mathcal{Q}}] = O, \quad \{\mathcal{Q}, \bar{\mathcal{Q}}\} = \mathcal{H}, \quad \{\mathcal{Q}, \mathcal{Q}\} = \{\bar{\mathcal{Q}}, \bar{\mathcal{Q}}\} = O,$$

where $\mathcal{H} = \begin{pmatrix} \mathcal{H}_\ell - \beta_{k_\pm}^2 & 0 \\ 0 & \mathcal{H}_{\ell\pm1} - \beta_{k_\pm}^2 \end{pmatrix}, \quad \mathcal{Q} = \begin{pmatrix} 0 & 0 \\ \mathcal{D}_{k_\pm} & 0 \end{pmatrix}, \quad \bar{\mathcal{Q}} = \begin{pmatrix} 0 & \mathcal{D}_{-k_\pm} \\ 0 & 0 \end{pmatrix},$

Spin-s field perturbation to Schwarzschild BH has supersymmetric structure

- odd-parity / even-parity are also supersymmetric [Chandrasekar, 1975]

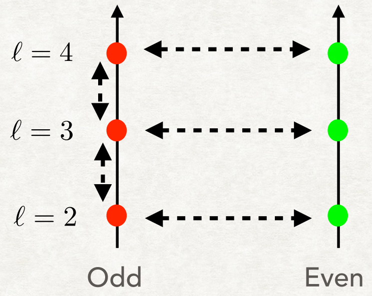

Linearized GR around Schwarzschild BHs has supersymmetric structure

arXiv: 2209.10469

Love numbers = 0 from radially conserved quantities

- Radially conserved quantities exist: $\mathcal{W}_\ell := (\mathcal{D}_{-k_\pm}\phi_{\ell\pm1})\left(\Delta\frac{d\phi_\ell}{dz}\right) - \left(\Delta\frac{d\mathcal{D}_{-k_\pm}\phi_{\ell\pm1}}{dz}\right)\phi_\ell.$
- For a pair of lowest multipole and originally ``unphysical” mode, (ϕ_s, ϕ_{s-1})

$$\frac{d}{dz}\mathcal{W}_s = 0 \quad \longrightarrow \quad \frac{d}{dz}\underbrace{[z^s\mathcal{D}_s\phi_s]}_{=:\,Y_s} = 0$$

Asymptotic sols.: $\phi_s|_{z\to1} \sim \text{const.}, \quad \ln(1-1/z)$

$\phi_s|_{z\gg1} \sim z^s, \quad z^{-s-1}$

$Y_s = 0$ for $\phi_s|_{z\to1} \sim \text{const.}$, $\phi_s|_{z\gg1} \sim z^s$ $\quad$ $Y_s \neq 0$ for $\phi_s|_{z\to1} \sim \ln(1-1/z)$, $\phi_s|_{z\gg1} \sim z^{-s-1}$

⇨ Horizon-regular sol. is purely growing at large distances, showing Love number = 0

[Cooper *et al*, 1994]

$\ast$ $Y_s = 0$ is similar to unbroken supersymmetry in SUSY quantum mechanics

Love numbers = 0 from radially conserved quantities

- Higher multipole can be mapped into the lowest one with ladder operators

Radially conserved quantity: $Y_\ell := z^s \mathcal{D}_s \tilde{\phi}_s$, where $\tilde{\phi}_s = \mathcal{D}_{s+1} \cdots \mathcal{D}_{\ell-1} \mathcal{D}_\ell \phi_\ell$

Asymptotic sols.: $$\phi_\ell|_{z\to 1} \sim \text{const.}, \quad \ln(1-1/z)$$ $$\phi_\ell|_{z\gg 1} \sim z^\ell, \quad z^{-\ell-1}$$

Y_ℓ implies that $\tilde{\phi}_s|_{z\to 1} \sim \text{const.}$ is $\tilde{\phi}_s|_{z\gg 1} \sim z^s$
because $\tilde{\phi}_s$ is the lowest multipole

Ladder operator $\mathcal{D}_{k\_}$ keeps the asymptotic feature:
the horizon-regular sol. is mapped into that and
the growing sol. at large distances is mapped into that.

⇨ Horizon-regular sol. of ϕ_ℓ is purely growing at large distances;

therefore, all the Love numbers = 0

Kerr BH case

- Static Teukolsky eq. can be reduced to static scalar fields in AdS2:

[Teukolsky, 1972]

$$\Delta^{-s}\frac{d}{dz}\left(\Delta^{s+1}\frac{d}{dz}\Phi^{(s)}_{\ell m}(z)\right) + \left(\frac{m^2\chi^2 + im\chi s(2z-1)}{\Delta} - \ell(\ell+1) + s(s+1)\right)\Phi^{(s)}_{\ell m}(z) = 0,$$

$$\Big\downarrow \qquad \Delta = z(z-1), \quad z = \frac{r-r_-}{r_+ - r_-}\,, \quad \chi \in [0,1) \qquad \boxed{\phi^{(s)}_{\ell m}(z) := \Delta^{s/2}\Phi^{(s)}_{\ell m},}$$

$$\left[\Box_{\mathrm{AdS}_2} - \left(\ell(\ell+1) - \frac{4m^2\chi^2 - s^2}{4\Delta} + im\chi s\frac{1-2z}{\Delta}\right)\right]\phi^{(s)}_{\ell m} = 0,$$

- Ladder operators and supersymmetric structure exist:

$$\mathcal{D}_{k_\pm} = \Delta\frac{d}{dz} - \frac{k_\pm}{2}\left(2z - 1 - i\frac{2m\chi s}{k_\pm^2}\right), \quad k_+ = -\ell-1, \quad k_- = \ell,$$

- Radially conserved quantities allow one to show Love numbers = 0

  without solving the perturbation equations

arXiv: 2209.10469

Summary

arXiv: 2209.10469

- First attempt to explain Love numbers = 0 from symmetric structure arising from spacetime symmetry in a unified manner for spin-s fields
- Perturbation field can be reduced into a set of infinite scalar fields in AdS2
- Linearized GR around 4-dim BHs in vacuum has supersymmetric structure arising from conformal symmetry of the effective AdS2 geometry
- Radially conserved quantity allows one to show Love numbers = 0 without solving the perturbation equations

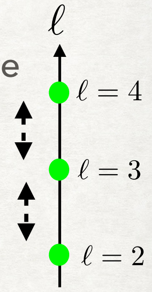

Comment

- Our ladder operator includes generators of hidden symmetry in previous works
- Time-dependent field with low frequencies also has supersymmetric structure
- Supersymmetric structure explains the result of higher-dim Schwarzschild BH

Ladder operator and generic potential

- Consider generic scalar fields in AdS2: $\boxed{\left[\Box_{\mathrm{AdS}_2} - \left(k(k+1) + P(z)\right)\right] \Psi_k(t,z) = 0.}$
- Requiring commutation relation:

$$\boxed{\left[\Box_{\mathrm{AdS}_2} - P, \mathcal{D}\right] = -2k\mathcal{D} + 2Q\left[\Box_{\mathrm{AdS}_2} - \left(k(k+1) + P\right)\right],}$$

$$\longrightarrow \left[\Box_{\mathrm{AdS}_2} - \left((k-1)\,k + P\right)\right] \mathcal{D}\Psi_k = \left(\mathcal{D} + 2Q\right)\left[\Box_{\mathrm{AdS}_2} - \left(k(k+1) + P\right)\right]\Psi_k.$$

- Assuming $\mathcal{D}$ is a 1st order derivative operator: $\mathcal{D} = V^a \nabla_a + \mathcal{K}$

$$\nabla_a V_b = \left(\nabla_c V^c\right) g_{ab}^{(\mathrm{AdS}_2)}$$ (Closed conformal Killing eq. in AdS2)

$$\Rightarrow \quad \nabla^a \mathcal{K} = -k V^a,$$

$$\Box_{\mathrm{AdS}_2}\mathcal{K} + V^a \nabla_a P = -2k\mathcal{K} - \left(\nabla_a V^a\right)\left[k(k+1) + P\right]$$

- $\mathcal{D}$ and $P(z)$ compatible with the above conditions are:

$$\boxed{\mathcal{D} = z(z-1)\partial_z - k\left(z - c_0\right), \quad P = \frac{k\left(1 - 2c_0\right) z + c_p}{z(z-1)},}$$

Schwarzschild-Tangherlini case

- Supersymmetric structure explains the result of the Schwarzschild BH in n dims

  Static scalar fields with $\ell \propto n-3$ have zero Love numbers [Hui *et al*, 2021]

- Problem can be reduced into a set of infinite scalar fields in AdS2:

$$\boxed{\left[\Box_{\mathrm{AdS}_2} - \hat{\ell}(\hat{\ell}+1)\right]\Phi_{\hat{\ell}} = 0\,,\ \hat{\ell} = \frac{\ell}{n-3}}$$

- Ladder operators exist but shift $\hat{\ell}$ into $\hat{\ell} \pm 1$

  ⇨ ϕ_ℓ with $\ell \propto n-3$ connects to the lowest multipole

- In the same manner as $n=4$,

  the radially conserved quantities exist, allowing to show
  Love numbers = 0 for $\ell \propto n-3$

C69

Quasi-periodic oscillations of a particle in the background of a deformed compact object

Audrey Trova & Shokoufe Faraji [1]

[1] University of Bremen, Center of Applied Space Technology and Microgravity (ZARM), 28359 Bremen, Germany

JGRG 31, The University of Tokyo, Japan

High Frequency QPOs and General Relativity

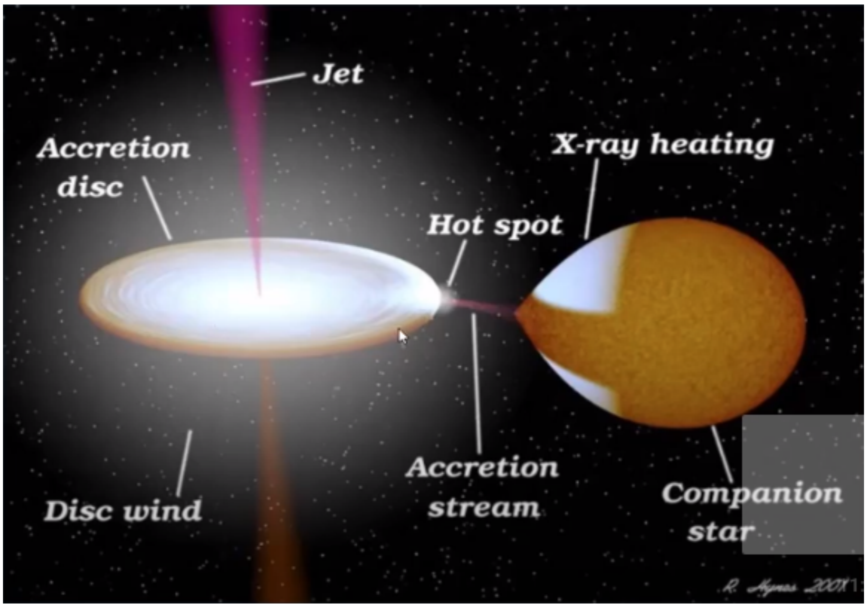

High Frequency QPOs and General Relativity

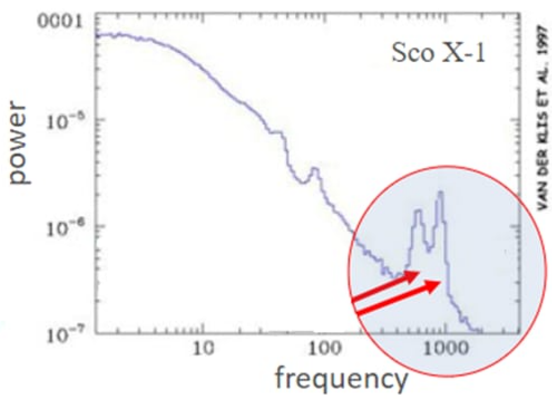

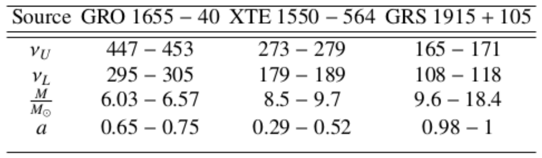

Source	GRO 1655 − 40	XTE 1550 − 564	GRS 1915 + 105
ν_U	447 − 453	273 − 279	165 − 171
ν_L	295 − 305	179 − 189	108 − 118
$\frac{M}{M_\odot}$	6.03 − 6.57	8.5 − 9.7	9.6 − 18.4
a	0.65 − 0.75	0.29 − 0.52	0.98 − 1

TABLE II. Observed HF QPO data for the three micro-quasars, independent of the HF QPO measurement, and based on the spectral continuum fitting.

QPOs in BH divided in various classes. QPOs in BH XRBs are normally divided into two large groups:

- the low frequency QPOs $\sim$ 50 Hz
- the high-frequency QPOs, above $\sim$ 100Hz up to $\sim$ 500Hz.

Model to explain HFQPOs

Large variety of ideas to explain the phenomenon of HF QPOs: Main idea is that it is related to the motion of the inner part of accretion disk

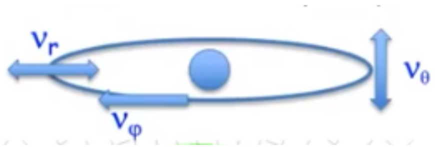

Local oscillations analysis
→ RP Model (Stella)
→ TD Model (Cadez)
→ WD Model (Kato)

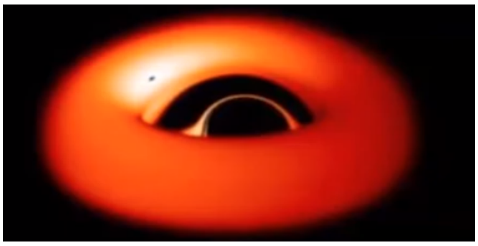

Global oscillations analysis
→ ER Model (Abramowicz & Kluzniak)
→ p-modes, c-modes,.. (Rezzolla, Kato ...)

Background metric : q-Metric
A static, axially symmetric metric that is non-spherically symmetric

$$ds^2 = -\left(\frac{x-1}{x+1}\right)^{(1+\alpha)} dt^2 + M^2(x^2-1)\left(\frac{x+1}{x-1}\right)^{(1+\alpha)} \left[\left(\frac{x^2-1}{x^2-y^2}\right)^{\alpha(2+\alpha)}\left(\frac{dx^2}{x^2-1}+\frac{dy^2}{1-y^2}\right)+(1-y^2)d\phi^2\right]. \quad (1)$$

- describes the exterior gravitational field of a static deformed compact object
- α positive for a oblate compact object and negative for an prolate one

Class of orbits that slightly deviate from the circular geodesics

$$\omega_x^2 = \partial_x U^x - \gamma^x_{\ \eta}\gamma^\eta_{\ x} = A_x\Omega^2, \quad (2)$$

$$\omega_y^2 = \partial_y U^y = A_y\Omega^2. \quad (3)$$

$$A_x = \frac{(1-1/x^2)^{-\alpha(2+\alpha)}}{(x^2-1)}\left[2(2S-x)(S-x)-\frac{(x^2-1)}{S}(1+\alpha)\right]$$

$$A_y = \frac{(1-1/x^2)^{-\alpha(2+\alpha)}}{S}(1+\alpha)$$

Schwarzschild case:

$$\omega_y^2 = \frac{1}{(x+1)^3},$$

$$\omega_x^2 = \frac{1}{(x+1)^3}\left(1-\frac{6}{x+1}\right)$$

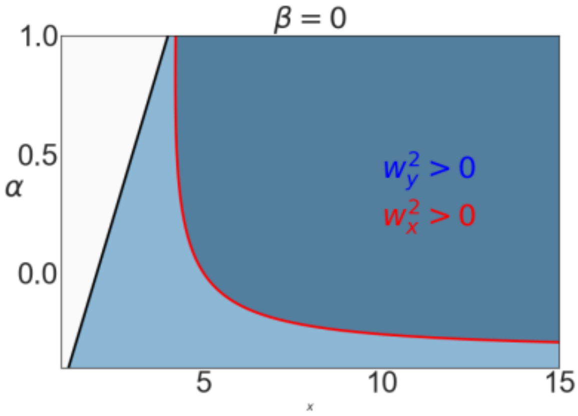

Class of orbits that slightly deviate from the circular geodesics: In a uniform magnetic field

$$\frac{d^2\xi^\mu}{dt^2} + 2\gamma^\mu_\eta \frac{d\xi^\eta}{dt} + \xi^\eta \partial_\eta U^\mu = F^\mu,$$

$$\begin{aligned} w_y^2 &= \left(\frac{x^2-1}{x^2}\right)^{-\alpha(2+\alpha)} \left[\Omega^2 \frac{x f_1(x) + S}{S} + (1 + f_1(x))\Omega\omega_{\rm B}\right], \\ w_x^2 &= \frac{\Omega^2(1-1/x^2)^{-\alpha(2+\alpha)}}{x(1-x^2)} \left[g_1(x,\alpha)\frac{x-S}{S} + g_2(x,\alpha)\right] \\ &+ \frac{(1-1/x^2)^{-\alpha(2+\alpha)}}{x(1-x^2)} \left[-\omega_B^2 x(S-x)^2 + \Omega\omega_{\rm B} g_2(x,\alpha)\right], \end{aligned} \qquad (4)$$

Epicyclic frequencies in the background of a deformed compact object

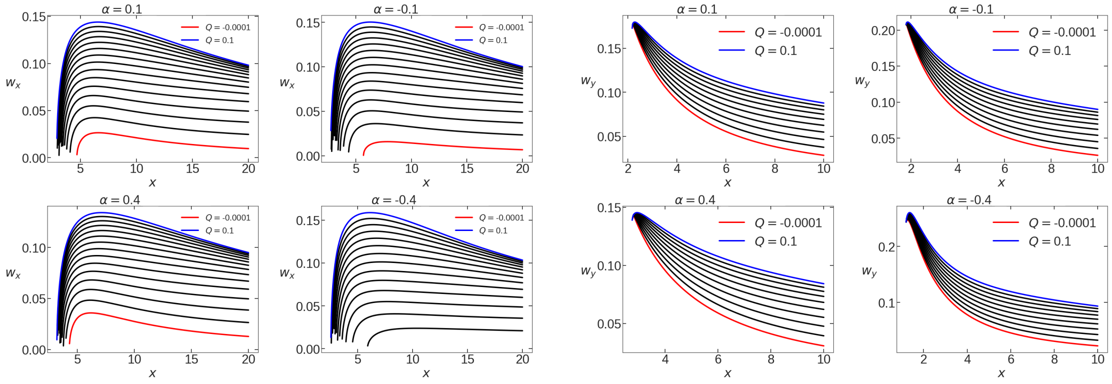

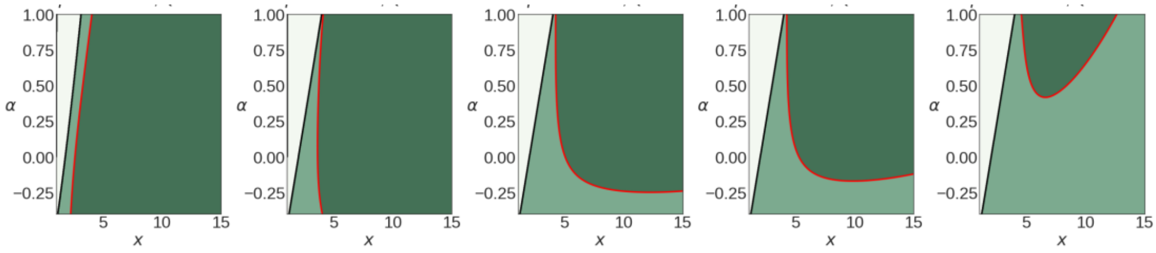

Epicyclic resonances: 3:2 frequency ratio

Effect of the quadrupole moment

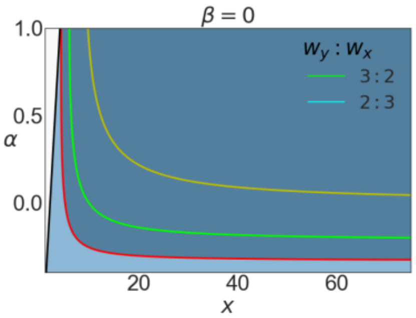

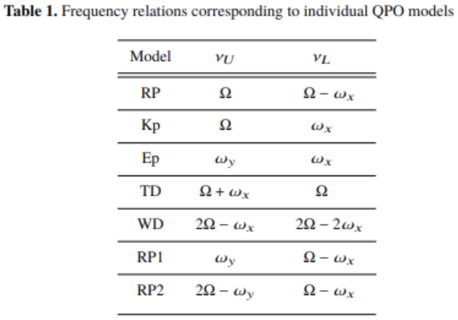
Table 1. Frequency relations corresponding to individual QPO models

Model	ν_U	ν_L
RP	Ω	$\Omega - \omega_x$
Kp	Ω	ω_x
Ep	ω_y	ω_x
TD	$\Omega + \omega_x$	Ω
WD	$2\Omega - \omega_x$	$2\Omega - 2\omega_x$
RP1	ω_y	$\Omega - \omega_x$
RP2	$2\Omega - \omega_y$	$\Omega - \omega_x$

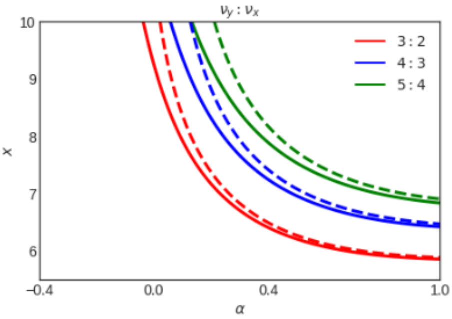

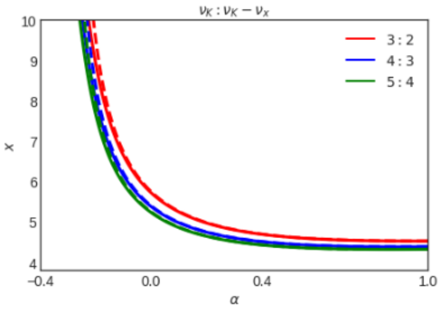

Epicyclic resonances: 3:2 frequency ratio

Effect of the magnetic field

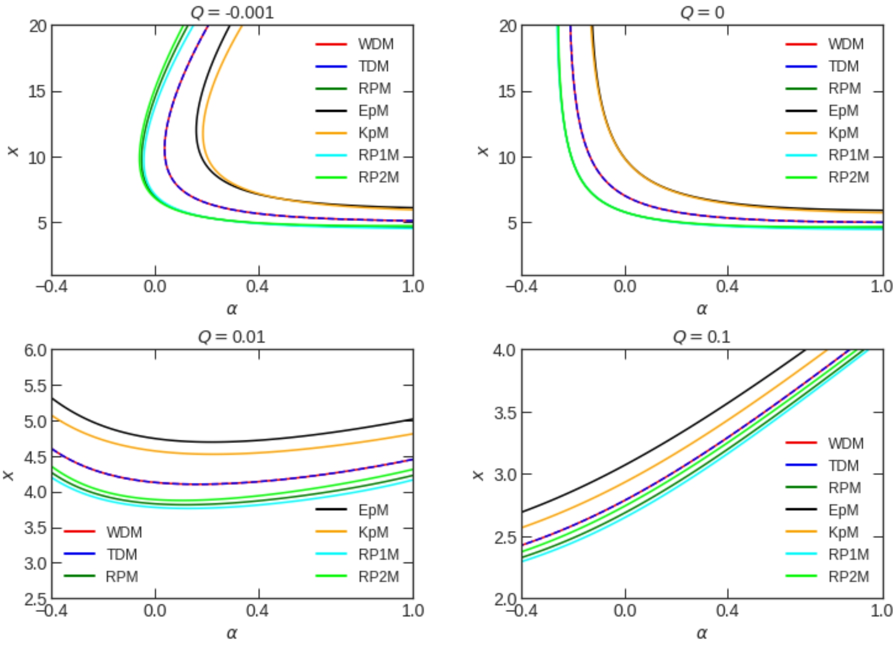

Data Fitting with Galactic Microquasars: 1/M relation

Effect of the quadrupole moment

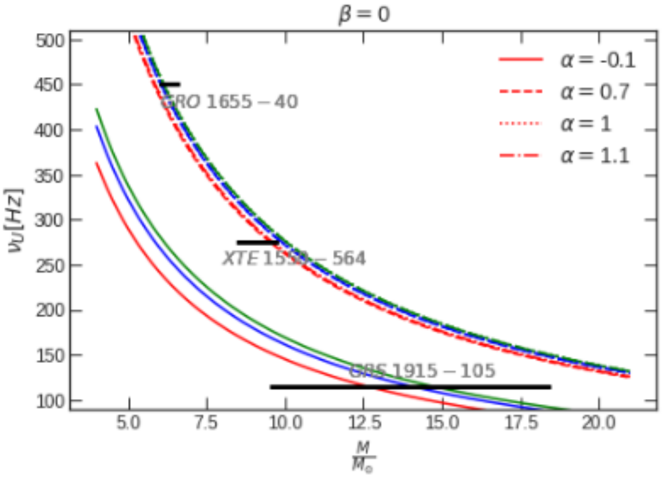

$$\nu_{Up} = \frac{1}{2\pi}\frac{c^3}{GM}\Omega_{Up}$$

Table 1. Frequency relations corresponding to individual QPO models

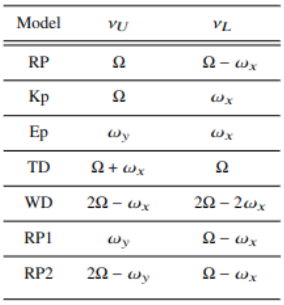

Model	ν_U	ν_L
RP	Ω	$\Omega - \omega_x$
Kp	Ω	ω_x
Ep	ω_y	ω_x
TD	$\Omega + \omega_x$	Ω
WD	$2\Omega - \omega_x$	$2\Omega - 2\omega_x$
RP1	ω_y	$\Omega - \omega_x$
RP2	$2\Omega - \omega_y$	$\Omega - \omega_x$

Data Fitting with Galactic Microquasars: 1/M relation

Effect of the magnetic field

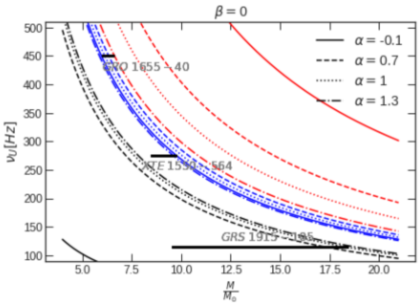

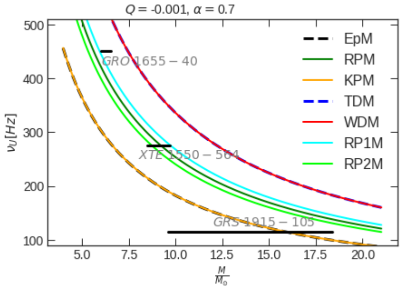

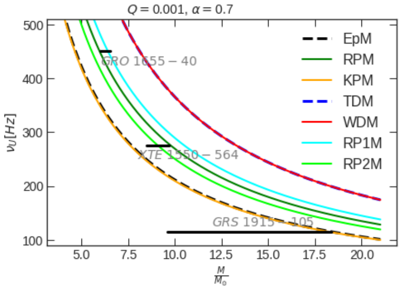

Table 1. Frequency relations corresponding to individual QPO models

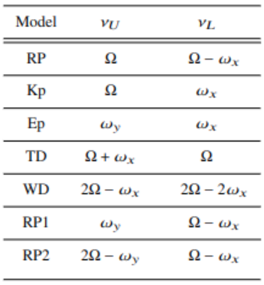

Model	ν_U	ν_L
RP	Ω	$\Omega - \omega_x$
Kp	Ω	ω_x
Ep	ω_y	ω_x
TD	$\Omega + \omega_x$	Ω
WD	$2\Omega - \omega_x$	$2\Omega - 2\omega_x$
RP1	ω_y	$\Omega - \omega_x$
RP2	$2\Omega - \omega_y$	$\Omega - \omega_x$

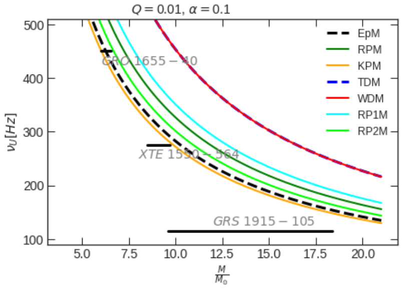

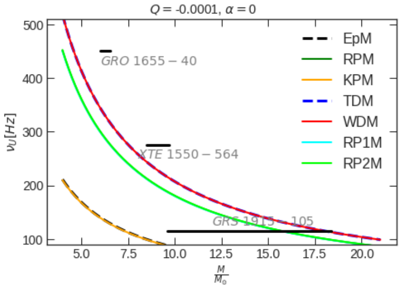

Conclusion

- The quadrupole moment and magnetic field alter the motion and epicyclic frequencies of charged particles moving in this background.
- cause strong deviation from the corresponding quantities in the Schwarzschild case
- the resonant phenomena of the radial and vertical oscillations at their frequency ratio 3:2 for different parameters can be adequately related to the frequencies of the twin 3:2 HF QPOs observed in the microquasars

Future work ? Question ?

- extend this work from a single particle to a complex system, such as accretion discs
- Global oscillations analysis

Class of orbits that slightly deviate from the circular geodesics

$$\frac{d^2x^{\mu}}{ds^2}+\Gamma^{\mu}_{\nu\rho}\frac{dx^{\nu}}{ds}\frac{dx^{\rho}}{ds}=0. \tag{6}$$

$x'^{\mu}=x^{\mu}+\xi^{\mu}$ and consider terms up to linear order in ξ^{μ}

$$\frac{d^2\xi^{\mu}}{dt^2}+2\gamma^{\mu}{}_{\eta}\frac{d\xi^{\eta}}{dt}+\xi^{\eta}\partial_{\eta}U^{\mu}=0,$$

$$\gamma^{\mu}{}_{\eta}=\left[2\Gamma^{\mu}{}_{\eta\delta}u^{\delta}(u^0)^{-1}\right]_{y=0},$$

$$U^{\mu}=\left[\gamma^{\mu}_{\eta}u^{\eta}(u^0)^{-1}\right]_{y=0}.$$

$$\frac{d\xi^{\eta}}{dt}+\gamma^{\eta}{}_{\nu}\xi^{\nu}=0, \tag{7}$$

$$\frac{d^2\xi^{x}}{dt^2}+\omega_x^2\xi^{x}=0, \tag{8}$$

$$\frac{d^2\xi^{y}}{dt^2}+\omega_x^2\xi^{y}=0, \tag{9}$$

where in the first equation η can be taken t, or ϕ; and

C71

Creating stars orbiting in AdS

Nihon University
Keiju Murata
with Youka Kaku, Jun Tsujimura

arXiv:2202.07807 [hep-th]

Steller motion around Sgr A*

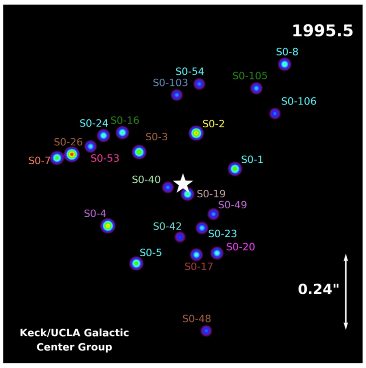

Keck/UCLA Galactic Center Group
https://www.astro.ucla.edu/~ghezgroup/gc/animations.html

Steller motion in
BH spacetime

⬇

- ●Existence of BH
- ●Information of BH geometry

Timelike geodesic in AdS/CFT

Can we create a star (timelike geodesic) orbiting around BH using AdS/CFT?

If it is possible,
can we observe the created star?

Extraction of information about BH geometry from QFT.

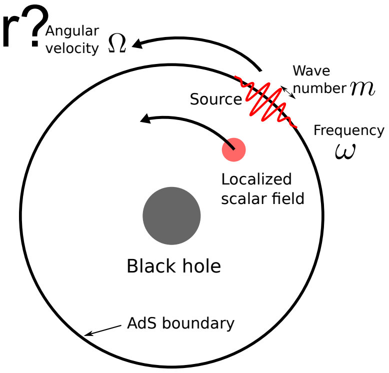

Setup: Massive scalar field in Sch-AdS4

$$ds^2 = -f(r)dt^2 + \frac{dr^2}{f(r)} + r^2\left(d\theta^2 + \sin^2\theta\, d\phi^2\right),$$

$$f(r) = 1 + r^2 - r_h(1 + r_h^2)/r$$

AdS radius=1

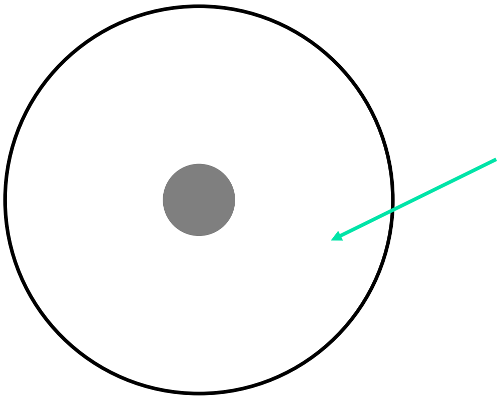

Probe scalar field

$$\Box\Phi = \mu^2\Phi$$

Source and response

Near AdS boundary $r \to \infty$

$$\Phi(t,r,\theta,\phi) \simeq \mathcal{J}(t,\theta,\phi)\, r^{-\Delta_-} + \langle \mathcal{O}(t,\theta,\phi)\rangle\, r^{-\Delta_+} \,,$$

non-normalizable
(boundary condition)

normalizable

$$\Delta_\pm = 3/2 \pm \nu \qquad \nu = \sqrt{9/4+\mu^2}.$$

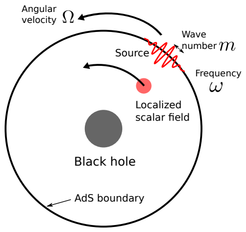

$\mathcal{J}$:Source (External field)
$\langle\mathcal{O}\rangle$:Its response

How should we apply the external field to create a star (particle-like configuration of scalar) in the bulk? (inverse problem)

Creation of radially localized scalar field

$$\Box\Phi = \mu^2\Phi$$

$$\Phi = r^{-1}\sum_{l'm'} \Psi_{l'm'}(t,x) Y_{l'm'}(\theta,\phi)$$

$$[\partial_t^2 - \partial_x^2 + V(x)]\Psi_{l'm'}(t,x) = 0$$

$$x = \int \frac{dr}{f(r)} \qquad V(x) = f(r)\left(\frac{l'(l'+1)}{r^2} + \mu^2 + \frac{1}{r}\frac{df}{dr}\right),$$

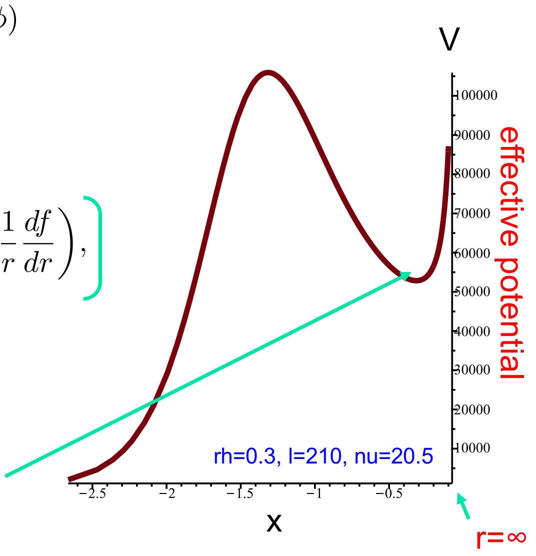

We create the localized scalar field here.
(Stable circular orbit)

Localized QNM

Quasi normal mode (fundamental tone)

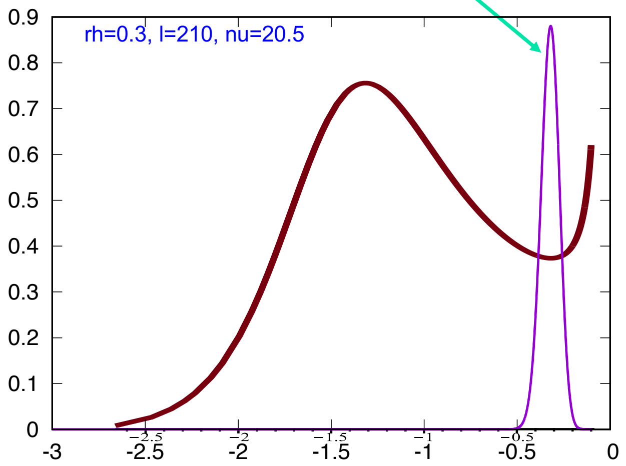

$$\mathrm{Re}\,\omega_{\mathrm{qnm}} \simeq 231$$

$$|\mathrm{Im}\,\omega_{\mathrm{qnm}}| < 10^{-16}$$

Almost normal mode

We create this QNM by choosing boundary condition of $\Psi_{lm}(t,x)$.

Toy example

How should we shake the endpoint of the string to realize the fundamental tone?

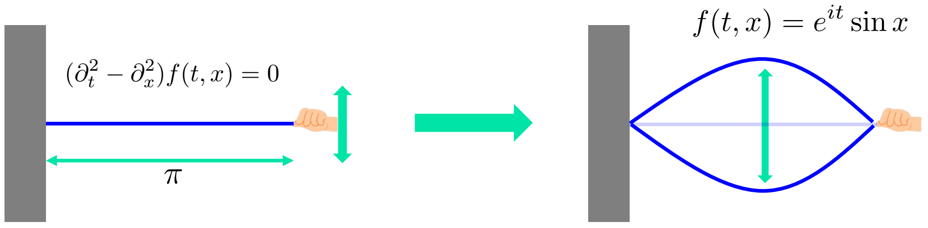

Eigenfrequency $\omega = 1, 2, 3, \cdots$

$$f(t, x=\pi) = \exp\left[-\frac{(t-T)^2}{2\sigma_t^2} - it \right]$$

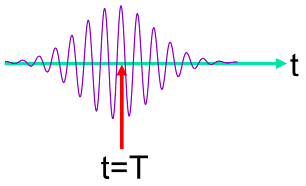

Localized QNM

$$r^{\Delta_- -1}\Psi_{l'm'}(t,x)|_{x=0} = \exp\left[-\frac{(t-T)^2}{2\sigma_t^2} - i\omega_{\rm qnm}t\right]$$

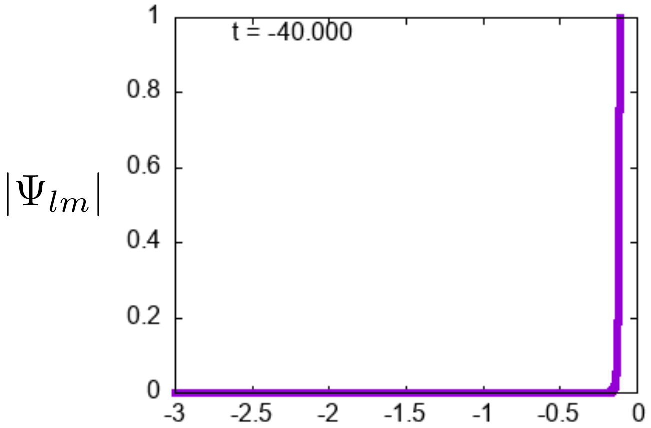

Creation of the radially localized solution for each (l’,m’).

Superposing (l’,m’)-modes

$$\Psi(t,x,\theta,\phi) = \sum_{l'm'} c_{l'm'}\Psi_{l'm'}(t,x)Y_{l'm'}(\theta,\phi)$$

For an appropriate $c_{l'm'}$

the solution can also be localized angular directions.

Creation of star in Sch-AdS (rh=0.3)

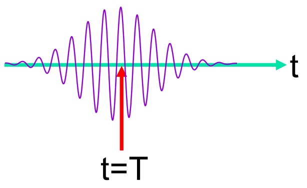

t=-40.00

rh=0.3, m=210, nu=20.5

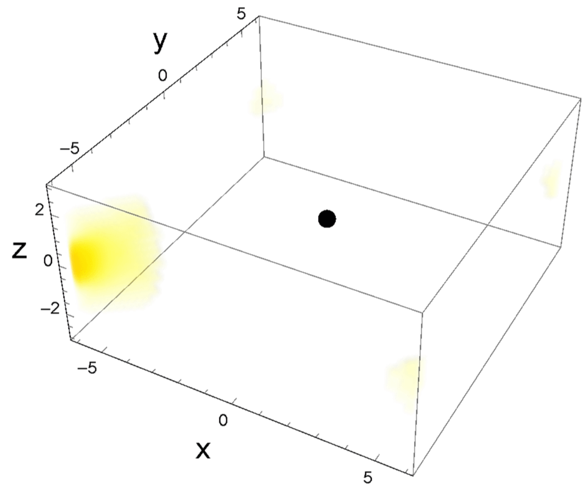

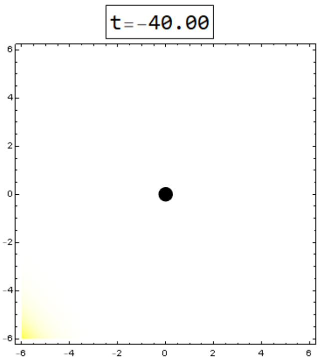

Equatorial plane

Linear response

$$\Phi(t,r,\theta,\phi) \simeq \mathcal{J}(t,\theta,\phi)\, r^{-\Delta_-} + \langle \mathcal{O}(t,\theta,\phi)\rangle\, r^{-\Delta_+} \ ,$$

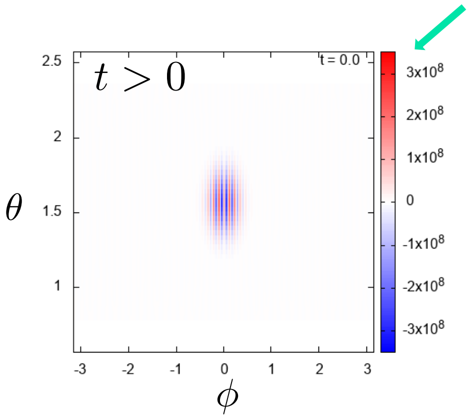

We can see the star from the response function.

Summary

We can create stars orbiting around BH in AdS bulk by applying appropriate source in QFT.

We can observe the created star from the response function.

⬇

We can read out the information about the geometry in the AdS bulk.

Appendix

rh=1

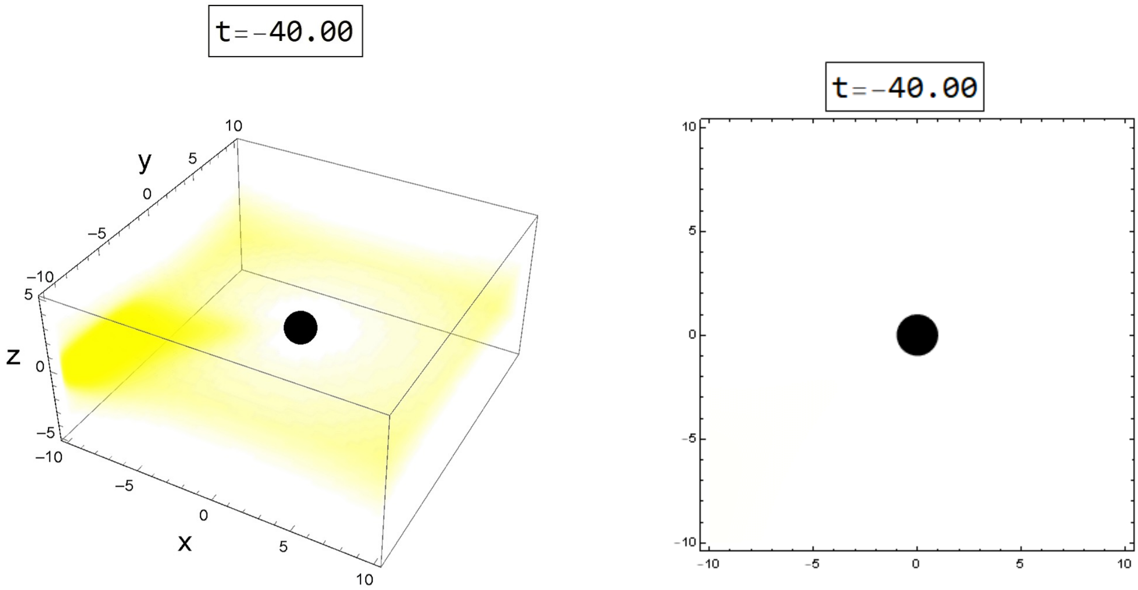
t=-40.00
y
x
z
10
5
0
-5
-10
t=-40.00
10
5
0
-5
-10

Pure AdS

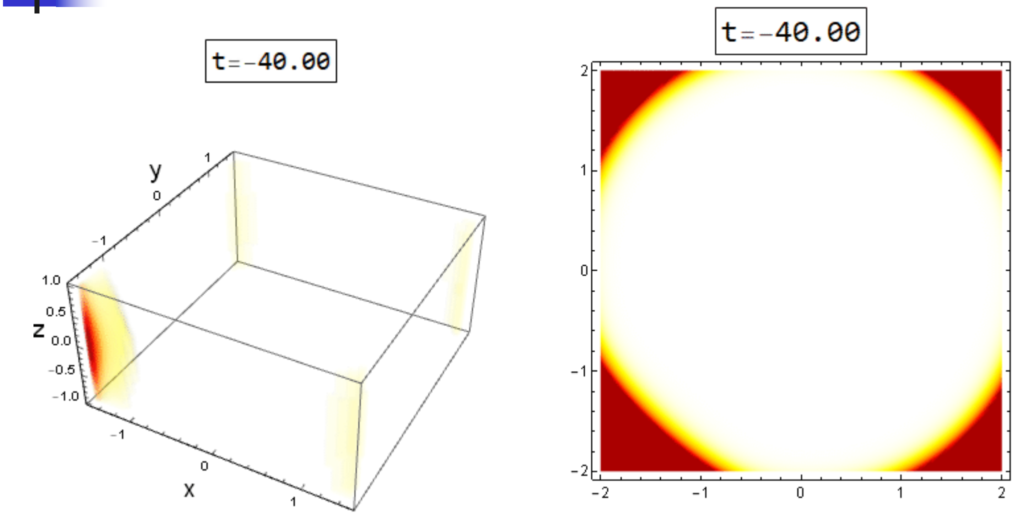
t=-40.00
y
x
z
1
0
-1
1.0
0.5
0.0
-0.5
-1.0
t=-40.00
2
1
0
-1
-2

Parameters of created star

Our source is

$$\mathcal{J}(t,\theta,\phi) = J_0 \exp\left[-\frac{(t-T)^2}{2\sigma_t^2} - \frac{(\theta-\pi/2)^2}{2\sigma_\theta^2} - \frac{(\phi-\Omega t)^2}{2\sigma_\phi^2} - i\omega t + im\phi \right]$$

Specific energy $\epsilon = \dfrac{\omega}{\mu}$

Specific angular mom $j = \dfrac{m}{\mu}$

Angular velocity Ω

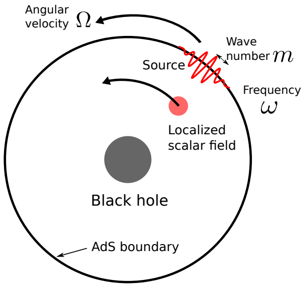

Implication to gauge/gravity

これは、任意のエネルギー・角運動量・公転角速度を持つ星を作れると言っているわけではない。

円軌道の測地線は、1-parameter ファミリー,
つまり、軌道半径を決めると、
エネルギー・角運動量・公転角速度がすべて決まるからである。

$$\epsilon^2 = \frac{2(R-r_h)^2(R^2+r_hR+r_h^2+1)^2}{R\{2R-3r_h(1+r_h^2))\}} ,$$

$$j^2 = \frac{R^2(2R^3+r_h^3+r_h)}{2R-3r_h(1+r_h^2)} , \quad \Omega^2 = \frac{2R^3+r_h^3+r_h}{2R^3} .$$

$$\epsilon \longrightarrow \begin{cases} j = j(\epsilon) \\ \Omega = \Omega(\epsilon) \end{cases}$$

計量が分からなくても、実際に実験で星が作れれば
円軌道する粒子のエネルギー・角運動量・公転角速度
の関係がわかる。 → 計量の情報

Future prospect

場の理論の外場をうまく選べば、重力系を操作出来る。
何を作れば面白いだろうか？

●null測地線

外場を与えてから,その応答が現れるまでに時間差があるはず。

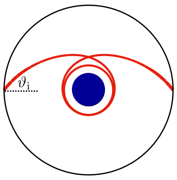

●非円軌道

“楕円”軌道・ブラックホールへ落下する軌道など。
角運動量=0の軌道 → BHがあるかないかの判定

Future prospect

●D-brane

D3-D7解は重力解として存在する。
pure AdSに外場をかけて、D3/D7系を作れるか？ Kirscha&Vaman, 05

SYMに外場をかけるとQCDになる?

●宇宙論

膨張宇宙をAdS内部に作れるか？

●天文学?

$\mu^2 > 0$ のスカラー場に外場を入れるときの注意

$$\Phi(t,r,\theta,\phi) \simeq \mathcal{J}(t,\theta,\phi)\, r^{-\Delta_-} + \langle \mathcal{O}(t,\theta,\phi)\rangle\, r^{-\Delta_+} \ ,$$

J≠0だと、Φ→∞. ➡ EM tensor→∞.

➡ Backreactionが無視できない。

r=Λでcutoffを入れてその内側のダイナミクスを考える。

カットオフの外側では、理論が変更されて、
うまく正則化されてると考える。

$$\mathcal{L}' = -(\partial\Phi)^2 - \lambda(\psi)^2\Phi^2 - (\partial\psi)^2 + 2\psi^2$$

$$\lambda(\psi) = \mu \tanh(\psi)$$

AdS/CFT対応

Maldacena, 97

➡ “現実的”な系への応用?
AdS/QCD, AdS/CMP

Condensed
matter physics

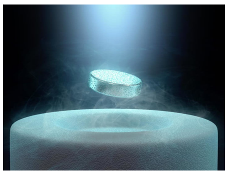

⟷

AdS black hole

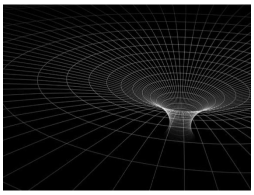

Hartnoll, Herzog & Horowitz, 08

本当に、ブラックホール描像を持つ
物質が存在するのか?

"ブラックホールらしさ"もしくは"重力らしさ"を見出したい。

本当に、重力双対を持つ物質があったら?

⬇

その物質を使って重力特有の現象を観測できるはず。

重力特有な現象？

重力レンズ効果?

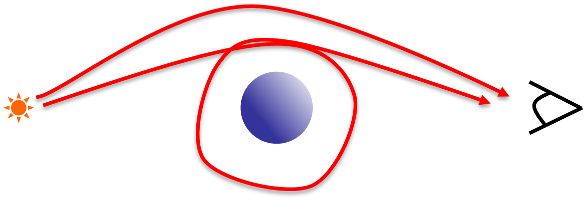

重力は光を曲げる。 ➡ 重力レンズ

ブラックホール存在の状況証拠のひとつ。

Taken from Astrophys. J. Lett. 875:L1

重力レンズ in AdS/CFT

K.Hashimoto, S. Kinoshita, KM, 18,
K.Hashimoto, S. Kinoshita, KM, 19,
Y.Kaku, KM, J.Tsujimura, 21

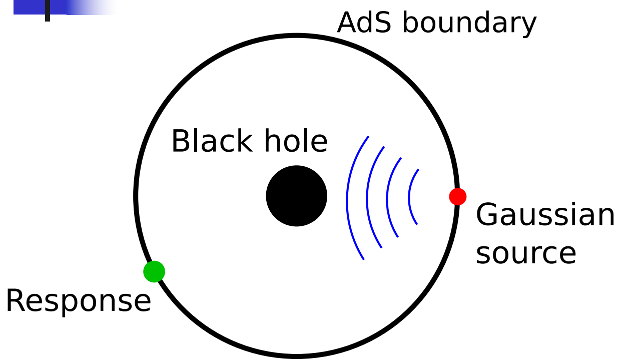

$$\Phi(t,r,\theta,\phi) \simeq \mathcal{J}(t,\theta,\phi)\, r^{-\Delta_-} + \langle \mathcal{O}(t,\theta,\phi)\rangle\, r^{-\Delta_+} \ ,$$

AdS black holeの像

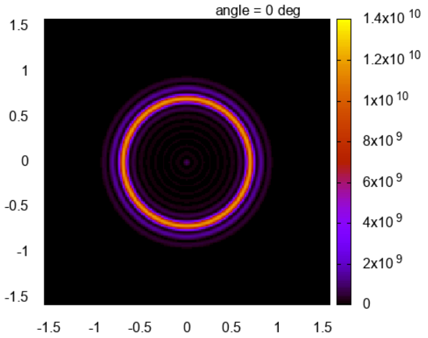

AdS時空中の“光”を使って、
AdS black holeの姿を見ることが出来る。

➡ 時間的測地線も考えられる?

場で測地線を表せるか?

$\Box\Phi = \mu^2\Phi$ を短波長近似で考えよう。

↳ $\Phi = a(x)\exp(iS(x))$ 位相が早く振動するとする。

➡ $-a(\nabla S)^2 + \cancel{2i\nabla a\cdot\nabla S + \Box a} = \mu^2 a$

[$S(x) \sim -\omega t + im\phi$ ➡ $\partial_\mu S \sim \omega, m \gg 1$]

➡ $\boxed{\partial_\mu S\partial^\mu S = -\mu^2}$

Klein-Gordon → 測地線

4元速度　$u_\mu \equiv \partial_\mu S/\mu$　とおけば

$\partial_\mu S \partial^\mu S = -\mu^2$ ⇒ $$u_\mu u^\mu = -1$$

$\partial_\mu S \partial^\mu S = -\mu^2$ を微分

⇒
$$
\begin{aligned}
0 &= \nabla_\nu(\partial_\mu S \partial^\mu S) = 2\partial^\mu S \nabla_\nu(\partial_\mu S) \\
&= 2\partial^\mu S \nabla_\mu(\partial_\nu S) = 2u^\mu \nabla_\mu u_\nu
\end{aligned}
$$

短波長近似では、Klein-Gordon方程式から、
測地線方程式が得られる。

測地線と場のパラメータの対応関係

$\Phi = a(x)\exp(iS(x))$

測地線のエネルギーと角運動量は

$E = -mu_\mu(\partial_t)^\mu$　　$L = mu_\mu(\partial_\phi)^\mu$

で与えられることを思い出すと、

単位質量あたりのエネルギー：　$\epsilon = -u_t$

単位質量あたりの角運動量：　$j = u_\phi$

一方，$u_\mu \equiv \partial_\mu S/\mu$　だったので，

$$\boxed{\epsilon = -\frac{1}{\mu}\partial_t S \ , \quad j = \frac{1}{\mu}\partial_\phi S \ .}$$

C72

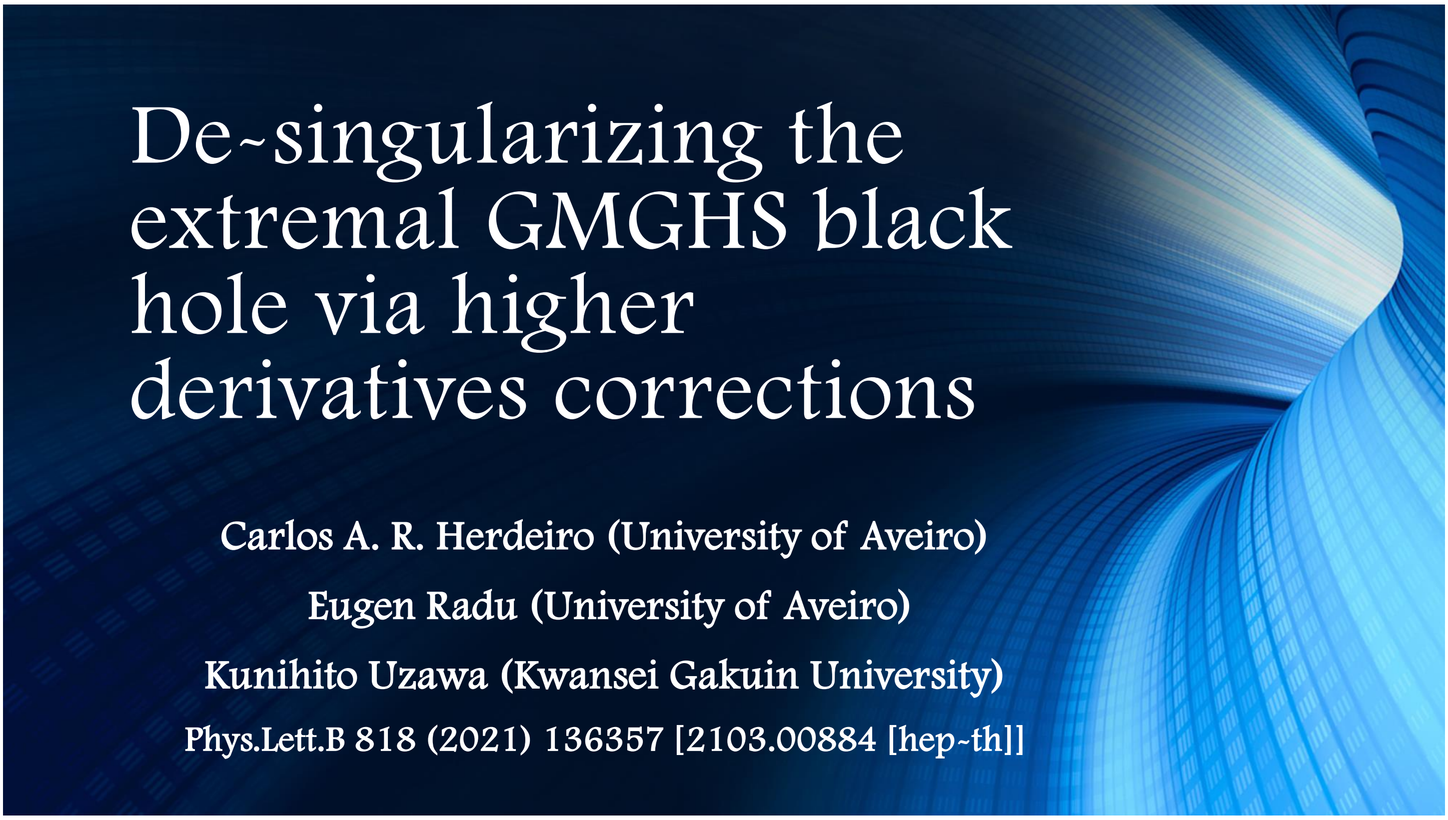

De-singularizing the extremal GMGHS black hole via higher derivatives corrections

Carlos A. R. Herdeiro (University of Aveiro)
Eugen Radu (University of Aveiro)
Kunihito Uzawa (Kwansei Gakuin University)

Phys.Lett.B 818 (2021) 136357 [2103.00884 [hep-th]]

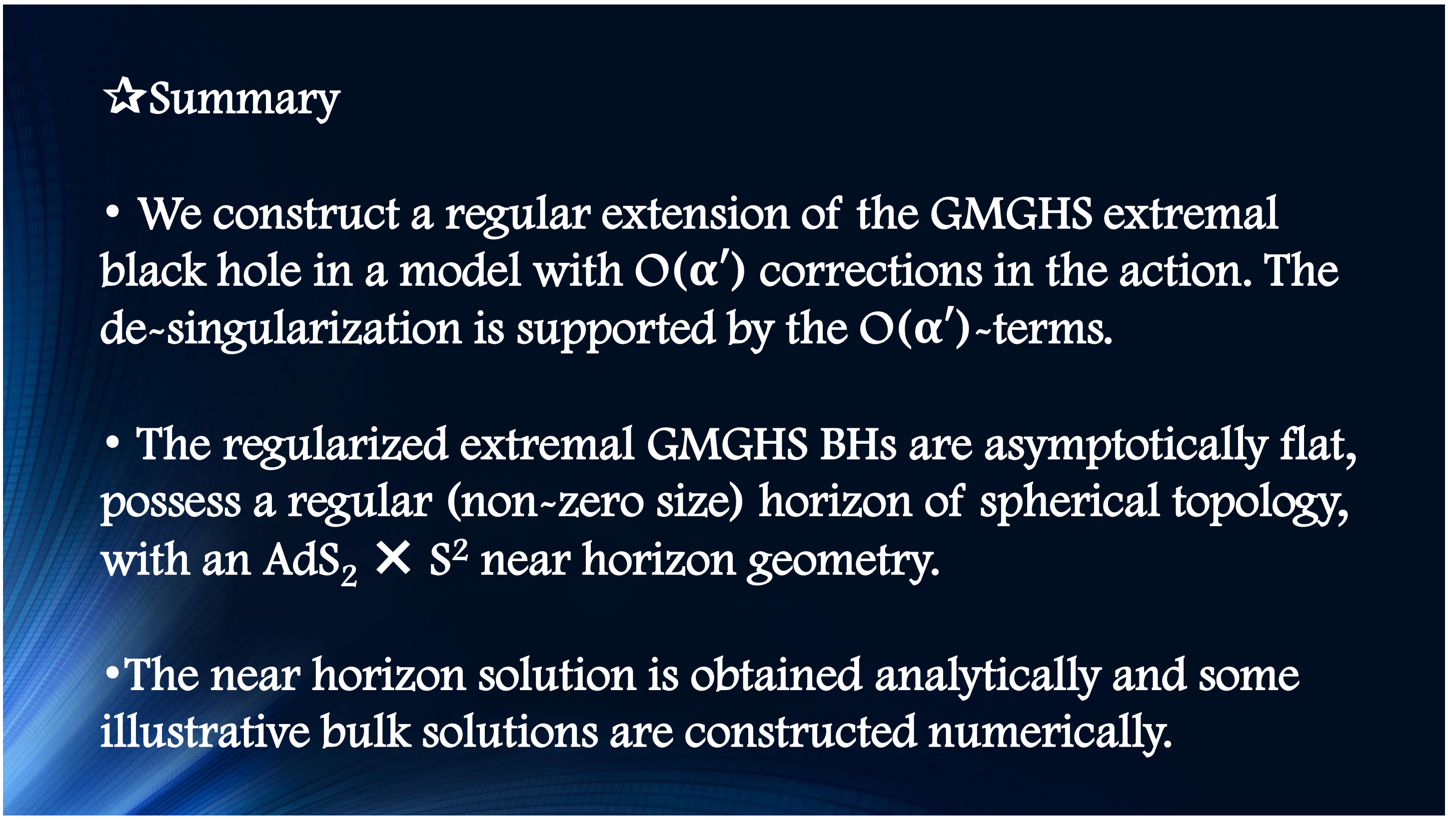

☆Summary

- We construct a regular extension of the GMGHS extremal black hole in a model with $O(\alpha')$ corrections in the action. The de-singularization is supported by the $O(\alpha')$-terms.

- The regularized extremal GMGHS BHs are asymptotically flat, possess a regular (non-zero size) horizon of spherical topology, with an $AdS_2 \times S^2$ near horizon geometry.

- The near horizon solution is obtained analytically and some illustrative bulk solutions are constructed numerically.

[1] Introduction

☆The Gibbons-Maeda-Garfinkle-Horowitz-Strominger (GMGHS) black hole is an influential solution of the low energy heterotic string theory compactified to four spacetime dimensions.
(G.W. Gibbons, K.i. Maeda, Nucl. Phys. B 298 (1988) 741)
(D. Garfinkle, G.T. Horowitz, A. Strominger, Phys. Rev. D 43 (1991) 3140)

☆Property of the GMGHS solution

- Its extremal limit is singular.

- The area of the spatial sections of the horizon shrinks to zero.

- The Kretschmann scalar blows up at the horizon.

Nobody knows whether the possible stringy α'-corrections could de-singularize the extremal solution in the Einstein-Maxwell-dilaton action.

Cf)
- There is a perturbative extension of the extremal magnetic GMGHS BH.
(M. Natsuume, Phys. Rev. D 50 (1994) 3949, arXiv:hep -th/9406079)

- The corrected solution inherits all basic properties of the extremal GMGHS BH.

- The horizon area still vanishes.

⇒ The task of constructing the fully non-linear BH solutions of the O(α′) corrected action has not yet been considered.

The main purpose of our work is to reply to the key question whether such corrections can de-singularize the extremal GMGHS solution.

---

[2] The model

- Starting with a general model for the O(α′) corrections to the Einstein-Maxwell-dilaton action.

$$S_s = \int d^4x\sqrt{-\tilde{g}}\,\mathrm{e}^{-2\phi}\Big[\tilde{R}+4\left(\tilde{\nabla}\phi\right)^2 - F^2 + \alpha'\Big\{a\left(\tilde{R}_{\mu\nu\rho\sigma}\tilde{R}^{\mu\nu\rho\sigma} - 4\tilde{R}_{\mu\nu}\tilde{R}^{\mu\nu} + \tilde{R}^2\right) \\ +b\left(F^2\right)^2 + cF^2\left(\tilde{\nabla}\phi\right)^2 + h\tilde{R}^{\mu\nu\rho\sigma}F_{\mu\nu}F_{\rho\sigma}\Big\}\Big]$$

Here, $F = dA$ is the U(1) field strength tensor, ϕ is a real scalar field and $a,\ b,\ c,\ h$ are constant coefficients.

✩α′=0 limit: the GMGHS solution

(M. Natsuume, Phys. Rev. D 50 (1994) 3949, arXiv:hep-th/9406079)

$$ds^2 = -\left(1-\frac{r_+}{r}\right)dt^2 + \left(1-\frac{r_+}{r}\right)^{-1}dr^2 + r^2\left(1-\frac{r_-}{r}\right)d\Omega^2\,,$$

$$A = \frac{Q}{r}dt\,, \qquad \mathrm{e}^{2\phi} = \frac{1}{2}\left(1-\frac{r_-}{r}\right)\,, \qquad M = \frac{r_+}{2}\,, \qquad Q = \left(\frac{r_-r_+}{2}\right)^{\frac{1}{2}}$$

The two free parameters $r_+,\ r_-$ (with $r_- < r_+$), corresponding to outer and inner horizon radius, respectively.

✩Horizon area A_H and Hawking temperature T_H :

$$A_H = 4\pi r_+^2\left(1-\frac{r_-}{r_+}\right)\,, \qquad T_H = \frac{1}{4\pi r_+}$$

- In the extremal limit, $A_H \to 0$ while T_H approaches a constant. (It gives singular solution)

$$A_H = 4\pi r_+^2\left(1-\frac{r_-}{r_+}\right)\,, \qquad T_H = \frac{1}{4\pi r_+}$$

- Magnetic version of the GMGHS solution

$$ds^2 = -\left(1-\frac{r_+}{r}\right)dt^2 + \left(1-\frac{r_+}{r}\right)dr^2 + r^2\left(1-\frac{r_-}{r}\right)d\Omega^2$$

$$A = Q\cos\theta d\varphi, \qquad \mathrm{e}^{-2\phi} = \frac{1}{2}\left(1-\frac{r_-}{r}\right)$$

- Magnetic solution is also singular in the extremal limit.

☆Setup: static spherically symmetric solutions with a purely electric U(1) potential

$$ds^2 = -a(r)^2 dt^2 + c(r)^2 dr^2 + b(r)^2 d\Omega^2, \qquad \phi \equiv \phi(r), \qquad A = V(r)dt$$

- The field equations of the full model possess an exact solution describing an AdS$_2$ × S^2 metric, an electric field and a constant dilaton.

- There is no counterpart of this solution with a magnetic charge.

- Our choice here is to work with

$$a = \frac{1}{8}\ , \qquad b, c: \ \ \text{arbitrary}\ , \qquad h = 0$$

☆ Ansatz:

$$ds^2 = v_0^2 \left(\frac{dr^2}{r^2} - r^2 dt^2 \right) + v_1^2 d\Omega^2_{(2)}, \qquad \phi(r) = \phi_0, \qquad V = qr$$

- Near horizon field configuration for the ansatz is consistent with the SO(2, 1)×SO(3) symmetry of AdS$_2$×S^2
(A. Sen, J. High Energy Phys. 0509 (2005) 038, arXiv:hep-th/0506177)

- We choose to determine the unknown parameters by extremizing an entropy function.
(A. Sen, Gen. Relativ. Gravit. 40 (2008) 2249, arXiv:0708.1270 [hep-th])

The entropy function is defined by

$$F(v_0, v_1, q, Q, \phi_0) = 2\pi \left(qQ - f(v_0, v_1, q, \phi_0) \right) \quad Q: \text{ electric charge of the solutions}$$

The black hole entropy $S_{\rm BH}$ is given by the value of the function F at the extremum with v_0 , v_1 , ϕ_0 :

$$S_{\rm BH}(q\ ,\ Q) = F\left(v_0\ ,\ v_1\ ,\ q\ ,\ Q\ ,\ \phi_0\right)$$

The Lagrangian density $f(v_0, v_1, q, \phi_0)$ can be evaluated as

$$\begin{aligned} f(v_0, v_1, q, \phi_0) &= \frac{1}{4\pi} \int d\theta d\varphi \sqrt{-g} \mathcal{L} \\ &= \frac{v_0^2 - v_1^2}{2} + e^{-2\phi_0} q^2 \frac{v_1^2}{2v_0^2} - \frac{1}{4} \alpha' e^{-2\phi_0} \left(1 - 4b \frac{e^{-4\phi_0} q^4 v_1^2}{v_0^6} \right) \end{aligned}$$

☆The scalar and the metric field equations in the near horizon geometry correspond to extremizing F :

$$\frac{\partial F}{\partial v_0} = 0\,, \qquad \frac{\partial F}{\partial v_1} = 0\,, \qquad \frac{\partial F}{\partial \phi_0} = 0\,, \qquad \frac{\partial F}{\partial q} = 0$$

- Solution :

$$v_0 = \frac{\sqrt{\alpha'} e^{-\phi_0}}{\sqrt{2}}\,, \qquad v_1 = \sqrt{\alpha'} e^{-\phi_0} \frac{\sqrt{2b}}{\sqrt{1 + 12b - \sqrt{1 + 16b}}}\,,$$

$$q = \sqrt{\alpha'} \frac{\sqrt{\sqrt{1 + 16b} - 1}}{4\sqrt{b}}\,, \qquad Q = \sqrt{\alpha'} e^{-2\phi_0} \frac{\sqrt{b(1 + 16b)(\sqrt{1 + 16b} - 1)}}{1 + 12b - \sqrt{1 + 16b}}$$

✩Bulk extremal BH

$$ds^2 = -\mathrm{e}^{-2\delta(r)} N(r) dt^2 + \frac{dr^2}{N(r)} + r^2(d\theta^2 + \sin^2\theta d\varphi^2)$$

If we assume the existence of a horizon located at $r = r_H > 0$, one finds the following approximate solution:

$$N(r) = N_2(r - r_H)^2 + \dots \ , \qquad \delta(r) = \delta_0 + \delta_1(r - r_H) + \dots \ ,$$

$$\phi(r) = \phi_0 + \phi_1(r - r_H) + \dots \ , \qquad V(r) = v_1(r - r_H) + \dots \ ,$$

with

$$N_2 = \frac{2}{\alpha'} \ , \qquad r_H = \frac{\mathrm{e}^{-\phi_0}\sqrt{\alpha'}\sqrt{2b}}{\sqrt{1 + 12b - \sqrt{1 + 16b}}} > 0 \ , \qquad v_1 = \frac{\mathrm{e}^{-\delta_0}\sqrt{\sqrt{1 + 16b} - 1}}{2\sqrt{\alpha'}\sqrt{b}}$$

✩For large r, the asymptotic form of the solution becomes

$$N(r) = 1 - \frac{Q^2 + Q_s^2}{r} + \dots \ , \qquad \phi(r) = \frac{Q_s}{r} + \dots \ ,$$

$$V(r) = V_0 + \frac{Q}{r} + \dots, \qquad \delta(r) = \frac{Q_s^2}{2r^2} + \dots \ .$$

Q_s : scalar charge

•These extremal BHs have finite global charges $M, \ Q$ as well as a finite scalar "charge" Q_s while their Hawking temperature vanishes.

☆ Profile of a typical BH solution

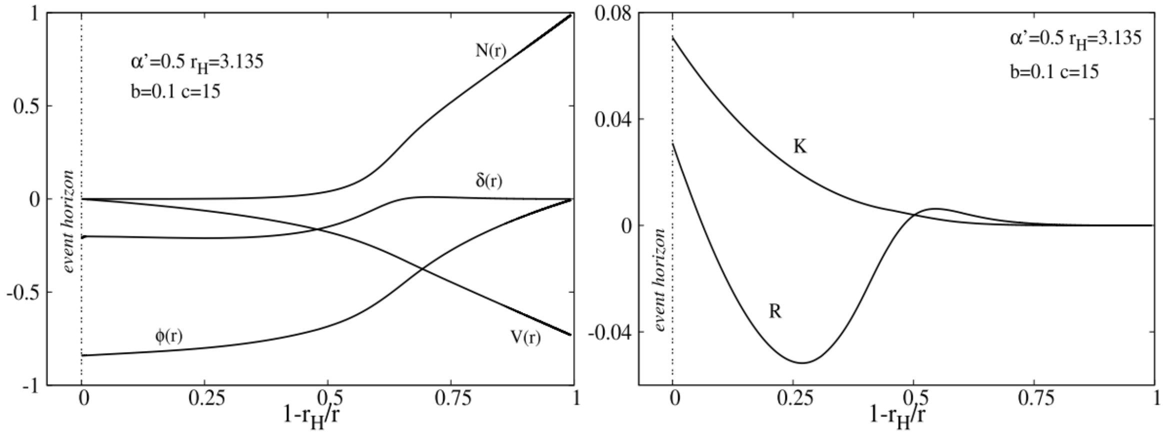

Profile functions of the extremal BH

Ricci (R) and Kretschmann (K) scalars

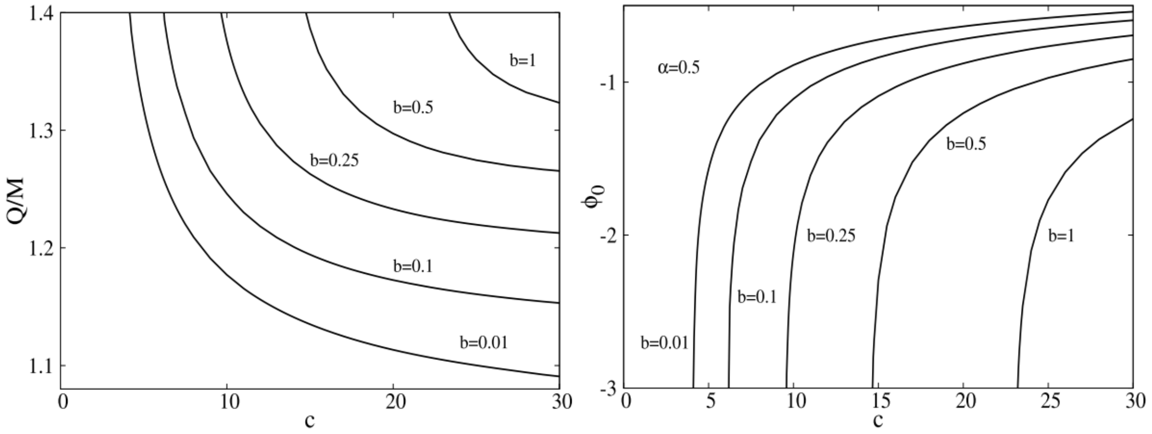

Charge to mass ratio

Value of dilaton

- The most interesting feature of the solutions found so far is that the charge-to-mass ratio Q/M is always greater than one.

- The ratio Q/M decreases when c increases for fixed b .

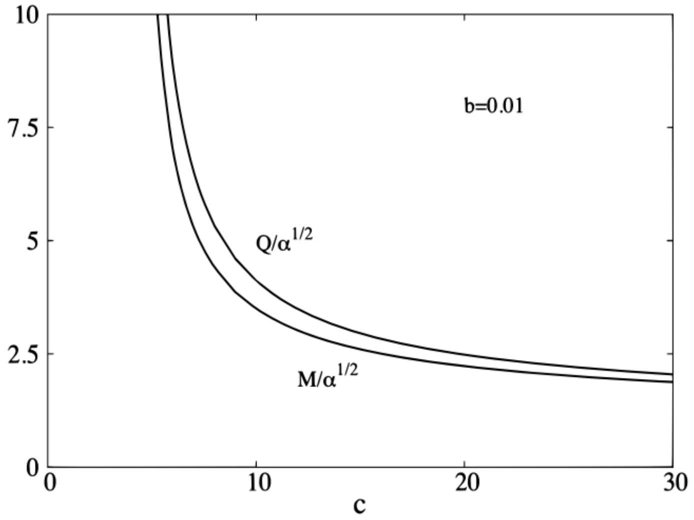

- As the parameter c grows, the BH mass M decreases for fixed value of b .

---

[3] Discussion and remarks

- In this work, we have focused on static BHs but there are also studies with rotating BHs with first order correction in α'.

- We have confirmed that α' corrections can de-singularize the extremal GMGHS solution, an influential stringy BH whose extremal limit is long known to be singular.

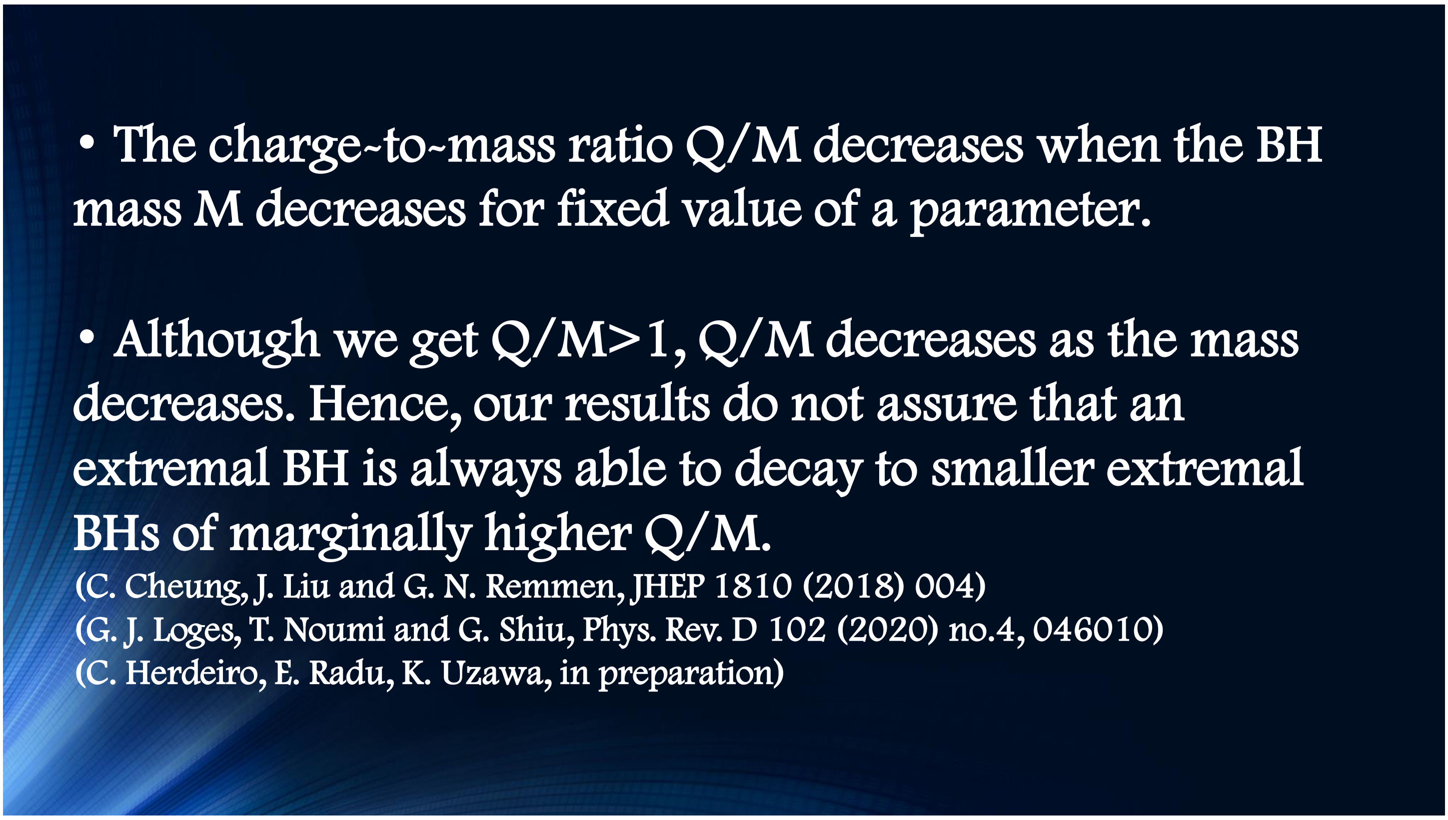

- The charge-to-mass ratio Q/M decreases when the BH mass M decreases for fixed value of a parameter.

- Although we get Q/M>1, Q/M decreases as the mass decreases. Hence, our results do not assure that an extremal BH is always able to decay to smaller extremal BHs of marginally higher Q/M.

(C. Cheung, J. Liu and G. N. Remmen, JHEP 1810 (2018) 004)
(G. J. Loges, T. Noumi and G. Shiu, Phys. Rev. D 102 (2020) no.4, 046010)
(C. Herdeiro, E. Radu, K. Uzawa, in preparation)

C73

Holographic Dark Energy from AdS Black Hole

Ratchaphat Nakarachinda

The Institute for Fundamental Study (IF), Naresuan U., Thailand

Collaborators: P. Wongjun, C. Pongkitivanichkul, D. Samart, L. Tannukij
Based on: Phys. Rev. D 105, 123524 (2022)

IF The Institute for Fundamental Study RGJ PhD. โครงการปริญญาเอกกาญจนาภิเษก WASEDA University

---

Outline

1. Holographic Dark Energy
   - Bounds of QFT system
   - HDE from AdS BH
2. Cosmological models
   - Hubble radius as IR length scale
   - Particle horizon as IR length scale
3. Summary

UV/IR Relationship

- Let us consider a system in a box volume L^3 for a conventional QFT with UV cutoff Λ_{UV}. The entropy of this system scales by its volume,

$$S \sim L^3 \Lambda_{UV}^3. \tag{1}$$

UV/IR Relationship

- Let us consider a system in a box volume L^3 for a conventional QFT with UV cutoff Λ_{UV}. The entropy of this system scales by its volume,

$$S \sim L^3 \Lambda_{UV}^3. \tag{1}$$

- It was found that the volume scaling entropy of QFT system is bounded by the area scaling entropy of a black hole as [Bekenstein, Phys. Rev. D. 23, 287 (1981)]

Bekenstein bound

$$L^3 \Lambda_{UV}^3 \lesssim S_{\rm BH} \sim L^2 M_{\rm P}^2. \tag{2}$$

UV/IR Relationship

Bekenstein bound (Entropy bound)

$$L^3\Lambda_{UV}^3 \lesssim S_{\mathrm{BH}} \sim L^2 M_{\mathrm{P}}^2. \qquad (2)$$

- For any value of Λ_{UV}, there exists a sufficiently large length scale (i.e., $L > M_{\mathrm{P}}^2/\Lambda_{UV}^3$) compatible with the IR cutoff in which the QFT breaks down ['t Hooft, arXiv:gr-qc/9310026].
- Obviously, the IR cutoff depends on the UV cutoff in this aspect.

Energy Bound

- Cohen et al proposed that the entropy of the quantum field theory never saturate to the Bekenstein bound. It is because the maximum energy of the matter in QFT corresponds to the Schwarzschild energy (mass) will be reached before.

  [Cohen et al, Phys. Rev. Lett. 82, 4971 (1999)]

Energy bound

$$L^3\Lambda_{UV}^4 \lesssim L M_{\mathrm{P}}^2. \qquad (3)$$

They also proposed that the states, when the energy bound is satisfied, can be described by QFT.

HDE model

- This is possible to interpret as the energy density for the holographic dark energy (HDE) [Hsu, Phys. Lett. B 594, 13 (2004); Li, Phys. Lett. B 603, 1 (2004)]

HDE

$$\Lambda_{UV}^4 \sim \rho_{HDE} = 3b^2 M_{\rm P}^2/L^2. \tag{4}$$

HDE model

- This is possible to interpret as the energy density for the holographic dark energy (HDE) [Hsu, Phys. Lett. B 594, 13 (2004); Li, Phys. Lett. B 603, 1 (2004)]

HDE

$$\Lambda_{UV}^4 \sim \rho_{HDE} = 3b^2 M_{\rm P}^2/L^2. \tag{4}$$

- The terminology “Holographic” in this context is conventionally used because this DE model is actually constructed from the physical quantities at boundary (i.e., $M_{\rm P}$ and L).

Hubble horizon

To describe the dynamics of the Universe, one can choose suitable IR length scale for this HDE model

- Choose $L = H^{-1}$

Energy Density

$$\rho_{de} = 3b^2 M_{\rm P}^2 H^2. \tag{5}$$

The Friedmann with this type of HDE reads

$$3M_{\rm P}^2 H^2 = \rho_M + 3b^2 M_{\rm P}^2 H^2. \tag{6}$$

Hubble horizon

To describe the dynamics of the Universe, one can choose suitable IR length scale for this HDE model

- Choose $L = H^{-1}$

Energy Density

$$\rho_{de} = 3b^2 M_{\rm P}^2 H^2. \tag{5}$$

The Friedmann with this type of HDE reads

$$3M_{\rm P}^2 H^2 = \rho_M + 3b^2 M_{\rm P}^2 H^2. \tag{6}$$

- It is seen that the Universe evolves as the MD epoch (scaled by b^2)

$$3M_{\rm P}^2 H^2 = \frac{\rho_M}{(1 - b^2)} \equiv \tilde{\rho}_M. \tag{7}$$

It is not possible to drive the accelerated expansion using this HDE. [Hsu, Phys. Lett. B 594, 13 (2004)]

Particle horizon

Energy Density

$$\rho_{de} = \frac{3b^2 M_{\mathrm{P}}^2}{R_h^2}, \qquad R_h = a(t)\int_0^t \frac{\mathrm{d}\bar{t}}{a(\bar{t})}. \tag{8}$$

Particle horizon

Energy Density

$$\rho_{de} = \frac{3b^2 M_{\mathrm{P}}^2}{R_h^2}, \qquad R_h = a(t)\int_0^t \frac{\mathrm{d}\bar{t}}{a(\bar{t})}. \tag{8}$$

The EoS parameter for HDE can be determined from the conservation eq,

$$\dot{\rho}_{de} + 3H(1 + w_{de})\rho_{de} = 0. \tag{9}$$

Then, one can compute ($\Omega_{de} \equiv \frac{\rho_{de}}{3M_{\mathrm{P}}^2 H^2}$)

$$w_{de} = -1 - \frac{1}{3H}\frac{\dot{\rho}_{de}}{\rho_{de}} = -1 + \frac{2}{3H}\frac{\dot{R}_h}{R_h} = -1 + \frac{2}{3}\left(1 + \sqrt{\frac{\Omega_{de}}{b^2}}\right)$$

Particle horizon

Energy Density

$$\rho_{de} = \frac{3b^2 M_P^2}{R_h^2}, \qquad R_h = a(t)\int_0^t \frac{d\bar{t}}{a(\bar{t})}. \tag{8}$$

The EoS parameter for HDE can be determined from the conservation eq,

$$\dot{\rho}_{de} + 3H(1 + w_{de})\rho_{de} = 0. \tag{9}$$

Then, one can compute ($\Omega_{de} \equiv \frac{\rho_{de}}{3M_P^2 H^2}$)

$$w_{de} = -1 - \frac{1}{3H}\frac{\dot{\rho}_{de}}{\rho_{de}} = -1 + \frac{2}{3H}\frac{\dot{R}_h}{R_h} = -1 + \frac{2}{3}\left(1 + \sqrt{\frac{\Omega_{de}}{b^2}}\right) > -\frac{1}{3}. \tag{10}$$

→ It cannot drive the accelerated expansion of Universe.

Future particle horizon

- Let us consider instead [Li, Phys. Lett. B 603, 1 (2004)]

$$R_f = a(t)\int_t^\infty \frac{d\bar{t}}{a(\bar{t})}. \tag{11}$$

Eventually, the EoS parameter becomes

$$w_{de} = -1 + \frac{2}{3}\left(1 - \sqrt{\frac{\Omega_{de}}{b^2}}\right). \tag{12}$$

→ The accelerated expansion can be explained by this DE model ($w_{de} = -1$ when $\Omega_{de} = b^2$).

Future particle horizon

- Let us consider instead [Li, Phys. Lett. B 603, 1 (2004)]

$$R_f = a(t)\int_t^{\infty}\frac{\mathrm{d}\bar{t}}{a(\bar{t})}. \tag{11}$$

Eventually, the EoS parameter becomes

$$w_{de} = -1 + \frac{2}{3}\left(1 - \sqrt{\frac{\Omega_{de}}{b^2}}\right). \tag{12}$$

→ The accelerated expansion can be explained by this DE model ($w_{de} = -1$ when $\Omega_{de} = b^2$).

- However, it obviously suffers the problem of causality.
- Many HDE models with other length scales are also investigated.

AdS-HDE

- Since the dark energy is defined as the energy bound corresponding to BH mass, it is possible to study HDE via some properties of BH.

AdS-HDE

- Since the dark energy is defined as the energy bound corresponding to BH mass, it is possible to study HDE via some properties of BH.
- In this work, we proposed the HDE model by modifying the mass of Schwarzschild BH to that of AdS BH,

$$M_{\mathrm{Sch}} = \frac{r_h}{2G}, \quad \rightarrow \quad M_{\mathrm{AdS}} = \frac{r_h}{2G}\left(1 + \frac{\Lambda}{3} r_h^2\right). \tag{13}$$

- The dimensional estimation of Cohen's energy bound is straightforwardly modified as

$$L^3 \Lambda_{UV}^4 \lesssim M_{\mathrm{AdS}} \sim M_{\mathrm{P}}^2 L(1 + \Lambda L^2). \tag{14}$$

This work

AdS-HDE energy density

$$\rho_{de} = 3b^2 M_{\mathrm{P}}^2 \left(\frac{1}{L^2} + \Lambda\right). \tag{15}$$

- This Λ is a constant which will be dominant at late-time similar to ΛCDM model.

This work

AdS-HDE energy density

$$\rho_{de} = 3b^2 M_{\mathrm{P}}^2 \left(\frac{1}{L^2} + \Lambda \right). \tag{15}$$

- This Λ is a constant which will be dominant at late-time similar to ΛCDM model.
- Interestingly, this constant associated to the AdS BH can somehow give the dS space in cosmological context.

This work

AdS-HDE energy density

$$\rho_{de} = 3b^2 M_{\mathrm{P}}^2 \left(\frac{1}{L^2} + \Lambda \right). \tag{15}$$

- This Λ is a constant which will be dominant at late-time similar to ΛCDM model.
- Interestingly, this constant associated to the AdS BH can somehow give the dS space in cosmological context.

- We are interested in investigating the cosmological model for this AdS-HDE with 2 types of length scale
  1. $L = H^{-1}$
  2. $L = R_h = a(t) \int_0^t \frac{d\bar{t}}{a(\bar{t})}$

Outline

1. Holographic Dark Energy
   - Bounds of QFT system
   - HDE from AdS BH
2. Cosmological models
   - Hubble radius as IR length scale
   - Particle horizon as IR length scale
3. Summary

Energy Density

$$\rho_{de} = 3b^2 M_{\rm P}^2 \left(H^2 + \Lambda \right), \tag{16}$$

- Friedmann eq

$$3M_{\rm P}^2 H^2 = \rho_{r,0} a^{-4} + \rho_{m,0} a^{-3} + 3M_{\rm P}^2 b^2 \left(H^2 + \Lambda \right). \tag{17}$$

- It can be rearranged as

$$\begin{aligned} 3M_{\rm P}^2 H^2 &= \left(\frac{\rho_{r,0}}{1-b^2} \right) a^{-4} + \left(\frac{\rho_m}{1-b^2} \right) a^{-3} + \frac{3M_{\rm P}^2}{1-b^2} \Lambda \\ &\equiv \tilde{\rho}_{r,0} a^{-4} + \tilde{\rho}_{m,0} a^{-3} + M_{\rm P}^2 \tilde{\Lambda}. \end{aligned} \tag{18}$$

This is identical to ΛCDM model.
(just rescale ρ_i by parameter b)

Outline

Energy Density

$$\rho_{de} = 3b^2 M_{\rm P}^2 \left(\frac{1}{R_h^2} + \Lambda \right), \qquad R_h = a(t) \int_0^t \frac{\mathrm{d}\bar{t}}{a(\bar{t})}. \tag{19}$$

- Define the dimensionless parameters as $\Omega_i \equiv \frac{\rho_i}{3M_{\rm P}^2 H^2}$. One then has the constraint eq as $1 = \Omega_M + \Omega_\Lambda + \Omega_R$.

Autonomous system

$$\Omega_M' = -3\Omega_M \left(1 + w_M + \frac{2\dot{H}}{3H^2} \right), \tag{20}$$

$$\Omega_\Lambda' = -3\Omega_\Lambda \left(\frac{2\dot{H}}{3H^2} \right), \tag{21}$$

with $$\frac{2\dot{H}}{3H^2} = -(1 + w_M)\Omega_M - (1 + w_R)(1 - \Omega_M). \tag{22}$$

Dynamical System Analysis

FPs	w_{de}	w_{eff}	Epoch	Stability
(a)	$-\frac{1}{3}+\frac{2}{3\lvert b\rvert}$	$-\frac{1}{3}+\frac{2}{3\lvert b\rvert}$	Ω_R-dom	saddle $\left(\lvert b\rvert>\frac{2}{1+3w_M}\right)$, unstable $\left(\lvert b\rvert<\frac{2}{1+3w_M}\right)$
(b)	-1	-1	Ω_Λ-dom	stable
(c1)	undefined	w_M	Ω_M-dom	unstable
(c2)	w_M	w_M	$\Omega_R+\Omega_M$	saddle (Exists only $\lvert b\rvert<2/(1+3w_M)$)

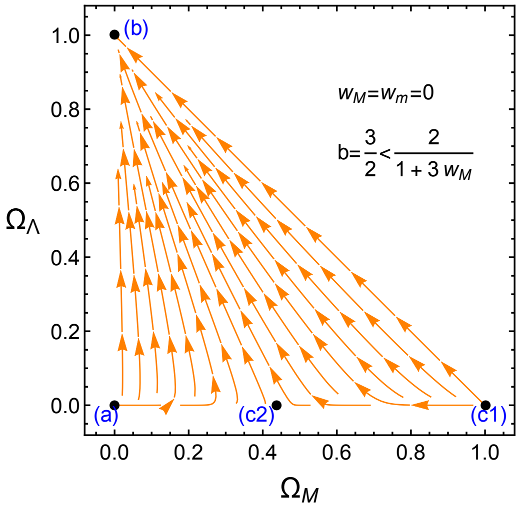

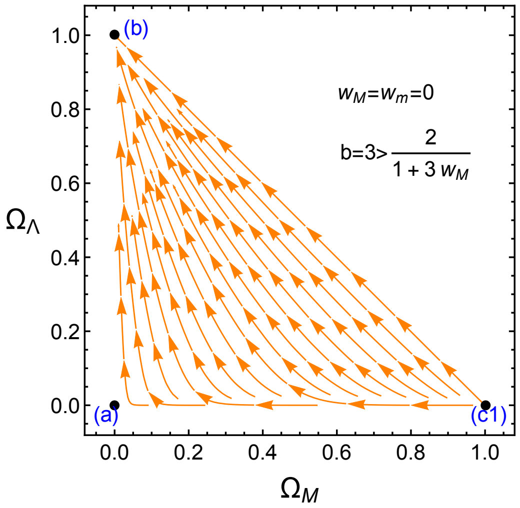

Numerical Results

- $\Omega_{R,0}=0.07$

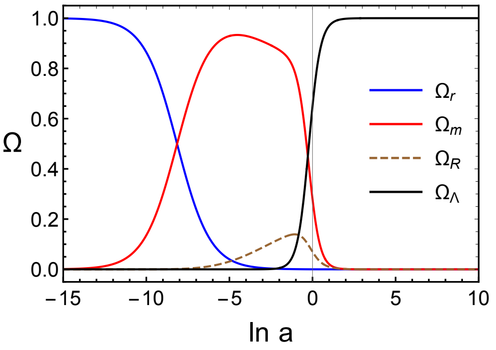

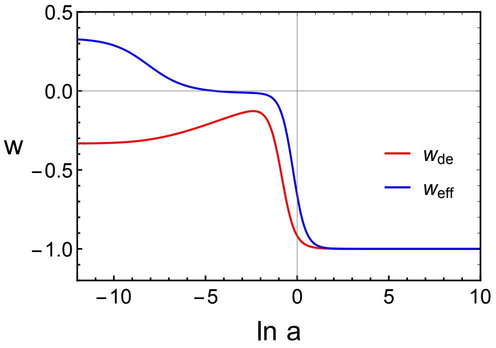

- $\Omega_{R,0}=0.12$

$\ast$ ICs: $\Omega_{r,0}=8.1\times10^{-5}$, $\Omega_{m,0}=0.28-\Omega_{r,0}$, $\Omega_{\Lambda,0}=0.72-\Omega_{R,0}$.

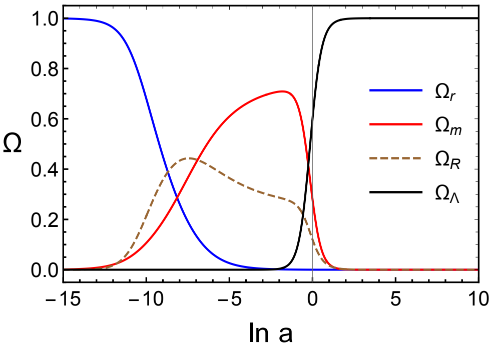

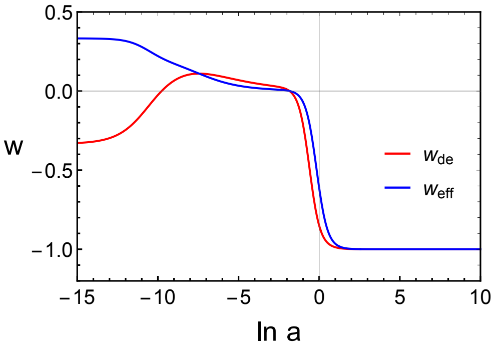

Summary and remarks

- We have studied 2 HDE models
    1. $L = H^{-1}$: it is identical to ΛCDM model.
    2. $L = R_h$: it is able to predict the late-time expansion without suffering the causality problem.
- This model cannot solve the coincidence problem since the dominant contribution at late-time is the constant similar to ΛCDM model.
- It is difficult to investigate the full perturbation analysis because the field description of HDE is still ambiguous.
- The result might lead to a proposal of the relation between dS (cosmology) and AdS (black hole).

Thank You for Your Attention

Brane Dynamics of Holographic BCFTs

Norihiro Tanahashi [Chuo U]

based on

Keisuke Izumi, Tetsuya Shiromizu, Kenta Suzuki, Tadashi Takayanagi & NT

“Brane Dynamics of Holographic BCFTs”

JHEP 10, 050 (2022) [arXiv:2205.15500]

Brane Dynamics of Holographic BCFTs

- ▶ Boundary conformal field theory (BCFT)
  Quantum field theory living on space with boundaries
- ✓ Applications to string theory, condensed matter physics, …

- ▶ AdS/BCFT correspondence
  BCFT ≈ Higher-dimensional gravity with a membrane (brane)
  [Takayanagi ’11; Karch+ ‘01, …]
- ✓ Dynamics in BCFT ≈ Dynamics of gravity and brane in higher dim.
- ✓ Energy-momentum tensor of BCFT = Gravitational perturbation in higher dim.

- ◆ Complete treatment of gravitational dynamics in AdS/BCFT
  → Dynamics of BCFT in general dimensions
- ◆ Properties of energy & momentum flux in BCFT in general dimensions

[Izumi, Shiromizu, Suzuki, Takayanagi, NT ’22]

Boundary conformal field theory (BCFT)

- BCFT = CFT + boundary preserving a part of conformal symmetries

d dim. CFT
$SO(2,d)$

↓

d dim. **BCFT**
$SO(2,d-1)$

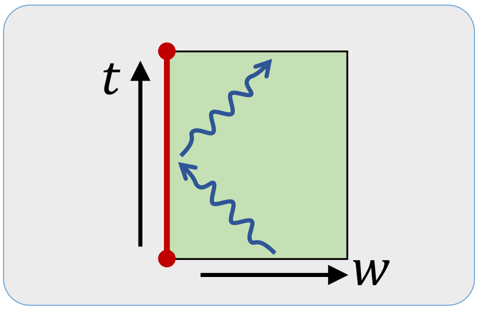

ex.) Conformal scalar ϕ in d dim. + Neumann boundary condition $\partial_w\phi = 0$ at $w = 0$

$$I = \frac{1}{2}\int d^dx \left[\partial_a\phi\partial^a\phi + \frac{d-2}{4(d-1)}R_0\phi^2\right]$$

$$\mathcal{T}_{ab} = \frac{d}{2(d-1)}\partial_a\phi\partial_b\phi - \frac{\delta_{ab}}{2(d-1)}(\partial\phi)^2 - \frac{d-2}{2(d-1)}(\partial_a\partial_b\phi)\phi + \frac{(d-2)\delta_{ab}}{2d(d-1)}(\partial^2\phi)\phi$$

→ $T_{wi}|_{w=0} = 0$; energy & momentum flux = 0 across the boundary
(Other components of $T_{\mu\nu}|_{w=0}$ non-vanishing in general)

Dynamics in AdS/BCFT

- AdS/BCFT correspondence: BCFT$_d$ = "braneworld" in AdS$_{d+1}$
- Dynamics in AdS/BCFT

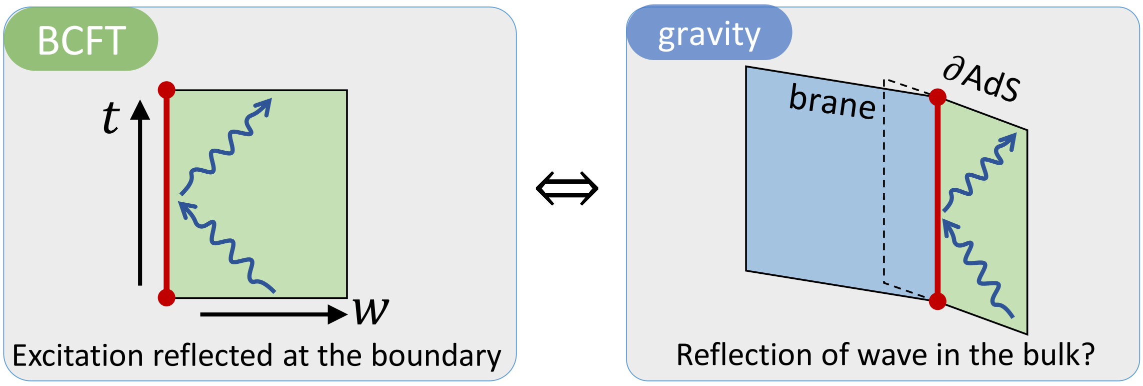

Excitation reflected at the boundary

Reflection of wave in the bulk?

- Scalar field in bulk spacetime
  → Corresponds to $\langle O\rangle$ (O: scalar operator) in BCFT
- Gravitational perturbation in bulk spacetime
  → Corresponds to $\langle T_{\mu\nu}\rangle$ in BCFT

→ Study **dynamics of bulk scalar & gravitational wave**
(≈ dynamics of holographic BCFTs)

Bulk geometry: AdS$_{d+1}$ spacetime & brane

- AdS$_d$ brane in AdS$_{d+1}$ spacetime

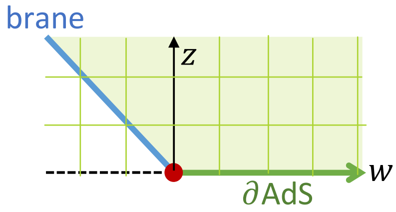

Spacetime metric:

$$ds^2 = \frac{1}{z^2}\left(dz^2 + dw^2 + \Sigma_{i=0}^{d-2}\, dx_i^2\right)$$

Brane with tension σ :

$$w + \lambda z = 0 \quad \left(\lambda = \frac{\sigma}{\sqrt{4(d-1)^2+\sigma^2}}\right)$$

- AdS$_d$ slicing of AdS$_{d+1}$ spacetime

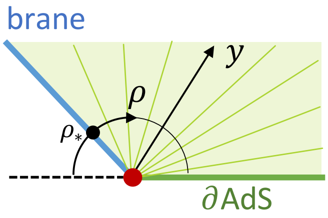

$\Leftrightarrow$

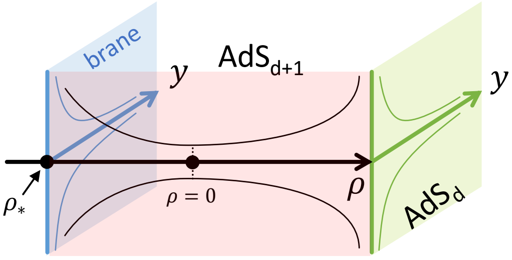

$$ds^2 = d\rho^2 + \cosh^2\rho\left(\frac{dy^2+\Sigma_{i=0}^{d-2}\, dx_i^2}{y^2}\right) \;; \quad \text{Brane at } \rho = \rho_* = -\sinh^{-1}\lambda$$

Gravitational perturbation in bulk

- Gravitational EoM: Einstein equation

$$R_{MN} - \frac{1}{2}R\, g_{MN} + \Lambda\, g_{MN} = 0$$

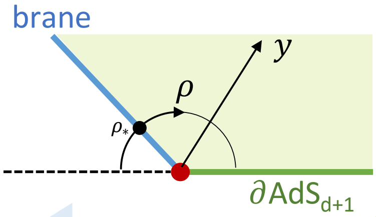

- Gravitational perturbations

$$ds^2 = d\rho^2 + \left(\cosh^2\rho \cdot g_{\mu\nu}^{(\mathrm{AdS}_d)} + h_{\mu\nu}\right) dx^\mu dx^\nu$$

Work in the transverse-traceless (TT) gauge

$$\tilde{\nabla}^\mu h_{\mu\nu} = 0, \qquad h^\mu{}_\mu = 0$$

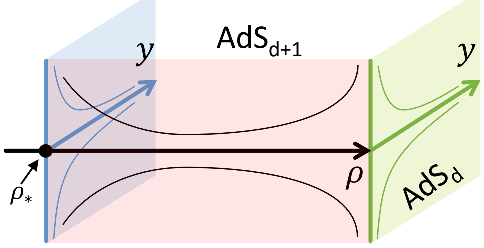

$\tilde{\nabla}_\mu$: covariant derivative of AdS$_d$

- Separation of variables w.r.t. ρ & y

$$h_{\mu\nu} = \cosh^2\rho\, R(\rho)\, Y_{\mu\nu}(y, t, \vec{x})$$

$$\begin{cases} R_{,\rho\rho} + d\tanh\rho\, R_{,\rho} = \dfrac{-\lambda_\rho}{\cosh^2\rho} R \\ (\tilde{\Box} + 2 - \lambda_\rho) Y_{\mu\nu} = 0 \end{cases}$$

$\tilde{\Box} = \tilde{\nabla}_\mu \tilde{\nabla}^\mu$: d'Alembertian in AdS$_d$

Gravitational perturbation in bulk

Boundary conditions

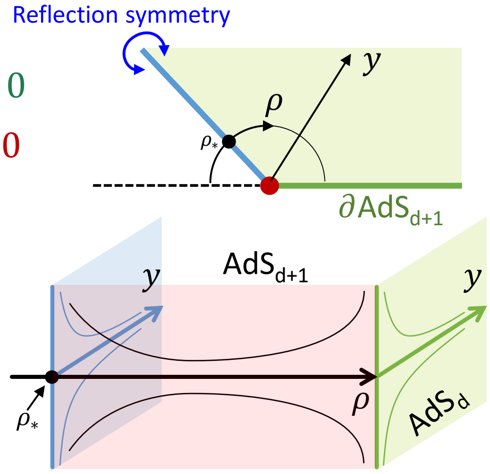

- Dirichlet condition at ∂AdS$_{d+1}$: $h_{\mu\nu}(\rho = \infty) \to 0$
- Dirichlet condition at ∂AdS$_d$: $h_{\mu\nu}(y = 0) \to 0$
- **Junction condition at the brane:**

$$K^{\mu}{}_{\nu} - K\delta^{\mu}{}_{\nu} = -\frac{\sigma}{2}\delta^{\mu}{}_{\nu}$$

- ➢ Condition for the reflection symmetry at brane
- ➢ $K_{\mu\nu} \sim \partial_\rho g_{\mu\nu} + \cdots$
- ➢ σ: tension of the brane : $T_{\mu\nu}^{(\mathrm{brane})} = \sigma g_{\mu\nu}$

◆ In the TT gauge we used to derive the EoM,
brane position fluctuates: $\rho = \rho_* - \varphi(x^\mu)$

→ Junction condition for becomes

$$\partial_\rho h_{\mu\nu} + \frac{\sigma}{d-1}h_{\mu\nu} = 2\left(\tilde{\nabla}_\mu\tilde{\nabla}_\nu - \gamma_{\mu\nu}\right)\varphi$$

$(\tilde{\Box} - d)\varphi = 0$:
brane bending φ behaves as a massive scalar on AdS$_d$

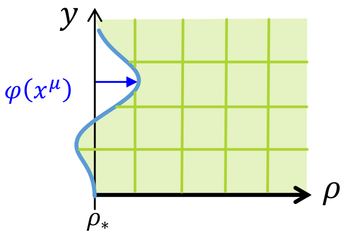

Gravitational perturbation in bulk

Summary: AdS$_{d+1}$ gravitational perturbations

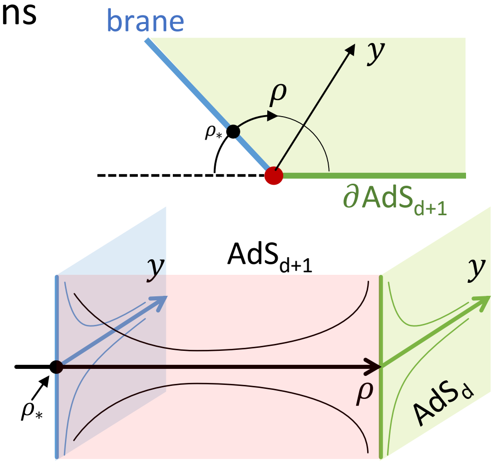

$$ds^2 = d\rho^2 + \left(\cosh^2\rho \cdot g_{\mu\nu}^{(\mathrm{AdS}_d)} + h_{\mu\nu}\right)dx^\mu dx^\nu$$

- EoM

$$h_{\mu\nu} = \cosh^2\rho \cdot R(\rho)\, Y_{\mu\nu}(y, t, \vec{x})$$

$$\begin{cases} R_{,\rho\rho} + d\tanh\rho\, R_{,\rho} = \dfrac{-\lambda_\rho}{\cosh^2\rho}R \\ (\tilde{\Box} + 2 - \lambda_\rho)Y_{\mu\nu} = 0 \end{cases}$$

- Boundary conditions at ∂AdS:
  $h_{\mu\nu}(\rho = \infty), h_{\mu\nu}(y = 0) \to 0$
- Junction condition at the brane: $\partial_\rho h_{\mu\nu} + \frac{\sigma}{d-1}h_{\mu\nu} = 2(\tilde{\nabla}_\mu\tilde{\nabla}_\nu - \gamma_{\mu\nu})\varphi$

$\varphi(x^\mu)$: brane displacement
s.t. $(\tilde{\Box} - d)\varphi = 0$

Two types of the modes

- Bulk graviton modes $(\varphi(x^\mu) = 0)$: ≈ bulk gravitational wave
- Brane-bending mode $(\varphi(x^\mu) \neq 0)$: ≈ bending of brane ≈ massive scalar field

Bulk graviton mode / brane-bending mode

EoM
$$\begin{cases} h_{\mu\nu} = \cosh^2\rho \cdot R(\rho)\, Y_{\mu\nu}(y,t,\vec{x}) \\ R_{,\rho\rho} + d\tanh\rho\, R_{,\rho} = \dfrac{-\lambda_\rho}{\cosh^2\rho} R \\ (\tilde{\Box} + 2 - \lambda_\rho) Y_{\mu\nu} = 0 \end{cases}$$

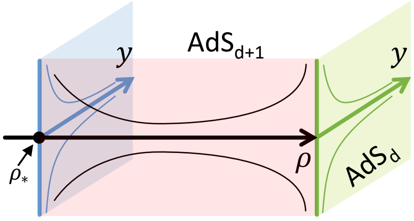

Bulk graviton modes ($\varphi(x^\mu) = 0$)

✓ ρ direction: $R(\rho)$ given by Legendre function

$$R(\rho) = P_l^{-\mu}(\zeta)(1-\zeta^2)^{\frac{d}{4}} \quad \left(\zeta = \tanh\rho,\ l = \frac{-1+\sqrt{(d-1)^2+4\lambda_\rho}}{2},\ \mu = \frac{d}{2}\right)$$

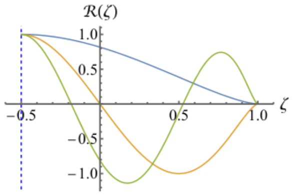

- Dirichlet condition at ∂AdS$_{d+1}$: $R(\rho = \infty) = 0$
- Junction condition at the brane: $\partial_\rho R(\rho = \rho_*) = 0$

→ Eigenvalue λ_ρ fixed

✓ y direction: $Y_{\mu\nu}$ given by massive tensor on AdS$_d$ $\quad d\tilde{s}^2 = \dfrac{1}{y^2}(dy^2 + \eta_{ij}dx^i dx^j)$

$$\begin{cases} (\tilde{\Box} + 2 - \lambda_\rho) Y_{\mu\nu} = 0 \\ Y_{\mu\nu} = \begin{pmatrix} Y_{yy} & Y_{yi} \\ Y_{iy} & Y_{ij} \end{pmatrix} \end{cases} \longrightarrow \begin{cases} \Box_0 Y_{yy} - \dfrac{d-2}{y}\partial_y Y_{yy} - \dfrac{\lambda_\rho}{y^2} Y_{yy} = 0 & \text{“scalar”} \\ \Box_0 Y_{yi} - \dfrac{d-4}{y}\partial_y Y_{yi} - \dfrac{d-2+\lambda_\rho}{y^2} Y_{yi} - \dfrac{2}{y}\partial_i Y_{yy} = 0 & \text{“vector”} \\ \Box_0 Y_{ij} - \dfrac{d-6}{y}\partial_y Y_{ij} - \dfrac{2d-6+\lambda_\rho}{y^2} Y_{ij} - \dfrac{2}{y}(\partial_i Y_{yj} + \partial_j Y_{yi}) + \dfrac{2}{y^2} Y_{yy}\eta_{ij} = 0 & \text{“tensor”} \end{cases}$$

Bulk graviton mode / brane-bending mode

EoM
$$\begin{cases} h_{\mu\nu} = \cosh^2\rho \cdot R(\rho)\, Y_{\mu\nu}(y,t,\vec{x}) \\ R_{,\rho\rho} + d\tanh\rho\, R_{,\rho} = \dfrac{-\lambda_\rho}{\cosh^2\rho} R \\ (\tilde{\Box} + 2 - \lambda_\rho) Y_{\mu\nu} = 0 \end{cases}$$

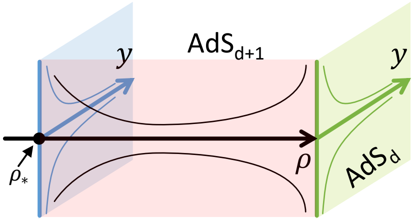

Brane-bending mode ($\varphi(x^\mu) \neq 0$)

- Boundary conditions at ∂AdS: $\quad h_{\mu\nu}(\rho = \infty), h_{\mu\nu}(y = 0) \to 0$
- Junction condition at the brane

$$\partial_\rho h_{\mu\nu} + \frac{\sigma}{d-1} h_{\mu\nu} = 2\left(\tilde{\nabla}_\mu \tilde{\nabla}_\nu - \frac{1}{d}\gamma_{\mu\nu}\tilde{\Box}\right)\varphi \qquad (\varphi(x^\mu)\text{: brane displacement, } (\tilde{\Box} - d)\varphi = 0)$$

✓ Brane bending $\varphi(x^\mu)$ → bulk graviton excited

$$Y^{(\varphi)}_{\mu\nu} = \left(\tilde{\nabla}_\mu \tilde{\nabla}_\nu - \frac{1}{d}\tilde{\Box}\gamma_{\mu\nu}\right)\varphi \ : \ \text{satisfies } Y_{\mu\nu} \text{ eq. with } \lambda_\rho = -(d-2)$$

$$\partial_\rho h_{\mu\nu} + \frac{\sigma}{d-1} h_{\mu\nu} = 2\left(\tilde{\nabla}_\mu \tilde{\nabla}_\nu - \frac{1}{d}\gamma_{\mu\nu}\tilde{\Box}\right)\varphi \ \rightarrow\ \partial_\rho R(\rho = \rho_*) = \frac{2}{\cosh^2\rho}$$

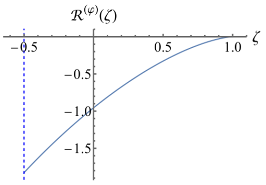

Holographic stress-energy tensor

- Holographic stress-energy tensor $T_{\mu\nu}$ of BCFT

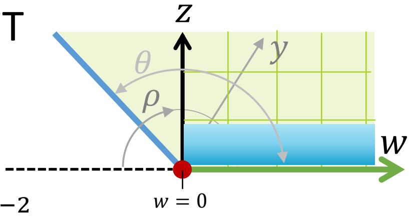

$$ds^2 = d\rho^2 + \left(\cosh^2\rho \cdot g_{\mu\nu}^{(\mathrm{AdS}_d)} + h_{\mu\nu}\right) dx^\mu dx^\nu$$

$$T_{\mu\nu} = \frac{d}{16\pi G_N} \lim_{z\to 0} \frac{1}{z^{d-2}} h_{\mu\nu}(x,w,z) = \frac{d}{16\pi G_N} \lim_{\rho\to\infty} \left(\frac{e^\rho}{2y}\right)^{d-2} h_{\mu\nu}(x,y,\rho)$$

- Behavior of $T_{\mu\nu}$ near the BCFT boundary

$$h_{\mu\nu} = \cosh^2\rho \cdot R(\rho)\, Y_{\mu\nu}(y,t,\vec{x}) \;\Rightarrow\; T_{\mu\nu} \propto Y_{\mu\nu}$$

- **Bulk graviton modes**

Traceless part of Y_{ij}

$$Y_{yy} \propto y^{\frac{d-1}{2}+\nu}, \quad Y_{yi} \propto y^{\frac{d-3}{2}+\nu}, \quad Y_{(ij)} \propto y^{\frac{d-5}{2}+\nu} \qquad \left[\nu = \sqrt{\frac{(d-1)^2}{4} + \lambda_\rho} > \frac{d-1}{2} \quad (\lambda_\rho > 0)\right]$$

$$\rightarrow \mathcal{T}_{ww} \propto w^{-\frac{d-3}{2}+\nu>1}, \quad \mathcal{T}_{wi} \propto w^{-\frac{d-1}{2}+\nu>0}, \quad \mathcal{T}_{(ij)} \propto w^{-\frac{d+1}{2}+\nu>-1};$$

$T_{wi} = 0$ at the boundary $(w=0)$

$$\left[\text{ex.) } d = 3: \quad \mathcal{T}_{ww} \propto w^{\frac{\pi}{\theta}n}, \quad \mathcal{T}_{wi} \propto w^{\frac{\pi}{\theta}n-1}, \quad \mathcal{T}_{(ij)} \propto w^{\frac{\pi}{\theta}n-2} \quad \left(\frac{\pi}{\theta} > 1, n = 1,2,3,\ldots\right)\right]$$

Holographic stress-energy tensor

- Holographic stress-energy tensor $T_{\mu\nu}$ of BCFT

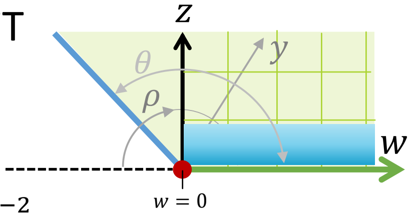

$$ds^2 = d\rho^2 + \left(\cosh^2\rho \cdot g_{\mu\nu}^{(\mathrm{AdS}_d)} + h_{\mu\nu}\right) dx^\mu dx^\nu$$

$$T_{\mu\nu} = \frac{d}{16\pi G_N} \lim_{z\to 0} \frac{1}{z^{d-2}} h_{\mu\nu}(x,w,z) = \frac{d}{16\pi G_N} \lim_{\rho\to\infty} \left(\frac{e^\rho}{2y}\right)^{d-2} h_{\mu\nu}(x,y,\rho)$$

- Behavior of $T_{\mu\nu}$ near the BCFT boundary

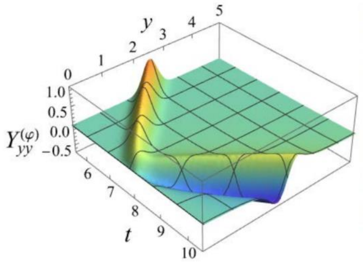

$$h_{\mu\nu} = \cosh^2\rho \cdot R(\rho)\, Y_{\mu\nu}(y,t,\vec{x}) \;\Rightarrow\; T_{\mu\nu} \propto Y_{\mu\nu}$$

- **Brane-bending mode**

Traceless part of Y_{ij}

$$Y_{yy} \propto y^{d-2}, \quad Y_{yi} \propto y^{d-1}, \quad Y_{(ij)} \propto y^d$$

$$\rightarrow \boxed{\mathcal{T}_{ww} \propto w^0, \quad \mathcal{T}_{wi} \propto w^1,} \quad \mathcal{T}_{(ij)} \propto w^2$$

$T_{wi} = 0$ at the boundary $(w=0)$

[ex.) Agrees with $d = 2$ (BCFT$_2$) results; dual to AdS$_3$ (brane-bending mode only)]

Summary: Brane Dynamics of Holographic BCFTs

- ◆ BCFT$_d$ satisfies the reflection boundary condition $T_{wi} = 0$
- ◆ Holographic dual of BCFT$_d$ = AdS$_{d+1}$ spacetime with a brane
  $T_{\mu\nu}$ of BCFT$_d$ = gravitational perturbation of AdS$_{d+1}$
- ◆ Scalar field & gravitational dynamics in AdS braneworld w/ junction condition at the brane

- ✓ Bulk gravity dynamics: bulk graviton modes & brane-bending mode
- ✓ $T_{wi} = 0$ satisfied for any dimensions, any brane tension; consistent with the BCFT$_d$ picture
- ✓ Complete description of dynamics in AdS$_{d+1}$/BCFT$_d$ correspondence

---

Summary: Brane Dynamics of Holographic BCFTs

We also explored … [Izumi, Shiromizu, Suzuki, Takayanagi, NT ’22]

- ☐ Duality between BCFT$_d$ & CFT$_d$+AdS$_d$ gravity
- ☐ Interaction of the bulk scalar field and the brane

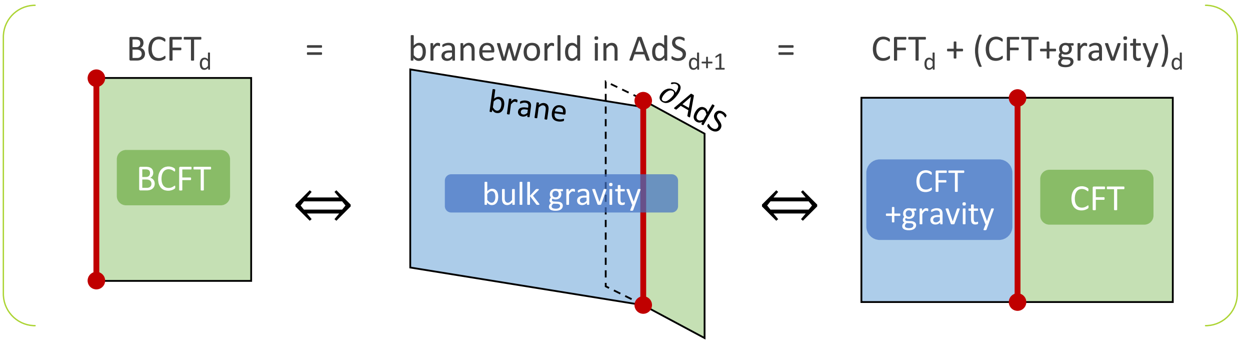

Future directions

- ◆ BCFT counterpart of bulk graviton modes & brane-bending mode?
- ◆ Any interesting dynamics in BCFT?
- ◆ Relationship between Liouville gravity & JT gravity? [Suzuki, Takayanagi ’22; Geng+ ‘22]

C77

JGRG31 28th Oct. 2022

PHOTON CYLINDER IN A STATIC CYLINDRICAL SYMMETRIC SPACETIME

Ryuya Kudo (Hirosaki Univ.)

Collaborator:
Hideki Asada (Hirosaki Univ.)

CONTENTS

1. Introduction

2. Equations of light rays and definition of photon cylinder

3. Properties of photon cylinder

4. Summary

CONTENTS

1. Introduction

2. Equations of light rays and definition of photon cylinder

3. Properties of photon cylinder

4. Summary

Backgrounds

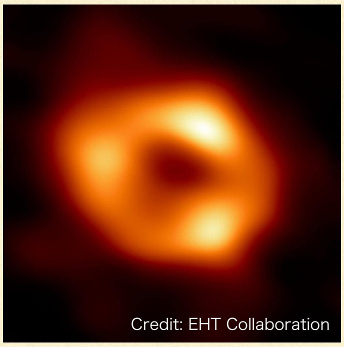

Sgr A* (2022)

- ✓ Imaging of black hole shadow

→ Observation and testing of strong gravity region have become possible

- ✓ The shape and the size of shadows are closely connected with the properties of the spacetime, e.g. , photon sphere

e.g. [A. Grenzebach + (2014), (2015)], [V. Perlick + (2021)]

- ✓ Photon sphere also plays an important role in gravitational physics; gravitational waves and gravitational lensing

e.g. [V. Caldoso + (2014)], [K. S. Virbhadra + (2002)]

Previous works

Behavior of light rays in any static spherically symmetric spacetime

Deflection angle of light

For an unstable photon sphere:

Divergent logarithmically

For a marginally stable photon sphere:

Divergent power functionally

[N.Tsukamoto (2017), (2020)]

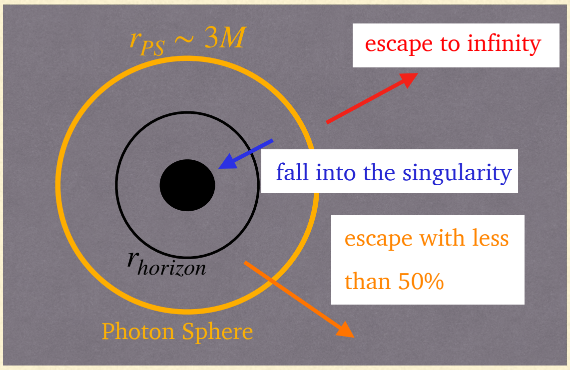

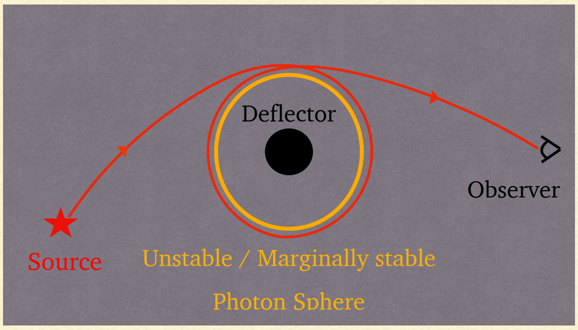

For a stable photon sphere (SPS)

[RK and H.Asada (2022)]

- ✓ Total angle change is described by inverse trigonometric function
- ✓ The light rays are bound orbits

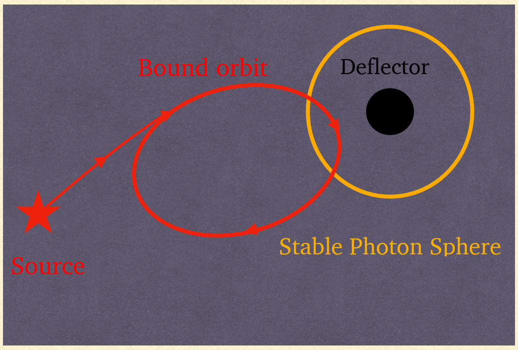

- If a source and an observer are located outside of SPS, then we cannot take the strong deflection limit ($r_0 \rightarrow r_{PS}$)

➡ Total angle change does not diverge

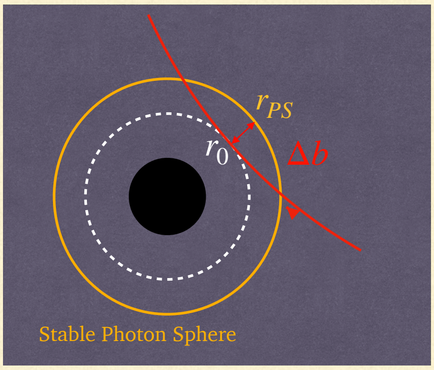

Motivation

To test the theory of gravity in the strong gravity region.

Investigate the behavior of light in the strong gravity region in less symmetric spacetimes

Clarify the difference between static spherically symmetric spacetime and static cylindrically symmetric spacetime

- ✓ Deflection angle of light
- ✓ Black hole shadow

CONTENTS

Equations of light rays

$G = c = 1$

✓ <u>Assumption:</u> static cylindrically symmetric spacetime

Metric: $ds^2 = -A(\rho)dt^2 + B(\rho)d\rho^2 + C(\rho)dz^2 + D(\rho)d\phi^2$

$$A > 0, \quad B > 0, \quad C > 0, \quad D > 0$$

Tangent vector: $k^\mu = \dfrac{dx^\mu}{d\lambda} =: \dot{x}^\mu$

✓ Null condition:

$$A(\rho)B(\rho)\dot{\rho}^2 + L_z^2 V(\rho) = E^2, \;\; V(\rho) := A(\rho)\left[P_z^2 L_z^{-2} C(\rho)^{-1} + D(\rho)^{-1}\right]$$

✓ Constants of motion:

$$E := -k_\mu \xi^\mu_{(t)} = A(\rho)\dot{t},$$

$$P_z := k_\mu \xi^\mu_{(z)} = C(\rho)\dot{z},$$

$$L_z := k_\mu \xi^\mu_{(\phi)} = D(\rho)\dot{\phi}$$

Definition of photon cylinder

$' \equiv d/d\rho$

$$\boxed{V(\rho_c) = E^2/L_z^2, \quad V'(\rho_c) = 0}$$

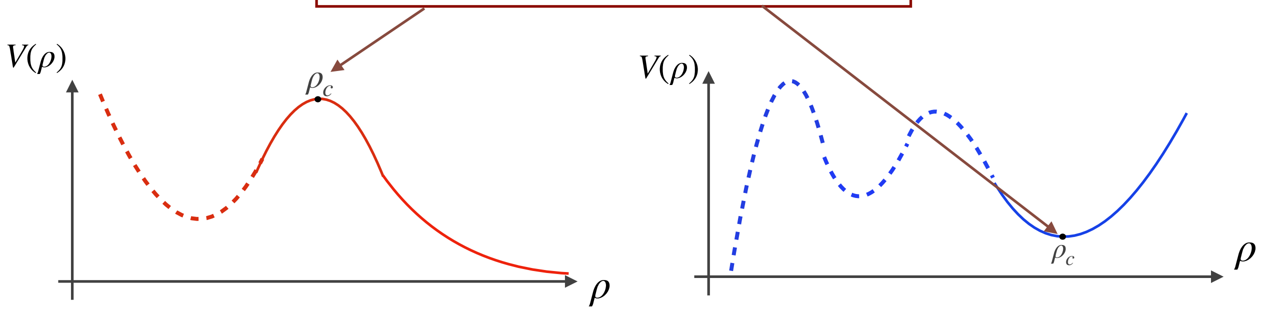

We define <u>Photon Cylinder</u> as the hypersurface $\{\rho = \rho_c\}$

$$V'(\rho) = A(\rho)\left[P_z^2/L_z^2 F(\rho)C(\rho)^{-1} + G(\rho)D(\rho)^{-1}\right]$$

$$F(\rho) := A'(\rho)A(\rho)^{-1} - C'(\rho)C(\rho)^{-1},$$

$$G(\rho) := A'(\rho)A(\rho)^{-1} - D'(\rho)D(\rho)^{-1}$$

Example (Levi-Civita Solution) [Levi-Civita (1919)]

Metric: $ds^2 = -R^{\frac{4\sigma}{\Sigma}}dt^2 + d\rho^2 + R^{-\frac{4\sigma(1-2\sigma)}{\Sigma}}dz^2 + a^{-1}R^{\frac{2(1-2\sigma)}{\Sigma}}d\phi^2$

$$0 < \sigma < 1/2, \quad R := \Sigma\rho, \quad \Sigma := 4\sigma^2 - 2\sigma + 1$$

Effective potential: $V(\rho) = R^{\frac{8\sigma(1-\sigma)}{\Sigma}}\left[\frac{P_z^2}{L_z^2} + R^{-\frac{2\sigma(1-4\sigma^2)}{\Sigma}}\right]$

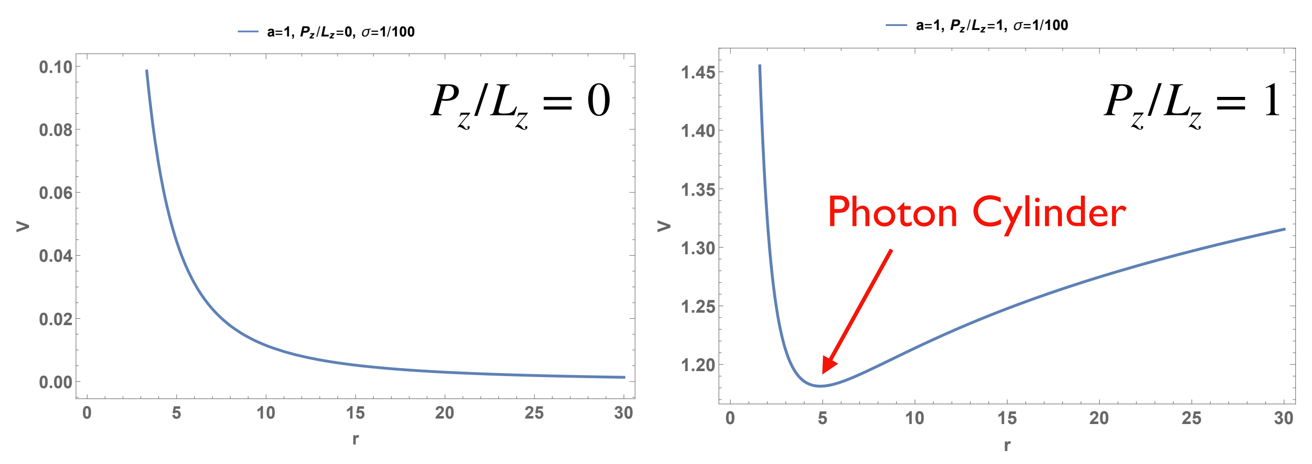

$P_z/L_z = 0$

$P_z/L_z = 1$

Photon Cylinder

CONTENTS

1. Introduction

2. Equations of light rays and definition of photon cylinder

3. Properties of photon cylinder

4. Summary

Photon cylinder $\Longleftrightarrow$ Photon surface?

Photon surface:

one of the generalized concepts of the photon sphere

based on only the property that any null geodesic initially tangent $S = \{r = 3M\}$ will remain tangent to S.

[C. M. Claudel + (2001)]

Let us check whether the hypersurface is a photon surface or not, by calculating the following equations;

$$\boxed{\begin{gathered}\chi_{ab}k^a k^b = 0, \quad \forall k^a \in T_pS \quad \forall p \in S \\ \Updownarrow \\ \sigma_{ab} = 0\end{gathered}}$$

$\chi_{ab} := \nabla_a n_b$: second fundamental form, $n_\mu dx^\mu = \sqrt{B}dr$: normal unit vector,

$\sigma_{ab} := \chi_{ab} - \dfrac{\chi}{3}h_{ab}$: trace-free part, $\chi = h^{ab}\chi_{ab}$, h_{ab} : induced metric

---

$$\chi_{ab}k^a k^b = -\frac{L_z^2}{2\sqrt{B}}\left[\frac{P_z^2}{L_z^2}\frac{F}{C} + \frac{G}{D}\right] = -\frac{L_z^2 V'}{2A\sqrt{B}}$$

$$\sigma_{tt} = -\frac{A}{6\sqrt{B}}(F+G), \quad \sigma_{zz} = \frac{C}{6\sqrt{B}}(G-2F), \quad \sigma_{\phi\phi} = \frac{D}{6\sqrt{B}}(F-2G)$$

$$\forall k^a \iff \forall P_z/L_z, \quad F(\rho) = G(\rho) = 0 \implies \chi_{ab}k^a k^b = \sigma_{ab} = 0$$

$S = \left\{\rho_m \in \mathbb{R} \,\middle|\, G(\rho_m) = 0, \ F(\rho_m) = 0\right\}$: Photon Surface

ρ_m is the radius of a photon surface

Stability of photon cylinder

$V''(\rho_c) > 0\ (<0, =0) \implies$ the photon cylinder is stable (unstable, marginally stable)

- ✓ For $F(\rho_c) \neq 0$ and $G(\rho_c) \neq 0$,

$$V''(\rho_c) = \frac{A_c}{D_c}\left[G_c' + G_c\left(G_c - F_c - \frac{F_c'}{F_c}\right)\right]$$

- ✓ For $F(\rho_m) = 0$ and $G(\rho_m) = 0$ (photon surfaces),

$$V''(\rho_m) = A_m\left[\frac{P_z^2}{L_z^2}\frac{F_m'}{C_m} + \frac{G_m'}{D_m}\right]$$

Example 1. (Levi-Civita Solution)

Metric: $ds^2 = -R^{\frac{4\sigma}{\Sigma}}dt^2 + d\rho^2 + R^{-\frac{4\sigma(1-2\sigma)}{\Sigma}}dz^2 + a^{-1}R^{\frac{2(1-2\sigma)}{\Sigma}}d\phi^2$

$$0 < \sigma < 1/2, \quad R := \Sigma\rho, \quad \Sigma := 4\sigma^2 - 2\sigma + 1$$

$$F(\rho) = \frac{8\sigma(1-\sigma)}{R} > 0, \quad G(\rho) = -\frac{2(1-4\sigma)}{R}$$

There exists **no** ρ_m such that $F(\rho_m) = G(\rho_m) = 0$

But

For $0 < \sigma < 1/4$, there exist $\{\rho_c\}$ such that

$$V'(\rho_c) = \frac{P_z^2}{L_z^2}\frac{F(\rho_c)}{C(\rho_c)} + \frac{G(\rho_c)}{D(\rho_c)} = 0$$

- ✓ Stability of photon cylinder

If $0 < \sigma < 1/4$ and $a > 0$,

$$V''(\rho_c) = \frac{4a(1-4\sigma)(1-2\sigma)(1+2\sigma)}{R_c^{4(1-\sigma)(1-2\sigma)/\Sigma}} > 0$$

➡ Photon cylinder in LC spacetime is stable

- ✓ Shape of photon cylinder

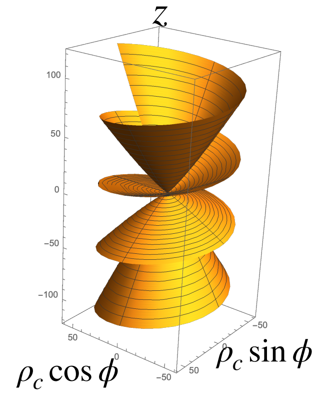

Insert $P_z^2/L_z^2 = -C(\rho_c)G(\rho_c)/D(\rho_c)F(\rho_c)$

into $$\frac{dz}{d\phi} = \frac{\dot{z}}{\dot{\phi}} = \frac{P_z}{L_z}\frac{D(\rho_c)}{C(\rho_c)}$$

And plot $\gamma_{\rho_c}(\phi) = \left(\rho_c \cos\phi, \rho_c \sin\phi, z(\phi)\right)$

Example 2. (Conformal Weyl Gravity)

[J. L. Said + (2012)]

Metric: $ds^2 = -f(\rho)dt^2 + f(\rho)^{-1}d\rho^2 + a^2\rho^2dz^2 + \rho^2d\phi^2$

$$f(\rho) = \frac{\beta}{\rho} + \sqrt{\frac{3\beta\gamma}{4}} + \frac{\gamma\rho}{4} + k^2\rho^2, \quad \beta < 0, \ \ \gamma < 0$$

$$F(\rho) = G(\rho) = \frac{1}{\rho^2 f(\rho)}\left(\sqrt{\frac{|\gamma|}{2}}\rho - \sqrt{3|\beta|}\right)^2$$

➡ There exists a photon surface at $\rho_m = 2\sqrt{3\beta/\gamma}$

It is marginally stable

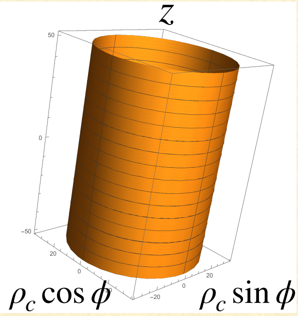

$$\because \quad V''(\rho_m) \propto \left(\sqrt{\frac{|\gamma|}{2}}\rho_m - \sqrt{3|\beta|}\right) = 0$$

CONTENTS

Summary

- Photon cylinder is defined as the hypersurface $\left\{\rho = \rho_c \mid P_z^2/L_z^2 F(\rho_c) C(\rho_c)^{-1} + G(\rho_c) D(\rho_c)^{-1} = 0\right\}$
- In static cylindrical symmetric spacetimes, Photon Surfaces are the hypersurface $\left\{\rho = \rho_m \,\middle|\, G(\rho_m) = 0, \;\; F(\rho_m) = 0\right\}$

Future works

- ✓ Investigate more details of structure of photon cylinder
- ✓ Calculate the shadows and the deflection angle
- ✓ Expand to stationary axisymmetric spacetime

C78

Amo, Izumi, Shiromizu, Tomikawa, Yoshino, in prep.

Generalization of photon sphere referring to null infinity

Masaya Amo YITP, Kyoto U

Collaborators: Keisuke Izumi, Tetsuya Shiromizu, Yoshimune Tomikawa, Hirotaka Yoshino

---

Black Holes

- Predicted by GR.
- Cannot be connected to $\mathscr{I}^+$ by causal curve.
- BHs have no effect on observers outside of BHs.

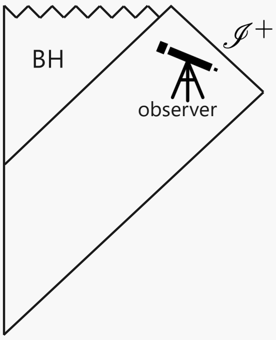

Redefining (something like) BH connected to $\mathscr{I}^+$ by causal curve

Photon sphere

- Defined in static & spherical symmetric spacetimes
- Collection of circular photon orbits ($r = 3M$ in Schwarzschild)
- Edge of BH shadow
- Mathematically rich structures

photon sphere

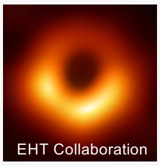

BH shadow

Generalize photon sphere to spacetimes w/o symmetry!

Previous attempts to generalize photon sphere

ex.) Yoshino et al. (2017), Yoshino et al. (2019), Siino (2021).

Applicable spacetimes for several attempts:

applicable not applicable

Def. 1 : 🙆 stationary spacetimes / 🙅 dynamical spacetimes.

Def. 2 : 🙆 some dynamical spacetimes / 🙅 rapidly rotating BHs.

Def. 3 : 🙆 rapidly rotating BHs / 🙅 photon spheres w/o BHs.

… anyway, case-by-case definitions, so far.

Let’s consider more comprehensive definition!

Outline

1. Introduction

2. Definition of dark horizon

3. Property of dark horizon

4. Examples

5. Conclusion

Def. of dark horizon

Escape Cone

spacelike hypersurface

Consider directions of photon reaching $\mathscr{I}^+$ projected on Σ.

→ Collection of these directions on two-sphere is escape cone.

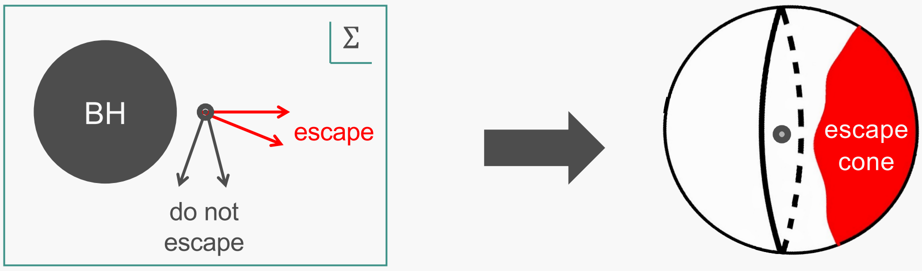

Escape cone in Schwarzschild

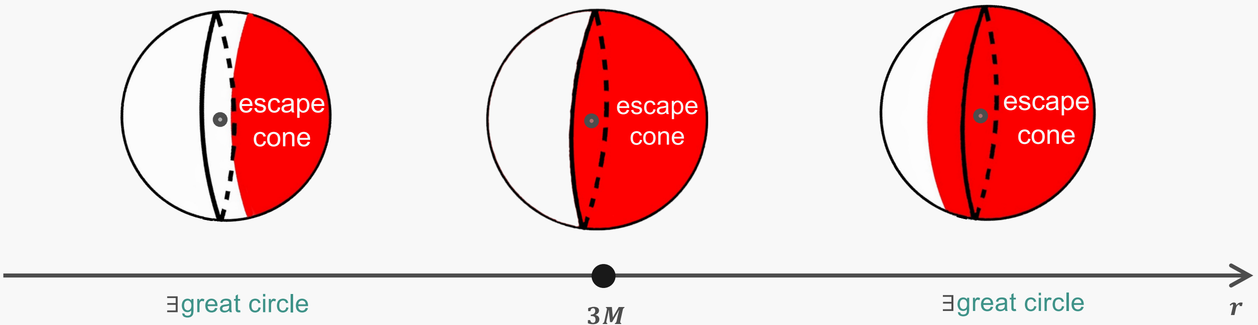

∃great circle
outside of escape cone

$3M$
photon sphere

∃great circle
inside of escape cone

※ great circle：inter section of sphere and plane containing the center of the sphere

---

※depend on projected hypersurface Σ

Generalization of photon sphere：dark horizon

Classify points in spacetime into three regions：

∃great circle
outside of escape cone

Set of points on this bdry.
is called ``inner dark horizon”

∀great circle
intersect bdry. of escape cone

∃great circle
inside of escape cone

Set of points on this bdry.
is called ``outer dark horizon”

distance
to BH

collectively called ``dark horizon”

Outline

1. Introduction
2. Definition of dark horizon
3. **Property of dark horizon**
4. Examples
5. Conclusion

Property of dark horizon

Spherical symmetric spacetime

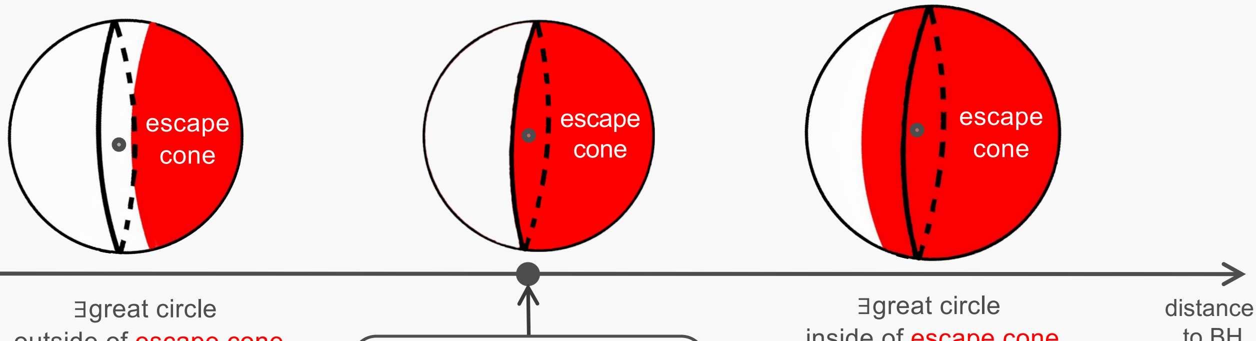

∃great circle
outside of escape cone

∃great circle
inside of escape cone

distance
to BH

inner dark horizon
= outer dark horizon
= photon sphere (if static)

Property of dark horizon

General properties (independent of spacetime symmetry)

Inner dark horizon is located ``inner” than outer dark horizon,
or they coincide.

based on Amo, Izumi, Shiromizu, Tomikawa, Yoshino (2021a, 2021b, 2022)

Two dark horizons both exist in BH spacetimes
when radiation is not so strong（compared to Planck luminosity）

Outline

Kerr BH

Amo, Izumi, Shiromizu, Tomikawa, Yoshino, in prep.

Mass： $M = 1$， Kerr parameter：a $(0 \leq a \leq 1)$

: inner dark horizon

: outer dark horizon

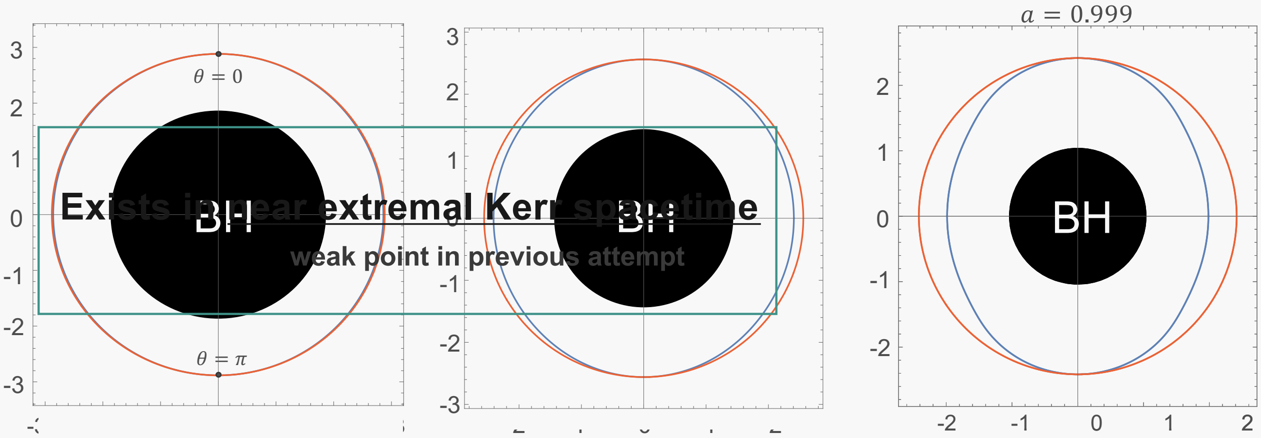

Exists in near extremal Kerr spacetime

weak point in previous attempt

Ingoing Vaidya

Amo, Izumi, Shiromizu, Tomikawa, Yoshino, in prep.
cf.) Koga, Asaka, Kimura, Okabayashi (2022).

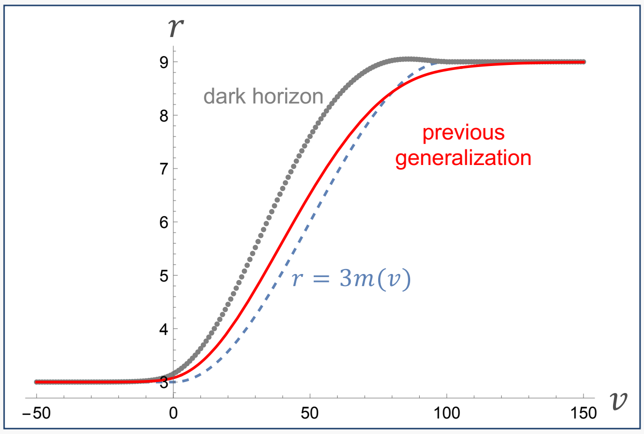

- Dark horizon exists.
- Differs from previous generalization (due to assumed position of light source)

Outline

1. Introduction
2. Definition of dark horizon
3. Property of dark horizon
4. Examples
5. **Conclusion**

Conclusion

Summary

- Proposed dark horizon, a generalization of photon sphere
- Explicit plot in Kerr & Vaidya
- Overcome some weak points in previous generalization

Future Work

- Dark horizon in other spacetimes?
- Correspondence to shadow observations?
- Dependence on spacelike hypersurface Σ?

Back Up

Area inequality

[A_P: area of outermost photon sphere, A_S: area of shadow, A_H: area of horizon, M: BH mass]

① Penrose inequality（conjecture, without assuming symmetry of spacetime）

$$\left(\frac{3}{2}\right)^2 A_H \leq 4\pi(\mathbf{3}M)^2$$

② Area inequality for photon sphere (static & spherical symmetry)

$$\left(\frac{3}{2}\right)^2 A_H \leq A_P \leq 4\pi(3M)^2$$

Discuss area inequality foer photon sphere without assuming symmetry of spacetime.

Outgoing Vaidya

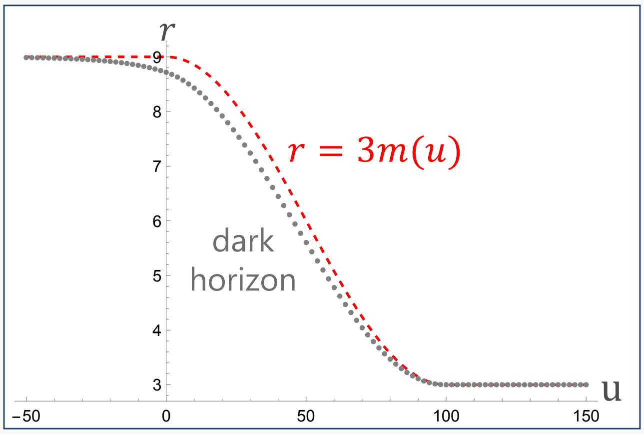

Minkowski spacetime

There is no boundary.

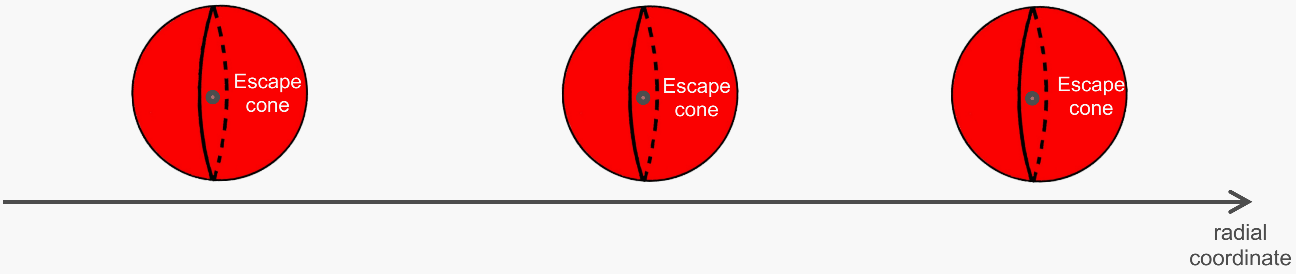

Dark horizon does not exists in Minkowski spacetime.

C79

JGRG31, Oct 28th

Four types of attractive gravity probe surfaces

Graduate School of Mathematics, Nagoya Univ.
Kangjae Lee

K. Lee, T. Shiromizu and K. Izumi, Phys. Rev. D 105, no.4, 044037 (2022)
K. Lee, T. Shiromizu, K. Izumi, H. Yoshino and Y. Tomikawa, Phys. Rev. D 106, no.6, 064028 (2022)

Contents

1. Introduction

Generalized gravity region from photon sphere

Trapped Surface (TS) : proposed for strong gravity region

➡ **singularity theorem** Penrose (1965) : proved by using TS

Penrose inequality Penrose (1973) : area inequality for apparent horizon

However, TS cannot be observed because blackhole envelope it!

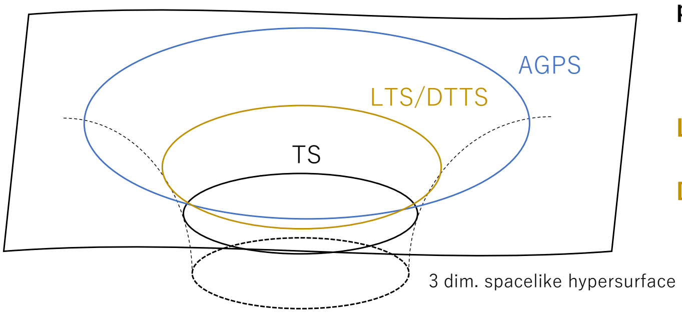

photon sphere : unstable circular photon orbit in Schwarzschild BH

⬇ **Generalize**

Loosely Trapped Surface (LTS)
Shiromizu, Tomikawa, Izumi and Yoshino (2017)

Dynamically Transversely Trapping Surface (DTTS)
Yoshino, Izumi, Shiromizu and Tomikawa (2020)

⬇ **Generalize LTS for weak gravity**

Attractive Gravity Probe Surface (AGPS)
Izumi, Tomikawa, Shiromizu and Yoshino (2021)

Area inequalities

A : area , $\mathcal{R}$: measure of size
m : mass
J : angular momentum

Minimal Surface (MS)	Loosely Trapped Surface (LTS) / Dynamically Transverse Trapping Surface (DTTS)	Attractive Gravity Probe Surface (AGPS)
Jang & Wald, Huisken & Ilmanen, Bray $m \geq \sqrt{\frac{A}{16\pi}}$	Shiromizu et al. / Yoshino et al. $m \geq \sqrt{\frac{A}{36\pi}}$	Izumi et al. $m \geq \frac{1+2\alpha}{3+4\alpha}\sqrt{\frac{A}{4\pi}} \quad (\alpha > -1/2)$
Anglada $m^2 \geq \frac{A}{16\pi} + \frac{J^2}{\mathcal{R}^2}$	**Our study**	

Area inequalities with ang. mom.

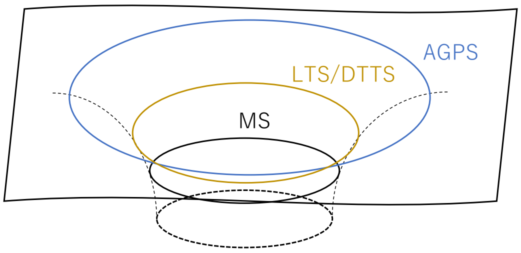

Refine area inequalities for AGPS by taking account of contribution from angular momentum, gravitational waves and matters

2. Attractive gravity probe surface

Classification of Attractive Gravity Probe Surface

LTS → **Longitudinal AGPS**
Loosely Trapped Surface generalize

- **LAGPS-k** : use mean curvature
- **LAGPS-r** : use scalar curvature

DTTS → **Transverse AGPS**
Dynamically Transversely Trapping Surface generalize

- **TAGPS-k** : use mean curvature
- **TAGPS-r** : use scalar curvature

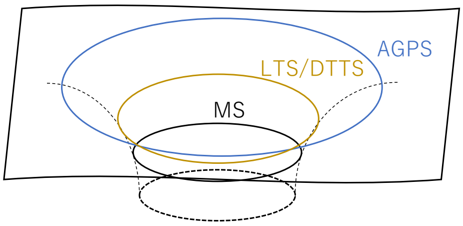

LAGPS : consider variation with respect to **orthogonal** to surface

TAGPS : consider variation with respect to **tangential** to surface

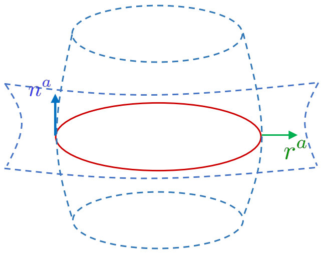

In this talk, I focus LAGPS-k

Longitudinal Attractive Gravity Probe Surface-k

MS photon sphere

For 2-sphere σ_0 in Schwarzschild spacetime, $k=\frac{2}{r}\sqrt{1-\frac{2m}{r}}$, ${}^{(3)}\pounds_r k = -\frac{2}{r^2}\left(1-\frac{3m}{r}\right)$ → k is maximal at $r=3m$

σ_0 : LTS $\overset{\text{def}}{\Longleftrightarrow}$ $\begin{cases} k>0 \\ {}^{(3)}\pounds_r k \geq 0 \end{cases}$
2-surface
in spacelike hypersurface

Shiromizu, Tomikawa, Izumi and Yoshino (2017)

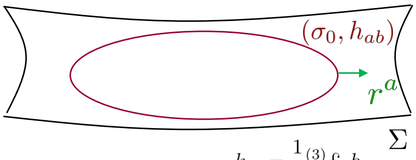

$k_{ab}=\frac{1}{2}{}^{(3)}\pounds_r h_{ab}$

Generalize LTS for weak gravity

σ_0 : LAGPS-k $\overset{\text{def}}{\Longleftrightarrow}$ $\begin{cases} k>0 \\ {}^{(3)}\pounds_r k \geq \alpha k^2 \quad (\alpha > -1/2) \end{cases}$
2-surface in spacelike hypersurface

Izumi, Tomikawa, Shiromizu and Yoshino (2021)

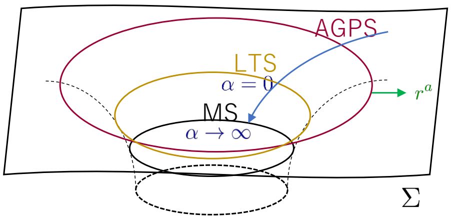

In Schwarzschild spacetime, $\frac{{}^{(3)}\pounds_r k}{k^2} \geq \alpha$ → $r \leq \frac{3+4\alpha}{1+2\alpha}m$

Area inequality for LAGPS-k

Assume： Asymptotic flat spacelike hypersurface Σ with ${}^{(3)}R \geq 0$
is foliated by $\{\sigma_y\}_{y\in\mathbb{R}}$ in inverse mean curvature flow where $\sigma_y \approx S^2$
and σ_0 is LAGPS-k. area of σ_y: $A(y) = A_0 \exp y$

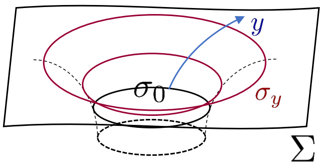

monotonicity of Geroch energy
& definition of LAGPS-k

$$\boxed{m_{\rm ADM} \geq \frac{1+2\alpha}{3+4\alpha}\mathcal{R}_{A0} \qquad (\alpha > -1/2)}$$

$$\begin{cases} \text{areal radius } \mathcal{R}_{A0} := \sqrt{\dfrac{A_0}{4\pi}} \\ m_{\rm ADM} \text{ : ADM mass} \end{cases}$$

Izumi, Tomikawa, Shiromizu and Yoshino (2021)

$$\begin{cases} \alpha \to \infty & (S_{\rm MS}) \quad \mathcal{R}_{A0} \leq 2m_{\rm ADM} \\ \alpha = 0 & (S_{\rm LTS}) \quad \mathcal{R}_{A0} \leq 3m_{\rm ADM} \\ \alpha \to -1/2 & (S_{\infty}) \quad \text{No upper bound of } \mathcal{R}_{A0} \end{cases}$$

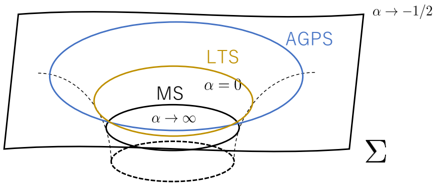

---

3. Refined area inequalities with angular momentum

Theorem (LAGPS-k)

Lee, Shiromizu and Izumi (2022)

Let Σ be asymptotic flat spacelike maximal hypersurface equipped by inverse mean curvature flow $\{\sigma_y\}_{y\in\mathbb{R}}$ with $\sigma_y \approx S^2$, where σ_0 is LAGPS-k. Assuming that the energy density of matters is nonnegative.

We have an inequality for the LAGPS-k σ_0,

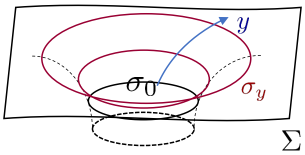

$$m_{\rm ADM} - \left(m_{\rm ext} + \frac{3}{3+4\alpha}m_{\rm int}\right) \geq \frac{1+2\alpha}{3+4\alpha}\mathcal{R}_{A0} + \frac{1}{\mathcal{R}_{A0}^3}\left(\frac{3}{3+4\alpha}\bar{J}_0^2 + \bar{J}_{\rm min}^2\right)$$

$$\geq \frac{1+2\alpha}{3+4\alpha}\mathcal{R}_{A0} + 2\frac{3+2\alpha}{3+4\alpha}\frac{\bar{J}_{\rm min}^2}{\mathcal{R}_{A0}^3} \quad (\alpha > -1/2)$$

$m_{\rm ADM}$: ADM mass , $\mathcal{R}_{A0}$: areal radius of σ_0

$m_{\rm ext} := 2\pi\int_0^\infty dy\mathcal{R}_A^3\bar{\rho}_{\rm tot}$: exterior energy , $m_{\rm int} := \frac{4\pi}{3}\mathcal{R}_{A0}^3\bar{\rho}_{\rm tot0}$: internal energy

$\bar{\rho}_{\rm tot}(y) := \frac{1}{A}\int_{\sigma_y} dA\rho_{\rm tot}(y)$, $\rho_{\rm tot} := \rho + \rho_{\rm gw}$, $8\pi\rho_{\rm gw} := \frac{1}{2}(\tilde{\kappa}_{ab}\tilde{\kappa}^{ab} + \tilde{k}_{ab}\tilde{k}^{ab})$: energy density of gravitational waves

$\left(8\pi\bar{J}(y)\right)^2 := \frac{A^2}{6\pi}\int_{\sigma_y} v_a v^a dA$: area averaged angular momentum , $v_a := h_a^b r^c K_{bc}$, $\kappa_{ab} := h_a^c h_b^d K_{cd}$

$\bar{J}_{\rm min} := \min\limits_{\{\sigma_y\}}\bar{J}(y)$

Sketch of proof

$$\begin{cases} m_{\rm ext} := 2\pi\int_0^\infty dy\mathcal{R}_A^3\bar{\rho}_{\rm tot} \\ m_{\rm int} := \frac{4\pi}{3}\mathcal{R}_{A0}^3\bar{\rho}_{\rm tot0} \\ \bar{\rho}_{\rm tot}(y) := \frac{1}{A}\int_{\sigma_y} dA\rho_{\rm tot}(y) \end{cases} \quad \begin{cases} \rho_{\rm tot} := \rho + \rho_{\rm gw} \\ 8\pi\rho_{\rm gw} := \frac{1}{2}(\tilde{\kappa}_{ab}\tilde{\kappa}^{ab} + \tilde{k}_{ab}\tilde{k}^{ab}) \end{cases}$$

$$\begin{cases} \left(8\pi\bar{J}(y)\right)^2 := \frac{A^2}{6\pi}\int_{\sigma_y} v_a v^a dA \\ v_a := h_a^b r^c K_{bc} \end{cases}$$

maximal slice, inverse mean curvature flow
and nonnegative energy density

Monotonicity of Geroch energy + asymptotically flatness

$$m_{\rm ADM} - \frac{\mathcal{R}_{A0}}{2} + \frac{\mathcal{R}_{A0}}{32\pi}\int_{\sigma_0} dAk^2 \geq 2\pi\int_0^\infty dy\mathcal{R}_A(y)^3\bar{\rho}_{\rm tot}(y) + \frac{1}{16\pi}\int_0^\infty dy\mathcal{R}_A(y)\int_{\sigma_y} dAv^a v_a \geq 0$$

Definition of LAGPS-k + maximal slice

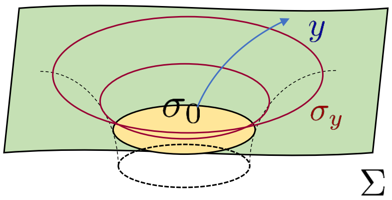

$$\left(1+\frac{4}{3}\alpha\right)\int_{\sigma_0} dAk^2 \leq \frac{16\pi}{3} - \frac{2}{3}\int_{\sigma_0} dA(16\pi\rho_{\rm tot} + 2v_a v^a) \leq \frac{16\pi}{3}$$

$$m_{\rm ADM} - \left(m_{\rm ext} + \frac{3}{3+4\alpha}m_{\rm int}\right) \geq \frac{1+2\alpha}{3+4\alpha}\mathcal{R}_{A0} + \frac{1}{\mathcal{R}_{A0}^3}\left(\frac{3}{3+4\alpha}\bar{J}_0^2 + \bar{J}_{\rm min}^2\right) \quad (\alpha > -1/2)$$

Result

$m_{\rm int}$: internal energy

$p_r^{({\rm int})}$: internal radial pressure

Longitudinal Attractive Gravity Probe Surface (LAGPS-k) $(\alpha > -1/2)$

$$m_{\rm ADM} - \left(m_{\rm ext} + \frac{3}{3+4\alpha}m_{\rm int}\right) \geq \frac{1+2\alpha}{3+4\alpha}\mathcal{R}_{A0} + \frac{1}{\mathcal{R}_{A0}^3}\left(\frac{3}{3+4\alpha}\bar{J}_0^2 + \bar{J}_{\rm min}^2\right)$$

Transverse Attractive Gravity Probe Surface (TAGPS-k)

$$m_{\rm ADM} + \frac{3}{3+4\beta}p_r^{({\rm int})} - m_{\rm ext} \geq \frac{1+2\beta}{3+4\beta}\mathcal{R}_{A0} + \frac{1}{\mathcal{R}_{A0}^3}\left(\frac{3}{3+4\beta}\bar{J}_0^2 + \bar{J}_{\rm min}^2\right)$$

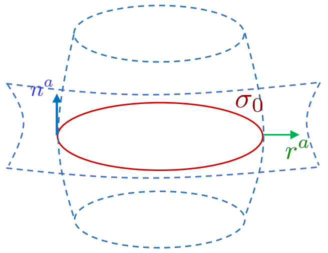

LAGPS-k, TAGPS-k → MS $(\alpha, \beta \to \infty)$

$$m_{\rm ADM} - m_{\rm ext} \geq \frac{\mathcal{R}_{A0}}{2} + \frac{\bar{J}_{\rm min}^2}{\mathcal{R}_{A0}^3}$$

$$\Rightarrow (m_{\rm ADM} - m_{\rm ext})^2 \geq \left(\frac{\mathcal{R}_{A0}}{2}\right)^2 + \frac{\bar{J}_{\rm min}^2}{\mathcal{R}_{A0}^2} + \left(\frac{\bar{J}_{\rm min}^2}{\mathcal{R}_{A0}^3}\right)^2 \geq \left(\frac{\mathcal{R}_{A0}}{2}\right)^2 + \frac{\bar{J}_{\rm min}^2}{\mathcal{R}_{A0}^2} \Rightarrow m^2 \geq \frac{A}{16\pi} + \frac{J^2}{\mathcal{R}^2}$$

Anglada (2018)

For equality, the area is same with $A_{\rm Kerr} := 8\pi m(m + \sqrt{m^2 - J^2/m^2})$

Inequality for mass and angular momentum

$$m_{\rm ADM} - \left(m_{\rm ext} + \frac{3}{3+4\alpha}m_{\rm int}\right) \geq \frac{1+2\alpha}{3+4\alpha}\mathcal{R}_{A0} + \frac{1}{\mathcal{R}_{A0}^3}\left(\frac{3}{3+4\alpha}\bar{J}_0^2 + \bar{J}_{\rm min}^2\right) \quad (\alpha > -1/2)$$

for vacuum & axially symmetric case,

prolate σ_0 ⇒ $m_{\rm ADM} \geq \eta_\alpha^{1/2}|J|^{1/2}$

$\eta_\alpha := \left[\frac{2(1+2\alpha)}{3+4\alpha}\right]^{3/2}(1+\chi_\alpha)^{1/2}$, $\frac{1}{3+4\alpha} \leq \chi_\alpha \leq \frac{5}{3+4\alpha}$

Komar angular momentum $J(y) := \frac{1}{8\pi}\int_{\sigma_y} v^a\phi_a dA$

ϕ^a : axial Killing vector

$v_a := h_a^b r^c K_{bc}$

$\alpha \to \infty$ **(MS),**

$m_{\rm ADM} \geq |J|^{1/2}$ Dain (2008) : For vacuum, axisymmetric, asymptotically flat, maximal Σ,
Dain proved this inequality where initial data close to extreme Kerr.

4. Summary

Summary

We proved area inequalities for AGPS taking account of contribution from angular momentum, gravitational waves and matters.

$$\text{LAGPS-k} \overset{\text{def}}{\Longleftrightarrow} \begin{cases} k > 0 \\ {}^{(3)}\pounds_r k \geq \alpha k^2 \end{cases}$$

Longitudinal Attractive Gravity Probe Surface (LAGPS-k)

$$m_{\mathrm{ADM}} - \left(m_{\mathrm{ext}} + \frac{3}{3+4\alpha} m_{\mathrm{int}} \right) \geq \frac{1+2\alpha}{3+4\alpha} \mathcal{R}_{A0} + \frac{1}{\mathcal{R}_{A0}^3} \left(\frac{3}{3+4\alpha} \bar{J}_0^2 + \bar{J}_{\mathrm{min}}^2 \right) \quad (\alpha > -1/2)$$

Transverse Attractive Gravity Probe Surface (TAGPS-k)

$$m_{\mathrm{ADM}} + \frac{3}{3+4\beta} p_r^{(\mathrm{int})} - m_{\mathrm{ext}} \geq \frac{1+2\beta}{3+4\beta} \mathcal{R}_{A0} + \frac{1}{\mathcal{R}_{A0}^3} \left(\frac{3}{3+4\beta} \bar{J}_0^2 + \bar{J}_{\mathrm{min}}^2 \right)$$

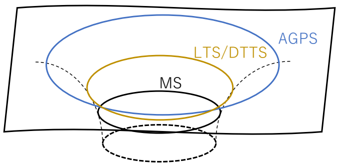

Contribution of charge and EM fields?

Non maximal spacelike hypersurface?

Relax restrictions of parameter?

$$\begin{cases} m_{\mathrm{ext}} := 2\pi \int_0^\infty dy \mathcal{R}_A^3 \bar{\rho}_{\mathrm{tot}} \ , \quad m_{\mathrm{int}} := \frac{4\pi}{3} \mathcal{R}_{A0}^3 \bar{\rho}_{\mathrm{tot0}} \ , \quad \bar{\rho}_{\mathrm{tot}}(y) := \frac{1}{A} \int_{\sigma_y} dA \rho_{\mathrm{tot}}(y) \\ p_r^{(\mathrm{int})} := \frac{4\pi}{3} \mathcal{R}_{A0}^3 \bar{P}_{r0}^{(\mathrm{tot})} \ , \quad \bar{P}_{r0}^{(\mathrm{tot})} = \frac{1}{A_0} \int_{\sigma_0} P_r^{(\mathrm{tot})} dA \\ \rho_{\mathrm{tot}} := \rho + \rho_{\mathrm{gw}} \ , \quad P_r^{(\mathrm{tot})} = P_r + P_r^{(\mathrm{gw})} \ , \quad 8\pi P_r^{(\mathrm{gw})} = \frac{1}{2} (\tilde{k}_{ab} \tilde{k}^{ab} + \tilde{\kappa}_{ab} \tilde{\kappa}^{ab}) = 8\pi \rho_{\mathrm{gw}} \\ \left(8\pi \bar{J}(y) \right)^2 := \frac{A^2}{6\pi} \int_{\sigma_y} v_a v^a dA \ , \quad v_a := h_a^b r^c K_{bc} \ , \quad \bar{J}_{\mathrm{min}} := \min_{\{\sigma_y\}} \bar{J}(y) \end{cases}$$

Appendix

Transverse Attractive Gravity Probe Surface-k

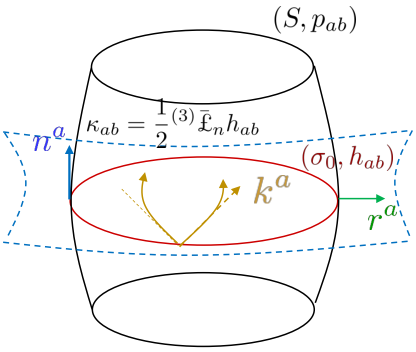

k^a : null tangent on S

$\bar{K}_{ab}$: extrinsic curvature on S

$\bar{K}_{ab} = \frac{1}{2}\pounds_r p_{ab}$

lapse function of n^a is constant

In Schwarzschild spacetime, for photon surface S, ${}^{(3)}\bar{\pounds}_n \kappa = \frac{2}{r^2}\left(1 - \frac{3m}{r}\right)$

σ_0 : DTTS $\overset{\text{def}}{\Longleftrightarrow}$ $\begin{cases} \kappa = 0 \ : ① \\ \max(\bar{K}_{ab}k^a k^b) = 0 \ : \text{transversely trapped} \\ {}^{(3)}\bar{\pounds}_n \kappa \leq 0 \ : ② \end{cases}$

2-surface
in spacelike hypersurface

①&② → maximal with respect to time

Yoshino, Izumi, Shiromizu and Tomikawa (2020)

Generalize DTTS for weak gravity

σ_0 : TAGPS-k $\overset{\text{def}}{\Longleftrightarrow}$ $\begin{cases} \kappa = 0 \\ \max(\bar{K}_{ab}k^a k^b) \leq -\beta k \\ {}^{(3)}\bar{\pounds}_n \kappa \leq 0 \end{cases}$

2-surface in spacelike hypersurface

Izumi, Tomikawa, Shiromizu and Yoshino (2021)

In Schwarzschild spacetime, $\max(\bar{K}_{ab}k^a k^b) \leq -\beta k$ ⇒ $r \leq \frac{3+4\beta}{1+2\beta}m$

Area averaged angular momentum

$$\left(8\pi \bar{J}(y)\right)^2 := \frac{A^2}{6\pi}\int_{\sigma_y} v_a v^a dA \qquad v_a := h_a^b r^c K_{bc}$$

For axisymmetric case, $\bar{J}^2 \geq \left(\frac{\mathcal{R}_A}{\mathcal{R}_\phi}\right)^4 J^2$

ϕ^a : axial Killing vector

Komar angular momentum $J(y) := \frac{1}{8\pi}\int_{\sigma_y} v^a \phi_a dA$

$\frac{8\pi}{3}\mathcal{R}_\phi^4 := \int_{\sigma_y} \phi_a \phi^a dA$

In Kerr spacetime, $\int_{\sigma_y} v^a v_a dA = 24\pi \frac{a^2 m^2}{r^4} + O(a^4)$

➡ $\bar{J}^2 \simeq a^2 m^2 + O(a^4)$

C80

The 31st Workshop on General Relativity and Gravitation in Japan

Gravitational lens on the optical constant-curvature background

Keita Takizawa* (PhD student)
Collaborator: Hideki Asada

Hirosaki University, Japan

- Outline -

- Introduction
- Background for Gravitational lens
- Optical constant-curvature background
- BG dependence of Deflection angle
- Summary

- Outline -

- **Introduction**
- Background for Gravitational lens
- Optical constant-curvature background
- BG dependence of Deflection angle
- Summary

Introduction

Gravitational Lens

◉ Conventional configuration

Gravitational lens equation is a basic equation of lensing which relates a deflection angle of light to angular positions at an observer.

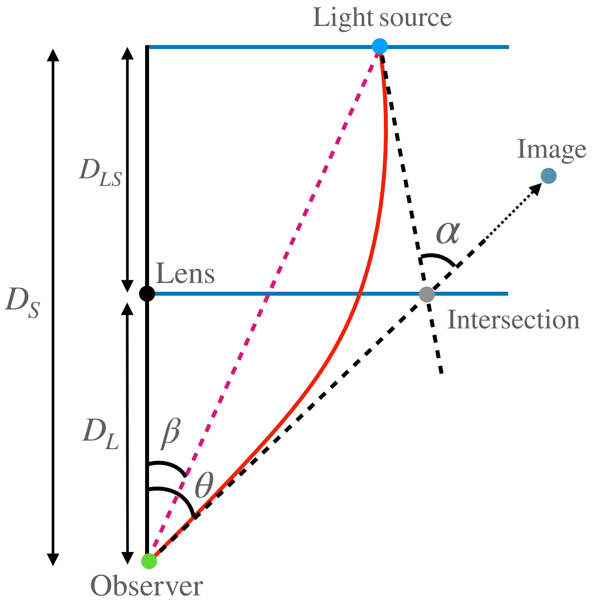

✓ Deflection angle of light

For Schwarzschild metric:

$$\alpha = \frac{4GM}{c^2 b} + O\left(\frac{M^2}{b^2}\right)$$

✓ Lens equation

$$\beta = \theta - \frac{D_{LS}}{D_S}\alpha$$

α : Deflection angle of light

β : Intrinsic position of light source

θ : Apparent position of light source (Observables)

Introduction

Conventional lensing method

- Assumptions in Conventional method

✓ Asymptotic flatness

A limit $r \to \infty$ is used for calculation of the deflection angle of light.

- It causes no problem in asymptotically flat spacetimes.

However,

- An asymptotically **non-flat** spacetime **does not allow** $r \to \infty$ limit

↳ A horizon crossing of a light ray can occur (Horizon crossing problem)

- In Astronomy, **distances between objects are finite**

↳ Contradiction: Lens equation includes distances as a finite value

---

Introduction

Extension beyond Conventional lensing method

- **Finite distance method**

✓ Deflection angle of light based on **Gauss-Bonnet theorem**
[Gibbons & Werner (2008)]

- Finite distance correction to the deflection angle of light [Ishihara+ (2016)]
- Improving to be valid even for asymptotically non-flat spacetimes [KT+ (2020a)]

✓ **Gravitational lens in Finite distance configuration**
[KT, Ono, Asada (2020b), KT & Asada (2021)]

- Lens equation consistent with the finite distance framework
- Application: Lensing in Weyl gravity model (Asymptotically non-flat spacetime)
- Finite distance effects in strong deflection limit

Is Minkowskian background valid for any spacetimes ?

- Motivation for Lensing on constant-curvature background

If the spacetime is **not Minkowskian asymptotically,**
can we take the flat BG ?

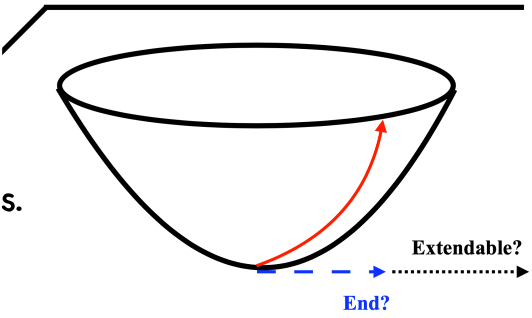

We investigate

a new the method which is valid for
GL on (optical) **constant-curvature** backgrounds.

- Outline -

- Introduction
- **Background for Gravitational lens**
- Optical constant-curvature background
- BG dependence of Deflection angle
- Summary

Background for Gravitational lens

Definition of Background

We consider that the light deflection
is caused by lens objects.

Lens parameter: $p_i = p_1\,,\, p_2\,,\cdots\, p_n$ (mass, spin, charge of BH, etc.)

Definition: Background spacetime as $p_i \to 0$

For a full metric including the lens objects:

$$ds^2 = g_{\mu\nu}(p_i)\,dx^\mu dx^\nu$$

a background metric is defined as

$$\bar{g}_{\mu\nu} \equiv g_{\mu\nu}(p_i)|_{p_i=0}$$

Background for Gravitational lens

Optical space

Unit: $c = 1\,,\, G = 1$

A static & spherically symmetric spacetime (Equatorial plane):

$$ds^2 = -A(r)dt^2 + B(r)dr^2 + C(r)d\phi^2$$

$$ds^2 = 0 \quad \longrightarrow \quad d\ell^2 \equiv \gamma_{IJ}dx^I dx^J$$
$$= \frac{B(r)}{A(r)}dr^2 + \frac{C(r)}{A(r)}d\phi^2$$

γ_{IJ} … <u>**Optical metric**</u> (Riemannian metric of light ray)

e.g. Asada & Kasai (2000),
Gibbons & Werner(2008)

Light ray: $\delta \int dt = 0$ (Fermat's principle)

$$\delta \int \sqrt{\gamma_{IJ}\left(\frac{dx^I}{dt}\right)\left(\frac{dx^J}{dt}\right)} = 0$$

We consider a space defined by γ_{IJ} where light rays are spatial geodesics.

Background for Gravitational lens

Background spacetime

◉ Background optical metric

Let a background be the optical metric with $p_i = 0$ as

$$\bar{\gamma}_{IJ} \equiv \gamma_{IJ}(p_i)|_{p_i=0}$$

✓ Background optical metric

$$\begin{aligned} d\bar{\ell}^2 &\equiv \bar{\gamma}_{IJ} dx^I dx^J \\ &= \frac{\bar{B}(r)}{\bar{A}(r)} dr^2 + \frac{\bar{C}(r)}{\bar{A}(r)} d\phi^2 \end{aligned}$$

Circumference radius: $\tilde{r} \equiv \sqrt{\frac{\bar{C}(r)}{\bar{A}(r)}} \quad \Rightarrow \quad \bar{\gamma}_{rr} \longrightarrow \bar{\gamma}_{\tilde{r}\tilde{r}} = F(\tilde{r})^{-1}$

$$d\tilde{\ell}^2 = F(\tilde{r})^{-1} d\tilde{r}^2 + \tilde{r}^2 d\phi^2$$

- Outline -

- Introduction
- Background for Gravitational lens
- **Optical constant-curvature background**
- BG dependence of Deflection angle
- Summary

Optical constant-curvature background

Optical constant-curvature space

◉ Spatial curvature of Background space

Gaussian curvature of the background optical space is

$$\tilde{K}^{\rm opt} = \frac{R_{\tilde{r}\phi\tilde{r}\phi}}{\det(\tilde{\gamma}_{\rm IJ})}$$

We focus on the space that have a "constant-curvature":

$$\frac{\partial \tilde{K}^{\rm opt}}{\partial \tilde{r}} = 0 \qquad \rightarrow \text{ 2nd order differential equation for } F(\tilde{r})$$

✓ Solution

$$F(\tilde{r}) = 1 + \kappa \tilde{r}^2 \qquad \text{(with the condition } F(\tilde{r})|_{\tilde{r}=0} = 1)$$

Optical constant-curvature background

Optical constant-curvature approach

◉ Optical constant-curvature background

Gaussian curvature under $F(\tilde{r}) = 1 + \kappa\tilde{r}^2$ is given by

$$\tilde{K}^{\rm opt} = -\kappa \quad \text{(const.)}$$

* e.g., de Sitter & anti-de Sitter $\cdots$ $\kappa = \Lambda/3$

Mannheim-Kazanas solution (in Weyl gravity) $\cdots$ $\kappa = \gamma^2/4 + k$

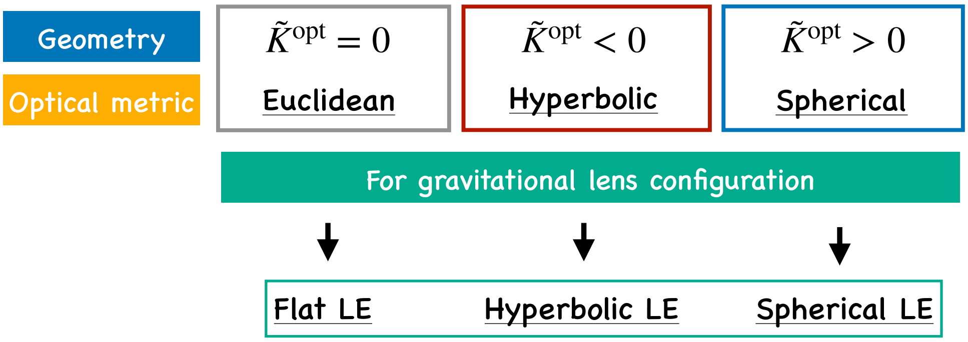

Geometry	$\tilde{K}^{\rm opt} = 0$	$\tilde{K}^{\rm opt} < 0$	$\tilde{K}^{\rm opt} > 0$
Optical metric	Euclidean	Hyperbolic	Spherical

For gravitational lens configuration

Flat LE | Hyperbolic LE | Spherical LE

→ already proven in [KT & Asada (2022)]

- Outline -

- Introduction
- Background for Gravitational lens
- Optical constant-curvature background
- **BG dependence of Deflection angle**
- Summary

Background dependence of Deflection angle

Deflection angle of light for Asymptotically non-flat spacetime

◉ Finite distance framework to Deflection angle

✓ Definition based on Gauss-Bonnet theorem [Ishihara+ 2016, KT+ 2020a]

$$\alpha \equiv \Psi_R - \Psi_S + \phi_{RS}$$
$$= \iint_{\Omega_R+\Omega_S} K \mathrm{d}S + \int_{P_R}^{P_S} \kappa_g \mathrm{d}\ell + \phi_{RS}$$

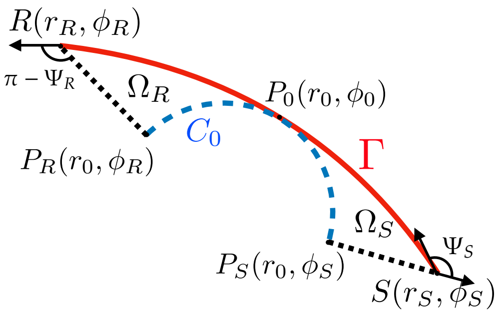

- This form is valid **even in asymptotically no-flat spacetimes** [KT+ 2020a]
- This is the **exact form** which does not assume BG

There should be a **background dependence.**

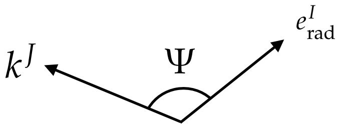

$$\cos\Psi = \gamma_{IJ} e^I_{\text{rad}} k^J$$

Background dependence of Deflection angle

Deflection angle of light as a function of parameters

- Parameters in the metric function

  p_i : Lens parameters q_j : Others (BG)

- Background dependence of α

  α is the function of these parameters: $\alpha(p_i\,,\ q_j)$

  What we have to do is to consider only the **contributions due to the lens objects.**

  Then, we denote α due to the lens object as

$$\underset{\text{Effects by Lens}}{\underline{\alpha(p_i)}} \equiv \underset{\text{Full }\alpha}{\underline{\alpha(p_i\,,\ q_j)}} - \underset{\text{BG effects}}{\underline{\alpha(p_i = 0\,,\ q_j)}}$$

- Outline -

- Introduction
- Background for Gravitational lens
- Optical constant-curvature background
- BG dependence of Deflection angle
- **Summary**

Summary

Optical constant-curvature approach for Gravitational lens

- We defined the background as a metric with the lens parameter $p_i \to 0$

✓ Optical constant-curvature approach (for SSS spacetime)

- We focused on "constant-curvature" background

↔ BG optical metric function: $\tilde{F}(r) = 1 + \kappa \tilde{r}^2$

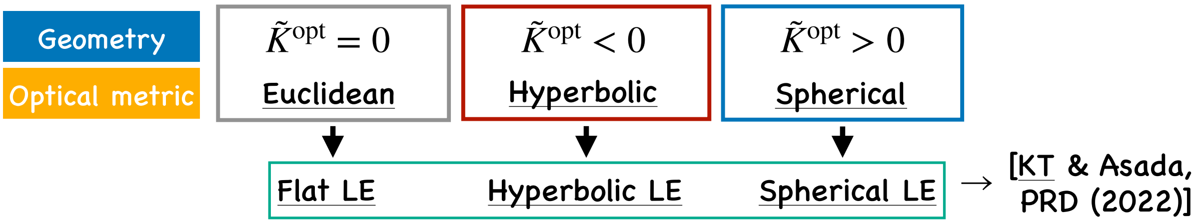

Geometry	$\tilde{K}^{\rm opt} = 0$ Euclidean	$\tilde{K}^{\rm opt} < 0$ Hyperbolic	$\tilde{K}^{\rm opt} > 0$ Spherical
Optical metric	Flat LE	Hyperbolic LE	Spherical LE

→ [KT & Asada, PRD (2022)]

✓ BG dependence of Deflection angle of light

- α which consists with the optical constant-curvature approach

✓ Working on

- Concrete example: Calculating lens effects on MK(Weyl gravity) background

---

Background geometry for Gravitational lens

Lens equation for Optical constant-curvature B.G.

✓ Non-flat extension for B.G. geometry

Depending on $\bar{K}^{\rm opt}$ of the optical constant-curvature space for B.G. …

Euclidean geometry

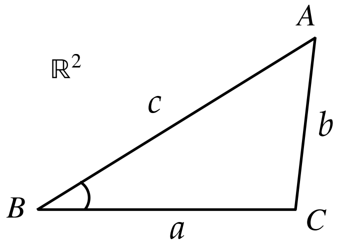

$$c^2 = a^2 + b^2 - 2ab\cos C$$

Hyperbolic geometry

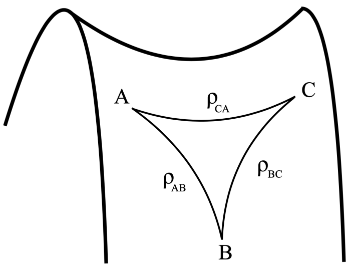

$$\cosh \rho_{AB} = \cosh \rho_{CA} \cosh \rho_{BC} - \sinh \rho_{CA} \sinh \rho_{BC} \cos C$$

Spherical geometry

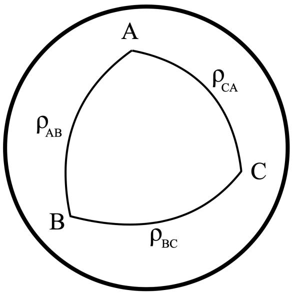

$$\cos \rho_{AB} = \cos \rho_{CA} \cos \rho_{BC} - \sin \rho_{CA} \sin \rho_{BC} \cos C$$

* ρ_{AB}, ρ_{BC}, ρ_{CA} are proper lengths based on the optical metric

* In hyperbolic & spherical geometry, length is the same dimension as angles **(dimensionless)**.

Gravitational lens equation

Lens equation for Flat background

- LE based on Flat trigonometry [KT+ (2020b)]

✓ Angular diameter distances

$$d_L \equiv r_L\,,\ d_{LS} \equiv r_{LS}\,,\ d_S \equiv r_S\,.$$

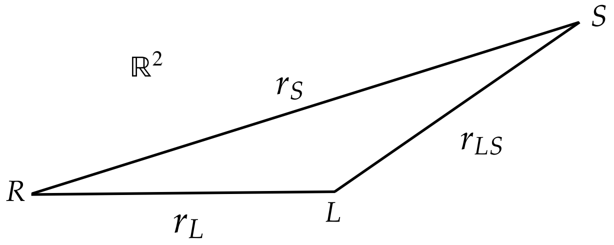

✓ Lens equation (Flat)

$$\alpha - \theta = \arcsin\left(\frac{d_L}{d_{LS}}\sin\theta\right) - \arcsin\left(\frac{d_S}{d_{LS}}\sin\beta\right)$$

θ : Apparent position , β : Intrinsic position ,
α : Deflection angle of light .

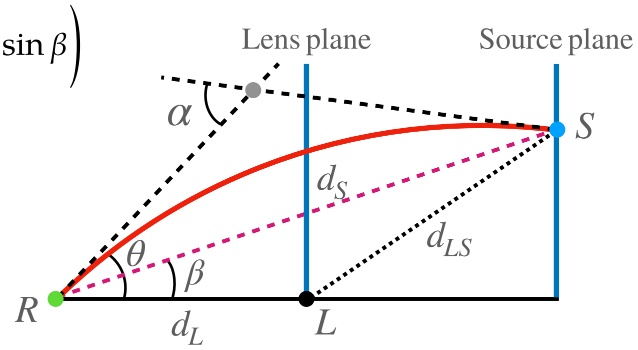

Gravitational lens equation

Lens equation for Spherical background

- LE based on Spherical trigonometry

✓ Angular diameter distances

$$\hat{d}_L \equiv \sin\rho_L\,,\ \hat{d}_{LS} \equiv \sin\rho_{LS}\,,$$
$$\hat{d}_S \equiv \sin\rho_S\,.$$

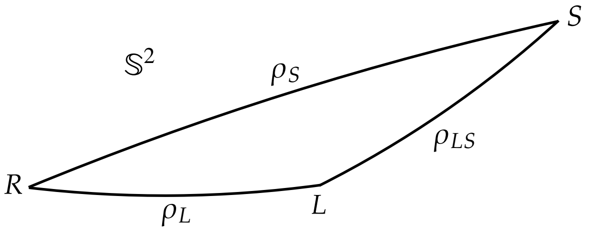

* Physical angular diameter distance is $d = \dfrac{\hat{d}}{\sqrt{\bar{K}^{\rm opt}}}$

✓ Lens equation (Spherical)

$$\alpha - \theta = \arcsin\left(\frac{\hat{d}_L}{\hat{d}_{LS}}\sin\theta\right) - \arcsin\left(\frac{\hat{d}_S}{\hat{d}_{LS}}\sin\beta\right)$$

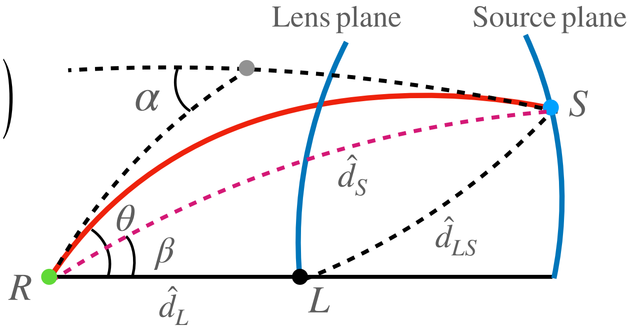

Gravitational lens equation

Lens equation for Hyperbolic background

- LE based on Hyperbolic trigonometry

✓ Angular diameter distances

$$\hat{d}_L \equiv \sinh \rho_L\ ,\ \ \hat{d}_{LS} \equiv \sinh \rho_{LS}\ ,$$
$$\hat{d}_S \equiv \sinh \rho_S\ .$$

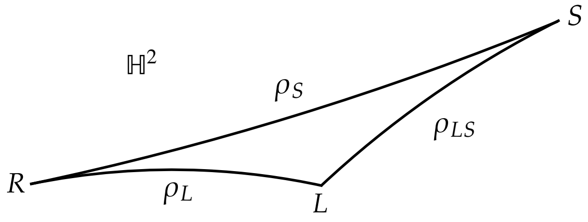

* Physical angular diameter distance is $d = \dfrac{\hat{d}}{\sqrt{-\bar{K}^{\mathrm{opt}}}}$

✓ Lens equation (Hyperbolic)

$$\alpha - \theta = \arcsin\left(\frac{\hat{d}_L}{\hat{d}_{LS}} \sin\theta\right) - \arcsin\left(\frac{\hat{d}_S}{\hat{d}_{LS}} \sin\beta\right)$$

LEs for each B.G. written by the angular diameter distance between 2-points can be expressed in the same form.

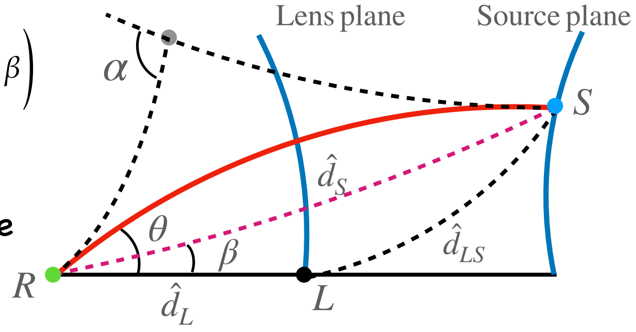

Gravitational lens equation

Lens equations in terms of distance between planes

✓ Unification of LEs

LE for **Euclidean B.G** in terms of distances between planes which does not use any approximations is as [KT, Ono, and Asada (2020b)]

$$\alpha - \theta = \arcsin\left(\frac{D_L \sin\theta}{\sqrt{(D_{LS})^2 + (D_S)^2 \tan^2\beta}}\right) - \arctan\left(\frac{D_S}{D_{LS}} \tan\beta\right)$$

Hence, we can unify write these LEs as below, by introducing a parameter K .

$$\alpha - \theta = \arcsin\left(\frac{\sqrt{1 + K\hat{D}_S^2 \tan^2\beta}}{\sqrt{\hat{D}_{LS}^2 + \hat{D}_S^2 \tan^2\beta}} \hat{D}_L \sin\theta\right) - \arctan\left(\frac{\hat{D}_{LS}}{\hat{D}_S} \tan\beta\right)$$

where

$$K = \begin{cases} +1 & \cdots\ \text{Spherical} \\ 0 & \cdots\ \text{Flat} \\ -1 & \cdots\ \text{Hyperbolic} \end{cases}$$

Gravitational lens equation

Iterative analysis

◉ Iterative method

✓ Approximation

Apparent position θ and Intrinsic position β , and Deflection angle of light α are small for the unit:

$$|\theta| \ll 1 \ , \quad |\beta| \ll 1 \ , \quad |\alpha| \ll 1$$

- Treating of angles

$$\theta = \sum_{k=1}^{\infty} \varepsilon^{(k)} \theta_{(k)} \ , \quad \alpha = \sum_{k=1}^{\infty} \varepsilon^{(k)} \alpha_{(k)} \ , \quad \beta = \varepsilon \beta_{(1)}$$

✓ Iterative solutions for LE

Each order of iterative solutions for LE can be **systematically** obtained as

$$\varepsilon \theta_{(1)} \ , \ \varepsilon^2 \theta_{(2)} \ , \ \varepsilon^3 \theta_{(3)} \ , \ \cdots$$

Gravitational lens equation (直す)

Iterative analysis

◉ Background effects

The deviation from the flat B.G. begins at the 3rd-order of the small angle.

$$\theta_{(3)} = \frac{\tilde{D}_{LS}}{\tilde{D}_L + \tilde{D}_{LS}} \alpha_{(3)} - \frac{\tilde{D}_S}{3(\tilde{D}_L + \tilde{D}_{LS})} \left(1 - \frac{\tilde{D}_S^2}{\tilde{D}_{LS}^2} \right) \beta_{(1)}^3$$
$$\boxed{- \frac{(1-K)\tilde{D}_L \tilde{D}_S^2}{2\tilde{D}_{LS}^2(\tilde{D}_L + \tilde{D}_{LS})} \beta_{(1)}^2 \theta_{(1)}} - \frac{\tilde{D}_L}{6(\tilde{D}_L + \tilde{D}_{LS})} \left(1 - \frac{\tilde{D}_L^2}{\tilde{D}_{LS}^2} \right) \theta_{(1)}^3$$

✓ New effects due to dS/AdS B.G.

$$\theta_{(3)}^{\text{New}} = K \frac{\tilde{D}_L \tilde{D}_S^2}{2\tilde{D}_{LS}^2(\tilde{D}_L + \tilde{D}_{LS})} \beta_{(1)}^2 \theta_{(1)}$$

$$K = \begin{array}{llll} & & \text{B.G.} & \text{New effects} \\ & +1 & \text{AdS} & \text{Positive} \\ \left\{ \vphantom{\begin{array}{l} 1 \\ 1 \\ 1 \end{array}} \right. & 0 & \text{Flat} & \text{———} \\ & -1 & \text{dS} & \text{Negative} \end{array}$$

The new effects in **Hyperbolic B.G.**$(K = 1)$ **increases** the lensed image position θ, while that in **Spherical B.G.**$(K = -1)$ **decreases** it.

Deflection angle of light

▶ Deflection angle of light on dS backgrounds

✓ Background dependence of α

We denote the deflection angle of light on dS B.G. as $\alpha^{\rm dS}(p_i, \Lambda)$.

* Lens system is characterized by $p_i\,(i = 1, 2, \cdots)$ (e.g., m) in addition to Λ.

For dS B.G., and thus

$$\alpha^{\rm dS} \equiv \alpha(p_i, \Lambda) - \underbrace{\alpha(p_i = 0, \Lambda)}_{\text{B.G. effects}}$$

For example, we obtain $\alpha^{\rm dS}$ in the case of SdS lensing as

$$\alpha^{\rm dS} = \frac{4m}{D_L\theta} - \frac{m\theta}{D_L}\left[1 + \left(\frac{D_L}{D_{LS}}\right)^2\right] + \frac{m\Lambda D_L\theta}{3} + \mathcal{O}(m^2, m\theta^3, m\Lambda D\theta^3, m\Lambda^2 D^3)$$

For also negative Λ (i.e., AdS B.G.), $\alpha^{\rm AdS}$ can be obtained in **the same form**.

C81

JGRG CCNU
2022/10/28

ADM formulation and Hamiltonian analysis of f(Q) gravity

arXiv:2204.12826
(Published in: Phys.Rev.D 106 (2022) 4, 044025)

Hu kun

Collaborators: Taishi Katsuragawa
(Central China Normal University)
Taotao Qiu
(Huazhong University of Science and Technology)

---

contents

- Introduction
  - Symmetric teleparallel gravity
  - f(Q) gravity and Coincident gauge
- Dynamics of constrained systems
- Hamiltonian analysis of f(Q) gravity
  - ADM decomposition of f(Q) gravity
  - Primary constraints and secondary constraints
- Summary

Symmetric teleparallel gravity (J.M. Nester, H-J Yo, 1999)

- In GR, gravity is described by curvature.

Curvature = energy density

$\Downarrow$ (torsion-free, metric-compatible)

Metric $g_{\mu v}$ Only variable

General Relativity

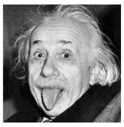

- But there exist two other equivalent ways to describe gravity.
  - The Teleparallel representation: (TEGR) > arXiv:1303.3897
  - Nonmetricity representation: (STEGR) > arXiv: 9809049

$$\boxed{Q_{\alpha\mu v} = \hat{\nabla}_{\alpha} g_{\mu v}}$$

Symmetric teleparallel gravity (J.M. Nester, H-J Yo, 1999)

- While the $\hat{\nabla}$ is corresponding to $\hat{\Gamma}^{\alpha}{}_{\mu\nu} = \left\{ {\alpha \atop \mu\nu} \right\} + K^{\alpha}{}_{\mu\nu} + L^{\alpha}{}_{\mu\nu}$
- The general quadratic action

$$\mathcal{S}_{\mathrm{GQ}} = \int \mathrm{d}^4 x (\sqrt{-g} Q_{\alpha\mu\nu} P^{\alpha\mu\nu} + \lambda_{\alpha}{}^{\beta\mu\nu} \hat{R}^{\alpha}{}_{\beta\mu\nu} + \lambda_{a}{}^{\mu\nu} T^{\alpha}{}_{\mu\nu}).$$

- If we choose our $\hat{\Gamma}^{\sigma}_{\nu\alpha}$ to be total inertial $\boxed{\hat{\Gamma}^{\sigma}_{\nu\alpha} = \frac{\partial x^{\sigma}}{\partial \xi^{\lambda}} \frac{\partial^2 \xi^{\lambda}}{\partial x^{\nu} \partial x^{\alpha}}}$
- Non-metricity scalar defined

$$Q = (-g^{\alpha\rho} g^{\beta\mu} g^{\sigma\nu} + 2g^{\alpha\nu} g^{\beta\mu} g^{\sigma\rho} + g^{\alpha\rho} g^{\beta\sigma} g^{\mu\nu} - 2g^{\alpha\beta} g^{\mu\nu} g^{\sigma\rho}) \cdot Q_{\alpha\beta\sigma} Q_{\rho\mu\nu}$$

- We can prove the relationship

$$0 = \hat{R}\left(\hat{\Gamma}^{\sigma}_{\nu\alpha}\right) = \underline{R(\{{}^{\sigma}_{\nu\alpha}\})} - \underline{Q\left(g_{\mu\nu}, \hat{\Gamma}^{\sigma}_{\nu\alpha}\right)} + \boxed{\nabla_{\alpha}\left(Q^{\alpha} - \tilde{Q}^{\alpha}\right)}$$

- After the integral of the action, GR and STEGR are equivalent.

f(Q) gravity and Coincident gauge (Lavinia Heisenberg, 2018)

Why f(Q) gravity

- In order to describe the accelerated expansion of the Universe. We need to modify this gravitational theories.

Extend to an arbitrary function of nonmetricity scalar

$$S_{STEGR} = \frac{1}{2}\int d^4x\sqrt{-g}\,Q \quad \Rightarrow \quad S_{f(Q)} = \frac{1}{2}\int d^4x\sqrt{-g}\,f(Q)$$

- But before that, we need to figure out the number of independent *d.o.f.* it possesses.
- For simplicity, we fix the gauge to *Coincident gauge.*

Diffeomorphism

$$x^\alpha = \xi^\lambda \quad \Rightarrow \quad \hat{\Gamma}^\sigma_{\nu\alpha} = \frac{\partial x^\sigma}{\partial \xi^\lambda}\frac{\partial^2 \xi^\lambda}{\partial x^\nu \partial x^\alpha} \to 0$$

Dynamics of constrained systems (Dirac-Bergmann, 1951)

- In gauge theories, redundant *d.o.f.* may exist, some of which are closely related to the gauge symmetry.

  In the Hamiltonian formalism, they are characterized by the presence of constraints. The symmetries inherent in a theory can be explored by performing a Hamiltonian analysis.

- For a general action $S = \int dt L(q_s, \dot{q}_s)$
- Euler-Lagrange equations $\frac{\partial L}{\partial q_s} - \frac{d}{dt}\left(\frac{\partial L}{\partial \dot{q}_s}\right) = 0 \qquad s = 1, ..., k$

$$\Downarrow$$

It can be rewrite as $\boxed{\frac{\partial^2 L}{\partial \dot{q}_r \dot{q}_s}}\ddot{q}_s = \frac{\partial L}{\partial q_r} - \frac{\partial^2 L}{\partial q_s \dot{q}_r}\dot{q}_s$

hessian matrix

Dynamics of constrained systems (Dirac-Bergmann, 1951)

- Conjugate momenta is defined by $p_s = \dfrac{\partial L}{\partial \dot{q}_s} \qquad s = 1, ..., k$

  If some of above momenta is not the function of velocities, it means that there exist independent relations among p *and* q. This relations are called *primary constraints.*

$$\boxed{\phi_\rho(q_s, p_s) = p_\rho - \xi(q_s, p_j)}$$

- We define Total Hamiltonian via Lagrange multipliers

$$L = p^j \dot{q}_j - H(q, p) + \underline{u^\rho} \phi_\rho$$

- For an arbitrary function of the phase space, the evolution reads

$$\dot{f} \approx \{f, H\} + u^\rho \{f, \phi_\rho\}$$

$$\Downarrow$$

$$\boxed{\{\phi_\sigma, H\} + \underline{u^\rho}\{\phi_\sigma, \phi_\rho\} \approx 0}$$ *(consistency equation)*

Dynamics of constrained systems (Dirac-Bergmann, 1951)

- If the consistency equations are not automatically satisfied, they form new constraints, called *secondary constraints.*

- Then we have two major possibilities:

  - Situation 1

if $\{\phi_\sigma, \phi_\rho\} = 0$

$\Downarrow$

Consistency equations does not contain u^ρ

$\Downarrow$

Evolution of the secondary constraints give *tertiary constraints*

$\Downarrow$

The process ends after consistency equations naturally satisfied

$\Downarrow$

The u^ρ stay arbitrary (Example: GR)

Dynamics of constrained systems (Dirac-Bergmann, 1951)

- Situation 2

$$\{F(x), G(y)\} := \int_{\Sigma_t} \mathrm{d}^3 z \sum_k \left(\frac{\delta F(x)}{\delta \Phi^k(z)} \frac{\delta G(y)}{\delta \Pi_k(z)} - \frac{\delta G(y)}{\delta \Phi^k(z)} \frac{\delta F(x)}{\delta \Pi_k(z)} \right)$$

(When we exchange the order of two functions in PBs, The only difference is a minus sign)

if $\{\phi_\sigma, \phi_\rho\} \neq 0$

⇩

The matrix $\{\phi_\sigma, \phi_\rho\}$ must be singular

⇩

We can not determinate all u^ρ from consistency equations

⇩

We "missed" the additional constraint

⇩

We need to formulate extra constraints ξ^n imposed by the null eigenvector of $\{\phi_n, \mathscr{H}_0\}$

⇩

All the u^ρ can be solved as functions of phase space variables

(Example: f(T), f(Q))

Hamiltonian analysis of f(Q) gravity (Kun Hu, T K, Taotao Qiu, 2022)

A. ADM decomposition of f(Q) gravity

- To facilitate the calculation, we introduce an auxiliary field, we rephrase the action

f(Q) gravity ⟷ scalar-nonmetricity theory

$$S_{f(Q)} = \frac{1}{2} \int d^4 x \sqrt{-g}\, f(Q) \quad \overset{}{\underset{\text{equivalent}}{\Longleftrightarrow}} \quad S_{f(Q)} = \frac{1}{2} \int d^4 x \sqrt{-g}\, [f'(\varphi) Q + f(\varphi) - \varphi f'(\varphi)]$$

- The Arnowitt-Deser-Misner (ADM) metric

$$ds^2 = -\boxed{N^2} dt^2 + \boxed{h_{ij}} \left(dx^i + \boxed{N^i} dt \right) \left(dx^j + N^j dt \right)$$

- There are 11 dynamical variables in total. we insert above metric into the scalar-nonmetricity action, and with the help of the relations

$$\mathcal{R}(\{\,\}) = Q - \nabla_\alpha \left(Q^\alpha - \tilde{Q}^\alpha \right) \qquad {}^3\mathcal{R} = {}^3Q - \mathcal{D}_l({}^3Q^l - {}^3\tilde{Q}^l)$$

Hamiltonian analysis of f(Q) gravity (Kun Hu, T K, Taotao Qiu, 2022)

- We reach the ADM decomposed action

$$\boxed{\begin{aligned} S_{f(Q)} = \int d^4x \Big\{ N\sqrt{h}\left[f + f'\left({}^3Q + K_{ij}K^{ij} - K^2 - \varphi\right) - \mathcal{D}_l[f'({}^3Q^l - {}^3\tilde{Q}^l)]\right] \\ + \frac{\sqrt{h}}{N}\dot{\varphi} f''\left(\partial_i N^i\right) - \frac{\sqrt{h}}{N}\dot{N}^i\partial_i f' - \frac{\sqrt{h}}{N}\partial_i f'\left(N^i\partial_j N^j - N^k\partial_k N^i\right)\Big\} \ . \end{aligned}}$$

B. Primary constraints and secondary constraints

- For N, N_i, h_{ij}, φ , conjugate momenta are defined by

$$\boxed{\begin{aligned} \pi^N &\equiv \frac{\delta S}{\delta \dot{N}} = 0 \ , \\ \pi^i &\equiv \frac{\delta S}{\delta \dot{N}_i} = -\frac{\sqrt{h}}{N}\partial^i f' \ , \end{aligned}} \longrightarrow$$

$$\pi^{ij} \equiv \frac{\delta S}{\delta \dot{h}_{ij}} = \sqrt{h}\left[f'\left(K^{ij} - h^{ij}K\right)\right] + A^{ij} \ ,$$

$$\boxed{p \equiv \frac{\delta S}{\delta \dot{\varphi}} = \frac{\sqrt{h}}{N} f''\left(\partial_i N^i\right)} \longrightarrow$$

$$\begin{cases} \phi_a : \pi_N \overset{!}{\approx} 0 \ , \\ \phi_i : \pi_i + \frac{\sqrt{h}}{N}\partial_i f' \overset{!}{\approx} 0 \ , \\ \phi_c : p - \frac{\sqrt{h}}{N} f''\left(\partial_i N^i\right) \overset{!}{\approx} 0 \end{cases}$$

(5 primary constraints)

Hamiltonian analysis of f(Q) gravity (Kun Hu, T K, Taotao Qiu, 2022)

- We define total Hamiltonian in f(Q) gravity

$$\begin{aligned} H &= \int_{\Sigma_t} \mathscr{H}\, d^3x \\ &= \int_{\Sigma_t} d^3x \left(\underline{\lambda^a}\pi_N + \underline{\lambda^i}\phi_i + \underline{\lambda^c}\phi_c + \mathscr{H}_0\right) \end{aligned}$$

while

$$\begin{aligned} \mathscr{H}_0 &:= \pi^{ij}\dot{h}_{ij} + \pi^i\dot{N}_i + p\dot{\varphi} - \mathscr{L} \\ &= NC + 2\mathcal{D}_i N_j \pi^{ij} - \frac{\sqrt{h}}{N}\partial_i f'\left(N^j\partial^i N_j - N^i\partial_j N^j + 2N^j\partial_j N^i\right) \end{aligned}$$

- The Poisson Brackets

$$C_{n'n} = \{\phi_{n'}, \phi_n\} = \begin{pmatrix} 0 & A_1 & A_2 & A_3 & -B \\ -A_1 & 0 & 0 & 0 & C_1 \\ -A_2 & 0 & 0 & 0 & C_2 \\ -A_3 & 0 & 0 & 0 & C_3 \\ B & -C_1 & -C_2 & -C_3 & 0 \end{pmatrix}$$

Unsurprisingly, the $\det(C_{n'n})$ vanish. This implies that we miss an equation to determine the Lagrange multipliers.

Hamiltonian analysis of f(Q) gravity (Kun Hu, T K, Taotao Qiu, 2022)

- However, there exist an *additional constraints* imposed by the null eigenvector

$$\boxed{\chi=\xi^n h_n=\xi^i\left(\{\pi_i,\mathscr{H}_0\}+\{V_i,\mathscr{H}_0\}\right)\overset{!}{\approx}0 \qquad h_n\equiv\left(\{\phi_n,\mathscr{H}_0\}\right)}$$

- The consistency conditions of above six constraints become *six equations* that contain unknow $u^{\rho}(q,p)$.

- We define a new matrix Φ_{mn} , and we check Φ_{mn} is full rank matrix. ⟶ All the $u^{\rho}(q,p)$ can be solved from this six equations.

$$(\Phi_{mn})\equiv\begin{bmatrix}C_{n'n}\\ \{\chi,\phi_n\}\end{bmatrix}=\begin{pmatrix}0 & A_1 & A_2 & A_3 & -B\\ -A_1 & 0 & 0 & 0 & C_1\\ -A_2 & 0 & 0 & 0 & C_2\\ -A_3 & 0 & 0 & 0 & C_3\\ B & -C_1 & -C_2 & -C_3 & 0\\ \{\chi,\phi_a\} & \{\chi,\phi_x\} & \{\chi,\phi_y\} & \{\chi,\phi_z\} & \{\chi,\phi_c\}\end{pmatrix}$$

(all the constraints are Second class!)

Hamiltonian analysis of f(Q) gravity (Kun Hu, T K, Taotao Qiu, 2022)

- Inserting back those Lagrange multipliers, the consistency conditions *must be* automatically satisfied.

$$\boxed{\begin{aligned}\mathcal{D}.o.f.&=\frac{1}{2}\cdot\left(\begin{array}{c}\text{Number of original}\\ \text{canonical variables}\end{array}-\begin{array}{c}\text{Total number}\\ \text{of constraints}\end{array}-\begin{array}{c}\text{Number of}\\ \text{gauge conditions}\end{array}\right)\\ &=\frac{1}{2}\cdot\left(\begin{array}{c}\text{Number of original}\\ \text{canonical variables}\end{array}-2\times\begin{array}{c}\text{Number of}\\ \text{FC constraints}\end{array}-\begin{array}{c}\text{Number of}\\ \text{SC constraints}\end{array}\right)\\ &=\frac{1}{2}\cdot(22-0-6)=8\ .\end{aligned}}$$

Summary

- **f(R), f(T), and f(Q), will not be equivalent to each other because the total derivative term is no longer boundary term.**

- **The geometrical trinity of gravity**

	Number of basic variables	Degrees of freedom	Symmetry breaking
$f(R)$	$10+1\ (g_{\mu\nu},\phi)$	$(22-8\times 2-0)/2=3$	No symmetry is broken
$f(T)$	$16+1\ (e_a^\mu,\phi)$	$(34-8\times 2-8)/2=5$	Local Lorentz is broken
$f(Q)$	$10+1\ (g_{\mu\nu},\phi)$	$(22-0-6)/2=8$	Diff. is broken

$$\boldsymbol{f(R)}\left\{\begin{array}{l}\left.\begin{array}{l}\pi_N,\pi_i\\ C_0,C_i\end{array}\right\}\text{4+4 FC}\\ \pi_{ij},p\end{array}\right.$$

$$\boldsymbol{f(T)}\left\{\begin{array}{l}\left.\Pi^{A0},C^A\right\}\text{4+4 FC}\\ \left.\begin{array}{l}\Gamma^{AB}\\ p\\ \chi\end{array}\right\}\text{6+2 SC}\end{array}\right.$$

$$\boldsymbol{f(Q)}\left\{\begin{array}{l}\pi_N,\pi_i\\ p\\ \chi\end{array}\right\}\text{8 SC}$$

- **In f(Q) gravity, all of constraints are second class, which imply the Diff-symmetry is broken. Because the gauge fixing. *(Coincident gauge)***

C83

Colliding gravitational waves and singularities

Sinya AOKI

Center for Gravitational Physics and Quantum Information,
Yukawa Institute for Theoretical Physics, Kyoto University

The 13th RESCEU International Symposium “JGRG31”
October 24-28, 2022
The 31st Workshop on General Relativity and Gravitation in Japan
Koshiba Hall, The University of Tokyo

I. Introduction/Motivation

Proposal for matter energy and conserved charge in general relativity

S. Aoki, T. Onogi, S. Yokoyama, Int. J. Mod. Phys. A36 (2021) 2150098,2150201.

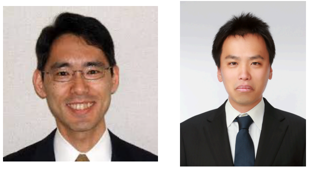

matter energy $\Sigma(x^0)$: a constant x^0 spacelike hypersurface

$$E(x^0) := \int_{\Sigma(x^0)} [d^{d-1}x]_\mu \underline{T^\mu{}_\nu}(x)\xi^\nu_E(x), \quad \xi^\nu_E(x) = -\delta^\nu_0$$

with coordinate condition $g_{0j} = 0$

Energy Momentum Tensor (EMT)

The charge for “time” translation, but is not conserved in general.

matter conserved charge

$$Q(x^0) := \int_{\Sigma(x^0)} [d^{d-1}x]_\mu T^\mu{}_\nu(x)\beta(x)\xi^\nu_E(x)$$

β satisfies $\nabla_\mu(T^\mu{}_\nu\beta\xi^\nu_E) = 0.$

The charge from the Noether’s 1st theorem. S. Aoki, arXiv:2206.00283[hep-th].

This charge can be regarded as entropy with the inverse temperature β for some cases such as FLRW universe.

A criticism against our proposal

A black-hole (like object) may be created by a collision of two gravitational waves.

$$T^{\mu}{}_{\nu} \neq 0 \longrightarrow Q \neq 0 \quad \Longleftrightarrow \quad T^{\mu}{}_{\nu} = 0 \longrightarrow Q = 0$$

contradiction

In this talk, I investigate how our proposal works/fails in a model of colliding plane gravitational waves by Szekeres.

S. Aoki, arXiv:2209.11357[gr-qc]

II-1. Model of colliding plane gravitational waves

P. Szekeres, J. Math. Phys. 13 (1972) 286.

left-moving GW + right-moving GW ⟶ singularities

$$ds^2 = -2e^{-M(u,v)}dudv + e^{-U(u,v)}\left(e^{V(u,v)}dx^2 + e^{-V(u,v)}dy^2\right), \qquad R_{\mu\nu} - \frac{1}{2}g_{\mu\nu}R = 0$$

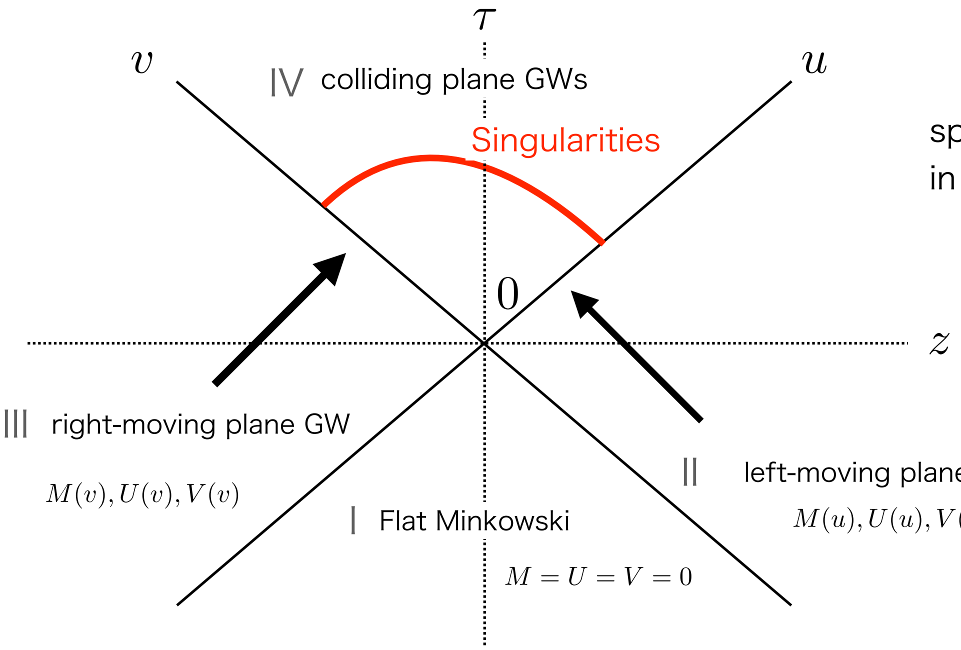

spacetime is uniform in x & y directions

II-2. Solutions and singularities

A class of solutions $R_{\mu\nu} - \frac{1}{2} g_{\mu\nu} R = 0$ P. Szekeres, J. Math. Phys. 13 (1972) 286.

$$M = -\log t^2, \; V = -\frac{k_{12}}{2} \log t^2 + \cdots, \; M = \frac{1}{2}\left(1 - \frac{k_{12}^2}{4}\right) \log t^2 + \cdots,$$

$$t^2 = f(u) + g(v), \; f(u) = \frac{1}{2} - (au)^{n_1} \theta(u), \; g(v) = \frac{1}{2} - (bv)^{n_2} \theta(v) \qquad k_{12} := k_1 + k_2, \; \frac{k_i^2}{8} = 1 - \frac{1}{n_i}$$

Continuity at u=0 or v=0 ⟶ $n_i \geq 4$, integer ⟶ singularities at $t^2 = 0$

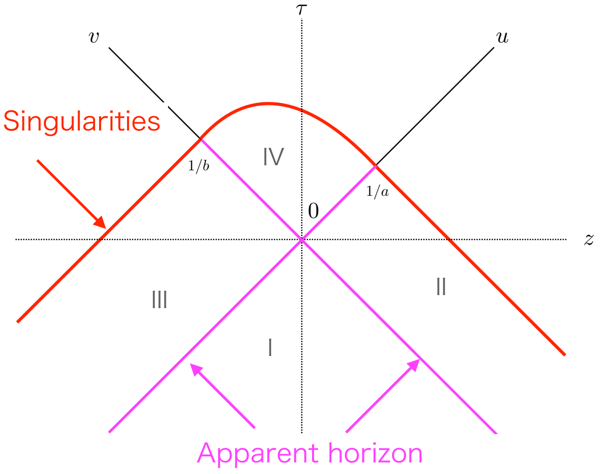

S. Aoki, arXiv:2209.11357[gr-qc]

cf. Kahn-Penrose. Nature 229 (1971)185.

$n_1 = n_2 = 2$

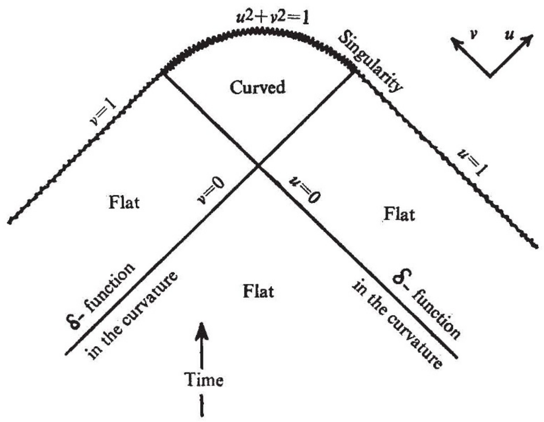

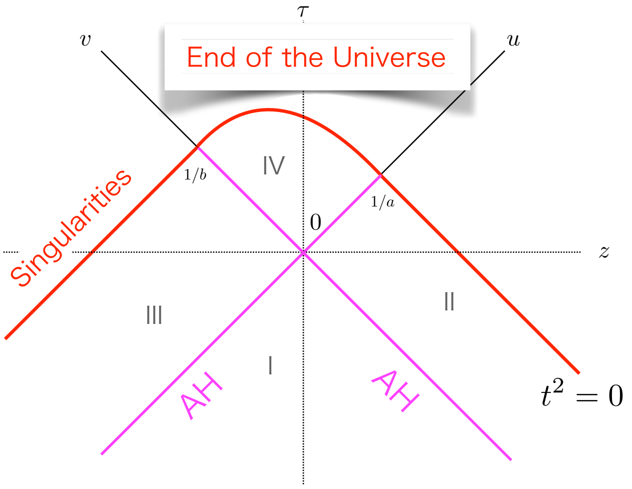

1. Plane GW has a singularity at $t^2 = 0$.

2. Singularities are protected by apparent horizons.

3. No spacetime beyond singularities.

4. University ends.

5. Non-zero EMT at singularities.

Energy Momentum Tensor at singularities

$$\sqrt{-g} T^u{}_u = \sqrt{-g} T^v{}_v = -\frac{f_u g_v}{8\pi G_N} \delta(t^2), \sqrt{-g} T^v{}_u = \frac{f_u^2}{8\pi G_N} \delta(t^2), \; \sqrt{-g} T^u{}_v = \frac{g_v^2}{8\pi G_N} \delta(t^2)$$

$$f_u := \frac{df}{du}, \; g_v := \frac{dg}{dv}$$

S. Aoki, arXiv:2209.11357[gr-qc]

III-1. Matter energy and conserved charge

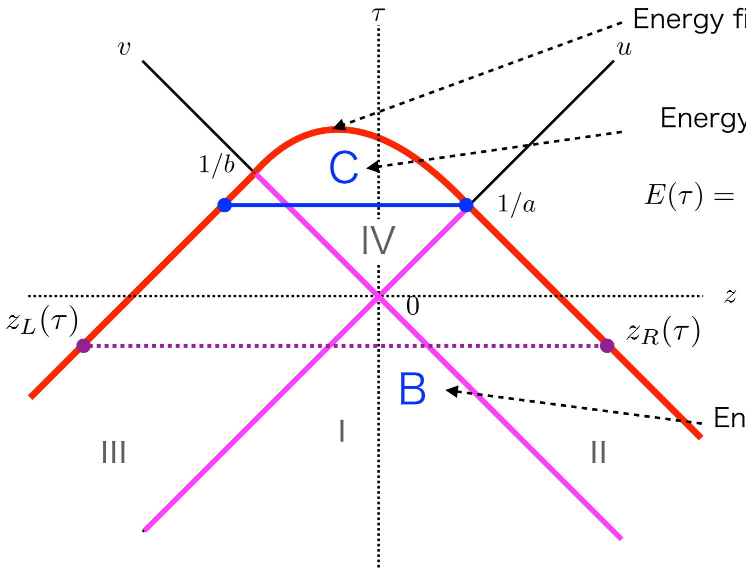

Energy finally vanishes at the “End of the Universe”.

Energy decreases during collision (region C)

$$E(\tau) = \frac{V_2}{8\pi G_N}\left(\left.\frac{g_v - f_u}{\sqrt{2}}\right|_{z=z_R(\tau)} + \left.\frac{f_u - g_v}{\sqrt{2}}\right|_{z=z_L(\tau)} \right)$$

$$V_2 := \int dxdy$$

Energy is conserved before collision (region B)

$$E(\tau) = \frac{V_2}{8\pi G_N}\frac{(n_1 a + n_2 b)}{\sqrt{2}}$$

The charge is always conserved but zero due to a cancellation of two GWs.

$$Q(\tau) = \frac{V_2\beta_0}{8\pi G_N}\left[\left.\frac{g_v - f_u}{|g_v - f_u|}\right|_{z=z_R(\tau)} + \left.\frac{g_v - f_u}{|g_v - f_u|}\right|_{z=z_L(\tau)} \right] = 0$$

=1, left-moving =-1, right-moving

Zero charge is consistent with the end of the Universe, where the charge must be zero.

III-2. Other spacetimes

S. Aoki, arXiv:2209.11357[gr-qc]

Scattering of GW (from left-moving to right-moving)

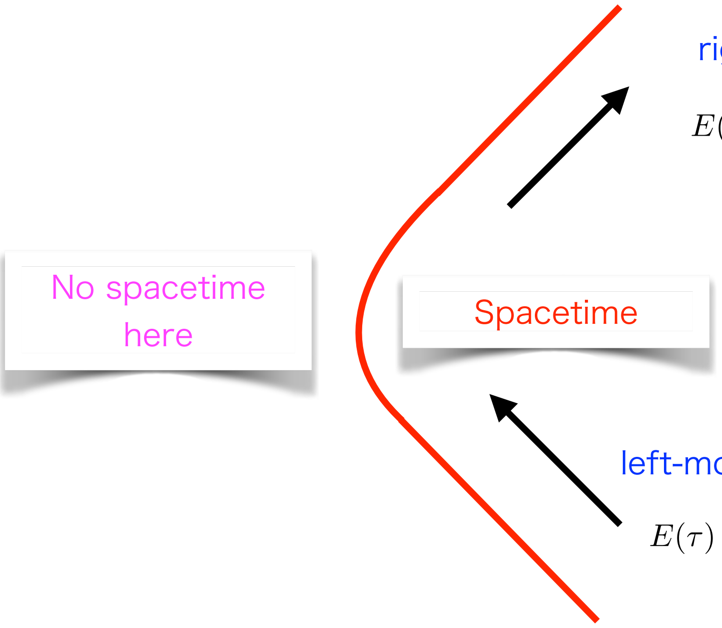

right-moving plane GW

$$E(\tau) = \frac{V_2}{8\pi G_N}\frac{n_2 b}{\sqrt{2}}$$

scattering GW

$$E(\tau) = \frac{V_2}{8\pi G_N}\left.\frac{f_u + g_v}{\sqrt{2}}\right|_{z=z_L(\tau)}$$

left-moving plane GW

$$E(\tau) = \frac{V_2}{8\pi G_N}\frac{n_1 a}{\sqrt{2}}$$

1. Energy is not conserved during the scattering.
2. The charge is conserved and non-zero.

$$Q(\tau) = \frac{V_2\beta_0}{8\pi G_N}\left.\frac{-g_v - f_u}{|g_v + f_u|}\right|_{z=z_L(\tau)} = -\frac{V_2\beta_0}{8\pi G_N}$$

III-3. Non-conservation of Komar integral

our charge Versus **Komar integral (Noether's 2n theorem)**

$$Q_{\rm ours}(x^0) = \int_{\Sigma(x^0)} [d^{d-1}x]_\mu J^\mu \qquad Q_{\rm 2nd}(x^0) = \int_{\Sigma(x^0)} [d^{d-1}x]_\mu K^\mu[\xi]$$

$$J^\mu = T^\mu{}_\nu \beta \xi^\nu_T \qquad \nabla_\mu J^\mu = 0 \qquad K^\mu[\xi] = \frac{1}{2\kappa}\nabla_\nu\left[\nabla^{[\mu}\xi^{\nu]}\right] \qquad \nabla_\mu K^\mu[\xi] = 0$$

conserved $Q_{\rm ours}(x^0) = Q_{\rm ours}(y^0)$ not conserved $Q_{\rm 2nd}(x^0) \neq Q_{\rm 2nd}(y^0)$

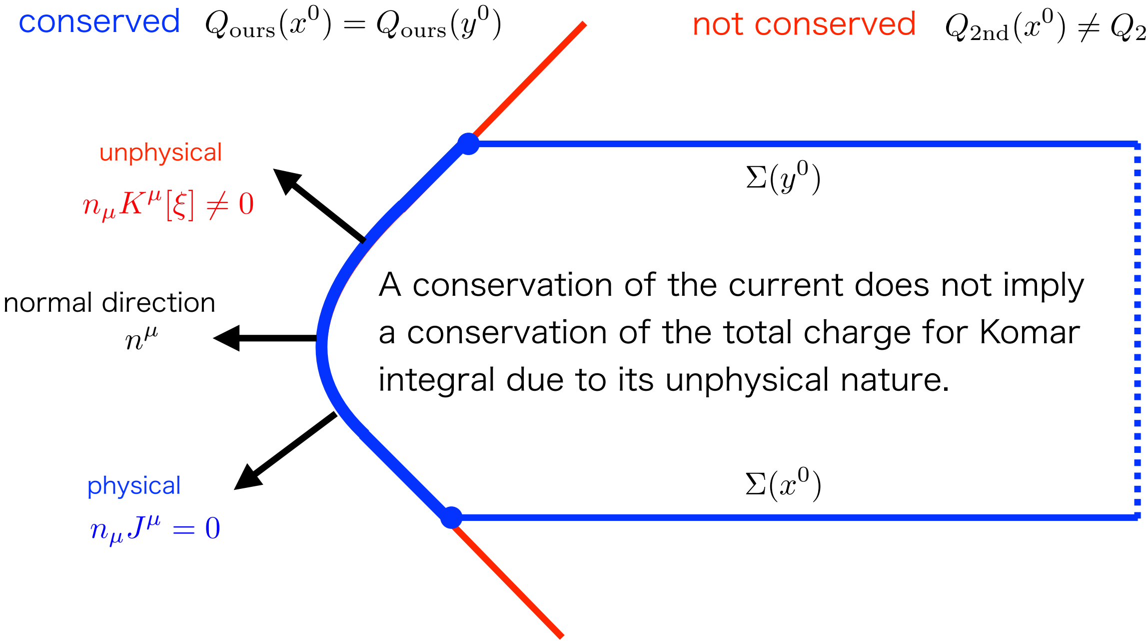

unphysical

$n_\mu K^\mu[\xi] \neq 0$

normal direction

n^μ

physical

$n_\mu J^\mu = 0$

$\Sigma(y^0)$

A conservation of the current does not imply a conservation of the total charge for Komar integral due to its unphysical nature.

$\Sigma(x^0)$

IV. Conclusion

1. A spacetime structure in the colliding plane gravitational waves by Szekeres is investigated.
2. The energy momentum tensor at singularities is evaluated.
3. The matter energy in our proposal is not conserved during the collision.
4. The matter conserved charge in our proposal is indeed always conserved.

Our proposal works for this spacetime, despite the criticism.

A new spacetime

A pair creation and annihilation of GWs
(Minkowski vacuum bottle)

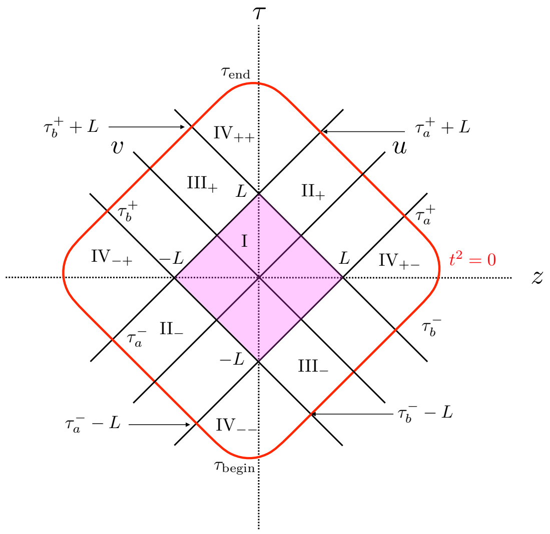

Thank you !

Periapsis shift of a quasi-circular orbit in a general static spherically symmetric spacetime

Tomohiro Harada[1]
with T. Igata[2], H. Saida[3], Y. Takamori[4]

[1]Rikkyo U, [2]Gakushuin U, [3]Daido U, [4]NIT, Wakayama College

JGRG31@U Tokyo
24-28/10/2022
arXiv:2210.07516

Introduction

- The periapsis (perihelion) shift is one of the first classical tests of GR.

$$\boldsymbol{\Delta\phi_{p,\mathrm{wf}}} = \frac{\boldsymbol{6\pi M}}{\boldsymbol{a(1-e^2)}} \text{ (weak field)},$$

$$\boldsymbol{\Delta\phi_{p,\mathrm{qc}}} = \boldsymbol{2\pi\left[\frac{1}{\sqrt{1-\frac{6M}{r}}}-1\right]}$$

(quasi-circular)

- The periapsis shift of S2 around Sgr A* has been observed. $\boldsymbol{f = 1.10 \pm 0.19}$ for $\boldsymbol{\Delta\phi_p = f\Delta\phi_{p,\mathrm{wf}}}$ (Abuter et al. (2020)).

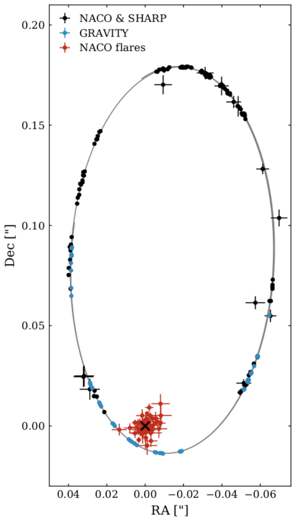

Figure: The orbit of S2 in 1992-2019 (Abuter et al. (2020))

Black hole candidate

- We do not know much about the central object.
  - The standard assumption is a Kerr (Schwazschild) BH.
  - Alternative possibities, such as a dense core, boson star, naked singularity, wormhole, dark matter spike and BH hair, are discussed.
- The periapsis shift can be "retrograde" in non-standard scenarios.

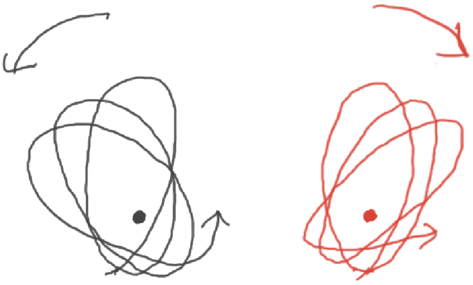

Figure: Prograde shift and retrograde shift

- Extended-mass effect in Newtonian gravity (Jiang and Lin (1985))
- We derive formulae for the periapsis shift of a quasi-circular orbit in a general static spherically symmetric spacetime.

Timelike geodesic

- Line element in the static spherically symmetric spacetime

$$ds^2 = -e^{\nu(r)}dt^2 + e^{\lambda(r)}dr^2 + r^2(d\theta^2 + \sin^2\theta d\phi^2).$$

- Gravitational mass $m(r)$

$$e^{\lambda(r)} =: \left(1 - \frac{2m(r)}{r}\right)^{-1},$$

where $r > 2m(r)$ must be satisfied.

- The geodesic equation with $g_{\mu\nu}\dot{x}^\mu\dot{x}^\nu = -1$ reduces to

$$\ddot{r} + V'(r) = 0, \quad \frac{1}{2}\dot{r}^2 + V(r) = 0,$$
$$V(r) := \frac{1}{2}e^{-\lambda}\left[\left(1 + \frac{L^2}{r^2}\right) - e^{-\nu}E^2\right]$$

where E and L are the energy and angular mometum, respectively, and the dot denotes the differentiation w.r.t. the proper time τ.

Periapsis shift of a quasi-circular orbit

- Circular orbit $r = r_0$
    - We can fix E, L and V''.
    - We concentrate on stable circular orbits, where $V'' > 0$.
- Periapsis shift $\Delta\phi_p$
    - $\delta r = r - r_0$ obeys a simple harmonic motion with ω_r, while orbiting with ω_ϕ, where

$$\omega_r = \sqrt{V''} \quad \text{and} \quad \omega_\phi = \dot{\phi} = \frac{L}{r^2}.$$

- $\Delta\phi_p$ is calculated to give

$$\begin{aligned} \Delta\phi_p &= 2\pi\left(\frac{\omega_\phi}{\omega_r} - 1\right) = 2\pi\left(\frac{1}{\sqrt{A}} - 1\right), \\ A &= re^{-\lambda}\frac{\nu'' - (\nu')^2 + (3/r)\nu'}{\nu'}(> 0). \end{aligned}$$

- $\Delta\phi_p > 0$, < 0 and $= 0$ if $A < 1$, > 1 and $= 1$, respectively.

Expression in terms of the gravitational mass

- Natural orthonormal basis: $\vec{e}_{\hat{0}} \propto \partial t$, $\vec{e}_{\hat{1}} \propto \partial r$, $\vec{e}_{\hat{2}} \propto \partial \theta$, $\vec{e}_{\hat{3}} \propto \partial \phi$
- General case
    - $A = A_{m0} + A_{m1}$ in terms of m and $G_{\hat{\alpha}\hat{\beta}}$, where

$$\begin{aligned} A_{m0} &= 1 - \frac{6m}{r}, \\ A_{m1} &= \left(1 - \frac{2m}{r}\right)\frac{G_{\hat{0}\hat{0}} + G_{\hat{1}\hat{1}} + 2G_{\hat{2}\hat{2}}}{\frac{2m}{r^3} + G_{\hat{1}\hat{1}}} + \frac{1}{2}(G_{\hat{0}\hat{0}} - 3G_{\hat{1}\hat{1}})r^2. \end{aligned}$$

- This with $G_{\hat{\alpha}\hat{\beta}} = 0$ reproduces the Schwarzschild formula.

$$A = 1 - \frac{6M}{r} = \frac{1 - 3r^2\omega_\phi^2}{1 + 3r^2\omega_\phi^2},$$

- A_{m1} stands for the discrepancy from the Schwarzschild value.

Expression in terms of the orbital angular velocity

- We cannot directly access m from r and ω_ϕ because

$$m = \frac{r^3\omega_\phi^2 - \frac{1}{2}G_{\hat{1}\hat{1}}r^3(1+r^2\omega_\phi^2)}{1+3r^2\omega_\phi^2},$$

whereas ω_ϕ is more accessible from the relation

$$\omega_\phi = \frac{dt}{d\tau}\frac{d\phi}{dt} = (1+z)\Omega_\phi.$$

- General case
  - $A = A_{\omega 0} + A_{\omega 1}$, where

$$\begin{aligned} A_{\omega 0} &= \frac{1-3r^2\omega_\phi^2}{1+3r^2\omega_\phi^2}, \\ A_{\omega 1} &= \frac{1}{\omega_\phi^2}\left[\frac{1}{2}\left(G_{\hat{0}\hat{0}} + 2G_{\hat{2}\hat{2}} + \frac{1+7r^2\omega_\phi^2}{1+3r^2\omega_\phi^2}G_{\hat{1}\hat{1}}\right)\right. \\ &\quad \left. + r^2\omega_\phi^2(G_{\hat{0}\hat{0}} + G_{\hat{2}\hat{2}})\right]. \end{aligned}$$

  - $A_{\omega 1}$ stands for the discrepancy from the Schwarzschild value.

Post-Newtonian regime near a massive compact object

- $\epsilon/\bar{\epsilon}, \Sigma/\bar{\epsilon}, \Pi/\bar{\epsilon} = O(\alpha)$ with $\alpha \ll 1$, where

$$G_{\hat{0}\hat{0}} =: 8\pi\epsilon,\ G_{\hat{1}\hat{1}} =: 8\pi\Sigma,\ G_{\hat{2}\hat{2}} = G_{\hat{3}\hat{3}} =: 8\pi\Pi,\ m =: \frac{4\pi}{3}r^3\bar{\epsilon}.$$

- Assuming the PN regime with $\alpha \ll 1$ simultaneously,

$$\Delta\phi_p = \frac{6\pi m}{r}\left(1 - \frac{\epsilon}{\epsilon_c}\right) + \text{higher order terms}$$

where we have defined the critical density

$$\epsilon_c := \frac{2m}{r}\bar{\epsilon} = \frac{3m^2}{2\pi r^4}.$$

  - $\Delta\phi_p > 0$, < 0 and $= 0$ if $\epsilon <$, $\epsilon >$ and $\epsilon = \epsilon_c$, respectively.
  - If $\Delta\phi_p > 6\pi m/r \simeq 6\pi r^2\omega_\phi^2$, then $\epsilon < 0$ must hold.

Implications to the Galactic Centre

- Let us apply (extrapolate) the formula to the elliptical orbit of S2.
  - Choose r to $a(1-e^2) \simeq 210$au. cf. $\Delta\phi_{p,\mathrm{wf}} \simeq 6\pi M/[a(1-e^2)]$
  - $\Delta\phi_p = f\Delta\phi_{p,\mathrm{wf}}$ can be recast to $\epsilon \simeq (1-f)\epsilon_c$.
- The observed value $f = 1.10 \pm 0.19$ implies

$$\epsilon = (-4.5 \pm 8.5) \times 10^{-6} M_\odot/\mathrm{au}^3 \left(\frac{m}{4.3 \times 10^6 M_\odot}\right)^2 \left(\frac{r}{210\mathrm{au}}\right)^{-4}$$

  - As stringent as Takamori et al. (2020)'s upper bound
  - Consistent with vacuum but ...
  - The best-fit value $f = 1.10$ is in the range of the WEC violation.
  - Caveat: large eccentricity and spin of the central object

Summary

- General formulae for the periapsis shift of a quasi-circular orbit
  - Reproduce the Schwarzschild formula in $R_{\mu\nu} = 0$ and the extended-mass effect in Newtonian gravity
  - The deviation from the Schwarzschild formula comes from a particular combination of the Ricci tensor components.
- PN regime near a massive compact object
  - Critical energy density ϵ_c beyond which the shift is retrograde
  - Prograde shift greater than the Schwarzschild value implies the breakdown of the WEC in GR.
  - Constraint on the energy density around the Galatic Centre

C85

Ultra-massive spacetimes

José M M Senovilla
マーティン セノビヤ 、 ホセ マリア

arXiv:2210.14585

Department of Physics, University of the Basque Country, UPV/EHU, Bilbao, Spain

Visiting: 京都大学基礎物理学研究所

JGRG31, 東京, 28th October 2022

Outline

Introduction

- In XXIst Century we have learnt there is a *positive* cosmological constant $\Lambda > 0$
- A positive Λ imposes restrictions on the area of marginally (outer) future-trapped surfaces if these are stable and the dominant energy condition holds (Hayward-Shiromizu-Nakao 1994)
- The area A for (stable) MTS is limited by

$$A < \frac{4\pi}{\Lambda}. \tag{1}$$

- M(O)TS are defined by a null mean curvature vector $\vec{H}$. This $\vec{H}$ defines the "outer" direction.
- MTSs are said to be stable if, when perturbed in some non-timelike outer directions, they become untrapped
- Thus, the stability assumption basically says that the MTS enclose a black hole (BH) region.

Introduction (continued)

- This is certainly puzzling... What happens if we keep sending mass into the BH?
- In principle a BH will simply become bigger by adding mass, so what can prevent such physical process?
- To understand this problem, I consider some simple models of spherical BHs that keep increasing their masses until stable MTS reach the area-limit value and beyond.
- The global structure of the resulting spacetimes is shown in convenient conformal diagrams.

The Vaidya-de Sitter metric

$$ds^2 = -\left(1 - \frac{2m(v)}{r} - \frac{\Lambda}{3}r^2\right)dv^2 + 2dvdr + r^2 d\Omega^2 \qquad (2)$$

- $d\Omega^2$ is the standard metric of the unit round sphere
- r is the areal coordinate (area $4\pi r^2$)
- $v \in (-\infty, \infty)$, $r \in (0, \infty)$ (or $r \in (-\infty, 0)$).
- $$T_{\mu\nu} = \frac{2}{r^2}\frac{dm}{dv}k_\mu k_\nu$$
  $$k_\mu dx^\mu = -dv, \qquad k^\mu \partial_\mu = -\frac{\partial}{\partial r}.$$
- massless particles propagate along null hypersurfaces $v =$ const. towards decreasing r (smaller area).
- DEC is satisfied if
  $$\frac{dm}{dv} \geq 0 \qquad (3)$$
- I will also assume $m \geq 0$ everywhere.

Case with $m = 0$: (partial) de Sitter

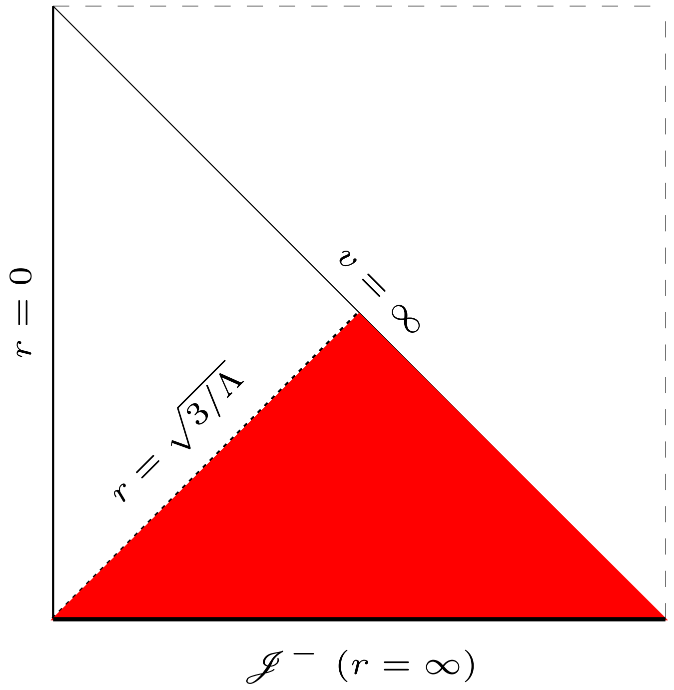

Cases with m =const. Kottler (1): $9m^2 < 1/\Lambda$

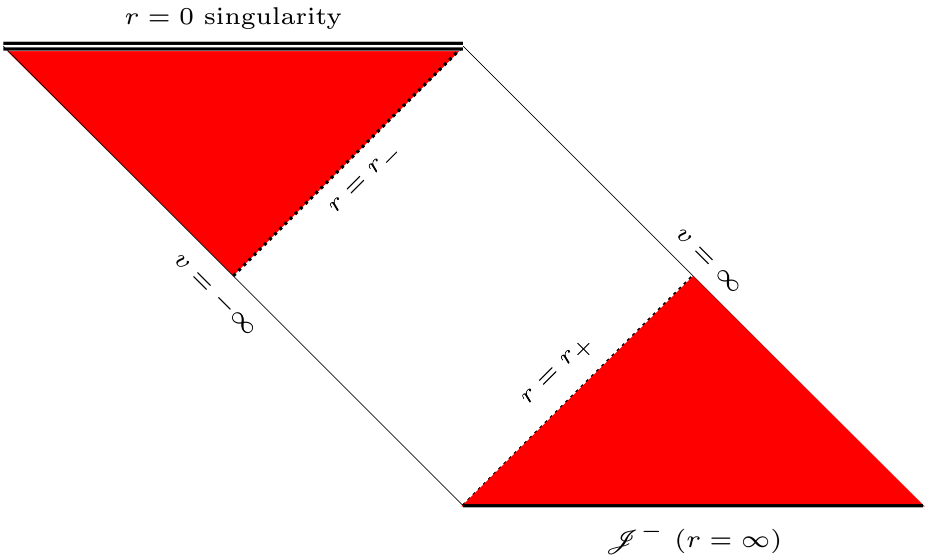

Cases with m =const. Kottler (1'): $9m^2 < 1/\Lambda$

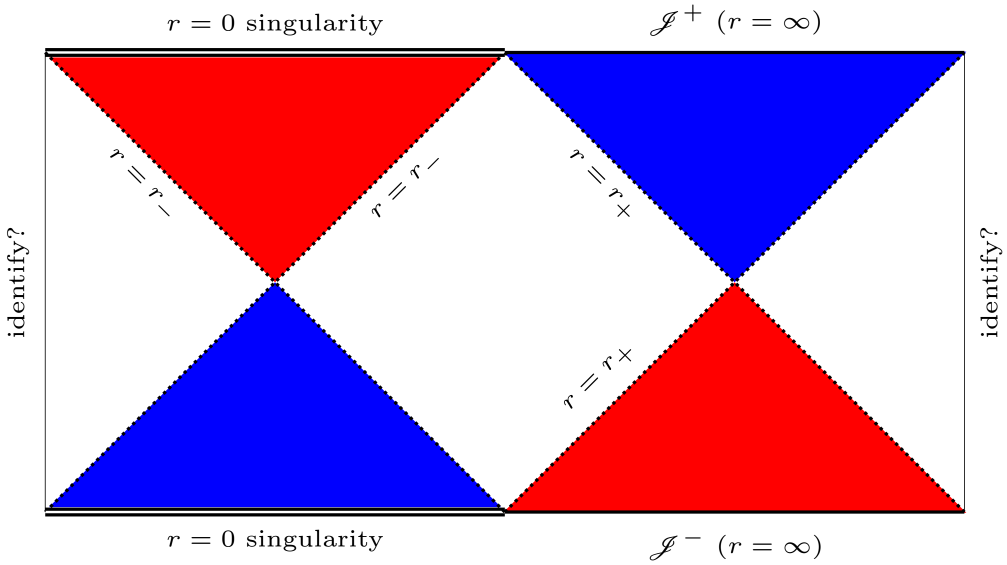

Cases with m =const. Kottler (2): $9m^2 > 1/\Lambda$

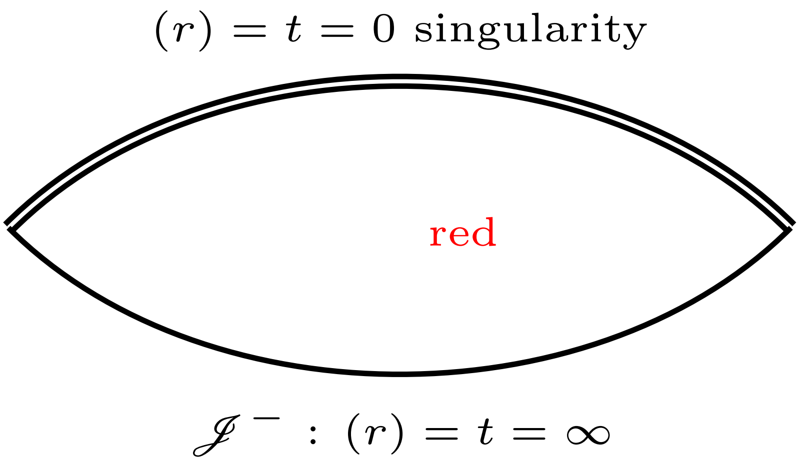

The idea

$$m(v \leq 0) = 0, \qquad m(v \geq v_1) = \mu$$

and interpolate with non-decreaasing $m(v)$ in $v \in (0, v_1)$.

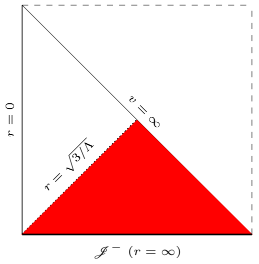

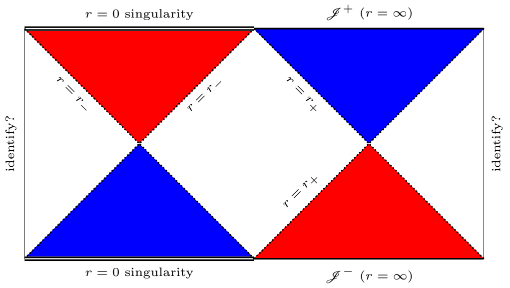

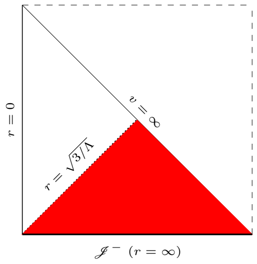

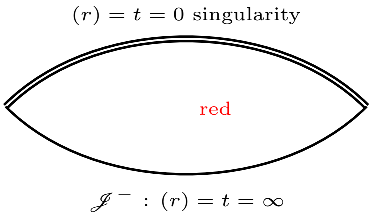

Vaidya-dS conformal diagram: $9\mu^2 < 1/\Lambda$

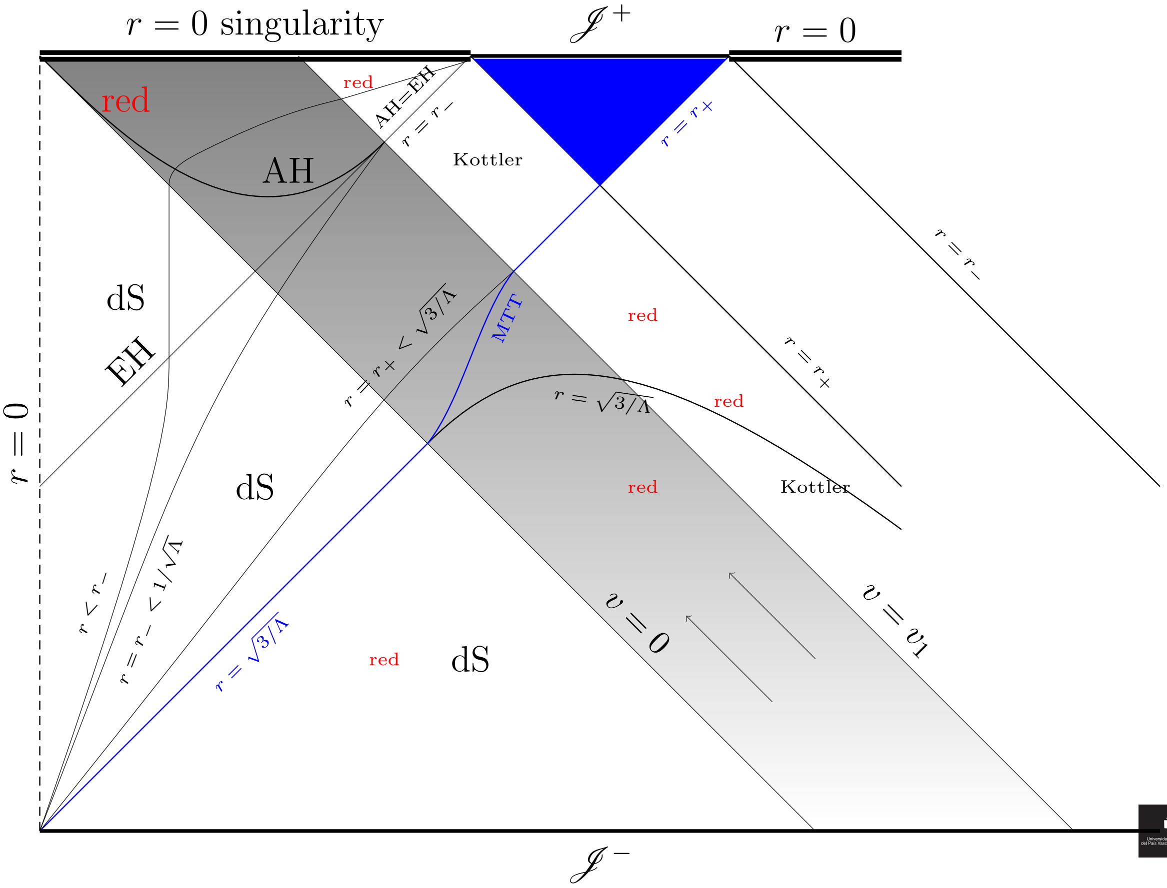

Vaidya-dS conformal diagram: $9\mu^2 > 1/\Lambda$

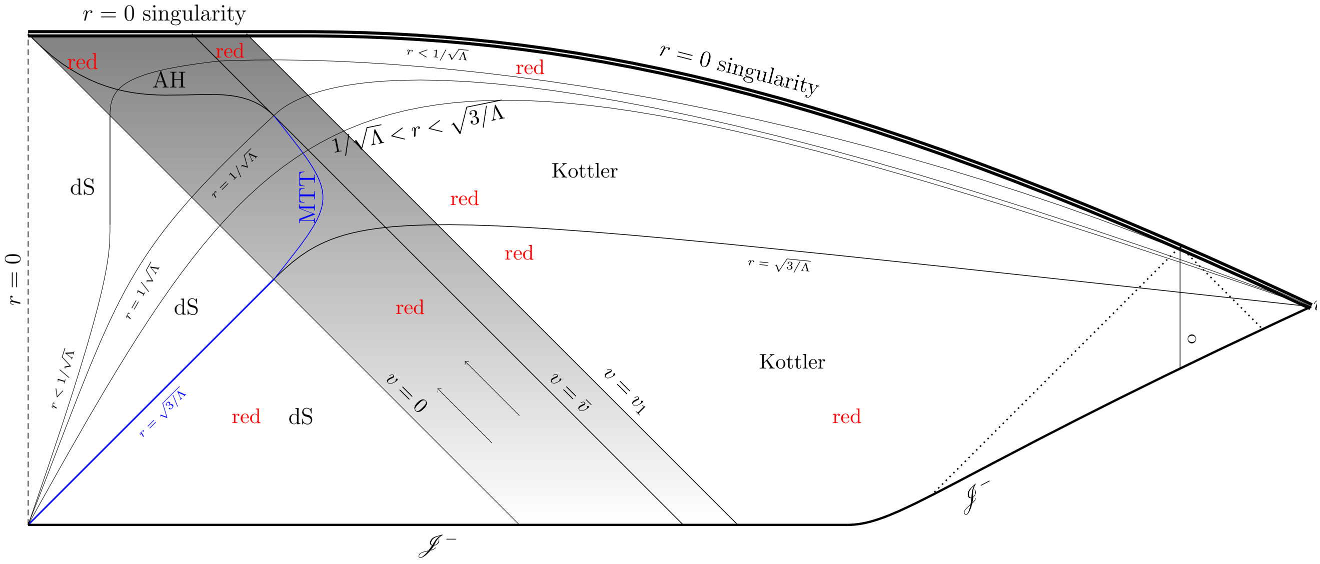

Observe that the (timelike) MTT and the (spacelike) AH merge at $r = 1/\sqrt{\Lambda}$, the round MTS of maximal area.

MTT and AH become null there.

No $\mathscr{I}^+$!

Vaidya-dS conformal diagram (2): $9\mu^2 > 1/\Lambda$

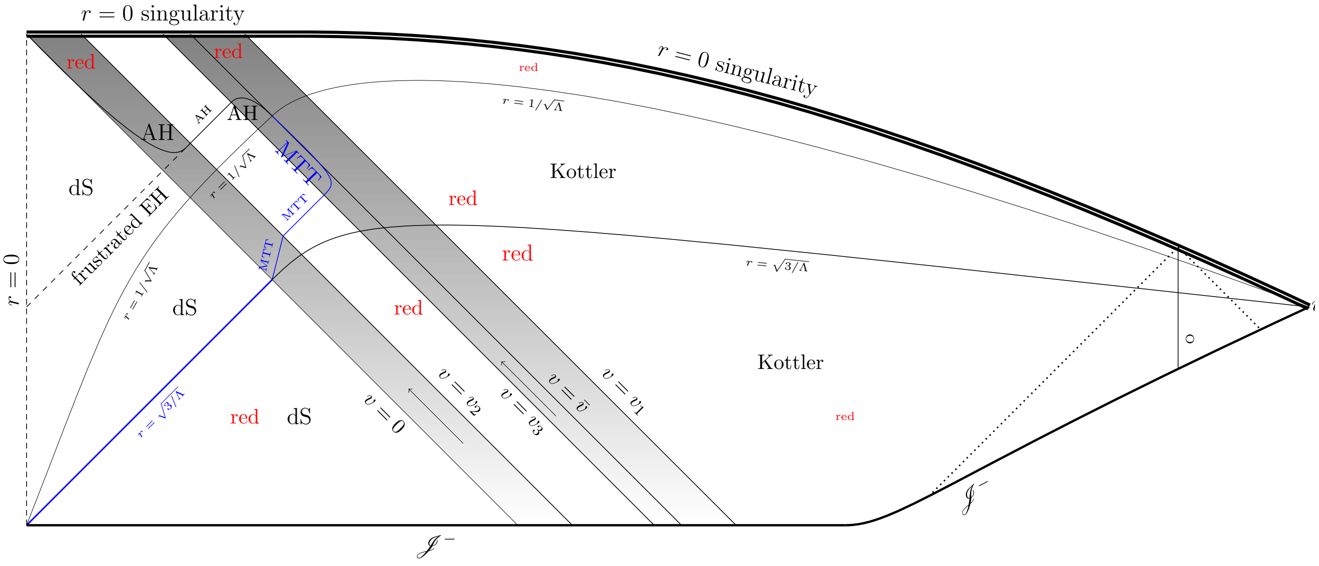

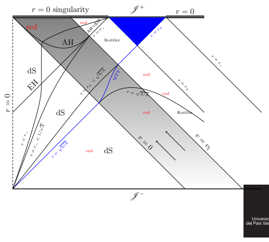

Oppenheimer-Snyder-dS conformal diagram

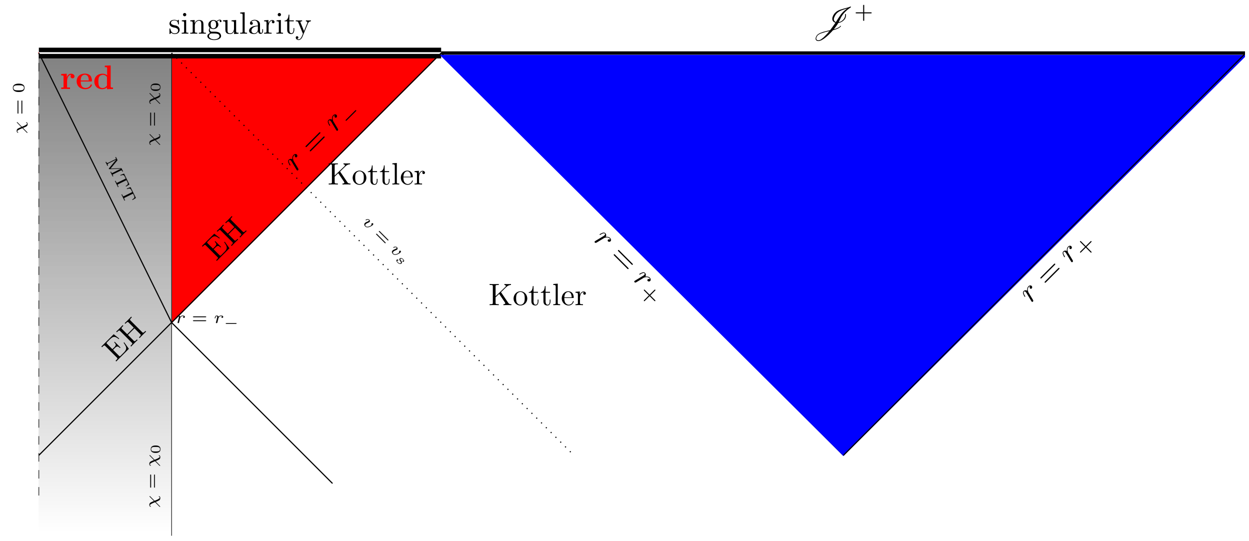

Oppenheimer-Snyder-Vaidya-dS conformal diagram: $9\mu^2 > 1/\Lambda$

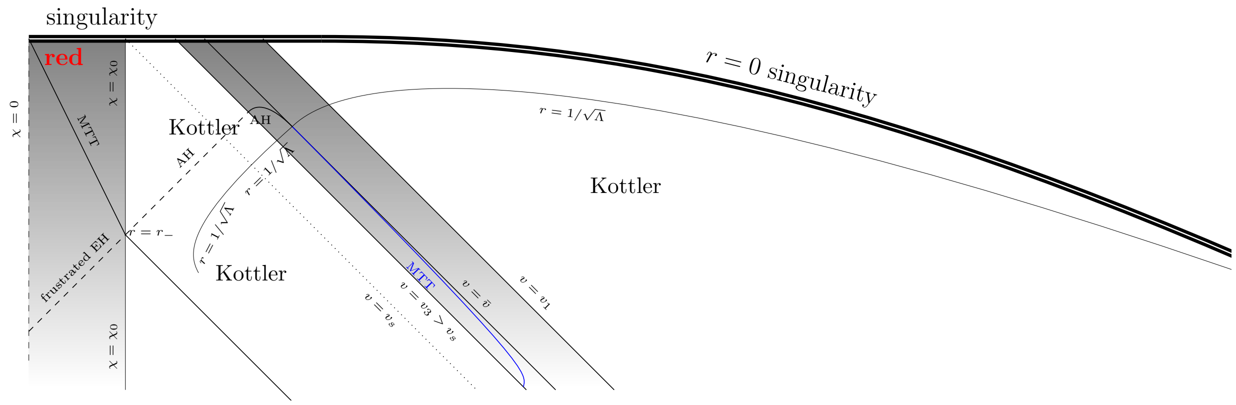

Discussion

- The limit (1) is not violated in any of the models, despite having huge total mass of the spacetime.
- MTSs simply approach one with the maximum area that *ceases* to be stable.
- Thus, the dynamical horizon foliated by stable marginally trapped spheres then simply ends its existence.
- The cosmological horizon totally vanishes.
- The global nature of event horizons is partly behind its dematerialization in these *ultra-massive* spacetimes.
- The main feature is the vanishing of future null infinity $\mathscr{J}^+$. This absence leads to 'frustrated event horizons'.
- The conclusions are robust in spherical symmetry, as follows from a simple analysis of initial data placed at $\mathscr{J}^-$
- I conjecture that the conclusion still holds without spherical symmetry.

Discussion: problematic questions arise

- An important puzzling question arises: is there any Hawking radiation?
- First, there is no Event Horizon.
- But even from the dynamical horizon AH, where will any such radiation go? There is no infinity that allows the system to radiate (lose) energy away!
- How quantum gravity might resolve this puzzle is uncertain.
- The results have implications on BHs mergers.
- The time reversals of ultra-massive spacetimes are worth considering (just look at the diagrams upside down).
- They describe a universal big-bang singularity in the past and expanding Universes such that mass-energy is radiated away towards $\mathscr{J}^+$ leaving behind either (i) a portion of de Sitter spacetime or (ii) an expanding FLRW universe.
- This may lead to several interesting speculations.

Discussion: how much mass is needed?

- The mass needed to produce ultra-massive spacetimes depends on the value of the cosmological constant Λ
- From the observed accelerated expansion of the visible Universe

$$\Lambda \simeq 1.1 \times 10^{-52} \text{m}^{-2},$$

- Then, the limit (1) requires a gravitational radius $2m$

$$2m \gtrapprox 6.4 \times 10^{25}\,\text{m}$$

- This translates into a total mass of about

$$2.2 \times 10^{22} M_{\odot} \sim 4.32 \times 10^{52} \text{Kg}.$$

- Estimated total mass of the observable universe now is

$$8.8 \times 10^{52} - 1.0 \times 10^{54} \text{Kg}$$

- There is enough mass in the already observed universe to produce such ultra-massive objects.

Thanks!

聞いてくれてありがとうございました

Thank you very much for your attention

Surface stress tensor and junction conditions on a rotating null horizon

Paolo Gondolo
University of Utah / Tokyo Tech / IPMU

Beltracchi, Gondolo, Mottola PRD 105 (2022) 2, 024001

- Junction conditions at the common 3-dimensional boundary of two parts of spacetime are the gravitational analog of the electromagnetic boundary conditions at the interface between two media (for example, $\Delta E_\perp = \sigma/\epsilon_0$, $\Delta E_{||} = 0$).

- Junction conditions in General Relativity have a long history. They are well understood when the boundary is everywhere spacelike or everywhere timelike, but obscure points remain when the boundary is null or is allowed to change signature.

- In a study of rotating exotic compact objects, we needed junction conditions on a rotating axisymmetric null horizon. The prescriptions we could find in the literature did not produce sensible results, so we worked out the junction conditions on our own.

Israel junction conditions

Applicable to spacelike or timelike boundary hypersurfaces

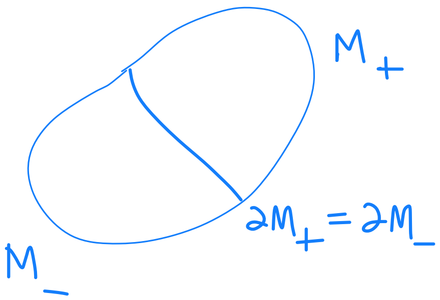

Specify the embeddings $x^\mu_\pm(\xi^i)$ of the common boundary hypersurface into each side, where $x^\mu_\pm$ are spacetime coordinates and ξ^i are hypersurface coordinates. Then $e_i^{\mu\pm} = \partial x^\mu_\pm / \partial \xi^i$ represent the same basis of vectors tangent to the boundary on either side. Let n^μ be the unit normal and ℓ the geodesic distance along the normal geodesic.

First junction condition:

(continuity of the induced metric)

$$e_i^+ \cdot e_j^+ = e_i^- \cdot e_j^- \equiv h_{ij}$$

Second junction condition:

(actually a recipe to compute the surface stress tensor)

$$^{(\Sigma)}T^{\mu\nu}_\pm = \delta(\ell)\ S^{ij}\, e_i^{\mu\pm}\, e_j^{\nu\pm}$$

$$8\pi G\, S_{ij} = -\,(n\cdot n)\,\big([K_{ij}] - [K]h_{ij}\big)$$

extrinsic curvature $K^\pm_{ij} = -\,n_\mu e_i^\nu \nabla_\nu e_j^{\mu\pm}$

$$[K_{ij}] = K^+_{ij} - K^-_{ij} \qquad K^\pm = K^\pm_{ij}\, h^{ij}$$

Barrabès-Israel junction conditions

For null boundary hypersurfaces

Null hypersurfaces do not have a unit normal vector.

Barrabes & Israel: replace the unit normal in Israel's conditions with a null vector $N^\pm$ along each side of the null surface satisfying

$$\boldsymbol{N}^\pm \cdot \boldsymbol{N}^\pm = 0, \quad \boldsymbol{N}^+ \cdot \boldsymbol{e}_i^+ = \boldsymbol{N}^- \cdot \boldsymbol{e}_i^-$$

The first junction condition remains the same as Israel's.

Define an "oblique exterior curvature" $\mathscr{K}_{ij}$ along the null surface as

$$\mathscr{K}^\pm_{ij} = -\,N_\mu e_i^\nu \nabla_\nu e_j^{\mu\pm}$$

Then the surface stress tensor $^{(\Sigma)}T^{\mu\nu}$ is *proportional to*

$$S^{\mu\nu} = [2\gamma^{(mu}n^{\nu)} - \gamma n^\mu n^\nu - \gamma^\dagger g^{\mu\nu} - (n\cdot n)\,(\gamma^{\mu\nu} - \gamma g^{\mu\nu})]/(16\pi)$$

where $\gamma^{\mu\nu}$ *satisfies* $2\gamma_{\mu\nu}e_i^\mu e_j^\nu = [\mathscr{K}_{ij}]$

Our work

A general stationary axisymmetric metric can be written as

$$ds^2 = -\,e^{2\nu}dt^2 + e^{2\psi}\big(d\phi - \omega\, dt\big)^2 + e^{2\alpha}dr^2 + e^{2\beta}d\theta^2$$

Combine the Killing vectors $\boldsymbol{K}_{(t)} = \boldsymbol{\partial}_t, \boldsymbol{K}_{(\phi)} = \boldsymbol{\partial}_\phi$ into $\boldsymbol{\ell} \equiv \boldsymbol{K}_{(t)} + \omega \boldsymbol{K}_{(\phi)}$, which is null at the horizon and tangent to it.

Introduce the frame $\{\boldsymbol{\ell}, \boldsymbol{N}, \boldsymbol{\partial}_\theta, \boldsymbol{\partial}_\phi\}$, where $\boldsymbol{\partial}_\theta, \boldsymbol{\partial}_\phi$ are spacelike and tangent to the horizon, and $\boldsymbol{N}$ is null and transversal to the horizon,

$$\boldsymbol{N}\cdot\boldsymbol{N} = 0, \quad \boldsymbol{N}\cdot\boldsymbol{\partial}_\theta = 0, \quad \boldsymbol{N}\cdot\boldsymbol{\partial}_\phi = 0, \quad \boldsymbol{\ell}\cdot\boldsymbol{N} = -\,1$$

The first junction condition is the same as Israel's.

Our work

The stress tensor density concentrated on the horizon at $r = R_H$ is

$${}^{(\Sigma)}T^i{}_j\ \underbrace{(-g)^{1/2}\ d^4x}_{\text{invariant volume}} = \mathcal{S}^i{}_j\ \underbrace{\delta(r - R_H)\ dr\ dA\ dt}_{\text{correct integration measure}}$$

where dA is the area element of the horizon, and

$$8\pi G\,\mathcal{S}^t{}_t = -\,\omega_H\,[\mathcal{J}] \qquad 8\pi G\,\mathcal{S}^t{}_\phi = [\mathcal{J}] \qquad 8\pi G\,\mathcal{S}^\theta{}_\theta = [\kappa]$$

$$8\pi G\,\mathcal{S}^\phi{}_t = -\,\omega_H\,[\kappa] - \omega_H^2\,[\mathcal{J}] \qquad 8\pi G\,\mathcal{S}^\phi{}_\phi = [\kappa] + \omega_H\,[\mathcal{J}]$$

Here ω_H is the angular velocity of the horizon, and $[\kappa], [\mathcal{J}]$ are the discontinuities at the horizon of the surface gravity $\kappa = N_\mu \ell_\nu(\nabla^\mu \ell^\nu)$ and of a new invariant quantity $\mathcal{J} = -\,N_\mu \ell_\nu(\nabla^\mu K^\nu_{(\phi)})$ proportional to the angular momentum density.

Our work

- We have checked that the conservation equations for the Komar mass and angular momentum fluxes lead to the same surface stress tensor $\mathcal{S}^i{}_j$.
- We have found a modification of the Israel junction conditions that leads to the correct null horizon limit, while the unmodified Israel junction conditions diverge.
- We have shown that the Barrabès-Israel prescription for junction conditions at null hypersurfaces leads to an incorrect surface stress tensor.
- We have computed the Weyl tensor and found that it has no $\delta(r - R_H)$ term at the horizon: there is no impulsive gravitational wave at a stationary axisymmetric rotating null horizon.

Summary

- We have obtained the stress energy tensor on a rotating stationary axisymmetric null horizon by direct calculation, and expressed in invariant terms, i.e., the discontinuities of the surface gravity and a new angular momentum invariant of the geometry.
- A key step is recognizing that an integration measure must accompany the Dirac δ-function, and that the correct integration measure follows from the stress-energy tensor density.
- Our result is a major improvement on previous prescriptions for the surface stress tensor on a null surface, which either diverge or do not give the physically correct surface stress.
- Our result applies to the stationary axisymmetric case, and a generalization is in progress.